PB89-172167

Proceedings: First Combined FGD (Flue Gas Desulfurization) and Dry S02 Control Symposium. Held in St. Louis, Missouri on October 25-28, 1988. Volume 2. Sessions 5 and 6

Radian Corp., Research Triangle Park, NC

Prepared for

Environmental Protection Agency
Research Triangle Park, NC

Mar 89

U.S. Department of Commerce
National Technical Information Service
NTIS

PB89-172167

EPA-600/9-89-036b
March 1989

PROCEEDINGS:
FIRST COMBINED FGD AND DRY SO_2 CONTROL SYMPOSIUM

Volume 2. Sessions 5 and 6

B. B. Emmel, Compiler

Radian Corporation
P.O. Box 1300
Research Triangle Park, NC 27709

EPA Contract 68-02-3994, Task 93

Project Officers:

Charles B. Sedman
U.S. Environmental Protection Agency
Air and Energy Engineering Research Laboratory
Research Triangle Park, NC 27711

P. T. Radcliffe
Electric Power Research Institute
Desulfurization Processes Program
Coal Combustion Systems Division
3412 Hillview Avenue
Palo Alto, CA 94304

AIR AND ENERGY ENGINEERING RESEARCH LABORATORY
OFFICE OF RESEARCH AND DEVELOPMENT
U.S. ENVIRONMENTAL PROTECTION AGENCY
RESEARCH TRIANGLE PARK, NC 27711

REPRODUCED BY
U.S. DEPARTMENT OF COMMERCE
NATIONAL TECHNICAL INFORMATION SERVICE
SPRINGFIELD, VA. 22161

TECHNICAL REPORT DATA
(Please read Instructions on the reverse before completing)

1. REPORT NO.
EPA-600/9-89-036b

2.

3. RECIPIENT'S ACCESSION NO.
PB89 172167/AS

4. TITLE AND SUBTITLE
Proceedings: First Combined FGD and Dry SO_2 Control Symposium, Volume 2. Sessions 5 and 6

5. REPORT DATE
March 1989

6. PERFORMING ORGANIZATION CODE

7. AUTHOR(S)
B.B. Emmel, Compiler

8. PERFORMING ORGANIZATION REPORT NO.

9. PERFORMING ORGANIZATION NAME AND ADDRESS
Radian Corporation
P.O. Box 13000
Research Triangle Park, North Carolina 27709

10. PROGRAM ELEMENT NO.

11. CONTRACT/GRANT NO.
68-02-3994, Task 93

12. SPONSORING AGENCY NAME AND ADDRESS
EPA, Office of Research and Development
Air and Energy Engineering Research Laboratory
Research Triangle Park, NC 27711

13. TYPE OF REPORT AND PERIOD COVERED
Proceedings; 10/88

14. SPONSORING AGENCY CODE
EPA/600/13

15. SUPPLEMENTARY NOTES AEERL project officer is Charles B. Sedman, Mail Drop 4, 919/541-7700. Volume 1 covers Sessions 1-4; Volume 2, Sessions 5 and 6; and Volume 3, Sessions 7 and 8 (and four unpresented papers).

16. ABSTRACT
The proceedings document presentations at the First Combined FGD and Dry SO2 Control Symposium, in St. Louis, MO, October 25-28, 1988. The symposium, jointly sponsored by EPA and EPRI, had as its objective the exchange of technical and regulatory information on sulfur oxide control technology, including wet and dry scrubbers, emerging processes, and international developments in clean coal/acid rain technologies. Topics covered included: retrofit economics, spray dryer technology, furnace sorbent injection topics (demonstration results, byproduct utilization, enhancement), wet FGD operation, municipal solid waste facilities, and post-combustion dry technologies. Also included were concurrent sessions on special topics of interest, including dry FGD, new technologies, and FGD improvement. The proceedings, published in three volumes, include 85 papers and 4 unpresented papers.

17. KEY WORDS AND DOCUMENT ANALYSIS

a. DESCRIPTORS		b. IDENTIFIERS/OPEN ENDED TERMS	c. COSATI Field/Group	
Pollution	Precipitation (Meteorology)	Pollution Control	13B	
Flue Gases		Stationary Sources	21B	04B
Desulfurization	Acidification	Clean Coal	07A, 07D	07C
Sulfur Dioxide	Economics	Acid Rain	07B	05C
Scrubbers	Sorbents	Spray Drying	13I	11G
Coal	Wastes	Municipal Waste	21D	14G

18. DISTRIBUTION STATEMENT
Release to Public

19. SECURITY CLASS *(This Report)*
Unclassified

20. SECURITY CLASS *(This page)*
Unclassified

21. NO. OF PAGES
508

22. PRICE

EPA Form 2220-1 (9-73)

PREFACE

The First Combined FGD and Dry SO_2 Control Symposium was held in St. Louis, Missouri, October 25 - 28, 1988. This Symposium, jointly sponsored by EPRI and EPA, had as its objective the exchange of technical and regulatory information on sulfur oxide control technology, including wet and dry scrubbers, emerging processes, and international developments in clean coal/acid rain technologies.

Eighty-five papers were presented by EPA and EPRI staff members, representatives of utility companies, equipment manufacturers, research and development companies, and university researchers. Specific topics discussed in symposium presentations included: retrofit economics, spray dryer technology, furnace sorbent injection topics (demonstration results, byproduct utilization, enhancements), wet FGD operation, municipal solid waste facilities, and post-combustion dry technologies. Also included were concurrent sessions on special topics of interest, including dry FGD, new technologies, and FGD improvement.

The Proceedings of this Symposium have been compiled in three volumes. Volume 1 contains papers from the following sessions:

• Session 1:	International Overview
• Session 2:	Retrofit Economics
• Session 3:	Spray Dryer Technology
• Sessions 4A/4B:	Furnace Sorbent Injection - Demonstrations/ Integration/Byproduct Utilization

Contained in Volume 2 are papers presented in these sessions:

• Sessions 5A/5B:	FSI Impacts/Enhancements/Wet FGD Operation
• Session 6:	Municipal Solid Waste Facilities

Contained in Volume 3 are papers presented in these sessions:

• Sessions 7A/7B/7C:	Special Topics: Dry FGD Fundamentals/New Technologies/FGD Improvement
• Session 8:	Post-Combustion Dry Technologies

The assistance of Holly Rossi, Radian Corporation, in preparing for the Symposium and in compiling these Proceedings is gratefully acknowledged.

CONTENTS

VOLUME 1

Paper Page

SESSION 1: INTERNATIONAL OVERVIEW
Chairman, J. Abbott, EPA

1-1 "FGD Research and Development Status in the U.S.," D. Delleney and J. Dickerman 1-1

1-2 "A Programme for Reducing SO_2 Emissions from UK Power Stations - Present and Future," W. Kyte 1-14

1-3 "Progress in European SO_x/NO_x Control," B. Forck 1-21

1-4 "Progress in European SO_2 and NO_x Emission Control," W. Ellison and H. Weiler 1-38

1-5 "Flue Gas Cleaning in Dutch Power Stations," F. van der Brugghen and J. Koppius-Odink 1-66

1-6 "Recent Developments in SO_2 and NO_x Abatement Technology in Japan and Far Eastern Countries," J. Ando and N. Kaplan 1-91

SESSION 2: RETROFIT ECONOMICS
Chairman, P. Radcliffe, EPRI

2-1 "The Design, Operation, and Performance of Current Generation Retrofit FGD Systems on Coal-Fired Utility Boilers," B. Laseke .. 2-1

2-2 "Site-Specific Evaluation of Six Sorbent Injection Processes," W. Frazier, P. Ireland, G. Brown, and P. Radcliffe 2-20

2-3 "Lime/Limestone FGD and Sorbent Injection Technology Retrofit Difficulty at 60 Coal-Fired Utility Power Plants," T. Emmel and N. Kaplan 2-38

SESSION 3: SPRAY DRYER TECHNOLOGY
Chairman, R. Glover, EPRI

3-1 "Results from the TVA 10-MW Spray Dryer/ESP Evaluation," C. Brown, G. Blythe, L. Humphries, R. Robards, R. Runyan, and R. Rhudy 3-1

3-2 "The GRDA Unit No.2 Dry FGD System: Performance and Operating Experience," J. Buschmann, T. Lillestolen, J. Mills, and J. Marcy 3-21

CONTENTS (Continued)

Paper Page

3-3 "Evaluation of a Combined $Ca(OH)_2/NH_3$ Spray Dryer System for SO_2 Removal on High Sulfur Coal," W. Davis, G. Reed, A. Pakrasi, G. Smith, and T. Keener 3-42

3-4A "Update of Joy/Niro U.S. Utility Spray Dryer FGD Systems," J. Donnelly, M. Quach, S. Wolf, and G. Fosher 3-56

3-4B "Update on Spray Dryer FGD Experience in Europe and in the People's Republic of China," K. Felsvang, R. Hahn, P. Necker, M. Novak, Y. Qing, N. Raffelsberger, E. Schumacher, H. Spannbauer 3-73

3-5 "Results from EPRI High Sulfur Spray Dryer Pilot Tests," G. Blythe, L. Lepovitz, R. Rhudy 3-94

SESSION 4A: FURNACE SORBENT INJECTION - DEMONSTRATIONS
Chairman, R. Stern, EPA

4A-1 "Operation of the LIMB/Humidifier Demonstration Unit at Edgewater (104 MWe), P. Nolan, R. Hendriks, and N. Kresovich 4-1

4A-2 "Prototype Evaluation of Dry Sorbent Injection with Humidification," G. England, B. Folsom, R. Payne, T. Sommer, J. Chappell, M. McElroy, and I. Huffman 4-15

4A-3 "Development and Demonstration of Sorbent Injection for SO_2 Control on Tangentially Coal-Fired Boilers ," M. Gogineni, J. Clark, R. Koucky, J. Marion, D. Anderson, A. Kwasnik, E. Gootzait, D. Lachapelle, and S. Rakes 4-35

4A-4 "Status of the LIFAC SO_2 and NO_x Removal Process," T. Kenakkala 4-51

4A-5 "Sorbent Slurry Injection for SO_2 Control," R. Mangal, M. Mozes, R. Thampi, and D. Tubman 4-66

4A-6 "Desulfurization Results for Three Different Firing Concepts," M. Chughtai 4-88

4A-7 "Austrian Experience with Furnace Limestone Injection," G. Staudinger, P. Melcher, and K. Eckerstorfer 4-109

4A-8 "Four Years of Operating Experience with Direct In-Furnace SO_2 Reduction at 600 MWe Unit of Provence Power Station," M. Vandycke, B. Auric, and J. Merry 4-121

CONTENTS (Continued)

Paper Page

SESSION 4B: INTEGRATION/BYPRODUCT UTILIZATION
Chairman, M. McElroy, EPRI

4B-1 "Improving Sludge Dewatering in Magnesium-Enhanced Wet Lime FGD Systems," L. Benson, R. D'Alesandro, J. Wilhelm, and A. Randolph 4-135

4B-2 "Recycle/Reuse of Boiler Chemical Cleaning Wastes in Wet Limestone FGD Systems," M. Stohs, D. Owens, and W. Micheletti ... 4-151

4B-3 "Design of Waste Management Systems for Furnace Sorbent Injection Technologies," G. Gumtz, M. Lees, D. Saylor, and D. Golden 4-169

4B-4 "Environmental Assessment of an FGD Sludge Disposal Site," I. Murarka and D. Rai 4-189

4B-5 "Spray Dry Absorption-Oxidation of SO_2/NO_x," A. Stromberg and H. Karlsson 4-204

4B-6 "Technology Development Status of Nitric Oxide Abatement Using Ferrous Chelates," D. Zabcik 4-224

4B-7 "Experiences with Active Coke Processes for Simultaneous Removal of SO_2 and NO_x," E. Richter, K. Knoblach, and W. Wunnenberg 4-229

4B-8 "Simultaneous NO_x/SO_2 Removal with Dry Sorbent Injection," M. Teague, R. Thompson, and L. Muzio 4-247

CONTENTS

VOLUME 2

Paper | Page

SESSION 5A: FSI IMPACTS/ENHANCEMENTS
Chairman, D. Drehmel, EPA

5A-1 "Design and Operation of Feeding Systems for High Reactivity Sorbents," P. Solt 5-1

5A-2 "Field and Laboratory Measurements of Fly Ash Properties and Precipitator Performance Parameters with Furnace Sorbent Injection," G. Faulkner, G. Marchant, Jr., E. Landham, Jr., and J. DuBard 5-13

5A-3 "The Ridox Project - A Summary Review," G. DeMichele 5-33

5A-4 "Mechanistic Studies of Sorbent Utilization Enhancement by Humidification," R. Dahlin and R. Beittel 5-55

5A-5 "Rate Controlling Processes in Humidification for Duct SO_2 Capture," J. Kramlich, D. Moyeda, G. Newton, and R. Payne 5-71

5A-6 "Pilot Plant Evaluation of Post-Combustion LIMB SO_2 Capture," C. Sedman, D. Drehmel, J. Chang, and C. Jorgensen 5-91

5A-7 "Effect of CaO Sorbent Physical Parameters Upon Sulfation," B. Gullett and K. Bruce 5-103

5A-8 "Laboratory and Commercial-Scale Results of Testing Surfactant-Modified Sorbents," D. Kirchgessner, W. Jozewicz 5-121

SESSION 5B: WET FGD OPERATION
Chairman, R. Moser, EPRI

5B-1 "Results of Wet FGD Tests at EPRI's High Sulfur Test Center," J. Burke, S. Gray, R. Moser 5-136

5B-2 "Advanced Simplified Wet FGD Designs," S. Dalton, R. Moser, D. Colley, and J. Burke 5-166

5B-3 "Corrosion Control in SO_2 Scrubbers by Impressed Current," G. Koch, S. Pednekar, and B. Syrett 5-183

5B-4 "Development of a Predictive Model for Limestone Dissolution in Wet FGD Systems," J. Jarvis, F. Meserole, T. Selm, G. Rochelle, and R. Moser 5-192

CONTENTS (Continued)

Paper Page

5B-5 "Performance Impact of Mist Eliminators and Wet Electrostatic Precipitators," E. Bakke and O. Sarmiento 5-216

5B-6 "Video Based In-Situ Droplet Concentration and Size Analyzer," J. McCain 5-230

5B-7 "Guidelines for Troubleshooting Utility Mist Elimination Systems," F. Jones, D. Colley, D. Balfour, R. Rhudy, and R. Keeth 5-244

5B-8 "Guidelines for Troubleshooting Excessive Stack Opacity," D. Balfour, R. Rhudy, R. Keeth 5-263

SESSION 5B: WET FGD OPERATION
(Continued) Chairman, C. Dene, EPRI

5B-9 "Performance and Operating Costs of the Somerset Wet Limestone FGD System," D. McCoy, B. Koch, W. Rogers, H. Crosby, and J. Smigelski 5-278

5B-10 "FGD Reliability Improvement at LG&E: Cane Run 6 Case Study and Overall Project Status," C. Weilert, D. Froelich, and M. Schmitt 5-293

5B-11 "Inhibited Sulfite Oxidation by Thiosulfate in Wet Lime/Limestone FGD Processes: Results of Laboratory Studies and Testing at EPRI's High Sulfur Test Center Mini-Pilot," D. Owens, G, Maller, F. Meserole, R. Chin, G. Rochelle, and R. Moser 5-310

5B-12 "Control and Reduction of Gypsum Scale in Wet Lime/Limestone FGD Systems by Addition of Thiosulfate: Summary of Field Experiences," R. Moser, D. Owens, and D. Colley 5-335

5B-13 "Design, Startup, and Operating Experience of FGD System with Gypsum Byproduct at Reidersbach No. 2 in Austria," P. Kneissl, G. Staudinger, and M. Weitzer 5-355

5B-14 "Simultaneous SO_2 and Particulate Removal in a Jet Bubbling Reactor," R. Sherwin, B. Gilbert, K. Kitamoto, Y. Yamagurhi, Y. Ogawa, and H. Koshizuka 5-379

5B-15 "The Bischoff Flue Gas Desulfurization Process," P. Kutemeyer and K. Hegemann 5-399

5B-16 "Operating Experience with Advanced FGD Technology in West Germany," M. Schutz, J. Glamser, and M. Eikmeier 5-416

CONTENTS (Continued)

Paper Page

SESSION 6: MUNICIPAL SOLID WASTE FACILITIES
Chairman, T. Brna, EPA

6-1 "A Comparison of HCL, SO_2 and Particulate Emissions from Three Different MSW Solid Waste-Fired Boilers," M. Sandell, V. Petti, and T. Porter 6-1

6-2 "Dry Scrubbing Process for Waste-To-Energy Applications--Operating Experience and Performance Data," P. Dhargalkar 6-19

6-3 "Characterization of Emissions for a Municipal Solid Waste Incinerator with a Dry Scrubber," T. Brna, C. Sedman, and C. Riley 6-31

6-4 "Operating Experience with a Spray Dry Scrubbing System on an RDF-Fired Boiler," G. Bresowar, D. Collins, and J. Accortt 6-53

CONTENTS

VOLUME 3

Paper | Page

SESSION 7: SPECIAL TOPICS

SESSION 7A: DRY FGD FUNDAMENTALS
Chairman: D. Mobley, EPA

7A-1 "An Experimental and Theoretical Study of the Fundamentals of the SO_2/Lime Reaction at High Temperatures," D. Pershing, C. Milne, and D. Kirchgessner 7-1

7A-2 "Dry Injection - Kinetic Studies," I. Bjerle and A. Karlsson 7-21

7A-3 "Laboratory Tests on Flue Gas Desulfurization by Dry Limestone Injection," F. Mayrhuber and G. Staudinger 7-40

7A-4 "Surface Chemical Reactivity of Different Calcium Based Sorbents with SO_2," D. Beruto, M. Giordani, R. Botter, G. Chiarello, A. Lumachi, F. Parmigiani, P. Ghetti, and G. DeMichele 7-55

7A-5 "Dry Sorbent Recycle Processes," T. Lott, D. Teixeira, L. Muzio, and M. Teague 7-66

7A-6 "Calcium Hydroxide Reactivity with Sulfur Dioxide from X-Ray Diffraction Peak Profiles," F. Briden and D. Natschke 7-83

SESSION 7B: NEW TECHNOLOGIES
Chairman, C. Sedman, EPA

7B-1 "Test Results on the Use of a Circulating Fluidized Bed Absorber (CFBA) for Control of SO_2," T. Keener, X. Jiang, and J. Jao 7-99

7B-2 "A Pilot Demonstration of the Limestone Emission Control (LEC) System," D. Furlong, J. Wright, and M. Prudich 7-105

7B-3 "SO_2 Recovery by Sodium Phosphate Solution Scrubbing," O. Erga 7-125

7B-4 "The 3-S Process: Simultaneous (Acid Gas and NO_x) Sodium-Based Sorption of Waste Gases," R. Lindbauer and F. Mair 7-135

7B-5 "Production of Lime/Fly Ash Absorbents for Flue Gas Desulfurization," G. Rochelle and J. Peterson 7-143

Paper Page

7B-6 "Physical and Chemical Activation of Fly Ash to Produce Reagent for Dry FGD Processes," H. Karlsson, T. Peterson, J. Peterson, and I. Bjerle 7-160

SESSION 7C: FGD IMPROVEMENT
Chairman, M. Maxwell, EPA

7C-1 "On-Line Electrochemical Corrosion Monitoring in a Flue Gas Heat Exchanger," D. Farrell, W. Cox, B. Syrett, and R. Keeth 7-180

7C-2 "The Evolution of Fluorelastomeric Coatings for Flue Gas Desulfurization," K. Brethauer and J. Montle 7-199

7C-3 "Life-Cycle Cost Model for FGD Components," J. Redmond, Y. Shah, V. DiGirolamo, and W. Plant 7-217

7C-4 "Performance of Linings in FGD Systems," H. Rosenberg, G. Koch, C. Kistler, Jr., W. Mueller, and P. Radcliffe 7-233

7C-5 "FGD Chemistry Video Series," N. Gates and R. Moser 7-252

7C-6 "Chemical Additives for Dry FGD Scrubbers," L. Lin, R. Shiely, E. Ekis, Jr., and M. Meyerkord 7-255

SESSION 8: POST-COMBUSTION DRY TECHNOLOGIES
Chairman, R. Rhudy, EPRI

8-1 "Full Scale Demonstration of Additive NO_2 Reduction with Dry Sodium Desulfurization," J. Hammond 8-1

8-2 "In-Duct Scrubbing Technologies for SO_2 Control," C. Drummond ... 8-24

8-3 "Technical and Economic Evaluation of HYPAS," D. Giovanni and R. Rhudy 8-75

8-4 "Operating Experience with a Dry FGD Plant Using a Circulating Fluid Bed (CFB) at the Lignite-Fired Power Station of PREAG in Borken, Federal Republic of Germany," H. Sauer 8-97

8-5 "Scale-Up Testing of the ADVACATE Damp Solids Injection Process," J. Chang, C. Sedman, and T. Pearson 8-122

8-6 "Dry Flue Gas Desulfurization Process Using Absorbent Made from Fly Ash," M. Narita, S. Kudo, T. Veno, N. Arashi, T. Nishimura, and T. Mizoguchi 8-139

CONTENTS (Continued)

Paper Page

8-7 "Hydrate and Process Parameters Controlling SO_2 Removal During Hydroxide Injection Near 1000°F," S. Bortz, V. Roman, and G. Offen 8-156

8-8 "E-SO_x Studies Pilot Evaluation," L. Hovis, R. Valentine, B. Jankura, P. Chu, and J. Chang 8-177

UNPRESENTED PAPERS

"The Ecotech Dry Scrubber--for the Simultaneous Dry Scrubbing of High Temperature Hard Particulate Matter, Condensable Solids, and Noxious Gases Entrained in a Gas Stream," J. Chambers U-1

"SO_2 Capture in a Coal-Fueled Gas Turbine System, S. Johnson, L. Walkauskas, and J. Morency U-18

"FGD System Cost Comparisons," C. Gaige, S. Smith, R. Norton, and P. Dyer U-38

"Combined SO_x/NO_x Removal in a High-Sulfur Spray-Dryer/Fabric-Filter System," D. Livengood, H. Huang, J. Allen, and P. Farber U-43

Appendix A - List of Attendees A-1

NOTICE

This document has been reviewed in accordance with U.S. Environmental Protection Agency policy and approved for publication. Mention of trade names or commercial products does not constitute endorsement or recommendation for use.

SESSION 5A: FSI IMPACTS/ENHANCEMENTS

Chairman, Dennis C. Drehmel, EPA/AEERL

DESIGN AND OPERATION OF FEEDING SYSTEMS FOR HIGH REACTIVITY SORBENTS

by: Paul E. Solt, Consultant
Pneumatic Conveying Consultants
Allentown, Pennsylvania 18104

Michael W. McElroy
Electric Power Research Institute
Palo Alto, California 94303

ABSTRACT

This paper reviews fundamental material handling issues and discusses design approaches for sorbent storage, feeding and conveying systems for the furnace sorbent injection process. The information is particularly relevant to systems using hydrated lime or other very fine powdered sorbents. Design and operating recommendations are based on conventional material handling principles, and on a review of experiences at several sorbent injection installations. The recommendations are intended to provide a reference to aid in designing reliable sorbent injection systems that are consistent with the low retrofit cost objectives of furnace sorbent injection.

INTRODUCTION

Furnace sorbent injection has been under extensive development over the last decade as a potential low cost retrofit SO2 control alternative to conventional flue gas desulfurization. The development efforts have culminated in tests of this technology on utility and industrial boilers in Europe, Canada and the U.S. In recent years, much information has been reported from these projects as well as from numerous laboratory development programs (1)(2). The majority of information available on field experiences has tended to focus on factors affecting SO2 removal performance, and on the impacts of sorbent injection on various aspects of the generating system such as boiler heat transfer and particulate control. Very little information has been reported on the operating experiences and design criteria for sorbent storage, feeding and conveying systems associated with these programs. As a consequence, there has been a general perception that these systems, since they typically rely on conventional material handling hardware proven in other applications, are not a major issue in the performance or reliability of the furnace injection process.

Recent experiences in handling hydrated lime sorbents at two current furnace injection projects (3)(4), and a subsequent survey of the sorbent handling experiences by others (5), have highlighted the need for a greater awareness about the uncertainties and potential problems with these systems when adapted to furnace sorbent injection, and the solutions that have evolved to overcome them.

This paper summarizes design and operational considerations and recommendations for furnace sorbent injection systems. The recommendations are based on a review of experience at several sorbent injection installations (see acknowledgements), and are particularly relevant to sorbent injection systems using very fine powdered sorbents such as hydrated lime. The recommendations are not intended to be absolute, but rather are provided as a general reference to aid in the development of future sorbent injection system designs.

FUNDAMENTALS OF HANDLING FINE POWDERED MATERIALS

As background for subsequent discussion of sorbent system design issues and recommendations, basic principles of handling fine powdered materials are reviewed below, with particular emphasis on hydrated lime sorbent. Hydrated lime has become the sorbent of choice in most installations, and in many ways poses the most difficult challenges from the standpoint of material handling, compared to other "coarser" sorbents such as pulverized limestone.

When designing a bulk material handling system several variables must be considered. These include (1) sorbent material characteristics, (2) conveying criteria, (3) system capacity, and (4) conveying distance.

MATERIAL CHARACTERISTICS

Particle Size: Particle size probably has the greatest influence on the design of a sorbent handling system. This is an especially critical factor for furnace sorbent injection systems using hydrated lime since the sorbent is considered ultra fine from a material handling standpoint (usually 100% minus 10 micron). In bulk handling of such materials, fine material size tends to impair fluidization and increases material "stickiness". These phenomena are due to the small, light weight particles being attracted to each other forming lumps (e.g., agglomeration). Fine particles also tend to accumulate on the walls of bins and in the conveying line, sometimes building up to the point of blocking further flow.

Electrostatic forces become a major influence on particle-to-particle and particle-to-wall interactions with these materials.

Particle Density: Particle density has a minor affect on bulk conveying. However, with the light materials like hydrated lime it is more difficult to feed into pressure conveying systems or to provide proper system venting because of the tendency for sorbent entrainment in venting air, in bypass air around pressure seals, etc.

Hygroscopicity: Hygroscopic materials (materials that attract water), like hydrated lime, require consideration of moisture in storage and transport. Increased moisture content in the fine powder increases the material stickiness.

Compaction: Compaction of fine materials prevents their steady, free discharge from storage. However, these same materials can be self fluidizing and become very difficult to restrain once flow has been initiated.

CONVEYING CRITERIA

Smooth steady flow, as required for continuous pneumatic transport of sorbent in the conveying lines to the boiler, requires special design considerations as compared to bulk unloading or transfer systems which intermittently move large quantities of material en masse from one point to another. For smooth flow the sorbent being transported must be conveyed above the saltation velocity.

Saltation velocity by definition is the minimum air velocity in a conveying system needed to maintain the solid material in suspension (constantly entrained by the air). This type of conveying is referred to as "stream flow." However, experience has also shown that an excessively high velocity can cause turbulence and unsteady flow conditions. Additionally, if the conveying velocity is below the saltation velocity, material will settle out in the conveying system resulting in a surging flow. This can best be understood as some stream flow taking place above a settled layer of material.

The required velocity of injection through the boiler nozzles may require air volumes to achieve good sorbent dispersion in the furnace that are larger than required to satisfy conveying air requirements. As a consequence, for example, it may be preferable that any additional injection air that is needed for sorbent jet momentum in the furnace be supplied directly to the furnace injection nozzles via a separate air system (an example of this approach is illustrated in Figure 4). In this way, the conveying system can be operated at the optimum transport air flows independent of furnace dispersion considerations.

CAPACITY

As the capacity of a system is increased, the transport air volume must also be increased to maintain a minimum air to material ratio. If this ratio is too low (insufficient air per pound of material) surging will be initiated in the conveying system, even if the conveying velocity is above the saltation velocity.

CONVEYING DISTANCE

The length of a conveying system does not directly impact the ability to maintain steady, stream flow conditions as long as the conveying system is designed within the proper air-to-material ratio and in the proper velocity range. Increased conveying distance does increase the system operating pressure which may pose increased difficulty (e.g., pressure sealing) in feeding the sorbent into the pressure conveying system. However, use of a larger diameter conveying line might reduce this system pressure to the desired range.

SORBENT HANDLING DESIGNS AND RECOMMENDATIONS

For purposes of discussion, the sorbent handling system is divided into three major sections (see figure 1):

- Sorbent Receiving and Storage: The sorbent is typically received from bulk delivery (usually self unloading bulk carrier trucks) and transferred into the storage silo from which it must later be discharged. Included in this area along with the storage silo are the conveying line for bulk loading, silo venting and dust control, inventory control and controlled discharge from the silo to the sorbent flow control section.

- Sorbent Flow Control: The discharged sorbent from the silo is controlled and weighed for injection into the boiler. This area includes provisions for controlling the feed rate to maintain a steady, known flow of sorbent to the furnace.

- Sorbent Conveying: Sorbent which is discharged from the flow control area is picked up and transported pneumatically and injected into the furnace. This system includes the conveying air supply, material injection into the transport line (line charger), the conveying line and line splitter. (The design and placement of sorbent injection nozzles which discharge the sorbent into the furnace are not discussed in this paper.)

Recommendations for each of these sections of the sorbent handling system are discussed below.

SORBENT RECEIVING AND STORAGE (Figure 2)

Delivery by Bulk Transport : Bulk delivery is normally via a 4" diameter line that runs to the top of the storage bin. The bulk delivery truck should be discharged as close to the bin as possible to keep the total length of 4" line as short as possible to minimize unloading time.

Storage Bin Dust Collector: A dust collector is typically mounted on top of the storage bin to filter the bulk truck unloading air and other vented air volumes. This unit should be sized for a minimum of 1000 scfm of air and must include a separate discharge fan to handle this volume. This will eliminate any stray dust during truck unloading.

Storage Silo: The storage silo can be of conventional design with straight sides and cone bottom. The cone angle is not critical, however, the standard design utilizes a 60° cone. This bin design will result in funnel flow discharge and not mass flow from the bin. Because of the uniformity of size and chemical properties of the sorbent, there is no necessity for a mass flow bin design.

Flow Aids: Flow aids are needed to initiate flow of the sorbent from the storage silo and maintain steady discharge. Aeration units (e.g., "air slides") would be appropriate. They may have an active width of 6" and a length which reaches the greater length of the cone. If a shallower cone angle than 60° is desired to reduce over-all height or increase storage capacity within a given silo height constraint, additional fluidization will be required to aid in discharging the sorbent. The cone bottom can possibly be as shallow as 15°, but then would likely require complete coverage of the cone surface with aeration membranes.

Fluidizing air is supplied to these aeration units normally at a pressure of 3 to 5 psig. This air can be supplied from a fan, blower or plant instrument air source. The air volume used is typically 5 scfm/sq.ft. of aeration surface. It is important to realize that most of the time low quantities of air will be used; maximum air quantities are needed intermittently. This would argue for the use of a constant pressure air supply system which can be provided by a fan. It is also important that these flow aids be turned on only when material is to be discharged, otherwise excessive quantities of air might over-fluidize (expand) the sorbent and be discharged with the sorbent. This extra air would arrive at the sorbent flow control area where excessive venting or metering problems may occur.

Vibrators are not recommended due to the high likelihood that they would result in compaction of the sorbent and sporadic flow or plugging of the discharge.

Storage Bin Discharge: Since a pneumatic conveying system is used to discharge the sorbent into the storage vessel from the bulk truck, the storage bin discharge must include a positive flow control device to prevent flooding of the sorbent during silo filling. If a screw conveyor or live bin bottom is used, serious material flooding can be encountered when new material is loaded into a nearly empty silo. For this reason it is recommended to use a rotary feeder or other positive sealing device to control discharge of the sorbent from the storage silo.

A manual cut off valve can be installed for maintenance purposes between the bin and the rotary feeder. This valve must be well constructed or fluidized material could leak out of the packing into the work area.

Inventory Control: It may be desirable to mount the storage silo on load cells, or install load cells to the structural members of the silo. This will provide accurate feed inventory control and a overall feed rate check.

SORBENT FLOW CONTROL (Figure 3)

Sorbent Feed Rate: There are several types of feed control methods which can be considered. Each has advantages and disadvantages. Selection may be highly dependent on the degree of accuracy in feed rate desired. The only device that does not require in-service calibration is a weigh hopper. With this approach, the sorbent is discharged rapidly from the storage silo into a smaller weigh hopper (typically up to 100 cu.ft. capacity). The material is discharged from the weigh hopper by a variable rate discharge unit. The recommended equipment for the discharge is a variable speed rotary feeder. The speed of the discharge unit is controlled by a loss in weight measurement of the weigh hopper. When the hopper is almost empty, the discharge unit is locked at its present speed, and the weigh hopper is quickly filled from the storage silo. As soon as the filling is completed, the loss in weight control takes over. the weigh hopper approach provides the highest accuracy but has the added complication of an intermediate weigh hopper and its associated hardware.

Other type weighing devices might also be considered. The screw type weigh feeder senses the weight in a screw and calculates the rate by assuming the material is moving at a constant speed (volumetric flow). Errors may occur as the flow rate of the sorbent varies, since the fluid density characteristic of the sorbent changes. A weigh belt feeder is less prone to the above problem. However, sorbent can flood through both the screw type and the belt type weigh feeder. Both of these systems require frequent calibration and are very sensitive to differential pressures caused by changes in the venting system.

Impact flow meters can also be used where the sorbent is allowed to drop on an impact plate from a known height. This force on the plate is then proportional to the mass flow rate. With these units it is difficult to maintain accurate calibration.

The rotary feeder at the storage silo discharge can be driven by a variable speed motor. This motor can then be slaved to the material weighing device and its speed increased or decreased as necessary to control the desired feed rate.

The accuracy required for the sorbent feed control may be entirely different between a test installation and a commercial power plant installation. A high degree of accuracy might be sought in a research or test installation, while in a commercial installation slight variations in feed rate may be acceptable. For example a commercial system required to maintain a target SO2 emission level may simply adjust the sorbent feed as needed, without requiring knowledge of instantaneous feed rate. In this case a simpler/cheaper and less precise feed control device may be appropriate.

System Venting: In sorbent feed systems which involve sorbent transport in pressurized conveying lines, there will typically be some amount of leakage of conveying air into the weighing system. A venting system, which may include a fabric filter vent discharge, should be used to maintain ambient pressure in the weighing system, as well as to control dust emissions that would result from an open vent. Venting is also needed to release air that is brought into the weighing system along with the sorbent due to fluidization in the silo, or from natural air entrainment from sorbent dropping into the weighing device.

Venting is also necessary when using gravimetric weighing systems in order to maintain pressure equalization across the feeder. Small changes in pressure across the feeder will affect the indicated weight.

Improper venting of leakage air after the weighing step can permit escape of some of the weighed sorbent through the vent system. A standard design for venting a pressure conveying feed system that eliminates this problem includes a vent hopper between the weighing device discharge and the line charger. This hopper should be as large as practical, say 10 cubic feet, and would typically include a dust collector with automatic reverse pulse filter bag cleaning. Vent connections before and after the weighing device should be connected to this hopper to permit pressure equalization.

SORBENT CONVEYING (Figure 4)

As discussed previously, stream flow conveying is required to obtain steady sorbent flow into the boiler. The design should also attempt to keep system pressure to a minimum. System pressures exceeding 10 psig may cause problems with excessive leakage into the weighing system and should be avoided.

Line Charger: The line charger injects the sorbent material into the conveying line as fast as it is delivered from the weigh system. If system pressure is expected to exceed 3 psig, only two methods are recommended for this service: (1) screw feeders (e.g., Fuller-Kinyon pump) and (2) rotary feeders. Both units will have to be sized to handle the maximum desired capacity at a very low bulk density condition since the sorbent will be highly fluidized at this point.

The rotary feeder system will require less horsepower. However, at low feed rates the rotary feeder might initiate pulses in the feed as each pocket discharges. A feeder rotor with many pockets is desirable. Another problem with the rotary feeder is a tendency for fine, light weight sorbent to hang in the pockets instead of dropping into the conveying line. This problem is increased as the line pressure increases or if any moisture is present in the sorbent.

The screw feeder has less transport air leakage than the rotary feeder. However, it requires substantially higher horsepower and will be limited to a maximum discharge pressure with light fine sorbent.

Other types of line chargers can be used in bulk transfer of sorbent but should not be used for continuous flow operation such as required for furnace sorbent injection. A venturi feeder or eductor require higher air-to-material ratios and are not efficient at the higher operating pressures required for injection, although such systems have been successfully used in small, laboratory-scale systems.

Pressure tanks are excellent for higher pressure feed of sorbent into pressure conveying systems, but the accurate control of the discharge rate is difficult.

Air Supply: A fan system is not recommended for sorbent injection since changes in feed rate will change system operating pressure with substantial changes in air flow. A positive displacement blower is preferred, supplying an almost constant air volume regardless of the system pressure. The air volume should be sized to supply between 3500 and 4500 feet per minute actual air velocity at the highest system pressure to keep velocities above the saltation velocity.

Conveying Line: Experience has shown that minus 10 micron material has a tendency to build up on the conveying line walls. This build up can increase until system pressure exceeds the available air supply. This accumulation can also be dislodged from the wall periodically causing surging in the feed to the injector nozzles. It has been shown in many installations that the use of a flexible hose in place of rigid pipe has greatly minimized this action. It has been postulated that the hose flexing breaks off the build up while it is still small and does not create a substantial surge.

The line diameter should be selected to obtain as low a system pressure as practical. This diameter will be dependent on the desired capacity of the sorbent feed, the total distance of transport, the number of bends in the line and the pressure drop through the splitter and nozzles. As mentioned previously, to alleviate problems in the sorbent feed system, the line pressure should not exceed 10 psig.

Conveying Line Splitter: The line splitter should be installed in a vertical orientation and be preceded by a minimum of vertical conveying line (usually about 15 feet). As a general rule the total area of the conveying lines after the splitter should be slightly greater than the area of the line preceding the splitter. The conveying lines after the splitter should be as uniform in length and number of bends as practical in order to provide an equal back pressure on each line to minimize line-to-line variations in flow.

CONCLUSIONS

The storage, feeding and conveying of sorbent for furnace injection has been demonstrated in numerous installations, although many of the installations have experienced problems that have typically been resolved through a process of trial and error. Although dry pulverized materials have been handled in bulk for over

50 years, sorbent injection systems as compared to normal bulk transfer require special considerations. A sorbent injection system can be designed that will be clean and reliable, providing a material handling system compatible with the low retrofit cost objectives of furnace sorbent injection.

Within the report are reasons and substantiation for recommending the following design for a furnace sorbent injection system:

STORAGE:
- Use conventional cone bottom storage
- Supply fluidization air (vibrators not recommended)
- Design to control fluidized material flooding
- Include dust collector with exhaust fan
- Consider installation of load cells for inventory control and for independent check on feed rate

FLOW CONTROL:
- For maximum accuracy, use loss in weight feed bin approach. (Other feed rate controls are acceptable depending on the need for accuracy and precision).
- Special venting is required for weighing/feeding equipment

CONVEYING:
- Use pressure conveying system
- Design for system pressure below 10 psig
- Use screw feeder or rotary feeder line charger
- Use positive displacement blower air supply
- Design for 3500 - 4500 feet per minute pickup velocity
- Use flexible conveying line
- Install line splitter in vertical line after 15' rise
- Increase total transport line area after splitter
- Keep uniform lines after the splitter

These recommendations have been put into practice at the EPRI/EPA furnace sorbent injection project at Richmond Power and Light, where the sorbent feed system depicted in Figure 5 has been operating successfully.

ACKNOWLEDGEMENTS

The authors wish to acknowledge the advice and support of P. J. Chappell of the U.S. Environmental Protection Agency, Research Triangle Park, in the development of this paper.

The authors are also grateful for the information provided by operators and contractors at the following sites who have provided the basis for many of the recommendations offered in this paper:

Whitewater Valley Station, Richmond Power and Light, Richmond Indiana;
Edgewater Station, Ohio Edison, Loraine Ohio;
Kreisinger Development Laboratory, Combustion Engineering, Windsor Connecticut;
Boundary Dam Station, Saskatchewan Power;
Lakeview Station, Ontario Hydro;
Rheinbraun-Brikettfabriken Wachtberg, Frenchen, W. Germany;
Lhoist-Dumont, Liege, Belgium;
Papierfabrik Leinfelder, Schrobenhausen, W. Germany

The work described in this paper was not funded by the U.S. Environmental Protection Agency and therefore the contents do not necessary reflect the views of the Agency and no official endorsement should be inferred.

REFERENCES

1. Proceedings: First Joint Symposium on Dry SO2 and Simultaneous SO2/NOX Control Technologies, EPRI Report C5-4178, Vols. 1 and 2, July 1985

2. Proceedings: 1986 Joint Symposium on Dry SO2 and Simultaneous SO2/NOX Control Technologies, EPRI Report C5-4966, Vols. 1 and 2, December 1986

3. Richmond Power & Light, Whitewater Valley Station: Prototype Evaluation of Furnace Sorbent Injection on a 61 MW Tangential-Fired Boiler, Jointly funded by EPRI (Research Project 2786-2) and EPA (Contract 68-02-4253). (See session 4A, this Conference)

4. Ohio Edison, Edgewater Station: EPA Demonstration of LIMB on a 104 MW wall fired boiler. (See Session 4A, this Conference)

5. EPA workshop on Material Handling and Particulate Control Experiences with LIMB, Research Triangle Park, February 23, 1988

FIGURE 1.

Sorbent Material Handling

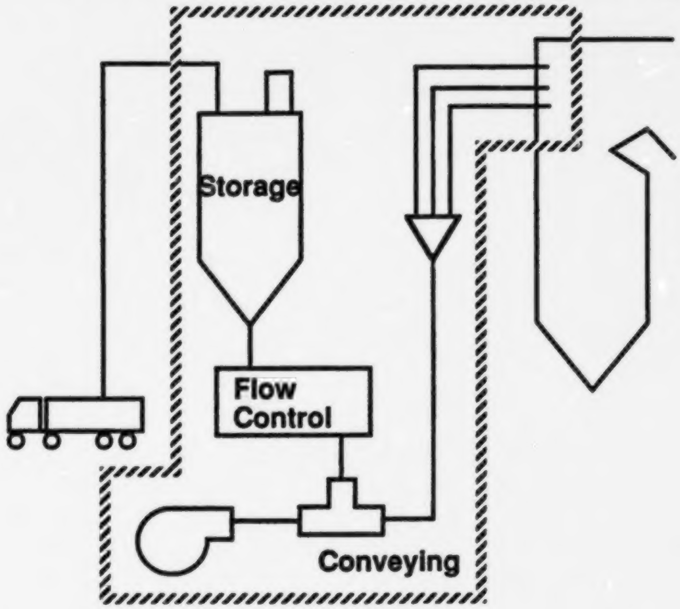
Storage
Flow Control
Conveying

FIGURE 2.

Sorbent Receiving & Storage

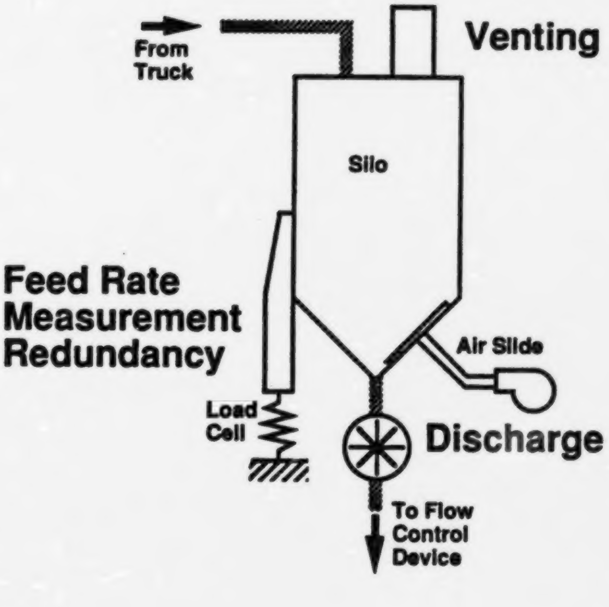
From Truck
Venting
Silo
Feed Rate Measurement Redundancy
Air Slide
Load Cell
Discharge
To Flow Control Device

FIGURE 3.

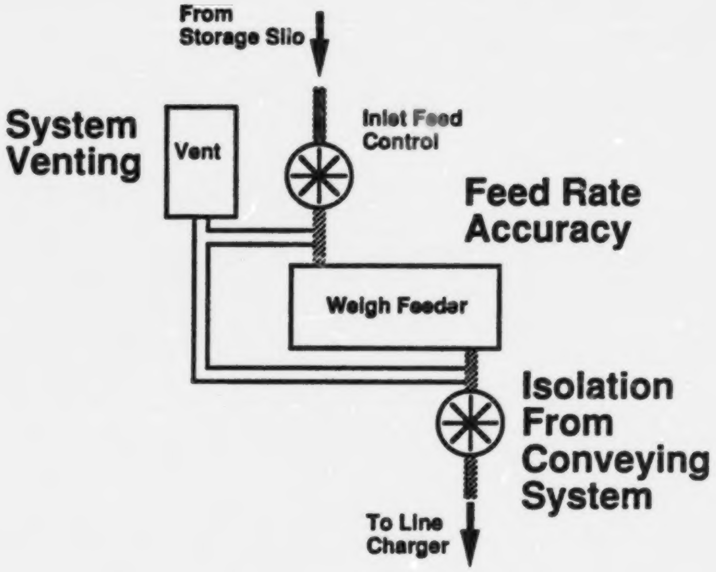

Sorbent Flow Control

From Storage Silo
System Venting
Vent
Inlet Feed Control
Feed Rate Accuracy
Weigh Feeder
Isolation From Conveying System
To Line Charger

FIGURE 4.

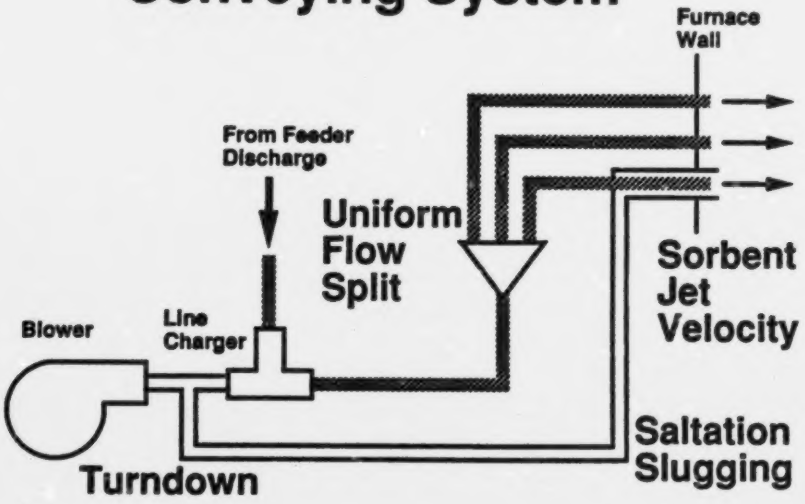

Conveying System

Furnace Wall
From Feeder Discharge
Uniform Flow Split
Sorbent Jet Velocity
Blower
Line Charger
Saltation Slugging
Turndown

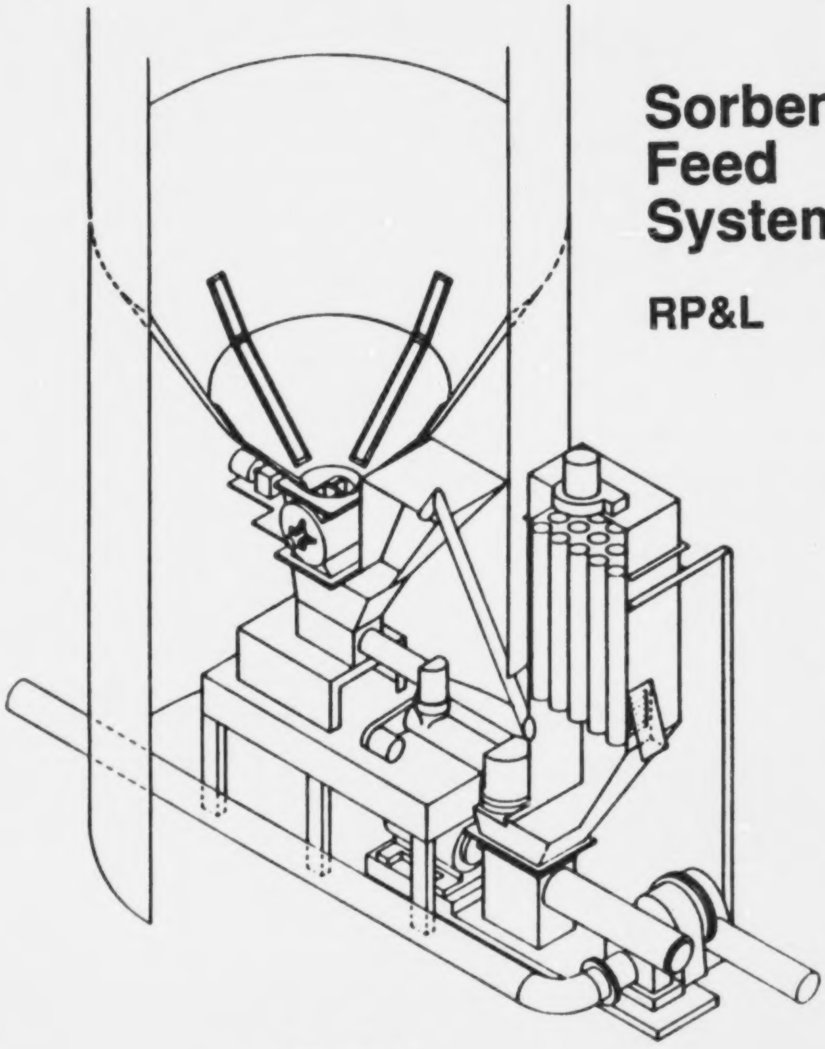

Sorbent Feed System

RP&L

FIGURE 5.

FIELD AND LABORATORY MEASUREMENTS OF FLY ASH PROPERTIES AND PRECIPITATOR PERFORMANCE PARAMETERS WITH FURNACE SORBENT INJECTION

by: M. G. Faulkner
G. H. Marchant, Jr.
E. C. Landham, Jr.
J. L. DuBard
Southern Research Institute
Birmingham, AL 35255-5305

ABSTRACT

Fly ash resistivity and particle size distribution have been measured at the Edgewater LIMB Demonstration with furnace injection of hydrated lime. The effect of the sorbent injection on precipitator voltage-current (V-I) characteristics and outlet plume opacity was determined, and the impact of sorbent injection on overall electrostatic precipitator (ESP) operation is discussed. Additional measurements and precipitator performance evaluations are planned with furnace injection of hydrated lime and downstream humidification for resistivity reduction.

Following the Edgewater LIMB Demonstration, a series of pilot-scale experiments were performed to evaluate the differences in ash collection and reentrainment characteristics as a function of LIMB injection and humidification process parameters. These tests examined V-I trends, surface and mechanical properties of the LIMB ash dust layer, and outlet plume opacities for different levels of humidification.

This paper has been reviewed in accordance with the U.S. Environmental Protection Agency's peer and administrative review policies and approved for presentation and publication.

INTRODUCTION

LIMB (Limestone Injection Multistage Burners) technology is a retrofit SO_x and NO_x emission control technology which may be applicable to a significant number of existing wall-fired and tangentially fired boilers. LIMB technology involves the injection of a calcium-based sorbent directly into a furnace that is equipped with low-NO_x burners. Since 1986, the development of LIMB technology has focused on furnace injection of hydrated lime, at about 2200°F (1200°C), with subsequent humidification of the combustion gas downstream of the heat exchangers. The particulate matter suspended in the combustion gas stream (fly ash and partially sulfated sorbent) must then be collected in an existing ESP.

Candidates among the existing boiler population for a retrofit application of LIMB technology are mostly equipped with small precipitators that were designed to collect low-resistivity fly ash from high-sulfur coal combustion. These precipitators typically have specific collection areas (SCA) less than 300 $ft^2/1000$ acfm (60 $m^2/m^3/s$). A retrofit application of LIMB technology will result in changes in the suspended particulate matter that present a difficult challenge to these precipitators.

The Air and Energy Engineering Research Laboratory of EPA is sponsoring a demonstration of LIMB technology at the Edgewater Station Unit 4 of Ohio Edison Company. Southern Research Institute (SRI) is providing technical support to EPA in the area of particulate control technology. The support activities have included extensive laboratory and pilot-scale studies, as well as preliminary on-site tests at Edgewater Unit 4.

The preliminary LIMB trials at Edgewater Unit 4 took place during September 1987. Following the preliminary LIMB trials, which were conducted without humidification of the combustion gas stream, extensive tests of the impact of humidification on ESP performance were conducted at SRI during January and February of 1988.

EDGEWATER UNIT 4 ESP EVALUATIONS

Unit 4 of the Edgewater Station of Ohio Edison Company is a 105 MW wall-fired boiler. The electrostatic precipitator at Edgewater Unit 4 is a large unit with a nominal SCA of 600 $ft^2/1000$ acfm at 528,000 acfm (118 $m^2/m^3/s$ at 249 m^3/s) of modern design that was retrofitted in 1982. There are six separately energized electrical fields in the direction of gas flow. The sixth field is designated as a spare because the precipitator is oversized for its usual present duty of cleaning flue gas from high-sulfur coal combustion. The ESP has 44 - 12 in. (30.5 cm) lanes and was designed to process 518,000 acfm (244 m^3/s) of gas at 280°F (138°C) with a gas velocity of 4.9 ft/s (1.5 m/s). Edgewater Unit 4 feeds a single stack which has an inner diameter 10.5 ft (3.2 m). This is an important parameter in regard to the optical opacity of the plume which emerges from the stack because the opacity is an exponential function of the optical path length through the plume.

During the period of September 7 to 25, 1987, SRI personnel assisted EPA in several evaluations of the operation and performance of the Edgewater Unit 4 ESP because the ESP performance had seriously deteriorated with the beginning of LIMB tests. Furnace injection of hydrated lime began during the first week of September without any humidification of the flue gas stream but stack plume opacity excursions made it impossible to continue the planned long-term sorbent injection program. Short-term sorbent injections continued until September 25, when the unit was taken off line for a scheduled major overhaul.

An internal inspection of the Edgewater Unit 4 ESP was conducted to determine if the poor performance with LIMB was due to equipment malfunction. Although the inlet fields had some dust deposits on the wires, they were not widespread enough to seriously limit the operation of the ESP. There was no evidence of mechanical problems. Alignment of electrodes was good, and dust layers on the collecting plates were minimal. The unit had been rapped overnight after shutdown; so some evidence may have been destroyed, but the ESP electrical operation indicated that the ESP was not limited by mechanical conditions.

ESP PERFORMANCE TESTS

Figure 1 presents the cascade impactor data for cumulative mass versus particle diameter. The lower curve shows data obtained without sorbent injection (baseline conditions for the 2.5% sulfur coal). The upper curve presents the data obtained while sorbent was injected at approximately 10,000 lb/h (4,550 kg/h), or a calcium-to-sulfur ratio of 2:1.

The corresponding cascade impactor data for dM/dlogD are given in Figure 2. This figure shows the incremental particulate mass loadings contained in incremental particle size ranges for baseline and LIMB data. The figure shows that in the particulate size range from 0.5 to 1.0 μm diameter there is a ten-fold increase in particulate mass loadings with LIMB. This is the particulate size range where precipitators are least efficient and where the particulate emissions contribute most strongly to plume opacity. (The light scattering is maximum where the particle diameters correspond to wavelengths of visible light.) The ten-fold increase in submicron particulate mass loadings with LIMB has also been observed in the pilot coal combustion facility in the Birmingham laboratories of SRI. This result indicates that opacity limits may be more restrictive on LIMB applications than mass emission limits.

For comparison with the mass train data obtained during LIMB tests, the total mass loadings indicated by the cascade impactors are listed here.

Date	Run	gr/ACF	gr/SCF	g/ACM
9/11/87	Baseline group	1.903	3.127	4.35
9/10,12,14/87	Sorbent at ~2:1	3.461	5.816	7.92

On September 8, 1987, comparative ESP electrical data were collected with and without sorbent injection. Sorbent injection was nominally 13,000 lb/h (5,910 kg/h), although some instability was encountered. Prior to the start of sorbent injection, baseline V-I curves were obtained on all operating fields of the ESP. The baseline curves for the second field are shown in Figure 3 and are indicated in the legend as "without LIMB." All fields exhibited good electrical operation with no evidence of high resistivity or back corona. All of the curves reached primary current limit without sparking. Stack opacity of 1-2% was indicated during this condition and was typical of normal operation without LIMB.

Sorbent injection was conducted for approximately 3 hours before stack opacity approached the 20% limit. A second set of V-I curves was obtained as the sorbent feed was being stopped. These V-I curves are identified as "with LIMB." Severe back corona is apparent from this second set of V-I curves, with little or no useful electrical power applied to the ESP fields. Back corona is produced almost simultaneously with corona onset at the discharge electrode.

Degradation of the ESP electrical operation began in the ESP inlet fields and gradually worked toward the outlet. In general, there was very little sparking and the controllers maintained current limit while voltage dropped due to back corona. The degradation process is illustrated in Figure 4, which plots the loss of operating voltage in each field as a function of the time from start of sorbent injection. The large size of this ESP enabled the unit to operate with less than 5% opacity until the fifth field began to degrade. At that time (approximately 3 hours elapsed time), the opacity began to increase very rapidly.

Only 15-20 minutes were required for the opacity to increase from 5% to nearly 20%.

When sorbent feed was discontinued, the ESP began to recover rapidly. Although the opacity dropped within minutes, there was a residual ESP performance degradation which lasted several hours.

ESP PERFORMANCE WITH IE

Intermittent energization (IE) was tried as a quick fix for the Edgewater Unit 4 ESP during the preliminary LIMB tests. On September 18, 1987, most ESP fields were operated with IE throughout the sorbent injection period to determine if performance degradation could be prevented. No increase in baseline opacity could be observed when the switch to IE was made. When the ESP was adjusted and stable, sorbent injection was set to 10,000 lb/h (4,550 kg/h). The ESP outlet opacity increased from 2% to approach 20% after a few hours of sorbent injection, even with IE constantly in use. Therefore, it was not possible to quantify how much performance improvement IE could provide under steady-state degraded ESP operating conditions.

BIRMINGHAM LABORATORY INVESTIGATIONS

Southern Research Institute operates a pilot-scale pulverized-coal-fired combustion research facility in its Birmingham laboratories. The plant features a 10^6 Btu/h (300 kW) vertical down-fired furnace of modular construction and a fully instrumented process monitor and control room. The simulation accuracy of the coal combustion facility has been validated by detailed comparisons of fly ash and flue gas properties with the properties measured at full-scale electric generating plants.

A laboratory ESP was installed on the gas stream in order to study ESP electrical operating characteristics (as controlled by the bulk electrical resistivity of the precipitated dust) and the electrode buildup and reentrainment properties of the precipitated dust. These types of performance data can be extrapolated to full-scale precipitators with sufficient accuracy to provide useful information about operating difficulties that may be experienced in full-scale precipitators. The laboratory ESP has a single lane with 9-in. (23 cm) plate spacing and six weighted-wire discharge electrodes. The active collecting plate area is 20x48 in. (51x122 cm). The nominal volume gas flow is 300 acfm (0.14 m^2/s) at 300°F (150°C) with a velocity of 4.0 ft/s (1.2 m/s), for an SCA of 44 ft^2/1000 acfm (8.7 $m^2/m^3/s$).

Measurements performed on line in the combustion gas stream were supplemented by extensive analytical laboratory investigations related to sorbent utilization and to physical and chemical properties of ash/sorbent mixtures. In several aspects related to ESP performance, the methods of combustion gas sampling and laboratory analyses were refined with experience. The measurements related to ESP performance include:

flue gas moisture and temperature,
dust resistivity measured in situ,
dust resistivity measured in the laboratory,
precipitator voltage-current characteristics, and
variations in the outlet gas stream opacity.

Because of the small size of the laboratory ESP and the high fraction of gas flow outside the electrified field, it is not possible to obtain absolute values of collection efficiency that are useful and meaningful in scaling up to full-size utility fly ash precipitators. Rather, the test data are interpreted in terms of relative values of ESP outlet gas stream opacity. Similarly, it is well known that greater spark-limited electrical power can be supplied to smaller electrified fields because of the smaller surface area of dust deposits where electrical breakdown can develop. The test data are interpreted in terms of relative changes in the ESP operating voltage and average current density on the collecting plate.

In addition to the conventional quantitative measurements listed above, qualitative observations of the severity of several important non-ideal effects were recorded: back corona, electrode deposit buildup, and dust reentrainment. Observations of electrode cleaning and dust reentrainment associated with plate rapping were correlated with electrical measurements of local plate accelerations with the ESP on line under normal process conditions. It is well known that gross electrode rapping effects do not scale up reliably to larger mechanical structures; so the rapping experiments were designed to correlate local effects - local plate accelerations and local dust cake reactions.

Finally, test data from both the SRI coal combustion facility and from the Edgewater Unit 4 site were used in numerical estimates of the performance of the Edgewater Unit 4 ESP during the LIMB demonstration.

ASH/SORBENT RESISTIVITY

The bulk electrical resistivity of dust is an important parameter because the electrical current in a precipitator passes through the collected dust layer to reach electrical ground. The collected dust layer forms a series resistance in the secondary circuit of each transformer-rectifier (T-R) set. The product of dust resistivity and local plate current density gives the local electric field within the dust layer, averaged over the thickness of the dust layer. When that electric field becomes high enough, electrical breakdown occurs within the dust layer and leads to sparking and/or back corona. Thus, high dust resistivity places an operating limit on the useful electrification of a precipitator.

Typical dependence of LIMB dust resistivity on environmental parameters, temperature and moisture, is illustrated in the laboratory data of Figure 5. For laboratory measurements, the volume percent of water in the heated air environments is fixed (at different values on different test days) and the temperature drops slowly as the oven cools. The bulk sample of LIMB dust was collected from the SRI coal combustion facility. The highest resistivity values in Figure 5 are four to five orders of magnitude higher than those measured for the fly ash from pulverized high-sulfur coal combustion, under typical flue gas conditions in utility fly ash precipitators. However, the resistivity values fall rapidly with decreasing temperature and increasing moisture. These data required the development of a new laboratory test protocol as it had been determined that the standard procedures for dust resistivity measurements in the laboratory (procedures based on experience with fly ash from pulverized coal combustion) were causing the physical and chemical properties of LIMB dust samples to change during the measurement.

In the LIMB process with cold-side humidification of the combustion gas stream, the evaporation of water causes the gas temperature to fall and the gas moisture to rise. The two variables are not separately controlled as in the laboratory. In situ resistivity data obtained after water injection into the combustion gas stream passing through an 8 in. (20 cm) pipe are shown in Figure 6.

Figure 6 also shows the very high value of resistivity (1x10^{14} ohm-cm) measured without any humidification. The comparison of spark data and V-I data in this figure is a comparison of two different methods of obtaining in situ resistivity values with the point-plane probe. The spark method is believed to be more accurate because it simulates the electrical stress that is experienced by dust layers collected on the ESP electrodes. However, the spark data appeared questionable because no values below 1x10^{11} ohm-cm could be obtained, even with a close approach to adiabatic saturation.

Concern about the validity of in situ resistivity data increased after the LIMB trials at Edgewater Unit 4 during September 1987. This concern led to changes in apparatus and procedure for the intensive studies of the effects of humidification on ESP performance during January and February of 1988. Calibration samples for the point-plane probe were fabricated and calibrated by the laboratory resistivity measurement procedure. During the final series of measurements of LIMB dust resistivity with the point-plane probe, it was verified (by comparison with the laboratory calibration data) that the probe readings were correct. It was found, however, that a non-representative sample of LIMB dust could be collected in the probe and could result in a non-representative value of resistivity. This source of measurement difficulty was discovered when the perforated shield that normally encloses the probe electrodes was removed. The biasing effect of the probe shield is not yet fully understood, but the resistivity data obtained without the probe shield show the expected effect of temperature and moisture.

During the final series of measurements, LIMB dust samples were removed from the laboratory ESP electrodes and subjected to laboratory resistivity measurements. The two curves in Figure 7 show the upper and lower bound of the resistivity data for the various samples. The trend of these curves upon approach to conditions corresponding to adiabatic saturation in the combustion gas stream (typically about 125°F (52°C) and 12% by volume moisture) is in good quantitative agreement with the in situ resistivity data. Given the coal, lime, and Ca/S stoichiometry used in the LIMB demonstration at Edgewater Unit 4, LIMB dust resistivity values below 1x10^{12} ohm-cm are expected within a 100°F (56°C) approach to adiabatic saturation, and values below 1x10^{10} ohm-cm within a 50°F (28°C) approach.

LABORATORY ESP ELECTRICAL OPERATION

Variations in the electrical operation of the laboratory ESP were measured along with variations in LIMB process conditions. Absolute values of operating voltage and plate current density cannot be extrapolated to full-scale utility fly ash precipitators, but relative values can provide some insight into the operation of the Edgewater Unit 4 ESP during the LIMB demonstration.

Figure 8 shows the rapid effect of water injection on the laboratory ESP V-I characteristics. The upper curve which shows very high values of plate current density does not indicate good electrification but rather a malfunction. The very high currents are caused by back corona from precipitated LIMB dust of high resistivity, and those currents are not useful for charging and collecting dust particles. The lower curve shows well-controlled, useful currents obtained after humidification. The remarkable thing about these data is the nearly instantaneous response of the ESP to the onset of water injection. The elapsed time between the onset of water injection and the curve measurement is only 2 minutes. The resistivity of the dust layers on the ESP electrodes apparently dropped rapidly after the sudden increase in gas moisture, in spite of the fact that the temperature of the dust layers must have remained high due to the thermal inertia of the ESP.

The ESP electrical operating data are shown in Figure 9. The left and right halves of this figure compare the V-I characteristics measured shortly after electrode cleaning and after the buildup of LIMB dust deposits. The most noticeable difference is a reduction in corona emission at low voltages with low levels of humidification. The more important information in this figure is the variation in corona emission with the level of humidification. At a given applied voltage, the average plate current density increases steadily with greater humidification and closer approach to adiabatic saturation. At an approach temperature of 26°F (14°C), the residual difference between the baseline V-I curve and the LIMB V-I curve can be attributed mainly to the corona quenching effect of the large increase in suspended particulate space charge with LIMB. Although the spark-limited operating voltages and currents can be expected to be much lower in a full-scale precipitator, these data indicate that some useful ESP electrification can be achieved with only a 100°F (56°C) approach to adiabatic saturation.

ESP EMISSIONS WITH HUMIDIFICATION

A Lear-Siegler transmissometer was installed on the combustion gas stream leaving the laboratory ESP in order to continuously monitor the variations in laboratory ESP performance with variations in LIMB process parameters. Of particular concern was the possibility of a catastrophic collapse of the precipitated LIMB dust layers, with massive reentrainment emissions of LIMB dust, as the water injection rate was increased to reach the point of adiabatic saturation. No such problem was observed. The precipitated LIMB dust layers did not exhibit excessive reentrainment as the water injection was increased even to the point of creating wet ash/sorbent deposits in the inlet duct.

Trends in the opacity data are plotted in Figure 10. The reference opacity values measured during LIMB without the ESP energized lie in the range of 50 to 60%. However, the calibration of the transmissometer was uncertain. Only relative changes in opacity are meaningful. The left-most series of bars in Figure 10 illustrates the data obtained without any humidification, when the baseline gas moisture was about 5% by volume and the gas temperature at the ESP outlet was about 240°F (115°C). A comparison of the two left-most hatched bars (opacity data obtained with the ESP energized) shows that the opacity increased ten-fold when sorbent injection was begun. The three remaining hatched bars show that the opacity decreased steadily with decreasing approach to adiabatic saturation. The decreasing opacity values correlate with the increasing ESP plate current density values shown in Figure 9.

Trends in the opacity data versus the elapsed time after beginning the test are plotted in Figure 11. The data were obtained with a residence time of 4.5 s, the elapsed time of travel of dust particles from the point of water injection to the inlet of the ESP. Earlier data obtained with a residence time of only 2.0 s showed that moisture conditioning was not complete in this time interval. Figure 11 also illustrates the importance of ESP electrode cleaning. Electrode rapping causes the opacity values to fall by several percentage points.

LABORATORY ESP DUST REENTRAINMENT

The spontaneous and rapping reentrainment characteristics of LIMB dust were investigated with the laboratory ESP on line under normal operating conditions. This work was based on considerations that a retrofit application of LIMB technology will:

- increase the rate of dust cake buildup on the electrodes near the front end of an existing utility fly ash precipitator, and

- change the physical/chemical properties, and possibly the cohesive properties, of the precipitated dust cake.

The collected dust layers were about 1/16-in. (0.16 cm) thick for these tests. The wires were cleaned every three to five tests, except during the tests with humidified LIMB dust when the wires had to be cleaned after every test. Only single raps were studied. Figure 12 shows the experimental arrangement used in these tests. For each rap, the local plate acceleration was measured, and the reaction of the dust cake was observed. The tri-axial accelerometer signal for the vertical in-plane acceleration was used in the data correlations. The accelerations measured in the other two axes of the heavy plate were similar.

Figure 13 compares the rapping characteristics of LIMB dust conditioned with H_2O and with SO_3. The two methods of flue gas conditioning can have similar effects on the electrical resistivity of LIMB dust but they have very different effects on the rapping characteristics of LIMB dust. The lines represent the percent of plate area cleaned by a single rap (as estimated by visual inspection through a window) versus the local plate acceleration. The straight lines are least-squares fits to the data.

The upper set of lines compare the rapping characteristics of the baseline fly ash and LIMB dust conditioned with SO_3. (It was not possible to test LIMB dust characteristics without flue gas conditioning because of the electrical malfunction of the precipitator.) Although SO_3 conditioning is not used for the precipitator at Edgewater Unit 4, it is an alternative means of conditioning LIMB dust and is discussed here for comparison. The substantial difference in slope of the two straight lines indicates a substantial difference in rapping behavior. With SO_3 conditioning, much more plate area was cleaned of LIMB dust with a gentle rap, but a much stronger rap was required to clean most of the plate. The plate was never completely cleaned with a single rap. With SO_3 conditioning the LIMB dust came off the plate too easily, with little or no rapping, but very intense multiple rapping was required to remove tenacious deposits adjacent to the plate.

The lower graph shows that the humidified LIMB dust was rapped more easily than the baseline fly ash. Furthermore, the two parallel lines in the lower graph indicate that the humidified LIMB dust was basically well behaved, within a 50°F (28°C) approach to adiabatic saturation.

The observations of spontaneous reentrainment were necessarily subjective in nature. Qualitative judgments about the behavior of the dust layer during formation, between rapping tests, are summarized in the following table.

Phenomenon	Baseline Fly Ash	LIMB Dust + SO_3	Humidified LIMB Dust 101°F (56°C) Approach	56°F (31°C) Approach	26°F (14°C) Approach	Near Saturation
Plate Deposit Growth Rate	slow	fast	fast	fast	fast	fast
Rapping Difficulty	medium	hard	hard	easy	easy	easy
Spontaneous Reentrainment	little	much	much	much	medium	medium
Wire Deposit Growth Rate	slow	slow	fast	fast	fast	fast

The LIMB dust layers conditioned with H_2O or SO_3 were much less stable and much more prone to spontaneous reentrainment than the baseline fly ash layers. However, this instability diminished with greater humidification and closer approach to adiabatic saturation. Furthermore, this instability was not manifested in the ESP outlet gas opacity measurements described in the preceding section. Apparently, the spontaneous reentrainment emissions occurred mainly in the form of dust agglomerates which were large enough to have little effect on light scattering in the ESP outlet gas stream. Large dust agglomerates would be quickly recharged and recollected under good electrical operating conditions in a full-scale ESP. All in all, the better behaved LIMB dust layers in the laboratory ESP were obtained with greater water injection and closer approach to adiabatic saturation. At this point, however, the gas velocity through the laboratory ESP was only about 3 ft/s (0.91 m/s).

The discharge electrode deposits were distinctively different with humidified LIMB dust, in marked contrast to all other test conditions. Heavy deposits developed rapidly (0.75 in. (1.9 cm) diameter deposits in 30 minutes) on energized wires downstream of the first energized wire, but not on quiescent wires. This behavior indicated the precipitation of positively charged dust particles. Furthermore, comparative mineral analyses of wire and plate deposits indicated that the wire deposits were significantly enriched in calcium.

ESP PERFORMANCE PROJECTIONS

A mathematical model of electrostatic precipitation, developed at Southern Research Institute, was used to project the performance of the Edgewater Unit 4 ESP during LIMB trials with flue gas humidification. The ESP Model performs a detailed numerical simulation of the charging and collecting of dust particles along one gas passage of an ESP and makes empirical corrections for non-ideal gas flow and rapping reentrainment. The correction factors are based on comprehensive tests of performance characteristics of fly ash precipitators installed on utility boilers firing pulverized coal.

Mathematical modeling was performed in order to estimate the steady-state performance limits of the Edgewater Unit 4 ESP during continuous LIMB trials with a minimum level of humidification corresponding to a 100°F (56°C) approach to adiabatic saturation. Laboratory data indicate that an approach to adiabatic saturation within 100°F (56°C) is required to moderate the LIMB dust resistivity sufficiently to obtain a minimum level of useful electrification of the Edgewater Unit 4 ESP. Consequently, the data measured at Edgewater were adjusted to 230°F (110°C) for modeling.

The nominal gas flow was reduced from 528,000 acfm (249 a m^3/s) to 373,000 acfm (176 a m^3/s), for a nominal SCA of 850 $ft^2/1000$ acfm (168 $m^2/m^3/s$) with all six fields energized. However, the modeling was performed with only five electrical fields energized for an SCA of 705 $ft^2/1000$ acfm (140 $m^2/m^3/s$) in order to obtain conservative projections of ESP performance with some T-R sets out of service. The gas flow was varied ±10% during the computations in order to obtain curves of ESP performance parameters (mass emissions and plume opacity) versus ESP SCA.

It was necessary to estimate the voltage and current values in each electrical field. The LIMB dust resistivity at a 100°F (56°C) approach to adiabatic saturation is expected to be about $1x10^{12}$ ohm-cm. Corresponding values of applied voltage and plate current density that are useful in charging and collecting dust particles can be estimated from measured performance characteristics of utility fly ash precipitators. However, the structural design of the discharge electrodes in the Edgewater Unit 4 ESP results in baseline operating voltage and current values that are less-than-average for utility fly ash precipitators having 12 in. (30.5 cm) plate spacing and collecting low-resistivity fly ash. On the other hand, the operating voltage values will tend to be higher in the inlet fields during LIMB trials (for given values of plate current density) because of the increased concentration of suspended particulate space charge. The final estimates of ESP electrical operating points are listed in the following table.

Field	kV	$\mu A/ft^2$	nA/cm^2
1	38	2	2.2
2	35	3	3.2
3	33	5	5.4
4	35	7	7.5
5	38	9	9.7

These values represent a low level of ESP energization compared to the measured baseline operation with fly ash from high-sulfur coal combustion.

The results of mathematical modeling are listed in the following table and plotted in Figure 14. The ESP Model cannot simulate frequent upsets in the ESP operation due to process malfunctions such as wide variations in sorbent feed or wide variations in gas temperature. Process malfunctions can cause changes in the precipitated dust deposits which can cause changes in the ESP electrical operation which can persist for days. Mathematical modeling can be used to project ESP performance only under stable and continuous process conditions.

SCA ft^2/kacfm	SCA $m^2/m^3/s$	Efficiency %	Emissions $lb/10^6$ Btu	Emissions ng/J	Opacity %
640	127	99.83	0.022	9.5	4.9
705	140	99.89	0.014	6.0	3.1
785	155	99.936	0.008	3.4	1.8

The conclusion of the mathematical modeling is that the performance of the Edgewater Unit 4 ESP will be controlled satisfactorily by its very large size if the LIMB dust resistivity is moderated enough for the T-R sets to supply only a small amount of useful electrical power in only five electrical fields.

SUMMARY

This section summarizes the principal findings related to the impact of LIMB on ESP performance, both from the preliminary LIMB trials at Edgewater Unit 4 and from tests in the SRI coal combustion facility with a laboratory precipitator installed on the combustion gas stream. The principal findings are organized under six major headings which describe ESP process, operation, and performance characteristics. Under each major heading, subheadings delineate the findings at Edgewater Unit 4 and in the SRI laboratories.

Dust Resistivity

Edgewater Unit 4

- During baseline operation, the dust resistivity measured in situ at the ESP inlet averaged $3x10^{10}$ ohm-cm at 350°F (177°C).

- During operation with LIMB, the dust resistivity was too high to be measured accurately with the point-plane in situ resistivity probe. The measured values were in the range of 1 to $5x10^{12}$ ohm-cm, at 300 to 360°F (150 to 182°C), but the actual values are believed to have ranged as high as $1x10^{14}$ ohm-cm.

SRI Laboratories

- Laboratory measurements of LIMB dust resistivity indicated values as high as $1x10^{14}$ ohm-cm at the operating temperatures experienced in the Edgewater Unit 4 ESP.

- Cold-side combustion gas stream humidification was found to be an effective means of moderating LIMB dust resistivity. The resistivity values (measured both in situ and in the laboratory) dropped over two orders of magnitude at temperatures of approximately 220°F (104°C), representing about a 100°F (56°C) approach to the adiabatic saturation temperature.

- LIMB dust resistivity is expected to be below $1x10^{12}$ ohm-cm within a 100°F (56°C) approach to saturation, and below $1x10^{10}$ ohm-cm within a 50°F (28°C) approach to saturation.

Electrical Operation

Edgewater Unit 4

- During baseline operation, there was no evidence in the measured T-R secondary V-I curves of any electrical or mechanical malfunction.

- During operation with LIMB, there was severe electrical malfunction caused by the high resistivity of the precipitated LIMB dust. Electrical degradation began in the ESP inlet field and progressed to the fifth field within 3 hours of operation with LIMB. Electrical degradation resulted in the immediate onset of back corona at the threshold voltage for primary corona. There was no working voltage range which would permit useful electrification of the precipitator.

SRI Laboratories

- Furnace sorbent injection caused severe electrical degradation of the laboratory precipitator. Humidification within a 100°F (56°C) approach to saturation was necessary to permit useful electrification of the precipitator.

- At a fixed operating voltage applied to the laboratory precipitator, the operating current increased with increasing humidification and closer approach to saturation.

Mechanical Operation

Edgewater Unit 4

- During an internal inspection of the ESP after furnace sorbent injection, there was no evidence of any serious electrode misalignments or electrode cleaning difficulties. The precipitator appeared to be in good mechanical operating condition. However, problems were encountered with the ash removal system during the LIMB tests.

Dust Loading and Particle Size Distribution

Edgewater Unit 4

- LIMB had an adverse impact on the mass loading and particle size distribution of dust entering the ESP. The overall mass loading increased by about a factor of two.

- During operation with LIMB, the mass loading increased by about a factor of ten in the particle size range from 0.5 to 1.0 μm. This is the particle size range where precipitators are least efficient and the particulate emissions contribute most strongly to plume opacity.

SRI Laboratories

- Furnace injection of hydrated lime resulted in changes in the suspended particulate matter that were consistent with data from the preliminary LIMB trials at Edgewater Unit 4. At a typical Ca:S stoichiometry of about 2:1, the overall mass loading increased by a factor of 2 to 3, and the fine particulate mass loading increased approximately tenfold.

Electrode Dust Accumulation and Cleaning

SRI Laboratories

- There was a rapid accumulation of dust deposits on the laboratory ESP electrodes during furnace sorbent injection and combustion gas stream humidification. Dust deposits on the high voltage discharge electrodes built up very rapidly.
- There was no difficulty in cleaning the ESP electrodes by mechanical rapping, even at a close approach to adiabatic saturation. LIMB dust was removed more easily than the fly ash from pulverized coal combustion.

Mass Emissions and Opacity

Edgewater Unit 4

- During baseline operation, the precipitator operated with a clear stack. Opacity readings were in the range of 1 to 2%.
- During operation with LIMB, the opacity rose rapidly to the 20% limit after electrical degradation began in the fifth ESP field. Steady state operation with LIMB was not achieved during the preliminary trials. Furnace sorbent injection had to be stopped after about 3 to 4 hours to avoid exceeding the opacity limit.
- Mathematical modeling of the precipitator performance during cold-side humidification of the combustion gas stream indicated that the performance will be satisfactory within a 100°F (56°C) approach to saturation because of the large size of the precipitator.

SRI Laboratories

- There was no catastrophic spontaneous reentrainment from the laboratory precipitator electrodes of humidified LIMB dust, as the humidification was increased all the way to the point of adiabatic saturation.
- Spontaneous reentrainment of precipitated LIMB dust occurred in large agglomerates which did not affect the measured outlet gas opacity. In an operating ESP, these agglomerates would be quickly recollected.
- The outlet gas opacity decreased (concurrently with the increasing operating current) with increasing humidification and a closer approach to saturation.
- The outlet gas opacity decreased by several percentage points after the laboratory ESP electrodes were rapped. This performance improvement is a result of the improved electrical operating conditions obtained with cleaner electrodes.

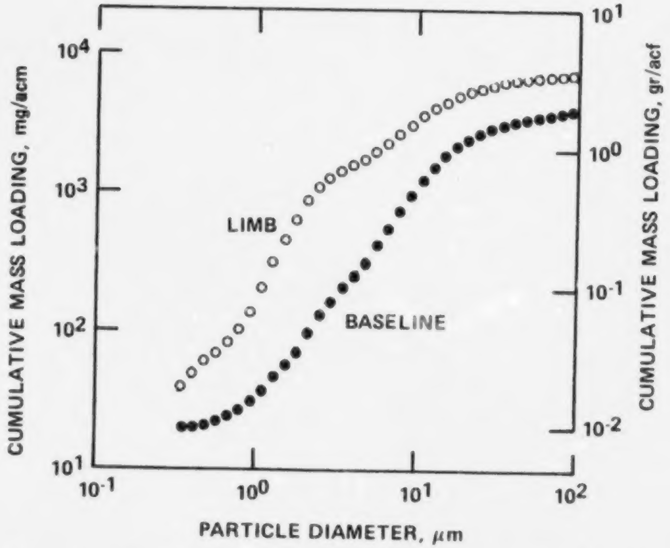

Figure 1. Cumulative mass loading versus particle diameter at the Edgewater Unit 4 ESP, 9/11/87.

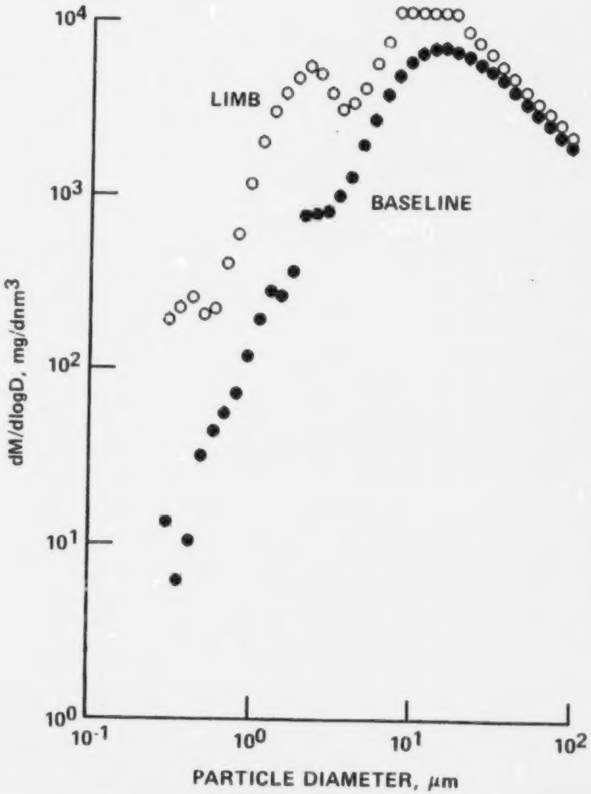

Figure 2. dM/dlogD versus particle diameter at the Edgewater Unit 4 ESP, 9/11/87.

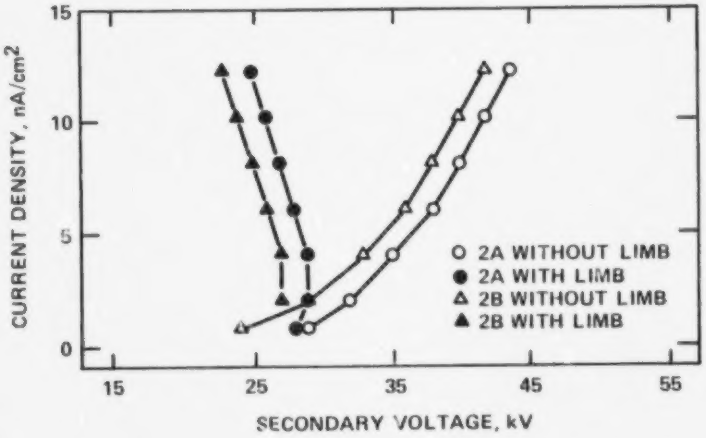

Figure 3. The effect of LIMB on Edgewater Unit 4 ESP electrical characteristics: second fields, 9/8/87.

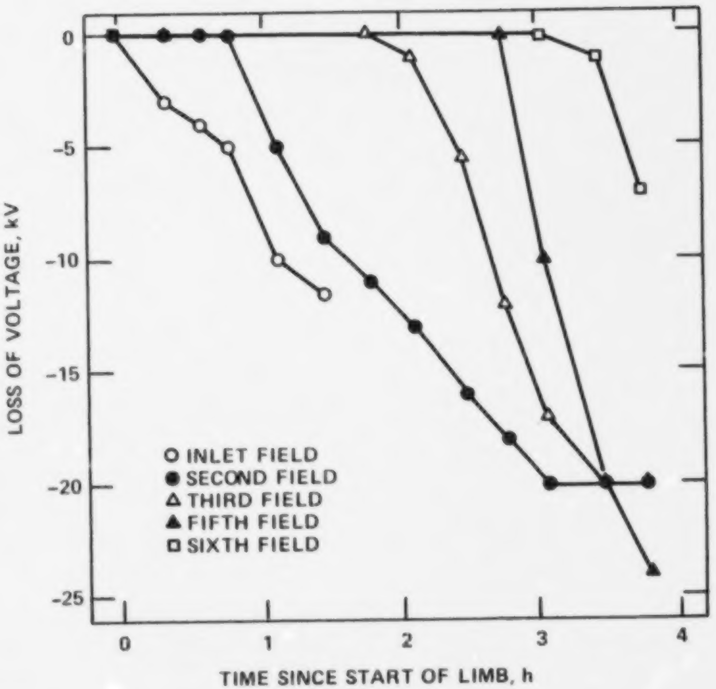

Figure 4. Edgewater Unit 4 ESP operating voltage loss as a function of time since the start of sorbent injection.

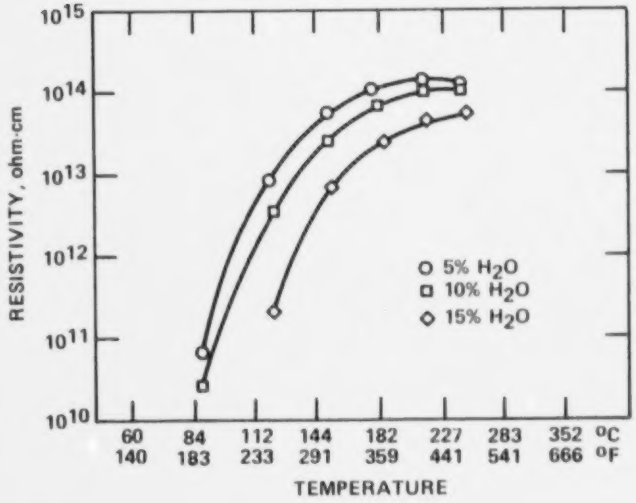

Figure 5. Laboratory measurements of LIMB dust resistivity versus temperature and moisture.

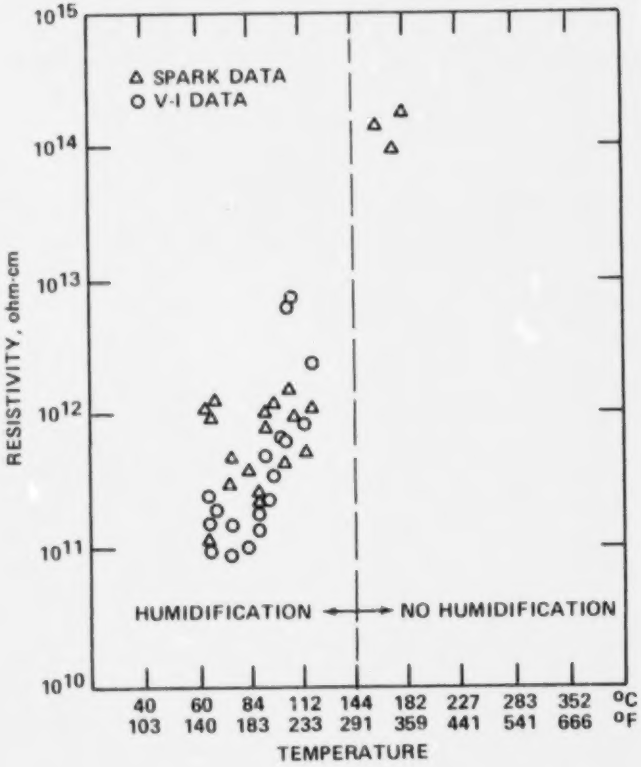

Figure 6. In-situ resistivity of LIMB dust as a function of temperature.

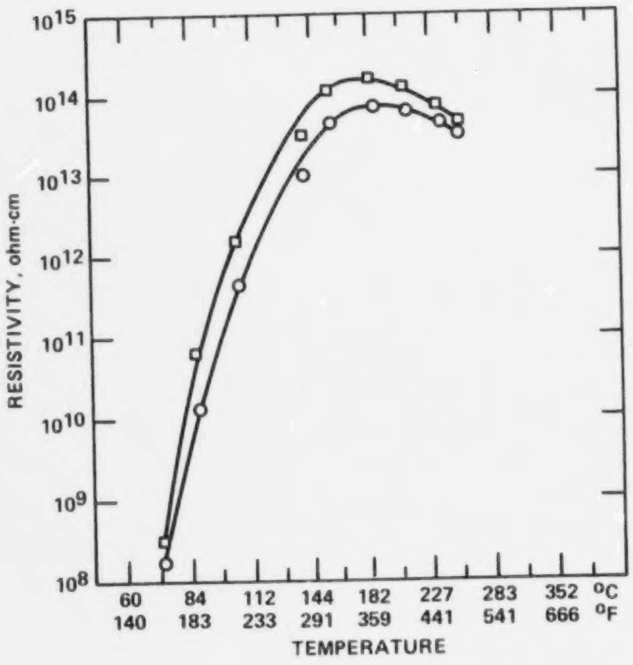

Figure 7. Laboratory resistivity of LIMB dust samples precipitated during in-situ measurements.

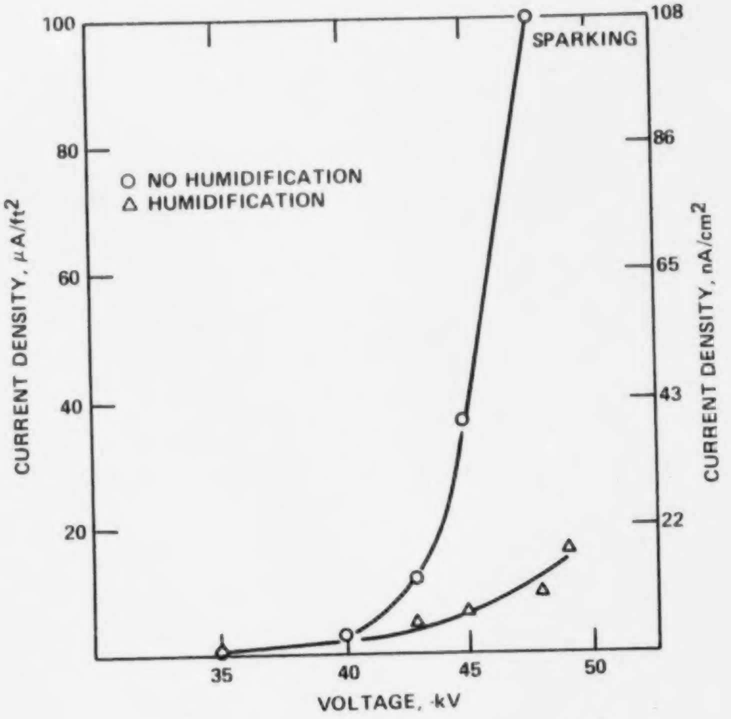

Figure 8. Effect of flue gas humidification on laboratory ESP V-I characteristics while collecting LIMB ash.

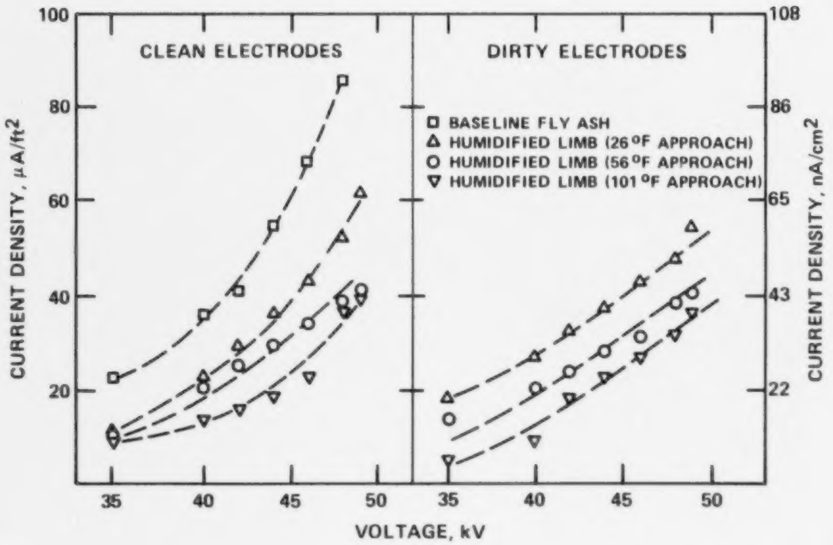

Figure 9. Effect of the approach to saturation on the laboratory ESP V-I characteristics.

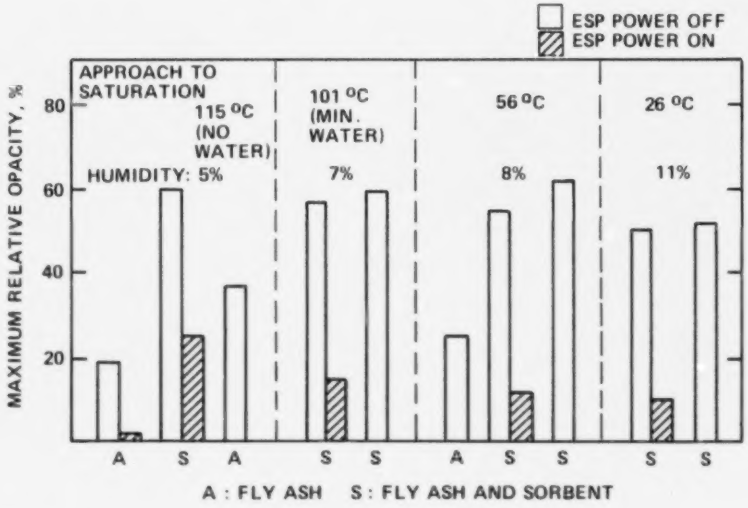

Figure 10. Opacity of flue gas at the laboratory ESP outlet during short-term LIMB tests.

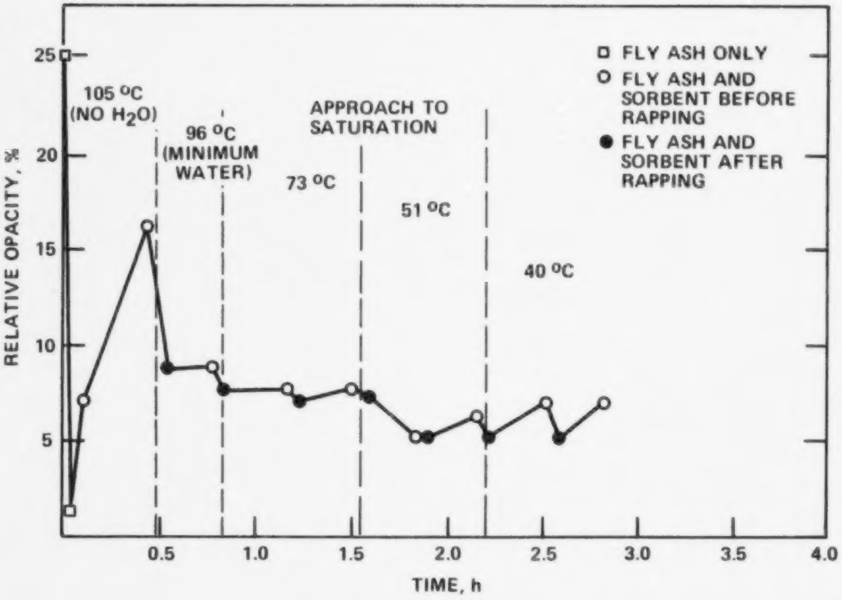

Figure 11. Opacity of flue gas at the laboratory ESP outlet with LIMB and humidification.

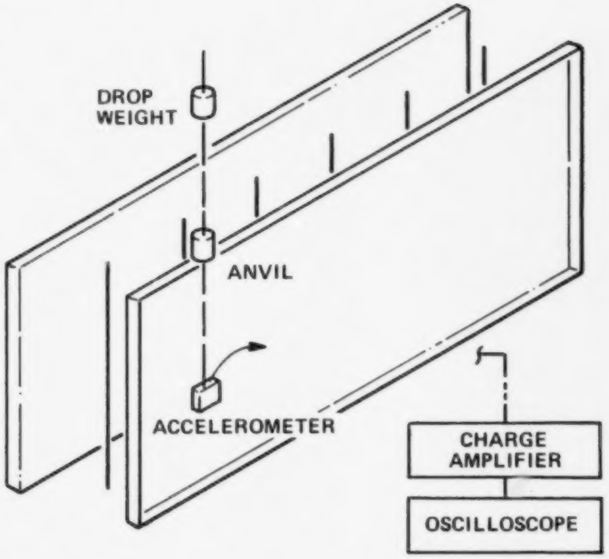

DROP WEIGHT
ANVIL
ACCELEROMETER
CHARGE AMPLIFIER
OSCILLOSCOPE

Figure 12. Schematic of laboratory ESP plate rapping mechanism.

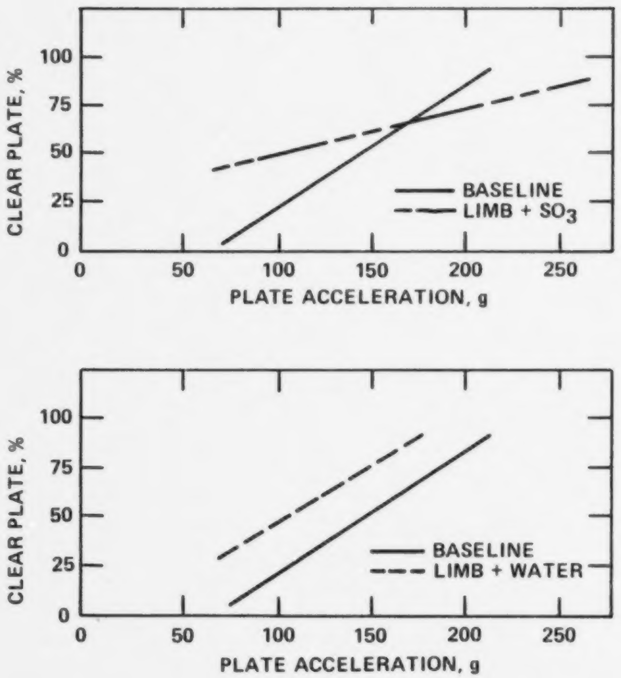

Figure 13. Rapping characteristics of LIMB dust conditioned with water and with SO_3.

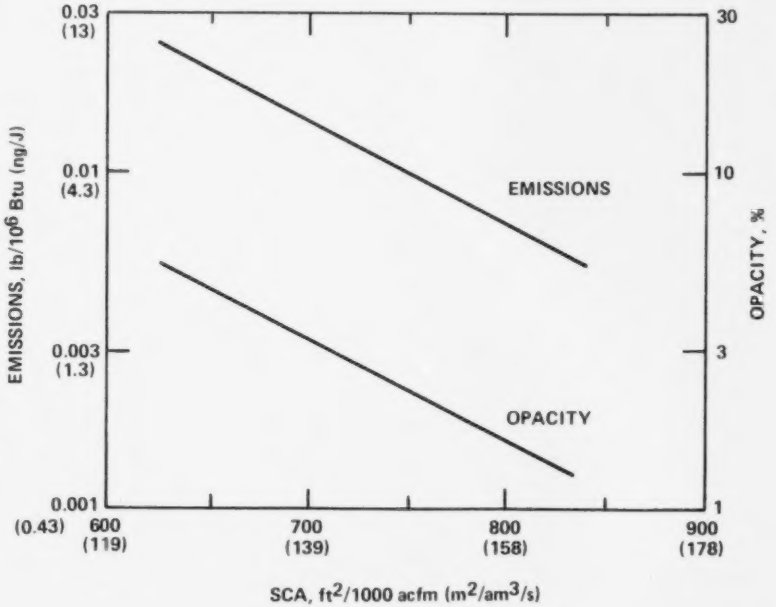

Figure 14. Performance projections of the Edgewater Unit 4 ESP with LIMB and humidification (100 °F approach to saturation).

THE RIDOX PROJECT - A SUMMARY REVIEW

G. De Michele*, M. Gatti**, G. Trebbi*
* ENEL-CRTN, Via A. Pisano, 120 - Pisa, Italy 56100
** ENEL, Via G.B. Martini, 3 - Roma, Italy 00198

ABSTRACT

The use of sorbent injection in oil-fired units is part of a large-scale research project carried out by ENEL called RIDOX.

The aim of the RIDOX Project is to prove the feasibility of a 50 % reduction in the emissions of SO_2 and NOx.

This paper describes the present state of the project with reference to SO_2 removal and deals in some detail with the fields in which the technology applied to oil-firing plants shows impressive differences compared to experiments with coal.

INTRODUCTION

In 1986 ENEL started a project with an environmental target called RIDOX, which includes the addition of calcium hydroxide and flue gas humidification to remove SO_2 and the testing of a combustion system for low NOx production.

The project is based mainly on demonstration tests and is essentially devoted to the retrofitting of oil-fired power stations, which are the majority of ENEL system, i.e. 60 % of thermoelectric generation.

This paper deals with the part of the RIDOX Project concerning SO_2 reduction; the present state of research on NOx abatement is reported elsewhere in the references /1/, /2/.

The use of sorbent injection in oil-fired boilers is a relatively new technique that needs specific research and demonstration because most of the experiments so far have been on coal-fired plants. This technique appears to be possible because these plants in ENEL generating system are equipped with electrostatic precipitators.

In setting up the research program the criterion adopted was that the investigation should be carried out directly on the power stations operating in various conditions, especially in view of the desirability of obtaining concrete results quickly. For this reason advantage was taken of the favourable circumstance that a very large experimental infrastructure was available, namely Unit # 1 and Unit # 2 at the Santa Gilla power station (Cagliari) /3/.

Unit # 1 was designed for coal-firing even if, at present, it is burning fuel oil. It is well equipped with instrumentation and was ready for use for the RIDOX Project. The experiments were extended and are, at the moment, in progress on Unit # 2 which has the same rating but, since it was designed fo fuel-oil firing, it has significantly different geometrical and functional characteristics.

In preparation for the Santa Gilla experiments, some fundamental research was carried out, essentially on a 50 kW test furnace and on a physical model of the boiler. For such specific activity, i.e. to localize the position of sorbent injection points on the boiler, mathematical modelling was extensively used.

CHOICE OF THE SORBENT

The choice of sorbent is of great importance especially for injection in oil-designed boilers where it is vital to reduce the sorbent flow-rate to a minimum, to avoid the boiler fouling.

Twenty commercial hydrated limes and special sorbents were tested using a differential reactor, a drop-tube furnace, a 50 kW test rig and a special TGA in which the sorbent can be easily exposed to high temperature reactive gas /4/.

It transpired that the desulphurization process is independent from the kind of fuel used (Fig. 1) and that, in the case of oil, it is promoted by certain additives, especially when limestone is used (Fig. 2) . On the contrary, when calcium hydroxide is used or for coal firing, the effect of the additive is negligible as has already been found by other authors /5/.

By operating both the drop tube and the 50 kW furnace, it was demonstrated that the main variable influencing sorbent reactivity is the particle-size distribution of the sorbent (Fig. 3).

An increased sintering resistance is very important for the use of sorbent injection in oil-designed boilers where residence time in the correct temperature range is very short. Some improvement in sintering resistance was obtained by modifying the structure of the sorbent by means of special treatment. Fig. 4 shows the percentage of SO_2 reduction at various temperatures when using a limestone, a commercial hydrated lime and a special sorbent. With the use of $S\text{-}Ca(OH)_2$ the maximum efficiency of desulphurization decreases but the reactivity of the sorbent is high over a wider temperature range. Fig. 5 shows the structure of each product.

A mathematical model based on the grain model is also available /6/. The model takes into account both the sintering processes and ionic diffusion. A number of results and data about the parameter used in the model are shown in

Fig. 2.

LOCATION OF SORBENT INJECTION POINTS

The Santa Gilla Power Station has two units. Unit # 1 is coal-designed while Unit #2 is oil-designed. Both the units are 35 MWe and are served by tangentially oil-fired boilers with eight burners on two levels (Fig. 6).

The sorbent is injected into the combustion chamber through up to six independent lines, each with a capacity of 700 Kg h^{-1}. The feed rates are controlled by a rotary valve on each hopper, and the hydrated lime is transported to the injectors by dried air with a 55 mm bore; the jet direction is variable.

Most of the tests were carried out on Unit # 1 and only certain preliminary experiments on Unit # 2.

The temperature in the boiler zone where the sorbent is injected is one of the most important variables affecting the efficiency of the desulphurization process. Experiments completed so far world-wide have ascertained that there is a "window" inside which SO_2 removal by sorbent reaches its maximum. The position of this window in the boiler depends on the load and on the combustion system configuration. To determine the location of these zones and then the injection points, both mathematical models and field measurements were used (Fig. 7).

MIXING OF THE SORBENT AND FLUE GAS

Adequate dispersion of the sorbent in the flue gas is a fundamental requisite for the efficiency of the desulphurization process and for minimizing the amount of sorbent used.

To study the mixing phenomena both cold physical models and mathematical models were used. The qualitative behaviour of the dispersion was obtained by using smoke and elium bubble tracers on a cold model.

The flow field in the combustion chamber was evaluated by means of a 3D code described elsewhere /7/ (Fig. 8); the model was validated by direct measurement of the velocity inside the combustion chamber as shown in Fig. 9.

The dispersion of solids in the combustion chamber is greatly dependent on the location of the injection ports even if they are on the same level (Fig. 10), and on the direction of the injectors. The mixing also depends on the configuration of the combustion system i.e. the tilting of the burners (Fig. 11).

The model also makes it possible to take into account the mixing obtained with multiple injection. Fig. 12 shows that the trend of a mixing factor on a plane at the furnace exit against sorbent flow-rate is the same as that of the desulphurization efficiency.

DESULPHURIZATION TESTS

The composition of the calcium hydroxide and of the oil used during the tests on the Santa Gilla # 1 and 2 Units are given in Tables 1 and 2.

The efficiency of the removal of sulphur dioxide from the gas is given in Fig. 13. It is of the same order of values obtained in Edgewater trials in the frame of LIMB project /8/.

BOILER FOULING

Sorbent injection increases the amount of solids that pass through the boiler and modifies the chemical and physical characteristics of the ash, especially in oil-fired units.

Tests using an air-cooled probe made it possible to measure the distribution of the deposits in the superheater zone and to link this to the geometry of the injection of air-borne calcium hydroxide.

Deposition rates were generally low (Fig. 14), but moderate rates were measured locally at a specific injection position. Material deposited in periods of up to 1 hour showed up to 70 per cent sulphation of the calcium. Such short-term deposits contained sufficient water-soluble compounds to make them easily removable by water-washing, but deposits aged for many hours were almost completely sulphated and their solubility was largely destroyed. The deposits were porous crystalline, of low mechanical strength (Table 3) and relatively easy to remove by soot-blowing.

Calcium injection did not increase the deposition of sodium sulphate derived from the fuel. At the end of the injection of calcium, a few hours passed before the fireside deposition of calcium actually ended.

Details of ENEL work in this field are reported in reference /9/.

SOLID PARTICULATE CAPTURING

The different nature and the greater load of particulate due to sorbent injection negatively affect the efficiency of electrostatic precipitators in coal-fired units. The high resistivity of the coal-ash/sorbent mixture was considered to be the main reason for the poor performance of the ESP and such techniques as the humidification of the flue gas and SO_3 injection were devised to reduce resistivity /10/.

In the case of oil-fired plants the situation is substantially different; because the resistivity of oil-ash is very low, the performances of ESPs are consequently poor (50-60 %). The injection of calcium into the boiler dramatically increases the resistivity of the particulate (Fig. 15), improving ESP operation. Apart from the presence of unburnt material derived from oil combustion, specific analyses have shown that low resistivity metallic oxides, essentially vanadium, are deposited on the calcium particles.

A good performance of the ESP was obtained by using a pilot precipitator fed by a stream split from Unit # 1 where the collection efficiency was 97 - 98 %. Tests on a full-size ESP which serves Unit # 2 gave a collection efficiency of the same order; ultimately, despite the sorbent injection, it seems to be possible to reduce the particulate emission produced by oil combustion.

GAS HUMIDIFICATION

Coolside desulphurization tests were included in the RIDOX Project and will be carried out in 1989 on the duct of Unit # 2 at Santa Gilla.

As shown elsewhere, water atomization is a key aspect in coolside technology /11/. Fundamental studies concerning water atomization are being carried out at ENEL Labs; the work concerns the characterization of the sprays obtained with two commercial twin-fluid nozzles and the correlation of the spray characteristics with the SO_2 abatement data obtained by CONOCO /12/ using the same atomizers.

Fig. 16 shows that the two nozzles give different reductions in SO_2 in spite of the approach and the mean spray-diameter are the same /13/. The atomization trials have shown that even if mean diameters are the same, the structure of the spray is considerably different (Fig. 17) and this produces different droplet drying-lengths. On the basis of these results atomizers able to produce optimal spray structure are being developed.

SORBENT REACTIVATION

CaO concentration in the particulate collected from the ESP is very high (Table 4) and sorbent reactivation appears to be very promising. Due to the absence of coal ash the particulate collected at the ESP can be easily activated again in a scavenging reactor.

Laboratory experiments show that it is possible to obtain an excellent hydratation of residual calcium oxide present in exhausted sorbent using hot water and an additive (Fig. 18).

The new active sorbent obtained in this way can be injected as a water slurry into the combustion chamber or into the duct upstream from the ESP, as is done in E-SOx technology. The capability of calcium hydrate water slurry to reduce SO_2 when injected into furnaces was also demonstrated in specific tests (Fig. 13).

CONCLUSIONS

Sorbent injection in oil-fired boilers is promising. Certain specific features of this technology are very different compared to coal.

Sorbent enhancement by means of additives is possible in oil-fired boilers and this appears to open up new possibilities as compared to coal.

The desulphurization efficiencies obtained in coal and oil-designed boilers

The desulphurization efficiencies obtained in coal and oil-designed boilers appear to be quite the same, being a compromise of different temperatures, residence time and mixing.

The boiler fouling was acceptable in the coal-designed plant, and no negative effect was produced by the combined effects of the sorbent and the oil-ash. Studies on fouling in oil-designed boilers are at present in progress.

The performance of the ESP with the particulate made of a sorbent - oil ash mixture appears to be very promising due to the good value of particulate resistivity.

Due to the composition of the solid collected at the ESP, it seems to be useful to carry out the scavenging and reactivation of the solids.

The demonstration at the Santa Gilla power station is still in progress and long-lasting tests are planned in Unit # 2 from the beginning of 1989. The experiments will deal essentially with fouling phenomena, the humidification of flue-gas and the reactivation and recirculation of the sorbent.

Following the success of the tests at the Santa Gilla Unit # 1, ENEL is studying the use of sorbent injection on a standard 320 MW coal-designed oil-fired unit. The project started with the evaluation of the flow field and temperature distribution in the furnace and the correct injection points were located using the mathematical model successfully tested at Santa Gilla.

REFERENCES

1. Baldacci, L., Bertacchi, S., De Michele, G. NOx reduction by gas reburning technology. IFRF Gaseous Fuels Panel; Roskilde, Denmark, 25-27 October 1988.

2. De Michele, G. et al. Development of an oil and gas low-NOx Burner. 1989 Joint Symposium on Stationary Combustion NOx Control; San Francisco, CA, 6-9 March 1989.

3. De Michele, G., Ligasacchi, S., Pasini, S. CWF Firing on an oil-designed utility boiler; 12th Internat. Conf. on Slurry Technology, New Orleans, March 31, April 3, 1987.

4. Bertacchi, S. et al. Evaluation of SO_2-Calcium sorbent reaction at high temperature by different scale experimental tests. The Combustion Institute, XIII Italian Section Meeting, Como, June 29, July 1, 1988.

5. Muzio, L.J. et al. The effectiveness of additives for enhancing SO_2 removal with calcium based sorbents. 1986 Joint Symp. on Dry SO_2 and Simultaneous SO_2/NOx Control Technologies. June 2-6, 1986, Raleigh, NC.

6. Bertacchi, S., Frandi, R. Influence of Promoters on the Effectiveness of Dry Sorbents for High Temperature Flue-Gas Desuplphurization. Joint

Meeting of French and Italian Sections of the Combustion Institute, 16-19 Giugno 1987, Amalfi, Italy.

7. De Michele, G., Pasini, S., Tozzi, A. Aerodynamics and Heat Transfer Modelling in Tangentially-Fired Boilers. Joint Meeting of the Aerodynamics, Flame Chemistry and Heat Transfer Panels, I.F.R.F., Stockholm, October (1985).

8. Nolan, P.S. et al. Demonstration of the Limb and Coolside Technologies at Ohio Edison's Edgewater Station. Fifth Annual Int. Pittsburgh Coal Conference, Sept. 12-16, '88.

9. De Robertis, U. et al. Studies of fireside deposit formation during calcium hydroxide injection in an oil-fired boiler. Eng. Foundation Conference, Mineral Matter and Ash in Coal, Santa Barbara, CA, February 22-26 (1988).

10. Dahlin, R.S., Gooch, J.P., and Kilgroe J.D. Effects of furnace sorbent injection on fly ash characteristics and electrostatic precipitator performance. In: Proceedings: First Joint Symposium on Dry SO_2 and Simultaneous SO_2/NO_x Control Technologies, Volume 2, EPA-600/9-85-020b, NTIS PB85-232361, p. 29-3, July 1985.

11. Yoon, H., Stouffer, M.R., Burke, F.P. Coolside Desulphurization Reactions and Mechanisms. 194th American Chemical Society National Meeting, New Orleans, August 30 - September 4 (1987).

12. Yoon, H., Stouffer, M.R., Rosenhoover, W.A., Withum, J.A., Burke, F.P. Pilot Process Variable Study of Coolside Desulphurization. AIChe 1987 Spring National Meeting. Houston, March 29 - April 2 (1987).

13. Graziadio, M. et al. Characterization of Flue Gas Humidification Nozzles. European ILASS Conference, Rouen, March 28-29 (1988).

DISCLAIMER

The work described in this paper was not funded by the U.S. Environmental Protection Agency and therefore the contents do not necessarily reflect the views of the Agency and no official endorsement should be inferred.

	per cent.
Water	0.6 to 1.0
Content of Ca (OH)	79 to 80
CaO	13.2 to 15.5
$CaCO_3$	5.5 to 6.5
Ca	48.6
Al	0.25
Si	0.63
Fe	0.10
Mg	0.45
K	0.03
Na	0.02
V	< 0.01
S	0.06

Tab. 1. Calcium hydroxide composition.

Density	15 C	0,971	g cm^{-3}
Viscosity	50 C	320	cS
	80 C	67,5	cS
	110 C	26,6	cS
Gross Calorific Value		42,7	MJ.kg
Water		0,03	per cent
Ash		0,081	
Asphaltene (ASTM 2007)		12,3	
(IP 143)		7,4	
Carbon		85,93	
Hydrogen		10,85	
Nitrogen		0,40	
Sulphur		2,87	
Composition of Ash (sulphated)			
SiO_2		20,8	per cent
Al_2O_3		0,68	
Fe_2O_3		0,21	
CaO		0,36	
MgO		0,44	
K_2O		0,08	

Tab. 2. Oil composition.

Microscopical examination of dry solid samples

SAMPLE	PRINCIPAL CONSTITUENT	PARTICLE SIZE µm	CENOSPHERES	
			PARTICLE SIZE µm	%
B	White amorphous agglomerate Loose agglomerates Non-dispersible aggregates	< 5 → 150 → 400	20 - 100	< 1
C	As B + cristalline, coloured lumps (about 1%)	200	20 - 100	< 0,5
D	As B aggregates	→ 1000	→ 120	< 1
E	As B. aggregates Aggregates include sub-micron particles → fawn color overall. A few yellow-fawn crystalline lumps.One contains a 80 µm cenospheres	→ 500 → 400	20 - 100	1 - 2
F	As E. Aggregates partly coloured yellow → orange → red-brown	→ 1000	→ 120	5
G	Entirely crystalline, colourless → brown, varying colour. Crystal size	→ 30 100	20 - 100	< 1
H	As B. Few aggregates	→ 400	20 - 100	< 0,5
X*	As B		10 - 100	1 - 2

* Dry solid from probe exposed during oil - firing whithout absorbent

Tab. 3. Characteristics of solid deposits.

Unburnt (%)	1.6
$Ca(OH)_2$ (%)	13.4
$CaCO_3$ (%)	15.6
CaO (%)	39.7
MgO (%)	1.5
$CaSO_4$ (%)	21.7
Diff. to 100 (%)	6.5

Tab. 4. ESP particulate composition.

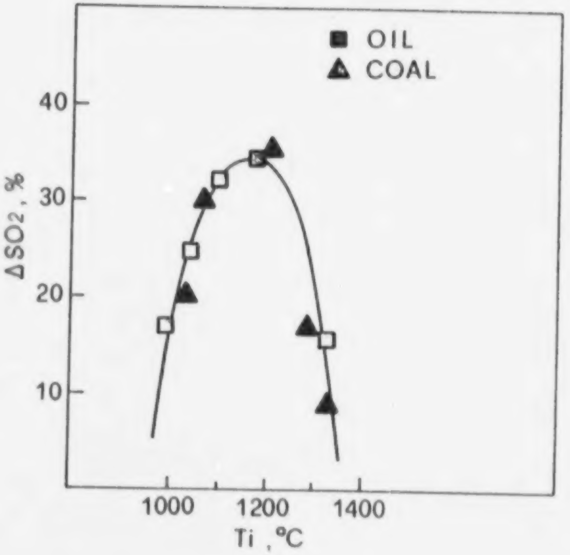

Fig. 1. Desulfurization efficiency ΔSO_2 vs injection temperature T_i for oil and coal. The data were obtained on 50 kW furnace for Ca/S=1.

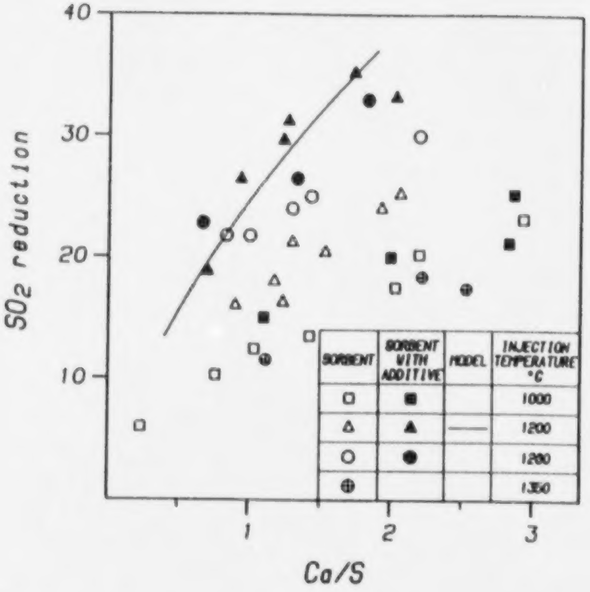

MODEL PARAMETERS

kinetic rate $k = 291 \exp(-7510/T)$ cm/s

product layer diffusion $D_s = 0.05 \exp(-14000/T)$ cm²/s

thermal sintering $S_t - S_{t-1} = 1.3E{+}8\,(S-3)^2 \exp(-29745/T)\Delta t$ m²/gs

combined pore diffusivity $= D_{Gt}\, C$

coefficient $C = S_t / S_{t-1}$

Fig. 2. Desulfurization efficiency ΔSO_2 vs Ca/S with and without additive for $CaCO_3$ injection.

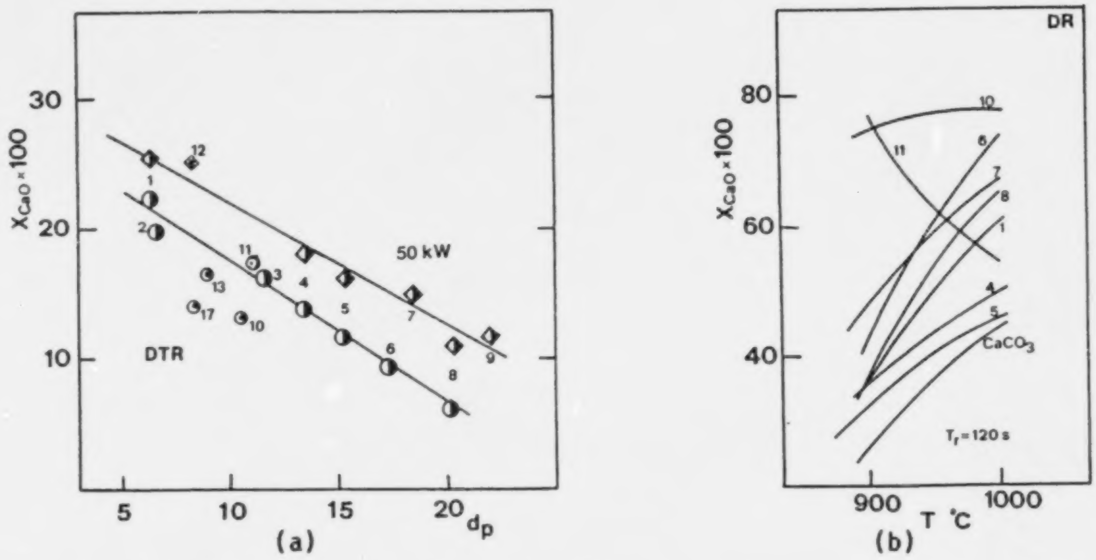

Fig. 3. Desulfurization efficiency for different sorbents vs temperature and particle mean diameter. (a) 50 kW furnace and drop tube reactor. The sorbents 10, 11, 12, 13 and 17 are modified starting from product # 1. (b) differential reactor.

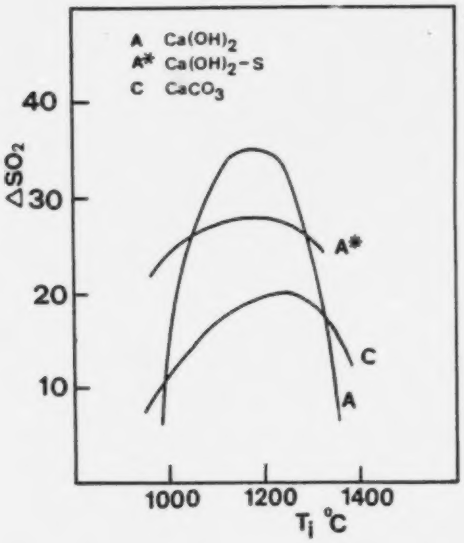

Fig. 4. Desulfurization efficiency vs injection temperature for commercial (A and C) and special (A^*) sorbent.

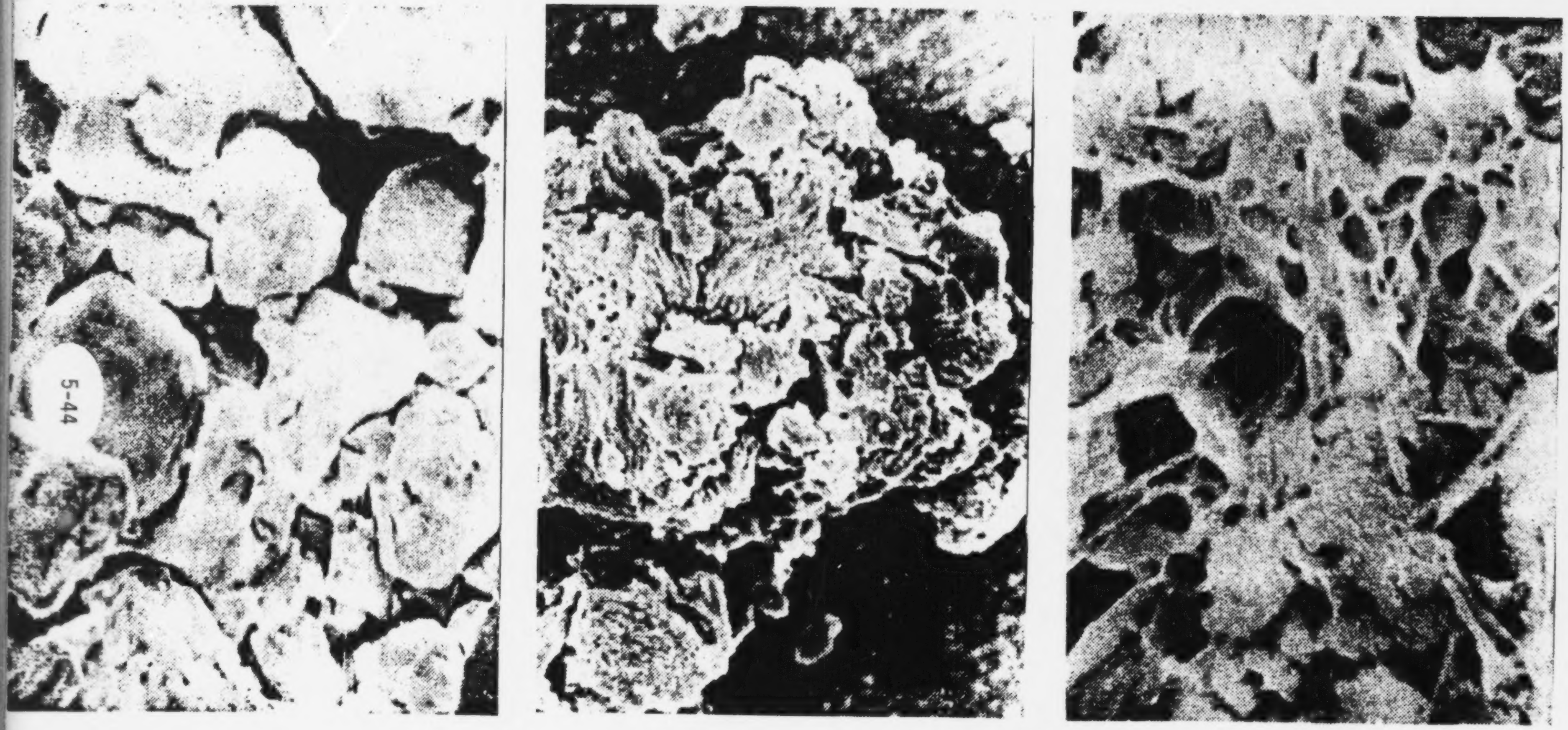

(C) (A) (A^*)

Reproduced from best available copy.

Fig. 5. Microstructure of two commercial sorbents (C and A) and a special product (A^*).

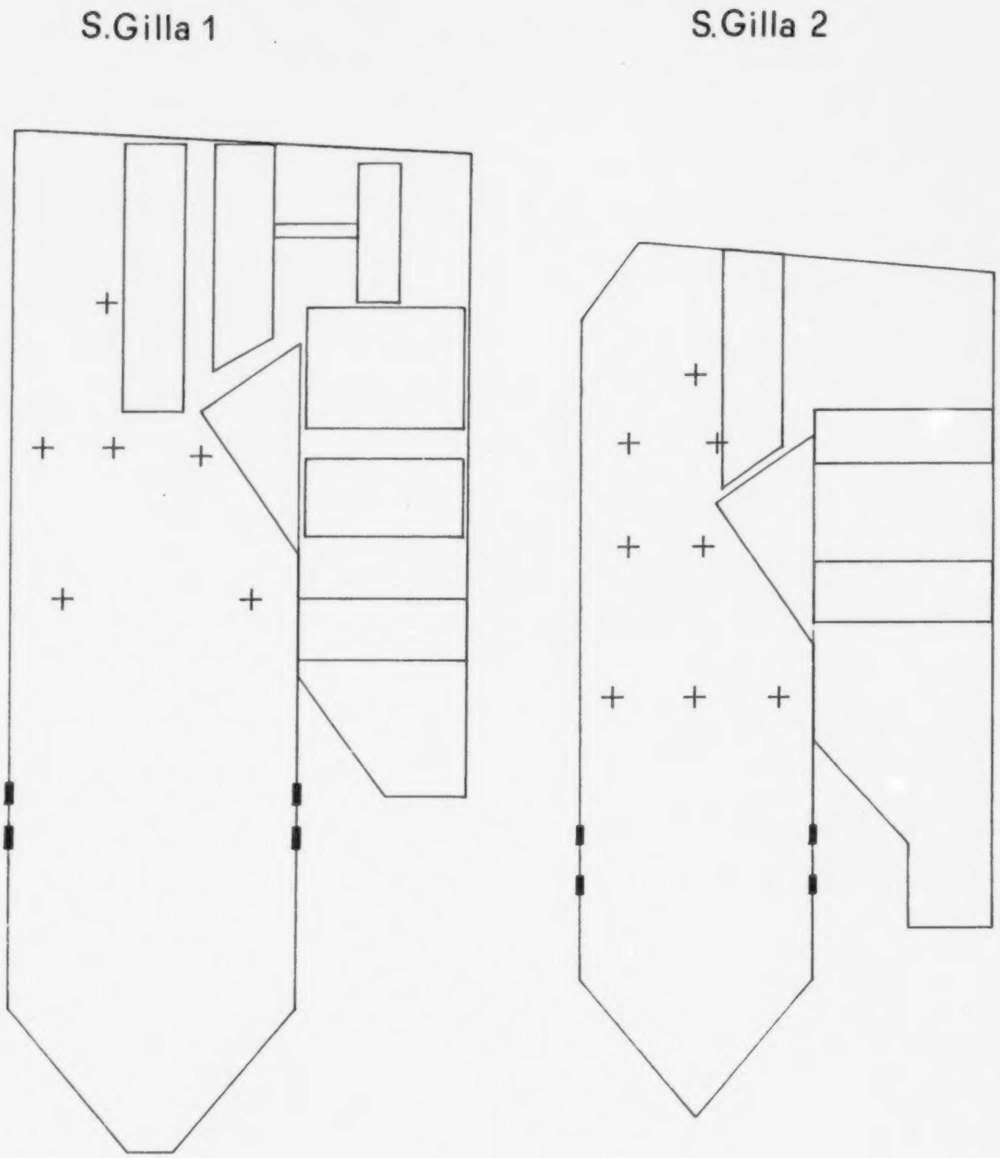

	UNITS	S.GILLA 1	S.GILLA 2
- PLAN AREA HEAT RELASE	MW/m^2	3.49	5.02
- BURNER ZONE HEAT RELASE	MW/m^2	1.65	2.31
- FURNACE LIBERATION RATE	MW/m^3	0.237	0.413
- HEAT RELASE/IRRAD. SURFACE	MW/m^2	0.233	0.376

Fig. 6. Geometrical characteristic of Santa Gilla # 1 and # 2 units.

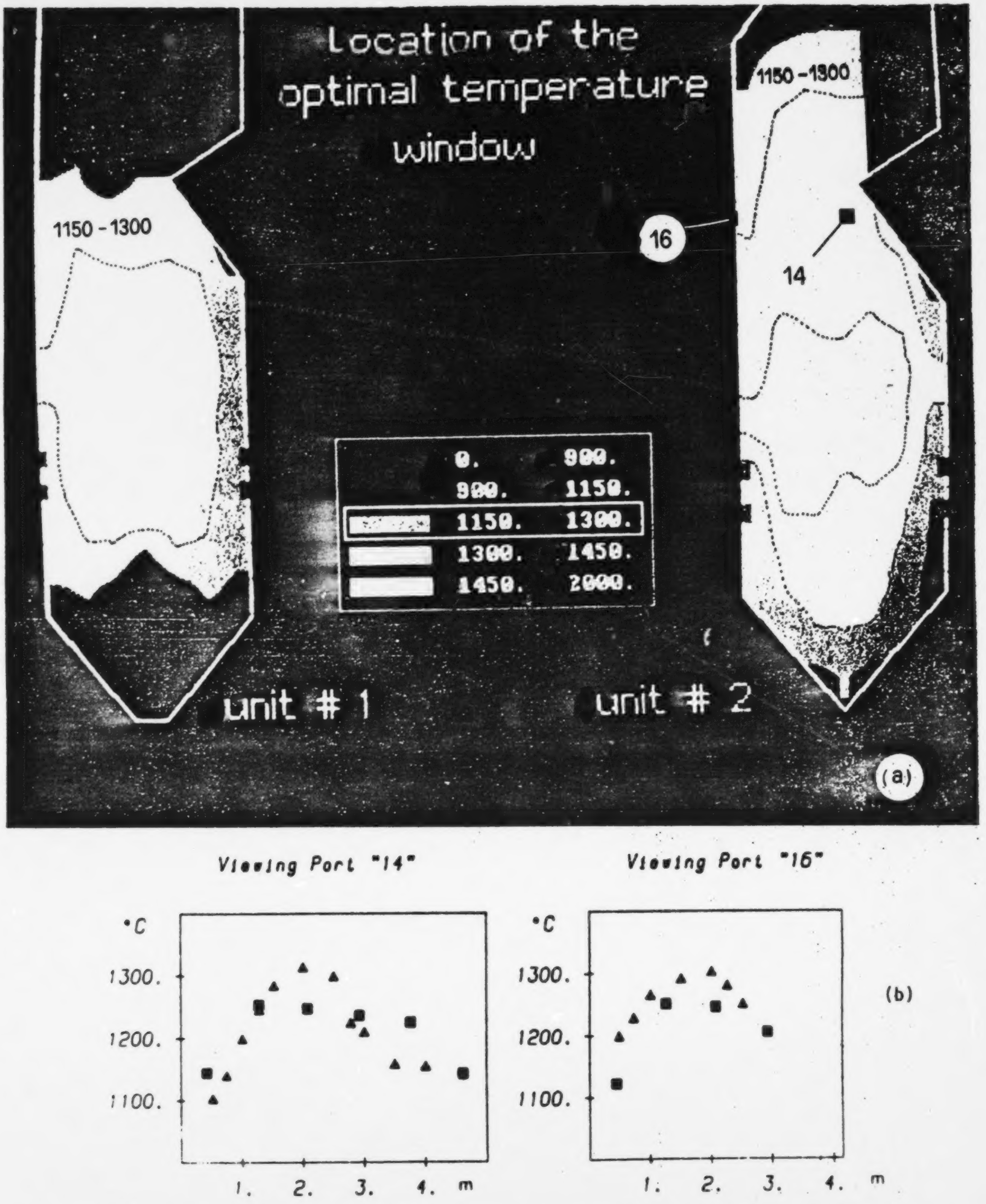

Fig. 7. (a) temperature distribution in the two Units (35 MW_e). (b) comparison between experimental (▲) and theoretical (■) predictions (S. Gilla // 2, 30 MW_e).

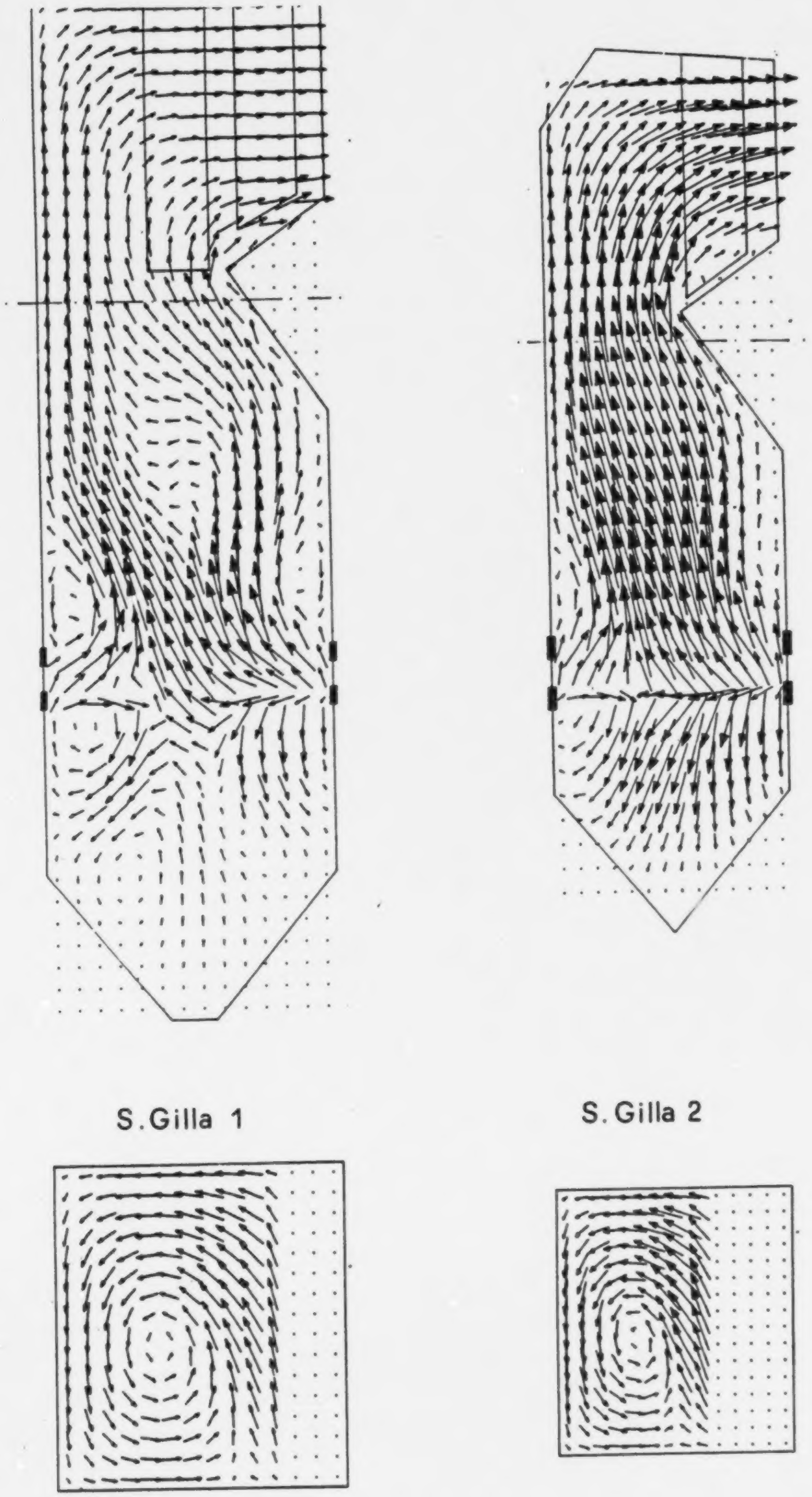

Fig. 8. Flow field in the furnace of the two Units obtained with a mathematical model.

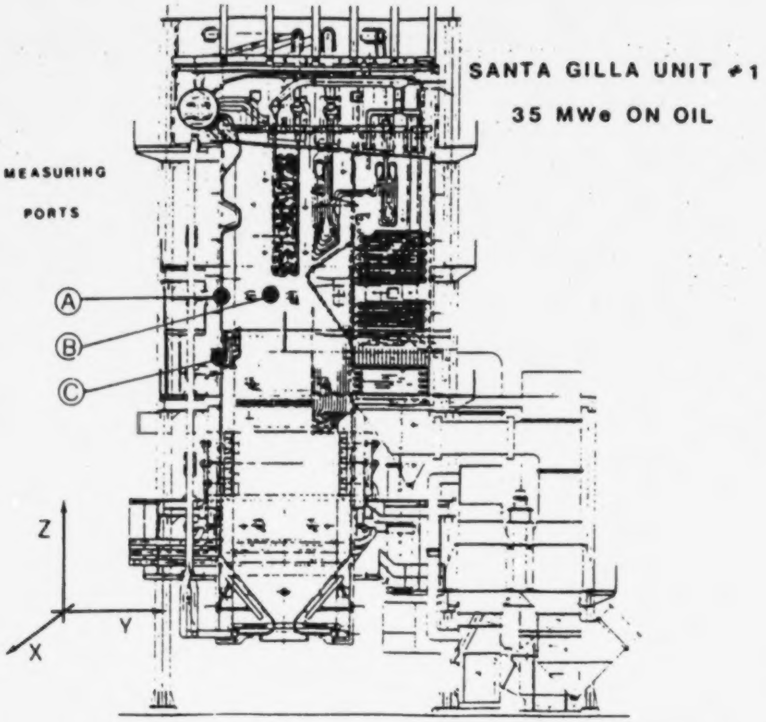
SANTA GILLA UNIT #1
35 MWe ON OIL
MEASURING PORTS
A
B
C
Z
Y
X

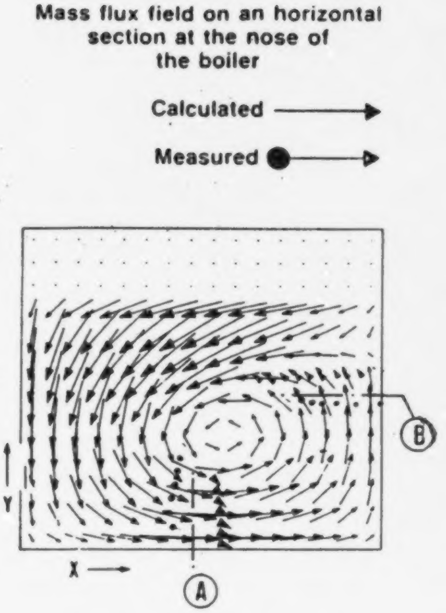

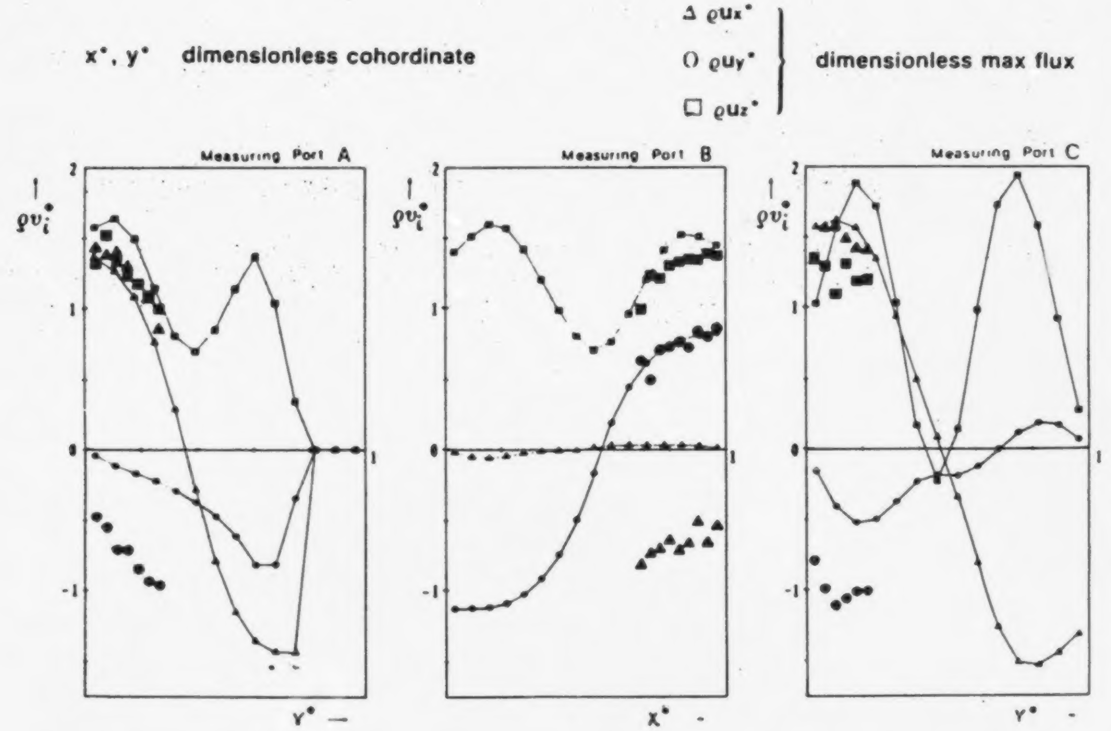

Fig. 9. S. Gilla # 1. Comparison between predicted (—▲—▲—) and measured (▲) mass fluxes.

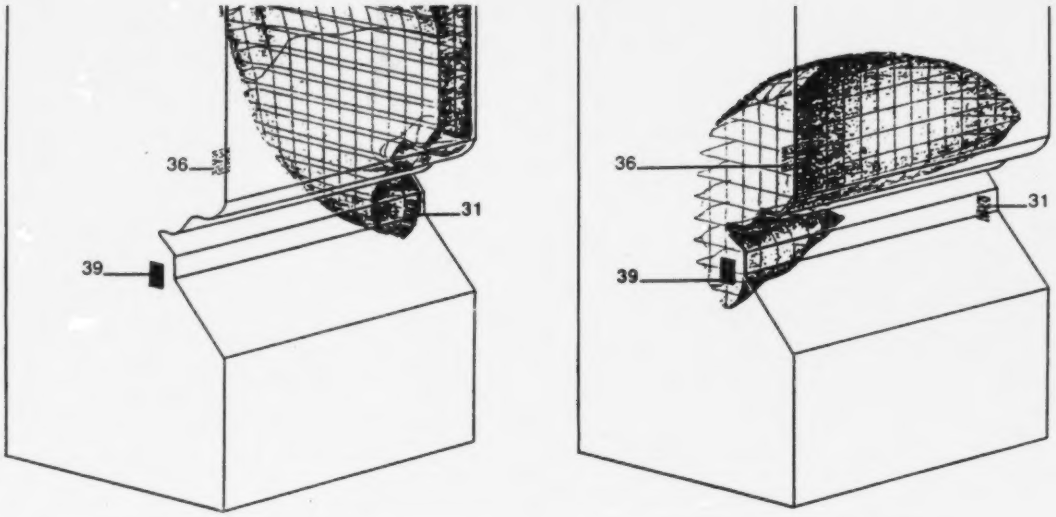

Load	32MWe
Port	31
Tilt	-24°
Fmix,t	23 %

Load	32MWe
Port	39
Tilt	-24°
Fmix,t	35 %

Fig. 10. S. Gilla ⌗ 1. Dispersion of sorbent injected in two ports at the same level.

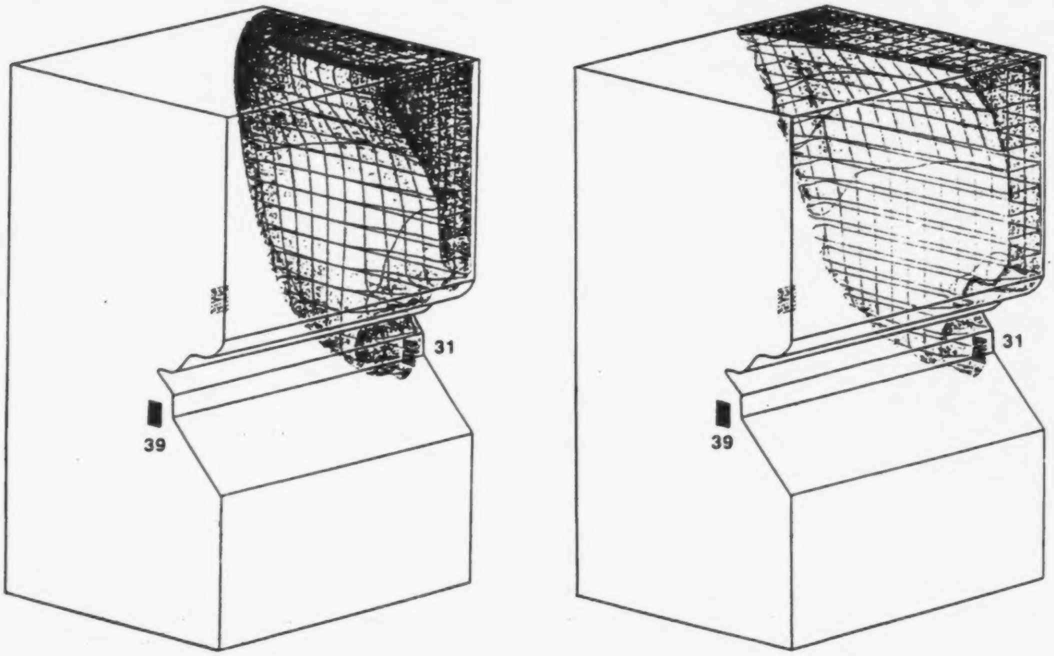

Load	32MWe
Port	31
Tilt	0°
Fmix,t	26,8 %

Load	32 MWe
Port	31
Tilt	-24°
Fmix,t	22,5 %

Fig. 11. S. Gilla ⌗ 1. Dispersion of sorbent with the combustion system in two different conditions.

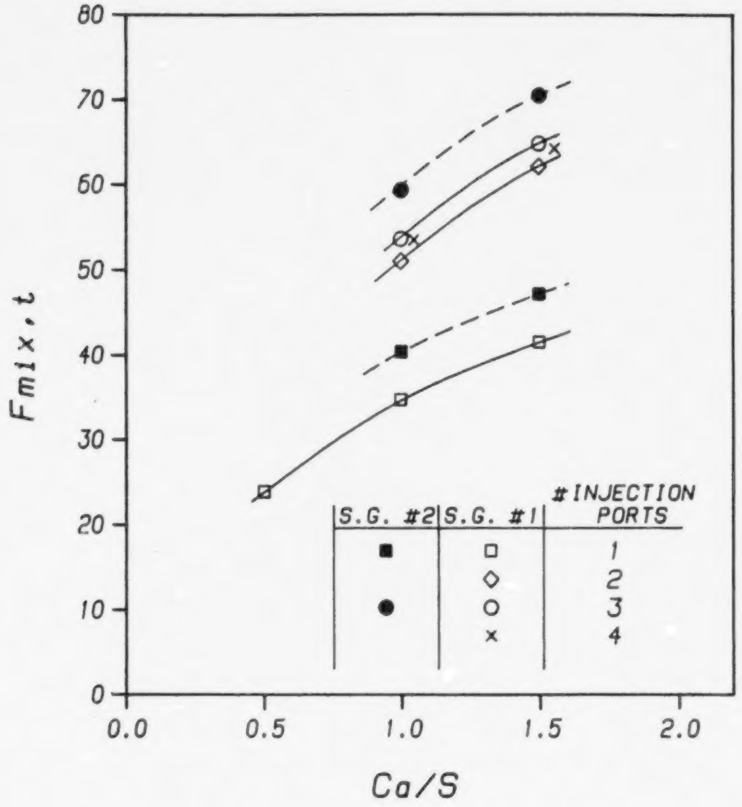

MIXING FACTORS

$$Fmix\,(i,j,k) = \min\left[\frac{C_{Ca\,(i,j,k)} * Frmax}{C_{SO_2\,(i,j,k)}} ; 1\right]$$

$$Fmix,t = \sum_{plane} \frac{Fmix\,(i,j,k) * Area * \rho u\,(i,j,k)}{Area,t * \rho u^{m}_{tot}}$$

Fig. 12. Mixing factor vs Ca/S, where F_{rmax} is the maximum calcium utilization factor.

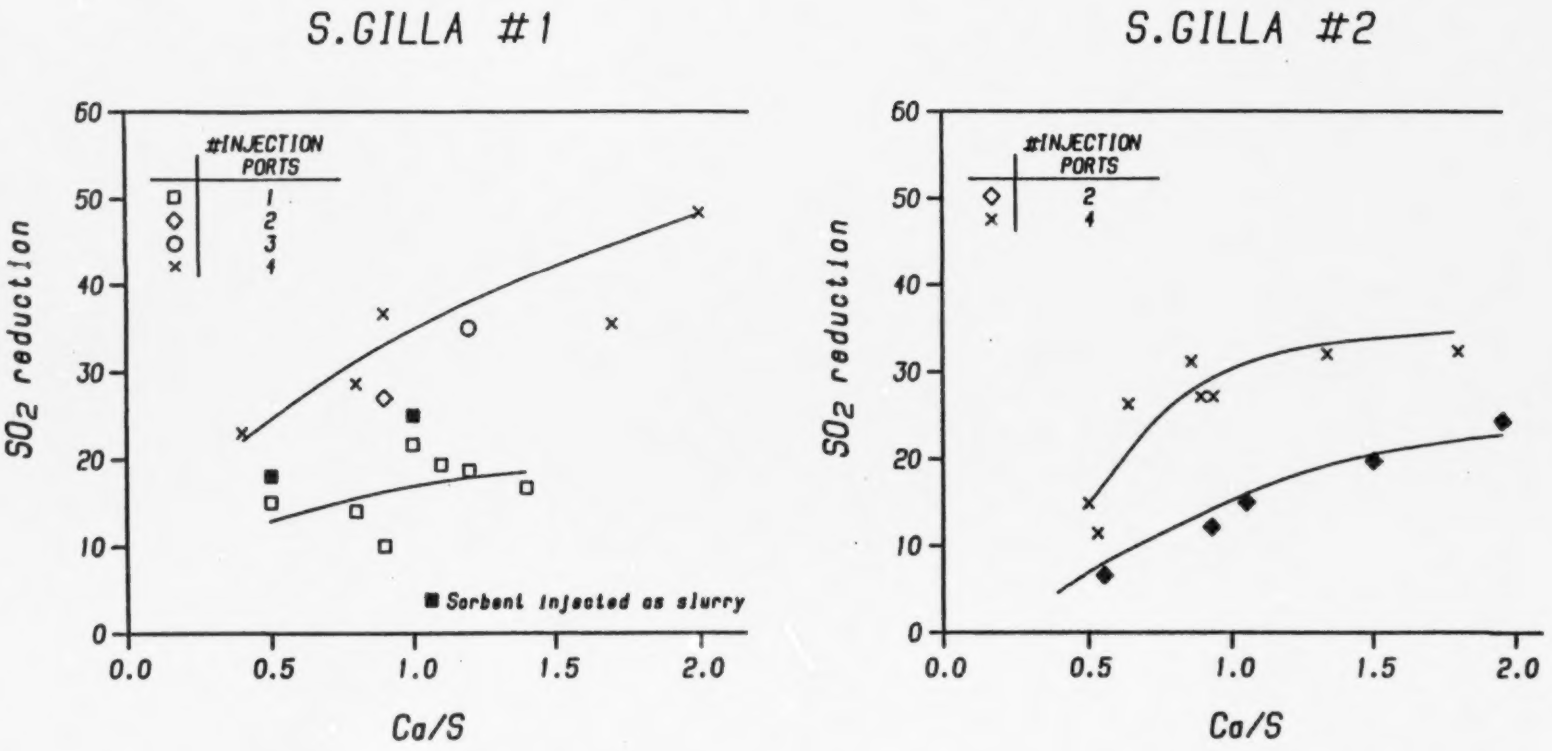

Fig. 13. Desulfurization efficiency vs Ca/S for various configurations of injecting system.

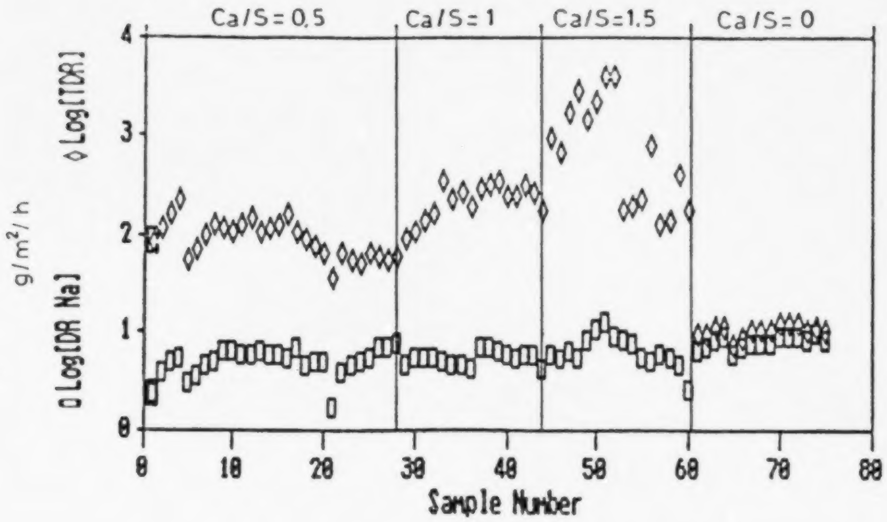

Fig. 14. Total and sodium deposition rates for different Ca/S.

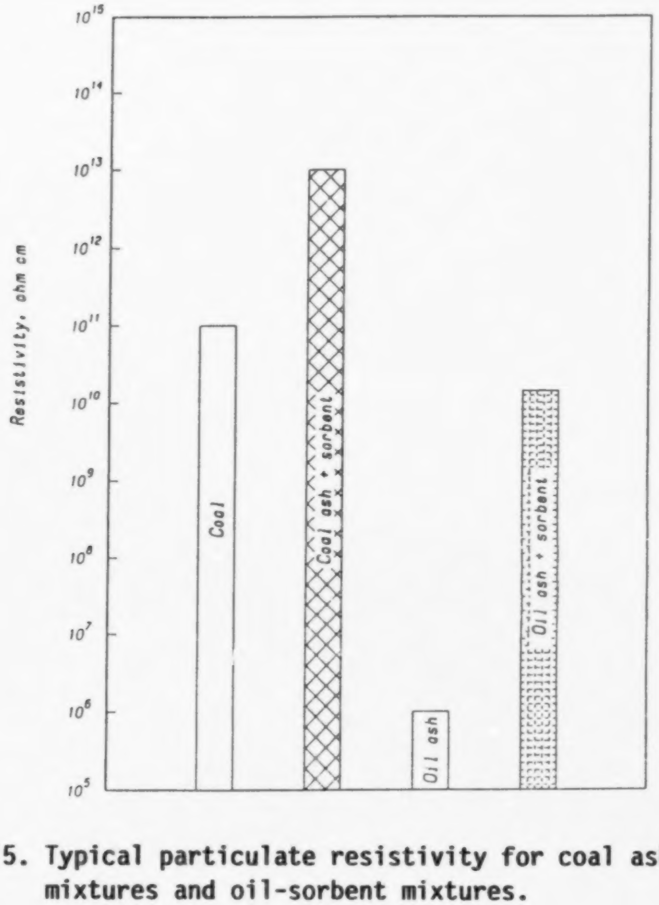

Fig. 15. Typical particulate resistivity for coal ash-sorbent mixtures and oil-sorbent mixtures.

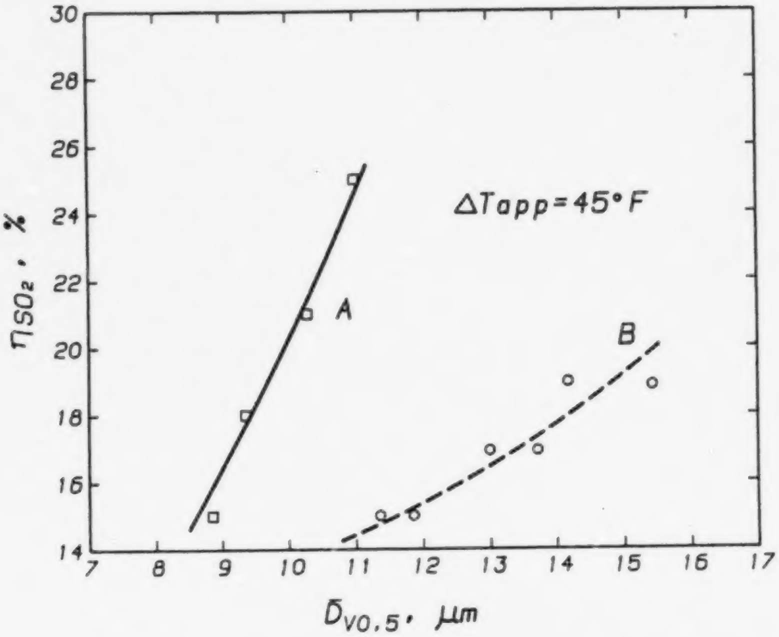

Fig. 16. Cool side sulfur reduction obtained with two commercial atomizers.

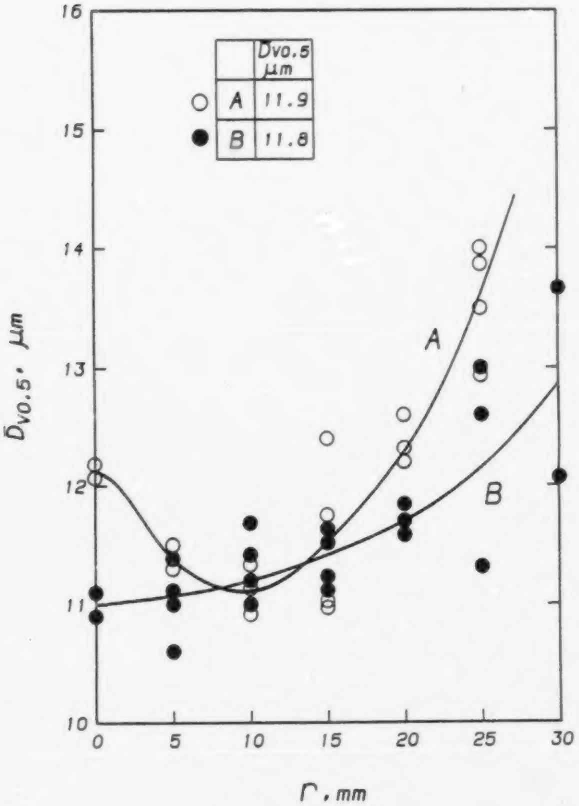

Fig. 17. Radial dorplet distribution for the two atomizers.

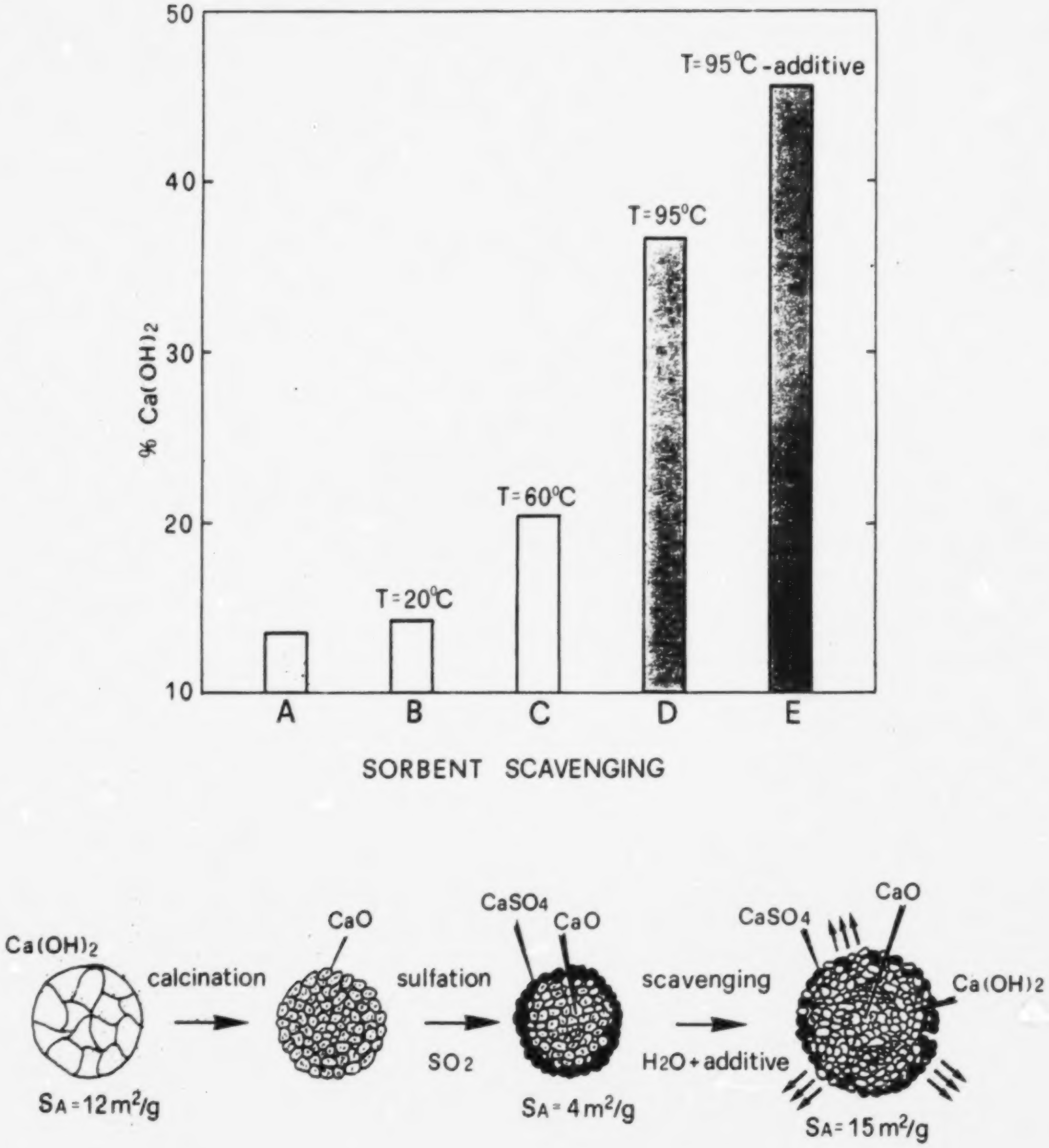

Fig. 18. Scavenging mechanism and calcium hydroxide concentration in reactived sorbent for different treatment of ESP particulate.

MECHANISTIC STUDIES OF SORBENT UTILIZATION ENHANCEMENT BY HUMIDIFICATION

by: Roderick Beittel
Robert S. Dahlin
Southern Research Institute
Birmingham, AL 35255-5305

ABSTRACT

This paper discusses the results of pilot tests and computer modeling of the enhancement of lime sorbent utilization by post-furnace humidification. The testing was performed in a 300 ft^3/min (0.14 m^3/sec) humidification chamber attached to a 1 x 10^6 Btu/hr (293 kW thermal) combustor firing SO_2-doped natural gas. Incremental changes in sorbent utilization across the chamber were measured with humidification by water vapor, humidification by water spray, and slurry injection. Increments of 1, 6, and 33%, respectively, were achieved with a sulfated calcine produced by furnace injection of hydrated lime. With fresh hydrated lime, increments of 10, 12, and 28% were achieved under similar conditions. The results show that the dominant mechanism of sorbent activation is sorbent/droplet collision, and comparison of slurry injection and spray humidification suggests that only 15% of the sorbent is wetted by this mechanism. Computer modeling suggests that the collision efficiency can be improved by increasing droplet size, but there are practical limitations on this approach due to wall impact and evaporation time.

This paper has been reviewed in accordance with the U.S. Environmental Protection Agency's peer and administrative review policies and approved for presentation and publication.

Presented at the First Combined FGD and Dry SO_2 Control Symposium
October 25-28, 1988
St. Louis, Missouri

INTRODUCTION

Post-furnace humidification is receiving attention as a means of enhancing the reaction of dry calcium-based sorbents with SO_2 at relatively low gas temperatures in ducts approaching the stack. In some instances, this technique is intended to increase the utilization of sorbents that are injected into the furnace to undergo primary reaction at high temperatures; for example, Yoon et al. (1) have described a process called "BLI Activation," in which limestone is injected in the boiler and the resulting calcine is activated by humidification in a low-temperature duct to undergo further reaction with SO_2. In other instances, the sorbent is injected only in the low-temperature duct; it undergoes all of its reaction in this zone and is highly dependent upon humidification to achieve significant reaction. One example of the low-temperature process has been referred to by Yoon et al. as "Straight Coolside;" it is based on $Ca(OH)_2$ as the sorbent and humidification with a spray of liquid water, which evaporates to further lower the reaction temperature. Low-temperature or duct-injection processes have been investigated under EPA- and EPRI-sponsored programs (2,3) and are currently under intensive development by the Department of Energy as a means of reducing the problem of acid rain.

One of the crucial issues associated with post-furnace humidification is whether activation can be achieved with water vapor alone or can only be accomplished by physical contact between sorbent particles and liquid water droplets prior to their evaporation. Another issue is how the effect of liquid droplets can be optimized by controlling droplet size, residence time, and other parameters. In ultimate efficiency, the interaction of sorbent particles and water droplets may approach that in a spray dryer. Comparison of vapor humidification and spray humidification with spray drying, therefore, is an appropriate way to gauge the effectiveness of the two humidification processes.

Post-furnace humidification has been viewed as a possible means of increasing the utilization of $Ca(OH)_2$ sorbent in EPA's LIMB (Limestone Injection Multi-stage Burners) demonstration. Humidification will be depended upon to satisfy one other essential goal--adjustment of the ash-sorbent electrical resistivity to a lower value consistent with efficient electrostatic precipitation. Obviously, the process will be even more useful if it also improves SO_2 removal. Post-furnace humidification at the LIMB demonstration would be a process similar to Consol's BLI Activation process; it would differ, however, in that the sorbent at the LIMB demonstration is hydrated lime, whereas that in Consol's process is limestone.

PILOT-SCALE STUDIES

EXPERIMENTAL APPARATUS

The main component of the experimental apparatus used for the post-furnace humidification studies was a cylindrical humidification chamber on a vertical axis, which is illustrated in Figure 1. This chamber was inserted between segments of the 4-in. (10-cm) duct normally channeling flue gas at a temperature around 300°F (150°C) to the system exit. The inlet and outlet of the chamber were flared outward to a diameter of 36 in. (91 cm); the length of the chamber was about 10 ft (3 m). Thermocouples were mounted at intervals along the length of the chamber. A Sonic Development ST47 two-fluid nozzle was placed at the centerline near the inlet for injecting water or an aqueous slurry. The total residence time of flue gas in the chamber was 10 to 15 sec, much longer than the time that would exist in an actual power-plant duct. The geometry, however, minimized collision of water droplets with the walls; moreover, the chief objective was to determine the upper limit of reaction. When water droplets were injected, their short lifetime (about 1 sec) rather than the total gas residence time was the controlling factor on the extent of reaction.

The nozzle was operated at an air pressure of 80 psi (550 kPa) and a water flow rate of 0.0913 gal./min (0.345 L/min). Sizing of the spray droplets with SRI's Video Droplet Analyzer indicated that the Sauter mean diameter was about 29 μm. The estimated time required for the droplets to undergo complete evaporation under the experimental conditions subsequently described was about 1.2 sec. The ST47 nozzle was also used for slurry injection on occasion, as a substitute for water injection. Dry solids, on the other hand, were injected in a stream of air at a location immediately upstream from the humidification chamber.

A dilution probe was used to sample entrained solids at the outlet of the reactor. This probe dilutes the sample with hot, dry air through a porous wall just inside the inlet and performs the vital function of quenching reaction at the instant of sampling. A filter was used to collect solids from flue gas sampled at about 0.18 ft^3/min (6.0 L/min) and a dilution of 10:1. Analysis of these solids provided the data that were used to compute the utilization of the sorbent. This procedure was eminently superior to the use of results based on the change in gas-phase SO_2 concentration, which was heavily influenced by reaction with long-lived wall deposits.

The ability of the dilution probe to quench the SO_2/lime reaction was verified by the following procedure. Hydrated lime was injected just upstream of the humidification chamber and followed by humidification to a total water concentration of 0.24 mole of water per mole of dry flue gas from an initial value of 0.17 mole/mole. The dilution probe was used to sample SO_2-free flue gas (from the combustion of natural gas) at the chamber outlet where the approach to saturation varied from 20 to 40°F (11 to 22°C) from experiment to experiment. The dilution air was spiked with 2000 ppm of SO_2; the dilution air volume was about four times the sample volume. Under these extreme conditions, the in-probe conversion of $Ca(OH)_2$ was about 2% or less.

An alternate sampling system—isokinetic with an in-duct filter—was used to determine the concentration of total suspended solids at the chamber outlet. It was also used on occasion at the inlet. There was no requirement at the outlet for the system to prevent further chemical reaction during sampling. On the other hand, the system was required to prevent reaction when used at the inlet (when sorbent was injected upstream from the inlet, prior to injection of water); the system was found satisfactory with respect to this requirement.

HUMIDIFICATION OF REINJECTED CALCINE

To facilitate a systematic study of humidification parameters, a large quantity of partially sulfated calcine was prepared for reinjection into the flue-gas stream immediately upstream from the humidification chamber. Reinjection of this material, followed by humidification, gave a simulation of the processes to be expected with post-furnace humidification at the LIMB demonstration. The material was produced by injecting $Ca(OH)_2$ into the SRI pilot combustor at a Ca/S ratio of 2:1 during the addition of SO_2 to the combustion products from natural gas. The material was collected on the fabric filter at the exit from the combustor. Chemical analysis showed that the composition of material on a weight basis was 33% CaO, 23% $Ca(OH)_2$, 7% $CaCO_3$, 30% $CaSO_4$, and 7% other components. The calculated atom ratio S/Ca in the solid corresponded to a utilization of 18% in the furnace.

The reinjected calcine was subjected to the effects of humidification by three processes, as depicted schematically in Figure 2. First, the dry solid was injected into flue gas containing excess water vapor, which had been precooled to 160°F (71°C). At no time during this process was liquid water introduced, and thus at no time did the calcine become physically wet. Literally speaking, there was no humidification in this process, but the effects simulated humidification by vapor addition and convective cooling, with heat discharged to the surroundings. Second, the dry solid was injected into flue gas at a temperature near 300°F (150°C) and then liquid water was introduced as a spray to cool the flue gas to 160°F (71°C). Third, the solid was briefly slurried with water and then introduced as a spray at 300°F (150°C), which subsequently lowered the gas temperature to 160°F (71°C). (To facilitate spraying the slurry, a small impingement target near the exit of the ST47 nozzle, known as the resonator, was removed; the resonator was usually retained for spraying plain water.) The features common to all three processes were these: 1) the flue gas was generated by the combustion of natural gas; 2) the SO_2 was added from an external source to a concentration of 1100 ppm; 3) reaction of SO_2 with the solids occurred at the same temperature, the same humidity level, and the same approach to adiabatic saturation. The temperature was 160°F (71°C), which represented a 30°F (17°C) approach to saturation; the water vapor concentration was 0.17 mole of water per mole of dry flue gas. One of the primary differences in conditions was in the O_2 level; to make it possible to humidify the combustion gas from natural gas to the final level desired, the gas was burned with excess air when liquid water or slurry was to be injected. Another difference was in the Ca/S ratio in the humidification chamber; the ratio was 2:1 in the first and second methods but only 1:1 in the third, with slurry injection.

Determinations of sorbent utilization following humidification revealed increments in utilizations over the 18% absolute level that had occurred previously in the furnace as follows:

Humidification method	Increment in utilization
Cooling to enhance the effect of water vapor already present	1%
Cooling and humidification with a water spray	6%
Slurrying with liquid water and spray injection	33%

Very little reaction of SO_2 with the calcine occurred when only water vapor was present. A six-fold increase in reaction, giving an increment in utilization of 6%, occurred when the dry solid was subjected to the effects of a water spray. An increment in excess of 30% occurred with slurry injection. Comparison of the results obtained with the water spray and the slurry spray indicates that the extent of low-temperature reaction was controlled by the fraction of sorbent particles actually colliding with water droplets and becoming physically wet. The added increment due to the water spray (5%) divided by the increment due to the slurry spray (33%) is indicative of a collision efficiency of 15% (5/33 x 100 = 15).

The slurry was prepared on-line in order to minimize the time available for reaction of the water and calcine. Slaking tests with quicklime and sulfated calcine have shown that the latter material hydrates more slowly, presumably due to the presence of a $CaSO_4$ layer. An initial concern was that this effect might prevent the activation of a sorbent particle in the time available in a humidifier. Although the estimated sorbent/water contact time of 30-60 sec was much longer than that available in an evaporating droplet, the results show that the presence of the $CaSO_4$ layer did not prevent activation of the sorbent.

HUMIDIFICATION OF HYDRATED LIME

To determine the effects of humidification on a sorbent that had not been subjected to high-temperature calcination, $Ca(OH)_2$ was injected into the flue-gas duct immediately upstream from the humidifier and allowed to react with SO_2 under the same conditions as those in the experiments with the partially sulfated calcine. The Ca/S mole ratio in each case was 2:1. The degrees of utilization observed following low-temperature reaction were as follows:

Humidification method	Extent of utilization
Cooling to enhance the effect of water vapor already present	9.6%
Cooling and humidification with a water spray	12%
Slurrying with liquid water and spray injection	28%

The results with the hydrated lime differ from those with the partially sulfated calcine primarily in terms of the effects produced by cooling alone and by the combination of spray humidification and cooling. Cooling alone gave a utilization of nearly 10% with the hydrated lime but an increment of just 1% with the calcine. The presence of water spray, on the other hand, increased the utilization of hydrated lime only from 10 to 12% but increased that of the calcine from 1 to 6%. Slurrying gave about the same result with both sorbents; this was a utilization of about 30% total with the hydrated lime or about 30% incrementally with the calcine.

The similar effects of slurrying the calcine and the hydrated lime are particularly striking. They indicate that the shell of $CaSO_4$ product surrounding a core of unused sorbent in the calcine particles is not a strong deterrent to the promotional effects of liquid water. Evidently, the $CaSO_4$ shell sloughs off rapidly when liquid water is present and does not markedly retard the wetting and partial dissolution of the underlying sorbent.

HUMIDIFICATION OF ENTRAINED CALCINE

For a more direct study of the humidification of partially sulfated calcine, $Ca(OH)_2$ was injected into the SRI pilot combustor, was thus subjected to calcination and sulfation in the furnace, and was then humidified at low temperature and subjected to further reaction with SO_2. Again the furnace was gas-fired and doped with SO_2 from an external source; a high level of excess air was used to produce humidity and temperature values at the humidifier that were comparable to those previously investigated. The burner was operated at either of two swirl angles for the secondary air. At 30°, there was a wide range of temperatures at the sorbent injection level—as high as 2780°F (1525°C), although the average was only

2070°F (1130°C). At 70°, on the other hand, the temperatures were more uniform at the injection level—maximum, 1990°F (1090°C); average, 1870°F (1020°C).

Utilization levels of the calcine measured at the inlet to the humidification chamber, as the result of sulfation in the furnace, were about 26%. Increments in utilization—due to humidification by the spray injection of liquid water—averaged 3.9% with 30° swirl in the furnace or 1.5% with 70° swirl in the furnace. Both increments reported are, of course, substantially lower than that of 6% observed for reinjected calcine with the same humidification method.

Several factors may have contributed to the difference noted above for entrained and reinjected calcine. First, the reinjected calcine was less extensively utilized before humidification (18% rather than 26%). Second, the reinjected calcine was exposed to an SO_2 concentration of about 1100 ppm in the humidifier, whereas the entrained calcine reacted at a lesser concentration of about 700 ppm. Finally, the reinjected calcine was coarser in particle size—a factor that promoted more efficient particle/droplet collisions. It is reasonable to assume that, in general, humidification and cooling with a water spray will promote further reaction to a degree that is governed by the extent of prior reaction in the furnace.

EFFECTS OF WALL DEPOSITS

Data on the utilization of suspended sorbent, based on analyses of solids removed in the dilution probe, usually indicated that the extent of SO_2 reaction was far below that signified by changes in the SO_2 gas-phase concentration. Reaction of SO_2 with the solids deposited on the in-stack filter ahead of the SO_2 analyzer was not a significant contributor to this discrepancy. Hence, reaction of SO_2 with solids deposited on walls within the reaction system was assumed to be the primary cause of the discrepancy.

To test the validity of this assumption, material balances were attempted during several of the tests described above. Before each test, the humidifier chamber was thoroughly cleaned by brushing and washing. After the test, as much material as possible was removed from different areas of the walls, weighed, and analyzed to determine the amounts of calcium and sulfur in the deposits. During the test, entrained solids were collected in the dilution probe and in a mass train.

The results of material-balance determinations can be illustrated in terms of two experiments. In the first, partially sulfated calcine was injected into humid flue gas (no water was added); in the second, the dry calcine was injected and followed with a water spray. Here is a summary of the results:

For injection into humid flue gas --

- Recovery of calcium—from entrained solids, 32%; from chamber walls, 45%; total, 77%. Recovery of sulfur—from the gas phase, 82%; from entrained solids, 0.5%; from chamber walls, 11.5%; total, 94%. About 64% of the SO_2 removal from the gas phase was found in the wall deposits.

For injection followed by water spray --

- Recovery of calcium—from entrained solids, 39%; from chamber walls, 47%; total, 86%. Recovery of sulfur—from the gas phase, 68%; from entrained solids, 5%; from chamber walls, 23%; total, 96%. Approximately 72% of the SO_2 removed from the gas phase was found in the wall deposits.

The incompleteness of calcium and sulfur recoveries does not detract from the conclusions reached. Whatever the disposition of unrecovered material may have been, the wall deposits recovered and analyzed still accounted for the fractions of SO_2 loss reported: in the first instance, 11.5/(100 - 82) or 64%; in the second instance, 23/(100 - 68) or 72%. Thus, in this system, up to 72% of the SO_2 removal may be attributed to wall effects. This contribution would be greatly reduced in a full-scale duct due to the much lower surface-to-volume ratio. Therefore, the quenched solids samples extracted from the flue gas provide the only reliable source of data for extrapolating to full-scale operation from small-scale systems.

MATHEMATICAL MODELING

OVERVIEW OF MODELING APPROACH

The process of in-duct desulfurization involves a complex set of mechanisms by which the sorbent is wetted and SO_2 is absorbed. To assist in understanding the operative mechanisms, a mathematical model was developed. This "first-generation" model treats the process in two steps. First, the "activation" of the sorbent is modeled in terms of the collisions between sorbent particles and water droplets. Second, the capture of SO_2 by the activated sorbent is modeled in terms of gas-phase diffusion of SO_2 to the sorbent/droplet ensemble, chemically enhanced absorption into the liquid phase, and liquid-phase mass transfer of the reacting species.

Based on the modeling results obtained thus far, the model appears to apply to the humidification of sorbent from either low-temperature or furnace injection. This suggests that the relatively low degree of sulfation achieved in furnace injection is not a limiting factor in the absorption of the SO_2 by the wetted sorbent. That is to say, the sulfate shell does not prevent the dissolution of a sufficient amount of lime into the droplet. This is basically a result of the very small fraction of the lime that must be dissolved in order to saturate the surrounding droplet. This will be discussed in more detail later.

SORBENT WETTING AND ACTIVATION

In the first-generation model, activation of the sorbent occurs only by physical contact between sorbent particles and water droplets. The model ignores the adsorption and transient condensation of water vapor on the sorbent particles. These mechanisms may contribute to sorbent wetting under certain circumstances. However, comparative tests with water sprays and steam humidification have shown that sorbent/droplet collision is the primary mechanism of sorbent activation (4). In any case, the model could be easily modified to accommodate the other wetting mechanisms.

Inertial impaction theory is used to model the collisions between sorbent particles and water droplets. In this treatment, the fraction of sorbent particles colliding with water droplets is a function of the relative velocity between the particles and droplets and the target efficiency for a given particle size and droplet size. The target efficiency is given by the Ranz and Wong correlation for impaction of two spheres (5). Particle size, droplet size, and relative velocity determine the target efficiency.

Since both the droplet velocity and the droplet size change during the humidification and desulfurization processes, the model must also account for the effects of droplet deceleration and droplet evaporation. The droplet leaves the nozzle at a velocity much higher than the flue gas velocity and is rapidly decelerated by the relatively stagnant gas. This process is modeled in terms of the well-known drag relationships for spheres moving through a gas. The drag is determined by the droplet size, relative velocity, gas density, and gas viscosity. Since the gas density and viscosity depend on temperature, the model includes a heat balance to calculate the cooling of the gas due to droplet evaporation.

As expected, the drag calculations predict that the small droplets used in most previous research are rapidly decelerated. This means that they travel only a very short distance away from the nozzle before the relative velocity becomes negligible and impaction ceases. The distance of travel, and hence the degree of impaction, becomes much greater, as the droplet size is increased. For example, for droplet sizes of 20 μm and 200 μm, the "stopping" distances are about 1 in. (2.5 cm) and 6 ft (1.8 m), assuming an initial velocity of 66 ft/sec (20 m/sec).

The droplet evaporation rate is calculated from the mass transfer coefficient and the driving force. The latter is based on the difference between the vapor pressure at the liquid interface and the partial pressure of water vapor in the bulk flue gas. The mass transfer coefficient is based on the Froessling correlation for mass transfer from a sphere (6). This correlation relates the mass transfer coefficient to the droplet size, relative velocity, gas density, gas viscosity, and the diffusivity of water vapor. The droplet evaporation rate predicted using this correlation is used to calculate the change in droplet size and simultaneously update the water vapor concentration in the flue gas.

Droplet evaporation and deceleration begin simultaneously as soon as the droplet leaves the nozzle and enters the flue gas stream. Thus, the droplet is shrinking while it is decelerating. For practical droplet sizes, however, the stopping distance is so short that the shrinkage during deceleration is negligible. Under these conditions, a plot of the stopping distance versus the droplet size should show the same trend as terminal velocity versus droplet size. Thus, an internal check on the model calculations is provided by comparing the size-dependence of these parameters. In this manner, the calculations have been confirmed over a range of conditions.

In order to accurately simulate various commercial lime sorbents and water spray nozzles, the model must take into account the particle and droplet size distributions. Thus, the model must integrate the inertial impaction calculations over the entire range of sorbent particle size and droplet size, taking into account the two size distributions. This is accomplished by first integrating over the particle size distribution to obtain the overall fraction of particles wetted by each droplet size. This result is then integrated over the droplet size distribution to obtain the overall fraction of sorbent wetted by all droplets. This fraction of the sorbent is assumed to be activated for SO_2 capture.

SO_2 CAPTURE

Calculations of SO_2 capture are applied to only the wetted fraction of sorbent particles. It is assumed that the sorbent/droplet ensembles can be treated in a manner analogous to the slurry droplets produced in a spray dryer. Therefore, this process is treated by a modified version of an existing spray dryer model. The basics of this model will not be discussed here, since they have been described in detail elsewhere (7). The original model was based on a mean slurry droplet size. However, our modeling work has shown that treatment of only the mean size can result in significant error compared to use of the actual size distribution (8). Therefore, the spray dryer model was modified to accommodate the size distribution of sorbent/ droplet ensembles predicted by the inertial impaction treatment.

The original spray dryer model also included the approximation that the Sherwood number remained constant at a value of 2. This assumption is valid only when the relative velocity becomes vanishingly small, which is not the case during droplet deceleration. Therefore, this assumption was replaced by a rigorous calculation of the Sherwood number based on a Froessling correlation analogous to that used in the droplet evaporation calculations. This modification can have a major impact on the results when the time required for droplet deceleration represents a significant portion of the total residence time. This is true only for the largest droplets in practical droplet size distributions.

Under typical spray dryer conditions, the chemical reaction between the dissolved lime and SO_2 provides a significant enhancement over purely physical absorption. Damle (7) has shown that this enhancement increases the liquid-phase mass transfer by a factor of 200 for a 50-μm slurry droplet at 120°F (50°C). Therefore, the rate-limiting mechanism is usually either the gas-phase diffusion of SO_2 to the droplet or the rate of lime dissolution.

When gas-phase diffusion is controlling, the spray dryer model should be directly applicable to the case of reactivating sorbent from furnace injection. However, the applicability of the model may be questioned when lime dissolution is controlling, since the sulfate shell on the sorbent may retard the dissolution rate. This effect may be examined by calculating the fraction of the sorbent that must be dissolved in order to saturate a droplet of given size.

For the mean sorbent and droplet sizes of 3.5 and 20 μm, complete dissolution of the sorbent would result in a lime concentration of 0.316 moles/L in the droplet. At 130°F (55°C), the solubility of lime in water is 0.016 moles/L (9). Thus, only about 5% of the sorbent must be dissolved in order to saturate the droplet. Since furnace injection generally results in less than 30% sorbent utilization, it appears likely that 5% of the sorbent could be available for dissolution. Therefore, the partial sulfation of the furnace injected sorbent does not necessarily preclude the possibility that a sufficient amount of lime can be dissolved. The dissolution of lime from the spent sorbent is also suggested by the rapid increase in pH when a spent sorbent is slaked (10).

Partially sulfated sorbent also releases heat when it is wetted due to the exothermic hydration of the lime. The practical effect on droplet temperature is minimal, however, since the relatively large water droplet acts as an infinite heat sink for the much smaller lime particle. For the case of typical mean particle and droplet sizes, the mass ratio is over 300. Based on a heat of hydration (11) of 490 Btu/lb (270 cal/g), the maximum droplet temperature rise would be 1.6°F (0.9°C). The effect of this small temperature rise is negligible.

LIMITING ASSUMPTIONS

For the impaction calculations, it is assumed that the sorbent particles and the water droplets are evenly distributed across the duct at the plane where impaction begins. This case may be approached when the sorbent is injected well upstream to allow good dispersion and the water is sprayed through a large array of nozzles. If the sorbent is stratified or the nozzles do not provide uniform coverage, the model will over-predict the degree of wetting.

The drag calculations assume that the droplets are immediately subject to the drag of the surrounding gas. This assumption is valid for a single-fluid nozzle where the injected droplets are immediately enveloped in flue gas. With two-fluid nozzles, however, the carrier air would insulate the droplets from the drag. The high-velocity carrier air would also create a low-pressure zone that would entrain sorbent particles into the jet. Calculations have shown that the net effect of the insulation and entrainment is a reduction in sorbent/droplet contacting (12). Thus, the model will tend to over-predict the degree of wetting achieved with two-fluid nozzles. However, there is no such limitation for single-fluid nozzles.

In the region near the water spray nozzle, where there is maximum droplet deceleration and maximum sorbent/droplet collision, the flow is assumed to be one-dimensional and incompressible. That is, the sorbent particles and water droplets travel along the axis of the spray nozzle, and impaction occurs when a droplet overtakes a sorbent particle. In reality, the spray trajectory is at an angle to the gas flow, which the fine sorbent particles tend to follow closely. This angle is greatest near the nozzle, where the droplet velocities are highest. In this region, the sorbent particles are effectively stagnant, so the relative velocity is independent of trajectory. Thus, the impaction calculations are still valid even though the particle and droplet streaklines are not co-directional (since the sorbent particles are effectively stagnant).

MODELING RESULTS

The mathematical model has been used to examine the dependence of predicted SO_2 capture on the approach to saturation (or amount of water injected), Ca/S ratio, residence time, and droplet size. The predicted effects of these parameters are illustrated in Figures 3, 4, and 5. As discussed in the Overview of Modeling Approach and SO_2 Capture, these modeling results may be applied to either low-temperature duct injection or reactivation of furnace injected sorbent. In the latter case, there is the tacit assumption that the sulfate shell does not prevent the dissolution of a sufficient amount of lime. Other differences between these two cases (e.g., differences in sorbent size distribution) are taken into account in the model input data.

Figure 3 shows the effect of approach to saturation and Ca/S ratio. These predictions are based on an assumed flue gas velocity of 50 ft/sec (15 m/sec), residence time of 2 sec, inlet flue gas temperature of 300°F (150°C), and inlet flue gas moisture content of 8% by volume. These parameters are believed to be reasonably representative of many pre-NSPS boiler retrofits. An initial droplet velocity of 460 ft/sec (140 m/sec) was chosen based on data supplied by Sonic Development Corporation for their ST-47 nozzle. The initial droplet size distribution was based on measurements made with a video droplet analyzer under cold-flow conditions. The Sauter mean and mass mean diameters were 29 and 24 μm, respectively. The minimum and maximum sizes were 15 and 71 μm, respectively.

All of the modeling was done using a sorbent particle size distribution obtained from cascade impactor measurements made in the SRI pilot combustor while firing coal and injecting hydrated lime. The sorbent size distribution was obtained by subtracting the fly ash distribution from the ash/sorbent distribution. The resulting sorbent distribution had a mass median diameter (mmd) of about 4 μm. This is comparable to the mmd of fresh hydrated lime sized by sedimentation in a dispersant liquid. This suggests that the high-temperature injection process results in very good dispersion of the hydrated lime. This degree of dispersion may not be attainable at low temperatures due to agglomeration. The effect of varying degrees of sorbent dispersion could be examined by using different sorbent size distributions in the model. This has not yet been done.

The effect of residence time on the predicted SO_2 capture is illustrated in Figure 4. This figure also illustrates how the mean droplet size changes with residence time. The figure shows that SO_2 removal ceases when the droplets are totally evaporated; this prediction, however, is a limitation of the present model, since even the residual dry solid will react at a finite rate. These predictions were based on a Ca/S ratio of 2:1 and an approach temperature of 20°F (11°C). The values of all other parameters were the same as those given previously.

Figure 5 shows the predicted effect of initial droplet size on the SO_2 capture and the time required for complete evaporation. While larger droplets give better removal, they also require more time to evaporate. For most retrofits, the available residence time would be less than 3 sec. For the conditions studied, this would limit the maximum droplet size to 110 μm, assuming that the droplet remained suspended in the flue gas and did not impact the duct wall prior to evaporation. These predictions are based on an approach temperature of 20°F (11°C) and Ca/S ratios of 1:1, 2:1, and 3:1, with all other independent variables held constant at the values given above.

The model predicts that there is an optimum droplet size with respect to SO_2 capture. This optimum corresponds to the maximum degree of sorbent wetting, or maximum sorbent/droplet collision rate. An optimum size exists due to the tradeoff between increasing stopping distance and decreasing coverage of the duct cross section. Larger droplets are able to penetrate farther into the flue gas and impact more sorbent particles. However, for a fixed flowrate of water (or fixed approach to saturation), larger droplets give less coverage of the duct cross section. This results is an optimum droplet size, which is typically about 150 to 200 μm for the conditions studied. Unfortunately, such a large droplet size is impractical due to the required evaporation time and problems with wall wetting. However, if a system could be designed to tolerate wall wetting and incomplete evaporation, much higher SO_2 removals could be achieved, as indicated in Figure 5.

CONCLUSIONS

When lime and water are injected separately, the SO_2 removal efficiency is governed by the degree of sorbent wetting by collisions between sorbent particles and water droplets. The sorbent/droplet collision rate is maximized by making the droplet size and velocity as large as possible. In actual practice, however, the droplet size must be well below the optimum value in order to ensure complete evaporation and avoid wetting of the duct walls. If the humidification process could be modified to allow larger droplets, it would be possible to significantly improve on the sulfur capture achieved.

In addition to droplet size and velocity, the sulfur capture is strongly influenced by approach to saturation, Ca/S ratio, and residence time. To maximize SO_2 removal, the approach should be as close as possible. However, it may be difficult to consistently maintain dry duct walls at approaches of less than 20°F (11°C). Increasing the sorbent injection rate, or Ca/S ratio, is also beneficial, but probably reaches a point of diminishing returns due to increased operating cost and particulate loadings. The effect of the latter on ESP performance must also be considered.

Increasing the residence time is only beneficial up to the point of complete droplet evaporation. Conversely, the residence time must be at least sufficient to allow complete evaporation. For most retrofit situations, the residence time will be fixed. This means that the droplet size must be selected to make maximum use of the available time without allowing droplets to reach the ESP. The model can be used to predict the optimum droplet sizing for a given duct residence time.

Strictly speaking, this mathematical model applies only to single-fluid nozzles, since each injected droplet is assumed to be immediately surrounded by the flue gas. That is to say, the entrainment and insulation associated with a two-fluid jet are not modeled. The net effect of these mechanisms is to reduce the sorbent/droplet collision rate compared to the single-fluid case. Therefore, the model predicts an upper limit on SO_2 removal achieved with two-fluid nozzles.

FUTURE WORK

The modeling results strongly suggest that larger droplet sizes (>29 μm) should be used to improve SO_2 removal. This improvement must be weighed against the longer residence time required for droplet evaporation. The potential for wall wetting must also be given consideration. Even with these considerations, it appears to be practical to use droplets larger than those produced by the Sonic Development ST-47 nozzle (Sauter mean = 29 μm). Sauter mean sizes on the order of 40 to 60 μm should be evaluated in future tests.

REFERENCES

1. Yoon, H., Stouffer, M.R., Rosenhoover, W.A., and Statnick, R.M. Laboratory and Field Development of Coolside SO_2 Abatement Technology. In: Proceedings of the Second Annual Pittsburgh Coal Conference. University of Pittsburgh and U.S. Department of Energy, Pittsburgh, PA, 1985. p. 223.

2. Jorgensen, C., Chang, J.C.S., and Brna, T.G. Evaluation of Sorbents and Additives for Dry SO_2 Removal. Environ. Prog. 6(1):26, 1987.

3. Blythe, G., Smith, R., McElroy, M., Rhudy, R., Bland, V., and Martin, C. EPRI Pilot Testing of SO_2 Removal by Calcium Injection Upstream of a Particulate Control Device. In: Proceedings: 1986 Joint Symposium on Dry SO_2 and Simultaneous SO_2/NO_x Control Technologies. Vol. 2. EPA-600/9-86-029b (NTIS PB87-120457), U.S. Environmental Protection Agency, Research Triangle Park, NC, October 1986. p. 35-1.

4. Yoon, H., Stouffer, M.R., and Burke, F.P. Coolside Desulfurization Reactions and Mechanisms. Paper presented at the National Meeting of the American Chemical Society, New Orleans, LA. August 30-September 4, 1987.

5. Ranz, W.E., and Wong, J.B. Impaction of Dust and Smoke Particles. Ind. Eng. Chem. 44:1371, 1952.

6. Froessling, N. The Evaporation of Falling Drops. Gerlands Beits. Geophys. 52:170, 1938.

7. Damle, A.S. Modeling of SO_2 Removal in Spray-Dryer Flue-Gas Desulfurization System. EPA-600/7-85-038 (NTIS PB86-136165), U.S. Environmental Protection Agency, Research Triangle Park, NC, December 1985.

8. Stokes, E.A. Southern Research Institute, Birmingham, AL. Personal Communication to D.C. Drehmel, March 2, 1987.

9. Jozewicz, W., and Rochelle, G. Modeling of SO_2 Removal by Spray Dryers. Paper presented at the Pittsburgh Coal Technology Conference, Pittsburgh, PA. September 17-21, 1984.

10. Dahlin, R.S., Lishawa, C.L., and Kaplan, N. Analysis of LIMB Waste Management Options. In: Proceedings: 1986 Joint Symposium on Dry SO_2 and Simultaneous SO_2/NO_x Control Technologies. Vol. 2. EPA-600/9-86-029b (NTIS PB87-120457). U.S. Environmental Protection Agency, Research Triangle Park, NC, October 1986. p. 39-1.

11. Boynton, R.S. Chemistry and Technology of Lime and Limestone, 2nd ed. Wiley-Interscience, New York, 1980. p. 324.

12. Muzio, L.J. Fossil Energy Research Corporation, Laguna Hills, CA. Personal Communication to J.P. Gooch, December 11, 1986.

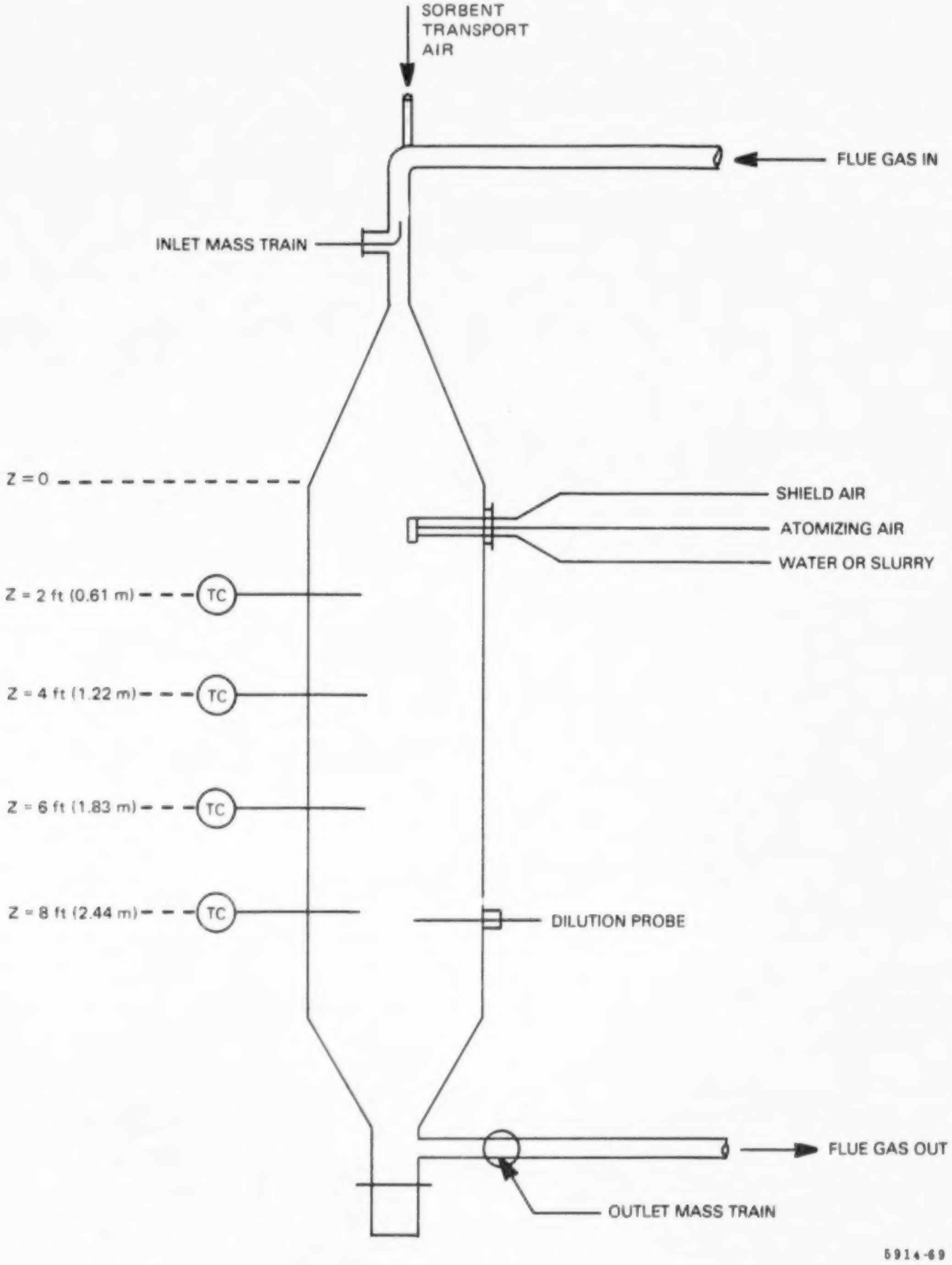
SORBENT TRANSPORT AIR
FLUE GAS IN
INLET MASS TRAIN
Z = 0
SHIELD AIR
ATOMIZING AIR
WATER OR SLURRY
Z = 2 ft (0.61 m)
TC
Z = 4 ft (1.22 m)
TC
Z = 6 ft (1.83 m)
TC
Z = 8 ft (2.44 m)
TC
DILUTION PROBE
FLUE GAS OUT
OUTLET MASS TRAIN
5914-69

Figure 1. Humidification chamber showing injection and sampling points.

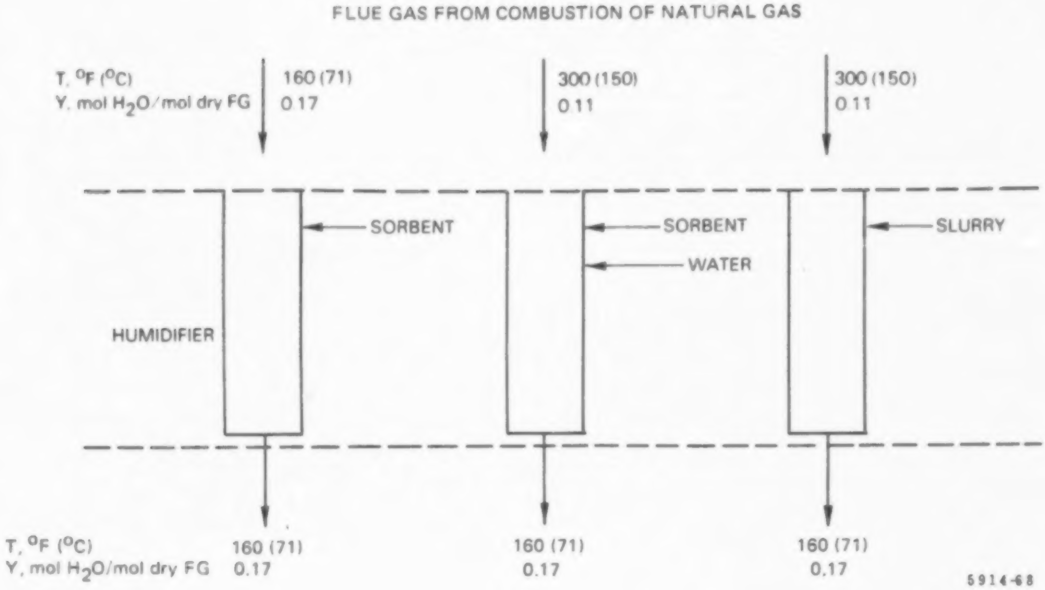
FLUE GAS FROM COMBUSTION OF NATURAL GAS
T, °F (°C)
Y, mol H2O/mol dry FG
160 (71)
0.17
300 (150)
0.11
300 (150)
0.11
SORBENT
SORBENT
WATER
SLURRY
HUMIDIFIER
T, °F (°C)
Y, mol H2O/mol dry FG
160 (71)
0.17
160 (71)
0.17
160 (71)
0.17
5914-68

Figure 2. Schematic representation of humidification modes.

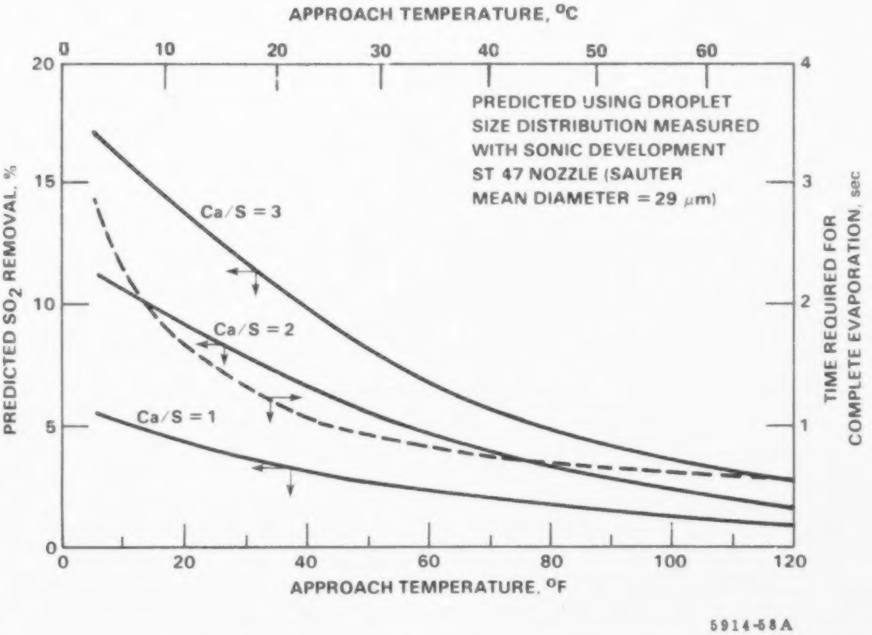

Figure 3. Effect of approach to saturation on SO_2 removal and evaporation time.

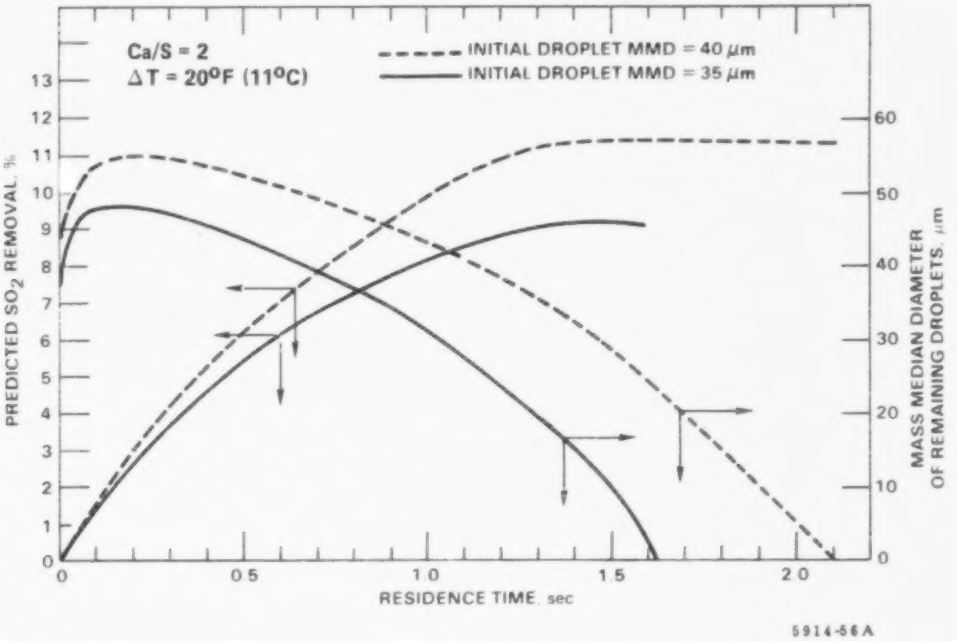

Figure 4. Predicted SO_2 removal and droplet MMD as a function of residence time.

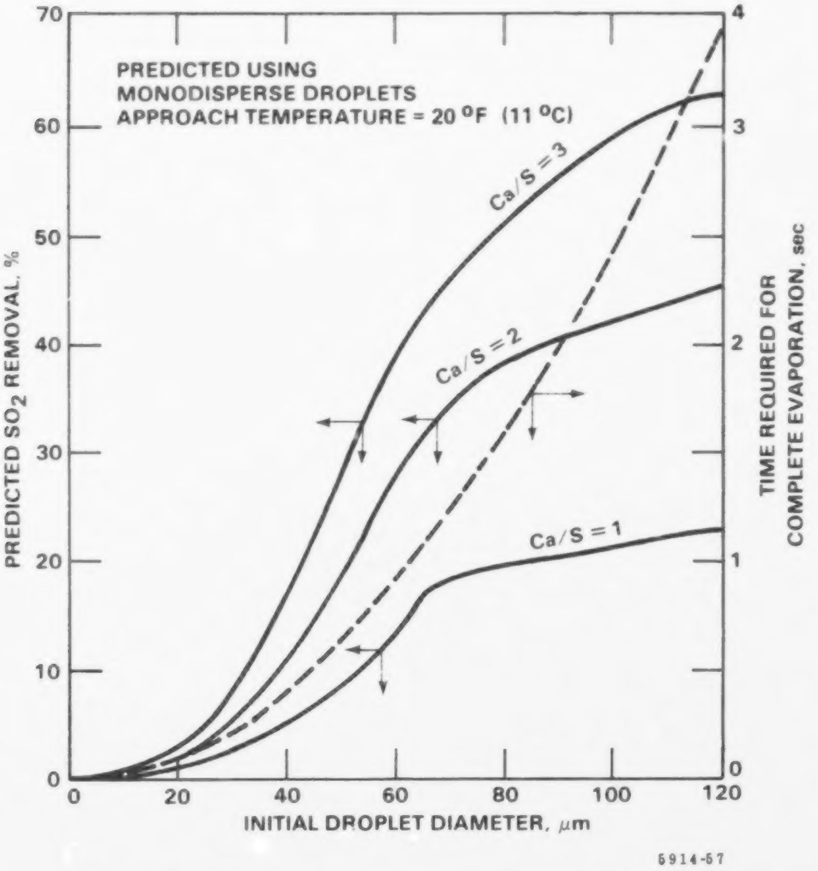

Figure 5. Effect of initial drop diameter on SO_2 removal and evaporation time.

RATE CONTROLLING PROCESSES IN HUMIDIFICATION FOR DUCT SO_2 CAPTURE

by: J. C. Kramlich, D. K. Moyeda, G. H. Newton, R. Payne
Energy and Environmental Research Corporation
18 Mason
Irvine, California 92718-2798

ABSTRACT

Two aspects of the reactivity of calcium hydroxide [$Ca(OH)_2$] toward sulfur dioxide (SO_2) were investigated under duct conditions. In the first, the capability of normal water sprays to physically wet the dry sorbent was investigated. A laser extinction technique was used to measure the collection rate of the sorbent particles into the droplets. The results show that sorbent collection efficiency is strongly dependent on spray characteristics (i.e., dropsize and droplet velocity), but only weakly dependent on the flow field or spray field. In the second phase of the work, the reactivity of slurry drops was investigated in a dilute phase reactor. The results indicate that calcium availability (i.e., dissolution into the liquid) and droplet lifetime are the principal constraints on sulfur capture.

Also, the internal porous structure of the sorbent is shown to contribute a significant quantity of calcium to the liquid phase, and the reactivity of a slurry drop, on a calcium-specific basis, decreases as slurry concentration is increased.

This paper has been reviewed in accordance with the U.S. Environmental Protection Agency's peer and administrative review policies and approved for presentation and publication.

INTRODUCTION

The use of calcium-based materials as in-furnace sorbents for sulfur dioxide (SO_2) has received considerable recent research attention as a low-cost approach to obtaining intermediate levels of SO_2 control. Two means of enhancing the attractiveness of the approach are to first find an inexpensive way of improving overall sorbent conversion to product, and second, develop an option for improving electrostatic precipitator (ESP) performance in collecting the furnace injected solids. One approach to both these problems is the adiabatic humidification of the duct gas immediately downstream of the air heater. Previous testing has shown that additional sulfur capture is possible within this region (1). Also, humidification reduces both the gas temperature (increases the ESP residence time) and the ash resistivity; both of these factors improve ESP performance.

Alternatively, a considerable amount of recent work has focused on sulfur capture by the injection of either dry $Ca(OH)_2$ (with separate humidification) or slurry sprays of $Ca(OH)_2$ downstream of the air heater. The reactivation of furnace injected sorbent shares much in common with injection of sorbent into the duct. For example, both occur within the same temperature regimes, both require humidification, and both involve the same reaction between $Ca(OH)_2$ and SO_2. This means that the literature on the injection of $Ca(OH)_2$ into the duct can provide useful information on the reactivation process. There are significant differences between the two processes that must be considered, however. For example, in the reactivation process the sorbent is a combination of calcium oxide (CaO), calcium carbonate ($CaCO_3$), and calcium sulfate ($CaSO_4$), while for once-through duct injection, the sorbent is fresh $Ca(OH)_2$.

In order to implement humidification, the principal design decision is to select the amount of humidification water and its method of introduction. The ideal situation is one in which the ESP performance is improved, duct sulfur capture is optimized, and problems such as wall deposits are avoided. In order to design for this condition, some indication of the processes that control the sulfur capture is needed. The objective of the work reported here is to define the rate limiting steps that control the capture of SO_2 in the duct humidification system.

The reaction kinetics of SO_2 with $Ca(OH)_2$ have been studied in sand bed reactors (2,3), in differential reactors (4,5), and in a packed bed baghouse element simulator (6). These results suggest that, even under highly humidified conditions, many minutes are required to obtain a significant conversion of sorbent to products. Thus, a sorbent particle with an equilibrium layer of adsorbed water is not sufficiently reactive to capture a significant amount of sulfur within dispersed phase duct residence times. However, pilot-scale experience shows that high captures are available within the few seconds available in the duct. Spray drying data suggest that these high reactivities are only possible if the sorbent particles are wetted by bulk moisture well beyond the equilibrium level. Three independent mechanisms by which this physical wetting can occur have been identified:

- Preslurrying and duct injection of the sorbent.
- Spraying of water into the duct, resulting in free-stream inertial impaction of the water droplet on the sorbent.
- Condensation, in which liquid collects on the surface of a cool (i.e., ambient temperature) particle injected into a warm, prehumidified gas stream.

Spraying water is the only likely candidate for the duct-reactivation of the furnace injected sorbent; condensation will not be favored because the sorbent is never colder than the surrounding gas. Thus, the only sorbent that is likely to be reactive in dispersed phase is that portion that directly collides with water droplets. Nozzle design should include a provision, if possible, for optimizing sorbent scavenging by water droplets via inertial impaction.

Once in the slurry phase, the reaction rate can be expected to be governed by one of the following processes:

- The rate at which SO_2 is transported from the free stream to the surface of the droplet.
- The rate at which water diffuses to the calcium ions through the liquid phase.

- The rate at which solid calcium becomes available in the liquid phase.

- The aqueous reaction rate, including ionization and direct product formation.

In addition, the $CaSO_3$ product will precipitate within the droplet. The location at which this precipitation occurs (e.g., homogeneously within the liquid phase or on the surface of the hydrate particles) will determine whether the product will act as a barrier to mass transport.

The objective of the work reported in this paper is to develop an understanding of the sorbent wetting process, which we have termed sorbent "scavenging," and to develop some understanding of the processes that limit SO_2 capture by drops of $Ca(OH)_2$ slurry. Thus, the work is generally divided into a "Scavenging" section and a "Sorbent Reaction" section.

PROCESS MODEL

A model of the relevant processes was assembled to aid in the experimental planning, data interpretation, and extrapolation to practical conditions. A full description of the model is available elsewhere (7), so only a list of the fundamental elements is presented here.

The model is a one-dimensional analysis that considers water droplets, sorbent particles, and SO_2 capture. A spray with a specified dropsize distribution is introduced into the gas with a specified slip velocity. Drag on the droplets is considered, and the droplets will relax to the gas velocity. While the droplets are slipping through the gas field, the droplets can collect sorbent due to inertial impaction. At each location and for each size class a separation number is determined from which the target efficiency can be calculated. Thus, between the time of droplet introduction and the time that the droplet ceases to slip through the gas, the amount of sorbent that is removed from the gas stream can be calculated, as well as the solids content of the resulting slurry droplets.

The droplets are also allowed to evaporate, humidify, and cool the duct gases. The driving force for evaporation is based both on temperature and on duct humidity. Concurrently, the rate of SO_2 removal from the gas-phase is governed by evaluating the combined resistances due to external SO_2 transport, transport of SO_2 in the liquid phase, and calcium dissolution and transport. A film theory is used to estimate the calcium availability, and the ionic product-forming reaction is assumed to be fast.

By appropriate simplification the model can consider slurry injection. Also, a second version of the model treats the case where room temperature sorbent is introduced into a prehumidified duct. Under these conditions, bulk water can condense onto the particle to the extent of several hundred monolayers; this is well beyond the few monolayers represented by equilibrium adsorption.

SCAVENGING

EXPERIMENTAL SYSTEMS

The overall approach for this study was to insert a nozzle into a subscale duct which contained a flowing sorbent suspension, and directly measure the amount of sorbent which was absorbed by the water droplets. The main technical challenges associated with the experiment were first, the selection of nozzles that yield the appropriate behavior, and second, the selection of a measurement technique. The facility shown in Figure 1 consists of a 20 cm diameter, 2.4 m long plastic tube. Air is fed into the top of the system from a rotary blower through a venturi flow meter. Sorbent is fed from a screw feeder, entrained in transport air, and introduced into the duct. The nozzles are supported on a long shaft that traverses the length of the tube. The shaft has provision for independent air and water passages for twin-fluid nozzles.

The measurement technique was developed during the course of this study. The approach is to pass an expanded, collimated laser beam through the sorbent/spray suspension. A focusing lens and a spatial filter are used on the opposite side to collect the light and focus it onto the detector. The use of a spatial filter ensures that all of the laser light that is absorbed, reflected, or diffracted by the spray/particles does not reach the detector. If the extinction signal for the spray alone, the sorbent alone, and the spray and sorbent together are compared, the amount of sorbent that is absorbed by the spray can be calculated by the Beer-Lambert law. Details of the approach are available (7).

RESULTS AND DISCUSSION

The initial results were obtained with small atomizers (a Delavan Type W-0.53-45 pressure atomized nozzle and a Delavan 30609-7 twin-fluid siphon nozzle). These initial results indicated essentially no scavenging was taking place. The model was exercised parametrically in order to identify whether scavenging would be expected under these circumstances. Figure 2 shows model predictions for scavenging efficiency as a function of dropsize and initial droplet velocity. The sorbent was assumed to be monosized at 2 μm. The figure illustrates that, at the present velocities (about 30 m/s) and dropsizes (15-25 μm), even with the one-dimensional idealization, only minimal scavenging could be expected. This suggests that a substantially larger dropsize and a higher droplet velocity are necessary to achieve measurable scavenging. High velocity drops travel farther than equal sized drops injected at slower velocities. High velocity drops therefore sweep out a larger volume of space and capture more particles than the slower drops. A high velocity also increases the collision efficiency between a drop and a particle. (Here, collision efficiency is defined as the fraction of sorbent in the cylinder swept out by the droplet's path that collides with the droplet.) For the cases studied here, however, collision efficiencies are very close to unity and the increased collision efficiency has a negligible influence. Increasing dropsize increases scavenging in the same manner as does higher velocity. Although a spray with larger drops has less projected area, a larger drop has more momentum and therefore travels farther than a smaller drop before decelerating to the gas velocity. A larger volume of space is again swept out by larger droplets. Further testing was therefore conducted on nozzles which maximized both droplet size and initial velocity.

Based on this evaluation, three nozzles were selected for further testing. These were:

- A Spray Systems J12 twin fluid nozzle
- A Y-jet nozzle (fabricated in-house)
- An Air Blast nozzle (fabricated in-house).

This last nozzle has the ability to produce a spray whose velocity is independent of the water flowrate. The air blast nozzle operates by producing a steady stream of large drops which are accelerated out the nozzle aperture by a stream of pressurized air.

Scavenging results for the Y-jet nozzle are shown as a function of water flowrate in Figure 3. This nozzle was designed with adjustable throat inserts so that spray dropsize could be adjusted. It was designed for heavy slurry atomization. It thus has larger internal clearances than the fine atomizers, and produces a correspondingly coarser dropsize.

Varying the water flowrate to a twin fluid nozzle affects scavenging in three ways. Increasing the water flowrate:

- Increases spray density (increases scavinging proportionally)
- Increases dropsize (increases scavenging)
- Decreases drop velocity (decreases scavenging).

These factors result in a scavenging curve which levels off at higher water flowrates.

Varying the air flowrate also results in opposing trends. Increasing the air to water ratio:

- Increases drop velocity (increases scavenging)
- Decreases dropsize (decreases scavenging).

These two influences can combine to give a curve such as that in Figure 4 for the J12 nozzle where a decrease in scavenging occurs at higher air flowrates.

Also shown in Figures 3 and 4 are performance predictions from the one-dimensional model. The dropsize distribution input for the model was obtained from direct laser diffraction measurements of the spray. The initial droplet velocity cannot normally be measured, and was estimated for this application. The procedure is as follows:

- Pressure Jet Nozzles: Use the measured pressure drop across the nozzle with Bernoulli's equation and an orifice coefficient of 0.8.
- Twin-Fluid Nozzles: Assume that the air flow is sonic at the contacting point between the air and water; assume perfect momentum exchange between the two streams at that point (i.e., both air and water finish at the same velocity).

No other adjustable parameters are used in the calculation. The close agreement between model and data suggests that the controlling processes are adequately represented. It also suggests that the correction to the one-dimensional model for two-dimensional effects is minor here.

A review of these results with the model suggests that the bulk of the scavenging takes place within a fairly limited cone immediately downstream of the nozzle. This cone, which we term the "high-efficiency zone," is the area where the greatest slip between droplets and gas takes place.

The data reported above indicate that only a fraction of the original sorbent is scavenged in real nozzle sprays. Since unscavenged sorbent appears to be quite unreactive in the short time provided by the duct flow, a means of improving sulfur capture is to enhance the percentage of the sorbent that is scavenged. A number of potential scavenging enhancement strategies were examined and tested.

One means of enhancing scavenging that was clearly demonstrated by the data is to tune atomizer performance to yield large, high velocity droplets. This, of course, can only be pursued to a limited extent because of increasing wall impingement, and evaporation time limits. Alternative strategies include:

- "One-dimensionalizing" the spray, so that the high-efficiency scavenging zone that exists immediately downstream of the nozzle is spread across the duct cross-section.

- Focusing the sorbent or flow-field into the high-efficiency zone.

However, expanding the spray across the duct will (i.e., by increasing the number of nozzles) also result in a dilution of the spray. Thus, this approach will only succeed if the sorbent is being depleted in the high-efficiency zone, and scavenging potential is being wasted. In this case, spreading the spray would improve overall scavenging. However, the low scavenging efficiencies measured here do not lead to sorbent depletion in the nominal high-efficiency zone. Therefore, doubling the size of the zone will halve the spray density, thus, to a first order approximation, the same amount of scavenging will be obtained.

Rather than "take the spray to the sorbent," the alternate approach is to "take the sorbent to the spray." In this case, the duct flow is focused onto the spray nozzle by a venturi or similar flow diversion device. This situation fails to improve scavenging because, although a higher fraction of the total flow passes through the high-efficiency zone, the residence time of the gas within this zone is proportionally reduced.

The only apparent means for improving scavenging, beyond the atomization parameters, is to concentrate the sorbent near the nozzle without changing the gas flow field. This would increase the sorbent density in the high-efficiency zone without changing the residence time within the zone. Unfortunately, this requires a means of physically separating the sorbent from a large fraction of gas within the duct.

SORBENT REACTION

EXPERIMENTAL

The previous section showed that the physical contact between the spray water and the dry sorbent can be a rate limiting process in sorbent activation. One means, therefore, for increasing capture is to enhance scavenging. However, once the sorbent is in slurry form, its reactivity can also constrain sorbent capture. Since the previous discussion detailed the factors that limit the collection of dry particles into slurry form, this section is directed toward the factors which limit SO_2 capture by slurry droplets. The objectives of this work were to first, evaluate the relative contributions of external and internal transport to the sorbent slurry droplet reaction with SO_2, and second, define the nature of the internal rate limiting mechanisms.

Since the objective of the work is to define controlling mechanisms, the ideal experimental system is one in which the capture of sulfur by a single slurry droplet is measured with time under well-controlled conditions. One approach to achieving this ideal is the dilute-phase flow reactor. A number of slurry droplets of known characteristics are introduced into a reaction gas. The droplet density is maintained at a sufficiently low level that the droplets behave as if they were in a single droplet environment (i.e., their evaporation changes neither the gas temperature nor humidity; their reaction does not deplete the SO_2 supply). After a suitable time the droplets are collected by extractive probing, and the sulfur capture measured by independent calcium and sulfur analysis of the collected materials. In its ideal form, such an experiment can be used to independently evaluate the influence of droplet parameters (size, slurry concentration, sorbent properties) and environment (temperature, humidity, SO_2 concentration) on the reaction rate.

A schematic of the test system used in these experiments is shown in Figure 5. Slurry droplets with known sorbent content are generated in the reactor by a rotary disk atomizer whose speed is continuously monitored by a tachometer. A skimmer cone is used to select and pass a small fraction of the spray into the reaction tube where it is entrained into a downward flow of reaction gas. The droplet size distribution produced by the rotary disk atomizer is characterized using a laser diffraction instrument (Malvern), and changes in the droplet velocity during evaporation and reaction are measured using a laser doppler anemometer. The exhaust stream from a natural gas flame is used to supply the reaction gas. SO_2 is doped into the natural gas line to provide the desired SO_2 concentration in the flue gas.

The droplets are collected in a heated cup (150°C). This is designed to flash vaporize the moisture and render the residue in the cup non-reactive. The residue is analyzed by wet chemical techniques for nitrogen and sulfur (6).

RESULTS AND DISCUSSION

Information on the influence of SO_2 concentration is valuable for determining the relative importance of internal and external resistances to reaction. Data taken in this study were therefore obtained primarily as a function of this variable. Calcium utilization as a function of SO_2 concentration is presented in Figure 6 for a dolomitic pressure hydrate (Genstar-S) and for a calcitic atmospheric hydrate (Genstar-N) at varying slurry concentrations.

The data show that, as SO_2 concentration is increased, utilization increases and then levels off at higher SO_2 concentrations. At each of the slurry concentrations shown, the leveling off occurs at different amounts of calcium utilization with the lower slurry concentration achieving the higher utilizations.

These trends indicate that at lower levels of SO_2 concentration the reaction is limited by SO_2 availability (i.e., external transport of SO_2 to the droplet surface). At higher SO_2 levels the reaction is no longer limited by SO_2 availability, so some internal step has become rate controlling.

The 2 percent dolomitic slurry had measured levels of utilization greater than 100 percent. Although the reason for this behavior is not known, possible explanations could include: 1) because of the low quantity of solids collected under this condition, there may be a high uncertainty in the experimental analysis, 2) since the sorbent was dolomitic, the magnesium may have participated and increased the apparent calcium utilization, and 3) at low slurry concentrations a bisulfite product, $Ca(HSO_3)_2$, may form, which would increase the apparent capture efficiency of the sorbent.

One key result is the finding that calcium utilization decreased at higher slurry concentrations. In a simplified view of the process, the following mechanism may be expected to occur:

- Above about 1000 ppm SO_2, internal processes control the reaction rate, and the utilization is insensitive to SO_2 concentration.

- Under this mode, a doubling of the slurry concentration doubles the amount of surface available for dissolution. This doubles the rate of calcium dissolution and the overall reaction rate.

- This doubled rate is spread over twice as much sorbent, with the net result that the utilization above 1000 ppm SO_2 should be independent of slurry concentration.

The result suggests that the additional sorbent is somehow deactivated, such that the incremental utilization of additional sorbent is quite poor.

A tentative conclusion that can be drawn from Figure 6 is that internal processes (i.e., calcium availability and/or reaction) control the overall reaction under realistic SO_2 concentrations. The exact mechanism of internal control is not so easily defined, however. Figure 7 reports results in which two factors that might be expected to influence the internal rate processes are addressed.

The first plot compares the reactivity of a calcitic atmospheric hydrate with that of calcitic pressure hydrate. The principal difference between the two is that the pressure hydrate consists of particles with a smaller mean size. Thus, this is a test of the importance of external surface area. The difference in external surface areas corresponds to a factor of 5.0 for these two materials. The fact that no improvement was noted suggests that the external surface of the particles does not significantly contribute to calcium availability.

In the second plot, the performance of two sorbents with markedly different specific surface areas is compared. The baseline sorbent is Genstar Type-N high calcium hydrate with a surface area of 16 m^2/g. The other two sorbents are alcohol prepared hydrates with surface areas in the 40-50 m^2/g range. The data suggest comparable utilizations at low SO_2 concentrations between the low and high surface area sorbents, but substantially better performance for the high surface area materials at higher SO_2 concentrations.

The superior performance of the alcohol hydrates shows that at least part of the internal pore structure participates in providing calcium for the reaction. At low SO_2 concentrations, data presented in previous figures suggested that external SO_2 mass transfer would control the reaction. In this regime, the high surface area materials would not be expected to show higher utilization. This is demonstrated in Figure 8 where model predictions for the limits of external mass transfer control and calcium dissolution control are shown with the low and high surface area data. (The calcium dissolution rate constant was set to match the low surface area utilization data.) At low SO_2 concentrations the data for both the low and high surface area materials fall near the limit of external mass transfer control. As SO_2 concentration increases, the low surface area materials enter a calcium starved regime where calcium utilization remains constant. The high surface area materials may, however, be able to provide sufficient calcium so that external SO_2 mass transfer is controlling at higher SO_2 concentrations. As the SO_2 concentration is further increased, the high surface area materials eventually cannot supply sufficient calcium and utilization will "level off" at a higher calcium utilization value. The influence of increasing surface area is, therefore, to move the external-internal control transition point to higher SO_2 partial pressures and higher sorbent utilizations.

In the practical case, it is possible that both mechanisms may actually limit calcium utilization in the reactor. This could result from the use of a spray with a wide size distribution. The larger drops in the distribution would most likely be limited by external SO_2 mass transfer while the smaller drops may be limited by internal calcium dissolution (since the rate of external mass transfer increases as the diameter decreases). It is, therefore, possible that control by both mechanisms may be observed. This possibility is supported by the apparent weak dependency (but not zero order) on SO_2 concentration at higher levels of SO_2. Utilization by large drops controlled by external mass transfer will increase linearly with SO_2 while utilization by the smaller, internally controlled drops remains constant. When utilization is integrated over the entire dropsize distribution a weak dependence (whose order will depend on the fraction of the distribution controlled by external SO_2 mass) may occur.

Since internal resistance to reaction was determined to be important, investigations into means to improve reactivity focused on internal mechanisms. The influence of various additives on calcium utilization is shown in Figure 9. The additives were selected to improve utilization by preventing agglomeration, adjusting slurry pH, or by modifying the product layer. None of these additives significantly increased utilization. The slurries were also subjected to an ultrasonic bath just prior to injection in an attempt to break up any agglomerates. Although the data in this figure show an improvement in utilization, it is not significant when compared with the normal range of experimental values. It should be emphasized that these data were obtained under conditions not entirely representative of an actual duct environment. The critical difference is that under duct humidification the sorbent is absorbed into the water droplet as a $CaO/CaSO_4$ mixture, rather than preslurried as $Ca(OH)_2$. Thus, the hydration process must occur within the droplet, and the opportunity exists for these additives to modify the hydrate. For example, an additive which produced a high surface area hydrate would likely improve utilization, as indicated by Figure 7. These additives may, therefore, improve utilization when used in a duct.

CONCLUSIONS

Efforts to improve the wetting of sorbent particles during duct humidification were examined. The literature suggests that high sorbent reactivities toward SO_2 cannot occur without this wetting. Inertial impaction of the humidification spray onto the sorbent particles is one means by which this bulk wetting can occur. The experimental results showed that particle scavenging does occur, but only in a relatively small cone-shaped region immediately downstream of the nozzle. Efforts to enhance scavenging showed the following:

- The expansion of the high-efficiency zone by increasing the number of nozzles failed to improve overall scavenging because the increase in zone size resulted in a proportional decrease in spray density.

- The focusing of the duct flow into the high-efficiency zone likewise failed to improve scavenging because, although more of the flow was exposed to the zone, the residence time of the flow within the zone was proportionally decreased.

Thus, the only apparent means of improving scavenging is to change nozzle characteristics, or to focus the sorbent onto the high-efficiency zone while leaving the bulk of the flow unchanged. Nozzle characteristics which favor scavenging include increasing both dropsize and initial droplet velocity; however, these parameters can only be adjusted to the point where wall wetting becomes a problem. To focus the sorbent onto the high-efficiency zone requires that the sorbent be separated from the duct gas. Since the sorbent size averages 2-4 μm, this is not an insignificant task. However, since higher concentration slurries appear to be less reactive, the benefits of enhanced scavenging would not result in a proportional increase in sulfur capture anyway.

The reactivity measurements showed that under the conditions covered by this study:

- Capture appears to be dominated by external SO_2 transport below about 500-1000 ppm, and controlled by internal processes above that value.
- Increased slurry concentration results in significantly reduced specific sorbent utilization.
- The internal availability of calcium, and hence the overall reaction, is enhanced by use of high surface area hydrates.
- The use of additives in the hydrate slurries to deagglomerate, or enhance calcium dissolution, failed to improve sulfate capture. The use of additives to enhance surface area development during dispersed phase hydration was not tested, but remains a promising possibility.

ACKNOWLEDGMENTS

The work reported here was supported by the U.S. Environmental Protection Agency under Contract No. 68-02-3995 to PEI Associates, Work Assignments No. 40, 41, and 44. Brian K. Gullett of the Engineering Applications Division, Air and Energy Engineering Research Laboratory, Research Triangle Park, NC, was the project officer. J. F. La Fond, D. M. Slaughter, T. C. Grogan, and J. McInerney of Energy and Environmental Research Corporation assisted in various experimental tasks.

REFERENCES

1. Staudinger, G., Schrofelbauer, H., and Meier, H. Laboratory tests on furnace limestone injection and development of a second desulfurization step with FLI ash through duct injection. In: Proceedings: 1986 Joint Symposium on Dry SO_2 and Simultaneous SO_2/NO_x Control Technologies. Volume 2. EPA-600/9-86-029b, U.S. Environmental Protection Agency, October 1986, NTIS PB87-120457.

2. Ruiz-Alsop, R. N. and Rochelle, G. T. Effect of Deliquescent Salt Additives on the Reaction of SO_2 with $Ca(OH)_2$. Preprints: 189th ACS National Meeting, American Chemical Society, 1985. p. 68.

3. Jozewicz, W. and Rochelle, G. T. Fly ash recycle in dry scrubbing. Paper presented at the AIChE Winter Annual Meeting, Chicago, Illinois. November 1985.

4. Borgwardt, R. H. and Bruce, K. R. EPA study of hydroxide reactivity in a differential reactor. In: Proceedings: 1986 Joint Symposium on Dry SO_2 and Simultaneous SO_2/NO_x Control Technologies. Volume 1. EPA-600/9-86-029a, U.S. Environmental Protection Agency, October 1986, NTIS PB87-120465.

5. Yoon, H., Withum, J. A., Rosenhoover, W. A., and Burke, F. P. Sorbent improvement and computer modeling studies for coolside desulfurization. In: Proceedings: 1986 Joint Symposium on Dry SO_2 and Simultaneous SO_2/NO_x Control Technologies. Volume 2. EPA-600/9-86-029b, U.S. Environmental Protection Agency, October 1986, NTIS PB87-120457.

6. Seeker, W. R., Chen, S. L., Kramlich, J. C., Greene, S. B., and Overmoe, B. J. Fundamental studies of low-temperature sulfur capture by dry calcitic sorbent injection. In: Proceedings: 1986 Joint Symposium on Dry SO_2 and

Simultaneous SO_2/NO_x Control Technologies. Volume 2. EPA-600/9-86-029b, U.S. Environmental Protection Agency, October 1986, NTIS PB87-120457.

7. Moyeda, D. K., Newton, G. H., LaFond, J. F., Payne, R., and Kramlich, J. C. Rate controlling processes and enhancement strategies in humidification for duct SO_2 capture. EPA-600/2-88-047, U.S. Environmental Protection Agency, August 1988, NTIS PB88-245915.

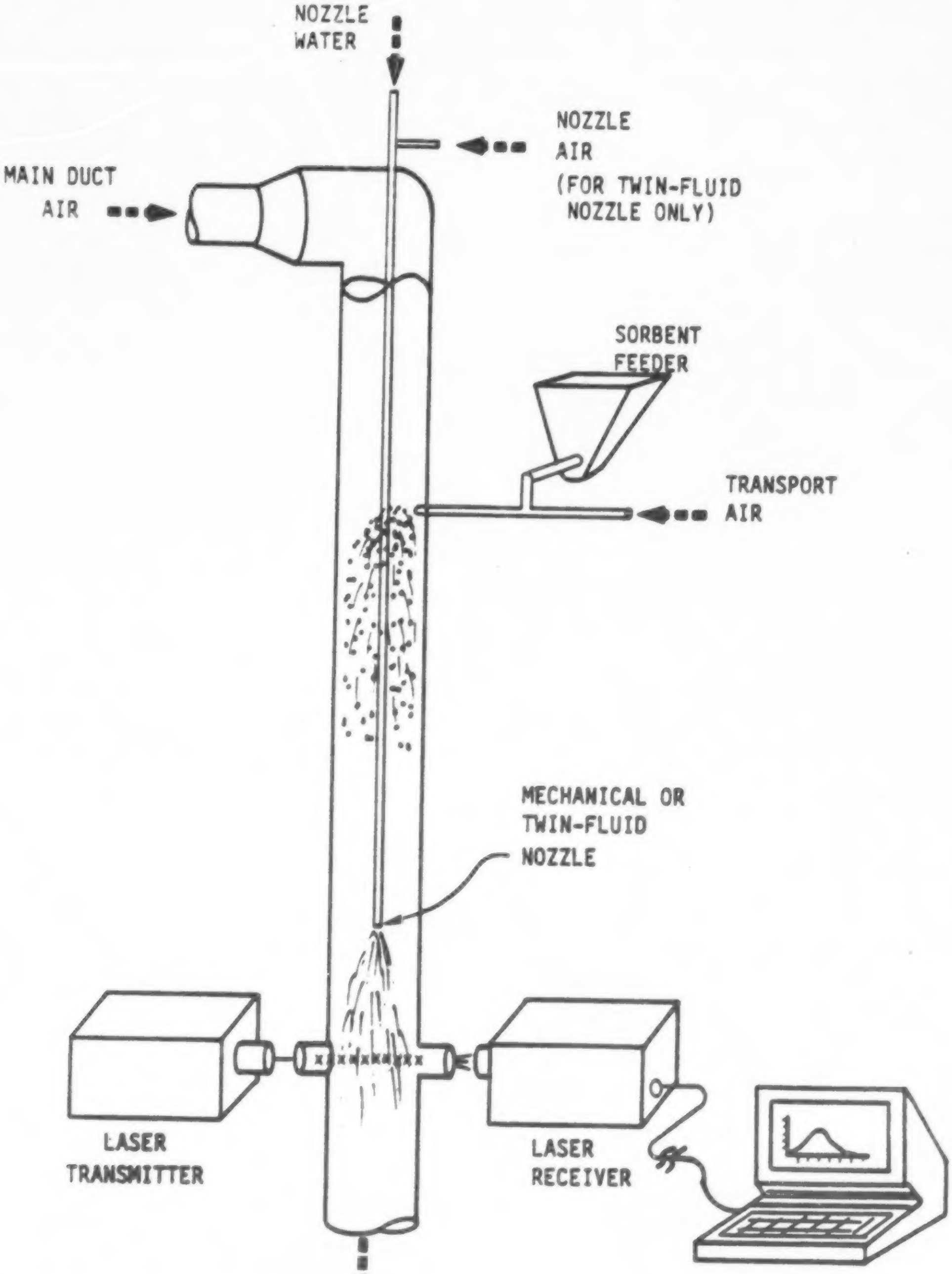
NOZZLE
WATER
NOZZLE
AIR
(FOR TWIN-FLUID
NOZZLE ONLY)
MAIN DUCT
AIR
SORBENT
FEEDER
TRANSPORT
AIR
MECHANICAL OR
TWIN-FLUID
NOZZLE
LASER
TRANSMITTER
LASER
RECEIVER
COMPUTER
EXHAUST

Figure 1. The scavenging rig.

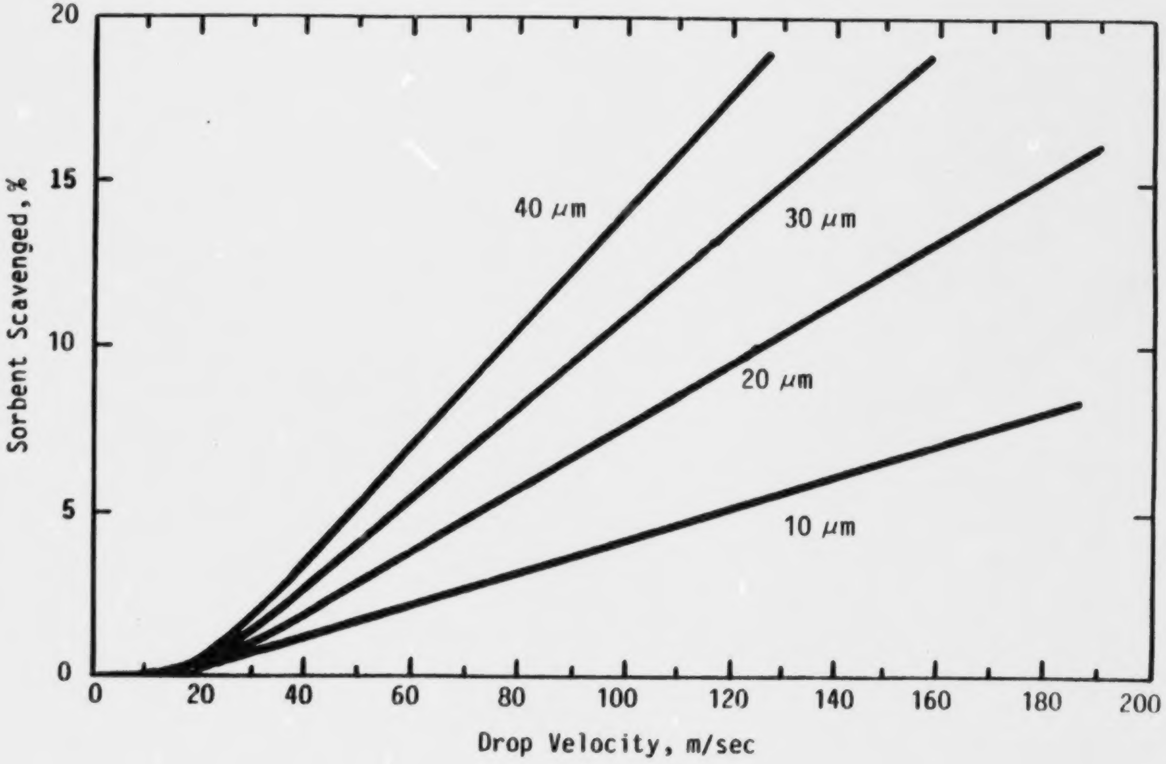

Figure 2. Predicted scavenging performance as a function of drop velocity and monosized droplet diameter.

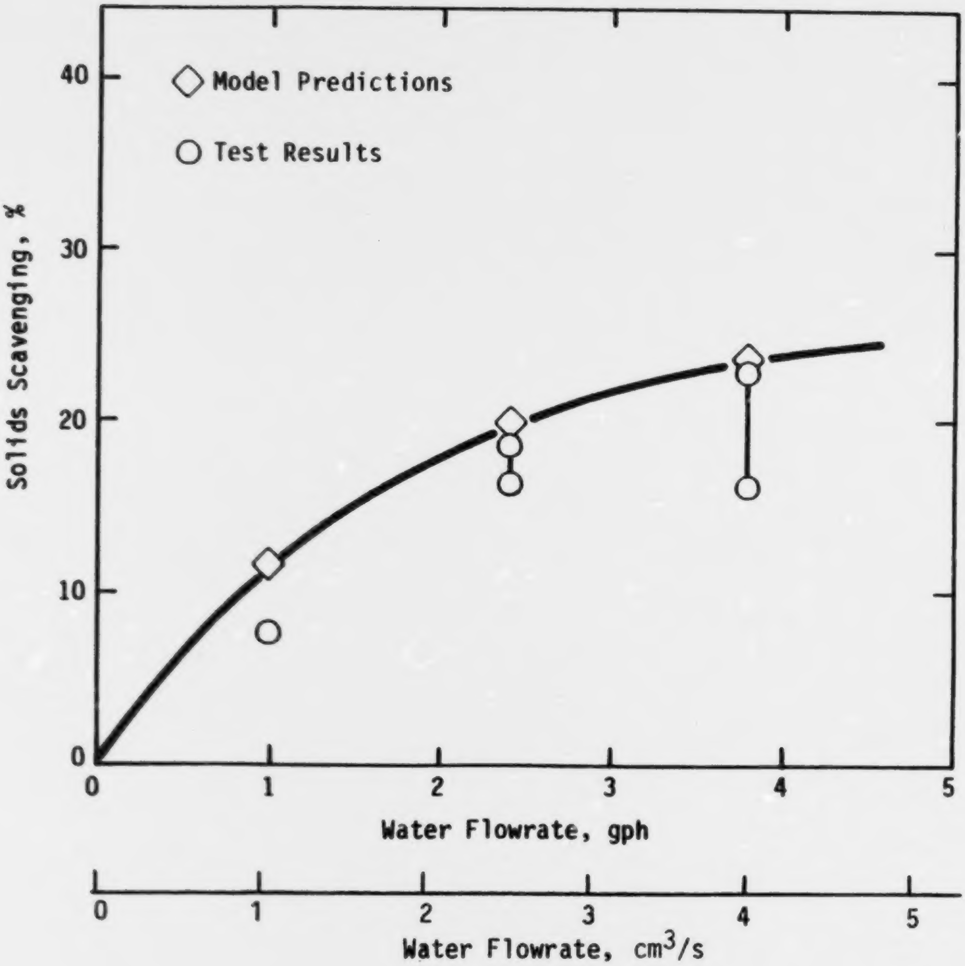

Figure 3. Scavenging results for the Y-jet nozzle compared to one-dimensional model predictions.

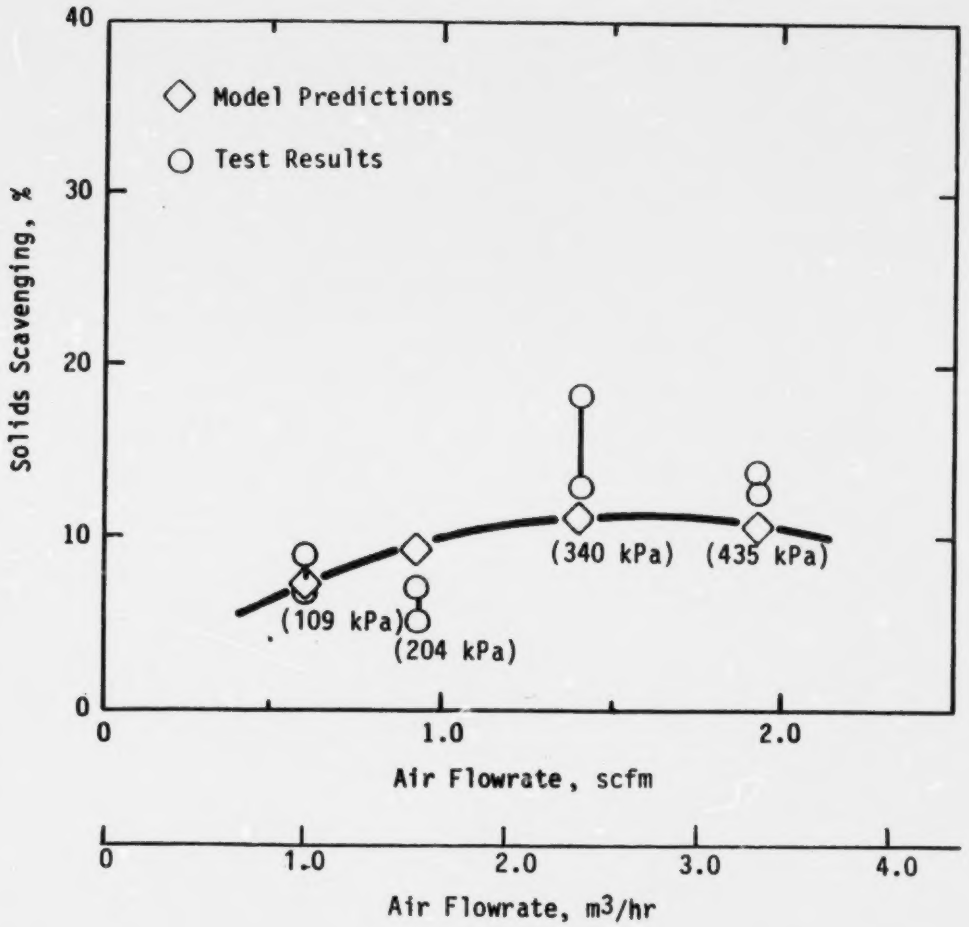

Figure 4. Impact of air flowrate on scavenging for Spraying Systems J12 nozzle at 4.0 cm^3/s water flowrate.

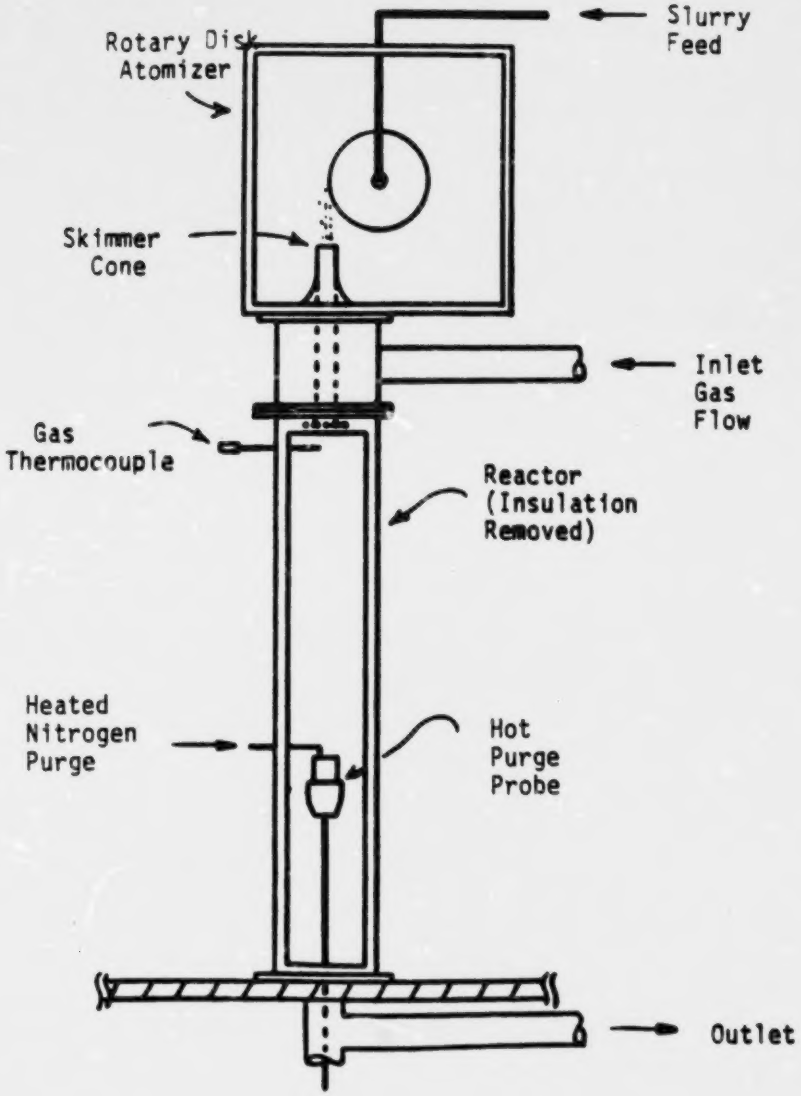
Slurry Feed
Rotary Disk Atomizer
Skimmer Cone
Inlet Gas Flow
Gas Thermocouple
Reactor (Insulation Removed)
Heated Nitrogen Purge
Hot Purge Probe
Outlet

Figure 5. Single-drop reactor.

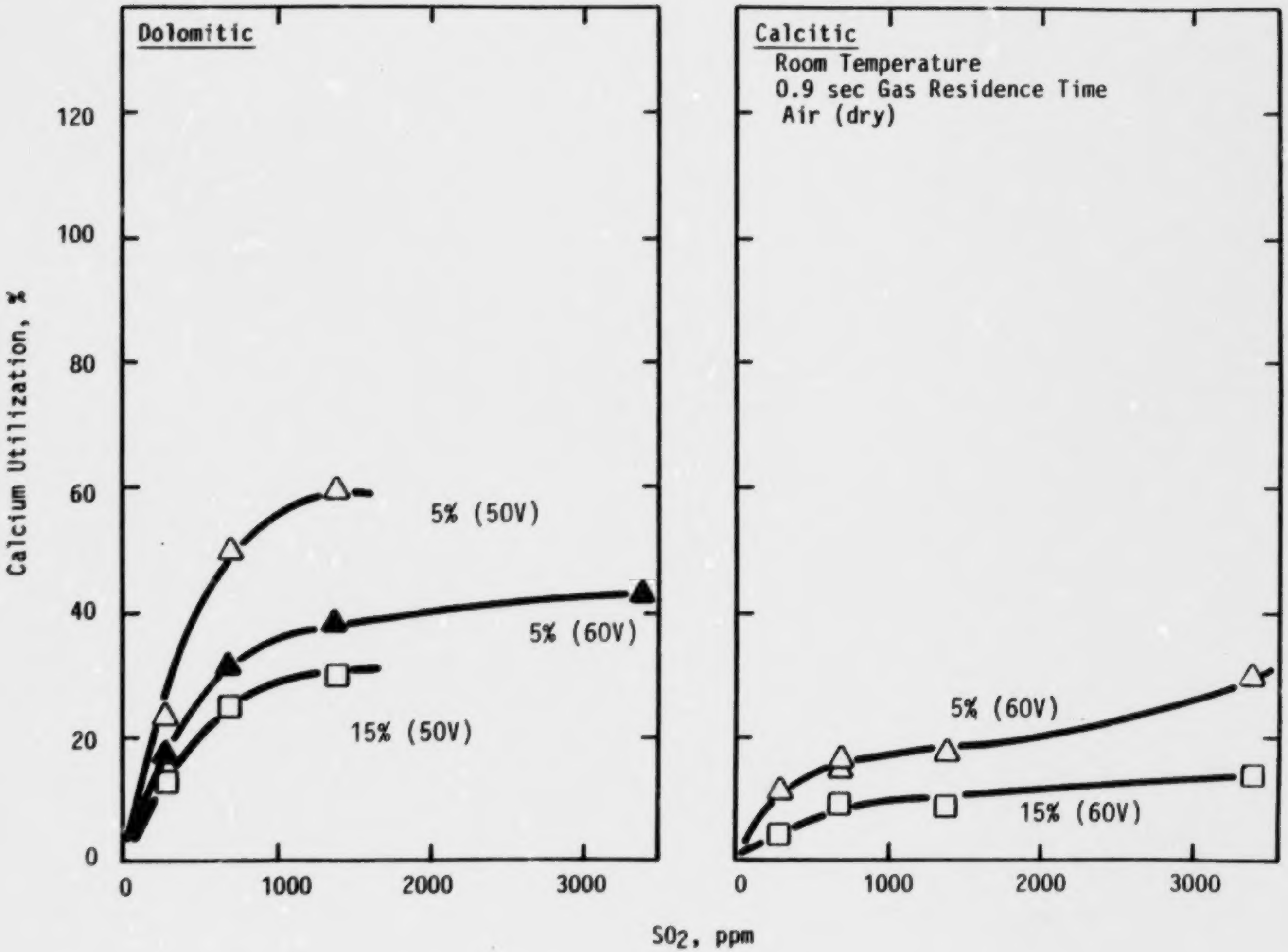

Figure 6. Calcium utilization as a function of SO_2 concentration at different slurry concentrations. First number represents the slurry concentration, and the second number represents the atomizer voltage (a higher value represents a finer spray).

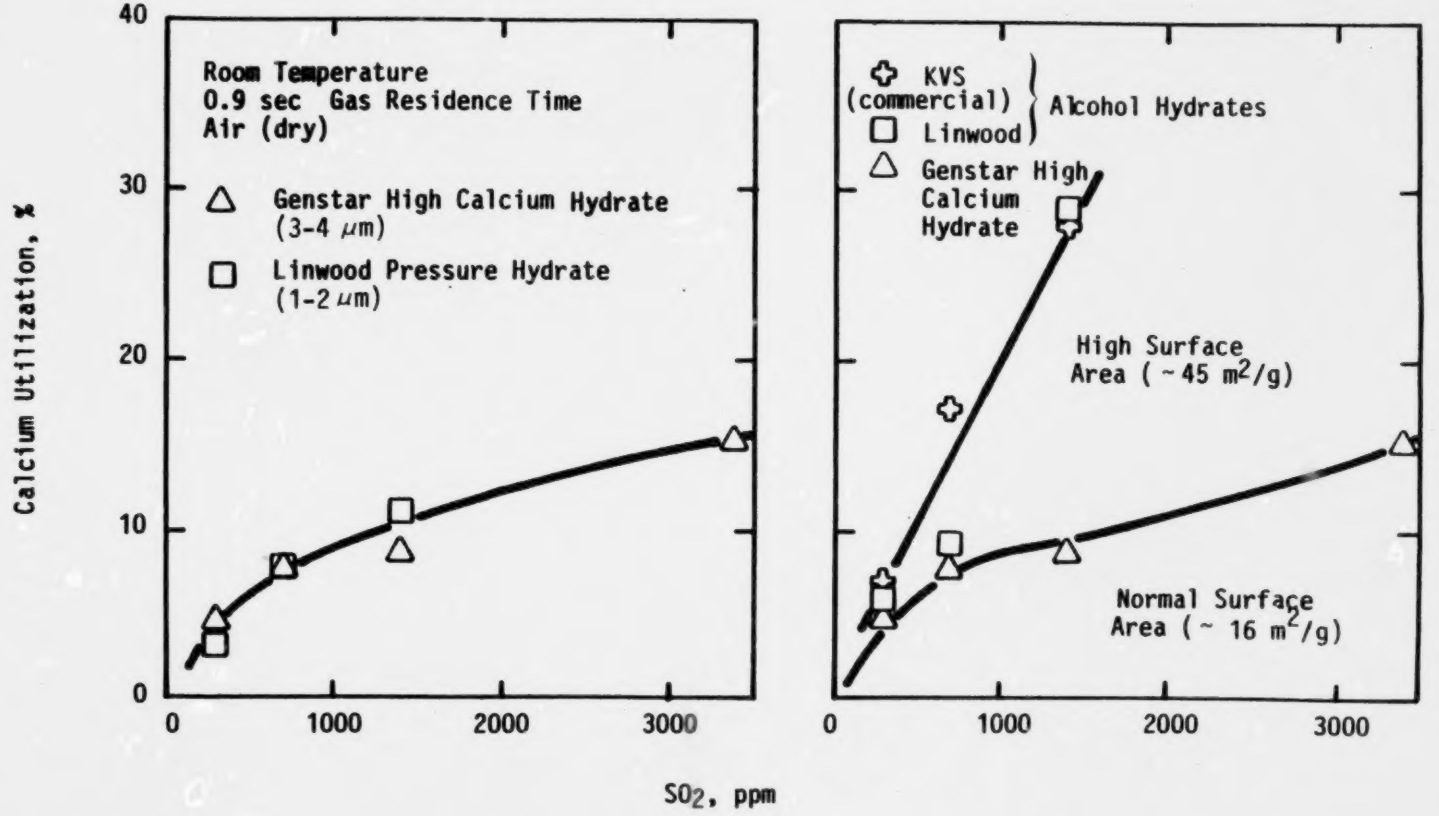

Figure 7. Influence of mass mean particle size and surface area on calcium utilization.

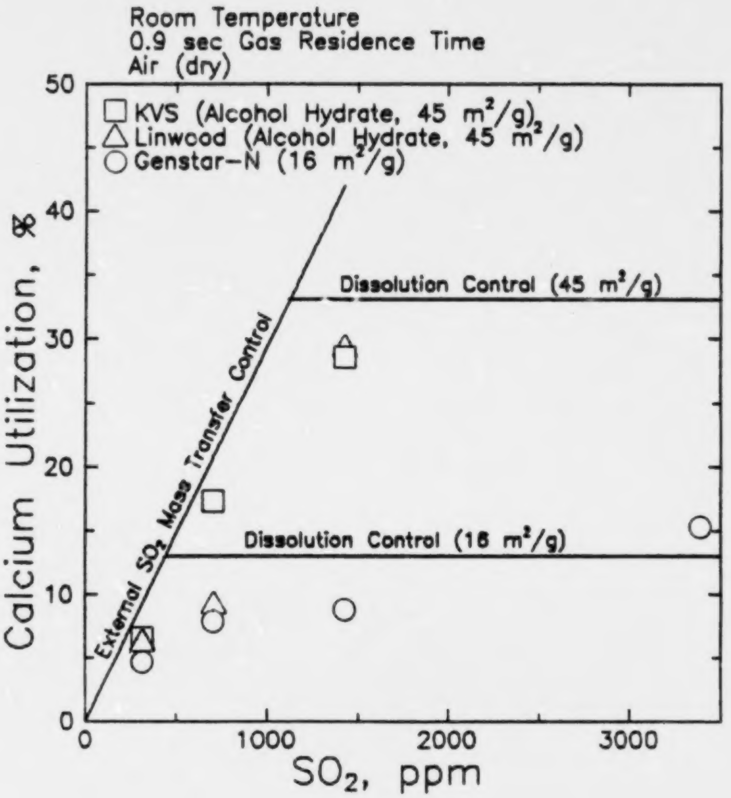

Figure 8. Limits of external mass transfer and internal dissolution compared to data.

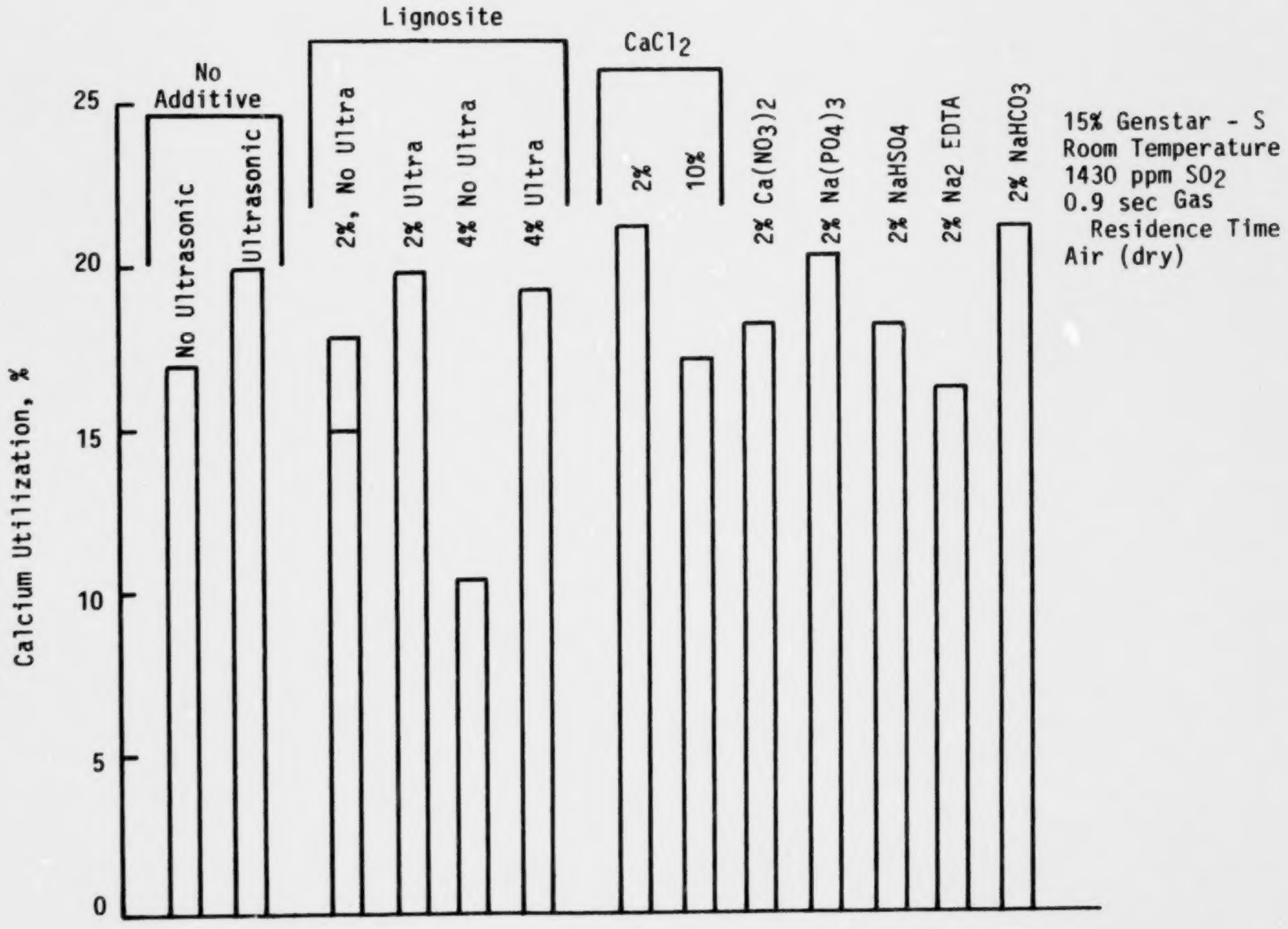

Figure 9. Influence of additives on utilization.

PILOT PLANT EVALUATION OF POST-COMBUSTION LIMB SO_2 CAPTURE

by: Claus Jorgensen* and John C.S. Chang
Acurex Corporation
Research Triangle Park, NC 27709

Charles B. Sedman and Dennis C. Drehmel
Air and Energy Engineering Research Laboratory
U.S. Environmental Protection Agency
Research Triangle Park, NC 27711

*currently employed at Environmental Elements Corporation,
Baltimore, MD

ABSTRACT

SO_2 capture by in-duct rewetting of furnace-injected calcium solids was evaluated on a 3400 m^3/hr pilot plant and compared to SO_2 removal by "reactivation" and reinjection of similar solids in an 85 m^3/hr pilot plant. First, simulated post-combustion flue gas solids from furnace lime injection, at a 2:1 calcium-to-sulfur molar ratio, were injected upstream of a spray dryer to determine SO_2 removal as a function of water spray droplet size and approach to saturation. In-duct SO_2 removal was found to increase by 30% as the approach to saturation decreased from 34 to 11 C°, for a fixed droplet size. At fixed $\blacktriangle T_{sat}$, SO_2 removal increased with droplet size. Solids deposits became severe when the theoretical droplet size was increased above 65 μm at 22 C° $\blacktriangle T_{sat}$ approach or 50μm at 11 C° approach. The combination of droplet size and approach to saturation shows best practical SO_2 removal anticipated at 10-20%.

Next, simulated solids were "reactivated" by slurrying at elevated temperatures for sufficient time to form a calcium silicate phase, dried, and injected at 10% surface moisture into a humidified gas stream (11 C° approach to saturation). At stoichiometric ratios of 1.5-3.5 calcium-to-sulfur, 25 to 55% SO_2 removal was observed, compared to 10% for dry recycle solids at the same stoichiometries.

Finally, the solids were "reactivated" as above then mixed with additional recycled LIMB solids, rather than dried. The silicate solids were injected at 20% surface moisture at similar conditions to the above and SO_2 removal was increased to 82% at a Ca/S of 2.5.

Conclusions to be reached are that: rewetting of furnace injected calcium solids increases SO_2 removal by a 10-20% increment under practical operating conditions; recycle of spent solids into a humidified gas stream increased SO_2 removal by up to another 10%; up to 40% incremental SO_2 removal is possible by reactivation to a silicate solids mixture, drying, and reinjection of solids; and greater than 80% incremental removal is possible through reactivation via the silicate reaction and reinjection as a damp powder. If 50% SO_2 removal is assumed in-furnace then the overall SO_2 removals are rewetting at 55-60%, rewetting and recycle at 60-65%, "reactivation" and dry injection at 70-75%, and "reactivation" and damp injection at 80-95%.

This paper has been reviewed in accordance with the U.S. Environmental Protection Agency's peer and administrative review policies and approved for presentation.

INTRODUCTION

Currently the Limestone Injection Multistage Burner (LIMB) process is being evaluated at three demonstration sites under EPA sponsorship. At the time the subject research was conducted, several aspects of the wall-fired LIMB demonstration at the Ohio Edison Edgewater site were being developed, including design of the humidification system downstream of the furnace. In particular, ways of improving SO_2 removal from retrofit levels (50-60%) to New Source Performance Standards (NSPS) (70-90%) were being contemplated, so that LIMB might be considered for new as well as existing sources.

Previous work by Jozewicz, et al. (1) on a bench-scale apparatus had shown that post-combustion, furnace injected calcium solids could be "reactivated" by slurrying at high temperatures (~90°C) for time periods longer than 1 hour. Subsequent efforts had shown similar reactivity improvement toward SO_2 with pressure hydration at only 1/2 to 1 hour reaction time. The mechanism involved is the creation of high-surface area calcium silicates/aluminates resulting from dissolution of lime and fly ash silica/alumina in water and reaction at the fly ash surface. It was proposed to conduct a series of pilot scale tests using this reactivation technique to produce a sorbent which would be reinjected either as a dry or a "damp" sorbent.

In addition, field work by Conoco (2) using furnace-injected lime had claimed considerable SO_2 capture by rewetting the sorbent passing through the humidifier. The mechanism here is dissolution of surface calcium into a liquid phase where SO_2 would be adsorbed and precipitate as a sulfite solid in the brief period between collision of the calcium solid with a water drop and evaporation to dryness. A series of tests were also planned in which furnace injected solids would be conveyed by simulated flue gas through a spray chamber and the extent of SO_2 capture measured as a function of humidity and droplet size.

Other potential enhancements considered included simple recycle of ESP collected solids either upstream or downstream of the humidifier, and spray drying of recycled solids.

Because of the very poor reactivity toward SO_2 of post-furnace solids, recycle was only briefly studied. Spray drying of recycled solids was discounted due to economics. The tests described here are comparatively evaluated reactivation and recycle, simple recycle, and rewetting under humidified gas conditions to determine the best path for post-combustion LIMB SO_2 capture.

POST-COMBUSTION REWETTING/HUMIDIFICATION EXPERIMENTS

A series of tests were conducted on the 3400 m^3/hr pilot plant at RTP (Figure 1) simulating the post-combustion flue gas conditions at Edgewater shown in Table 1. A solids mixture was injected at a point about 1/2 second upstream of a rotary atomizer/spray dryer vessel where simultaneous hydration of solids and humidification/adiabatic cooling of the flue gas took place. The most important parameters/variables were assumed to be droplet size (determines extent of rewetting collisions between drops and solid particles) and approach to saturation, which should affect the time for wetted particles to dry as well as the rate of subsequent SO_2 absorption on dried sorbent particles.

The rotary atomizer wheel speed was varied from 24,000 to 12,000 rpm, which translates, according to the Spray Drying Handbook (3), to a 40 to 75 μm mean droplet size. This was determined by:

$$D_{mean}\ (\mu m) = 1.6\ \frac{M_L^{0.2}\ X\ 10^4}{N^{0.8}\ X\ d^{0.6}\ X\ (nh)^{0.2}}$$

where M_L = water flow (kg/hr), typically 100 kg/hr
N = atomizer speed (rpm)
d = wheel diameter (m) = 0.15
n = number of vanes = 36
h = height of vanes (m) = 0.02

Figure 2 shows the results of tests performed, expressed as % SO_2 removal across the spray dryer vessel versus wheel rpm/droplet diameter. What is clear from the data is the dramatic drop in SO_2 removal with droplet size and with increasing approach to saturation temperature. Another interesting feature is the "critical line" superimposed over the data, at which solid deposits began to build up irreversibly. This occurred whenever a combination of larger droplets and lower approach to saturation resulted in a theoretical drying time for the mean droplet diameter of greater than 0.6 seconds (see Figure 3). Also the maximum practical SO_2 removal was thus fixed at just over 30% for a 10-second residence time humidifier, using only water to wet once-through LIMB solids. Based on the subsequent design of the Edgewater humidifier, the anticipated SO_2 removal is shown in the shaded area of Figure 2; i.e., 10-20% SO_2 removal.

A second exercise was performed to verify the droplet size calculated from the above equation, since there was no practical way to directly measure droplet size due to the difficulty in getting access to the spray dryer mixing zone. A 10% solution of sodium bicarbonate in water was sprayed into the flue gas, and the dried spray particles were sampled under isokinetic conditions using an MRI-1 Impactor. Using the rotary atomizer equation for a feed flow m = 63.5 kg/hr and atomizer speed N = 18,600 rpm gives the theoretical droplet size:

$$D_{mean} = 16,000\ \left[\frac{(63.5)^{0.2}}{(18,600)^{+0.8}\ (0.15)^{0.6}\ \ (0.72)^{0.2}}\right] = 47\ \mu m$$

If it is assumed that spherical droplets evaporate leaving a spherical solid particle and no "shell" formation occurs, then:

$$D_o = D_1 \sqrt[3]{\frac{V_o}{V_1}}$$

where V_o = Initial droplet volume
V_1 = Final particulate volume
D_o = Initial droplet diameter
D_1 = Final droplet diameter

The droplet and particulate volume may be expressed in terms of mass and density, so that when substituted:

$$D_o = D_1 \sqrt[3]{\frac{\rho_1}{(M_1/M_o)\,\rho_o}}$$

where ρ_o = solution density (g/ml) = 1.06
ρ_1 = particle density (g/ml) = 2.20
M_1 = final particle mass = 0.10 M_o
M_o = initial droplet mass

D_1 was found by sampling to have a mean value of 15 μm which, when substituted into the above equation, gives

$$D_o = 15 \sqrt[3]{\frac{2.2}{0.10 \times 1.06}} = 41\ \mu m$$

which is in very close agreement with the theoretical value of 47 μm.

From the first series of tests, and given the practical limits of duct humidification (e.g., nozzles, droplet drying restrictions in a more reasonable size humidifier of say 1-2 seconds for residence time), it is apparent that the maximum SO_2 removal to be expected is in the order of 20% above furnace removal, provided relatively large (40-50 μm) droplets can be generated and dried at a final approach to saturation of 17 C° without irreversible dust deposits being formed.

REACTIVATION AND REINJECTION OF LIMB SOLIDS

The potential reactivation of simulated LIMB solids from the 3400 m^3/hr facility was investigated in a separate test series using a smaller, 85 m^3/hr, pilot plant as shown in Figure 4. In this facility the flue gas is humidified to the desired approach to saturation prior to the introduction of solids. For each test the humidification was set so that the exit approach to saturation (at a point 2.0 seconds downstream of the solids injection point) was consistently 11 C°. Figure 5 illustrates test results from the 85 m^3/hr pilot plant as discussed in the following paragraphs. All data reflect in-duct and cyclone SO_2 removal, except where noted.

First LIMB solids from the 3400 m^3/hr facility (i.e., that had previously been re-wetted and dried) were injected at stoichiometric ratios varying from 1.3 to 4.0. The resulting SO_2 removal never exceeded 10%, including SO_2 removal in the baghouse, verifying previous bench-scale findings that totally dry SO_2 removal processes are limited to 15-20% lime utilization at duct conditions, for extended sorbent residence times.

A portion of the 3400 m^3/hr solids were then slurried at 80-100°C for 12-16 hours, filtered, and dried. Injection of this product as a dry powder resulted in 25% SO_2 removal at a stoichiometric ratio (SR) of 1.5 and 55% at 3.5 SR, indicating considerable "reaction" by the high temperature slurrying.

The third and most extensive set of data involved recycle of LIMB solids and reactivation of LIMB solids with "damp" solids injection. In these runs, the flue gas was only humidified down to 66-82 °C, with the moisture in solids accounting for the remaining 17-33 C° drop in flue gas temperature to reach 11 C° $\blacktriangle T_{wt}$ (usually 49-50 °C). Then a portion of the LIMB solids were slurried at ~90 °C for 12-16 hours, filtered, and mixed with solids recycled from earlier 85 m^3/hr runs at a ratio of 1:1.5-2.5 in a simple cement mixer, with a final sorbent moisture of about 20%. This embodiment takes advantage of the high moisture carrying capability of calcium silicates, where 20-30% of the sorbent mass is surface moisture, yet the aggregate is free-flowing and dry to the touch. As shown in Figure 5, the SO_2 removal dramatically increased from 40% at 1.15 SR to 84% at 2.5 SR. In this case the SR refers to external stoichiometry of lime or the lime present in the reactivated sorbent. The improved performance over the previous test series is likely due to a combination of increased moisture level on the sorbent surface and higher internal stoichiometries due to recycle.

A process model was developed for the last series of tests. Figure 6 depicts the proposed process on a 300 MWe boiler firing 2.2% sulfur coal with furnace sorbent injection at a 2.0 Ca/S ratio and recycle solids at 1.5 recycle ratio (RR). Using this model, plots of overall SO_2 removal versus RR were made as shown in Figure 7. Depending on the assumption of furnace SO_2 removal at Ca/S = 2.0, the ultimate performance of LIMB + reactivated silicate recycle varies from 82 to 96% at a RR (ratio of recycle stream solids mass to exit stream solids mass) of 1.5. At a RR of 1.5 the grain loading has increased to 2.5 times the loading for LIMB-only operation and 4 times the loading with coal-firing only. Therefore operation above 1.5 RR is not contemplated without a significant modification to the particulate collector.

Costs of this technology were also estimated on the same basis; i.e., a 300 MWe retrofit, 2.2% S coal, SR = 2.0, and RR = 1.5 where all duct and boiler hardware was assigned a multiplier of 1.6 for retrofit. Table 2 shows that the addition of a humidifier + reactivated LIMB recycle (damp silicate) increases the base capital cost by 60% ($70.9 to $103.3/kW), but the additional SO_2 removal improves cost-effectiveness for the 50 and 60% in-furnace reduction cases, and only slightly increases cost-effectiveness in the 70% in-furnace case. In all cases, the cost-effectiveness is considerably less than $1100/tonne on a 15 year levelized basis.

FUTURE R&D EFFORTS

A slipstream evaluation of the damp recycle sorbent concept (the ADVACATE Process) is scheduled for early Fall of 1988 at the Edgewater site. The equipment layout consists of a 3400 m^3/hr mobile ESP, a continuous weight loss feeder for reactivated sorbent injection, and an on-site sorbent preparation plant, essentially a pressure hydrate mixer, sorbent storage, and a "bucket brigade" to keep recycled sorbent and reactivated sorbent flowing in and out of the batch process. Sorbent will be stockpiled and injected continuously during test runs.

Initial runs at Edgewater will attempt to verify the data in Figures 5 and 7 using actual flue gas and furnace injected solids, and will establish the reasonable limits of recycle ratio and approach to saturation as a function of ESP size. (ESP size can be varied by de-energizing sections, varying the gas flow rate, or isolating the flow within the ESP.)

Solids will be collected and returned to RTP for further pilot plant evaluation. If successful, a second series of tests, using improved sorbent and optimized conditions for SO_2, and possibly NO_x, removal, will be conducted in 1989 at Edgewater.

SUMMARY AND CONCLUSIONS

1. Based on the limitations of in-duct humidification (i.e., 40-50μm droplets and 17-22 C° approach to saturation), our pilot plant evaluation using an optimized mixing chamber (rotary atomizer/spray dryer with 10 second residence time) shows that a maximum increment of 10-20% SO_2 is achievable over the in-furnace reduction level.

2. The rotary atomizer empirical equation of Masters, et al., has been verified on the 0.15 m diameter rotary atomizer in the operating range more frequently used (18,600 rpm) using a solution of sodium bicarbonate. Therefore we feel confident in the data comparing SO_2 removal as a function of droplet size and approach to saturation.

3. Recycle into a humidified stream showed less than 10% additional SO_2 removal at very high stoichiometries.

4. Reactivation by a high temperature, extended time reaction in an aqueous slurry yielded substantial SO_2 removal of 25-55% when the sorbent was injected as a dry powder.

5. Reactivation and injection as a damp but free-flowing powder at 20% surface moisture effected the highest SO_2 removal, ranging from 40% at SR = 1.2 to 84% at SR = 2.5.

6. Process modelling and cost analyses show that LIMB with the ADVACATE damp sorbent injection will boost overall SO_2 removal in the 80 to 90% range at costs well under $1000/tonne for a 300 MWe, 2.2% sulfur retrofit case.

7. Field evaluations are planned at the Edgewater Demonstration on a slipstream with two mobile ESPs to verify the pilot plant findings and optimize the LIMB + ADVACATE process for scale-up.

REFERENCES

1. W. Jozewicz, J.C.S. Chang, T.G. Brna, and C.B. Sedman, "Reactivation of Solids from Furnace Injection of Limestone For SO_2 Control," Environ. Sci. Technol. 21:664 (1987).

2. H. Yoon, M.R. Stouffer, W.A. Rocsenhoover, and R.M. Statnick, "Laboratory and Field Development of Coolside SO_2 Abatement Technology," Proceedings of the Second Pittsburgh Coal Conference, U.S. DOE, Pittsburgh, PA, 1985.

3. K. Masters, Spray Drying Handbook, 3rd Edition, John Wiley & Sons, New York, N.Y. 1979 p. 181.

TABLE 1. TEST CONDITIONS FOR REWETTING OF LIMB SOLIDS

DURATION OF TEST, hr	2.0 - 5.5
SOLIDS FEED, lb/hr. NR	43 - 50
ATOMIZER SPEED, rpm	12,400 - 23,600
WATER INJECTION, lb/hr	175 - 262
SO_2 FEED, lb/hr	8.3 - 14.4
SPRAY DRYER TEMPERATURES, °C:	
INLET, DRY BULB	173 - 178
INLET, WET BULB	49 - 60
OUTLET, DRY BULB	66 - 89
FLUE GAS FLOW, acfm	1740 - 1980
SO_2 CONC.:INLET, ppmv dry	670 - 1020
OUTLET, ppmv dry	260 - 730

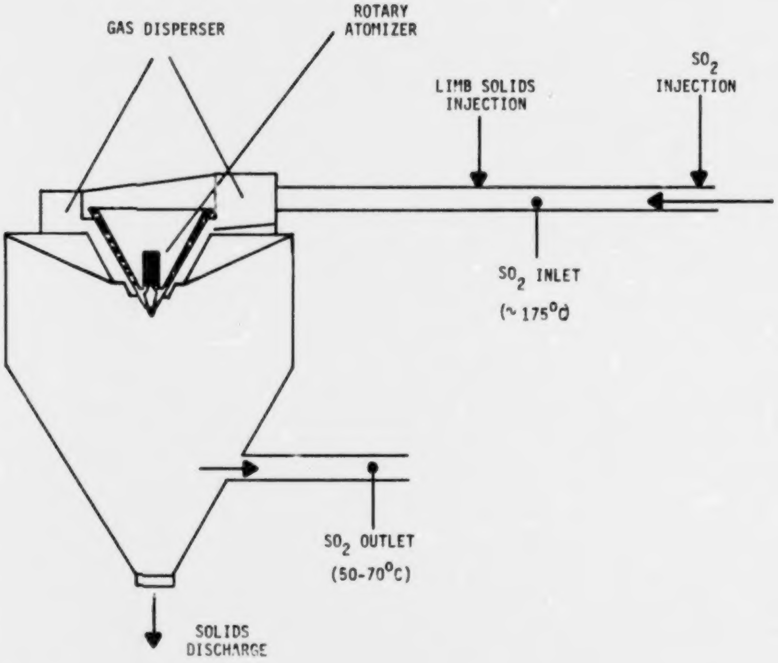
GAS DISPERSER
ROTARY ATOMIZER
LIMB SOLIDS INJECTION
SO2 INJECTION
SO2 INLET (~175°C)
SO2 OUTLET (50-70°C)
SOLIDS DISCHARGE

Figure 1. Rewetting of LIMB solids on 3400 m^3/hr pilot plant.

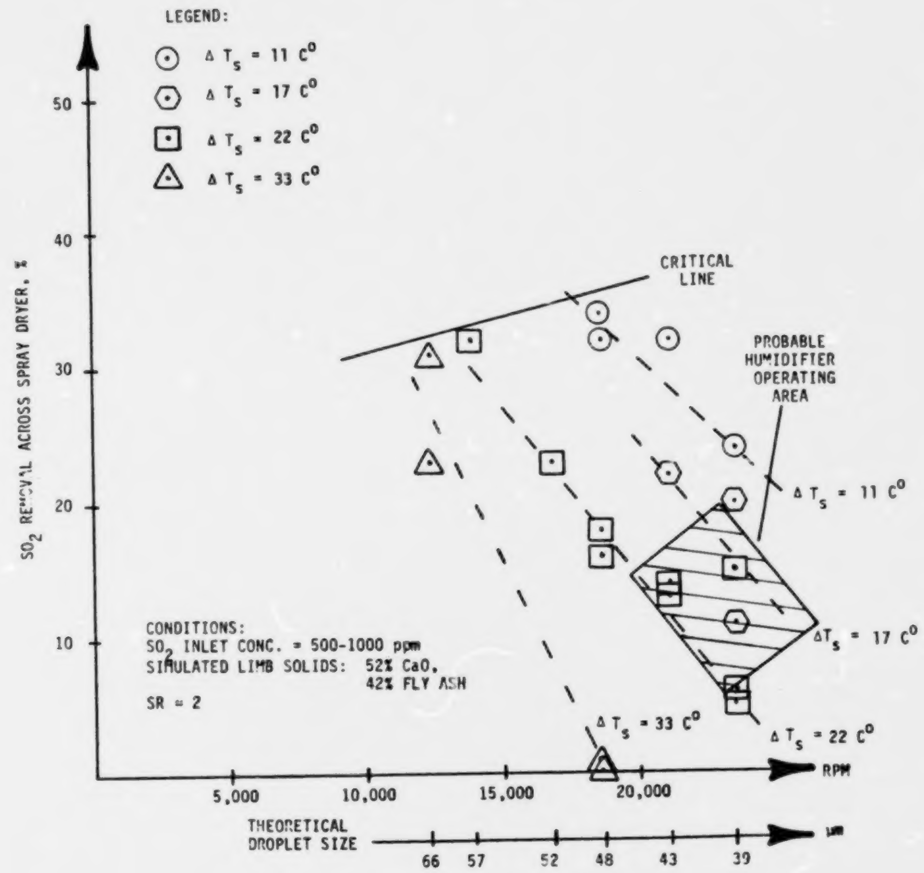

Figure 2. Humidification studies - 3400 m^3/hr facility SO_2 removal vs. atomizer speed.

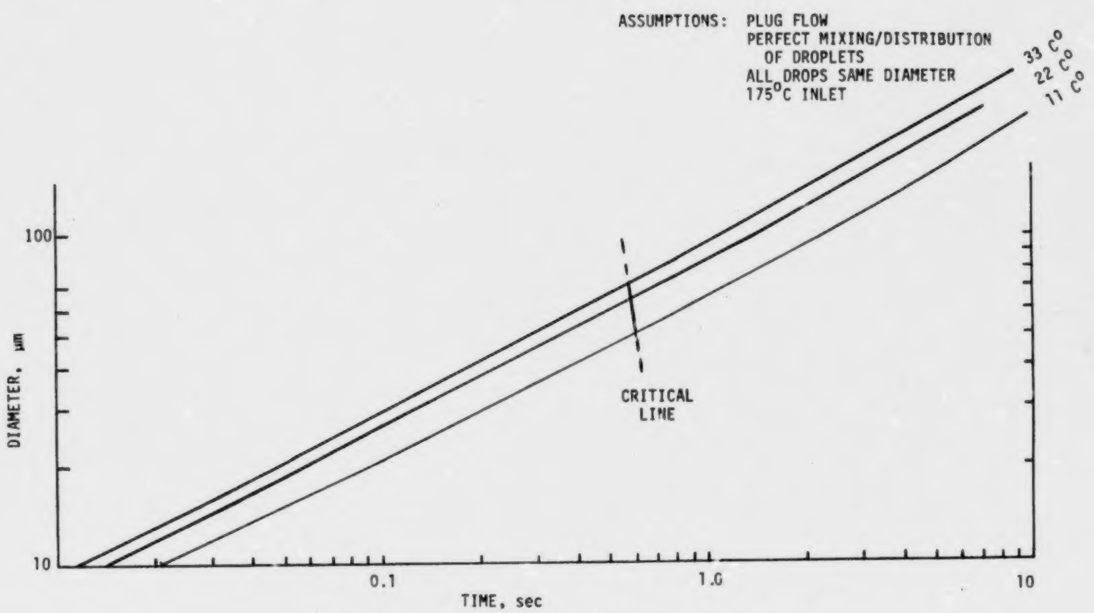

Figure 3. SRI model drying time vs. drop diameter as a function of ΔT_s.

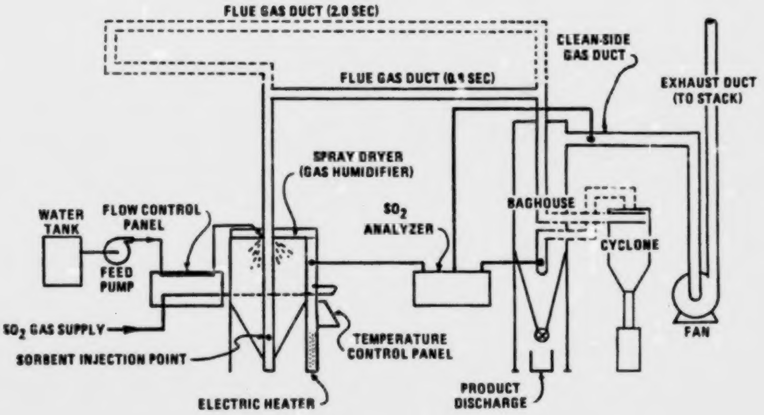
FLUE GAS DUCT (2.0 SEC)
FLUE GAS DUCT (0.9 SEC)
CLEAN-SIDE GAS DUCT
EXHAUST DUCT (TO STACK)
SPRAY DRYER (GAS HUMIDIFIER)
WATER TANK
FLOW CONTROL PANEL
FEED PUMP
SO_2 ANALYZER
BAGHOUSE
CYCLONE
SO_2 GAS SUPPLY
SORBENT INJECTION POINT
TEMPERATURE CONTROL PANEL
ELECTRIC HEATER
PRODUCT DISCHARGE
FAN

Figure 4. Schematic of 85 m^3/hr duct injection/pilot plant facility.

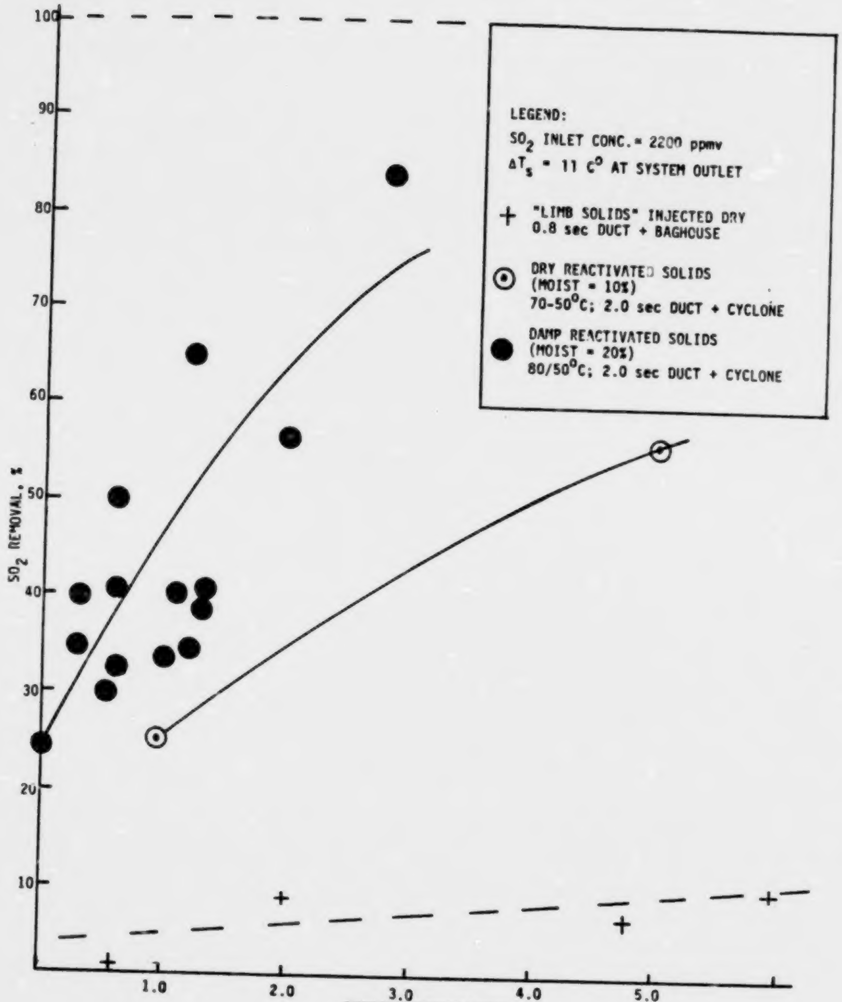

Figure 5. Comparison of SO_2 removal for LIMB solids reactivation.

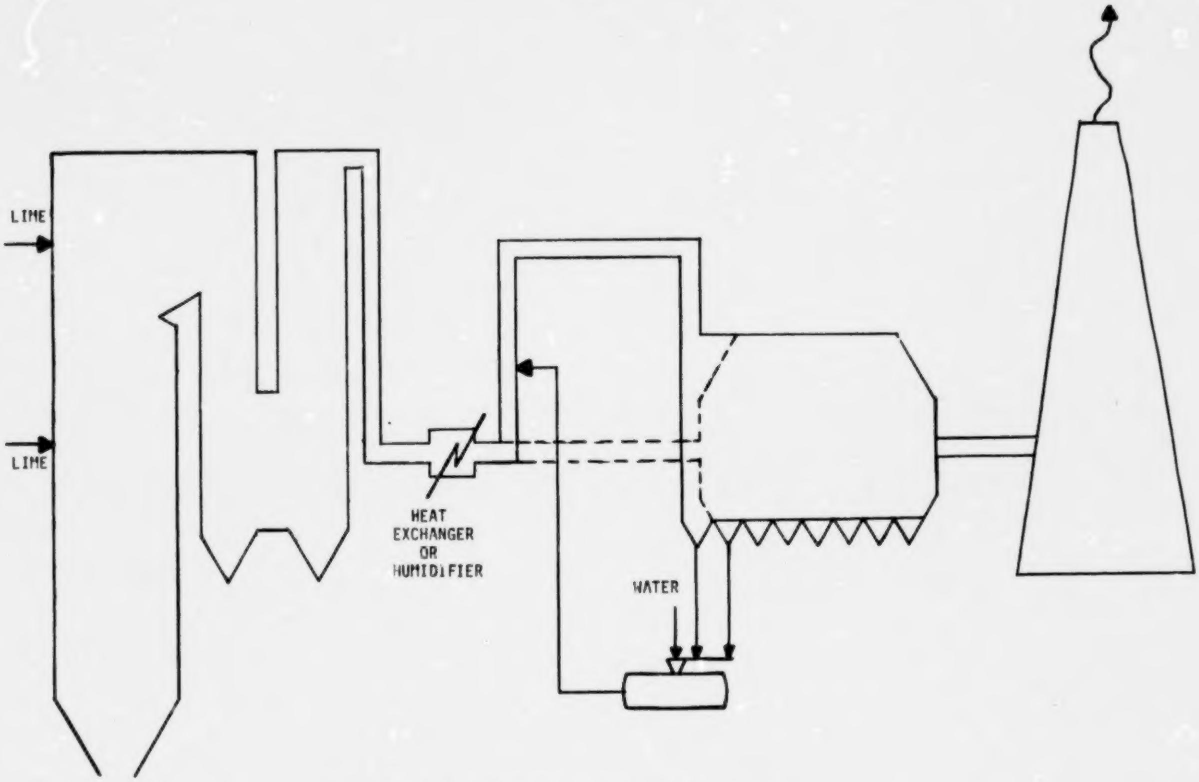
LIME
LIME
HEAT EXCHANGER OR HUMIDIFIER
WATER

Figure 6. Furnace injected sorbent with reactivated sorbent (silicate) recycle.

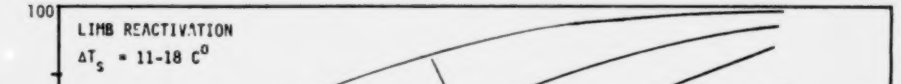

Figure 7. Total SO_2 removal vs. recycle ratio for damp recycle, reactivated LIMB sorbents.

EFFECT OF CaO SORBENT PHYSICAL PARAMETERS UPON SULFATION

by: Brian K. Gullett
U.S. Environmental Protection Agency
Office of Research and Development
Air and Energy Engineering Research Laboratory
Research Triangle Park, NC 27711

Kevin R. Bruce
Acurex Corporation
Research Triangle Park, NC 27709

ABSTRACT

Calcium-based sorbents have been studied for the effects of type [$Ca(OH)_2$, calcium hydroxide, vs. $CaCO_3$, calcium carbonate], particle size, porosity, surface area, and pore size distribution upon their high temperature reactivity with sulfur dioxide. Results show particle size to be inversely related to sorbent conversion by the 0.20 to 0.35 power of particle size. However, independent of particle size, there is still a large effect of initial calcium oxide (CaO) surface area. Experimental results suggest that the sorbent pore size distribution has only a minor effect upon reactivity. The overall sample porosity appears more important to limiting sorbent reactivity: sorbent conversion is related to developed porosity, although sintering and sorbent expansion phenomena complicate the relationship. Reactivity variation due to sorbent type is likely only a second order effect, reflecting physical differences due to particle size and sintering susceptibility, although sorbent grain shape has been shown to have a minor effect.

This paper has been reviewed in accordance with
the U.S. Environmental Protection Agency's peer
and administrative review policies and approved
for presentation.

INTRODUCTION

The effect of sorbent physical parameters upon the high temperature CaO/SO_2 (sulfur dioxide) sulfation reaction has been the subject of extensive investigation by the Environmental Protection Agency (EPA). At the 1986 Joint Symposium on Dry SO_2 and SO_2/NO_x Control Technology, investigators were reporting significant reactivity advantages of $Ca(OH)_2$ sorbents over $CaCO_3$ sorbents (1, 2). Since that time, considerable work has been done to identify the physical features of $Ca(OH)_2$ that lead to greater SO_2 capture than $CaCO_3$.

One of the most significant sorbent features relating to reactivity is particle size. Smaller particle sizes are more reactive in general because a greater mass percentage of the reactant sorbent is exposed to the reactant gas. Similarly, for a porous sorbent, the diffusion path of the gaseous reactant is shorter for the smaller diameter particle, increasing the effectiveness factor, or roughly the ratio of the interior reactivity to that of the exterior.

Repeated testing of $Ca(OH)_2$ and $CaCO_3$ has demonstrated typical SO_2 captures of about 55 and 35%, respectively ($Ca/S = 2/1$) (1, 3). The majority of this advantage is likely due to particle size effects. Indeed, the process of hydrating CaO to form $Ca(OH)_2$ results in considerable reduction in the particle size distribution. Although numerous variables are known to affect the amount of reduction (4), typical mass median diameters (MMD) for commercial processes remain around 4 μm. Additional size reduction can be achieved by hydrating with an excess of water although the product requires considerable drying.

The available sorbent porosity should limit the amount of reaction when the product volume is greater than that of the reactant. For $CaSO_4$ vs. CaO, the molar volume ratio, Z, is 3.09. The effect of greater product volume could be to close off the internal pore structure prior to complete reaction (pore plugging) or it could just provide an upper theoretical limit upon reaction as the available pore volume is filled with product (pore filling). Theoretical limits to sulfation are 51 and 49% conversion for $CaCO_3$ and $Ca(OH)_2$, respectively, when calcination or dehydration to the CaO form reaches theoretical porosities of 0.54 and 0.49.

Sorbent reactivity has been related to the square of calcined surface area (5). Extension of these results to uncalcined sorbent surface area has been less successful; tests with high surface area, alcohol-modified hydroxides did not show nearly proportional advances in reactivity over the unmodified hydroxides (6). The current thought suggests that increases in surface area decrease the mean pore size, making intra-particle diffusion more limiting. When this is the case, sulfation occurs mainly on the particle surface, causing pore blockage and leading to reaction control by product layer diffusion.

Studies attempting to investigate optimal pore size distributions have principally been theoretical in nature (7), due to the difficulty of controlling pore size distributions for testing. Experimental studies have shown varying reactivities for sorbents with different pore size distributions (8), but these results were not independent of variation in other physical parameters, namely porosity and surface area.

The objective of this paper is to discuss results from EPA efforts to determine the effects of these sorbent physical parameters upon the sulfation reaction.

EXPERIMENTAL

This paper covers experimental results obtained from four different reactors. The EPA differential reactor (DR) is an isothermal, electrically heated, fixed-bed reactor capable of temperatures up to 1000°C. A sorbent sample is placed on a quartz wool bed and inserted into the reactor on a quartz probe. Under normal operating conditions, sorbent exposures at residence times greater than or equal to 5 s are possible. This reactor is described more fully by Borgwardt et al. (9).

The EPA flow reactor (FR) is an electrically heated furnace about 3 m in length capable of operating isothermally up to 1050°C. Process gases pass through an outer annulus where they are heated to the reactor temperature prior to mixing with the injected sorbent and passing through the inner annulus. Solid samples are separated from the gas stream and collected at the reactor bottom in a cyclone after passing through an air-cooled heat exchanger. Nominal operating conditions result in sorbent residence times from 0.5 to 2.0 s.

The graphite element furnace reactor (GFR) at EPA is an electrically heated flow reactor capable of operating nominally at 1200°C or lower. Its sorbent feeding system entrains particles into an injector tube from a partially fluidized sorbent reservoir with an attached vibrator. The stainless steel sorbent injector and the quartz sample collection probe are, respectively, water and air cooled. The as-sampled sorbent residence time in the GFR is 0.74 s (nominal temperature of 1100°C) as determined from an algorithm developed by Langhaar (10) for solution of the Navier-Stokes equations in the transition region of a straight tube.

The EPA reactors were operated with 3000 ppm SO_2 (typically), 5% O_2, and the balance N_2. Sorbent carrier gas flowrates were generally below 5% of the total process gas flow.

The short time reactor (STR) is a furnace at Energy and Environmental Research Corporation (EER), an EPA contractor, with capabilities of short time sorbent sampling and reactivity measurement. It is 2.54 m in length with radial and axial sampling capabilities. The STR uses a CO-fired flame with back-fired heating channels to make the furnace isothermal from 930 to 1370°C with solids residence times of 35 to 400 ms. Sulfur dioxide capture was determined by gas phase sampling followed by a non-dispersive ultraviolet SO_2 analyzer. Solid samples were analyzed for porosity and pore size distribution at the EPA.

Conversion analyses of EPA sorbent samples were completed by atomic absorption spectroscopy and ion chromatography. Pore size distributions and porosities were done by nitrogen adsorption/desorption and mercury porosimetry. In the former, porosities were determined by inclusion of all volume below approximately 10% of the particle MMD. In the latter, porosities were determined by including all volume below that associated with interparticle voids as determined from inflection points on a plot of mercury intrusion versus pore size. Comparison of results between the two techniques showed agreement. Particle sizing was done by inertial cascade impactors and gravity sedimentation.

RESULTS AND DISCUSSION

PARTICLE SIZE

Laboratory investigations of particle size effects have been done by two methods: 1) sizing prior to reactivity testing, and 2) sizing by in situ methods after reaction. Both of these methods have shown considerable reactivity advantage for the smaller sorbents. Results using the first method have shown greater sulfur capture for $Ca(OH)_2$ and $CaCO_3$ as particle size decreases from 30 to 2 μm and 20 to 10 μm, respectively (11). The second method was used at EPA (12) with post-reactor sorbent collection by a heated seven stage inertial impactor. These stages collected sorbent particles with MMDs ranging from 0.44 to 7.8 μm, with the preimpactor stage collecting all particles with MMDs larger than 12.1 μm. The results from this testing showed that reactivity was inversely related to particle diameter by the 0.22 to 0.32 power. Fig. 1 shows the data from this testing and, for comparative purposes, from Ishihara et al., (13). This figure also demonstrates the reactivity advantage of $Ca(OH)_2$ compared to $CaCO_3$ even when examining similar particle sizes. EPA's work (12) also showed that $Ca(OH)_2$ sorbents had an extreme propensity to agglomerate as fed into the reactor (Fig. 2) and that overall agglomerate size similarly affected reactivity, despite being composed of much smaller constituent particles. The extension of this agglomeration problem to the full scale application and its impact upon sorbent capture is untested.

The effect of CaO [derived from $Ca(OH)_2$ and $CaCO_3$] surface area independent of particle size was analyzed by calcining sorbents to known surface areas prior to reactivity testing (14). The effect of increasing surface area at constant particle size [Fig. 3, CaO from $Ca(OH)_2$] raises the sorbent reactivity, indicating that film diffusion control is unimportant. Fig. 4 shows the effect of surface area at several constant particle sizes [CaO from both $Ca(OH)_2$ and $CaCO_3$]. Here the CaO conversion to $CaSO_4$ was inversely related to particle diameter by the 0.20 to 0.35 power, in agreement with the above tests of raw $Ca(OH)_2$ and $CaCO_3$ injection results. Fig. 4 also shows substantial conversion at low surface areas, suggesting reactant diffusion through a product layer on the outer particle surface.

The effect of sorbent type is also seen in Fig. 1. These results show the effect of the uncalcined sorbent size for Linwood $Ca(OH)_2$ produced under atmospheric and pressurized conditions along with a Fredonia 3.2 μm sized carbonate, and other $CaCO_3$ results (12, 13).

POROSITY

Sorbent conversions greater than expected based upon pore volume filling have been routinely obtained in laboratory research. Early work (5) demonstrated conversion at 1125°C up to 90% for presintered sorbents (ϵ_0=0.028), supported by more recent fixed bed reactor work (8) showing 3 μm MMD $CaCO_3$ reacting to 60% conversion (800°C, 7000 ppm, 250 s) and slaked $Ca(OH)_2$ reaching 80% conversion under similar conditions.

Kocaefe et al. (15) have incorporated a method into several of the published gas-solid reaction models allowing for sorbent conversions as high as 90%. This is accomplished by allowing diffusion, and subsequent reaction, through the solid product layer after filling of surface pores. While their model modifications have reflected the higher conversions experimentally achievable, their models hold particle radius as a constant and, therefore, are unable to explain the mechanism by which a particle can react beyond the filling of all pore volume with solid product.

These high conversion results could only be accomplished with particle expansion, a theory first verified for 250 μm $CaCO_3$ by mercury porosimetry (16) and later by nitrogen (14) and mercury porosimetry (14). The mercury porosimetry data for sulfated (800^{o}C, 3000 ppm SO_2, DR) slaked Fredonia $Ca(OH)_2$ and Fredonia $CaCO_3$ (Figs. 5 and 6) show residual porosity beyond the point of theoretical maximum converison (49 and 51% for $Ca(OH)_2$ and $CaCO_3$, respectively). Particle expansion is shown by the increasing values of total particle volume (solid volume added to pore volume).

Extension of this finding to laboratory conditions more closely simulating the full scale injection process has further verified this phenomenon: GFR tests (3000 ppm SO_2, nominal temperature of 1100^{o}C, sampled solids residence time of 0.74 s) have shown reaction in 1, 5, and 10 μm $Ca(OH)_2$ and $CaCO_3$ sorbent particles beyond the values expected for complete pore volume filling (Fig. 7). High conversions at low porosities, similar to results at low surface area (Fig. 4), continue to indicate the necessity for reactant diffusion through the product layer.

The extent to which sorbent expansion applies to the full scale process has not been tested nor has an attempt been made to correlate a sorbent's propensity to expand with its physical characteristics.

The role of porosity in limiting the sulfation of sorbents was further examined in the EER (7) short time reactor (STR). Solid samples were taken from the isothermal, CO-fired STR at times as short as 35 ms. The pore size distributions and porosities were determined at EPA from nitrogen porosimetry techniques. Porosities of Linwood $Ca(OH)_2$ in a calcination (SO_2-free) environment showed considerable porosity decline from the theoretical amount for sampling times between 32 and 369 ms. Porosities determined from sulfation runs resulted in similarly low porosity values (about 0.10 to 0.25). When the sample's conversion value, X, (Fig. 8) was used to determine the volume of product-filled porosity loss and this value was added to the remaining porosity measured after sulfation, ϵ_m, a calculated original porosity, ϵ_{CO}, value was determined:

$$\epsilon_{CO} = \epsilon_m + \frac{X\ (Z - 1)}{1 + X\ (Z - 1)}$$

Looking at these values (Fig. 9), one observes that the calculated original porosity, e_{CO}, under optimal sulfation conditions (1150 to 1200^{o}C) reaches the theoretical value, while at lower or higher temperatures, the value drops off. A competing mechanism of sulfation vs. sintering has been proposed (7) to explain this phenomenon. At optimal sulfation conditions, sulfation of the sorbent's interior structure competes favorably with the rate of sintering, maintaining a more open pore structure for sulfation. At lower temperatures, CO_2-promoted sintering [discussed, for example, by Borgwardt et al. (17)] dominates sulfation, closing the pore structure and leading to lower values of the calculated original porosity. At higher temperatures of 1270^{o}C, the porosity decline is again significant, likely due to thermally induced sintering.

The phenomenon of sulfation limitation by porosity loss was also investigated in the STR (7) for $CaCO_3$ (a 7 µm size cut of Vicron 45-3) and two $Ca(OH)_2$ sorbents of comparatively varying reactivities (Linwood and Mississippi). Results showed that the Vicron carbonate was more susceptible to porosity loss than the hydroxide. The results of the hydroxide testing showed that the less reactive Mississippi sorbent attained lower calculated original porosities than the Linwood. This, along with Mississippi's larger particle size, accounts for the difference in sorbent reactivity.

The porosity effect of $Ca(OH)_2$ reactivity was similarly investigated in the entrained flow GFR operating over five temperature ranges. Fig. 8 shows the Linwood $Ca(OH)_2$ sorbent reactivity over the full range of temperatures investigated. These results are similar to those of the STR, showing an optimal temperature for reaction. Porosity measurements (Fig. 9) again reflect a considerable decline in porosity that is fairly constant across the temperatures investigated. The ϵ_{CO} values from the GFR show a peak value at the optimum temperature, similar to the STR results. However, in contrast, ϵ_{CO} values are shown above the maximum theoretical porosity, providing further evidence that sorbent expansion must occur. Porosity and surface area measurements at these same conditions are underway to further investigate the effect of a CO_2-free environment upon porosity and sulfation.

THEORY ON COMBINED EFFECTS OF PARTICLE SIZE, POROSITY, AND SURFACE AREA

The relative contributions of particle size, surface area, and porosity are difficult to experimentally segregate. They have been analyzed on a theoretical basis through use of the dimensionless Thiele modulus (14):

$$\Phi = R \left(\frac{k_v}{D_e} \right)^{1/2}$$

The value of the Thiele modulus indicates the magnitude of the reaction rate (limited by either chemical or product layer diffusion kinetics) relative to the rate of reactant diffusion into the porous sorbent matrix. Developing this expression and using some simplifying assumptions (principally, first order and irreversible reaction) led to a modified Thiele modulus:

$$\Phi' = \left(\frac{S_0^2 (1 - \epsilon_0)}{\epsilon_0} \right)^{1/2}$$

When experimentally determined values of S_0 and ϵ_0 were substituted into this equation (particle size was held constant), Φ' could be plotted against either S_0 (Fig. 10) or ϵ_0 (Fig. 11). The figures show that, for these precalcined sorbents, the intermediate surface areas (30 to 50 m^2/g) and porosities (0.3 to 0.4) provide the optimal area/pore volume combination for reducing possible limitations due to pore diffusion. This theory provides insight into why tests with high surface area alcohol hydrates (80 m^2/g) had only marginal improvement in SO_2 capture (6).

Extension of these results should be tempered with several caveates. The surface area/porosity relationship is by no means constant throughout sulfation. Therefore, the relative importance of pore diffusion will vary as the sorbent characteristics change. Also, the relative position of CaO derived from $Ca(OH)_2$ versus CaO derived from $CaCO_3$ on Figs. 10 and 11 is likely to change with experimental calcination conditions due to variation in surface area and porosity development.

PORE SIZE DISTRIBUTION

The pore size distribution and its changes as reaction occurs were investigated (8) by nitrogen porosimetry for both CaO precursors: $CaCO_3$ and $Ca(OH)_2$. The isotherms of the unreacted materials both exhibit a Type IV isotherm yet their characteristic hysteresis loops are distinct (Fig. 12). The CaO derived from the $CaCO_3$ (termed c-CaO) has a type A hysteresis, associated with cylindrical pores as well as agglomerates of uniform spherical particles, while the CaO derived from the $Ca(OH)_2$ (termed h-CaO) has a type B hysteresis, commonly associated with slit-shaped pores or the space between parallel plates. These structural conclusions support similar isotherm results of Beruto et al. (18), photomicrograph evidence by Gooch et al. (6), and SEM (scanning electron microscopy) results of Milne and Pershing (19).

Based upon the isotherm interpretation of the physical shape of the pore structure, a cylindrical geometry based on an adaptation (20) of the method of Barrett et al. (21) was used to model the c-CaO and a parallel-plate model (22) was used for the h-CaO. The pore structures for both materials show similar peak volume pore sizes, around 100 to 200 Å. However, if the same model were used to predict the pore size distribution for both sorbents, the pores of the h-CaO would be much larger, with the peak volume size approximately doubling that of the c-CaO. This is because the cylindrical pore diameter in the Kelvin equation is equivalent to twice the plate separation (22).

Sulfation of either CaO pore structure (0 to 60 s, DR, 800°C, 7,000 ppm SO_2) results in pore volume decline throughout the entire range of pore sizes. The c-CaO sorbents lose their pore volume more rapidly and to a greater extent than the h-CaO sorbents.

The effect of sintering upon the sorbent's pore structure (800°C, N_2 atmosphere) is to reduce the surface area while causing only slight decline in the pore volume and in the sorbent conversion to $CaSO_4$. The peak pore size increases about 50 Å depending upon the sorbent type.

Whereas it was noted previously that $CaCO_3$ was more susceptible to porosity loss by sintering, other testing (800°C, 7,000 ppm SO_2) showed that sulfation-induced porosity loss was also considerably more rapid for c-CaO than h-CaO (Fig. 13).

The extent to which the grain shape of the CaO solid, as determined by the pore shape, affects the sulfation reaction was analyzed experimentally and theoretically by Bruce et al. (23). A product layer diffusion model, differing only in the grain shape, was used with experimental data to show that the flat, plate-like grain shape of the h-CaO resulted in slightly higher reactivity than the spherical c-CaO grain, at equal surface areas and porosities. This is due to a faster rate of diffusion of reactant through the growing $CaSO_4$ layer, yielding higher conversions with increased time, temperature, and progressive pore filling (Fig. 14).

CONCLUSIONS

The reactivity of calcium based sorbents is dependent upon particle size, sorbent type, surface area, and pore volume and shape. Reactivity is inversely dependent upon particle or agglomerate size to the 0.20 to 0.35 power. At a common particle size, surface area still has an effect upon relative reactivity, as does sorbent type. $Ca(OH)_2$-derived sorbents of similar particle size and surface area react to greater extents in this work than $CaCO_3$-derived sorbents, in part due to their differences in grain shape. Evidence suggests that the flat plate structure of the activated $Ca(OH)_2$ grains allows greater rates of product layer diffusion than the spherical form of the activated $CaCO_3$. Sorbent reactivity is limited by developed porosity, which is decreased by sintering processes. However, substantial laboratory evidence suggests that sorbent particles can undergo limited expansion during sulfation, allowing the sorbent to partially compensate for sintering porosity loss and react beyond the limits imposed by $CaSO_4$ product-filling of the available porosity. However, the implications of this phenomenon for large scale sorbent injection and sorbent development remain unexplored.

NOMENCLATURE

D_e	effective diffusivity
k_v	rate constant per unit CaO volume
R	radius at particle surface
S_0	initial specific surface area per unit weight of CaO
X	conversion of CaO to $CaSO_4$
Z	molar volume ratio of $CaSO_4$ to CaO, 3.09
ϵ_0	initial porosity of CaO
ϵ_{CO}	calculated original porosity
ϵ_m	measured porosity with SO_2 present
Φ	Thiele modulus
Φ'	modified Thiele modulus

ACKNOWLEDGMENTS

Major EPA construction and operational activities were supervised by George R. Gillis, U.S. EPA/Air and Energy Engineering Research Laboratory. Laboratory analyses were conducted by Laura O. Beach, John A. Blom, Richard T. Cunningham, and W. C. Pendergraph of Acurex Corporation. Work on the STR was performed at Energy and Environmental Research Corporation (EPA Contract 68-02-4239) under John C. Kramlich and Gerald H. Newton.

REFERENCES

1. Snow, G.C., Lorrain, J.M., and Rakes, S.L. Pilot Scale Furnace Evaluation of Hydrated Sorbents for SO_2 Capture. In Proceedings: 1986 Joint Symposium on Dry SO_2 and Simultaneous SO_2/NO_x Control Technologies, Volume 1, EPA-600/9-86-029a (NTIS No. PB87-120465), October 1986, p. 6-1.

2. McCarthy, J.M., Chen, S.L., Kramlich, J.C., Seeker, W.R., and Pershing, D.W. Reactivity of Atmospheric and Pressure Hydrated Sorbents for SO_2 Control. In Proceedings: 1986 Joint Symposium on Dry SO_2 and Simultaneous SO_2/NO_x Control Technologies, Volume 1, EPA-600/9-86-029a (NTIS No. PB87-120465), October 1986, p. 10-1.

3. Overmoe, B.J., McCarthy, J.M., Chen, S.L., Seeker, W.R., and Pershing, D.W. Reactivity Study of SO_2 Control with Atmospheric and Pressure Hydrated Sorbents. EPA-600/7-86-040 (NTIS PB87-129250), U.S. Environmental Protection Agency, Air and Energy Engineering Research Laboratory, Research Triangle Park, NC, November 1986.

4. Kirchgessner, D.A., Gullett, B.K., and Lorraine, J.M. Physical Parameters Governing the Reactivity of $Ca(OH)_2$ with SO_2. In Proceedings: 1986 Joint Symposium on Dry SO_2 and Simultaneous SO_2/NO_x Control Technologies, Volume 1, EPA-600/9-86-029a (NTIS No. PB87-120465), October 1986, p. 8-1.

5. Borgwardt, R.H. and Bruce, K.R. Effect of Specific Surface Area on the Reactivity of CaO with SO_2. AIChE J., 32: 239, 1986.

6. Gooch, J.P., Dismukes, E.B., Beittel, R., Thompson, J.L., and Rakes, S.L. Sorbent Development and Production Studies. In Proceedings: 1986 Joint Symposium on Dry SO_2 and Simultaneous SO_2/NO_x Control Technologies, Volume 1: Sorbents, Process Research, and Dispersion, EPA-600/9-86-029a (NTIS PB87-120465), October 1986. p.11-1.

7. Newton, G.H., Moyeda, D.K., Kindt, G., McCarthy, J.M., Chen, S.L., Cole, J.A., and Kramlich, J.C. Fundamental Studies of Dry Injection of Calcium-Based Sorbents for SO_2 Control in Utility Boilers. Final Report, EPA Contract No. 68-02-4239. U.S. Environmental Protection Agency, Air and Energy Engineering Research Laboratory, Research Triangle Park, NC, October 1988 (In Press).

8. Gullett, B.K. and Bruce, K.R. Pore Distribution Changes of Calcium-Based Sorbents Reacting with Sulfur Dioxide. AIChE J., 33: 1719, 1987.

9. Borgwardt, R.H., Roache, N.F., and Bruce, K.R. Surface Area of Calcium Oxide and Kinetics of Calcium Sulfide Formation. Environ. Prog., 3: 129, 1984.

10. Langhaar, H.L. Steady Flow in the Transition Length of a Straight Tube. J. Appl. Mech., 9: A-55, 1942.

11. Cole, J.A., Kramlich, J.C., Seeker, W.R., and Silcox, G.D. The Influence of Sorbent Physical Properties upon Reactivity with Sulfur Dioxide. EPA-600/2-87-105 (NTIS PB 88-143987), U.S. Environmental Protection Agency, Air and Energy Engineering Research Laboratory, Research Triangle Park, NC, December 1987.

12. Gullett, B.K. and Blom, J.A. Calcium Hydroxide and Calcium Carbonate Particle Size Effects on Reactivity with Sulfur Dioxide. React. of Solids, 3: 337, 1987.

13. Ishihara, Y., Asakawa, C., and Fukuzawa, H. Studies on Sulfur Oxides Removal from Flue Gas by Dry Limestone Injection (II). Effects of Reaction Conditions on Sulfur Oxides. Nenryo Kyokaishi (J. Fuel Soc. Jpn.), 54: 175 (1975).

14. Gullett, B.K., Blom, J.A., and Cunningham, R.T. Porosity, Surface Area, and Particle Size Effects of CaO Reacting with SO_2 at 1100°C. Accepted for publication in React. of Solids, 1988.

15. Kocaefe, D., Karman, D., and Steward, F.R. Interpretation of the Sulfation Rate of CaO, MgO, and ZnO with SO_2 and SO_3. AIChE J., 33: 1835, 1987.

16. Borgwardt, R.H. and Harvey, R.D. Properties of Carbonate Rocks Related to SO_2 Reactivity. Env. Sci. & Tech., 6: 350, 1972.

17. Borgwardt, R.H., Roache, N.F., and Bruce, K.R. Method for Variation of Grain Size in Studies of Gas-Solid Reactions Involving CaO. Ind. Eng. Chem. Fund. 25: 165, 1986.

18. Beruto, D., Barco, L., Searcy, A.W., and Spinolo, G. Characterization of the Porous CaO Particles Formed by Decomposition of $CaCO_3$ and $Ca(OH)_2$ in Vacuum. J. Am. Cer. Soc., 63: 439, 1980.

19. Milne, C.R. and Pershing, D.W. Time Resolved Sulfation Rate Measurements for Sized Sorbents. In Proceedings: Fourth Annual Pittsburgh Coal Conference, University of Pittsburgh, School of Engineering, Pittsburgh, PA, 109, 1987.

20. Faas, G.S. Correlation of Gas Adsorption, Mercury Intrusion, and Electron Microscopy Pore Property Data for Porous Glasses. M. Sc. Thesis, Georgia Inst. Technol., Atlanta, GA, 1981.

21. Barrett, E.P., Joyner, L.G., and Halenda, P.P. The Determination of Pore Volume and Area Distributions in Porous Substances. I: Computations from Nitrogen Isotherms. J. Am. Chem. Soc. 73: 373, 1951.

22. Innes, W.B. Use of a Parallel Plate Model in Calculation of Pore Size Distribution. Anal. Chem., 29: 1069, 1957.

23. Bruce, K.R., Gullett, B.K., and Beach, L.O. Comparative SO_2 Reactivity of CaO Derived from $CaCO_3$ and $Ca(OH)_2$. Accepted for publication in AIChE J., 1988.

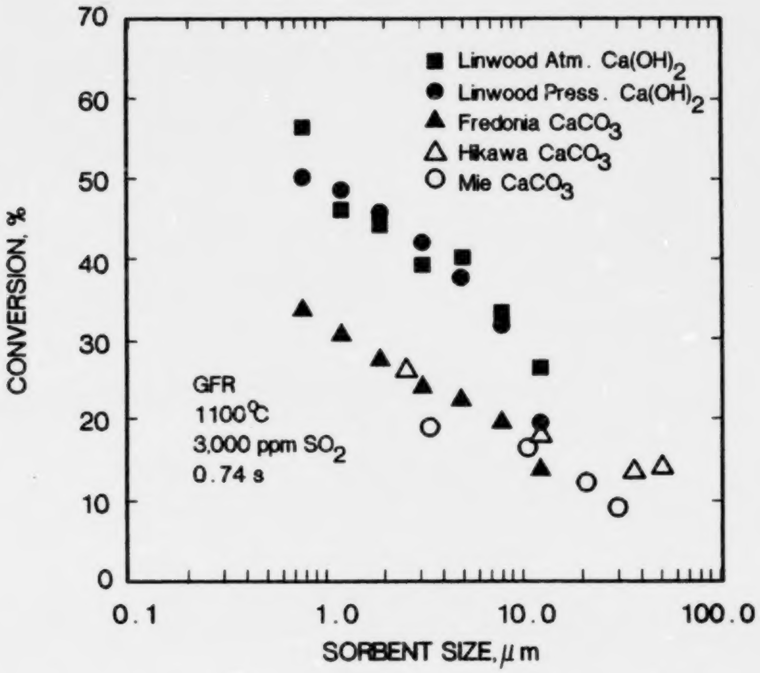

Figure 1. Sorbent size effects upon the reactivity (1100°C) of Linwood pressure hydrate $Ca(OH)_2$, Linwood atmospheric hydrate $Ca(OH)_2$, and Fredonia $CaCO_3$ (<3μm) compared to the results of Ishihara et al. (1975) for Hikawa $CaCO_3$ and Mie $CaCO_3$.

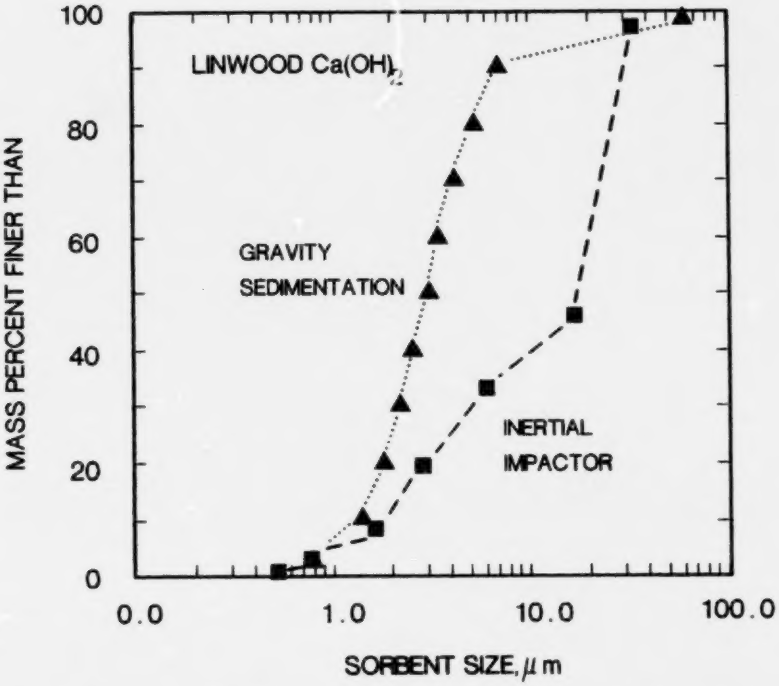

Figure 2. Sorbent size distribution of Linwood $Ca(OH)_2$ from gravity sedimentation and the inertial impactor.

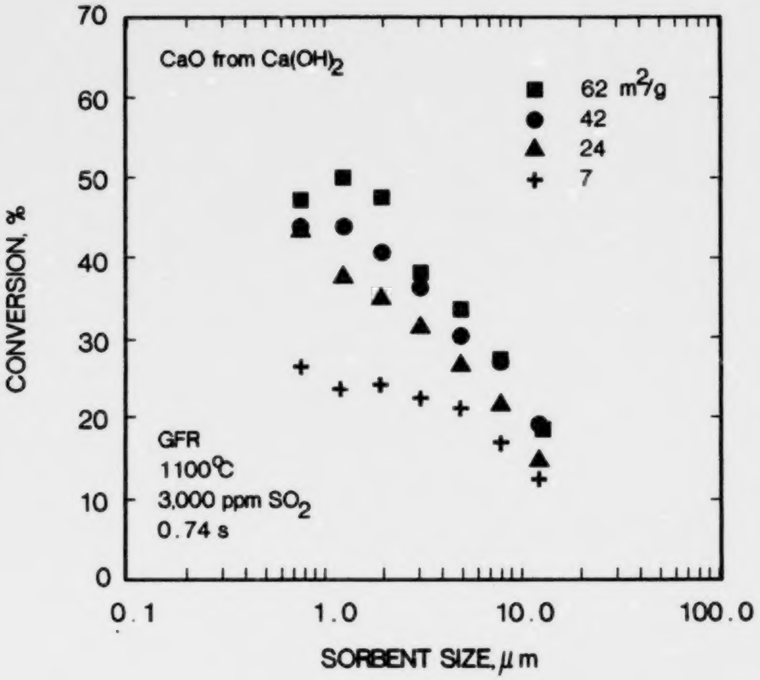

Figure 3. Effect of particle size and initial surface area upon CaO [from slaked Fredonia Ca(OH)$_2$] conversion at 1100°C and a residence time of 0.74 s.

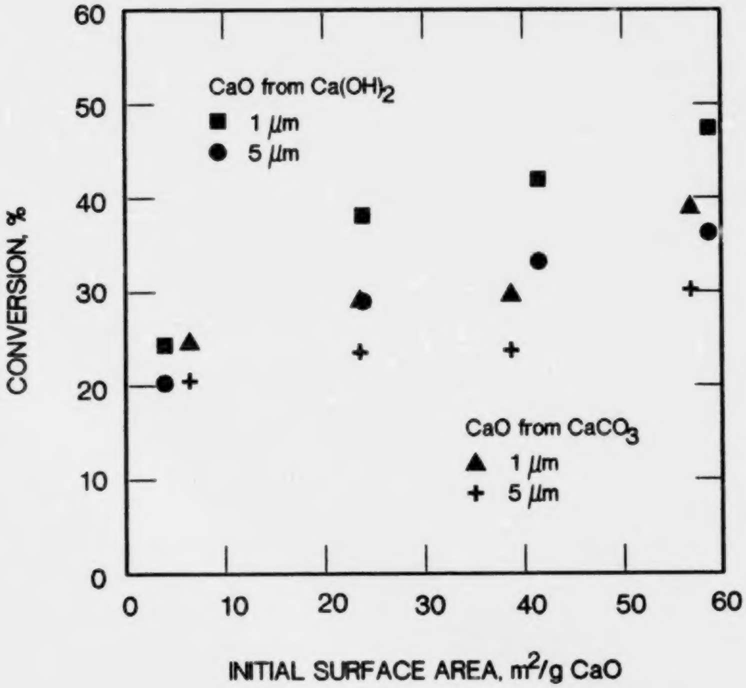

Figure 4. Effect of initial surface area upon conversion for CaO [from slaked Fredonia Ca(OH)$_2$ and 3.2 μm Fredonia CaCO$_3$] at 1 and 5 μm.

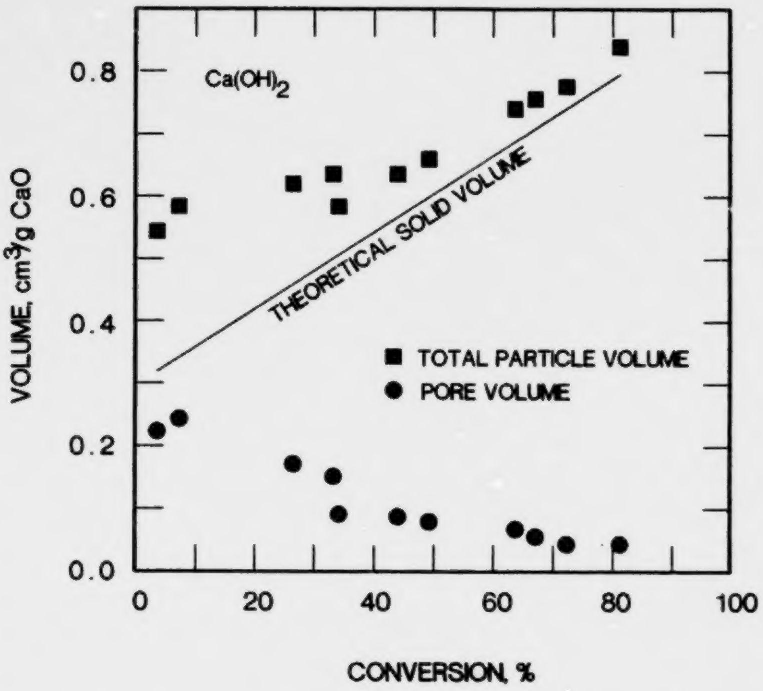

Figure 5. Effect of reaction upon pore volume for CaO [from slaked Fredonia Ca(OH)$_2$] versus theoretical solid volume and total particle volume.

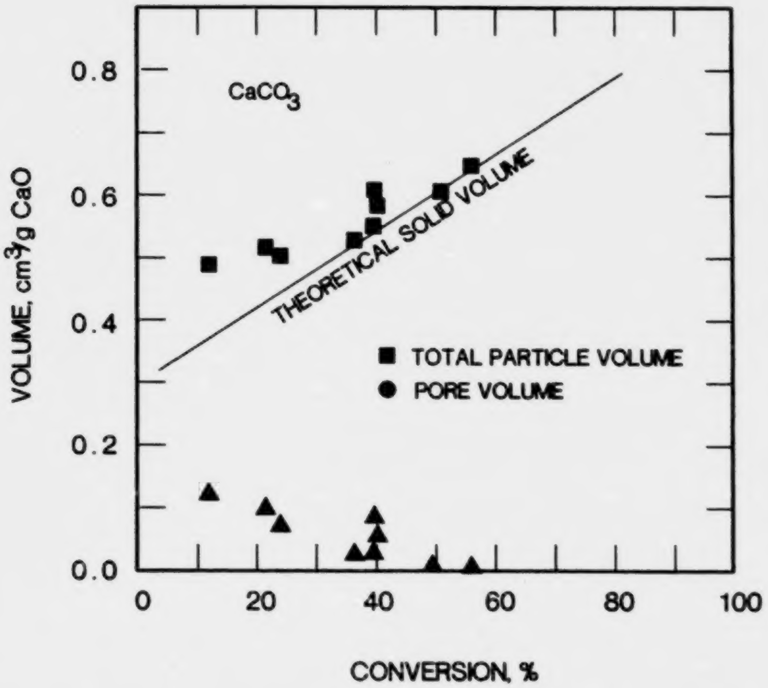

Figure 6. Effect of reaction upon pore volume for CaO [from 3.2 μm Fredonia CaCO$_3$] versus theoretical solid volume and total particle volume.

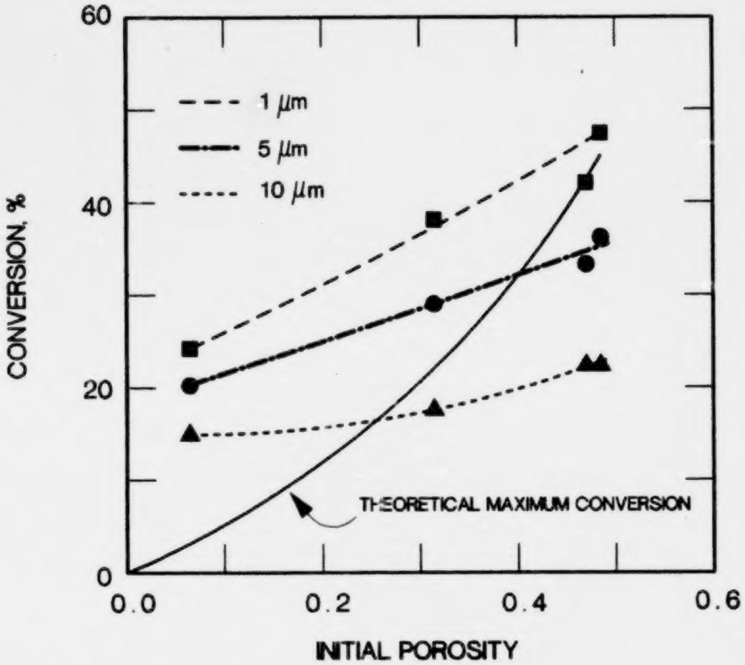

Figure 7. Effect of initial porosity upon conversion for both sorbents of Fig. 4 at 1, 5, and 10 μm versus the theoretical conversion/pore volume relationship.

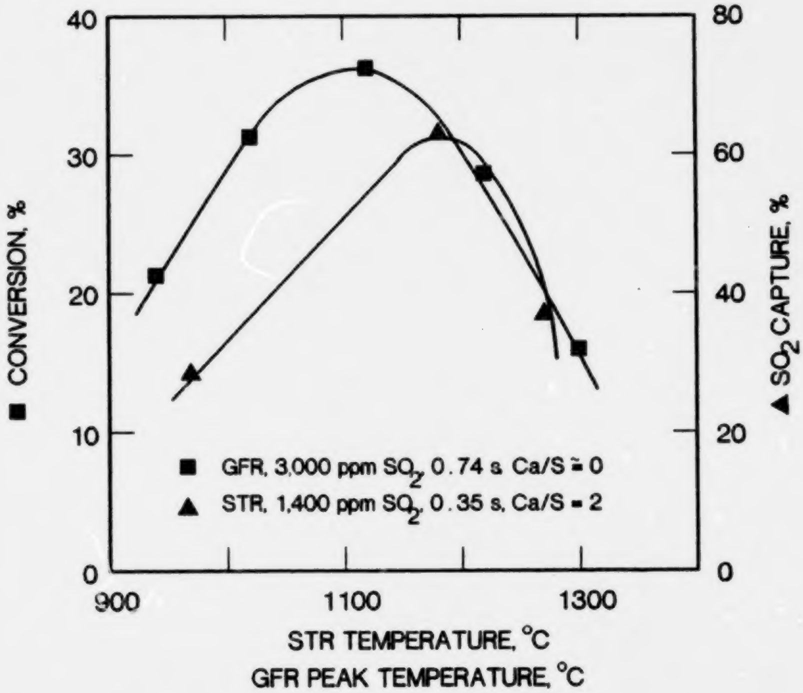

Figure 8. Sorbent reaction as a function of temperature for Linwood $Ca(OH)_2$ in the STR and the GFR.

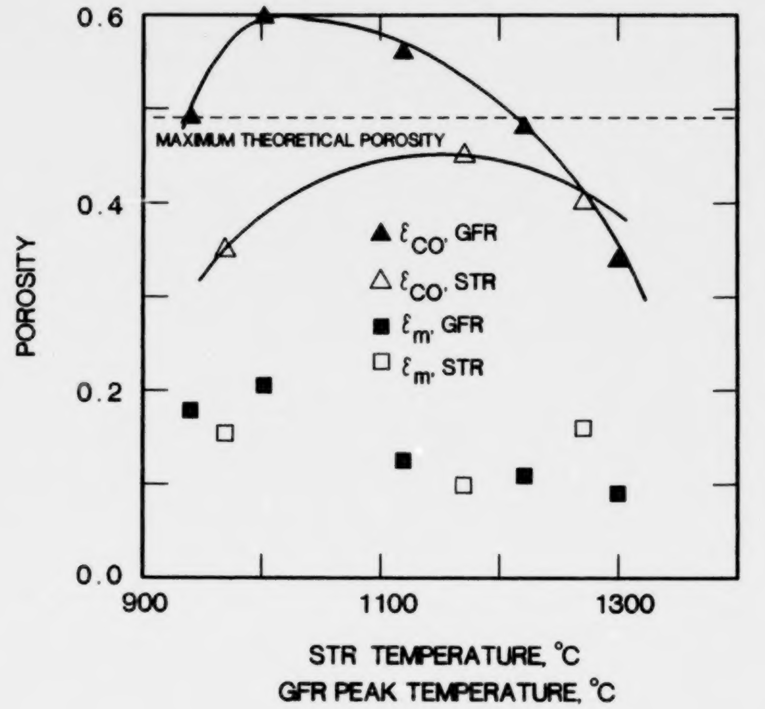

Figure 9. Measured porosities after sulfation and calculated original porosities for Linwood $Ca(OH)_2$ at conditions of Fig. 8.

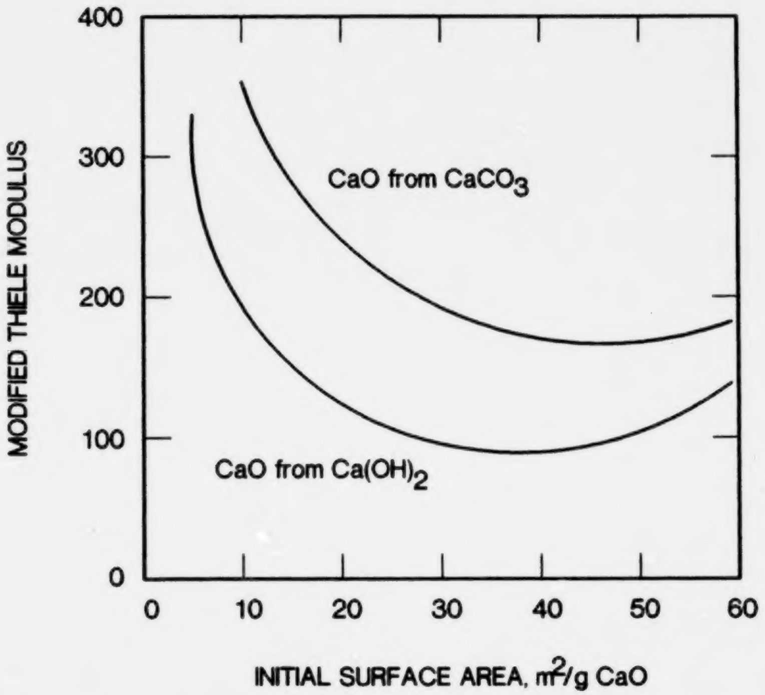

Figure 10. The effect of initial surface area on the modified Thiele modulus for CaO sorbents derived from $Ca(OH)_2$ and $CaCO_3$.

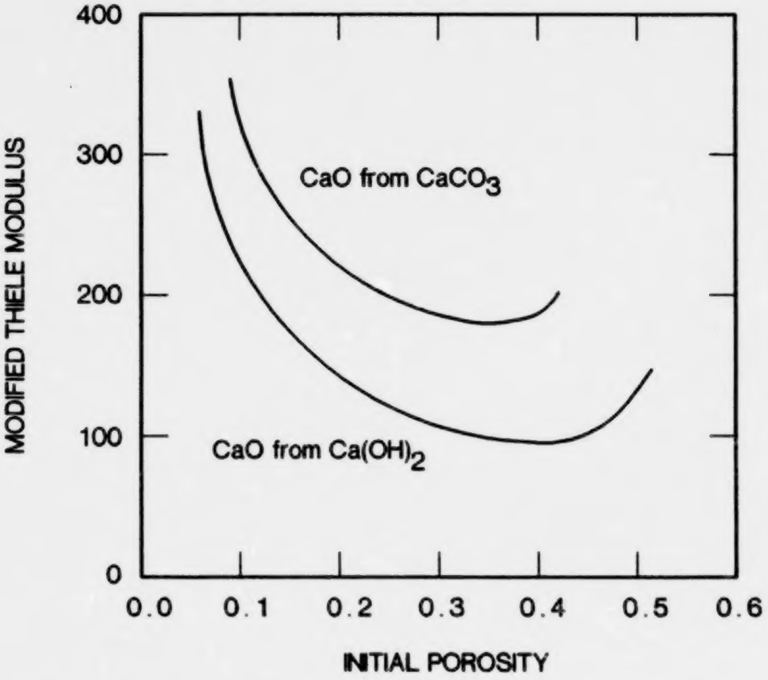

Figure 11. The effect of initial porosity on the modified Thiele modulus for CaO sorbents derived from $Ca(OH)_2$ and $CaCO_3$.

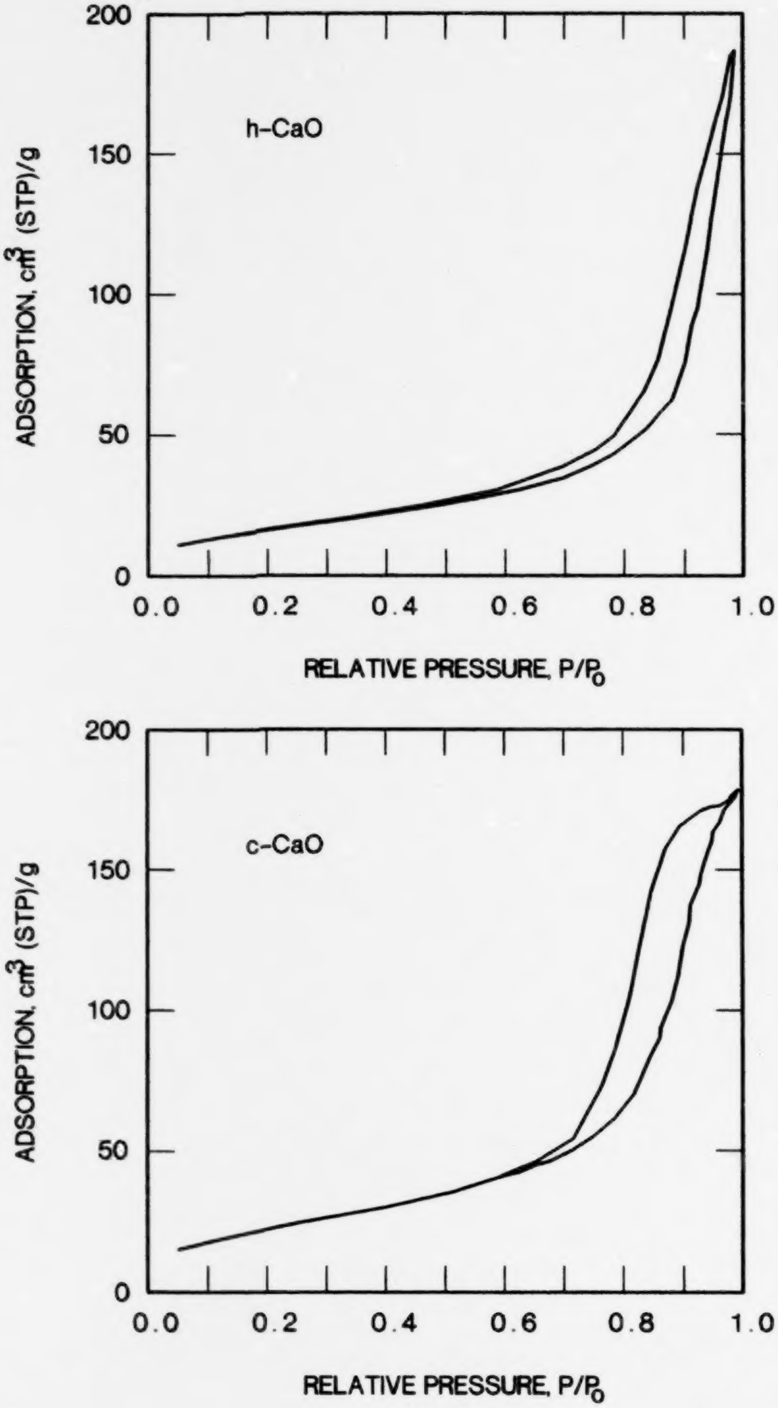

Figure 12. Nitrogen adsorption/desorption isotherms for CaO sorbents of Figs. 5 and 6.

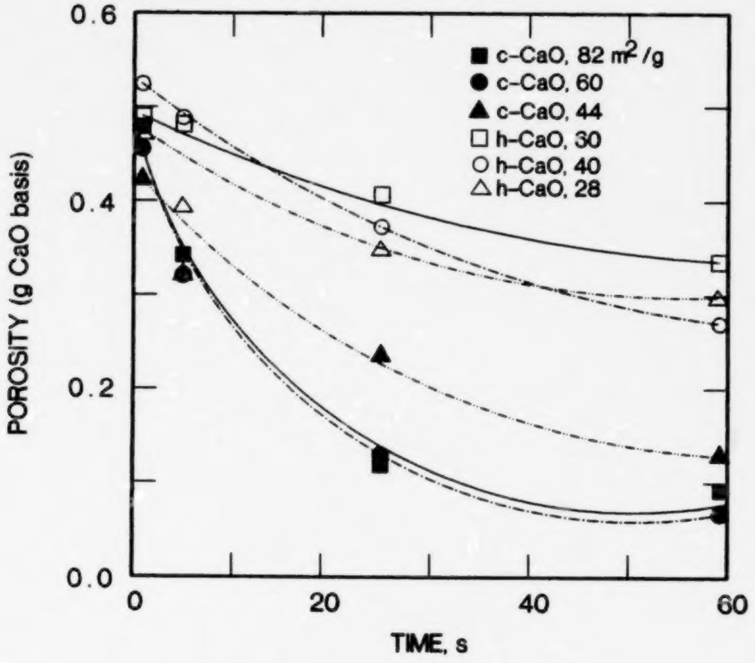

Figure 13. Porosity changes in precalcined sorbents from Figs. 5 and 6 at 7000 ppm SO_2, 800°C in the fixed bed DR.

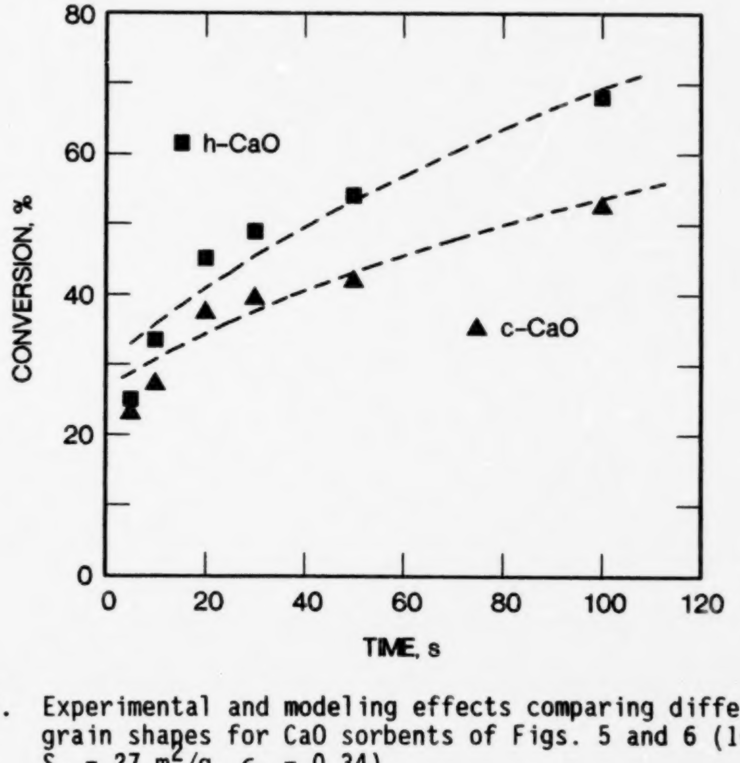

Figure 14. Experimental and modeling effects comparing differing grain shapes for CaO sorbents of Figs. 5 and 6 (1000°C, $S_0 = 27$ m²/g, $\epsilon_0 = 0.34$).

LABORATORY- AND COMMERCIAL-SCALE RESULTS OF TESTING SURFACTANT-MODIFIED SORBENT

by: D.A. Kirchgessner
U.S. Environmental Protection Agency
Air and Energy Engineering Research Laboratory
Research Triangle Park, NC 27711

W. Jozewicz
Acurex Corporation
Research Triangle Park, NC 27709

ABSTRACT

Efforts to improve the ability of commercially available, calcium-based sorbents to capture sulfur dioxide (SO_2) in EPA's limestone injection multistage burner (LIMB) system have resulted in the development of a calcium hydroxide [$Ca(OH)_2$] modified with calcium lignosulfonate. Initial laboratory-scale reactivity testing of this novel sorbent showed that it was capable of achieving a 20 percent relative increase in SO_2 capture over unmodified sorbents. When the new sorbent was produced commercially and tested at various pilot scales, reactivity increases of 6 to 15 relative percent were observed. Preliminary commercial-scale testing at Edgewater has shown a relative increase in SO_2 capture of about 4 percent at a Ca/S ratio of 2. Flow reactor studies suggest that the surfactant-modified sorbent's enhanced ability to capture SO_2 derives, in part, from its lower propensity to agglomerate in some applications. A more important characteristic of the new sorbent, however, appears to be its resistance to thermal sintering.

This paper has been reviewed in accordance with the U.S. Environmental Protection Agency's peer and administrative review policies and approved for presentation and publication.

INTRODUCTION

In the course of developing EPA's LIMB process, research has shown that $Ca(OH)_2$ reacts with SO_2 to a greater extent than either calcium carbonate ($CaCO_3$) or calcium oxide (CaO) during furnace injection (1, 2, 3, 4). While commercially available $Ca(OH)_2$ appears to be capable of meeting the SO_2 capture goal of 50 to 60 percent at a Ca/S ratio of 2, a cost effective method of enhancing sorbent reactivity would be desirable.

Studies have shown that the reactivity of $Ca(OH)_2$ sorbents can be modified. Borgwardt et al. (5) have shown that the addition of alkali metals to CaO increases sulfation. When additives are applied prior to calcination, however, no enhancement is observed due to the ability of these metals to catalyze the sintering of CaO, reducing its reactive surface area. Slaughter et al. (6) were also successful in using alkali metals to increase sulfation but noted that, during coal firing, most of the volatile additive was redeposited on the more abundant coal ash, and was unavailable to promote SO_2 capture by the sorbent.

Recent research at EPA has explored the use of surfactants to modify the reactivity of $Ca(OH)_2$. Since the effect of particle size on reactivity has been well documented (7, 8, 9), the initial goal of the research was to increase reactivity by reducing the sorbent particle size. Calcium lignosulfonate was chosen as the surfactant to be added to the water of hydration during the production of $Ca(OH)_2$. It was believed that this type of additive could reduce the fundamental crystal size of the hydrate and/or reduce the tendency of the sorbent to agglomerate. The first effect would be achieved by reduction of surface energy at the nucleus/solution interface during hydration, with a resulting increase in nucleation rate and smaller crystal size. The second effect would be produced through the introduction of a hydrophobic material to prevent hydrogen bonding between adjacent adsorbed water layers.

Subsequently a $Ca(OH)_2$ modified with 1.5 percent calcium lignosulfonate was produced commercially by the Marblehead Lime Company, and tested in a number of pilot- and commercial-scale gas- and coal-fired units ranging in size from 65 kW to 104 MW. Increases in percent SO_2 capture from 4 to 15 percent were achieved and are shown in Table 1. Enhancement in sulfation of this material was not accompanied by any significant particle size reduction, suggesting that a factor in addition to particle size was affecting the results. The remainder of the paper describes the results of research aimed at identifying the additional factor.

EXPERIMENTAL

In early experiments investigating the effect of additives on the particle size of sorbent and subsequent reactivity with SO_2 in the flow reactor, $Ca(OH)_2$ was produced in the laboratory from a parent material of calcined Presque Isle limestone. Limestone was calcined to CaO at 1000°C for 16 hr in a Lindberg furnace under a nitrogen flow of 6 l/min. Hydration was conducted in a laboratory-scale hydrator consisting of a 0.4 l Pyrex beaker suspended in a constant 100°C bath. A mechanically propelled stirrer was used to mix the water and lime. Each hydration was conducted by loading 10 g of dry lime into the hydrator and allowing the lime to achieve thermal equilibrium in the bath. The stirrer was started, and a single, rapid addition of 100°C water was syringed into the hydrator in the molar ratio of $H_2O/CaO = 2.6$. After 15 min, the hydration vessel was purged of remaining water vapor with nitrogen, leaving a thoroughly dry product. Modified hydrates were produced by dissolving a sufficient amount of additive in the hydration water to produce the desired mass concentration of additive in the product $Ca(OH)_2$. Mass percentages of lignosulfonate (based on CaO) in the hydration water were varied from 0 to 4 percent in an attempt to find the optimal concentration.

Hydrates discussed in the remainder of this paper were produced in a steam-jacketed Ross Ribbon Blender. To produce conventional $Ca(OH)_2$ the blender was loaded with 6.8 kg of pulverized CaO and allowed to reach a temperature of 30 to 50°C. A total of 3.7 kg of water was then added at a constant rate for 40 min. The blender was run for an additional 20 min while the heat of reaction drove off excess water, leaving a dry $Ca(OH)_2$ product [DH-$Ca(OH)_2$]. The procedure of producing surfactant-modified $Ca(OH)_2$ [SM-$Ca(OH)_2$] was identical except that 3.7 kg of water contained 0.102 kg of Lignosite. This yields a SM-$Ca(OH)_2$ product containing approximately 1 percent by weight of calcium lignosulfonate, a concentration that was shown (10) to be optimal for enhancement of SO_2 capture.

The electrically heated, isothermal reactor into which the hydrates are injected is shown in Figure 1 and described in detail elsewhere (11). The reactor is operated at nominal temperatures of 700-1000°C, and nominal residence times of 0.6-2.0 sec. Residence time was adjusted by varying the gas flow from 17.77 to 4.07 l/min at standard temperature and pressure (25°C, 760 mm Hg). Gas composition is 95 percent N_2 and 5 percent O_2. In experiments where Ca utilization is of interest, 3000 ppm SO_2 is used. Determinations of properties as a function of particle size are made by using a Gelman inertial impactor downstream from the flow reactor.

The degree of dehydration in samples is determined using a DuPont 951 Thermogravimetric Analyzer. Specific surface area, porosity, and pore size distribution are measured by N_2 adsorption/desorption in a Micromeritics Digisorb 2600 Autoanalyzer. Ca utilization is calculated after analyses for calcium by atomic absorption spectrophotometry and for sulfate by ion chromatography. No sulfur species other than sulfate have been detected.

RESULTS AND DISCUSSION

Early laboratory testing of surfactant-modified $Ca(OH)_2$ indicated that calcium lignosulfonate was capable of decreasing median particle size and substantially enhancing reactivity with SO_2. The results of sulfation testing have been reported elsewhere (10) and are redrawn in Figure 2. It can be seen that approximately 1.5 percent calcium lignosulfonate produces the highest relative increase in Ca utilization of 20 percent. Figure 3 shows the results of aerodynamic particle size analyses using a cascade impactor. Particle size decreases from a mass median diameter of 12 μm for unmodified $Ca(OH)_2$ to 3 μm for $Ca(OH)_2$ containing 3 percent calcium lignosulfonate. It has been suggested that Ca utilization does not increase through the full range of particle size reductions because of the ability of excessive amounts of lignosulfonate to block access by SO_2 to the sorbent's pore structure. Sedigraph analyses on the fundamental particle size of the same materials showed a similar trend, but much smaller size reduction.

Other surfactants were also investigated during this study, and they are presented in Table 2. Also given in Table 2 are the concentrations of surfactants that were used as well as the resulting median particle diameters of SM-$Ca(OH)_2$. For the additives tested, median particle size varied from 2.9 to 10.2 μm.

Each chemically modified sorbent was reacted with SO_2 in the flow reactor. The flow reactor was operated at 1000°C, 1 sec residence time, and 3000 ppm SO_2 (with 5 percent oxygen and the balance nitrogen) for this series of experiments. The results are presented in Figure 4, which shows Ca utilization increase in relative percentage as a function of median particle size in micrometers. Surfactant modification can reduce sorbent particle size but, although beneficial, particle size reduction does not seem to be a prerequisite for increased SO_2 capture, especially below 5 μm. Reducing the median particle size from 10 to 5 μm resulted in a relative increase in Ca utilization of 3 to 17 percent. Further reduction to 3.5 μm particle size resulted in a relative increase of as much as 20 percent. The recent study by Simons (12), that used a validated model and assumed a porosity of CaO of 60 percent, predicted increases of reactivity for corresponding particle diameters of 10 and 15 percent. The comparison of those data with the data obtained during this study indicates that some effect other than particle size decrease must be responsible for the enhanced reactivity of surfactant-modified sorbent. Lignosite was the additive selected for further testing; therefore, batches of unmodified and modified (with 1 weight percent of Lignosite) sorbents were prepared in the Ross Ribbon Blender.

To document the effect of particle size in more detail, the data in Figure 5 were produced. Ca conversion as a function of particle size and residence time are shown for modified and unmodified $Ca(OH)_2$. The increase in Ca utilization as particle size decreases is expected, and shows that, where particle size can be reduced, SO_2 capture can be increased. The more important observation to be made from the data is that, for any given particle size, the modified sorbent is always more reactive than the unmodified sorbent showing, again, that particle size reduction is not a prerequisite for increased reactivity.

When lignosulfonate is used during the hydration of CaO, hydration becomes more difficult as evidenced by a slower rate of temperature rise. It was assumed, therefore, that dehydration of modified $Ca(OH)_2$ would be faster than for unmodified $Ca(OH)_2$. The advantage of this was believed to be that the reactive CaO species would be available longer for reaction with SO_2. Figure 6 shows that, at all residence times and temperatures, modified $Ca(OH)_2$ does dehydrate more quickly than unmodified $Ca(OH)_2$ as expected.

To determine whether accelerated dehydration is responsible for the increased reactivity of surfactant-modified sorbent, the Ca utilization achieved by a modified and unmodified $Ca(OH)_2$ is compared to that achieved by precalcines made from the same materials (SM-CaO and DH-CaO). Should dehydration alone be responsible for the increased reactivity of surfactant-modified sorbent, then both precalcined sorbents should react to the same extent. The precalcines were produced in such a fashion that the CaO made from each parent material had a similar surface area and porosity, eliminating structure as a possible explanation for differences in reactivity. Figure 7 shows, as has been observed before, that hydrates are more reactive than oxides. More importantly, it shows that the CaO made from modified $Ca(OH)_2$ exhibits a higher Ca utilization than the CaO made from unmodified $Ca(OH)_2$, suggesting that the rate of dehydration does not explain the observed differences in reactivity.

During pilot-scale testing of the surfactant-modified sorbent it was observed that, at higher temperatures, the enhancement in SO_2 capture was greater. This observation led to the suggestion that modified $Ca(OH)_2$ may be more resistant to sintering than unmodified $Ca(OH)_2$. To test the possibility, the flow reactor was operated without SO_2 so that changes in structure could be observed without the influence of product layer accumulation.

Figure 8 shows the decrease in surface area with increasing residence time for a series of temperatures. At all times and temperatures it can be seen that the modified $Ca(OH)_2$ retains more of its initial surface area than the unmodified $Ca(OH)_2$. Figure 9 shows that modified $Ca(OH)_2$ also retains more of its initial porosity, with the difference in modified and unmodified $Ca(OH)_2$ becoming greater at higher temperatures. Both of these figures suggest a reduced rate of sintering in the modified $Ca(OH)_2$.

Additional evidence for the difference in sintering behavior between DH-$Ca(OH)_2$ and SM-$Ca(OH)_2$ is given in Figure 10, which shows the surface area of calcines plotted as a function of particle size. This set of data was produced with a heated Gelman inertial cascade impactor attached directly downstream of the flow reactor. This setup minimized the contact of freshly calcined material with the ambient air. The flow reactor was operated at 1000°C, 1.25 sec residence time, with the process gas composed of 5 volume percent oxygen and the balance nitrogen. As can be seen in Figure 10, for each particle size measured, calcined SM-$Ca(OH)_2$ retained a higher surface area than calcined DH-$Ca(OH)_2$. The difference is particularly pronounced for particles smaller than 3 μm. For example, for the 1.83 μm particle size, measured surface area was 13.5 and 26 m^2/g for calcined DH-$Ca(OH)_2$ and SM-$Ca(OH)_2$, respectively. From the decreasing surface area with decreasing particle size of DH-$Ca(OH)_2$, it can be interpreted that sintering is more advanced in fine particles of DH-$Ca(OH)_2$. For the whole range of SM-$Ca(OH)_2$ particle size measured (11.9 to 0.74 μm), the surface area revealed little change, varying between 23.5 and 26 m^2/g. The comparison of results for DH-$Ca(OH)_2$ and SM-$Ca(OH)_2$ presented in Figure 10 indicates that surfactant-modified sorbent underwent significantly decreased sintering compared with conventional dry hydrated lime. With a reduction of particle size (below 5 μm) having been shown to be of secondary importance and an enhanced dehydration rate ineffective in increasing the reactivity of the modified sorbent with SO_2, a reduced rate of sintering appears to be the most acceptable explanation.

Since the sintering process of CaO proceeds by the mechanism of solid state diffusion it would seem that calcium lignosulfonate or its residue interferes with the diffusion mechanism. It is suggested that the presence of lignosulfonate or its residue may inhibit the exchange of CaO species with lattice vacancies. Since the molecular diameter of hydrated lignosulfonate is about 100 Å it is too large to enter the $Ca(OH)_2$ crystal structure; therefore, it is most likely to retard exchanges along pore surfaces and the migration of species along crystal boundaries.

CONCLUSIONS

The following conclusions are drawn from this study:

1) modification of $Ca(OH)_2$ with calcium lignosulfonate is effective in enhancing SO_2 capture by as much as 20 relative percent;

2) surfactant modification can reduce sorbent particle size in some applications but, although beneficial, particle size reduction is not a prerequisite for increased SO_2 capture;

3) surfactant-modified $Ca(OH)_2$ dehydrates more quickly than unmodified $Ca(OH)_2$ during furnace injection, but this does not appear to be the mechanism by which SO_2 capture is increased; and

4) surfactant-modified $Ca(OH)_2$ sinters more slowly than unmodified $Ca(OH)_2$ thereby preserving more reactive surface area and porosity. This appears to be the principal mechanism by which SO_2 capture is enhanced in modified sorbents.

ACKNOWLEDGMENT

This research was supported by the U.S. Environmental Protection Agency's Air and Energy Engineering Research Laboratory (AEERL). The authors wish to recognize the assistance of Monsie Bazemore, Kevin Bruce, and Laura Beach of the Acurex Corporation, and George Gillis of AEERL.

REFERENCES

1. Overmoe, B., Chen, S., Ho, L., Seeker, W., Heap, M., and Pershing, D. Boiler Simulator Studies on Sorbent Utilization for SO_2 Control. In Proceedings: First Joint Symposium on Dry SO_2 and Simultaneous SO_2/NO_x Control Technologies, Volume 1: Fundamental Research and Process Development, EPA-600/9-85-020a (NTIS PB85-232353), July 1985.

2. Beittel, R., Gooch, J., Dismukes, E., and Muzio, L. Studies of Sorbent Calcination and SO_2-Sorbent Reactions in a Pilot-Scale Furnace. In Proceedings: First Joint Symposium on Dry SO_2 and Simultaneous SO_2/NO_x Control Technologies, Volume 1: Fundamental Research and Process Development, EPA-600/9-85-020a (NTIS PB85-232353), July 1985.

3. Bortz, S. and Flament, P. Recent IFRF Fundamental and Pilot Scale Studies on the Direct Sorbent Injection Process. In Proceedings: First Joint Symposium on Dry SO_2 and Simultaneous SO_2/NO_x Control Technologies, Volume 1: Fundamental Research and Process Development, EPA-600/9-85-020a (NTIS PB85-232353), July 1985.

4. Slaughter, D., Silcox, G., Lemieux, P., Newton, G., and Pershing, D. Bench Scale Evaluation of Sulfur-Sorbent Reactions. In Proceedings: First Joint Symposium on Dry SO_2 and Simultaneous SO_2/NO_x Control Technologies, Volume 1: Fundamental Research and Process Development, EPA-600/9-85-020a (NTIS PB85-232353), July 1985.

5. Borgwardt, R., Bruce, K., and Blake, J. An Investigation of Product-Layer Diffusivity for CaO Sulfation. Ind. Eng. Chem. Res. 26: 1993, 1987.

6. Slaughter, D., Chen, S., and Seeker, W. Enhanced Sulfur Capture by Promoted Calcium-Based Sorbents. In Proceedings: 1986 Joint Symposium on Dry SO_2 and Simultaneous SO_2/NO_x Control Technologies, Volume 1: Sorbents, Process Research, and Dispersion, EPA-600/9-86-029a (NTIS PB87-120465), October 1986.

7. McCarthy, J., Chen, S., Kramlich, J., Seeker, W., and Pershing, D. Reactivity of Atmospheric and Pressure Hydrated Sorbents for SO_2 Control. In Proceedings: 1986 Joint Symposium on Dry SO_2 and Simultaneous SO_2/NO_x Control Technologies, Volume 1: Sorbents, Process Research, and Dispersion, EPA-600/9-86-029a (NTIS PB87-120465), October 1986.

8. Borgwardt, R. and Bruce, K. EPA Study of Hydroxide Reactivity in a Differential Reactor. In Proceedings: 1986 Joint Symposium on Dry SO_2 and Simultaneous SO_2/NO_x Control Technologies, Volume 1: Sorbents, Process Research, and Dispersion, EPA-600/9-86-029a (NTIS PB87-120465), October 1986.

9. Cole, J., Kramlich, J., Seeker, W., Silcox, G., Newton, G., Harrison, D., and Pershing, D. Fundamental Studies of Sorbent Reactivity in Isothermal Reactors. In Proceedings: 1986 Joint Symposium on Dry SO_2 and Simultaneous SO_2/NO_x Control Technologies, Volume 1: Sorbents, Process Research, and Dispersion, EPA-600/9-86-029a (NTIS PB87-120465), October 1986.

10. Kirchgessner, D., and Lorrain, J. Lignosulfonate-Modified Calcium Hydroxide for Sulfur Dioxide Control. Ind. Eng. Chem. Res. 26: 2397, 1987.

11. Kirchgessner, D., Gullett, B., and Lorrain, J. Physical Parameters Governing the Reactivity of $Ca(OH)_2$ with SO_2. In Proceedings: 1986 Joint Symposium on Dry SO_2 and Simultaneous SO_2/NO_x Control Technologies, Volume 1: Sorbents, Process Research, and Dispersion, EPA-600/9-86-029a (NTIS PB87-120465, October 1986.

12. Simons, G. Parameters Limiting Sulfation by CaO. AIChE J. 34: 167, 1988.

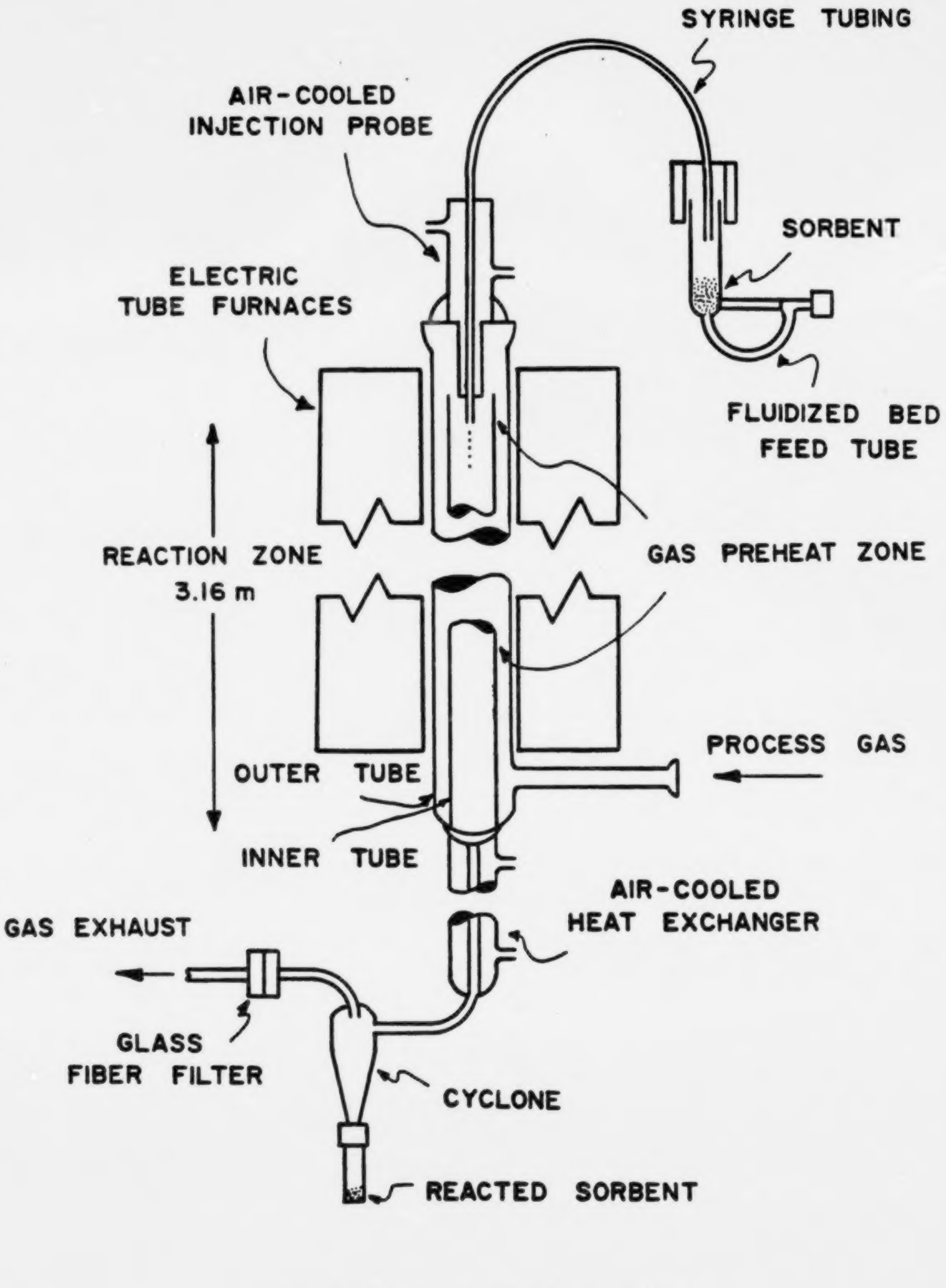
SYRINGE TUBING
AIR-COOLED INJECTION PROBE
SORBENT
ELECTRIC TUBE FURNACES
FLUIDIZED BED FEED TUBE
REACTION ZONE 3.16 m
GAS PREHEAT ZONE
PROCESS GAS
OUTER TUBE
INNER TUBE
AIR-COOLED HEAT EXCHANGER
GAS EXHAUST
GLASS FIBER FILTER
CYCLONE
REACTED SORBENT

Figure 1. Isothermal flow reactor.

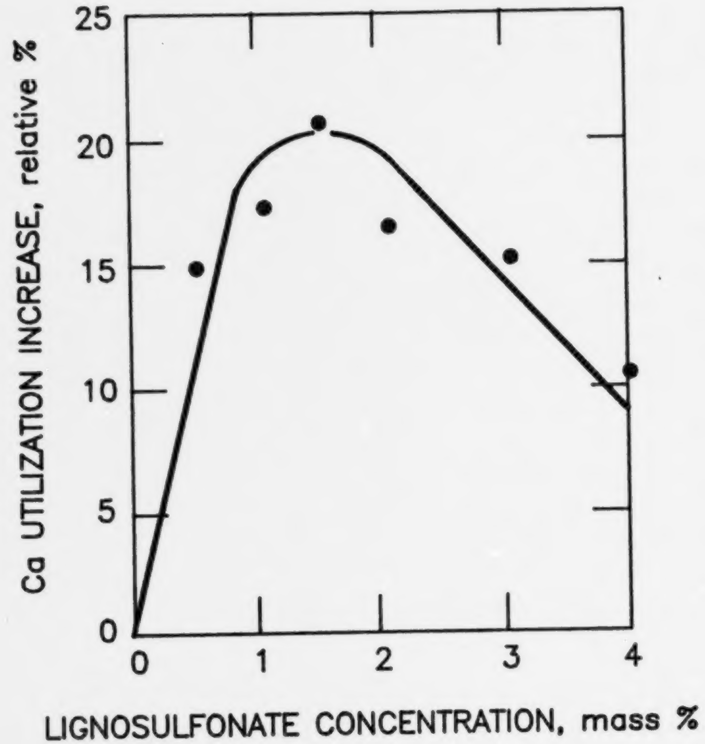

Figure 2. Effect of calcium lignosulfonate concentration on calcium utilization of $Ca(OH)_2$.

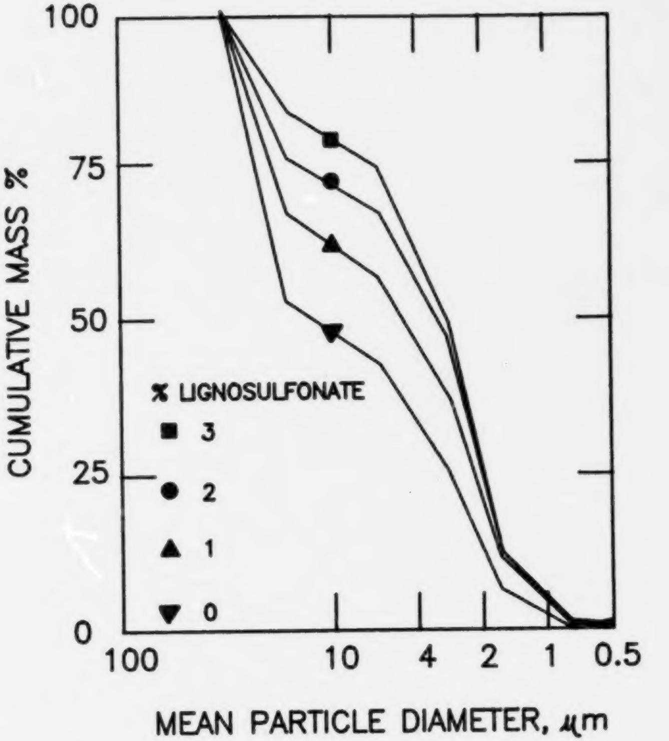

Figure 3. Effect of calcium lignosulfonate concentration on particle size distribution of $Ca(OH)_2$.

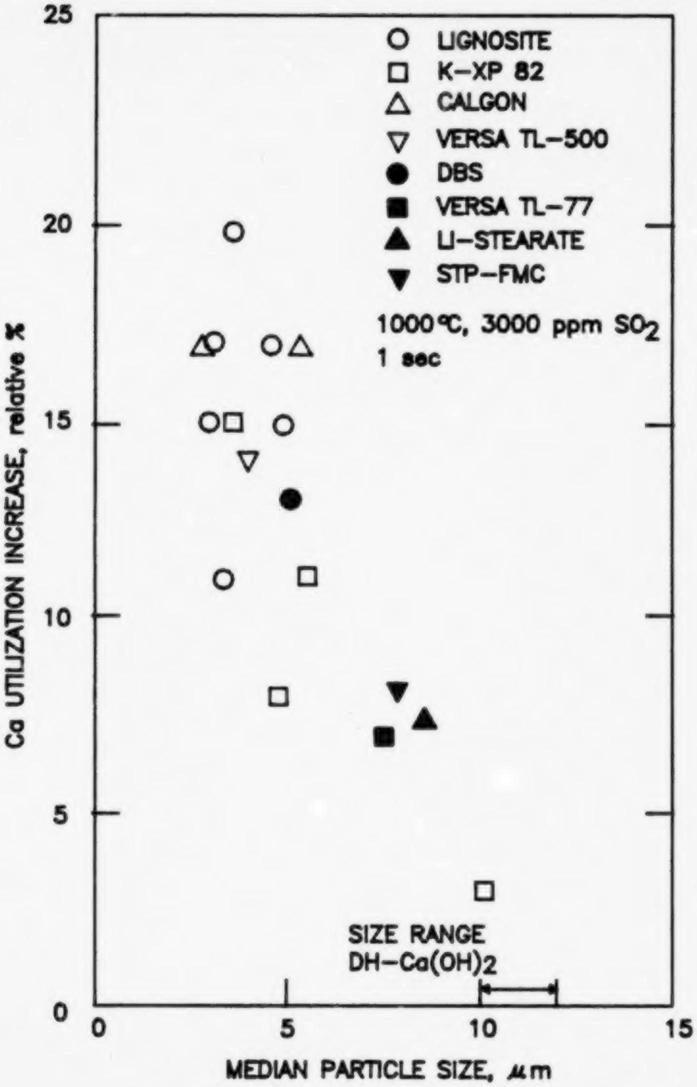

Figure 4. Effects of selected surfactants on Ca utilization and median particle size of $Ca(OH)_2$.

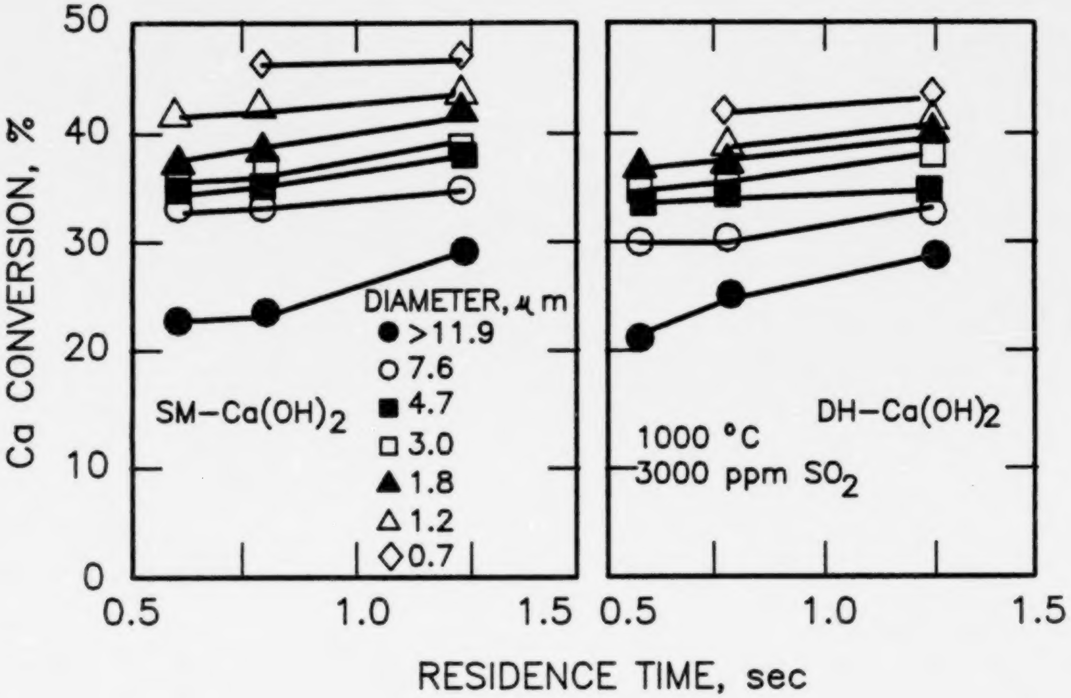

Figure 5. Calcium conversion as a function of particle size for modified and unmodified $Ca(OH)_2$.

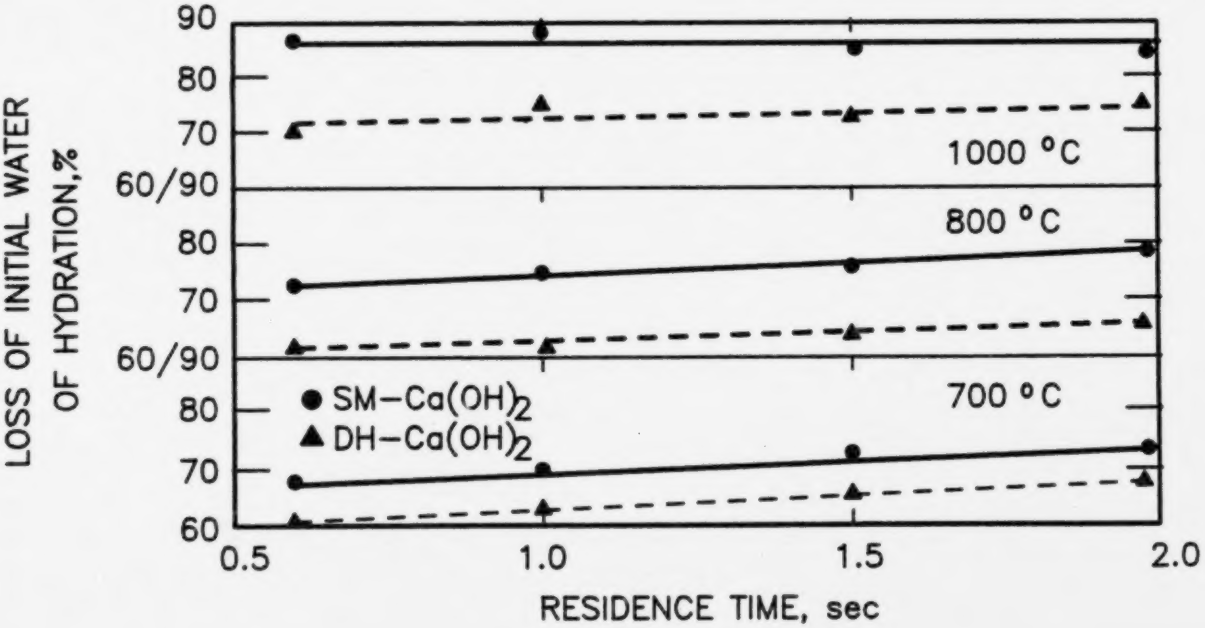

Figure 6. Loss of water of hydration as a function of time and temperature in modified and unmodified $Ca(OH)_2$.

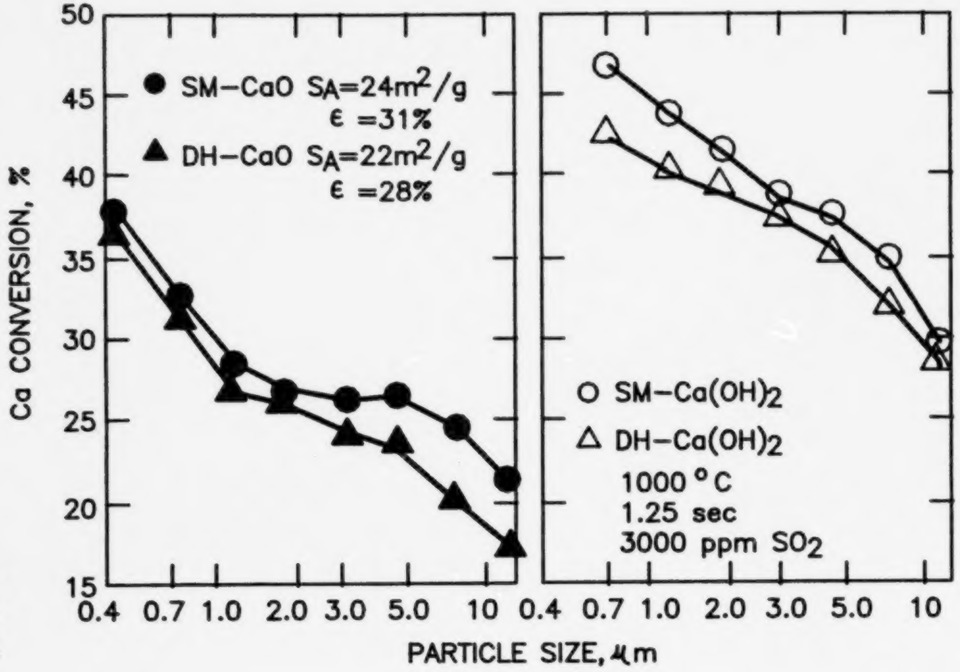

Figure 7. Calcium conversion as a function of particle size for modified and unmodified Ca(OH)$_2$ and for precalcines derived from them.

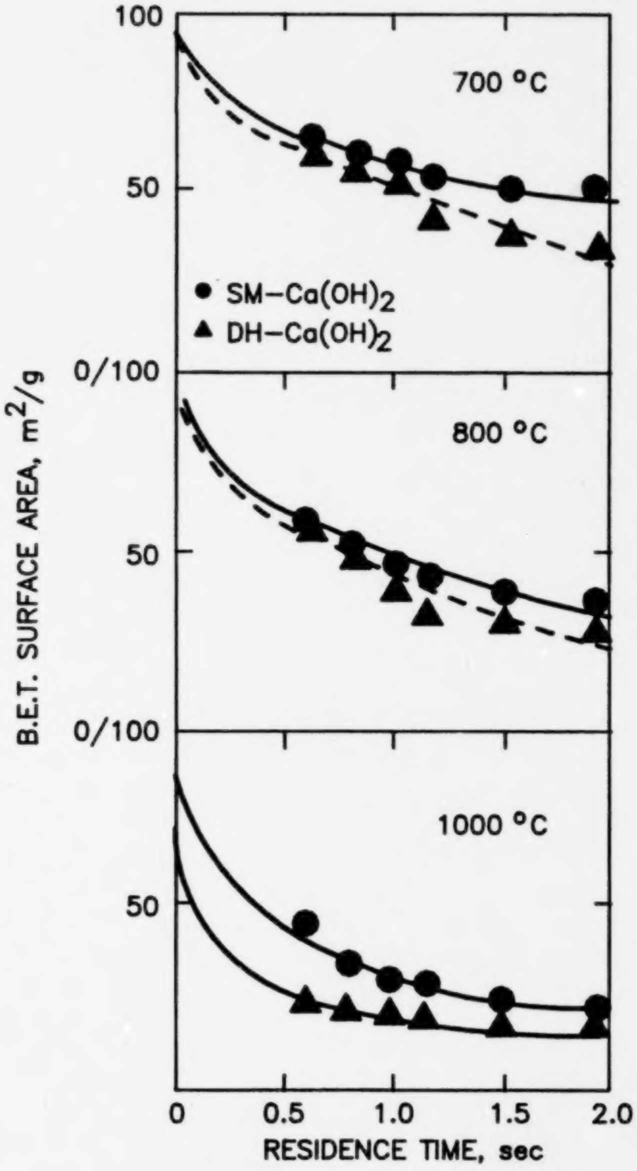

Figure 8. Reduction in specific surface area through sintering for modified and unmodified Ca(OH)$_2$ as a function of time and temperature.

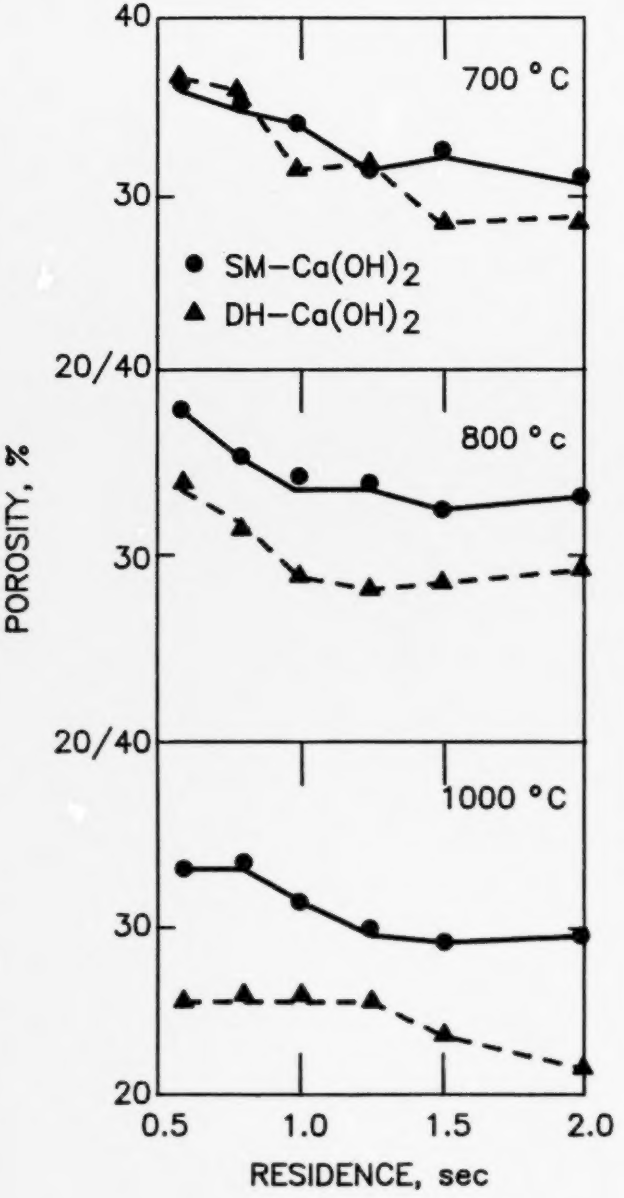

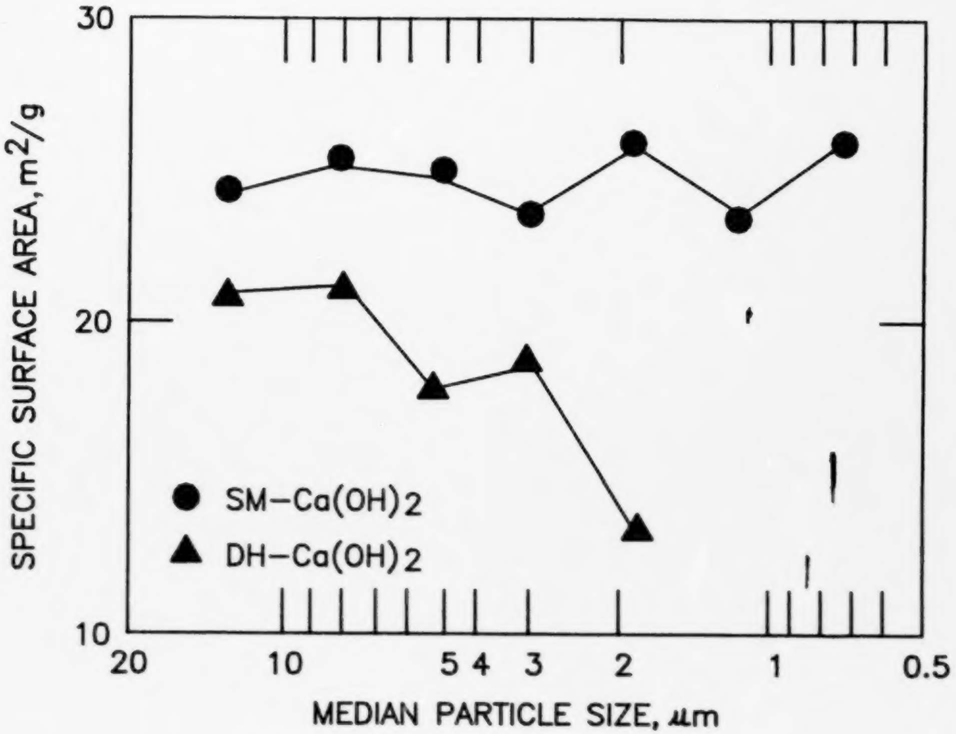

Figure 10. Reduction in specific surface area through sintering as a function of median particle size for modified and unmodified $Ca(OH)_2$.

Figure 9. Reduction in porosity through sintering for modified and unmodified $Ca(OH)_2$ as a function of time and temperature.

TABLE 1. RESULTS OF TESTING COMMERCIALLY PRODUCED CALCIUM-LIGNOSULFONATE-MODIFIED $Ca(OH)_2$

Facility	Size	Fuel	Increase in SO_2 Capture, relative percent
University of Utah	65 kW	Gas	15
Combustion Engineering	5 MW	Coal	13
Southern Research Institute	293 kW	Coal	6
Edgewater Plant	104 MW	Coal	4

TABLE 2. ADDITIVES USED TO PRODUCE CHEMICALLY MODIFIED SORBENTS

Name		Formula	Vendor	Weight concentration of additive, %	SM-$Ca(OH)_2$ D_{50}, µm
Trade	Chemical				
Lignosite	Calcium lignosulfonate	[a]	Georgia-Pacific	0.5	4.85
Lignosite	Calcium lignosulfonate	[a]	Georgia-Pacific	1.0	4.60
Lignosite	Calcium lignosulfonate	[a]	Georgia-Pacific	1.5	3.60
Lignosite	Calcium lignosulfonate	[a]	Georgia-Pacific	2.0	3.20
Lignosite	Calcium lignosulfonate	[a]	Georgia-Pacific	3.0	2.96
Lignosite	Calcium lignosulfonate	[a]	Georgia-Pacific	4.0	3.30
K-XP 82	Polyacrylic acid (partially neutralized)	$CH_3CHCOOHX$	B.F. Goodrich	10^{-3}	4.80
K-XP 82	Polyacrylic acid (partially neutralized)	$CH_3CHCOOHX$	B.F. Goodrich	$2 \cdot 10^{-4}$	6.50
K-XP 82	Polyacrylic acid (partially neutralized)	$CH_3CHCOOHX$	B.F. Goodrich	10^{-4}	3.70
K-XP 82	Polyacrylic acid (partially neutralized)	$CH_3CHCOOHX$	B.F. Goodrich	$5 \cdot 10^{-5}$	10.20
Calgon	Sodium hexametaphosphate	$(NaO)_2PO(NaOPOO)_n(NaO)_2POO$[b]	Beecham Products	1.0	5.30
Calgon	Sodium hexametaphosphate	$(NaO)_2PO(NaOPOO)_n(NaO)_2POO$[b]	Beecham Products	5.0	2.90
Versa TL-500	Sodium polystyrene sulfonate	$[CH_3CHC_6H_4SO_3Na]_n$[c]	National Starch & Chemical	1.0	4.00
Versa TL-77	Sodium polystyrene sulfonate	$[CH_3CHC_6H_4SO_3Na]_n$[d]	National Starch & Chemical	1.0	7.50
DBS	Sodium dodecylbenzene sulfonate	$C_{12}H_{25}C_6H_4SO_3Na$	Aldrich	1.0	5.10
Li-Stearate #306	Lithium stearate	$CH_3(CH_2)_{16}COOLi$	Witco Chemical	1.0	8.50
STP	Sodium tripolyphosphate	$Na_5P_3O_{10}$	FMC	1.0	7.80

[a] Estimated formula: $C_6C_{2.93}H_{7.86}O_{2.07}(OCH_3)_{0.88}(OOH)_{0.26}(SO_3M)_{0.48}(COOH)_{0.03}$.

[b] n = 15 - 20.   [c] Molecular weight = 500,000   [d] Molecular weight = 70,000

RESULTS OF WET FGD TESTING AT EPRI'S HIGH-SULFUR TEST CENTER

by: Robert E. Moser
Project Manager
Electric Power Research Institute
Palo Alto, California 94303

Jack M. Burke
Senior Staff Engineer

And

Sterling M. Gray
Engineer
Radian Corporation
Austin, Texas 78759

ABSTRACT

EPRI is managing the operation and testing of different FGD technologies at the High-Sulfur Test Center. Test work at this facility began in July, 1987 and significant results are now emerging. This paper summarizes the results of tests completed on two wet FGD test systems; one is a 4 MWe pilot scale system and one an 0.4 MWe mini-pilot system.

Results from the pilot-scale system have provided some useful data on the factors which affect limestone utilization and sulfite oxidation in a limestone FGD system. In addition, tests were conducted which quantify the effects of changing absorber feed tank volume and inlet SO_2 concentration on FGD system performance. While these results can be useful in specific situations, they will become more useful when they can be generalized using EPRI's FGD process integration and simulation model (FGDPRISM).

The tests completed on the mini-pilot system have investigated the chemistry of thiosulfate ion in limestone FGD systems. Significant results from these tests include:

- The existence of a threshold thiosulfate concentration. Above this concentration the thiosulfate degradation rate and the sulfite oxidation rate are very slow. The rates of degradation and oxidation increase rapidly below the threshold concentration.
- Trithionate is the only significant thiosulfate degradation product produced in the system. Over time, trithionate will hydrolyze to re-form thiosulfate. In addition, thiosulfate is lost through coprecipitation with the calcium sulfite waste solids produced in the system.
- Under certain circumstances, thiosulfate can have a significant effect on the dewatering properties of waste solids from a limestone system. A significant increase in the solids settling and filtration rates were observed at very low levels of sulfite oxidation (below 10 percent).

EPRI'S HIGH-SULFUR TEST CENTER

July 1987 marked the beginning of a multi-year research effort at the Electric Power Research Institute's High-Sulfur Test Center (HSTC). The HSTC is a research facility which is dedicated to aiding the utility industry in developing more cost effective and environmentally sound emission control technologies for use with high-sulfur coals. With the debate surrounding the sources of, and methods for reducing acid rain, the start-up of the HSTC is timely. It is anticipated that near-term research conducted at this facility will lead to reduced operating costs and improved reliability for flue gas desulfurization (FGD) systems now in operation. In addition, future work at the facility will help identify more cost effective FGD system design options for both new and retrofit applications. This work could save the utility industry hundreds of millions of dollars if future legislation mandates FGD retrofit.

The HSTC is located adjacent to New York State Electric & Gas (NYSEG) Corporation's 640-MW Somerset station which is about 45 miles northeast of Buffalo. The primary sponsor and manager of the HSTC research effort is EPRI. However, the potential impacts of acid rain legislation have sparked interest in the HSTC research agenda and EPRI has received major co-funding from a number of sources including:

- The New York State Electric & Gas Corporation;
- The Empire State Electric Energy Research Corporation;
- The New York State Energy Research and Development Authority;
- The Consolidation Coal Company; and
- The United States Department of Energy.

Together with EPRI, these co-sponsors form a steering committee to provide philosophical direction for the research projects at the HSTC.

HSTC CAPABILITIES

One of the key aspects of the HSTC design which will ensure that the facility fulfills EPRI's goals is its flexibility. Figure 1 is a simplified illustration of the various environmental control options which can be combined at the HSTC. The facility now includes three particulate control devices, pilot, mini-pilot, and bench-scale wet FGD systems, a pilot spray dryer FGD system, a lime-based dry injection system, and a paste slaker and ball mill grinding circuit for reagent preparation. For the most part, these particulate control, SO_2 control and reagent preparation sub-systems can be combined in any order to form an overall emissions control system.

Flexibility also exists within each sub-system. For example, the pilot wet FGD system can employ a number of waste solids dewatering options including a thickener, a horizontal centrifuge, a vacuum belt filter, and/or a hydrocyclone classifier. These options can be tested in various combinations to evaluate different primary and secondary dewatering schemes. This same degree of flexibility also exists in the modular fiberglass absorbers, the distributed process control system, and the physical configuration of the tanks and pumps which make up each process. Overall, the HSTC has the unique capability to simulate most current FGD system designs. It is also possible to modify the systems to incorporate new design options as they are identified.

HSTC WET SCRUBBERS

This paper presents preliminary test results from the HSTC pilot and mini-pilot wet FGD systems. The results presented are highlights of the research completed during the first 15 months of testing.

As mentioned, there are three wet FGD systems operating at the HSTC including:

- A pilot system which treats 12,000 acfm of flue gas;
- A mini-pilot system which treats 1000, acfm of flue gas; and
- A bench-scale system which treats 5 acfm of flue gas.

These three system sizes provide EPRI with the capability to investigate and develop promising new concepts in wet FGD technology. For example, a new performance additive can be quickly screened on the bench-scale system. Then, if the additive looks promising, it can be evaluated under more realistic conditions and for relatively low cost on the mini-pilot system. Assuming the additive continues to show promise, tests on the pilot-scale system can be used to further characterize the additive's performance and ultimately provide data which can be used to predict additive performance on commercial systems. In just such a screening process, tests using thiosulfate as an FGD additive are currently underway on the mini-pilot system and future thiosulfate tests are planned on the pilot scrubber.

Table 1 presents additional facts and figures on the HSTC pilot and mini-pilot systems. This table illustrates the range of operating conditions which can be achieved by each of these systems. As shown, several absorber configurations can be tested over a wide range of gas and slurry flow rates, inlet SO_2 concentrations, and reaction tank volumes. Both lime and limestone reagents can be tested and a range of reagent characteristics can be obtained.

HSTC TEST PLANS

The overall goal of the HSTC wet FGD research program is to investigate ways of reducing the operating costs and improving the reliability of existing lime and limestone wet FGD systems. In addition, the test work should provide data which can be used to improve future wet FGD system designs. To meet this goal, EPRI has outlined two-year test plans for both the pilot and mini-pilot systems. These test plans comprise a series of individual test blocks which will focus on specific aspects of FGD system design or operation. The 1988 and 1989 test schedules for the pilot and mini-pilot systems are presented in Figure 2.

As Figure 2 shows, this test plan includes an 18-month series of additive tests on the mini-pilot system. These tests are scheduled to evaluate a number of different additives which can be used to modify FGD system operation. The additives tested will include oxidation inhibitors (e.g., the sodium thiosulfate tests now in progress), crystal growth modifiers (e.g., citric acid), and SO_2 removal efficiency enhancers (e.g., adipic acid). Additives will be tested both individually and in selected combinations to evaluate synergistic effects.

The additive tests on the mini-pilot system will be followed by a group of tests which will evaluate alternate reaction tank design concepts. It is expected that these tests will identify a tank design which will improve both the dewatering properties of waste solids and the limestone reagent utilization while minimizing the scaling potential within an FGD system.

On the pilot system, the major group of tests scheduled for 1988 are a series of baseline tests. The objective and results of these tests are discussed in detail later in this paper. Tests in 1988 will also include the first of five scheduled system-specific test blocks. In these tests, the pilot system will be configured and operated to address a specific problem or question for an EPRI member utility. In the first system-specific block, the tests will evaluate some of the issues involved in converting NYSEG's Somerset system from natural to forced oxidation operation.

Pilot system tests for 1989 are scheduled to begin with a series of reagent preparation tests. These tests will evaluate the performance of several different limestone reagents in an effort to correlate laboratory measurements with actual system performance. Following the reagent preparation tests, a second block of system specific tests will be conducted. (The research agenda for this block of tests has not been finalized.) Then, a series of additive tests will begin. The pilot scale additive tests will represent a further screening of additives or additive combinations identified during the extensive mini-pilot additive test block.

PILOT TEST RESULTS

A number of tests have been completed on the pilot wet FGD system since the unit began operation in 1987. The tests completed to date include:

- A series of tests using sodium carbonate reagent. The objective of these tests was to measure the gas-liquid contacting efficiency of different spray, tray, and packed absorber arrangements. The results of these tests will be available in an EPRI technical report in the near future.

- A series of tests aimed specifically at improving the SO_2 removal efficiency of the pilot absorber while using limestone reagent. In general, these tests dealt with the problem of minimizing the wall effects (i.e., the loss of SO_2 removal which results from slurry sprays impinging on the wall of the absorber) in the pilot absorber and are of little general interest.

- A series of baseline tests using limestone reagent. The overall goal of these tests was to measure the performance of the FGD system as a function of the more basic FGD design and operating variables such as pH and liquid-to-gas ratio. These tests will provide a basis for understanding the results of future tests (i.e., tests which modify the basic FGD system operation through the use of performance additives, alternate limestones, modified reaction tank designs, forced oxidation, etc.). These tests have also provided some fundamental information on limestone FGD systems which may prove immediately useful to system designers and operators.

The discussion which follows presents a synopsis of the baseline limestone tests completed to date and it highlights some of the more interesting results from these tests. It should be noted that efforts are currently underway to further generalize the baseline test results using EPRI's FGD process integration and simulation model (FGDPRISM). It is anticipated that the modeling effort should expand the usefulness of the tests results and it may also help provide direction for future tests.

TEST OBJECTIVES AND APPROACH

The overall goal of the pilot system baseline tests was to provide a foundation for the test work to follow. These tests were designed to characterize the behavior of the FGD system in response to basic system design variables so the effects of more complex changes can be evaluated. More specifically, Table 2 shows the process conditions which were varied and performance indicators which were measured during these tests.

Several approaches were considered for the baseline test plan including a statistical experimental design. Because a statistical design would require an excessive length of time to evaluate the seven process variables shown in Table 2, an "engineering" test plan was finally selected. This type of test plan quantifies the effects of different process variables by defining a "baseline" condition and then measuring system performance when a single process set point is changed from the baseline condition. For example, the baseline operating pH for the pilot FGD system is 5.5. The effect of pH on system operation was evaluated by conducting tests at pH 5.3 and 5.7 while all other variables were held constant. This approach allows the results of three or four tests to be evaluated independent of the remaining tests and it helps to quickly identify areas of investigation which offer the most promise.

SYSTEM DESCRIPTION AND TEST PROCEDURES

Figure 3 is a schematic of the pilot FGD system as it was operated during the baseline tests. Approximately 15,000 acfm of flue gas is withdrawn from NYSEG's Somerset station upstream of the electrostatic precipitator (ESP). This flue gas then passes through the HSTC pilot-scale ESP. At that point, some of the flue gas (approximately 12,000 acfm) is drawn into the pilot system gas loop where it is spiked with SO_2 before it enters the 5' diameter pilot absorber. Flue gas which bypasses the pilot absorber may either enter the mini-pilot system or be returned unscrubbed to NYSEG's stack. Flue gas flow to the absorber is controlled using a variable speed fan and a venturi flow meter. Just upstream of the pilot absorber, the flue gas is quenched with a blend of service water and recycled process liquor. This quench step prevents solids build-up at the point where the flue gas enters the pilot absorber.

In the absorber, flue gas flows up where it is contacted with slurry sprayed down through one or two spray levels located in the upper portion of the absorber. The distances from the center line of the absorber inlet to the lower and upper spray headers are 16' and 23' respectively. Each spray header is equipped with four Bete spiral spray nozzles (Model No. TF88XPN). One nozzle is located in the center of each quadrant of the absorber and the nozzles are angled toward the absorber's center to minimize the quantity of slurry sprayed directly on the absorber walls. Approximately 9' above the upper spray header the flue gas passes through a 2-stage mist eliminator before being returned to the Somerset duct just upstream of the stack.

Up to 1300 gpm of slurry can be fed to the absorber by two variable speed pumps (one for each spray header). Absorber effluent slurry returns to the absorber feed tank through an 8" diameter downcomer which enters the side of the tank. During the baseline tests, the absorber L/G was varied by removing one spray header from service although it is also possible to adjust flow using the variable speed pumps. The absorber feed tank is 9' in diameter and its level can be varied from 6' to 18' to provide a wide range of tank volumes for testing.

Limestone reagent for the pilot system is prepared on-site in a pilot scale closed loop grinding circuit using a 6' x 6' KVS ball mill. The grinding circuit is equipped with several sizes of hydrocyclone classifiers to provide a wide range of reagent grind sizes.

Calcium-sulfur waste solids are discharged from the system in a bleed stream from the absorber feed tank. This dilute stream is fed directly to a horizontal centrifuge where the solids are concentrated from about 12 percent to over 60 percent and then discharged into disposal bins and ultimately to NYSEG's FGD landfill. Clear liquor from the centrifuge is returned directly to the absorber feed tank and is also blended with service water. This blend is used for both mist eliminator washing and flue gas quenching.

As Figure 3 illustrates, the pilot system configuration was kept relatively simple during the baseline tests to minimize operating problems and to ensure that process conditions could be closely controlled. In particular, the use of the horizontal centrifuge for both primary and secondary dewatering of the waste solids minimized the system liquid volume and thus helped allow the calcium and chloride concentrations in the system to be maintained at a relatively constant level. The use of service water for reagent preparation also helped minimize system liquid volume although this did make closed-loop operation (with respect to process liquor) more difficult.

Figure 3 also identifies control loops for key process variables on the pilot system. Automatic, feedback controls are used to maintain gas flow, inlet temperature, inlet SO_2 concentration, absorber feed slurry pH, and absorber feed slurry flow at constant levels throughout a test. The dissolved calcium concentration is maintained at a constant level by daily addition of technical grade calcium chloride salt. Tank volume is manually maintained by adjusting the service water addition rate to the system to control tank level while the absorber feed slurry solids concentration is controlled by manually adjusting the centrifuge feed rate based on manual measurements of the solids content. After initial start-up problems, this set of controls has provided very stable system operation as evidenced by the low variability of the process performance indicators. For example, the standard deviation of the SO_2 removal efficiency measured during the baseline test was only 0.1 percent.

The specific procedures for each test involved several steps including:

- Establish the desired operating conditions by adjusting set points, spiking calcium chloride, etc.. Initial centrifuge feed rates were determined by material balance calculations.
- Allow the system to operate at the specified test conditions for three solid-phase residence times.
- Collect at least three sets of solid- and liquid-phase samples from the absorber feed tank over a two to three day period while operating conditions were maintained at specified levels. In the case of system upsets or shutdowns, tests were extended to ensure that at least three sets of samples could be collected at representative operating conditions.

The key criterion for all the tests was collecting representative solid and liquid phase samples from the absorber feed tank. These samples allowed measurement of limestone utilization, gypsum relative saturation, sulfite oxidation, solids settling rate, and solids filtration rate. The absorber's SO_2 removal efficiency was determined by continuously monitoring the inlet and outlet O_2 and SO_2 concentrations.

At the conclusion of each test, any required system maintenance would be performed and then conditions would be established for the next test. As part of the QA/QC effort, operating conditions were periodically returned to their baseline levels to ensure that SO_2 removal efficiency would also return to the baseline value. Other QA/QC measures included calibration of the absorber feed slurry flow meters, velocity traverses to check the venturi flue gas flow meter, twice-daily calibration of the feed slurry pH probes, and extensive daily calibration checks of the continuous SO_2 and O_2 analyzers.

OVERALL TEST RESULTS

Table 3 summarizes the results of the baseline tests completed as of September 30, 1988. As shown 17 of 21 planned tests have been completed. While the data in Table 3 provide a general overview of the test results, a more detailed review of these data are required to understand the implications of the baseline tests. The discussion which follows highlights some of the most significant findings of the tests completed to date. Specific areas which are addressed are:

- Factors which affect limestone utilization in the system;
- Factors which affect sulfite oxidation in the system;
- The effect of tank volume on process performance indicators; and
- The effects of inlet SO_2 concentration on process performance.

Limestone Utilization Results

A key measure of FGD process performance is the limestone utilization obtained in the system. Utilization is important for a number of reasons. For example, poor utilization increases FGD operating costs by increasing the quantity of reagent which must be purchased and and then processed in the limestone grinding circuit. Poor utilization also increases the volume of waste solids produced by an FGD system and thus the costs of waste disposal. And finally, there is a large volume of experimental evidence which shows that poor utilization increases the chances of mist eliminator plugging and scaling.

Utilization can also be too high. Operation at very high limestone utilizations requires low absorber feed slurry pHs. At low pHs, SO_2 removal efficiency will be adversely affected or the costs to achieve that removal efficiency will be excessive. Experience has shown that the optimum range for limestone utilization is in the 85 to 95 percent range.

By understanding the factors which control reagent utilization in an FGD system, existing systems can be made more cost effective and reliable and new FGD systems can be designed more intelligently. The baseline limestone tests represent the start of a significant data base on the factors which influence reagent utilization in an FGD system. Some of the more significant findings are reviewed in the discussion which follows.

Effect Of Calcium Carbonate Relative Saturation--

In most limestone FGD systems, the pH of the absorber feed slurry tank is the only variable which can be adjusted to control limestone utilization. A variable which is strongly dependent on pH is the calcium carbonate relative saturation. The pilot baseline test results have shown that one of the most significant factors affecting limestone utilization during the tests was the calcium carbonate ($CaCO_3$) relative saturation in the absorber feed tank. This is not surprising since the $CaCO_3$ relative saturation is a measure of the solubility of limestone as shown in Equation 1.

$$CaCO_3\ R.S. = [a_{Ca^{++}}] \cdot [a_{CO_3^{=}}] / k_{sp}[CaCO_3\ (s)] \qquad (1)$$

where k_{sp} is the solubility product constant for limestone and $[a_{Ca^{++}}]$ and $[a_{CO_3^{=}}]$ are the activities* of the calcium and carbonate ions in the FGD process liquor.

Figure 4 shows the relationship between limestone utilization and absorber feed $CaCO_3$ relative saturation for the baseline tests in which limestone grind, slurry solids concentration, and tank volume were held constant. Operating conditions which were varied during these tests include pH, L/G, inlet SO_2 concentration, and the dissolved calcium concentration. As shown, the dependence of limestone utilization on the $CaCO_3$ relative saturation is nearly linear over a wide range.

There are several well documented examples of how this information applies to FGD systems including the effect of elevated coal chloride concentrations and the effect of forced oxidation operation on limestone utilization. In the case of elevated coal chloride concentrations, the result is a high dissolved chloride concentration in a closed-loop FGD system. High chloride levels produce correspondingly high calcium concentrations which increase the $CaCO_3$ relative saturation and thus decrease limestone utilization. In the case of in-loop forced oxidation, the oxidation air tends to strip CO_2 from the process liquor, thus lowering the $CaCO_3$ relative saturation and increasing the limestone utilization.

What are the practical implications of the results illustrated in Figure 4? The data may be useful in situations where some degree of control can be exercised over the $CaCO_3$ relative saturation in the reaction tank. One possibility is to use air to reduce the $CaCO_3$ relative saturation. It may be possible to achieve the beneficial effects of stripping CO_2 observed in forced oxidation systems using a fraction of the air normally used for oxidation. For example, if small quantities of air are sparged into the reaction tank, it may be possible to improve utilization and more than off-set the cost for the air addition system. The feasibility of this concept obviously depends on the quantity of air needed and represents an area which will be evaluated in future HSTC screening tests.

Another situation where this knowledge could be useful is when a waste water stream is being used as FGD makeup. Given the choice of two streams, the one with the lower chloride concentration should be selected to minimize the impact on the $CaCO_3$ relative saturation of the FGD process liquor.

Effect Of Inlet SO_2 Concentration--

Another result of the relationship between $CaCO_3$ relative saturation and limestone utilization is the effect of inlet SO_2 concentration on limestone utilization. Figure 5 illustrates how a change in the inlet SO_2 concentration in the flue gas affected the $CaCO_3$ relative saturation in the absorber feed tank. As shown, the increase in the inlet SO_2 concentration caused a corresponding increase in the $CaCO_3$ relative saturation. This result is significant because it shows that an increase in inlet SO_2 concentration (i.e., coal sulfur content) should be expected to adversely affect limestone utilization.

Why does this occur? A material balance around the absorber feed tank shows that, as the inlet SO_2 concentration increases, the quantity of limestone which dissolves in the tank must also increase. Assuming that the carbonate concentration of the slurry exiting the absorber is relatively constant (i.e., in equilibrium with the flue gas), then an increase in the limestone dissolved in the absorber feed tank will elevate the $CaCO_3$ relative saturation in the tank and thus decrease the utilization. The decrease in utilization should be a direct function of how much additional limestone must dissolve in the feed tank.

---

* Activity is used to account for the non-ideal behavior of ions in solution. The activities of ions commonly found in limestone FGD systems can be calculated using EPRI's FGD LIQEQ program for MS-DOS™ compatible computers.

Sulfite Oxidation Results

In many FGD systems, the rate at which absorbed SO_2 (i.e., aqueous sulfite ion - $SO_3^=$) is oxidized to sulfate ion can significantly affect the reliability of the system. The reason this occurs is that, under certain circumstances, sulfite oxidation produces just enough sulfate ($SO_4^=$) to require a small quantity of gypsum ($CaSO_4 \cdot 2H_2O$) to precipitate. If the surface area of gypsum crystals available in the absorber feed slurry is too low, then gypsum will tend to grow on absorber walls and internals, mist eliminator surfaces, and on surfaces in the absorber feed tank. This typically occurs when the sulfite oxidation fraction is above 15 percent. As the oxidation fraction increases above 15 percent, the gypsum surface area will also increase and the tendency for scaling will decline. Limestone FGD systems are especially susceptible if the oxidation fraction varies widely within this range during normal operation (e.g., as a result of daily load swings). Below this level of oxidation, any sulfate ion produced coprecipitates with calcium sulfite as $CaSO_4 \cdot {}^1/_2H_2O$.

One measure of the gypsum scaling potential in a limestone FGD system is the gypsum relative saturation which can be calculated using Equation 2.

$$CaSO_4 \cdot 2H_2O \text{ R.S.} = [a_{Ca^{++}}] \cdot [a_{SO_4^=}] \cdot [a_{H_2O}]^2 \,/\, k_{sp}[CaSO_4 \cdot 2H_2O\ (s)] \qquad (2)$$

where k_{sp} is the solubility product constant for gypsum and $[a_{Ca^{++}}]$ and $[a_{SO_4^=}]$ are the activities of the calcium and sulfate ions and $[a_{H_2O}]$ is the activity of water in the FGD process liquor. If the gypsum relative saturation is below 1.0, this indicates that gypsum will tend to dissolve. At sulfite oxidation fractions less than about 15 percent, the gypsum relative saturation is typically below 1.0 since any sulfate which forms subsequently coprecipitates with calcium sulfite. As the gypsum relative saturation increases above 1.0 the scaling potential also increases. At gypsum relative saturations above about 1.3 the gypsum scaling potential increases very dramatically.

Recently, many utilities have experimented with the use of thiosulfate ion ($S_2O_3^=$), an additive which has been shown to inhibit sulfite oxidation. Given sufficient quantities of $S_2O_3^=$ in solution it is possible to maintain the sulfite oxidation fraction below the 15 percent level and thus maintain operating conditions where gypsum will not precipitate in the FGD system. In fact, if the oxidation fraction of sulfite is kept below 15 percent, existing gypsum deposits can actually dissolve.

The baseline pilot system tests were conducted without the use of $S_2O_3^=$ additive. Combined with the results of mini-pilot thiosulfate tests (discussed later in this paper) these data are improving our understanding of the factors which control sulfite oxidation in limestone FGD systems. The discussion which follows outlines the results of the pilot baseline tests with respect to sulfite oxidation.

Effect Of Absorber Feed Slurry pH And L/G--

One operating variable which would be expected to have an effect on the rate of sulfite oxidation in a limestone FGD system is the pH of the absorber feed slurry. A change in pH causes the concentration of several key species involved in the sulfite oxidation reaction to change. Specifically, the concentration of sulfite ion will increase as the pH increases while the concentrations of dissolved metals such as iron and manganese (which are believed to catalyze the oxidation reactions) can decrease. To some extent, these two changes will tend to off-set each other. But, in limestone FGD systems, a reduction in the concentration of dissolved metals can overwhelm a change in the sulfite ion concentration.

Figure 6 illustrates the measured effect of pH on the rate of sulfite oxidation for two L/Gs. As shown, pH appears to have only a minor effect on the oxidation rate over the range of pHs tested. Further, the directional effect of pH on the oxidation rate appears to differ at the two L/Gs tested. While this may be indicative of scatter in the test data and not a real trend, the significant result illustrated by Figure 6 is that little if any change in the rate of oxidation occurs over a reasonable range of pHs (i.e., a range which might be available to an FGD system operator). This indicates that, for the HSTC pilot system, little control of oxidation can be achieved by adjusting only pH. However, it is important to note that this result may be an artifact of the low sulfite ion activity* measured during these tests, of the specific pH range examined, or of the type and concentration of trace metal species dissolved in the FGD process liquor. Extrapolation of the test results to other regimes of limestone FGD system chemistry cannot be done at this time but it should become possible as the HSTC test work proceeds.

Figure 6 also illustrates effect of L/G on the sulfite oxidation rate. As shown, L/G has a very significant effect on the rate of sulfite oxidation. In fact, the sulfite oxidation rate was reduced 50 percent when the L/G was reduced from 120 to 60 gal/macf. This result implies that, for a relatively constant system chemistry, the rate of oxidation is related to the rate of oxygen absorption in the absorber which in turn, is a direct function of the absorber L/G.

Effect Of Inlet SO_2 Concentration--

Tests were conducted at three inlet SO_2 concentrations. Figure 7 illustrates how the change in SO_2 concentration affected both the rate of sulfite oxidation and the fraction of absorbed sulfite which was oxidized. As shown, the fraction of sulfite oxidized decreased dramatically as the inlet SO_2 concentration was increased. The change was so dramatic that the system went from operating in a regime with gypsum crystals present in the slurry to a regime where no gypsum was present. This type of behavior is well documented and is not surprising. What was more interesting, however, was the effect of inlet SO_2 concentration on the rate at which absorbed sulfite is oxidized.

Figure 7 shows that, while there was a large change in the fraction of sulfite oxidized, there was essentially no change in the rate of sulfite oxidation during these tests. This indicates that, even though the rate of SO_2 removal and the slurry chemistry in the absorber changed dramatically during the inlet SO_2 concentration tests, there was no change in the factor(s) which control the rate of sulfite oxidation.

How can these results be used by utility engineers? For one thing, it may allow FGD system designers to more accurately anticipate the fraction of absorbed sulfite which would be oxidized in an FGD system. And it may be possible to design systems which would have low levels of sulfite oxidation. For example, a system designed for low L/Gs and high inlet SO_2 concentrations would be expected to have a low natural oxidation rate and it might be possible to operate such a system without any gypsum present. This type of system could meet current SO_2 emission limits by incorporating adipic acid or some other SO_2 removal performance additive into the design. Of course the cost of such an additive would have to be justified by the savings associated with operating at reduced L/G (i.e., fewer recycle pumps to operate and maintain) and not by the expected impact on sulfite oxidation.

---

* Sulfite ion activity is reduced as the ionic strength of the FGD process liquor is increased. For the moderate flue gas chloride levels encountered at the HSTC, an ionic strength of 0.4 to 0.5 results during closed-loop, steady-state operation.

The baseline test results also provide additional understanding of the effects of changing load on oxidation rates. Because boiler excess air levels generally increase as the unit load decreases, the flue gas SO_2 concentration will decrease. Even assuming that the flue gas oxygen concentration has no effect on the rate of sulfite oxidation (this assumption appears to be valid for the HSTC pilot system), the sulfite oxidation fraction would be expected to increase due to the drop in the flue gas SO_2 concentration. If the oxidation rate does remain constant, then the change in sulfite oxidation fraction can be predicted by the change in SO_2 concentration. This type of analysis could be used to identify times when the gypsum scaling potential is high and steps could be taken to address the problem. For example, it might be possible to reduce the L/G in the absorber as the SO_2 concentration drops and this may provide enough flexibility to off-set the drop in inlet SO_2 concentration.

There are, of course other scenarios in which the oxidation results might be used. However, the maximum benefit from these results will come when future tests are conducted and a more complete understanding of the factors which control the rate of sulfite oxidation is obtained. Given such an understanding, it should then become possible to eliminate gypsum scaling as an operating problem in limestone FGD systems either by modification of system operation (e.g., the use of thiosulfate ion) or by careful design of new systems.

Effects Of Absorber Feed Tank Volume On FGD Performance

Slurry feed tank volume is considered a key design variable for limestone FGD systems because a number of important chemical reactions occur in this tank. Specifically, the tank must be sized to provide adequate time for limestone solids to dissolve and for calcium sulfite and sulfate solids to precipitate. If the tank is too small, poor limestone utilization may result. Another possible consequence of an undersized absorber feed tank is an increase in both the calcium sulfite and calcium sulfate relative saturations of the absorber feed slurry.

On the other hand, a tank which is oversized should provide good performance from a chemistry standpoint but it will result in excessive capital costs for the system. Therefore, an optimized tank design would be large enough to permit the dissolution and precipitation reactions to approach completion while minimizing the cost of the tank.

Three tests were conducted to evaluate the effects of changing the volume of the absorber slurry feed tank on the performance of the pilot FGD system. One of these tests was the baseline condition with a tank volume of 6000 gallons. This tank volume was selected to provide a slurry residence time of approximately 5 minutes and a solids residence time of about 12 hours (at 10 percent solids). These values are in the range of many utility FGD systems although the slurry residence time is on the low end of the range due to the high L/G ratio used in the pilot scrubber. The remaining two tests were conducted at volumes of 75 and 50 percent of the baseline volume. The objective of these tests was to quantify the changes which occur as the tank volume is reduced and to identify the optimum tank volume for the pilot FGD system.

Figure 8 presents selected results from the pilot tank volume tests. As shown, the $CaSO_3 \cdot {}^1/2H_2O$ and $CaSO_4 \cdot 2H_2O$ relative saturations actually declined slightly as the tank volume was reduced over the range of tank volumes tested. To understand the implications of this surprising result, the rate expression for the calcium sulfite and calcium sulfate precipitation reactions must be examined.

Equation 3 is a rate expression which has been shown to correlate experimental data for the precipitation of calcium sulfite and sulfate over the range of relative saturations typically encountered in limestone FGD systems.

$$r_p = k_p \cdot A \cdot (RS-1) \qquad (3)$$

where $\mathbf{r_p}$ is the precipitation rate, $\mathbf{k_p}$ is the precipitation rate constant, **A** is the crystal surface area available for precipitation, and **RS** is the relative saturation of the precipitating species. In an FGD system, as the reaction tank volume is reduced, the mass of crystals is also reduced. This would be expected to reduce the crystal surface area. Since the precipitation rate (i.e., SO_2 removal rate) is unaffected by changes in the tank volume, the relative saturations of the precipitating species would be expected to increase to satisfy the rate expression in Equation 3.

Why didn't the sulfite and sulfate relative saturations increase as the tank volume was reduced? Apparently, even though the total mass of crystals in the reaction tank was reduced at lower tank volumes, the total crystal surface area must have increased slightly. In other words, even though there were fewer crystals available as precipitation sites, the crystals had a higher surface area per unit mass (i.e., smaller crystals were formed at reduced tank volumes).

Figure 9 presents experimental evidence which confirms the trend toward smaller crystals. This figure illustrates how the filtration rate and the settling rate (as measured by the unit area required to obtain 30 percent solids in the thickener underflow) of the calcium-sulfur solids changed as the tank volume was reduced. As shown, the filtration rate decreased from 198 to 126 $lb/hr \cdot ft^2$ while the thickener unit area increased from 21.2 to 33.9 ft^2/tpd. Thus, for the HSTC pilot system, it appears that one of the most significant effects of reduced absorber feed tank volumes was not an increase in the scaling potential in the system but a degradation in the dewatering properties of the waste solids produced. One likely cause of this change is an increase in the energy per unit volume of slurry (i.e., specific energy) in the pilot system. As the tank volume was reduced, energy supplied by the recycle pumps and the tank agitator remained relatively constant. Since the energy added to the system determines the rate of crystal breakage, this increase in energy added to the slurry must have been responsible for the reduction in crystal size.

As discussed earlier, limestone utilization was also expected to be affected by the change in tank volume. Figure 10 illustrates how the utilization changed as the tank volume was reduced. As shown, the initial reduction in tank volume (from 6000 to 4500 gallons) did not appear to affect the utilization. However, the second change in volume (from 4500 to 3000 gallons) did cause a significant drop in reagent utilization. Overall, the observed trend in limestone utilization is consistent with the reduced time available for dissolution as the tank volume was lowered. However, the fact that the first reduction in volume did not affect the limestone utilization is indicative of a complex mechanism for limestone dissolution. Further tests are needed to completely understand the factors which affect limestone utilization in an FGD system.

Overall, the results of the reaction tank volume tests have added to the understanding of the role which tank volume plays in the FGD system design. For one thing, the test data show that it may be possible to operate with tank volumes which are much smaller than those found in most existing limestone FGD systems without encountering gypsum scaling problems. This may depend on the specific energy imparted to the slurry by pumps and agitators. The data also suggest that it may be possible to off-set changes in solids properties by increasing the solids content in the absorber feed tank. This option will be investigated in a future test.

Before these test results can be applied to systems with dissimilar aqueous chemistries (e.g., low calcium and chloride concentrations, high magnesium concentrations, etc.) additional review of the test data is required. This is one area where EPRI's FGDPRISM may permit generalization of the test results to other cases.

Effects Of Inlet SO_2 Concentration On SO_2 Removal Efficiency

The concentration of SO_2 entering an FGD system represents a major design variable, especially for very high sulfur systems where removal efficiencies must exceed 90 percent to meet the Federal New Source Performance Standards. System operators who must deal with varying coal sulfur levels also find this to be an important variable affecting the operation of their FGD system. In some cases, a load of high sulfur coal may force a unit derating to allow the FGD system to remain in compliance with emission limits.

Tests were conducted to evaluate the effect of inlet SO_2 concentration on the performance of the HSTC pilot system. As discussed previously, the change in SO_2 concentration was found to affect both the limestone utilization and the fraction of absorbed sulfite which is oxidized. The same tests have also provided some interesting results concerning the effect of inlet SO_2 concentration on the SO_2 removal efficiency. Figure 11 presents the results of two groups of tests which measured the change in SO_2 removal as the inlet concentration changed. Figure 11 actually shows SO_2 pickup (rather than removal) as a function of the inlet SO_2 concentration. SO_2 pickup represents the quantity of SO_2 absorbed per gallon of slurry recirculated through the absorber and is calculated by Equation 3.

$$SO_2 \text{ pickup} = \frac{k \cdot \text{Gas Flow} \cdot \text{Inlet } SO_2 \text{ Concentration} \cdot SO_2 \text{ Removal Efficiency}}{\text{Slurry Flow}} \quad (3)$$

where k is a constant containing the proper conversion factors to determine SO_2 pickup in units of mM.

As Figure 11 shows, the measured change in SO_2 pickup was a linear function of the inlet SO_2 concentration over the range of SO_2 concentrations tested. This result is significant because it allows the HSTC pilot system's SO_2 removal efficiency to be estimated very accurately for any inlet SO_2 concentration. If this result can be generalized, it could provide a utility engineer with a useful tool for projecting the impact of changing coal sulfur levels on the performance of an existing FGD system. Given SO_2 pickup rates at two inlet SO_2 concentrations, it is probably possible to accurately interpolate SO_2 removal efficiencies and it may also be reasonable to extrapolate the data to some extent. For example, extrapolation of the data at the lower SO_2 concentrations in Figure 11 (1500 and 2500 ppm) to the higher SO_2 concentrations predicts SO_2 removal efficiencies of 86.1 percent and 56.6 percent at high and low L/G respectively. These estimates compare to actual removal efficiencies of 85.2 and 57.0 percent respectively.

SUMMARY OF PILOT TEST RESULTS

A total of 16 baseline limestone tests have been completed on the HSTC pilot scrubber. These tests were conducted to provide a basis for comparing the results of subsequent tests which involve significant variations from the "basic" limestone FGD system design (i.e., natural oxidation, no additives, spray tower absorber). While meeting this objective, the tests have also provided insight into the fundamental mechanisms which control important rate processes in limestone FGD systems. New data on sulfite oxidation, limestone utilization, and the effects of key design variables represent tools which can be used by both system designers and utility engineers with existing FGD systems. It is anticipated that further review and analysis of the test data using EPRI's FGD PRISM program along with additional tests at carefully selected conditions will allow further generalization of the HSTC pilot results.

MINI-PILOT TEST RESULTS

The initial work on the HSTC mini-pilot system paralleled the tests conducted on the pilot system. The first tests used sodium carbonate reagent to evaluate the gas-liquid contacting characteristics of different absorber configurations. These tests were followed by a series of limestone baseline tests. Then, in early 1988, an extensive series of tests began to evaluate the use of thiosulfate ion (added as sodium thiosulfate) as an additive. The discussion which follows highlights some of the more significant findings from the thiosulfate tests. In addition, some general guidelines for thiosulfate use are presented. A more thorough evaluation of the mini-pilot thiosulfate test results is contained in a companion paper which covers the theoretical implications of the HSTC test results in combination with the results of laboratory scale tests sponsored by EPRI.

TEST OBJECTIVES AND APPROACH

The fraction of absorbed SO_2 which is naturally oxidized to sulfate ion can have a significant impact on the O&M costs and the reliability of a limestone FGD system. When the sulfite oxidation fraction is above 15 percent, conditions can exist which result in precipitation of gypsum on surfaces within the FGD system. Such deposits tend to grow and can eventually require a system outage for cleaning. However, if the sulfite oxidation fraction can be maintained below 15 percent, the system will be subsaturated with respect to gypsum. Under these conditions, gypsum will not form and existing gypsum deposits can actually dissolve.

Until recently, the fraction of absorbed SO_2 which is naturally oxidized to sulfate was considered an inherent characteristic of an FGD system which could not be changed easily. The use of forced oxidation, in which all of the absorbed SO_2 is oxidized using compressed air, represents one way to control oxidation. Another approach is to add a compound to the FGD system which inhibits the rate of the sulfite oxidation reactions and thus maintains the oxidation fraction below 15 percent. One such compound is sodium thiosulfate. The thiosulfate ion ($S_2O_3^{=}$) interferes with the sulfite oxidation reactions which normally occur in a limestone FGD system.

Prior to 1988, the use of thiosulfate in limestone systems had been the subject of limited pilot scale test work. In addition, several utility FGD systems had been using thiosulfate to control gypsum scaling on a permanent basis. However, the cost of sodium thiosulfate had limited the application of this additive to systems where gypsum scaling represented a severe economic penalty. Recently, however, utility interest in using thiosulfate has expanded. This is a result of tests at Public Service Of Indiana's Gibson Station which have shown that thiosulfate can be produced in a limestone FGD system from the addition of elemental sulfur. By using elemental sulfur as an additive, a given thiosulfate concentration can be maintained for 10 to 20 percent of the cost of adding sodium thiosulfate. This has greatly expanded the number of systems which can consider thiosulfate as a cost-effective technique for controlling gypsum scaling.

Because of the expanded potential for application of thiosulfate to utility limestone FGD systems, EPRI decided to focus the initial HSTC mini-pilot tests on this additive. The overall goal of these tests was to develop data and guidelines which would assist utility engineers considering the use of thiosulfate in existing systems. In addition, the specific objectives of the thiosulfate tests were to determine how the effectiveness and consumption rate of the thiosulfate additive are affected by basic FGD system operating variables such as pH, thiosulfate concentration, inlet SO_2 concentration, L/G, and the process solution chemistry (e.g., the dissolved sulfite concentration). Key process performance indicators to be measured during these tests included gypsum relative saturation, limestone utilization, sulfite oxidation, and the concentration of thiosulfate by-products such as trithionate ion ($S_3O_6^=$). As with the pilot system, and engineering test plan design was selected as the best approach for evaluating the thiosulfate additive.

SYSTEM DESCRIPTION AND TEST PROCEDURES

Figure 12 is a process schematic for the HSTC mini-pilot system. As this figure illustrates, the mini-pilot system is, in most respects, a 1/12 scale version of the pilot system. Approximately 1000 acfm of flue gas is drawn from the HSTC ESP loop at a controlled rate. The SO_2 concentration of this gas stream is controlled to a set level (typically 2500 ppm) by spiking before it enters the mini-pilot absorber. In the absorber, the gas is quenched using a blend of service water and recycled process liquor before it turns up and is contacted with the alkaline limestone slurry.

It is in the absorber where the principal difference between the pilot and mini-pilot systems exist. Because of the mini-pilot absorber's small diameter (18"), it is impossible to obtain representative SO_2 removal efficiencies using only spray nozzles (the sprayed slurry contacts the absorber wall almost immediately). Therefore the mini-pilot absorber contains a single spray nozzle in combination with a counterflow tray to provide gas-slurry contact. The tray has a hole-size (1-3/8") and an open area (27 percent) which are characteristic of many utility FGD systems. Above the spray, the flue gas passes through a single stage mist eliminator before being returned to the Somerset flue gas system.

Control loops on the mini-pilot system are also similar to those on the pilot. Automatic, feedback control loops regulate gas flow, inlet SO_2 concentration, inlet flue gas temperature, absorber feed slurry pH, and the absorber slurry feed flow rate. Tank volume is controlled by manually adjusting service water addition to the centrate tank while the slurry solids concentration is controlled by adjusting the centrifuge feed rate based on manual slurry density measurements. The dissolved calcium concentration is also maintained at a constant level by spiking technical grade calcium chloride to the system or in some cases, by operating with a controlled liquid blowdown from the process liquor loop.

Two types of thiosulfate tests have been conducted on the mini-pilot system; steady-state and spike tests. In the steady-state tests, either elemental sulfur or sodium thiosulfate solution is added to the absorber feed tank on a continuous basis to maintain a constant concentration of thiosulfate ion in the feed slurry. In a spike test, a quantity of solid sodium thiosulfate is added to the absorber feed tank to raise the thiosulfate concentration of the slurry to a specific level. Then the thiosulfate concentration is allowed to decline with time and the response of the system to this decline is measured.

The initial test plan called for most of the thiosulfate tests to be operated in the steady-state mode using emulsified elemental sulfur to generate thiosulfate ion in-situ. However, after several tests, it was determined that spike tests using sodium thiosulfate were easier to control and these tests actually provided more useful information than the steady-state type tests. Therefore, the majority of the thiosulfate tests have been spike tests.

As mentioned, the procedure for conducting the sodium thiosulfate spike tests involved an initial spike of solid sodium thiosulfate followed by a period (typically from five days to a week) during which the thiosulfate concentration gradually declined. Measurements of process performance were made as the thiosulfate concentration dropped. These measurements included twice daily samples for thiosulfate and trithionate (the primary product of thiosulfate degradation), and a complete analysis of the solid- and liquid-phases of the absorber feed slurry every other day. When combined with continuously collected process data, the chemical data allowed the effects of thiosulfate ion on process performance to be quantified. It was also possible to quantify the effects of changing process conditions on the rate of thiosulfate consumption by the system by using an unsteady-state material balance calculation.

OVERALL TEST RESULTS

The thiosulfate tests which have been completed on the mini-pilot system have provided some new insights into the use of thiosulfate in limestone FGD systems. For the most part the test results represent a refinement in the current understanding of the mechanisms involved in sulfite oxidation and the way in which the thiosulfate ion interacts with the oxidation reactions. These results are covered in depth in a companion paper titled "Inhibited Sulfite Oxidation by Thiosulfate:Laboratory Studies of Thiosulfate Chemistry and Reactions as Applied to Wet Lime/Limestone FGD Processes". However, some of the test results, which are of general interest, are summarized in the discussion which follows.

Thiosulfate Degradation And Loss Mechanisms

The first thiosulfate test conducted on the mini-pilot system was a spike test designed to identify the optimum thiosulfate concentration for use in subsequent tests. Sodium thiosulfate was spiked to a concentration of 2000 ppm and then the concentration was allowed to decline over a two week period. During this period, the operation of the mini-pilot system was exceptionally reliable and the system was operated continuously. As a result it was possible to complete accurate material balance calculations which allowed the rate of thiosulfate degradation to be estimated.

Before reviewing the results of the thiosulfate spike test, some background information is needed on sulfite oxidation and the role of thiosulfate in these reactions. Previous investigators have shown that sulfite oxidation proceeds by a free radical, chain reaction mechanism which consists of initiation, propagation, and termination steps. Example reactions for each of these steps include:

Initiation: $$SO_3^{=} + Fe^{+3} \rightarrow Fe^{+2} + SO_3^{\dot{-}}\text{[*]} \tag{4}$$

Propagation: $$SO_3^{\dot{-}} + O_2 \rightarrow SO_5^{\dot{-}} \tag{5}$$

$$SO_3^{=} + SO_5^{\dot{-}} \rightarrow SO_5^{=} + SO_3^{\dot{-}} \tag{6}$$

---

[*] $SO_3^{\dot{-}}$ is the sulfite free radical (i.e., the sulfite ion minus an electron).

$$SO_5^{=} + Fe^{+2} \rightarrow Fe^{+3} + SO_5^{\dot{-}} \qquad (7)$$

Termination: $$SO_3^{\dot{-}} + SO_3^{\dot{-}} \rightarrow S_2O_6^{=} \qquad (8)$$

Thiosulfate ion inhibits this chain of reactions by quenching the propagation step as illustrated by:

Quenching: $$S_2O_3^{=} + SO_3^{\dot{-}} \rightarrow SO_3^{=} + S_2O_3^{\dot{-}} \qquad (9)$$

$$SO_3^{\dot{-}} + S_2O_3^{\dot{-}} \rightarrow S_3O_6^{=} \qquad (10)$$

The major by-product of the quenching reactions is trithionate ion ($S_3O_6^{=}$) which ultimately reacts with water to regenerate thiosulfate ion:

Regeneration: $$S_3O_6^{=} + H_2O \rightarrow S_2O_3^{=} + SO_4^{=} + 2H^{+} \qquad (11)$$

This reaction path implies that the ratio of the thiosulfate to trithionate concentration will depend on the relative rates of the quenching and regeneration reactions. If the quenching reactions are fast relative to the regeneration reaction, a lower thiosulfate to trithionate ratio will exist at steady-state. If the regeneration reaction is faster, a higher thiosulfate to trithionate concentration ratio will result.

Figure 13 presents the measured change in thiosulfate and trithionate ion concentrations as a function of time for the 2000 ppm spike test. This figure also shows how the trithionate concentration should vary assuming that any thiosulfate not lost with the waste sludge liquor is converted to trithionate. As shown, the actual trithionate concentration is much lower than the predicted trithionate concentration. This indicates that the conversion of thiosulfate to trithionate and the subsequent loss of thiosulfate and trithionate in the waste sludge liquor is not the only mechanism for thiosulfate consumption.

In a search for alternate thiosulfate loss mechanisms, ion chromatographic analyses of process liquor samples were completed in an attempt to identify other species which might be formed by thiosulfate degradation. No species other than trithionate were found in significant concentrations. This indicates that thiosulfate was either being degraded to some species such as sulfate (which cannot be distinguished from background sulfate levels) or that the thiosulfate or trithionate was being coprecipitated with the calcium sulfite waste solids. Semi-quantitative analysis has subsequently shown that significant concentrations of thiosulfate do coprecipitate with calcium sulfite in the waste solids.

Another significant result illustrated by Figure 13 is the fact that the trithionate concentration was essentially constant over the entire range of concentrations measured during the 2000 ppm spike test. If thiosulfate degradation to trithionate is function of the thiosulfate concentration, the trithionate concentration should have declined as the thiosulfate concentration declined. The fact that the trithionate concentration was actually constant, however, implies that the rate at which thiosulfate is converted to trithionate was also constant. In other words, the rate of thiosulfate degradation to trithionate is independent of the thiosulfate concentration under the conditions of the 2000 ppm spike test. Why does this occur? The most likely explanation is that the rate of the quenching reactions, in which thiosulfate is converted to trithionate (Equations 9 and 10) are controlled by the rate at which the sulfite free radical is generated (Equation 4).

Another important result from the 2000 ppm spike test is the effect of thiosulfate concentration on the calcium sulfate relative saturation in the absorber feed slurry. Figure 14 shows that before thiosulfate addition, the gypsum relative saturation ranged from about 0.9 to 1.1. Following the addition of thiosulfate, the gypsum relative saturation dropped to less than 0.1 and remained at this level even though the thiosulfate concentration declined from 2000 ppm to 200 ppm during the test. This indicates that the ability of thiosulfate to inhibit sulfite oxidation was not a function of the thiosulfate concentration over the range of thiosulfate concentrations measured during this test. In other words, operation at 200 ppm thiosulfate provided the same benefits as operating at 2000 ppm thiosulfate but for a lower cost in thiosulfate additive. The fact that no further benefit resulted at higher thiosulfate concentrations is related to the discovery of a threshold thiosulfate concentration which is discussed below.

Thiosulfate Threshold Concentration

Perhaps the most significant finding of the thiosulfate tests on the mini-pilot system is that, under certain operating conditions, there is a thiosulfate threshold concentration. Above this concentration, both the rate of thiosulfate degradation to trithionate and the rate of sulfite oxidation are slow. Any increase in the thiosulfate concentration above the threshold level does not provide a further decrease in the rate of oxidation. Once the thiosulfate concentration falls below the threshold level, both the thiosulfate degradation rate and the sulfite oxidation rate increase dramatically.

Figure 15 presents measured thiosulfate concentrations as a function of time for spike tests at pH 5.2 and 5.5. As shown, at pH 5.2, the thiosulfate concentration declines rapidly once the concentration drops below about 300 ppm. At the same time the rate of sulfite oxidation increased dramatically. At pH 5.5, on the other hand, the decline in thiosulfate concentration is very gradual as the thiosulfate concentration drops from near 400 down to about 100 ppm. Subsequent tests at pH 5.0 have shown a threshold concentration closer to 500 ppm thus indicating the strong pH dependence of this phenomenon.

For the test at pH 5.2, the threshold thiosulfate concentration was approximately 300 ppm. If the thiosulfate concentration is maintained above this concentration, oxidation will remain low and the thiosulfate degradation rate will also be reduced. Material balance calculations show that operation at a thiosulfate concentration below 300 ppm actually results in higher thiosulfate use rates than operation at a concentration of 350 ppm.

How can this threshold level be explained and what does it mean to utility FGD engineers? The existence of the threshold level appears to be a function of the complex sulfite oxidation reaction path. If enough thiosulfate is present to destroy the sulfite free radicals formed by the reaction shown in Equation 4, then the oxidation chain reaction cannot propagate. However, if enough sulfite radicals are produced to participate in the propagation steps, even more sulfite free radicals are formed and the rate of thiosulfate degradation accelerates. The pH dependence of the threshold concentration is appears to be related to increased solubility of ferric iron at reduced pHs.

The practical application of the test data are relatively simple. First, a system which is considering using thiosulfate should operate the absorber feed tank at as high a pH as possible (consistent with good limestone utilization). And second, the quantity of thiosulfate maintained in the system should be just above the threshold concentration to maximize the benefits (i.e., reduced gypsum relative saturations) and minimize thiosulfate consumption. The threshold concentration for a given system can be determined by conducting a spike test similar to those done on the mini-pilot system. As a rule of thumb, higher threshold concentrations will occur at lower pHs and higher dissolved sulfite concentrations (e.g., in magnesium-enhanced systems).

Effect Of Thiosulfate On Waste Solids

Previous research has shown that the use of thiosulfate can have a significant impact on the characteristics of calcium sulfite waste solids produced in a limestone FGD system. Under conditions where the sulfite oxidation rate is reduced to very low levels and a very pure calcium sulfite crystal is produced, the calcium sulfite crystals grow larger and have a more regular shape. These crystals settle much more rapidly and actually seem to have dewatering properties similar to gypsum. Pilot tests which documented this phenomenon were conducted by TVA, and TVA researchers hold a patent (United States Patent 4,454,101 - June 12, 1984) on the use of thiosulfate for the purpose of improving the FGD waste dewatering properties.

Tests at the HSTC have provided additional insight into the phenomenon of improved dewatering when thiosulfate is used. Figure 16 shows scanning electron micrographs of sulfite crystals produced in the mini-pilot system with and without thiosulfate in the slurry. Operating conditions for the tests in which these samples were collected were otherwise identical. As shown, the sulfite crystals produced in the presence of thiosulfate have significantly different size and shape characteristics. The the settling rates for these two crystal types differed by about a factor of 10.

One implication of these results is the possibility that thiosulfate could produce crystals which would cause problems in existing dewatering equipment. In particular, a sludge thickener which was designed to handle the smaller, slower settling sulfite crystals typically produced without thiosulfate could encounter plugging or rake torque problems if larger crystals are produced. Test data have shown that these type of crystals only tend to form when the sulfite oxidation fraction is reduced to very low levels (less than 10 percent). A system where sulfite oxidation can easily be reduced to such low levels is one with high dissolved calcium and chloride concentrations (i.e., greater than 5000 ppm chloride). Under these conditions, the sulfite ion activity is very low and thiosulfate is particularly effective at reducing sulfite oxidation.

SUMMARY OF MINI-PILOT TEST RESULTS

A number of thiosulfate addition tests have been completed on the mini-pilot system. The results of these tests have some practical use for utility engineers considering the addition of thiosulfate for eliminating gypsum scale control. Specifically:

- The test data have shown that trithionate is the only significant degradation product from the use of thiosulfate in an FGD system;
- A threshold thiosulfate concentration exists under some operating conditions. Operating at thiosulfate concentrations just above this threshold level will maximize the benefit of using thiosulfate and it can actually reduce the costs of using thiosulfate relative to the cost of operating below the threshold concentration.
- Operating at higher pHs results in a reduced threshold concentration and in reduced levels of thiosulfate consumption.
- Operating at thiosulfate concentrations significantly above the threshold concentration does not appear to provide any further reduction in the gypsum relative saturation in the absorber feed liquor. Therefore, the "optimum" thiosulfate concentration is just above the threshold level.

- Under some circumstances, the use of thiosulfate can significantly alter the dewatering properties of the waste calcium sulfite solids. Care should be exercised to prevent serious operating problems in existing thickeners. Systems with high chloride concentration appear to be more likely to encounter this type of problem.

One goal of the thiosulfate test program which has not yet been met is the ability to predict the concentration of thiosulfate needed for a given FGD system. It is anticipated that future tests will help attain this objective.

DISCLAIMER

The work described in this paper was not funded by the U.S. Environmental Protection Agency and therefore the contents do not necessarily reflect the views of the Agency and no official endorsement should be inferred.

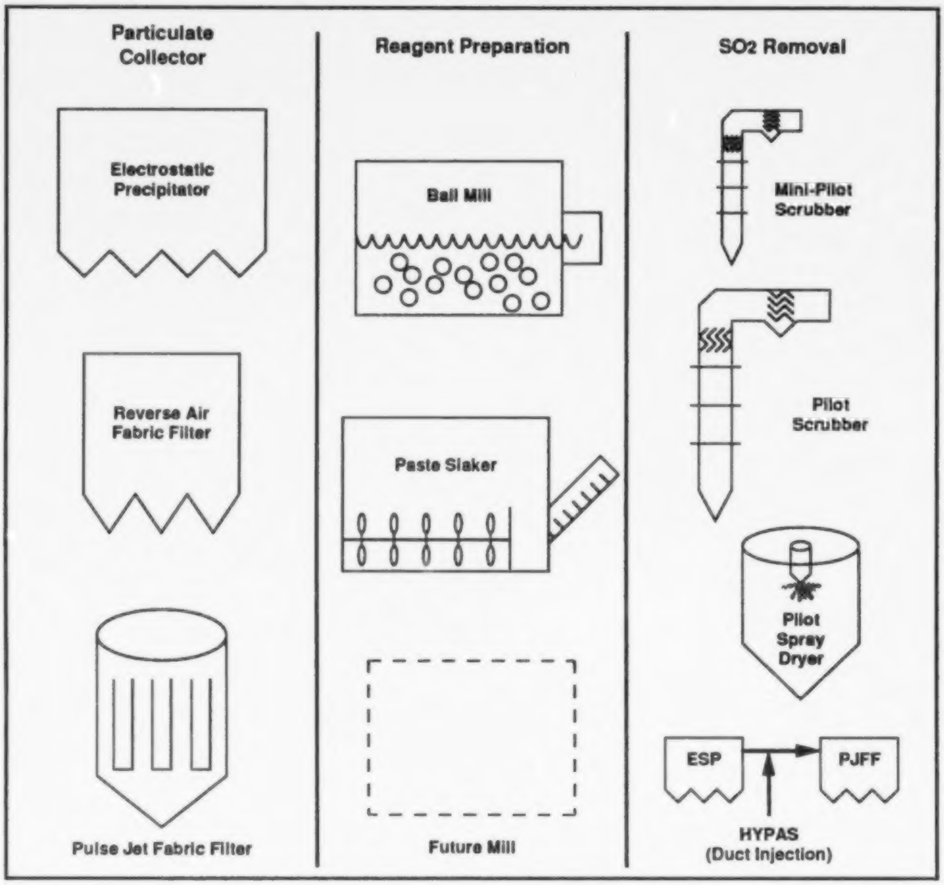
Particulate Collector
Reagent Preparation
SO2 Removal
Electrostatic Precipitator
Ball Mill
Mini-Pilot Scrubber
Reverse Air Fabric Filter
Paste Slaker
Pilot Scrubber
Pilot Spray Dryer
ESP
PJFF
HYPAS (Duct Injection)
Pulse Jet Fabric Filter
Future Mill

Figure 1. HSTC Equipment Configuration Options.

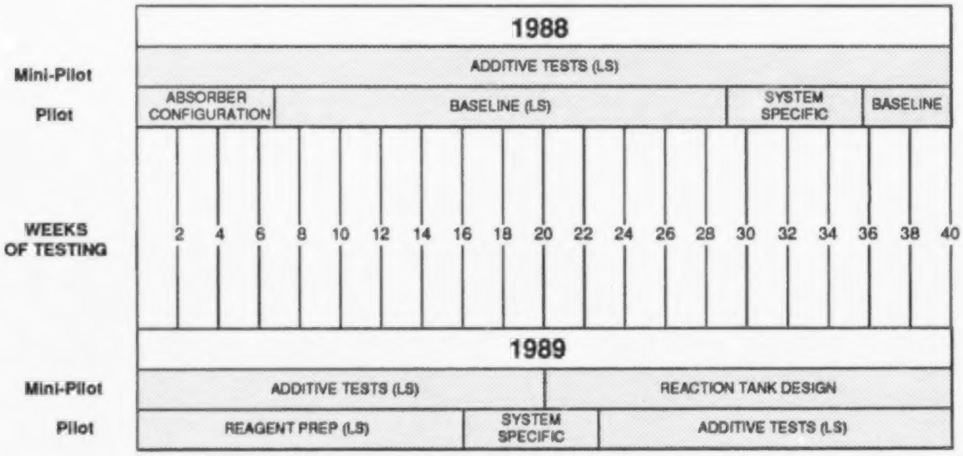

Figure 2. Two year HSTC wet scrubber test schedule.

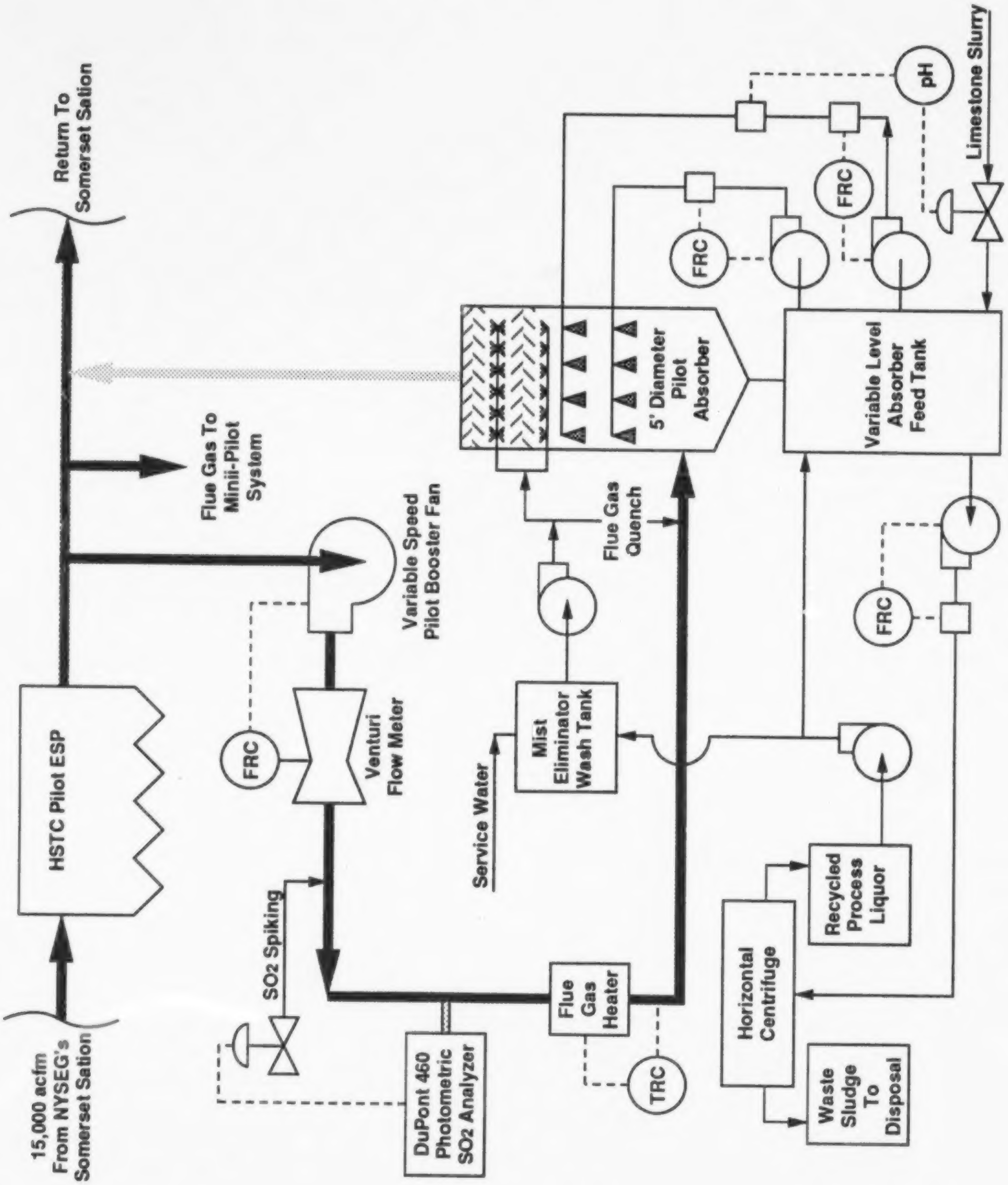
15,000 acfm
From NYSEG's
Somerset Sation
HSTC Pilot ESP
Return To
Somerset Sation
Flue Gas To
Minii-Pilot
System
Variable Speed
Pilot Booster Fan
FRC
Venturi
Flow Meter
SO2 Spiking
DuPont 460
Photometric
SO2 Analyzer
Flue
Gas
Heater
TRC
Service Water
Mist
Eliminator
Wash Tank
Flue Gas
Quench
5' Diameter
Pilot
Absorber
Variable Level
Absorber
Feed Tank
FRC
FRC
pH
Limestone Slurry
FRC
Horizontal
Centrifuge
Recycled
Process
Liquor
Waste
Sludge
To
Disposal

Figure 3. HSTC pilot FGD system flow schematic.

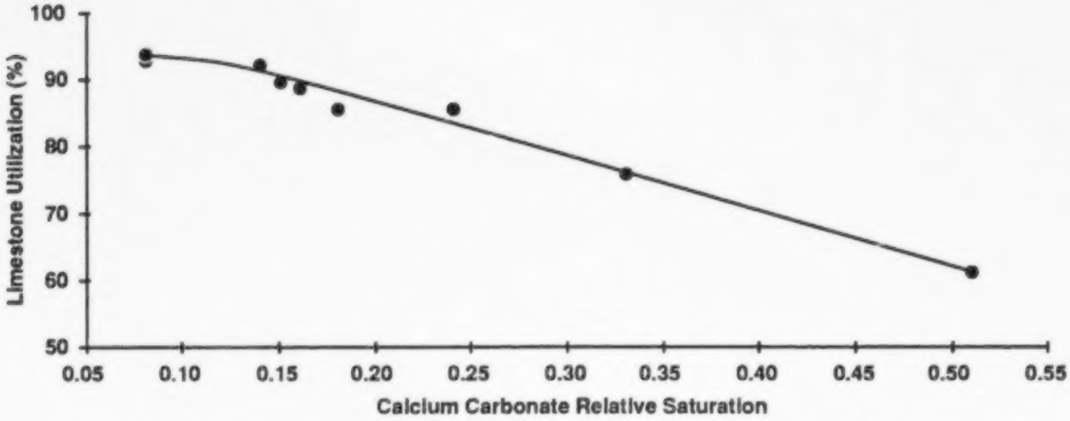

Figure 4. Limestone utilization vs. calcium carbonate relative saturation for the baseline tests.

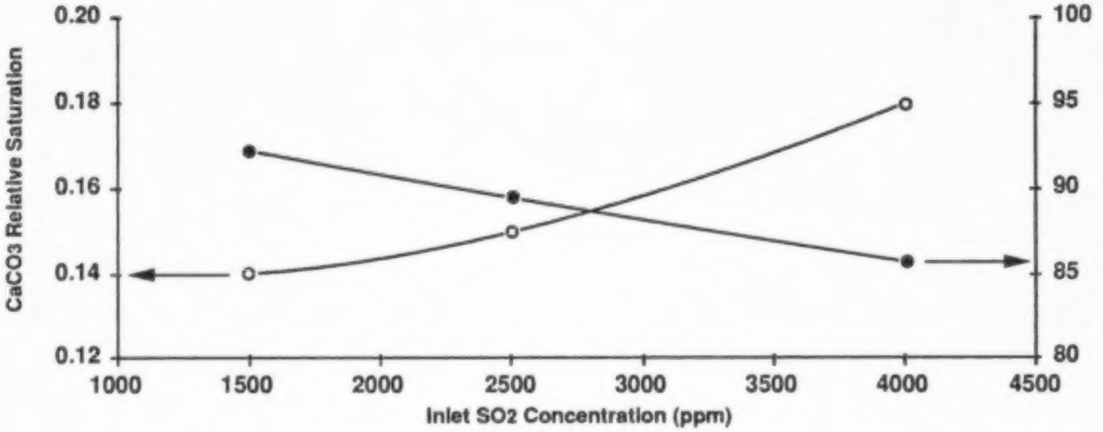

Figure 5. Effect of inlet SO2 concentration on CaCO3 relative saturation and limestone utilization.

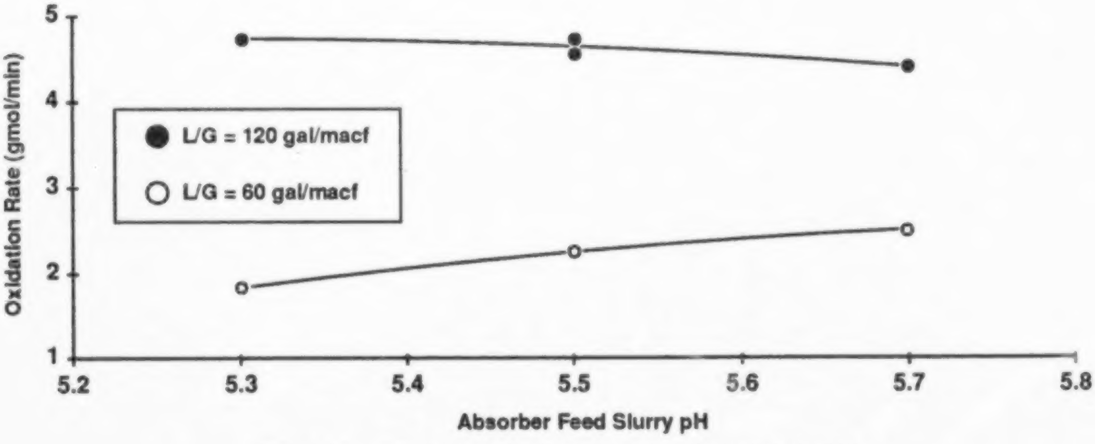

Figure 6. Effect of pH and L/G on the sulfite oxidation rate.

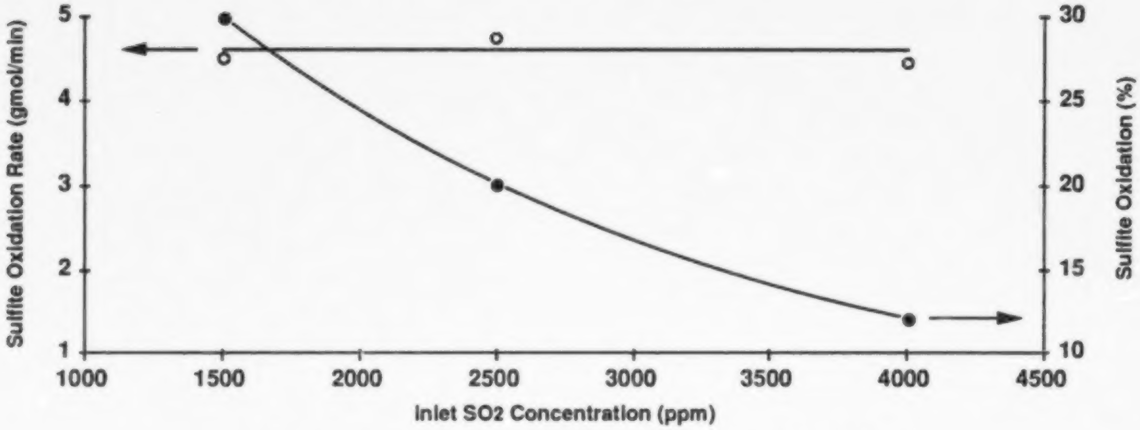

Figure 7. Effect of inlet SO_2 concentration on sulfite oxidation.

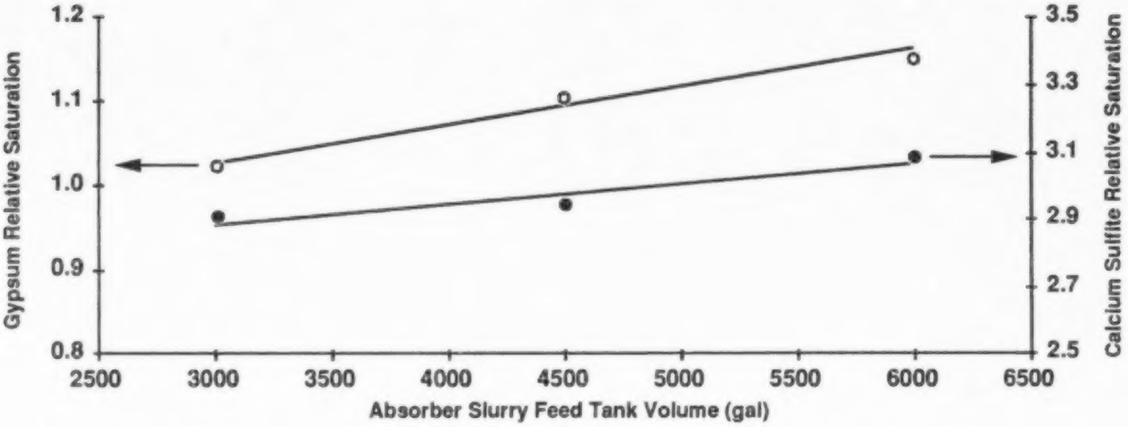

Figure 8. Effect of absorber slurry feed tank volume on calcium sulfate and sulfite relative saturations.

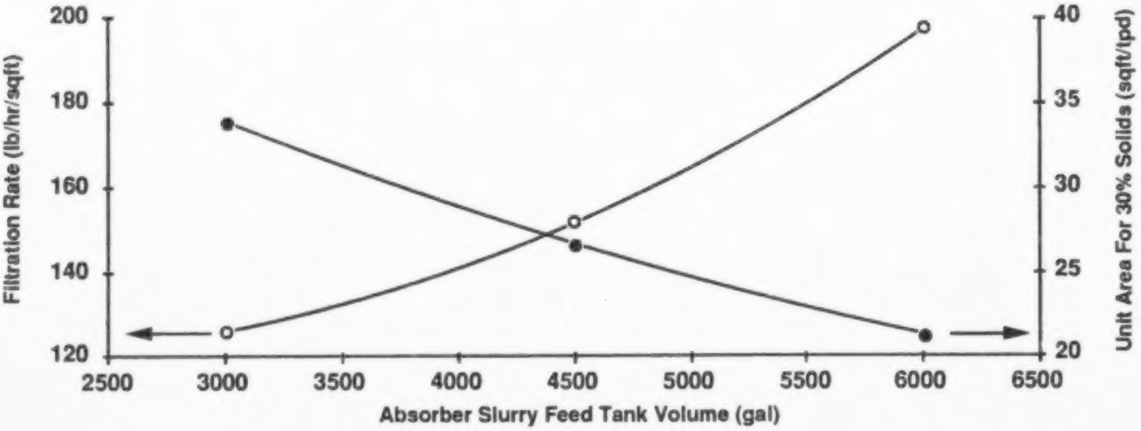

Figure 9. Effect Of Absorber Slurry Feed Tank Volume On Solids Dewatering Properties

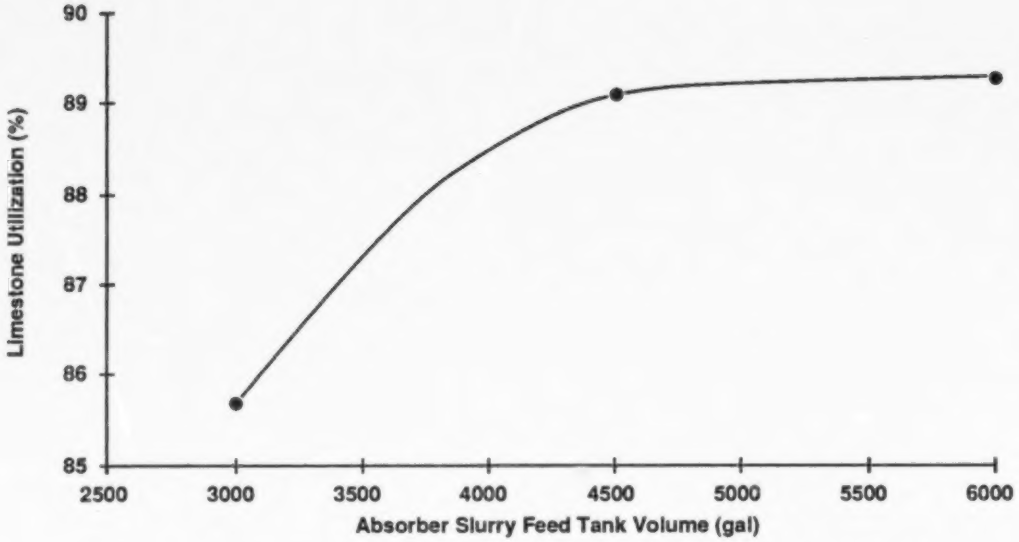

Figure 10. Effect of absorber slurry feed tank volume on limestone utilization.

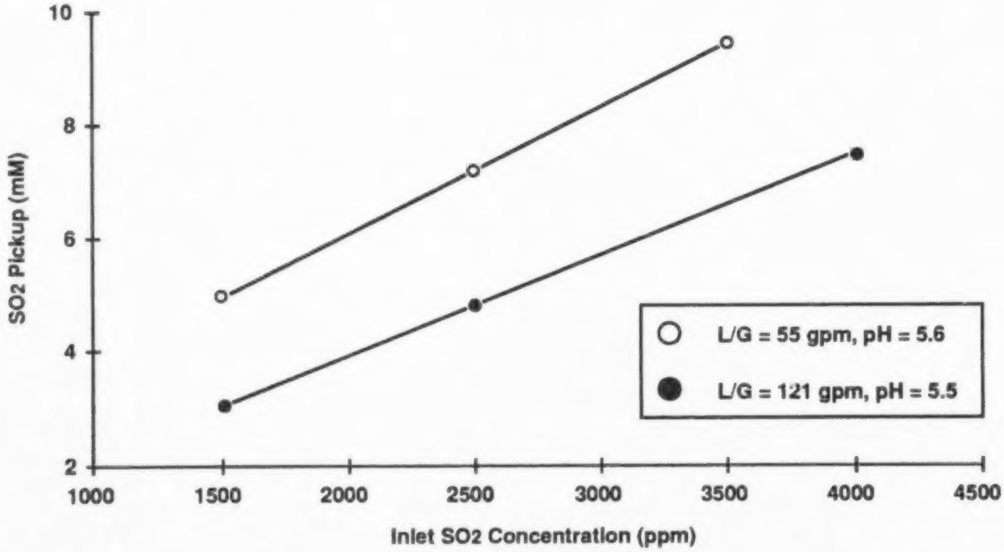

Figure 11. Effect of inlet SO_2 Concentration on SO_2 pickup.

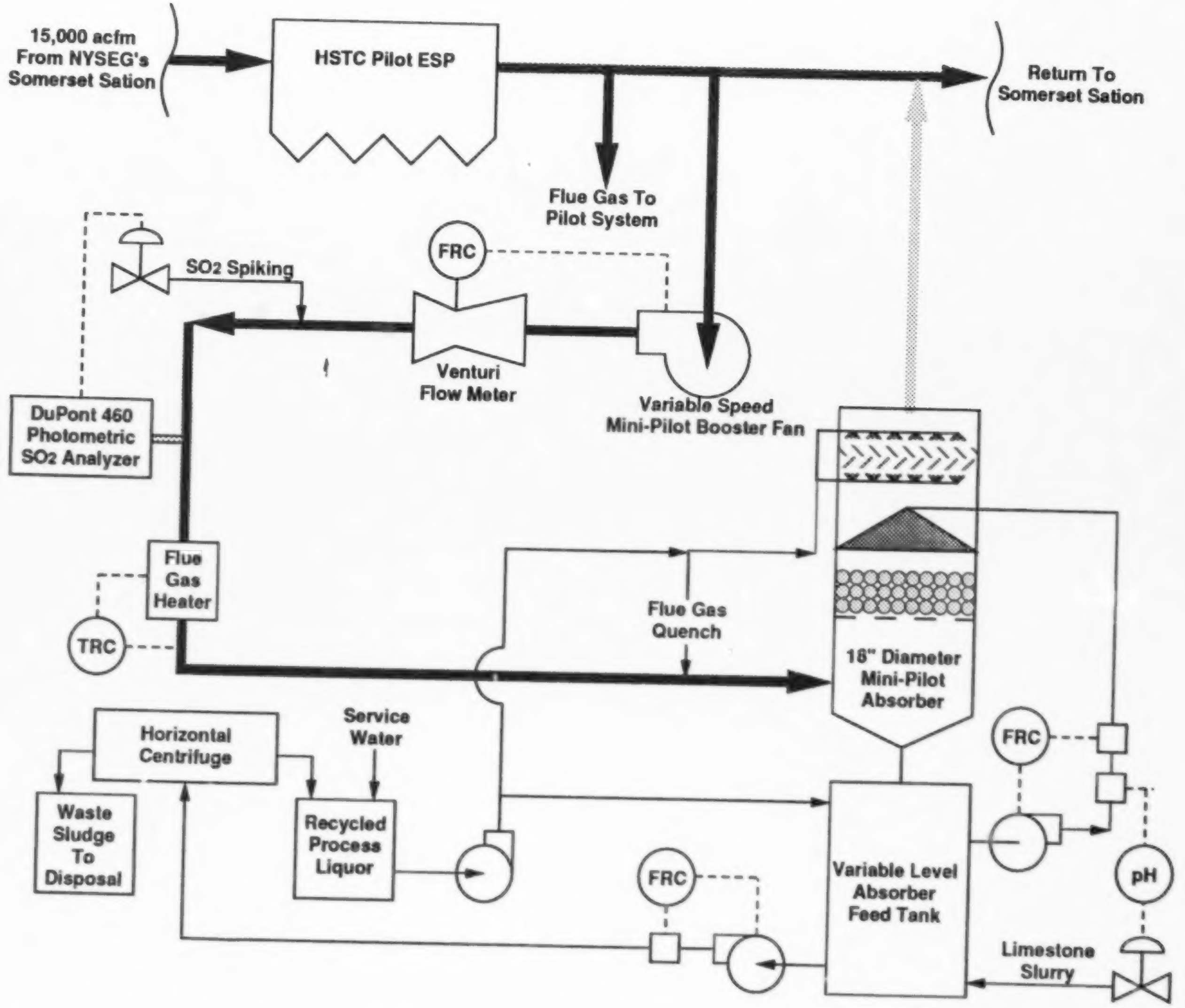
15,000 acfm
From NYSEG's
Somerset Sation
HSTC Pilot ESP
Return To
Somerset Sation
Flue Gas To
Pilot System
FRC
SO2 Spiking
Venturi
Flow Meter
Variable Speed
Mini-Pilot Booster Fan
DuPont 460
Photometric
SO2 Analyzer
Flue
Gas
Heater
TRC
Flue Gas
Quench
18" Diameter
Mini-Pilot
Absorber
Horizontal
Centrifuge
Service
Water
Waste
Sludge
To
Disposal
Recycled
Process
Liquor
FRC
Variable Level
Absorber
Feed Tank
FRC
pH
Limestone
Slurry

Figure 12. HSTC mini-pilot FGD system flow schematic.

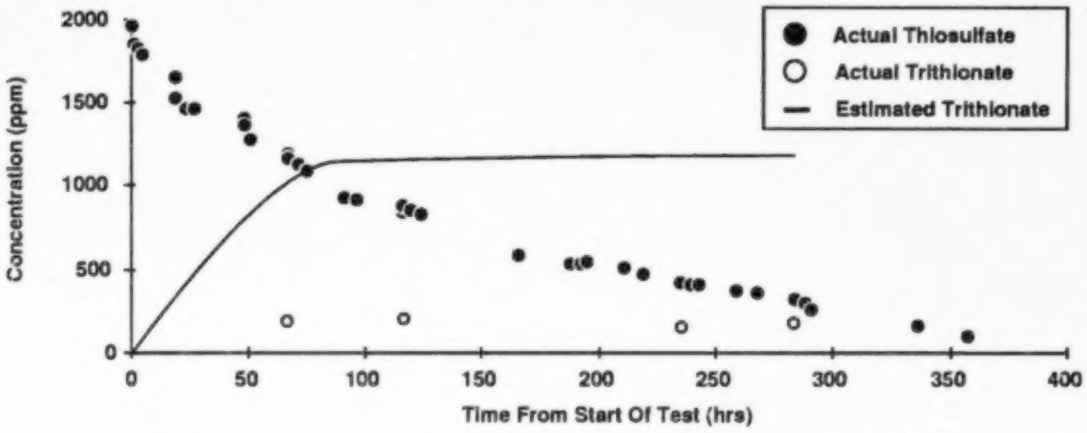

Figure 13. Actual and estimated concentrations for the 2000 ppm thiosulfate spike test.

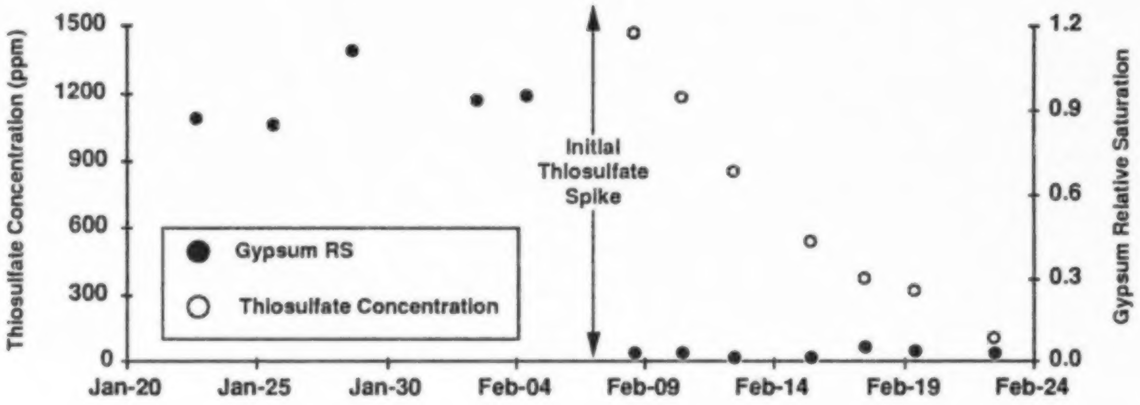

Figure 14. Gypsum relative saturations before and after thiosulfate addition.

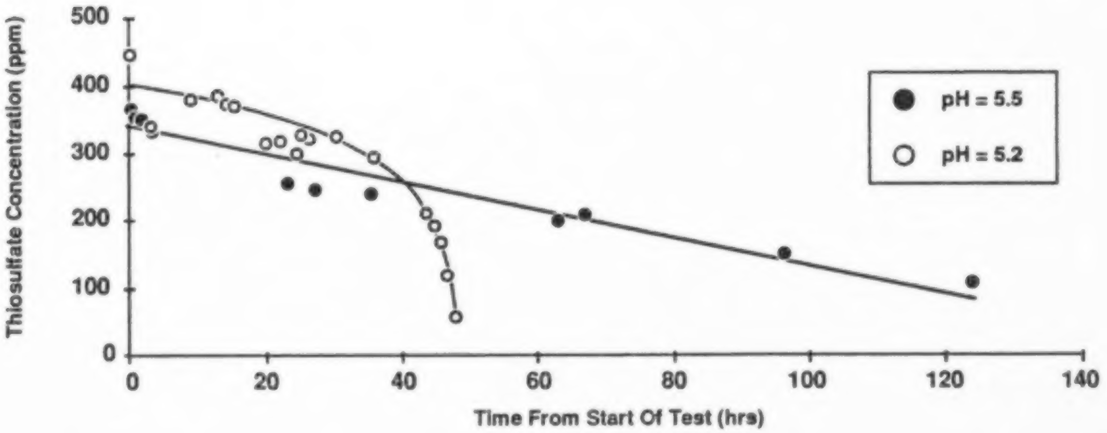

Figure 15. Thiosulfate concentration trends vs. pH.

Reproduced from
best available copy.

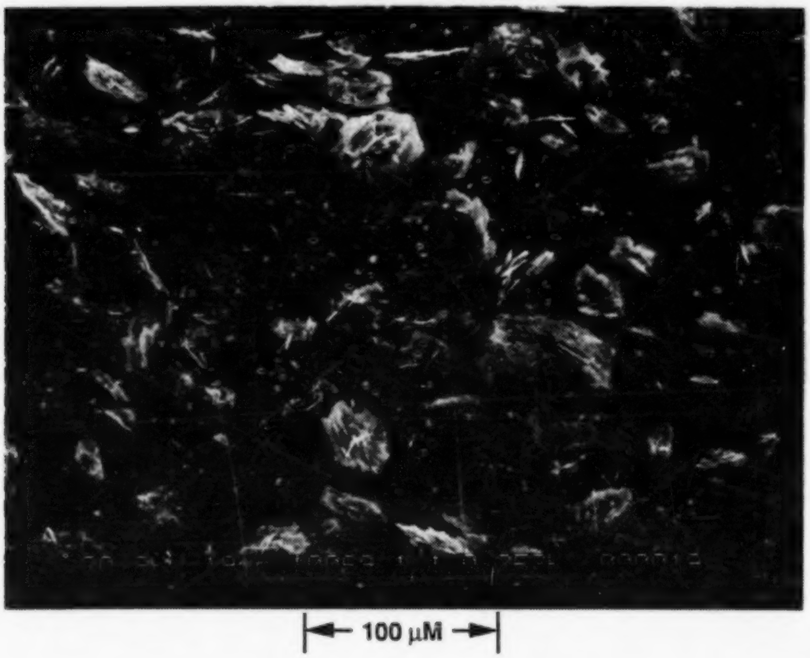

Calcium sulfite solids produced without thiosulfate present.

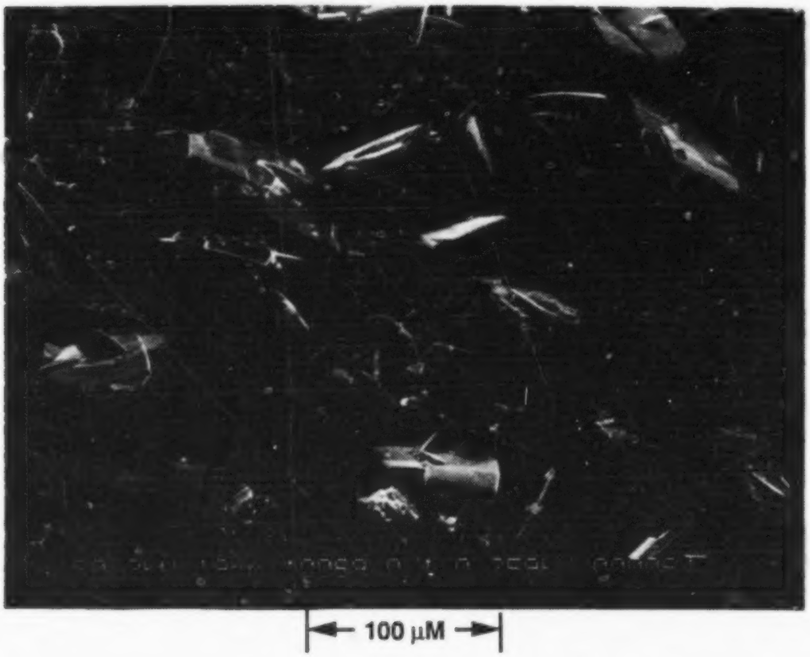

Calcium sulfite solids produced with thiosulfate present.

Figure 16. Scanning electron micrographs of mini-pilot waste solids produced with and without thiosulfate in the system.

TABLE 1. HSTC wet scrubber capabilities.

Capability	Range
	General
Inlet SO_2 (ppmv)	5000 to 1500
Limestone Grind	80% past 200 mesh to 98% past 325 mesh
L/G (gal/macf)	40 to 120
Solids Residence Time (hr)	8 to 24
Slurry Residence Time (min)	3 to 30
Absorber Gas Velocity (fps)	6 to 12
Inlet Gas Temperature (°F)	250 to 350
Reagent	Lime, Limestone, or Sodium Carbonate
	Pilot
Absorber	1 to 6 Spray Levels 1 or 2 Trays 1' or 2' of Packing Single or Dual Loop
Primary Dewatering	Thickener Hydrocyclone Horizontal Centrifuge
Secondary Dewatering	Vacuum Belt Filter Horizontal Centrifuge
Mist Eliminator	Vertical or Horizontal Gas Flow
	Mini-Pilot
Absorber	1 to 3 Spray Levels 1 or 2 Trays Single or Dual Loop
Dewatering	Horizontal Centrifuge
Mist Eliminator	Vertical or Horizontal Gas Flow

TABLE 2. Process variables and performance indicators for the pilot limestone baseline tests.

Process Variable	Performance Indicator
• pH	• SO_2 Removal
• L/G	• Sulfite Oxidation
• Inlet SO_2 Concentration	• Gypsum Scaling Potential
• Limestone Grind	• Limestone Utilization
• Reaction Tank Volume	• Solids Settling Rate
• Slurry Solids Concentration	• Solids Filtration Rate
• Calcium (Chloride) Concentration	

Table 3. Independent Variables And Measured Process Performance Indicators For The Pilot Variable Tests Completed Through September 1, 1988

Test ID	pH	L/G (gal/macf)	Inlet SO_2 (ppm)	Ca Activity (mmolar)	Solids (wt %)	Grind (% < 325)	Tank Volume (gal)	SO_2 Removal (%)	Limestone Utilization (%)	Sulfite Oxidation (%)	Gypsum Relative Saturation	Filtration Rate (lb/hr·ft^2)	Unit Area (ft^2/TPD)	$CaSO_3 \cdot 1/2H_2O$ Relative Saturation
PVT-1	5.5	120	2500	30	12	90	6000	88.3	89.3	19.0	1.15	198	21.2	3.09
PVT-2	5.3	120	2500	30	12	90	6000	84.4	93.0	*	1.19	*	*	2.95
PVT-3	5.5	120	2500	30	12	90	6000	88.4	88.9	*	1.07	*	*	2.57
PVT-4	5.7	120	2500	30	12	90	6000	91.8	76.5	*	1.18	*	*	3.46
PVT-5	5.3	60	2500	30	12	90	6000	59.0	93.8	*	0.92	*	*	2.28
PVT-6	5.5	60	2500	30	12	90	6000	62.2	89.7	*	1.08	*	*	2.97
PVT-7	5.7	60	2500	30	12	90	6000	72.7	61.3	*	0.74	*	*	2.77
PVT-9	5.5	120	2500	30	12	90	4500	89.8	89.1	22.0	1.10	152	26.6	2.95
PVT-10	5.5	120	2500	30	12	90	3000	89.3	85.7	17.9	1.02	126	33.9	2.91
PVT-12	5.5	120	2500	30	8	90	6000	88.9	84.2	16.5	1.10	129	42.2	3.13
PVT-13	5.5	120	4000	30	12	90	6000	85.2	86.0	12.1	0.90	197	21.7	2.80
PVT-14	5.5	120	1500	30	12	90	6000	92.7	92.5	31.5	0.98	129	32.3	2.91
PVT-15	5.5	120	2500	30	12	95	6000	88.5	90.9	*	1.01	*	*	2.71
PVT-16	5.5	120	4000	30	12	95	6000	85.0	89.4	*	0.94	*	*	2.69
PVT-17	5.5	120	2500	50	12	95	6000	90.3	85.6	*	1.05	*	*	2.73
PVT-18	5.5	120	2500	50	12	90	6000	90.5	85.0	19.4	1.10	141	34.1	2.94

* The objective of these tests was to define how SO_2 removal and limestone utilization vary with changes in process operation. The tests were not long enough to provide meaningful data on solids properties.

ADVANCED SIMPLIFIED WET FGD DESIGNS

by

Stuart M. Dalton
&
Robert E. Moser
Electric Power Research Institute

and

Jack M. Burke
&
J. David Colley
Radian Corporation

Abstract

Experience in the U.S. in the design and operation of flue gas desulfurization (FGD) systems has been accumulating since the early 70's. While significant improvements have been made in the performance and reliability of FGD systems, and in our understanding of FGD process chemistry, the technology still seems to be perceived as expensive and troublesome to operate. By combining the experience accumulated with our latest insights in process chemistry, it is possible to envision simplified designs which could substantially reduce the costs of installing and operating FGD systems. This is a very important consideration in light of the increasing likelihood that acid rain legislation may be enacted, opening up a potentially large retrofit FGD market. This paper discusses component and system design improvements which should be considered for an "advanced, simplified" wet FGD system design, offers several examples of improved wet FGD system designs, and presents a rough estimate of the potential cost reductions which might be expected.

The "Conventional" U.S. FGD System Designs

Prior to addressing the topic of advanced, simplified wet FGD system designs, it is important to establish the starting point - to what level has the "conventional" FGD system evolved in the U.S.? An obvious difficulty in doing this results from the fact that very few FGD systems have been constructed in the last five years, and those that were, were designed around 1980. More often than not these designs reflected copies of earlier designs, as opposed to innovative designs. In an attempt to define the "conventional" FGD system, an examination of the various processes and the evolution of the design of major components of an FGD system is in order.

Since the very first FGD system designs in the late 1960's, FGD systems using calcium-based reagents (lime and limestone) have been in the majority. In 1976, 82% of the operating wet FGD capacity (7519 out of 9207 MW) used calcium-based reagents. As of 1985, nearly 88% of the operating wet FGD systems (56,915 out of 64,981 MW) used calcium-based reagents. This trend is expected to continue. In 1985, sodium-based wet FGD systems are a distant second with approximately 11%, split almost evenly among once-through sodium systems, sodium dual alkali systems, and regenerable sodium-based systems. Magnesium-based regenerable FGD systems constituted the remaining 1%. Clearly, the "conventional" wet FGD system should be considered to be a calcium-based system. Since limestone systems continue to outnumber lime systems by approximately 2:1, this paper will assume that the advanced, simplified wet FGD system will utilize limestone as the reagent.

The heart of any FGD system is the gas-contacting device. Many early scrubbers were designed to remove both particulates and sulfur dioxide. These designs required fairly high gas-side pressure drops to remove particulates, and their demonstrated particulate removal efficiencies were not adequate to meet the more stringent particulate requirements enacted during the 1970's. The presence of large quantities of flyash in the absorber tends to take its toll on system components such as pipes, valves, pumps, and spray nozzles. Also, scaling can be aggravated and reagent utilization adversely affected by the presence of large quantities of flyash, as those who are still struggling to maintain and operate these early designs can attest.

Many of the early sulfur dioxide scrubbers used vertical countercurrent absorber towers with some sort of internal gas/liquid mass-transfer devices such as packing materials, ping pong balls, and/or grid systems to provide additional surface area for SO_2 mass-transfer. Without a good understanding and control of the process chemistry, such absorbers were extremely vulnerable to scaling, and few of these designs were repeated. Often the packing material was removed or replaced in an effort to make the absorbers more reliable. Thus, the breed of open vertical countercurrent spray towers emerged in the late 1970's. In fact, only a few of the FGD system suppliers have offered simple countercurrent spray towers. Several suppliers offer countercurrent spray tower systems which contain dual loops with segregated effluent streams, and other suppliers offer spray towers which incorporate a perforated tray or small amounts of packing to enhance SO_2 removal. Horizontal (crosscurrent) spray towers have been installed. A cocurrent spray tower design, incorporating a grid system for enhanced gas/liquid contact is offered by one supplier. There are, obviously, a variety of tower designs available. Each type has different characteristics and its own set of operating caveats. Each has had to work through operating problems, and for the most part, has evolved into a workable design. Most FGD systems have spare absorbers so maintenance can be accomplished in a particular tower without having to reduce the unit load.

The auxiliary components associated with FGD systems - reagent preparation systems, mist elimination systems, dewatering systems, dampers, duct designs, reheat systems, controls - have all undergone improvements with experience. However, with the exception of advances in digital distributed control systems, few have experienced very dramatic design changes. Accurate on-line measurements of pH and density of the absorber feed slurry, two of the more essential things to know in controlling the process, are still problematic. We certainly know more about keeping mist eliminators clean, but the actual designs have not seen dramatic changes. Gas maldistribution and locally high velocities still can create carryover problems even if scaling is not an issue. Advances in reagent preparation system designs have been minimal through two decades of experience. The awareness gained in correlating limestone grind characteristics to improved dissolution in the FGD system has accentuated the importance of maintaining good control of the product quality. Dewatering equipment has been problematic in many cases. Thickeners and vacuum filters or centrifuges are conventionally used. While we understand more about keeping this equipment operational, there really have not been any dramatic improvements in the design of this equipment.

Few, if any, U.S. FGD systems have been designed to take advantage of the use of performance additives. Performance additives available today fall into two categories: gypsum scale control or SO_2 removal enhancement. By understanding the process chemistry associated with these additives, reliability can be improved significantly. With adequate monitoring and control of the process chemistry, gypsum scaling can be controlled, if not eliminated completely. A properly designed and operated forced-oxidation FGD system can operate reliably without scaling. If forced oxidation is not employed, and the natural oxidation of sulfite to sulfate is in the 20 to 60% range, then an oxidation inhibitor should be used to control gypsum relative saturations to levels well below 1.0 to assure that gypsum scaling will not occur. This mode of operation will actually dissolve any existing gypsum scale. The demonstration of in-situ production of thiosulfate by the addition of sulfur to the FGD slurry has made this option a very affordable alternative to manual methods or high-pressure washing for removal of gypsum scale.

In the area of SO_2 removal, several additives can be used to enhance removal efficiency of a limestone FGD system. Organic acids, (DBA, a mixture of organic acids, the major component of which is glutaric acid, with smaller quantities of succinic and adipic acids, is the most commonly used), and magnesium (added as magnesium-lime) have been used successfully as additives in a number of utility limestone FGD systems as remedial action to bring these systems up to SO_2 removal performance requirements. Very few of these systems, and none of the DBA-enhanced systems, were designed with the use of additives in mind.

Thus, the "conventional" wet FGD system uses limestone as the reagent, probably achieving 90% SO_2 removal efficiency in some variation of a countercurrent spray tower, incorporating some spare absorber capacity. The auxiliary systems incorporate the latest improvements in design based on operating experiences, including improved instrumentation and data acquisition systems. The system uses either forced-oxidation or inhibited-oxidation to control gypsum scaling.

Design Criteria for Advanced Wet FGD

An advanced FGD system should be capable of achieving greater than 90% SO_2 removal efficiency (ideally, 95% or better), with system reliabilities of greater than 99%. Currently, some limestone systems achieve greater than 90% SO_2 removal efficiency. Sodium and magnesium-enhanced lime FGD systems can be designed to exceed 95% SO_2 removal efficiencies. Getting 95% SO_2 removal efficiency with a limestone wet FGD at reasonable L/Gs will almost certainly require the use of an SO_2 removal enhancement additive.The median availability of limestone FGD systems in 1985 was approximately 91%, and this reflects the existence of spare modules. Accomplishing a system reliability of 99% will require good designs and a very serious utility commitment to operate these systems well.

An advanced limestone FGD should utilize the reagent more effectively. Usually, 90% limestone utilization is considered a good target value for currently operating system. An improvement to 95% limestone utilization seems a reasonable goal for the advanced limestone wet FGD system.

An advanced limestone FGD system should have an energy consumption of less than 2% of the station energy input. Current designs typically use 3-5%. FGD system gas-side pressure drop (fan horsepower) and pumping power are the major areas where savings in power consumption would have to be accomplished. Auxiliary steam from the boiler should not be used for indirect flue gas reheat, thus allowing the unit to generate more megawatts.

Both installed costs and operating costs for the advanced FGD system should be significantly less than the costs of existing systems. Reductions of 25 to 30% for each are realistic short-term goals. Longer-term goals should seek to reduce costs even more as designs are further improved and simplified.

Ideally, the FGD system should produce a usable byproduct, rather than a material for landfill. Sulfur or sulfuric acid production from a limestone-based FGD process has not been found to be practical. However, the production of synthetic FGD gypsum should be pursued where it makes economic sence. While market forces ultimately will prevail, every effort should be made to produce an FGD synthetic gypsum which can be useful within the existing gypsum industry. Even if the synthetic gypsum would not produce revenue for the utility, it would eliminate the cost of waste disposal. Where a market for FGD synthetic gypsum does not exist, calcium sulfite or gypsum solids can be produced, hopefully with a simplified dewatering scheme, and stabilized for safe landfill disposal.

Elements of Design for Simplified Wet Limestone FGD

The design criteria detailed above define an advanced limestone wet FGD system which will remove SO_2 more effectively, operate with greater reliability, achieve better utilization of the reagent, use less energy, will produce a usable byproduct, and will cost less to build and operate. All of these are worthy goals, but can this realistically be done? The remainder of this paper will present some ideas which should be considered in attempting to achieve these goals.

An essential concept upon which all of these system improvements and benefits are based is that utilities will make the necessary commitment to operate these "advanced" designs in a manner consistent with the latest knowledge of FGD process chemistry. It will be necessary to staff the systems with knowledgeable supervisors, and to train operators so that they are aware of the implications of their actions (or inactions) while operating these systems. A staffed FGD analytical laboratory will be required to effectively monitor the status of the FGD system, and a data tracking and reporting scheme is also assumed. A dedicated maintenance staff that is not rotated to other plant functions has also proved beneficial.

While this assumption of utility commitment seems fairly simple, it is the cornerstone upon which these advanced designs are built. The design philosophy suggested for the "advanced" FGD system incorporates the following concepts:

- Larger absorber module designs: There would seem to be no reason why the absorber modules could not be designed to treat more flue gas. This trend was already emerging when the last U.S. FGD systems were coming off of the drawing boards in the early 1980's. However, the largest spray towers in use in the U.S. treat only about half as much flue gas as the 700 MW module at the Takehara station of EPDC in Japan. Larger towers would have economy of scale, and, assuming larger towers equate to fewer towers, the entire FGD system would have fewer auxiliary components associated with the absorbers, like pumps, piping, valves, agitators, ductwork, dampers, mist eliminators, and instrumentation, to name a few. The use of larger towers is closely linked to the use of spare absorber modules which is discussed in more detail in a later section of this paper.

The converse to larger towers would be towers capable of treating the flue gas at higher gas velocities. Current spray towers are designed for superficial gas velocities of 8 to 10 feet per second. A goal of increasing this to velocities approaching 20 feet per second is not inconceivable. The standard design criteria of 8 to 10 feet per second superficial gas velocity in a countercurrent spray tower may be improved upon. However, in a countercurrent spray tower there would be a severe pressure drop associated with the higher gas velocities. The crosscurrent (horizontal) spray towers have been found to have some problems in gas distribution due to compression of the gas in the lower portion of the tower. This could rule out trying to significantly increase the gas velocity through this design of tower. The best potential for achieving satisfactory performance at higher gas velocities lies, perhaps, in the use of a cocurrent spray tower design. EPRI and TVA tested the cocurrent scrubber in 1976 and 1977 at both the 1MWe and 10 MWe sizes, with results indicating that it may be possible to design a cocurrent absorber tower to treat flue gas at up to 20 feet per second gas velocity. This approach would be even more beneficial cost-wise than the economy of scale benefit of larger modules, since the result would be smaller towers and/or a major reduction in the number of total towers required. This would result in a dramatic decrease in the amount of steel required for absorbers.

- No spare absorber modules: There are a several FGD systems in operation in the U.S., and many in Japan and Europe, which do not currently have any spare absorbers, so this may not seem to be a very futuristic proposal. However, most U.S. FGD systems have been designed with spare absorber capacity. The use of spare modules in the U.S. has largely been dictated by regulation, not by prudent design. The sizes, number of modules and sparing philosophy is dictated by the specific wording in the June 11, 1979 Rules and Regulations for New Stationary Sources Performance Standards; Electric Utility Steam Generating Units. During emergency conditions the owner or operator may bypass around a malfunctioning FGD system provided "...the FGD system has been constructed with a spare module...". This single provision in the regulation has dictated absorber size and system complexity for most new units ever since it was promulgated. The U.S. utilities have had to comply with the regulations, and have been unable to use a single large module because if they designed such a module, it could never be bypassed during an emergency. The requirement of having a spare module means that designs were optimized based on how many spares they would need. Since a spare was needed , they could consider one big module plus one 100% spare, but the cost was prohibitive. A more economical design with a spare might be 3 modules @ 33 1/3% plus one spare @ 33 1/3%, and this has been typical. This dictates not only sparing philosophy, but module size as well (since three modules might treat a unit, rather than one module).

The relatively short emissions averaging time reporting requirements also made the presence of spare towers a necessity since it is difficult to make up for poor short term operation without a spare. Of course, once they have the spare, FGD operating personnel use that spare to perform periodic maintenance on a particular tower without requiring a reduction of unit load. However, it can also be reasonably argued that having a spare tower available allows looser control of operation, maintenance and scrubber chemistry. If you need to be shutting down towers for emergency maintenance due to less-than-optimum control of the process chemistry (i.e., due to wholesale scaling of the tower), having a spare absorber may in fact cost more in maintenance expenses over the long run. This is one area where regulatory flexibility could save millions of dollars while still accomplishing the SO_2 emissions reduction desired. Depending on how future legislation is worded, it may be possible that specific emissions reductions from a unit, in terms of tons of SO_2 reductions on an annual basis, may be the requirement. In such a case, there could be a great deal more flexibility for the utility to undergo an emergency shutdown of the scrubber periodically and still meet the regulations. The West German approach, setting a maximum number of hours per week and per year during which uncontrolled emissions are permitted in the event of a breakdown, appears to offer this flexibility while at the same time providing adequate guarantees against excessive pollution.

Combining these two design elements leads to the least conservative, lowest cost absorber alternative imaginable - the single module design. The ultimate design simplification would be to have a one-module design treating flue gas at up to 20 feet per second gas velocities. Imagine how simple the ductwork arrangement would be for a one-module FGD system design. Dampers would be eliminated except for any bypass. Our original assumption, that utilities make the commitment to operate these systems diligently, would certainly be extremely important in this type of situation. However, the potential cost savings merit consideration of this type design for future FGD systems.

- No bypass capability: If a utility makes the commitment to operate the FGD system in a manner that allows them to have no spares, then the bypass capability also may be considered for elimination. There are units in both Europe and Japan where no bypass capability exists. It is not unreasonable to assume that for new units, when the boiler is operating, then the FGD system must also be operating. In the U.S., if retrofit is to be considered the major market for FGD, then it is likely that nearly all retrofit FGD systems can be designed without designing new flue gas bypass capability. The rationale behind this is that it is very likely that a new stack will be required for the FGD system retrofit. Since this is likely to be the case, the tie-in for the retrofit FGD system can be designed to allow the original stack (and ductwork to that stack) to be used as the bypass of the retrofit FGD system.

- Wet stack operation: Unless there is a regulatory requirement to the contrary, we believe future FGD systems should be designed to operate with a wet outlet duct and wet stack arrangement, i.e., no reheat of the outlet gas stream. The cost of the steam required to do this (~ 1% of the plant energy input) does not seem justified by the benefits obtained from flue gas reheat. The use of untreated, bypassed flue gas for reheat (called bypass reheat), mixed in a mixing section in the outlet ductwork, creates probably the most severe corrosion problem for existing FGD systems, and if the gases are not evenly heated entering the brick liner of the stack, the liner may develop a lean problem. In contemplating a retrofit situation where achieving a specific tonnage SO_2 emission reduction is the goal, the often the cheapest way to do that would be to treat all the gas of a few units to the highest level of SO_2 removal possible (without bypass). The advanced FGD system should have the outlet duct and stack liner designed with the idea of operating in a wet mode, sloping the outlet duct for drainage, installing liquid disentrainment devices in the outlet duct and the stack liner, and providing adequately sized and sealed drain capabilities.

- Use of performance additives: The advanced FGD system should be designed to take advantage of the use of performance-enhancing additives. Increasing SO_2 removal capabilities while decreasing the liquid to gas ratio is a very worthwhile goal. This could further reduce the size of the towers, and would certainly reduce absorber recirculation pumping costs. Additives can also be used in different concentrations, yielding differential SO_2 removal enhancement. This could be very significant if, for instance, a boost in efficiency were required to offset an emergency shutdown.

Oxidation-inhibiting additives to control gypsum scaling should be used if forced-oxidation is not being used to produce a marketable gypsum byproduct. The generation of thiosulfate in-situ from sulfur addition has proven to be an effective and economical means of controlling gypsum scaling in nearly all of the places where it has been tried. EPRI is currently in the process of patenting a combination of additives to effectively reduce sulfite oxidation even in those cases where thiosulfate has been only marginally effective. Future research programs at the High Sulfur Test Center at bench and pilot scales will examine the use of other additives for SO_2 removal enhancement and oxidation inhibition.

There are several other areas in a wet limestone FGD system where the use of additives could become important. It may be possible to use additives in catalyzing oxidation in forced-oxidation systems. The cost of these additives would have to be compared to potential savings in air compressor horsepower. Also, there may well be crystal habit modifiers added to tomorrow's FGD systems to produce larger, better settling, more easily dewatered calcium solids. If this can eliminate any equipment from the dewatering area, the cost will be easily justified. Maybe another additive will be introduced into the reaction tank to promote limestone dissolution, with its cost weighed against improvement in limestone utilization. Research into additives for these areas are planned at bench-scale and pilot-scale at the HSTC. Another possible area for additives may be as corrosion inhibitors. EPRI has been researching this possibility for several years.

- Improved materials of construction: Cladding of carbon steel with a thin layer of highly corrosion resistant copper/nickel alloys has become a popular fix for a number of FGD systems which have experienced severe corrosion problems in areas such as prequenchers, absorbers and downcomers, and outlet ductwork. These clad materials appear to work well in the FGD environment, and should very definitely be considered for the advanced FGD system. With the experience acquired in repairing existing FGD systems via wallpapering of these higher grade alloys in the field, shop manufacture for new FGD system designs using clad materials should be relatively trouble-free, and should represent a cost savings.

Linings for FGD systems have had mixed experiences. A great deal has been learned about the QA/QC requirements for rubber linings, for instance, and about which kinds of rubber to use. Future installations of rubber liners for FGD absorbers should be expected to perform far better than past applications. Various organic linings (epoxys, fluoroelastomers, polyesters, urethanes, vinyl esters) have been applied to absorber towers and outlet ducts, with varying degrees of success. The experience gained should be beneficial in offering improved organic liners for future FGD systems. Inorganic linings have also been applied in a number of utility FGD systems. Borosilicate blocks have enjoyed reasonably good success in outlet duct service, after working out some installation bugs. Calcium silicate cements have also been used as linings in outlet ducts, with varying degrees of success. EPRI has been researching the use of impressed current in a inorganic refractory-based liner for corrosion protection. This is being field tested now at the HSTC.

An option which has recently been receiving increased attention is the use of fiberglass reinforced plastic (FRP) for fabricating the absorber and outlet ductwork. FRP has the potential of reducing costs, and is expected to exhibit excellent corrosion resistance. Questions need to be answered on how large could FRP absorbers be constructed. QA/QC on both the resin formulation and absorber fabrication would be very important. A 100-MW bubbling reactor absorber will be demonstrated in the recently-selected Southern Company Services CT-121 Clean Coal Technology 2 project. FRP as the preferred material of construction for absorbers may be hard to beat, but there will be stiff competition from alloy claddings and improved liner systems, which should help to produce cost savings.

Another development in the materials area may come from mollifying the corrosiveness of the FGD slurry so that lower grade stainless steels may be suitable in certain applications. Chloride removal is the emphasis currently in this approach. An electrodialysis reversal (EDR) unit is currently being evaluated on a 4 MW pilot scale at the HSTC, in joint work with New York State Electric & Gas. Other possibilities exist and will also be looked at to remove chloride from FGD systems. Reduction and control of FGD slurry chloride concentrations has other implications. If forced-oxidation is employed for synthetic gypsum production, control of chloride in the final product is very important. From a process chemistry point of view, reducing chloride concentrations will have beneficial effects on both SO_2 removal and limestone utilization.

- Simplified dewatering schemes: Thickeners take up a lot of space. Space is not something that is likely to be readily available in many retrofit situations. Eliminating the thickener is a worthwhile goal. Using hydroclones as the primary liquid/solids separation device, followed by a centrifuge or horizontal vacuum filter may be a feasible alternative. During the thiosulfate testing at the HSTC mini-pilot, a 95% pure calcium sulfite material was dewatered to above 72% solids by routing absorber blowdown directly to a horizontal bowl centrifuge. As more is learned about the factors which affect calcium sulfite and calcium sulfate precipitation and crystal growth characteristics, it is reasonable to expect that improved reaction tank designs, coupled with the possible use of crystal habit modifier additives, will lead to simplified dewatering system designs.

- Integrated system design: This is nothing more than putting all of these things together in a manner that makes sense. The design of the absorber and reaction tank affect the design of the dewatering system. The mist elimination system affects the outlet duct design. Limestone grind can affect absorber SO_2 removal performance and scaling potential in the mist eliminator. The source of makeup water can dramatically affect mist eliminator scaling and alter the process chemistry. The design of each component must be considered in light of how it fits into the total FGD system design. Total integration includes the requirement that the FGD system be carefully monitored and controlled. A lack of effort and commitment by the utility to the proper operation of the FGD system is likely to defeat any design, however.

Cost Implications of Simplified Wet FGD Systems

This section will present estimates of the economic implications of these design modifications. These cost estimates were derived using EPRI's RETROFGD FGD cost estimating PC program. This computer program uses the economic evaluations of FGD processes carried out by EPRI in the 1982-1984 time frame. We are currently in the midst of producing a second round of economic evaluations which will update our information to 1988 dollars. Since the program estimates are based on a design of six years ago, and with costs which were estimated six years ago, the precision of these numbers may be less than exact. However, the point of this exercise is to look at the order of magnitude changes in capital, operating and levelized costs as a result of the design modification noted. The inputs for these estimates are based upon the standards being used for EPRI's latest round of economic estimates. The major changes are the size of the unit (a 300 rather than 500 MW unit) and the coal sulfur content (2.6% rather than 4.0%). All dollars shown are based upon a construction start date of 1/1/89 and a FGD system startup of 1/1/92.

TABLE 1

CAPITAL, OPERATING AND LEVELIZED COST COMPARISON
1982 VS. 1988 "CONVENTIONAL" WET LIMESTONE FGD DESIGNS

	Capital Costs ($/kW)	First-Yr Operating Costs		30-Yr Levelized Costs	
		Fixed (10^6\$)	Variable (10^6\$)	(mills/kWh)	($/ton SO_2 rem'd)
"Conventional" Wet Limestone 1982 Design	281	3.90	4.00	15.2	656
1988 "State-of the-Art" Design	263	2.87	4.00	13.0	559

For comparison purposes, Table 1 lists the costs for the new conditions of the "conventional" limestone FGD system defined in Volume 1 of EPRI report CS-3342, Economic Evaluations of FGD Systems, with a design date of 1982, compared to the "state-of-the-art" design defined earlier in this paper. The primary differences are that the absorbers were enlarged to three towers at 50% total design capacity each (from four towers at 33%), and that the FGD system maintenance factor has been reduced to account for tha decreased maintenance requirements when using thiosulfate for gypsum scale control.

As can be seen, the 1988 state-of-the-art design is estimated to reduce capital costs by 6% and levelized operating costs by 13%, compared to the 1982 "conventional" design. Using the 1988 "state-of-the-art" design as the base design, the following cost savings were estimated for each of the design modifications noted previously. Table 2 illustrates the predicted savings for each.

TABLE 2

COST SAVINGS OF VARIOUS DESIGN MODIFICATIONS

	Capital Costs ($/kW)	First-Yr Operating Costs ($10^6$$)		30-Yr Levelized Costs	
		Fixed	Variable	(mills/kWh)	($/ton SO2 rem'd)
Eliminate spare absorber	54	0.33	-	1.6	72
Wet Stack Operation	8	0.05	0.57	0.9	37
Eliminate Eergency Bypass Duct	6	0.03	-	0.2	7
Add DBA for SO2 Rem'l Enhancement	4	0.03	0.16	0.3	13
Simplified Dewatering	3	0.02	-	0.1	4
Integrated Inhibited Oxid. LS FGD System	75	0.46	0.73	3.1	133
% SAVINGS	29	16	18	24	24

As the gas-contacting device is the heart of the process, so is it the most expensive part of an FGD system. As can be noted in Table 2, the elimination of the spare tower reduced capital costs 20%, and reduced 30-year levelized costs about 13% for these conditions. Far and away, the largest capital savings are to be found in ~~the~~ SO_2 removal equipment. The "wet stack" option eliminates the capital costs of an indirect air/steam reheat system. The elimination of the steam costs reduce the variable operating costs nearly 15% all by itself. The use of DBA as an SO_2 removal enhancement assumes 90% SO_2 removal efficiency is maintained at an L/G reduction of 15%. The simplified dewatering represents replacing a thickener with a bank of hydroclones prior to vacuum filtration.

The net effect of incorporating all of these design modifications would be a reduction in capital costs of nearly 30%, with total first-year operating costs reduced nearly 20%, and 30-year levelized costs reduced nearly 25%. These modifications do not represent any radical advancements in design, but rather represent simplifying today's FGD system design. All of these improvements could be incorporated into an FGD system going on the drawing boards tomorrow.

To note again, the significance of the savings listed in Table 2 is in the order of magnitude of savings resulting from these changes. Eliminating the spare absorber tower has the largest effect on the system capital and levelized costs. All of the changes together represent some very real savings which can be realized if a utility is willing to make a commitment to carefully operate these FGD systems.

All these savings can also be illustrated in the following figure showing the percent savings by these various changes:

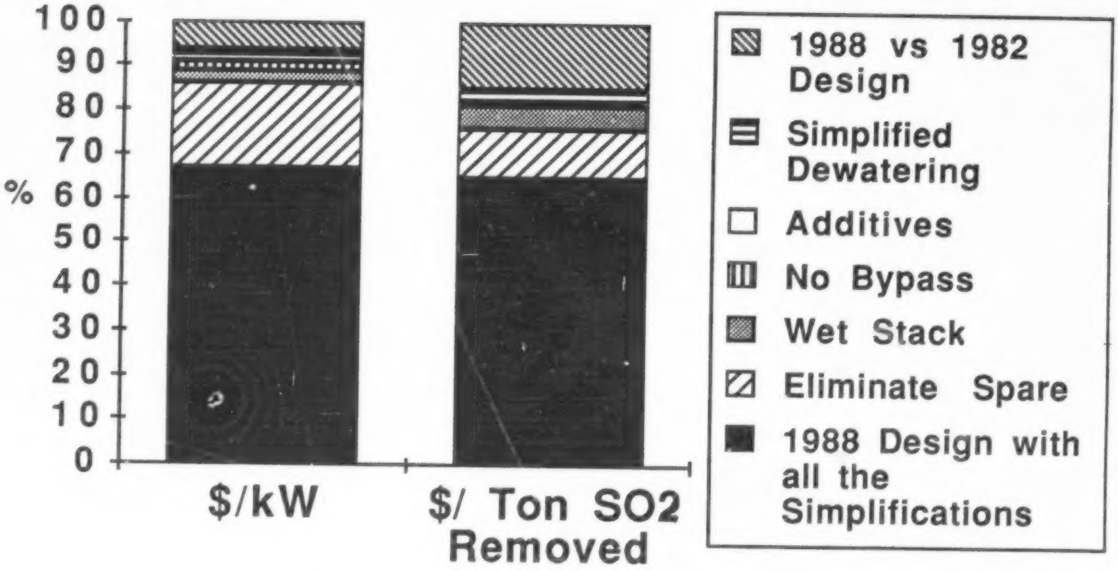

Figure 1: Savings from Design Simplification

"Advanced" Wet FGD System Designs

An"advanced" design implies some significant improvement over existing designs. An "advanced" wet FGD system design need not use a spray tower at all. The bubbling reactor designs have much to offer from a process perspsective, and the CT-121 process was evaluated in the initial round of EPRI economics to be among the lowest in both capital and levelized costs. The "advanced" design need not use limestone as the reagent. The excellent SO2 removal capabilities of the magnesium-enriched lime FGD process may make it a prime candidate for process optimization and significant cost reductions. It would certainly be desirable for an "advanced" design to produce a useful byproduct rather than an end-product requiring disposal. The SOXAL process, a sodium-based regenerative process using membrane technology for regeneration of the sodium absorbent, produces sulfuric acid or sulfur as byproducts and can absorb SO_2 very effectively. EPRI's initial round of economic evaluations indicate that this process may well compete with lime or limestone throwaway FGD processes.

Since the main emphasis of this paper has been on limestone wet FGD, the following process design suggestions reflect our feelings of where an "advanced" wet limestone FGD system using tomorrow's spray tower may be heading.

A promising concept for an advanced absorber design is the use of a cocurrent scrubber (with gas and slurry flowing cocurrently), a concept that was tested by EPRI and TVA in 1976 and 1977 at 1 MWe scale, then at the 10 MWe pilot at TVA's Shawnee Steam Plant 11. This offers a number of potential advantages for both new and retrofit applications. The principal advantages are:

- Substantially reduced absorber/FGD system gas side pressure drop. This would be especially important in a retrofit application;
- The potential for operating at high gas velocities (20 ft/sec) and thus reduced absorber sizes relative to conventional vertical absorbers. This would reduce the overall area required by the FGD system and thus make it a good retrofit design; and
- The ability of the absorber to handle higher than design gas flows without serious problems. This could substantially reduce the amount of spare absorber capacity required by a design.

As envisioned, the cocurrent scrubber design would include a horizontal mist eliminator designed to operate at a gas velocity between 10 and 20 ft/sec and an integral reaction tank with side mounted agitators. The possibility of using variable speed recycle pumps should also be considered in evaluating absorber costs since such pumps would provide increased load following capability and could pay for the added capital cost in operating cost savings (e.g., the pump speeds could be easily adjusted to maximize SO_2 emissions at the regulated limit thus reducing costs for limestone and for power to operate the pumps). Two design options are presented here although other variations are possible. These options are termed "conservative" and "advanced". Table 3 identifies key features of each design.

TABLE 3

POSSIBLE COCURRENT DESIGNS

"Conservative Cocurrent" Design	"Advanced Cocurrent" Design
• 2 modules/500 MW unit	• 1 module/500 MW unit
• 10 fps design velocity	• 20 fps design velocity
• Design for additive use reduced L/G	• Design for high additive and conc.and possibly reduced L/G
• Can be operated at 20 fps with higher additive concentration for 100% spare capacity	• No spare capacity

Process Options with the Cocurrent design

Two major process options which should be considered are forced and inhibited oxidation operation. Each design offers advantages and the selection of one over the other would depend on a number of factors including the possibility of selling waste gypsum, the proximity of a disposal site for waste material, and the costs for developing and maintaining a waste disposal site. Table 4 presents some key features of both process options.

TABLE 4

FORCED VS INHIBITED OXIDATION DESIGN PARAMETERS

Forced Oxidation	Inhibited Oxidation
• Reaction tank same diameter as absorber x 20' deep	• Reaction tank same diameter as absorber x 15' deep
• DBA (dibasic acid) enhanced	• Sulfur enhanced • Mg or DBA enhanced
• Limestone grind 90% < 200 mesh	• Limestone grind 90% < 325 mesh
• Dewatering Options - Hydroclone-gypsum stacking - Hydroclone-basket centrifuges - Hydroclone-vacuum belt filter	• Dewatering Options - Horizontal centrifuge only - Hydroclone-filter - Hydroclone-vacuum belt filter

Key features of the forced oxidation design include a relatively small diameter reaction tank which has at least a 20' depth to permit good in-loop oxidation. A greater tank depth may be necessary and the costs of increasing the tank depth should be evaluated. The design should also include the use of DBA additive to reduce the required L/G in the absorber and the use of a relatively coarse limestone grind since forced oxidation operation increases the limestone dissolution rate in the system.

For dewatering, two options should be evaluated. Both options employ hydroclones for primary dewatering. For secondary dewatering, a gypsum stack technique could be used for some plants where space is not a problem while a basket centrifuge or vacuum belt filter should be considered for utilities which have limited space and which will sell the gypsum. Basket centrifuges have the potential to produce an extremely dry gypsum cake which can increase the revenues generated by gypsum sales.

The inhibited oxidation system should be designed to use both sulfur and either DBA or magnesium as additives. The use of sulfur plus DBA may permit the production of very large sulfite crystals (i.e., crystals which have settling properties similar to gypsum). This could allow the dewatering equipment size to be reduced substantially. The additives will also allow the design to incorporate reduced L/Gs and smaller reaction tank volumes.
There are also two options for dewatering for the inhibited oxidation system. If large sulfite crystals can be produced, the

use of hydroclones followed by a vacuum filter can be considered. Another good option may be to use vertical centrifuges for both primary and secondary dewatering. Potential advantages for the horizontal centrifuge include reduced space requirements for the dewatering equipment and substantially reduced tankage requirements since no thickener or filter feed tank is needed. Potential problems with the horizontal centrifuge include high operation and maintenance costs. The trade-offs between these factors should be evaluated.

Summary

This paper has tried to cover a number of the ideas that can improve the much-maligned wet scrubber in terms of performance, reliability and cost. Many of the ideas are not earth-shattering, such as a strong commitment to operate the system properly and to use the latest experience in developing the systems, but these ideas need to be incorporated in all aspects of design, construction, operation, and maintenance. Some of the ideas represent a departure from "conventional" U.S. design, such as the use of no reheat, no spares, and large single modules, but this is more a function of the regulation than of the willingness of U.S. organizations to take risk. The bulk of these changes are not "futuristic" but represent realistic advances in the technology based on U.S. and foreign designs.

There are certainly advances yet to be made. Some of the technologies represented in the later sections of the paper, and now being considered for funding under the Clean Coal 2 initiative from the U.S. Department of Energy will fill some of the needs in the near future. Still others will be brought forward at the market develops with the incentive of acid rain legislation at a federal or state level.

EPRI stands ready to support the U.S. electric utility industry in its efforts to develop and implement the most cost effective, efficient and timely answers to these needs.

Literature Cited

1. Devitt, T.W., G.A. Isaacs, and B.A. Laseke, "Status of FGD in the United States", Proceedings: Symposium on Flue Gas Desulfurization, New Orleans. EPA report EPA-600/2-76-136a, May, 1976.

2. Melia, M.T.,R.S. McKibben, F.M. Jones, and J.L. Kelly, "Trends in Commercial Applications of FGD", Proceedings: Tenth Symposium on FGD. EPRI report CS-5167, May, 1987.

3. Radian Corporation, Evaluation of 10-MW Shawnee Cocurrent Scrubber, EPRI report CS-1806, April, 1981.

4. Stearns Catalytic Corporation, Retrofit FGD Cost Estimating Guidelines: Computer User's Manual, EPRI report CS-5408-CCM, September, 1987.

5. Stearns-Roger Engineering Corporation, Economic Evaluation of FGD Systems (5 Volumes), EPRI report CS-3342, December, 1983 through October, 1986.

DISCLAIMER

The work described in this paper was not funded by the U.S. Environmental Protection Agency and therefore the contents do not necessarily reflect the views of the Agency and no official endorsement should be inferred.

CORROSION CONTROL IN SO_2 SCRUBBERS BY IMPRESSED CURRENT

by: G. H. Koch and S. Pednekar
Battelle Columbus Division
505 King Avenue
Columbus, Ohio 43201

B. C. Syrett
Electric Power Research Institute
P. O. Box 10412
Palo Alto, California 94303

ABSTRACT

A major problem in maintaining the reliability of wet FGD systems is the corrosion of the outlet ducting in the thin films of acidic condensate that form on the duct walls. EPRI and Battelle have developed a means of protecting carbon steel or stainless steel outlet ducts through control of the electrochemical potential of the walls by impressed currents. This paper discusses the general technique and presents results obtained in simulated duct environments created in the laboratory and in actual duct environments in a pilot plant facility at EPRI's High Sulfur Test Center (HSTC).

INTRODUCTION

Corrosion of the walls of outlet ducts in wet flue gas desulfurization (FGD) systems is a major problem in maintaining the system's reliability. Outlet ducts carry cooled, scrubbed flue gas, sometimes reheated, from the absorber to the stack. The wet gas condenses on the duct walls creating a highly corrosive, low pH, chloride containing environment. The overall cost of materials has historically been high, since the choice has been between corrosion resistant materials of high initial cost that require little maintenance, and less corrosion resistant, low cost materials that over time cost as much or more because of frequent maintenance.

As a third alternative, EPRI and Battelle have developed an electrochemical technique to provide protection to inexpensive metallic materials of construction, which by themselves are not sufficiently resistant to corrosion.

This method is economically highly attractive because both initial and maintenance costs are lowered. The electrochemical technique developed is based on control by impressed current cathodic protection, which is widely used to provide corrosion protection for underground structures such as pipelines and tanks, marine structures such as offshore equipment and ships, and rebar in concrete structures.

In cathodic protection, a current is applied to the structure to be protected, such that the structure is polarized to a potential cathodic to (more negative than) the free corrosion potential. Under these circumstances, the primary electrochemical reaction on the steel surface is a reduction reaction. The oxidation, or corrosion, reactions decrease to negligible rates. In order to be able to apply cathodic protection to a structure, this structure as well as the anode and reference electrode must all be immersed in the same ionically conductive environment. Cathodic protection of carbon and stainless steels in an outlet duct of an SO_2 scrubber is complicated by the fact that only a relatively thin film of condensate forms on the duct surface. A thin film of condensate cannot generally accommodate a cathodic protection system. Moreover, the acidity of the condensate would seem to render the use of cathodic protection impractical because of large current requirements. However, EPRI and Battelle have developed a method of making cathodic protection work in thin acidic films of condensate (1,2). Some details of this Electrochemical Potential Control (EPC) method are proprietary and available only under license from EPRI. EPRI member utilities and architect/engineers working for member utilities may receive this license free of charge. While the proprietary aspects of the technology cannot be divulged in this paper, the benefits derived from EPC can be described. The results of laboratory tests in a simulated outlet duct environment and of tests in an actual outlet duct environment in EPRI's High Sulfur Test Center (HSTC) are presented here.

APPROACH

In the first phase of the work, carbon steel and stainless steel (Alloy 904L) panels containing the EPC system were exposed to a simulated outlet duct environment. The phase was performed to test the various system components such as anode material and reference electrode, and to establish the potential criteria for cathodic protection. The simulated wet flue gas was created in a modified fog cabinet by atomizing an acid solution containing species at concentrations representative of those found in actual outlet duct condensates (2), see Table 1. The test panels were part of the cabinet wall so that, as a result of the cold wall effect, thin film condensate would form on the panel surfaces.

The potential criteria for cathodic protection were established on 6 in. x 6 in. panels over a 4 week exposure time. The potentials were controlled potentiostatically at values between -0.6 to -1.2 V SCE for the carbon steel and -0.1 to -1.0 V SCE for the stainless steel. Once the EPC components were selected and the proper cathodic protection potential was established, 6 week experiments were performed to evaluate the complete system on 24 in. x 20 in. panels. One of the methods used to evaluate the effectiveness of the ECP system was to measure the potential distribution over the panel in relation to the controlling reference electrode.

Following the laboratory studies, field studies were initiated at the HSTC to further evaluate the EPC system as defined in the laboratory phase, under actual operating conditions. Several duct sections, each 30 in. long and approximately 28 in. diameter, are being installed as part of the outlet duct of the pilot scale 4-MW wet scrubber, see Figure 1. During 3 month exposure periods, several system parameters will be evaluated. Also, one carbon steel and one stainless steel duct section with the optimal EPC systems are being tested at potentials of -0.9 V SCE and -0.5 V SCE respectively, for a total period of 18 months.

For practical reasons, the cathodic current for the long term experiments is being applied using a rectifier. The performance of the EPC system in the various duct sections is being monitored by measuring the potential and current distribution. Also, the corrosion rate as a function of time is being determined from weight loss coupons removed from the duct wall at regular intervals. Further, condensate that forms on the inside of the duct is being extracted and analyzed.

RESULTS

Based on the laboratory studies, the potential criteria for cathodic protection of carbon steel and the stainless steel in simulated SO_2 scrubber outlet duct condensate were selected to be -0.9 V SCE and -0.5 V SCE, respectively. In the case of carbon steel, polarization at potentials more noble (i.e., more positive) than -0.85 V SCE resulted in visible corrosion, while at potentials more active (i.e., more negative) than -1.0 V SCE hydrogen evolution occurred, which had a detrimental effect on the EPC system. In the case of the stainless steel, pitting attack would occur at potentials more noble than -0.3 V SCE and also, hydrogen evolution occurred at potentials more active than -1.0 V SCE.

Typical results of a 6-week experiment on a 24 in. x 20 in. carbon steel panel with the EPC system and polarized to -0.9 V SCE are presented in Figure 2. The figure shows the potential distribution on the panel as a function of the distance from the panel edge, after 42 days of exposure. As a result of the EPC system the potential distribution is very homogeneous, suggesting complete protection of the carbon steel exposed to the acidic condensate. Indeed, post-test examination of the panel evinced a surface free from corrosion. Similarly, a stainless steel panel with the EPC system and polarized to -0.5 V SCE did not show any sign of general corrosion or pitting after a 6-week exposure to the acidic condensate.

During the exposure of the duct sections at the HSTC's wet scrubber pilot plant the potential distribution was recorded. Figures 3 and 4 show the potential distribution along the carbon steel and stainless steel duct sections. The figures indicate that the potentials are close to the applied potentials of -0.9 V SCE for carbon steel and -0.5 V SCE for the stainless steel, suggesting that neither material was subject to corrosion. Weight loss coupons removed from the duct sections after 1, 2, and 3 months indicated the maximum corrosion rates of the carbon steel was less than 3 mpy, while on the stainless steel coupons no corrosion, general or pitting, could be detected. These observations are significant in view of the fact that the condensate collected from the duct surface was very acidic (pH 1.8) and contained high concentrations of chlorides and fluorides, see Table 2.

DISCUSSION

The objective of the work presented in this paper was to develop and evaluate an EPC system that can provide corrosion protection to metallic materials of construction in aggressive outlet duct environments. These materials would not, by themselves, be sufficiently resistant to the condensate that forms on the duct walls. The laboratory experiments have indicated the feasibility of the EPC system, and preliminary economic analysis has suggested that the system is very cost competitive with alternative methods of corrosion control, such as using an Alloy C-276 "wallpaper" or applying and maintaining an organic coating.

The first important question to be answered was the range of potentials to which the metallic duct walls need to be polarized to ensure protection from corrosion. In the case of carbon steel, protection is obtained at potentials equal to or more negative than -0.85 V SCE. Lowering the potential to values more negative than -1.0 V SCE is not advisable since hydrogen gas evolution might occur on the metal surface, causing problems with the EPC system. In the case of the stainless steel, protection from corrosion is obtained at potentials equal to or more negative than -0.4 V SCE. Again, potentials more negative than -1.0 V SCE are undesirable because of hydrogen evolution.

Having determined the feasibility of the EPC system under laboratory conditions, a series of tests has been started to evaluate the system under realistic outlet duct conditions in the 4-MW wet pilot scrubber at EPRI's High Sulfur Test Center. Results to date have indicated that the EPC system can indeed adequately protect against corrosion of carbon steel or stainless steel duct walls exposed to acidic condensates derived from the flue gas.

REFERENCES

(1) G. H. Koch and N. G. Thompson, "Controlling Corrosion in SO_2 Wet Scrubbers Using Impressed Currents: Phase I", EPRI Report CS-5665L, May, 1988.

(2) G. H. Koch, D. G. Vutetakis, G. O. Davis, S. P. Pednekar, "Controlling Corrosion in SO_2 Wet Scrubbers Using Impressed Currents: Phase II", EPRI report on Project RP1871-15.

(3) G. H. Koch, N. G. Thompson, and J. L. Means, "Effect of Trace Elements in Flue Gas Desulfurization Environments on the Corrosion of Alloys--A Literature Review", EPRI Report CS-4374, January, 1986.

DISCLAIMER

The work described in this paper was not funded by the U.S. Environmental Protection Agency and therefore the contents do not necessarily reflect the views of the Agency and no official endorsement should be inferred.

Table 1

COMPOSITION OF TEST SOLUTION ATOMIZED IN THE FOG CHAMBER

Species	Concentration, g/m^3
Cl	25,000
F	2,500
NO_3	1
PO_4	100
Mg	2,500
Ca	500
Al	10,000
Cr	500
Cu	100
Fe	2,000
Mo	100
pH	1, adjusted with H_2SO_4

Table 2

COMPOSITION OF CONDENSATE COLLECTED FROM THE OUTLET DUCT OF THE 4-MW PILOT SCRUBBER

Species	Concentration, g/m^3
Cl	943
F	220
NO_3	94
Mg	44
Ca	100
Al	265
Cu	$\leqslant 0.1$
Fe	28
Na	2,115
SiO_2	103
SO_4	1,258
pH	1.8

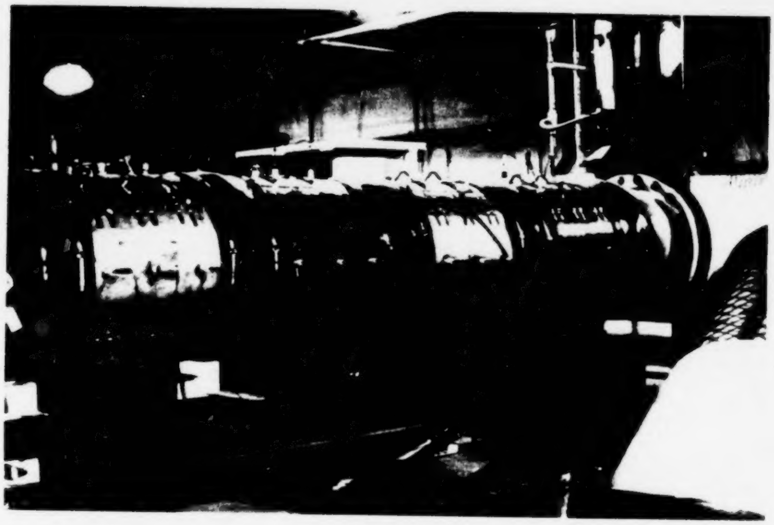

Figure 1. Photograph showing the test duct section as part of the outlet duct of the 4-MW wet scrubber. Four different test duct sections are separated by rubber expansion joints. Each duct section is equipped with reference electrodes and weight loss coupons at different longitudinal and clockwise positions.

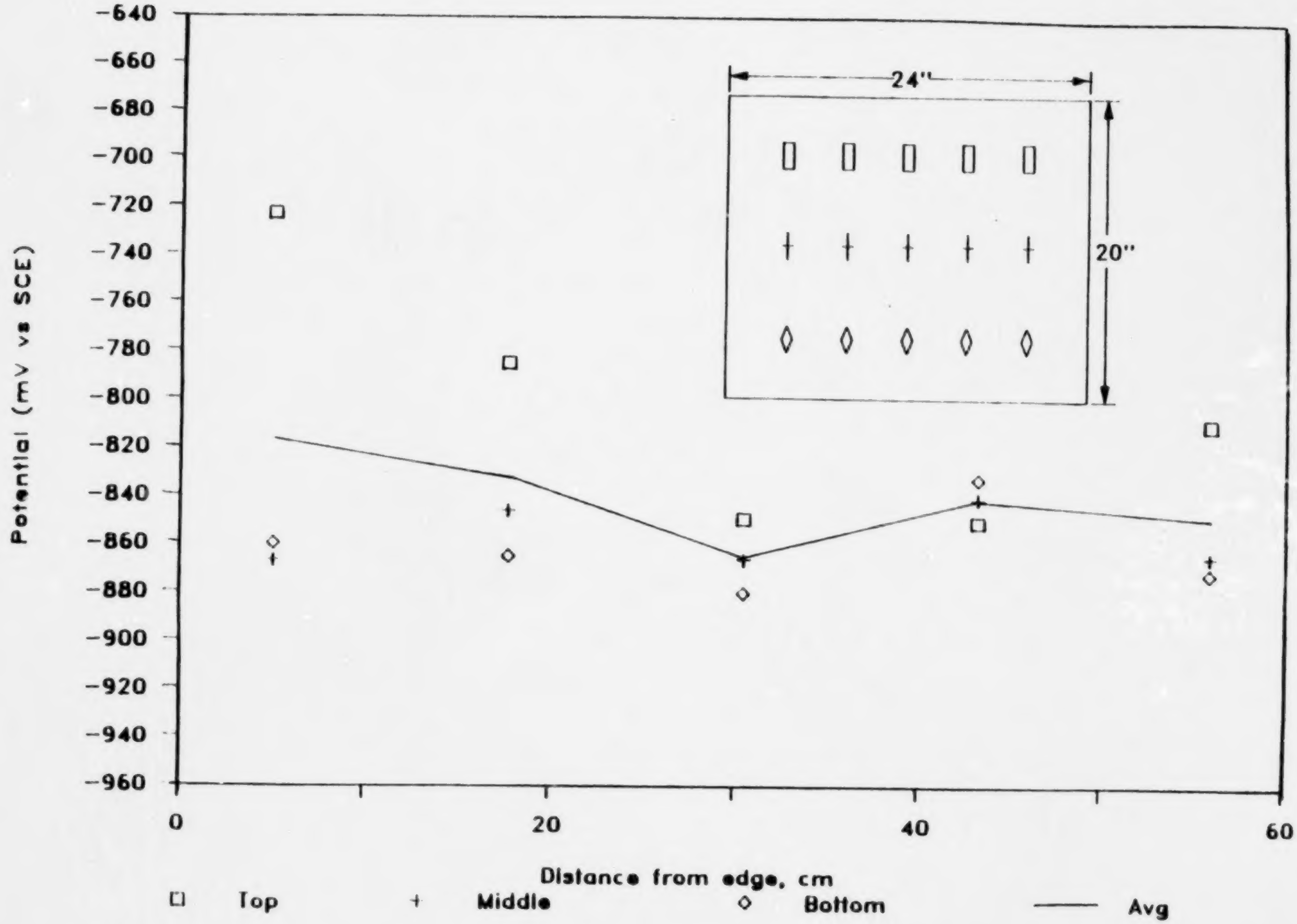

Figure 2. Panel F: Potential Distribution at the 15 Ports at 17 Days

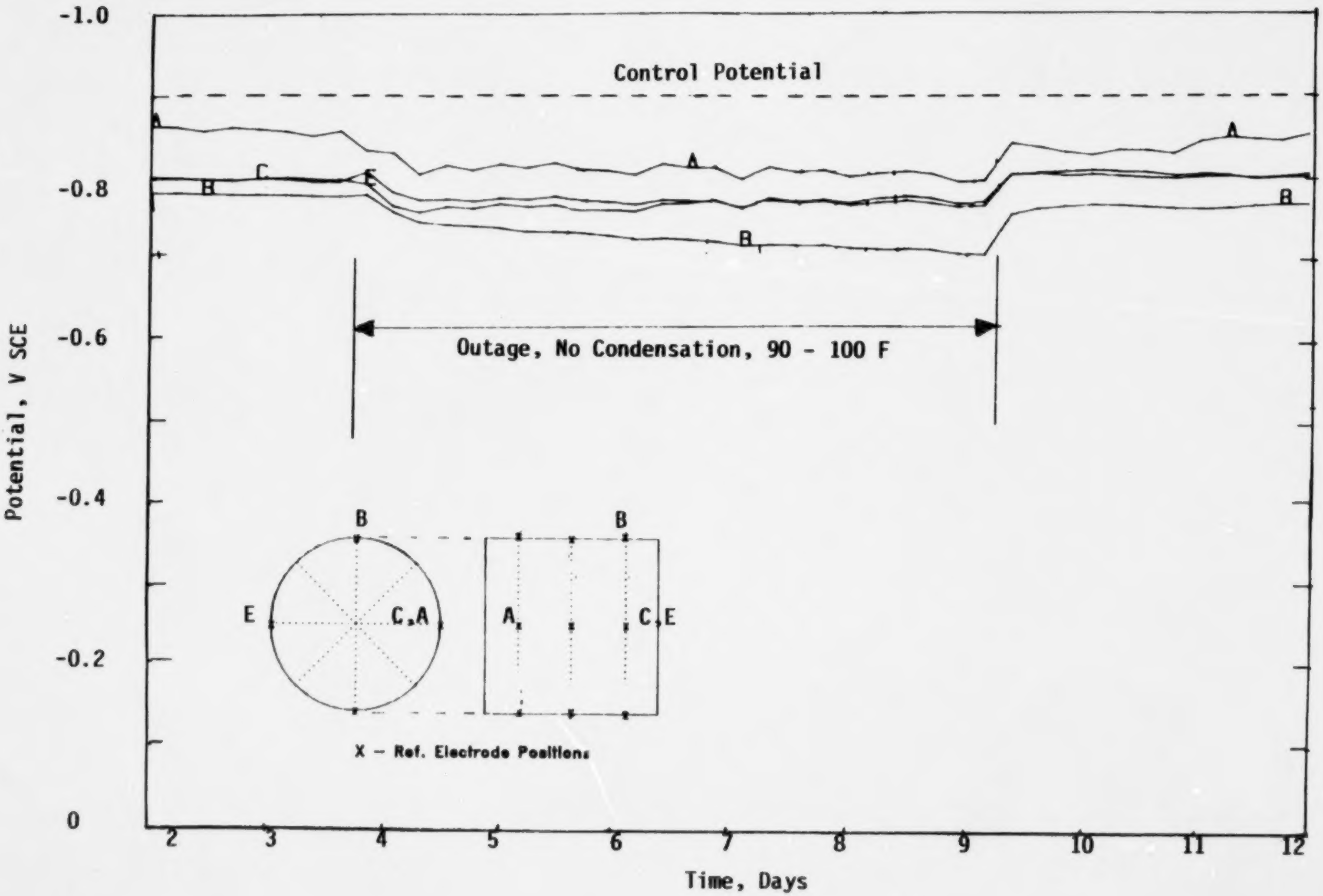

Figure 3. Potential at four locations on carbon steel section powered by rectifier.

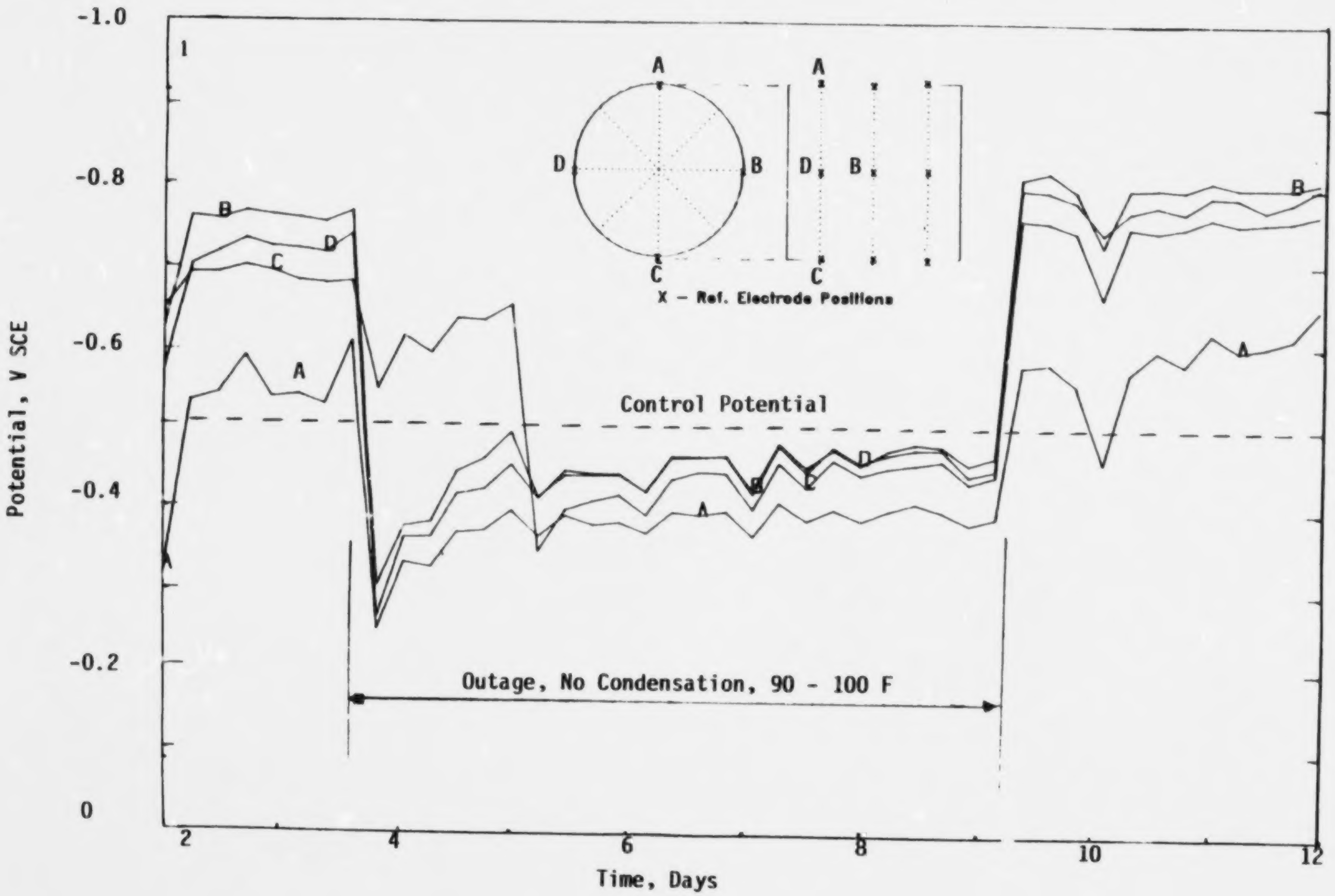

Figure 4. Potential at four locations on stainless steel sections on rectifier control.

DISCLAIMER

The work described in this paper was not funded by the U.S. Environmental Protection Agency and therefore the contents do not necessarily reflect the views of the Agency and no official endorsement should be inferred.

DEVELOPMENT OF A PREDICTIVE MODEL FOR LIMESTONE DISSOLUTION IN WET FGD SYSTEMS

by: James B. Jarvis, Frank B. Meserole, and Thomas J. Selm
Radian Corporation
Austin, TX 78766

Gary T. Rochelle and Cynthia L. Gage
The University of Texas at Austin
Austin, TX 78712

Robert E. Moser
Electric Power Research Institute
Palo Alto, CA 94303

ABSTRACT

This paper presents the results of an experimental study designed to develop an empirical model for limestone dissolution in wet FGD systems. The limestone dissolution model has been incorporated into EPRI's wet FGD process integration and simulation model (FGDPRISM). FGDPRISM can be used to predict the effect of process changes on many of the operations important to wet FGD systems.

One of the major objectives of the study was to develop a data base of experimental results for the effects of solution composition and sulfite on limestone dissolution. Sulfite, which is present in all FGD systems, was found to inhibit limestone dissolution and cause other significant changes in the way limestone dissolves. Ten different limestones, many of which are used in full-scale FGD systems, were tested during the study.

The experimental techniques developed during this study offer an improved method of determining the reactivity of limestones for use in FGD systems. FGDPRISM, which includes the limestone dissolution model developed during this program, will be a useful tool for predicting the effects of process changes on FGD system operation. The work described in this paper was not funded by the U.S. Environmental Protection Agency and therefore the contents do not necessarily reflect the views of the Agency and no official endorsement should be inferred.

INTRODUCTION

This paper describes interim results from an EPRI-funded project to model limestone dissolution in wet FGD systems. At this time, the first phase of experimental testing has been completed. An empirical limestone dissolution model has been developed which accounts for the effects of solution composition and pH, and the inhibiting effects associated with sulfite and certain metal ions. The limestone dissolution model gives good predictions of limestone utilization when compared to measured values at the EPRI High Sulfur Test Center (HSTC) but has yet to be tested at a full-scale FGD system.

Prepared for presentation at the EPA/EPRI First Combined FGD and Dry SO_2 Control Symposium, St. Louis, MO, October 25-28, 1988.

The results of this research have been incorporated into an FGD process integration and simulation model (FGDPRISM) capable of simulating many of the important chemical processes occurring in wet FGD systems. The model incorporates gas/liquid and solid/liquid mass transfer routines to predict the rates of SO_2 removal, calcium sulfite and sulfate precipitation, and limestone dissolution, and performs overall process material balances.

The results from a number of investigations of the limestone dissolution process are available in the literature. However, sulfite, which is present in all FGD systems, was not generally included as a test variable. The limited data which are available demonstrate that sulfite significantly inhibits the dissolution of limestone (1). Unfortunately, it has proven impossible to develop a predictive limestone dissolution model from either these data, or from full-scale operating data, due to the complexity of the dissolution phenomenon. Therefore, one objective of this program was to develop a more extensive data base which would characterize limestone dissolution in the presence of sulfite. A second objective was to demonstrate that a model based on these test results could provide accurate estimates of limestone utilization over a wide range of operating conditions.

This paper describes the results of experimental testing designed to determine the effects of important chemical variables on limestone dissolution. A key factor in the program was the development of an apparatus capable of providing unambiguous dissolution data under conditions representative of operating FGD systems. During the experimental program, tests were done over a wide range of conditions characteristic of operating FGD systems. Test variables included pH, Ca++, Mg++, Na+, SO_3=, SO_4=, CO_3=, Fe+++, Mn++, thiosulfate, adipic acid, limestone type, particle size, agitation rate, and temperature. The results of the experimental tests have been used to develop an empirical model which can predict limestone dissolution in various parts of the FGD system over a wide range of operating conditions.

Poor limestone utilization is a problem common to many full-scale FGD systems. In addition to the cost of wasted reagent, poor limestone utilization can impact the SO_2 removal capability of the absorber and can lead to reliability problems including a greater tendency for gypsum scaling in the mist eliminator. The experimental techniques developed during this program, along with FGDPRISM, will be useful in helping utility FGD operators solve problems associated with poor limestone utilization.

OBJECTIVES

The overall objectives of the test program were to identify the factors affecting limestone dissolution in the presence of sulfite and demonstrate that a model based on these findings could be used to predict limestone utilization in full-scale FGD systems. In order to accomplish these objectives, several secondary objectives were identified, including:

1) Development of an experimental apparatus capable of providing unambiguous limestone dissolution data at conditions representative of operating FGD systems;

2) Perform experimental tests to develop a data base quantifying the effects of chemical factors on the limestone dissolution rate;

3) Develop procedures for modeling the dissolution rate as function of particle size, solution composition and pH, and inhibitors which affect the dissolution rate;

4) Validate the model with data from the High Sulfur Test Center (HSTC); and

5) Use the model (and the experimental procedures developed during the program) to help identify and solve problems for utility system operators.

Information was generated during the test program addressing each of the above objectives. The remainder of the paper describes some of the significant experimental results and how they have been used to develop the limestone dissolution model. Then, a discussion is provided illustrating how the model can be used to solve problems for full-scale FGD system operators.

THEORY

THE MASS TRANSFER MODEL

One of the most valuable tools available within FGDPRISM is a mass transfer routine which can be used to interpret many of the mass transfer phenomena occurring in FGD systems. The mass transfer model is used primarily to calculate SO_2 absorption at the gas/liquid interface within the scrubber.

The mass transfer model can also be applied to limestone dissolution. While the limestone dissolution model is largely empirical, the mass transfer model provides the basis for estimating dissolution rates. The theoretical basis for the model is outside the scope of this paper and is documented in the references (2). However, it is important to have a feeling for what the mass transfer model does in order to appreciate the significance of the results presented later. Therefore, a brief description of the mass transfer model is provided here.

The mass transfer model is based on the classical "film theory" in combination with equilibrium (fast) chemical reactions. In film theory, it is proposed that a thin stagnant liquid film exists around the limestone particle. The bulk solution adjacent to the liquid film is assumed to be well-mixed and at equilibrium. Calcium and carbonate-containing species from the dissolving limestone surface diffuse through this film in order to reach the bulk solution. Similarly, acidic species diffuse through the film towards the limestone surface. Due to the presence of the film, the composition of the liquid adjacent to the limestone surface is different from that of the bulk solution. This concentration difference provides the driving force for diffusion of chemical species through the film.

With the exception of CO_2 hydrolysis, all liquid phase reactions are fast relative to the time taken by each species to diffuse through the film (CO_2 hydrolysis is discussed later in the paper). Therefore, the solution is essentially at equilibrium at all positions within the film. The equilibrium distribution of species within the film is estimated using a computer model which incorporates the constants for each of these equilibrium reactions. This program is a slightly modified version of EPRI's FGDLIQEQ program which is in use at many utilities (3). The data base used for the mass transfer model also includes estimates of the diffusivity for each diffusing component.

Steady-state material balances can be written across the film for each component in solution. As an example, the equation for carbonate is;

$$0 = D_{(CO_3=)} \frac{d^2[CO_3=]}{dx^2} + D_{(HCO_3-)} \frac{d^2[HCO_3-]}{dx^2} + \ldots \qquad (1)$$

where D is the diffusivity of each species and x is the position within a stagnant film of thickness δ. Terms are provided in Equation 1 for each species (including ion pairs) that contain carbonate (i.e., $CO_3=$, HCO_3-, H_2CO_3, $CaSO_3^o$, $MgCO_3^o$, $NaCO_3-$, $CaHCO_3+$, $MgHCO_3+$, $NaHCO_3^o$, and CO_2). Similar equations can be written for other components in the system including Ca++, Mg++, Na+, $SO_3=$, $SO_4=$, Cl-, NO_3-, H+, and buffers such as adipic acid.

For each component in the system, a material balance constraint can be applied to the diffusion equation. In the limestone dissolution problem, the net flux of non-dissolving components must be zero:

$$F_{(SO_3=)} = F_{(SO_4=)} = F_{(Mg++)} = \ldots = 0 \qquad (2)$$

Also, the flux of calcium must match the flux of carbonate:

$$F_{(CO_3=)} = F_{(Ca++)} \qquad (3)$$

The mass transfer model was set to treat hydrogen ion as a non-dissolving component, applying the constraint in Equation 2. This is equivalent to requiring that the sum of all of the fluxes is charge-balanced. Note, however, that the charge balance at any point within the film is not completely satisfied.

With appropriate boundary conditions, this system of equations can be solved to provide a numerical solution for the flux of each component through the film. The output is expressed as the composition of the solution at the solid/liquid interface. Using the composition differences across the film, the limestone dissolution rate can be calculated from the total carbonate (or calcium) flux according to the twice-integrated form of Equation 1;

$$\text{Carbonate Flux} = \frac{D_{(CO_3=)}\ \Delta[CO_3=]}{\delta} + \frac{D_{(CaHCO_3-)}\ \Delta[CaHCO_3-]}{\delta} + \ldots \qquad (4)$$

where Δ represents the concentration difference for each species between the solid/liquid interface and the bulk solution. Again, terms are included in Equation 4 for all species (including ion pairs) which contain carbonate.

An important boundary condition, which must be specified in order to solve the mass transfer equations, involves the activity of $CaCO_3$ at the solid/liquid interface. Data presented later in this paper shows that in the absence of inhibitors such as sulfite, accurate predictions of the dissolution rate can be obtained by specifying that the solution at the solid/liquid interface is saturated to $CaCO_3$. That is, the limestone can dissolve as fast as necessary to replace the calcium and carbonate diffusing away from the limestone surface. Therefore, the limestone dissolution rate is limited only by diffusion through the film.

When sulfite is present, however, limestone dissolution is inhibited and the limestone surface is not at equilibrium with respect to $CaCO_3$. To account for this, we have incorporated a kinetic model in which the limestone dissolves at a finite rate dictated by the composition of the solution at the interface. Under these conditions, the limestone dissolution rate is controlled by two (series) resistances; the finite reaction rate at the limestone surface, and the diffusion rate through the film. The mass transfer model calculates the interface composition where these two rates are equal.

In summary, a mass transfer model, based on film theory, is used to estimate the effect of the film on the solution composition and pH at the limestone surface. The inhibiting effect of sulfite is predicted by incorporating an empirical model in which finite-rate surface reactions add an additional resistance to dissolution. Data are presented later in this paper which show that the mass transfer model does a good job of predicting limestone dissolution over a wide range of conditions.

In addition to sulfite, however, other species were identified which inhibit limestone dissolution. The most important inhibitor for FGD systems is aluminum fluoride. Magnesium and adipic acid also inhibit dissolution but to a much lesser extent. The mass transfer model fails when these species are present and must be adjusted empirically to account for their effects. The techniques used to accomplish this are described later in the paper.

EFFECT OF PARTICLE SIZE ON FILM THICKNESS

In order to apply the mass transfer model, it is necessary to have a relationship describing the thickness of the stagnant film (δ in Equation 4). A number of correlations have been developed in order to estimate film thickness as a function of particle size (4). The most widely used correlations have the form;

$$\delta = \frac{d}{2 + K(Re)^{0.5}(Sc)^{0.33}} \tag{5}$$

where d is the particle diameter, Re is the Reynolds Number (a function of the solution density, the particle velocity relative to the liquid phase, the particle diameter, and the solution viscosity), and Sc is the Schmidt Number (a function of solution viscosity, density, and the diffusivity of the diffusing species).

In order to obtain values for the film thickness, it is necessary to specify a relationship between particle diameter and particle velocity relative to the liquid phase. We have assumed that the particles are moving at their terminal velocity. Then, the results from experimental tests, performed in the absence of inhibitors, were used to determine the value of K in Equation 5. At conditions typical of those used in the experimental apparatus, Equation 5 reduces to:

$$\delta = \frac{d}{2 + 1.26\text{x}10^{4}(d)^{1.5}} \tag{6}$$

A plot showing the relationship between particle size and film thickness is shown in Figure 1. Note that at particle diameters above about 20 microns, the film thickness is relatively constant and independent of particle diameter. At particle diameters below about 20 microns, however, the film becomes much thinner and approaches d/2 for very small particles. This means that smaller particles will dissolve more quickly per unit area than larger particles which is significant in FGD systems where finely ground limestone is used.

Experimental tests have been performed during this program to verify the validity of the the correlation between film thickness and particle diameter. The results, which are not described in detail in this paper, showed that the correlation provides good estimates of the dissolution rate as a function of particle size. Specifically, the initial dissolution rates of as-ground limestone samples could be predicted both with and without sulfite. This is necessary in order to estimate the limestone dissolution rate in FGD systems where the ground limestone typically contains a wide range of particle sizes.

While good predictions of the effect of particle size were obtained, other experimental results showed that the terminal velocity assumption used in Equation 6 is not very accurate. In the absence of sulfite, agitation rate had a significant effect on the dissolution rate (40 percent decrease from 1800 to

300 rpm). This means that the velocity of the particles, and therefore, the thickness of the film, is affected by agitation rate. Therefore, equation 6 only applies to the experimental apparatus operated at 1800 rpm. However, when sulfite is present, a kinetic resistance to dissolution is also involved. This significantly decreases the influence of film thickness on the dissolution rate. And, tests with sulfite showed a significantly diminished effect of agitation rate (5 percent decrease from 1800 to 300 rpm). Therefore, Equation 6 should do an adequate job of predicting the effects of particle size in FGD systems where sulfite and other inhibitors are present.

EXPERIMENTAL TEST PROGRAM

Over 200 tests were conducted during the initial phase of the limestone dissolution test program. Test variables included solution composition and pH, limestone type and particle size, temperature, and agitation rate. The specific test variables and the variable ranges used during these tests are summarized in Table 1. Table 1 also shows the values of each variable used to establish the baseline operating conditions. As indicated in Table 1, 10 different limestones were tested during the program. Information on each of these limestones is provided in Table 2. Note the limestones obtained from specific full-scale systems have been given a letter designation (A, B, etc.) because these utilities have not yet been informed of the test results.

The key to the experimental program was the development of an apparatus capable of providing unambiguous dissolution data over a wide range of conditions. The apparatus operates at constant composition and was designed to eliminate many of the problems which limit the usefulness of other limestone dissolution techniques. This apparatus, which is illustrated in Figure 2, utilizes a 2-liter sealed reactor and operates in flow-through liquid/batch solids mode. A single charge of limestone (typically 0.5 g/l) is added to the reactor and is completely dissolved during an experiment. The solids are retained in the reactor by a filter located at the bottom of the reactor. Experiments can be conducted with narrow particle size fractions so that the approximate size of the limestone is known at any point in the experiment as a function of the fraction dissolved. As-ground limestone samples, containing a broad particle size distribution can also be tested.

The apparatus operates in the flow-through liquid mode. A split-feed arrangement is used to supply the acid for dissolving the limestone. These streams also include calculated amounts of other salts required to maintain a constant solution composition in the reactor. Anions which form soluble calcium salts (Cl- and NO_3-) are combined with the dissolving acid in one tank. Anions which form insoluble calcium salts (SO_3=, SO_4=, F-, and CO_3=) are added as sodium or magnesium salts in a second tank. This tank is basic which prevents evolution of SO_2 or CO_2. Streams from each tank are fed in equal amounts and mixed together just before entering the reactor, or alternatively, fed to the reactor as separate streams. Typically, about 2.5 reactor volumes of combined acid feed are used to dissolve the limestone charge. This minimizes the acid concentration which helps prevent local pH gradients within the reactor. Using the flow-through split-feed arrangement, it is possible to operate the reactor at nearly any desired liquid-phase composition and maintain the composition at a constant predetermined level throughout the experiment. It is also possible to operate with process liquor from an actual FGD system. In this case, the acidified process liquor is fed from a sealed bag to prevent SO_2 or CO_2 evolution.

The reactor is sealed to prevent CO_2 evolution. Therefore, it is possible to operate at a constant elevated CO_2 partial pressure without the need for sparging the reactor. The sealed reactor also aids in minimizing sulfite oxidation since the sealed reactor is not in contact with air. However, a slight amount of sulfite oxidation still occurs, even though the reactor is sealed. Therefore, a small amount of sodium EDTA (0.25 mM) is added to prevent oxidation by complexing oxidation catalysts such as iron and manganese. The EDTA did not appear to affect the dissolution rate in experiments with sulfite.

Experimental techniques were developed which allowed the reactor to operate at $CaSO_3$ relative saturation levels up to 5.0 before nucleation of calcium sulfite solids. This covers the range of $CaSO_3$ relative saturation levels typically seen in FGD systems.

SUMMARY OF RESULTS

Important test results obtained during the program are summarized in this section. This includes results from tests with and without sulfite and test results using process liquor obtained from EPRI's High Sulfur Test Center (HSTC). Selected results are presented in the following section which illustrate the results summarized below. At the same time, a discussion is presented showing how the test results were incorporated into a model capable of predicting the effect of process changes on limestone utilization.

TEST RESULTS WITHOUT SULFITE

1) Dissolved CO_2 can hydrolyze and enhance the limestone dissolution rate by assisting in the transport of hydrogen ions to the limestone surface. However, the hydrolysis rate is known to be much slower than other reactions occurring within the stagnant film. Test results with variable carbonate levels, and a comparison of predicted and experimental results, showed that this reaction can be modeled by prohibiting the hydrolysis of CO_2 within the stagnant film. Under FGD conditions, where other buffers such as sulfite are present, enhancement in the limestone dissolution rate due to CO_2 hydrolysis is insignificant.

2) The mass transfer model, modified to neglect CO_2 hydrolysis, gives good predictions of the limestone dissolution rate over a wide range in solution composition and pH. This includes variations in the concentrations of Ca^{++}, Na^{+}, $SO_4^{=}$, Cl^{-}, and $CO_3^{=}$. In the absence of sulfite or other inhibitors, the dissolution rate is limited only by diffusion through the stagnant film. The dissolution rates for any limestone grind can be estimated using the relationship between particle diameter and stagnant film thickness given previously in Equation 6.

3) A comparison of the predicted and experimental dissolution rates showed that some species inhibit limestone dissolution. Significant inhibition was observed with sulfite and aluminum fluoride complexes. Minor inhibition was observed with magnesium and adipic acid.

4) Most high calcium limestones had about the same dissolution rate in the absence of sulfite (within about ±10%). A few limestones were tested, however, which gave lower dissolution rates. These included limestones containing dolomite (a solid solution containing $CaCO_3$ and $MgCO_3$).

5) Photomicrographs of partially dissolved limestones show that the limestone surface becomes relatively smooth when dissolved in the absence of sulfite. This behavior indicates that the limestone surface is uniformly reactive and the dissolution rate is limited only by film diffusion.

TEST RESULTS WITH SULFITE

1) For most limestones, sulfite enhances the dissolution rate above that without sulfite. This is expected since sulfite is a buffer and should assist in the transport of hydrogen ions to the limestone surface. However, the experimental dissolution rates are as much as a factor of 30 below that which would be possible if dissolution were limited only by diffusion. This represents sulfite inhibition or "blinding". Sulfite probably absorbs on the surface of the limestone and prevents it from dissolving. The degree of inhibition is a function of the calcium sulfite relative saturation.

2) In the presence of sulfite, the dissolution rate is controlled by both film diffusion and finite-rate reactions at the limestone surface. Evidence supporting this conclusion includes changes in the effects of agitation and particle size on the dissolution rate, and a change in the appearance of the limestone surface. An empirical correlation was developed which predicts the effect of sulfite, and all other variables, on the initial surface reaction rate with an average error of less than ±15 percent. However, the rate constant varies for different limestones.

3) Photomicrographs of limestone dissolved in the presence of sulfite show unusual surface features. On the more crystalline limestones, peaks of undissolved limestone form as the stone dissolves which indicate that the surface of the limestone is no longer uniformly reactive. That is, the reactions which control the dissolution rate have different rates on different areas of the limestone surface.

4) Limestones which show about the same reactivity without sulfite have very different dissolution rates when sulfite is present (a range of about a factor of three). Therefore, the average reactivity of the surface varies for different limestones. In general, more crystalline limestones tended to dissolve more slowly while limestones composed of aggregates of smaller particles dissolved more quickly. Iceland Spar, a highly crystalline limestone, had the lowest dissolution rate. This suggests that dissolution may occur preferentially at active sites or dislocations on the limestone surface. These active sites are more difficult to blind and dissolve more quickly whereas the more uniform crystal surface appears to dissolve more slowly.

5) The dissolution rate per unit surface area decreases significantly as the as the limestone dissolves in the presence of sulfite. This so-called "aging" effect means that particles with the same nominal size can dissolve at different rates depending on how long the particle has been in the system. This behavior varies in severity with the type of limestone and is only significant when sulfite is present. Apparently, the more reactive areas on the surface dissolve leaving less reactive areas undissolved. The net effect is a reduction in the average reactivity of the surface as the limestone dissolves. The effect can be correlated as a function of the fraction dissolved, rather than the particle size. This simplifies the modeling of this effect. Test results indicate that the blinding and aging affects described above will persist after the limestone passes through the absorber. That is, exposure to the low pH environment in the absorber does not un-blind the limestone.

6) Recent test results have shown an improvement in limestone utilization at full-scale FGD systems with the use of thiosulfate (5). Several tests were performed with thiosulfate and no effect on the limestone dissolution rate was observed. Therefore, improvement in limestone utilization associated

with thiosulfate is probably the result of other changes in system chemistry caused by thiosulfate (e.g., reduced calcium concentration), rather than an effect of the thiosulfate itself. The effects of thiosulfate on system chemistry are complex and are described in the references (5 and 6).

HSTC SIMULATION RESULTS

1) Tests were performed with actual and simulated liquor from the HSTC. The objective of these tests were to determine if trace species were present in the actual process liquor which were inhibiting limestone dissolution. The results showed that the dissolution rates with the actual process liquor were about 30 to 40 percent lower than with the simulated process liquor, indicating the presence of inhibitors. Similar tests for full-scale FGD systems could help to identify if poor utilization was the result of unreactive limestone or the presence of inhibitors.

2) Limestone dissolution rates were measured using process liquor and as-ground limestone from the HSTC. These results were used to predict the limestone utilization at the HSTC for several pH levels. The results were very close to the utilizations measured at the HSTC. This indicates that the limestone dissolution model can give good predictions of utilization if all factors which influence the dissolution rate are accounted for. It also indicates that the limestone dissolution apparatus gives realistic dissolution rates which can be applied to actual systems.

DISCUSSION OF RESULTS

The mass transfer model provides the basis for the empirical limestone dissolution model. However, the experimental results indicate that the mass transfer model must be modified in order to accurately predict dissolution rates when sulfite or other inhibitors are present. Selected results are presented which illustrate key experimental findings. Then, the modifications used to account for these effects are described. The result is an empirical model which can be used to predict limestone utilization over a wide range in conditions. The model itself is described in the following section.

EFFECT OF CARBONATE

Carbonate species are present in limestone FGD systems in several forms. These include solid $CaCO_3$ (limestone) and dissolved carbonate species such as carbonate ($CO_3{=}$), bicarbonate (HCO_3-), carbonic acid (H_2CO_3), and CO_2. In addition, ion pairs containing carbonate and bicarbonate are also present (e.g., $CaHCO_3+$ and $MgCO_3^o$). The composition of a solution containing carbonate species is a function of the solution pH and the concentrations of other ions in solution.

Carbonate species should affect the limestone dissolution rate in two ways. First, carbonate ($CO_3{=}$) is a product of the dissolution of limestone. Therefore, higher carbonate (or calcium) concentrations should reduce the limestone dissolution rate through the common ion effect. This effect, which is incorporated in the mass transfer model, becomes more important as the bulk solution approaches equilibrium with respect to $CaCO_3$.

Second, carbonic acid (H_2CO_3) and dissolved CO_2 should increase the limestone dissolution rate. Under conditions where diffusion of hydrogen ions limits the dissolution rate, carbonic acid and CO_2 can diffuse to the limestone surface and react to serve as an additional source of hydrogen ions. The equilibrium concentration of carbonic acid is very low relative to dissolved

CO_2. Since carbonic acid can dissociate rapidly, the net reaction can be represented as:

$$CO_2 + H_2O \rightleftharpoons H^+ + HCO_3^- \qquad (7)$$

Most liquid phase reactions important in FGD systems are fast reactions and are essentially at equilibrium. In contrast, reaction 7 is known to proceed rather slowly. The presence of finite rate reactions within the liquid film complicates the mathematical solution of the mass transfer model. At present, the mass transfer model cannot solve the diffusion problems where liquid phase finite-rate reactions are involved. It is possible, however, to completely shut off the reaction within the stagnant liquid film to simulate a very slow reaction rate. For conditions found in limestone FGD systems, this appears to be a reasonable approximation.

Experimental results illustrating this conclusion are shown in Figure 3. This figure shows the initial dissolution rates for two limestones as a function of solution pH. Figure 3 also shows two predicted curves provided by the mass transfer model. These curves represent the predicted dissolution rates with both fast and slow CO_2 hydrolysis. The experimental data fall close to the predicted curve in which the CO_2 hydrolysis rate is slow. Note that the potential enhancement due to CO_2 hydrolysis is significant. For example, at pH 5.5, a dissolution rate about 20 times greater than the measured value would be expected if CO_2 hydrolysis were fast.

The agreement between the experimental and predicted curves is indirect evidence that the CO_2 hydrolysis rate is slow and can be neglected. However, direct experimental evidence was also obtained. The tests in Figure 3 were performed at a carbonate concentration of 2 mM. Additional tests were performed at carbonate concentration up to 8 mM at pH levels of 5.0 and 5.5. No enhancement in the dissolution rate was seen at the higher carbonate levels.

It should be noted that CO_2 hydrolysis may provide significant enhancement at pH levels higher than those tested in these experiments. At pH levels closer to equilibrium (approximately pH 6.6 for this solution composition), the hydrogen ion concentration in solution is very low. Under these conditions, even slow CO_2 hydrolysis acid could provide some degree of enhancement in the dissolution rate. In FGD systems, however, there are other buffers present, such as sulfite, which provide much greater buffering capability than carbonic acid. Carbonic acid dissociation can be safely neglected under these conditions. From a practical viewpoint, the lack of enhancement due to carbonic acid dissociation over the pH range tested allows the mass transfer model to be used for evaluating the effects of other changes in solution composition.

EFFECT OF SOLUTION COMPOSITION FOR SPECIES OTHER THAN SULFITE

The results in Figure 3 show that good predictions of the dissolution rate were obtained as a function of solution pH when CO_2 hydrolysis was prohibited. Similar plots have been prepared showing the effects of the other variables listed in Table 1. However, space limitations prevent a complete discussion of all the test results. Some of the more important observations are summarized below.

The mass transfer model gives reasonably good predictions for variations in the concentrations of Ca++, Na+, SO_4=, CO_3=, and Cl-. Dissolution rates decreased with increasing Ca++ and CO_3= since these species decrease the solubility of $CaCO_3$ at the limestone surface. No significant effects were noted with changes in the concentrations of Na+, SO_4=, or Cl-. It is interesting that sulfate, which has a slightly soluble calcium salt, does not inhibit limestone dissolution in a manner analogous to sulfite.

Trace metals including Fe++, Fe+++, Mn++, and Al+++ (as AlF_3) were also tested. At a concentration of 5 ppm, iron and manganese had no effect on the dissolution rate. Aluminum fluoride, which exists as a complex ion, caused a significant reduction in the dissolution rate. The effects of aluminum fluoride are described in more detail later in the paper.

The mass transfer model predicts a considerable increase in the dissolution rate with adipic acid. While experimental dissolution rates were much higher with adipic acid, the degree of enhancement was only about 70 percent of that predicted by the mass transfer model. This may be due to uncertainty in the diffusivities or equilibrium constants of species containing adipate ions. However, photomicrographs of limestone dissolved in the presence of adipic acid showed surface features similar to those seen with sulfite. This indicates that finite-rate reactions may be involved when adipic acid is present. The inhibition due to adipic acid, however, is much less significant than that due to sulfite.

Some evidence of inhibition was also observed with magnesium. The experimental dissolution rates with magnesium were about 25 percent below that predicted by the mass transfer model. However, these differences are relatively minor and were only observed at high magnesium concentrations (100 mM).

EFFECT OF SULFITE ON THE INITIAL LIMESTONE DISSOLUTION RATE

Quantifying the inhibiting effects of sulfite was one of the primary objectives of this program. Sulfite inhibition has been observed in previous studies (1). However, the data describing this effect are limited. Since sulfite is present in all FGD systems, it is crucial that its effects be understood in order to model the dissolution process.

The nature of sulfite inhibition is illustrated in Figure 4. This figure shows the measured initial dissolution rates under baseline conditions for the HSTC limestone, along with the dissolution rate predicted by the mass transfer model (with no surface reaction limitations), as a function of the calcium sulfite relative saturation level. First, consider the experimental results. As shown in Figure 4, the dissolution rate increases with increasing sulfite up to a calcium sulfite relative saturation level of about 1.0. Then, the dissolution rate begins to decrease at higher calcium sulfite relative saturations. This same behavior was seen over a wide range of conditions with all of the limestones tested during the program.

The predicted dissolution rate, as shown in Figure 4, increases rapidly and continues to increase at high calcium sulfite relative saturations. This predicted increase in the dissolution rate is the result of the increasing buffer capacity of the liquid with increasing sulfite. Roughly the same type of behavior is predicted when a buffer such as adipic acid is used in place of sulfite. With adipic acid, however, the experimental dissolution rates are much higher at equivalent buffer capacity.

The difference between the predicted and experimental dissolution rates shown in Figure 4 is an indication of the magnitude of sulfite inhibition. In Figure 4, the difference between the experimental and predicted rates is about a factor of 18 at a calcium sulfite relative saturation level of 4.

An empirical model has been developed which accounts for the effect of sulfite in terms of a finite-rate reaction mechanism. The empirical model provides a surface reaction rate which is a function of the calcium sulfite and calcium carbonate relative saturations at the limestone surface;

$$\text{Surface Reaction Rate} = \frac{K(1 - \text{RS CaCO}_3)^{0.5}}{(\text{RS CaSO}_3)(\text{RS CaCO}_3)} \qquad (8)$$

where relative saturation is defined as the product of the activities of Ca++ and CO_3= (or SO_3=) divided by the K_{sp} of $CaCO_3$ (or $CaSO_3$). Note that solutions are saturated at RS=1.

Equation 8 indicates that the surface reaction rate is inversely proportional to the calcium sulfite relative saturation. As the calcium sulfite relative saturation goes to zero, the surface reaction rate goes to infinity. Under these conditions, the dissolution rate is entirely controlled by mass transfer through the film. As the calcium sulfite relative saturation increases, however, the surface reaction rate decreases. Similarly, at low calcium carbonate relative saturations, the denominator goes to zero and the surface reaction rate goes to infinity. As the calcium carbonate saturation goes to 1.0, the numerator and the surface reaction rate go to zero.

The value of K in Equation 8 must be determined experimentally and is different for different limestones. To do this, the mass transfer model is used to calculate the solid/liquid interface composition at the measured initial dissolution rate. Then, equation 8 is evaluated at this interface composition to obtain the value of K. The value of K was found to be constant for a particular limestone over a wide range of operating conditions. For the HSTC limestone, the value of K is 4.87×10^{-6} gmoles/s-m^2. Once K has been determined, predictions of the dissolution rate are obtained by varying the $CaCO_3$ relative saturation at the solid/liquid interface until an interface composition is found at which the diffusion rate (Equation 4) and the surface reaction rate (Equation 8) are equal.

The ability of the model to predict dissolution rates in the presence of sulfite is demonstrated in Figure 5. This figure shows a comparison between the measured and predicted dissolution rates for the baseline (HSTC) limestone. The data in Figure 5 include the variable ranges shown in Table 1 for pH, Ca++, Mg++, Na+, SO_3=, SO_4=, CO_3=, Cl-, and adipic acid. The results in Figure 5 show that the empirical model gives excellent predictions of the initial dissolution rate for dissolution rates over nearly two orders of magnitude. The average error between the experimental and predicted results is less than ±15 percent.

Note that tests conducted with aluminum fluoride, along with tests conducted at the highest magnesium concentrations (100 mM), are not shown in Figure 5. These species also inhibit limestone dissolution. However, there is not yet sufficient data to develop a rate form similar to Equation 8. Therefore, an empirical adjustment to the dissolution rate is required to account for their effects. Techniques which can be used to do this are described later in the paper.

OTHER EFFECTS OF SULFITE

In addition to the reduction in the initial limestone dissolution rate, sulfite causes a number of other important changes in the way limestone dissolves. As noted in the summary, these include much greater variation in the dissolution rates of different limestones when sulfite was present, an "age" effect in which the dissolution rate per unit area decreases as the limestone dissolves, and a change in the appearance of the limestone surface.

Experimental data illustrating the first two effects are provided in Table 3. This table shows the initial dissolution rates for 10 limestones, both with and without sulfite. The table also shows the ratio of the dissolution rate per unit area (at 50 and 80 percent dissolved) to the initial dissolution rate.

The data in Table 3 show that the initial dissolution rates without sulfite were about the same for each of the 10 limestones tested. When sulfite was present, however, the initial dissolution rates for these limestones varied by about a factor of 3. It is interesting to note that Iceland Spar gave the lowest dissolution rate in the presence of sulfite. This limestone is highly crystalline and is nearly pure calcium carbonate. This suggests that uniform, crystalline surfaces are particularly susceptible to sulfite blinding. The test results also imply that dissolution tests done in the absence of sulfite will not provide a true indication of the reactivity of limestones in FGD systems where sulfite is present.

Table 3 also shows the ratio of the dissolution rate per unit area (at 50 and 80 percent dissolved) to the initial dissolution rate. In tests without sulfite, this ratio remains at about 1.0 for many of the limestones. This means that the dissolution rate per unit area stays at a roughly constant level as the limestone dissolves (note that these tests were done over a particle size range where the film thickness is roughly constant). There was a decrease in the rate per unit area for some of the stones, particularly the Maysville and Gibson stones which contain a significant quantity of dolomite. When sulfite was present, however, the decrease in the dissolution rate per unit area was more dramatic for nearly all of the limestones tested. This behavior was seen over a wide range of operating conditions, including tests at low pH (4.5).

The "age" effect illustrated in Table 3 is the result of the finite-rate mechanism which controls limestone dissolution when sulfite is present. As indicated in photomicrographs presented later in the paper, the limestone surface is not uniformly reactive when sulfite is present. Therefore, some areas of the limestone surface dissolve more quickly than others. As the limestone dissolves, the average reactivity of the limestone surface decreases. As a result, the dissolution rate per unit area also decreases. These results lead to the conclusion that the dissolution rate of a particular limestone particle in the presence of sulfite is a function of its age as well as its size.

It should be noted that as a result of the "age" effect, the limestone dissolution model described previously can only be used to predict the initial limestone dissolution rate. That is, the model is not yet capable of predicting the depletion of the more reactive areas on the limestone surface. Therefore, an empirical adjustment is required to account for the age effect.

Experimental data were obtained during this program which simplifies this process considerably. An example of these results are shown in Figure 6. This figure shows the results of dissolution tests for three initial size fractions of Monteagle limestone under baseline conditions with sulfite. In Figure 6, a normalized dissolution rate, defined as the dissolution rate per unit area divided by the initial rate per unit area, is plotted against the fraction of the limestone which has dissolved.

The results in Figure 6 show that the normalized dissolution rate decreases as the limestone dissolves. By contrast, the normalized dissolution rates without sulfite stay at approximately 1.0 and do not drop as sharply as the fraction dissolved increases. Note, however, that the decrease in the normalized dissolution rate is about the same for each of the three size fractions tested. This means that the age effect is independent of the initial particle size and can be treated as a function of the fraction dissolved. This greatly simplifies the modeling process since the age effect can be characterized with one experiment and then applied to all other initial particle sizes as a function of the fraction dissolved.

The shapes of the curves in Figure 6 depend somewhat on the sulfite concentration. For example, at 80 percent dissolved, the Monteagle stone gives normalized dissolution rates of 0.64, 0.40, and 0.59 at calcium sulfite relative saturations of 0.27, 1.91 and 3.97, respectively. There were similar differences noted as a function of pH. However, these differences are relatively small and do not have a very significant effect on the predicted limestone utilization. In general, it appears that more reactive limestones can be adequately characterized with a single correlation between the normalized dissolution rate and fraction dissolved. This correlation can be applied to dissolution in both the hold tank and the absorber. However, for less reactive limestones (e.g., the last four limestones listed in Table 3), it will be necessary to use a correlation which is a function of solution composition (most likely as a function of bulk pH or calcium carbonate relative saturation).

Photomicrographs of partially dissolved limestones were obtained during many of the experiments conducted during this program. These photomicrographs reveal information about the mechanism of limestone dissolution both with and without sulfite. Examples of some of these photomicrographs are provided in Figures 7 through 14.

Figure 7 shows Iceland Spar limestone dissolved in the absence of sulfite. The particles are rounded indicating that the limestone surface is uniformly reactive. Similarly, rounded particles are seen with the HSTC limestone and limestone B in Figures 8 and 9, respectively.

Figure 10 shows the Iceland Spar limestone dissolved in the presence of sulfite. As shown in the figure, there is a dramatic change in the appearance of Iceland Spar dissolved in the presence of sulfite compared to Figure 7. The surface is considerably rougher and there are peaks of undissolved limestone covering the surface. This indicates that the limestone surface is no longer uniformly reactive but dissolves more quickly in some areas than in others.

Similar surface effects were seen with the other limestones tested during the program. Figures 11, 12, 13, and 14 show the HSTC limestone, limestone A, limestone C, and Edwards limestone dissolved in the presence of sulfite. These photomicrographs show that peaks similar to those seen on the Iceland Spar limestone have formed on all of these limestones. The effects are less dramatic with these limestones because they are not as highly crystalline as Iceland Spar. Similar surface features have been observed on photomicrographs of solids from several full-scale FGD systems.

LIMESTONE DISSOLUTION INHIBITION BY OTHER SPECIES

In addition to sulfite, several other species were identified which inhibit limestone dissolution. The relatively minor inhibition noted with magnesium and adipic acid has already been discussed. Aluminum fluoride complexes, however, have a much greater inhibiting effect and can inhibit dissolution at much lower concentrations (7). Aluminum can enter the FGD system in the fly ash or as a component of the limestone. Fluoride is absorbed from the flue gas where it is present as hydrofluoric acid. Neither aluminum nor fluoride is soluble at conditions typical of FGD systems. However, if both are present, aluminum fluoride complexes can form which are soluble. Severe limestone utilization problems have been experienced in full-scale FGD systems which have significant concentrations of aluminum fluoride complexes in solution (8).

Experimental tests were performed with sulfite in which the limestone dissolution rate was measured as a function of the aluminum fluoride concentration. The results are provided in Table 4. As shown in the table, the presence of small quantities of aluminum fluoride severely inhibited the limestone dissolution rate.

Severe aluminum fluoride blinding in full-scale FGD systems is a relatively rare phenomena and is usually associated with poor ESP performance. However, small quantities of aluminum are present in most FGD systems. Even at these levels, aluminum would be expected to inhibit limestone dissolution to some degree.

Several experimental tests were performed which illustrate this effect. Dissolution rates were obtained as a function of pH using process liquor obtained from the High Sulfur Test Center (HSTC). Additional tests were performed using simulated liquor which contained the same concentrations of only the major ions (Ca++, Mg++, Na+, SO_3=, SO_4=, NO_3-, Cl-, and CO_3=). The results of these tests are shown in Figure 15. The results show that the dissolution rate in the actual process liquor was, on average, about 35 percent lower than that seen in the tests with the simulated process liquor. Unfortunately, an analysis of the HSTC process liquor for aluminum was not performed on the process liquor used in these tests. However, the aluminum concentration in the HSTC pilot system typically runs about 3-10 ppm. Therefore, the decrease in the dissolution rate with the actual process liquor is consistent with the effect of aluminum presented in Table 4.

LIMESTONE DISSOLUTION MODEL

A limestone dissolution model has been developed which incorporates the results of the experimental test program. The model works well for the HSTC but has not yet been tested at other systems. The mathematical formulation of the model is;

$$\text{Dissolution Rate} = (\text{Initial Dissolution Rate})(Fa)(Fi) \qquad (9)$$

where:

Dissolution Rate = the dissolution rate for any particle present in the system;

Initial Dissolution Rate = the initial dissolution rate predicted by the empirical mass transfer model which accounts for the effect of sulfite;

Fa = a factor which accounts for the "aging" effect of sulfite; and

Fi = a factor which accounts for the inhibition due to trace species such as Al.

The mass transfer model provides an estimate of the initial dissolution rate which is dependent on the solution composition, pH, and the film thickness (δ). In the absence of inhibitors other than sulfite, the mass transfer model provides a good estimate of the initial limestone dissolution rate. As described previously, the mass transfer model was also modified to neglect enhancement due to the finite-rate hydrolysis of CO_2.

Fa is a factor which accounts for the particle aging effect in the presence of sulfite. It is an empirical function of the fraction dissolved, the limestone type, and solution composition, and must be determined experimentally using data similar to that presented in Figure 6. For more reactive limestones, Fa appears to be a weak function of solution composition as long as some sulfite is present. However, limestones which show a severe aging effects may require a value for Fa which is also a function of pH or calcium carbonate relative saturation.

Fi is a factor which accounts for inhibitors other than sulfite. These can include Mg++, Al+++, and other potential inhibitors. The value of Fi can be estimated from the magnesium and aluminum concentrations in the system. However, it is better to compare the results of tests conducted with both actual and simulated process liquor. This will simultaneously account for the effects of all species which act to inhibit limestone dissolution.

Due to the differences in the dissolution rates of limestones in the presence of sulfite, experimental tests are needed in order to model a specific FGD system. However, if actual process liquor and limestone are used, the factors K, Fa, and Fi can be determined with only a limited number of experimental tests. This procedure will also minimize errors associated with the mass transfer model. The result of this procedure is a calibrated model which should accurately predict the effects of changes in process conditions on the limestone dissolution rate.

In the application of the model, the limestone dissolution rates (calculated for both the hold tank and absorber modules) from the above model are combined with a particle balance which accounts for particle washout with the blowdown stream. The result is an estimate of the limestone utilization.

The test results for the dissolution rates using actual HSTC process liquor (in Figure 15) have been used to estimate limestone utilization in the HSTC system. These estimates were based on a particle size analysis of the HSTC as-ground limestone and a particle balance which incorporates the effects of solid phase residence time. Estimates were prepared for operation at pH 5.5 and 5.7. A comparison of these estimates with operating data from the HSTC is presented in Figure 16. These results show good agreement between the actual HSTC limestone utilization and that predicted from the experimental tests. This indicates that if all of the factors affecting limestone dissolution are accounted for, good estimates of the limestone utilization can be obtained. Then, the limestone dissolution model can be used to estimate the effect of changes in system operation on limestone utilization.

MODEL APPLICATIONS

The modeling capabilities developed during this test program should be useful to utilities in several ways. First, the experimental apparatus can be used to determine the reactivity of limestones for use in FGD systems and help to identify causes of poor utilization. Second, the limestone dissolution model, in conjunction with FGDPRISM, should be useful in a variety of ways. Several examples are provided which illustrate the potential uses of the test apparatus and the limestone dissolution model.

The experimental apparatus can be used to identify the causes of poor utilization in operating FGD systems. Tests can be done using limestone along with both simulated and actual process liquor from full-scale systems. The results will show two things. First, the results can indicate the reactivity of the limestone in sulfite. This is important since previous dissolution tests may have been performed in the absence of sulfite. As shown previously in Table 3, dissolution data in the absence of sulfite will not indicate the true reactivity of the limestone in FGD systems. Second, the results should indicate if inhibitors are present which are causing impaired utilization. Combined, these results could pinpoint the cause of poor utilization and provide direction for solving the problem. The test apparatus could also be useful for utilities considering a change in limestone type for some other reason. The test results would indicate which of the candidate limestones are more likely to provide good performance in an FGD system.

The limestone dissolution model has been developed as a part of an overall FGD process integration and simulation model (FGDPRISM). FGDPRISM includes unit operations modules for the absorber, hold tank, and thickener. The process model calculates gas/liquid mass transfer rates in the absorber, the precipitation rates of calcium sulfite and sulfate solids, the limestone dissolution rate, and performs overall system material balances.

The process model is capable of estimating the effects of changes in a wide range of variables on the operation of the FGD system. The types of operations which can be simulated by the process model include, but are not limited to, contactor configuration (L/G, trays, etc.), inlet gas composition and temperature, limestone type and grind, additives, make-up water quality, suspended solids concentration, residence times (solid or liquid), sulfite oxidation, and solids settling. The limestone dissolution model is an integral part of the overall process model.

REFERENCES

1. Rochelle, G. T., Chan, P. K. R., and Toprac, A. T. Limestone dissolution in flue gas desulfurization processes. EPA600/7-83-043 (PB83-252833). U.S. Environmental Protection Agency, Washington, DC, 1983. 101 pp.

2. Faist, M.B., Hebets, M.J., and Gevirtzman, L. Development of a chemistry and process engineering simulator (CAPES) capable of modeling chemistry and engineering problems in wet lime/limestone flue gas desulfurization. U.S. Department of Energy, DOE Contract No. DE-AC21-80MC14549, Morgantown, West Virginia, 1983.

3. Smith, T.P., Hebets, M.J., and Faist, M.B. FGD chemistry and analytical handbook. EPRI CS3612-CCM, Volume 3: Instructions for the Use of Computer Program FGDLIQEQ. Project 1031-4, Electric Power Research Institute, Palo Alto, CA, 1984.

4. Bird, R. B., Stewart, W. E., and Lightfoot, E. N. Tranport Phenomena. John Wiley & Sons, New York, NY, 1960.

5. Colley, J. D., et al. Control and reduction of gypsum scaling in wet lime/limestone FGD systems by addition of thiosulfate: Summary of field experiences. Presented at the EPA/EPRI First Combined FGD and Dry SO_2 Control Symposium, St. Louis, MO. October 25-28, 1988.

6. Rochelle, G. T., Owens, D. R., Chang, J. C. S., and Brna, T. G. Thiosulfate as an oxidation inhibitor in flue gas desulfurization processes: A review of R and D results. JAPCA 36. pp 1138-1146, 1986.

7. Farmer, W. R., and Jarvis, J. B. Effects of aluminum/fluoride chemistry on wet limestone flue gas desulfurization. Paper 78f. Presented at the 1987 Spring National AIChE Meeting in Houston, TX. March 29 - April 2, 1987.

8. Colley, J. D., et al. Investigation of flue gas desulfurization chemical process problems. Research project 2248-1. Draft interim report to the Electric Power Research Institute, Palo Alto, CA. 1988.

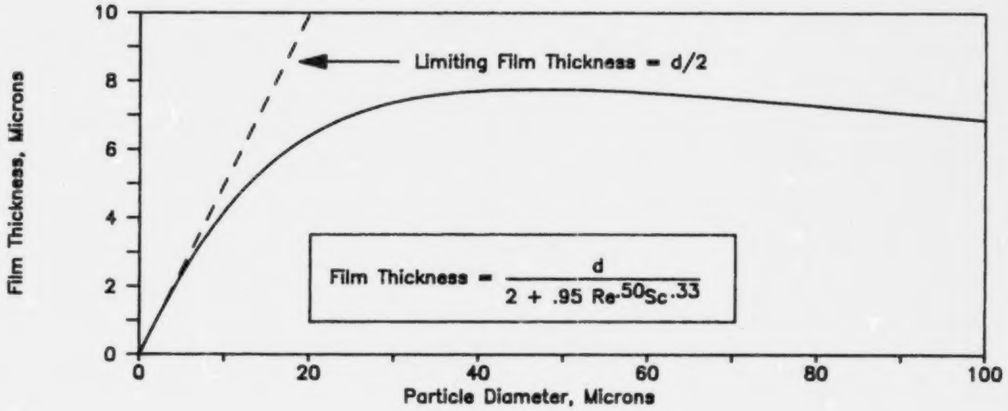

Figure 1. Relationship between the nominal particle diameter and the stagnant film thickness.

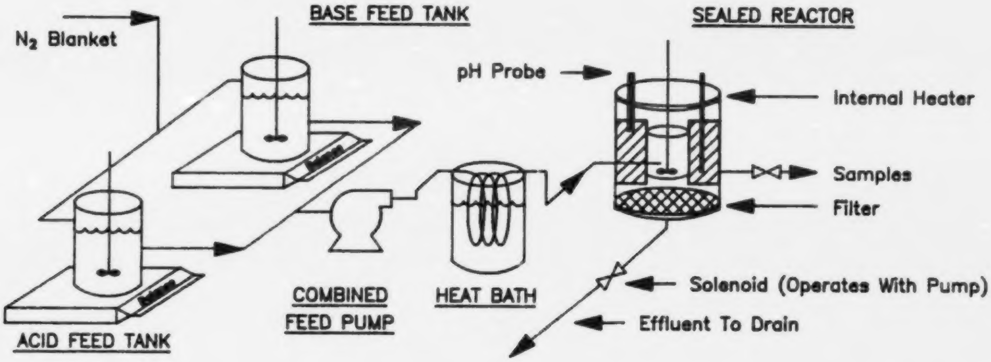
N₂ Blanket
BASE FEED TANK
SEALED REACTOR
pH Probe
Internal Heater
Samples
Filter
Solenoid (Operates With Pump)
Effluent To Drain
COMBINED FEED PUMP
HEAT BATH
ACID FEED TANK

Figure 2. Diagram of the experimental limestone dissolution apparatus.

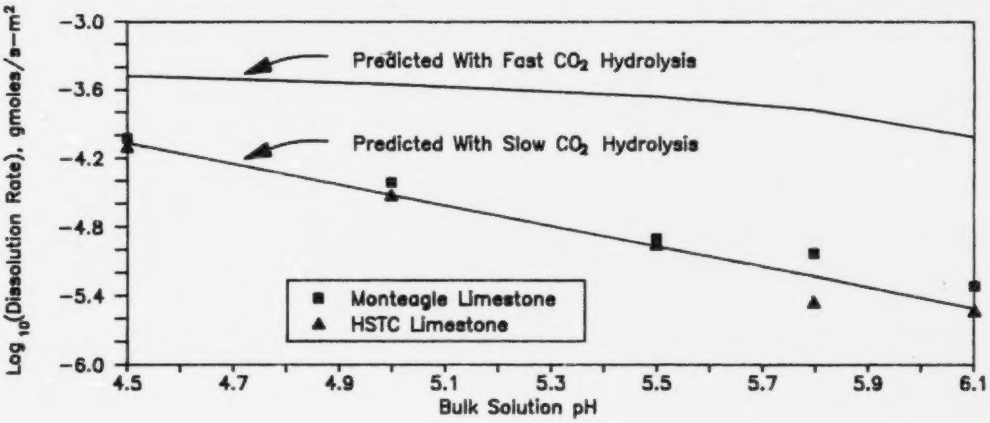

Figure 3. Experimental and predicted limestone dissolution rates versus pH at baseline conditions without sulfite.

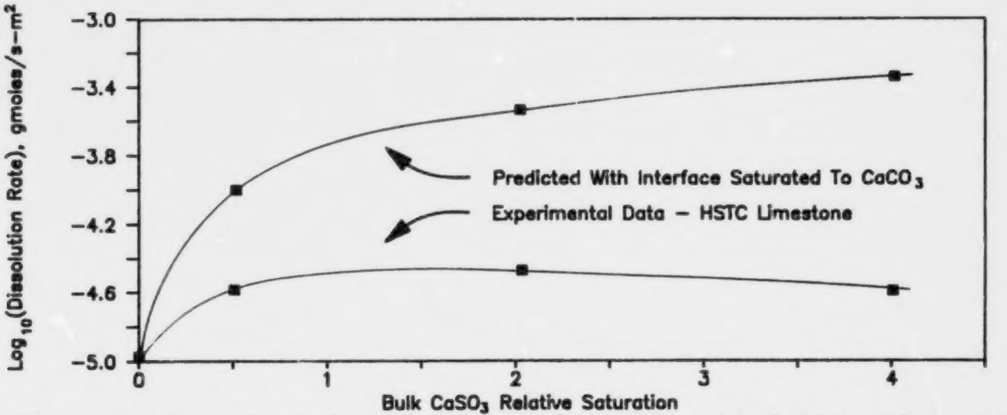

Figure 4. Experimental and predicted limestone dissolution rates versus calcium sulfite relative saturation for the HSTC limestone at baseline conditions.

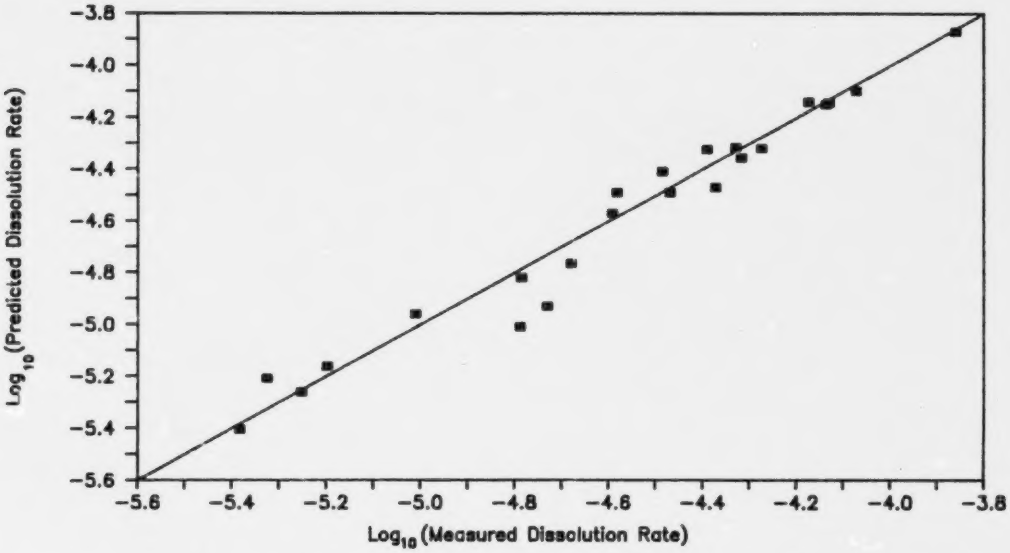

Figure 5. Predicted versus experimental limestone dissolution rates for all HSTC limestone tests with sulfite.

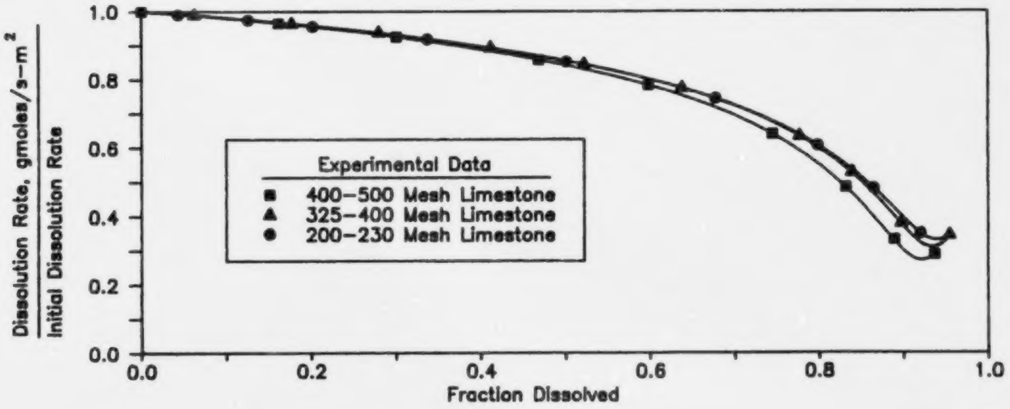

Figure 6. "Age" effect with sulfite - Normalized Monteagle dissolution rate per unit area versus fraction dissolved for three size ranges.

Reproduced from
best available copy.

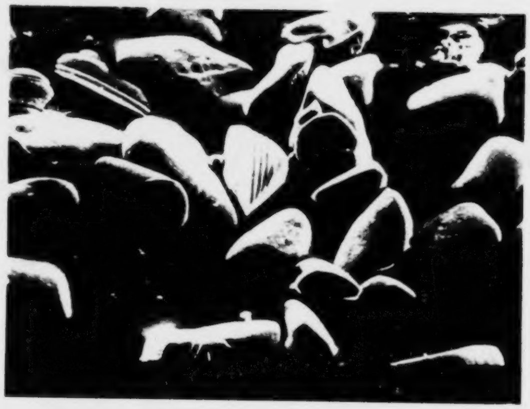

Figure 7. Iceland Spar limestone; no sulfite; 75% dissolved; 310X.

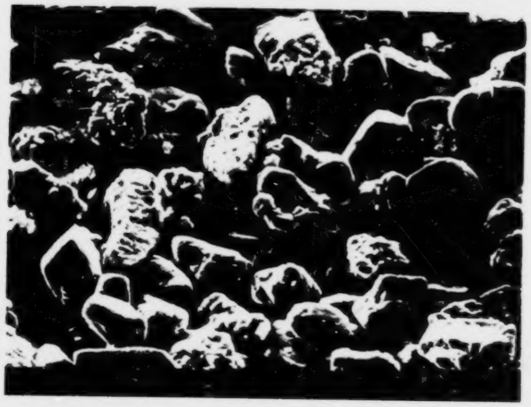

Figure 8. HSTC limestone; no sulfite; 50% dissolved; 500X.

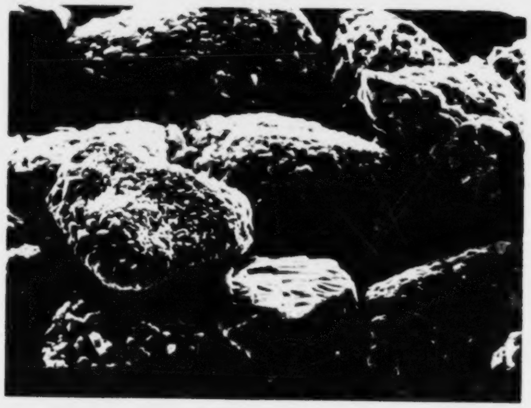

Figure 9. Limestone B; no sulfite; 50% dissolved; 1000X.

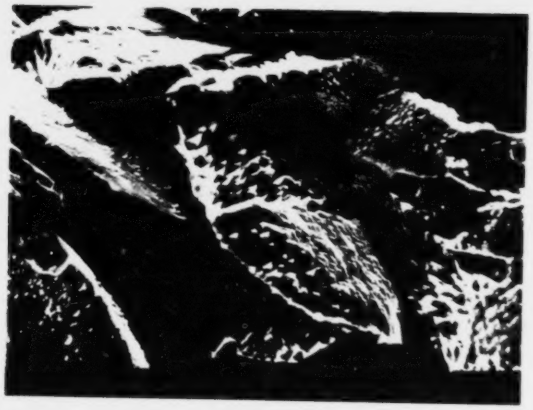

Figure 10. Iceland Spar; with sulfite; 50% dissolved; 1000X.

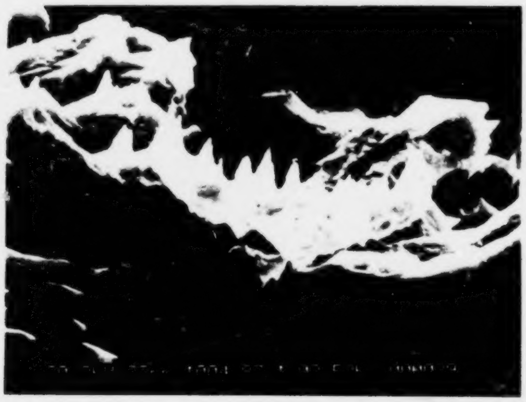

Figure 11. HSTC limestone; with sulfite; 50% dissolved; 3500X.

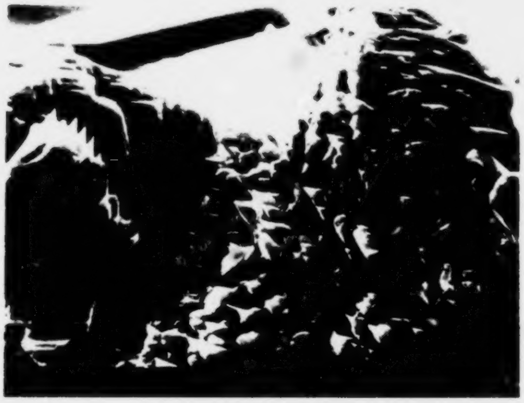

Figure 12. Limestone A; with sulfite; 50% dissolved; 3500X.

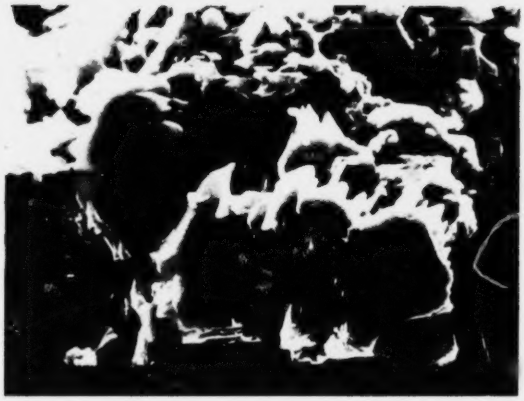

Figure 13. Limestone C; with sulfite; 50% dissolved; 3500X.

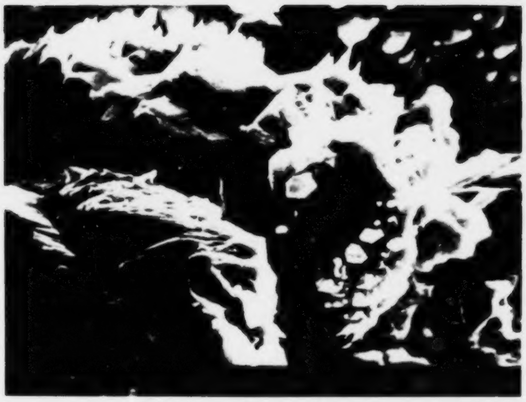

Figure 14. Edwards limestone; with sulfite; 50% dissolved; 3300X.

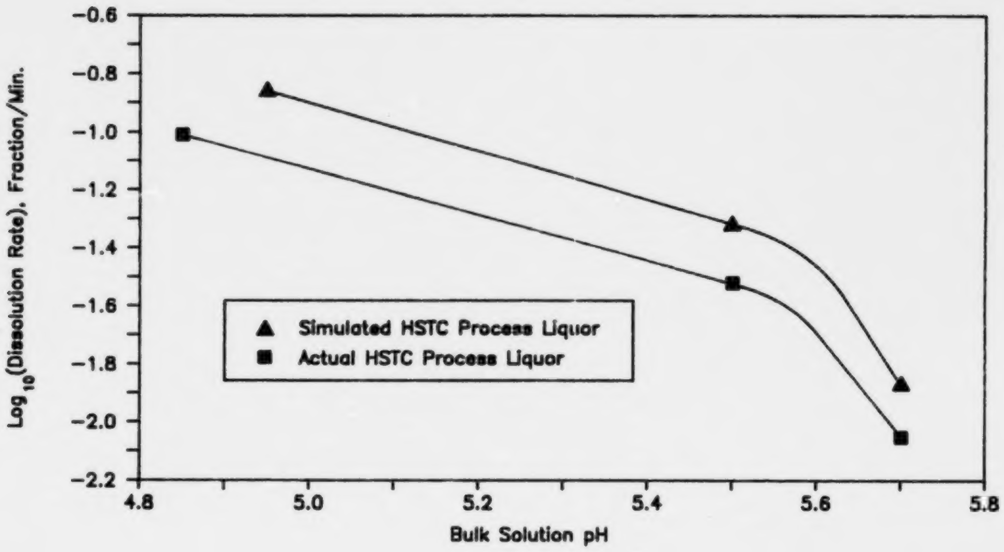

Figure 15. Effect of inhibitors in the HSTC pilot system - comparison of the HSTC as-ground limestone dissolution rate for actual and simulated HSTC process liquor.

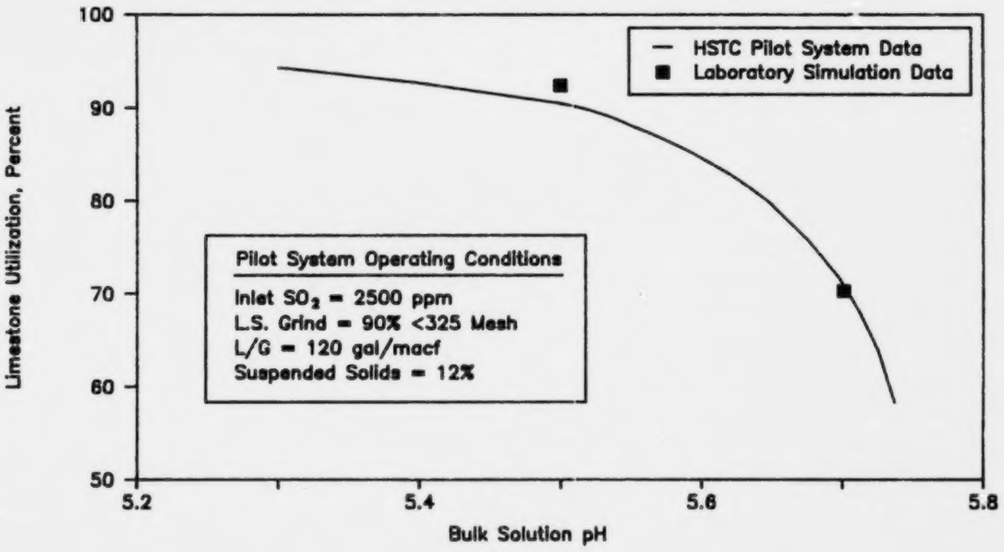

Figure 16. Comparison of the predicted and measured limestone utilization for the HSTC pilot system as a function of pH.

TABLE 1. RANGE OF TEST VARIABLES USED IN THE EXPERIMENTAL TEST PROGRAM

Variable	Variable Range	Baseline Levels (Without and With SO_3=)
pH	4.5 - 6.4	5.5
Ca++, mM	5 - 150	40
Mg++, mM	0 - 100	15
Na+, mM	15 - 110	33 and 27
SO_3=, mM	0 - 40	0 and 6
SO_4=, mM	0 - 50	15
CO_3=, mM	2 - 8	2
$CaSO_3 \bullet 1/2\ H_2O$ RS[1]	0 - 5	0 and 4
$CaSO_4 \bullet 2\ H_2O$ RS	0 - 1	0.9
$CaCO_3$ RS	0.0003 - 0.40	0.025
P*CO_2, atm.	0.05 - 0.40	0.083
Limestone Type	10 Limestones[2]	HSTC
Particle Size, mesh[3]	400-500; 325-400; 200-230; as-ground	325-400
AlFn, mM	0.0 - 0.6	0
Adipic Acid, mM	0 and 6	0
Thiosulfate, mM	0 and 9	0
Fe+2, Fe+3, ppm	0 and 5	0
Mn+2, ppm	0 and 5	0
Temperature,°C	35 - 65	50
Stir Rate, rpm	300 - 1800	1800

[1] Relative saturation is defined as the product of the liquid phase activities of the ions in a solid divided by the K_{sp} of the solid. Solutions are saturated at an RS of 1.0.

[2] Information on these limestones is presented in Table 2.

[3] Average nominal particle sizes are 69, 41.5, and 31.5 microns for the 200-230, 325-400, and 400-500 mesh size cuts. The as-ground limestone size range was 90 percent passing 325 mesh (44 microns).

TABLE 2. COMPOSITION OF THE LIMESTONES INCLUDED IN THE DISSOLUTION TESTS

Limestone	Magnesium Content, %	Inerts, %
Iceland Spar	0.04	0.01
HSTC[1]	0.2	0.9
Monteagle	0.6	4
Maysville[2]	1.7	4
Edwards	0.1	0.2
Arapahoe[3]	0.12	10
Limestone A[4]	0.19	7
Limestone B	0.1	0.7
Limestone C	0.0	6
Limestone D[2]	3.1	5

[1] Limestone used at EPRI's High Sulfur Test Center (HSTC).

[2] Contains dolomite.

[3] Limestone used at EPRI's Arapahoe test facility.

[4] Lettered limestones obtained from operating utility FGD systems.

TABLE 3. LIMESTONE DISSOLUTION RATES FOR DIFFERENT LIMESTONES[1]

	Tests Without Sulfite			Tests With Sulfite		
	Initial Rate[2]	Norm. Rate at 50% Dissolved[3]	Norm. Rate at 80% Dissolved	Initial Rate	Norm. Rate at 50% Dissolved	Norm. Rate at 80% Dissolved
HSTC	12.6	1.06	1.09	27.4	0.91	0.78
Arapahoe	13.1	0.99	1.02	27.3	0.93	0.83
Iceland Spar	13.5	0.94	0.85	14.0	0.94	0.88
Monteagle	13.1	0.94	0.85	36.6	0.86	0.59
Limestone A	12.6	0.98	0.95	24.0	0.85	0.63
Limestone B	12.9	0.99	0.97	47.1	0.89	0.71
Limestone C	12.2	0.89	0.62	27.2	0.86	0.37
Edwards	10.5	0.93	0.80	18.5	0.75	0.07
Maysville	11.0	0.75	0.35	45.7	0.56	0.10
Limestone D	10.6	0.63	0.19	29.6	0.15	0.05

[1] Baseline test conditions at a $CaCO_3$ relative saturation of 4.0 using a 324-400 mesh limestone grind.

[2] Rates given in gmoles/sec-m^2 (x10^6).

[3] Normalized rate is the ratio of the rates per unit surface area at 50% and 0% dissolved (or 80% and 0% dissolved).

[4] Data illustrating the normalized dissolution rates versus fraction dissolved for this limestone were presented in Figure 6.

TABLE 4. EFFECT OF ALUMINUM FLUORIDE COMPLEXES ON LIMESTONE DISSOLUTION[1]

Aluminum Concentration, ppm[2]	Normalized Initial Dissolution Rate
0	1.00
3	0.51
8	0.24
15	0.09

[1] Results in this table are for HSTC limestone dissolved under baseline conditions with sulfite.

[2] Aluminum and fluoride added at a ratio of 1:3 (AlF_3).

PERFORMANCE IMPACT OF MIST ELIMINATORS AND WET ELECTROSTATIC PRECIPITATORS

by: Even Bakke and Otto Sarmiento

Flakt Inc.
Peabody Process Systems Division
201 Merritt Seven
Norwalk, CT 06852

ABSTRACT

Design considerations and performance of state-of-the-art mist eliminators in wet FGD systems are discussed and the impact on reheat strategies and particulate emissions is evaluated. Experience in the United States is compared to Japanese and European experience.

The impact of retrofitting wet FGD to high sulfur coal fired boilers in terms of particulate emissions, S03 emissions and stack opacity is discussed. The use of wet electrostatic precipitators for mist elimination, fine particulate and S03 emissions reduction when firing high coal sulfur coals is also presented.

The capital and operating costs of mechanical mist elimination and wet electrostatic precipitators and their impact on reheat economics are presented.

DISCLAIMER

The work described in this paper was not funded by the U.S. Environmental Protection Agency and therefore the contents do not necessarily reflect the views of the Agency and no official endorsement should be inferred.

INTRODUCTION

Mist eliminator operation and performance has been identified by many investigators to be one of the most critical items in reliable wet flue gas desulfurization (FGD) operation. It has also been found that operation on higher sulfur coals with closed FGD water loop puts additional strains on reliable mist eliminator operation.

Today, there are two basic mist eliminator mechanisms used in wet FGD systems; by mechanical impaction or interception on a surface, fiber or blade or by electrostatic charging and collection on a tube or plate electrode. The former method is by far the most prevalent, and the latter is used when a high degree of mist elimination and/or particulate emission reduction are required.

The mist eliminator performance, or lack thereof, will have a direct impact on stack emissions and stack opacity. The performance of the flue gas reheat system and energy requirement for reheat will also be impacted by mist eliminator performance.

With the large amount of wet FGD retrofit work going on in the world and the upcoming acid deposition reduction program in the United States and Canada, it is essential that reliable and high performance mist eliminator methods are identified and implemented, especially since in most retrofit installations, due to space limitation, there will be no spare scrubber module and each module will be built as large as possible. Therefore, even at low loads, there will be limited opportunities to shut down a scrubber module for mist eliminator service while the boiler is in operation.

More stringent emission limits are foreseen and in retrofit scenarios, further reduction in particulate emissions is definitively a possibility. This will impose additional performance requirements on mist eliminators and, in some cases, require the installation of a wet electrostatic precipitator (WESP) down stream of the SO2 scrubbing section.

MIST ELIMINATOR DESIGN AND PERFORMANCE

When absorbing SO2 in a lime or limestone scrubber, the gas entrained droplets exiting the SO2 absorption zone must be removed by a mist eliminator section. Due to the inherent solids build-up potential when operating with a slurry, the mist eliminator must be cleaned constantly, but still function as a mist eliminator. These are two contradictory requirements; an efficient mist eliminator requires relatively narrow spaced and deep elements which inherently makes it difficult to clean the internal surfaces. A compromise between efficiency and washability mist therefore be made, and this is a delicate balance that must be recognized and established.

Most of the mist eliminator elements or blades used in early wet FGD installations were developed for droplet removal in solution (clear liquor) scrubbing, where the blades were more or less self cleaning. Some of the blades were developed for horizontal flow and simply adapted to vertical flow installation or vice versa. There was little thought given to in-place continuous washing requirements or manual cleaning of the blades. The fact that workers would walk on top of the blades during inspection, repair and cleaning was more or less neglected. Rapid replacement of damaged or plugged mist eliminator sections was given low priority by the designers, since there was usually an unused spare module available at all times. The FGD scrubber water loop was open or perceived open and the amount and quality of the washing water required was simply a guess from the designer's point of view. It was not always recognized that the mist eliminator section was an integral part of the scrubbing system where S02 absorption, calcium sulfite and sulfate crystallization were continuing. The fact that the space between the blades could fill up solid with a combination of dried slurry and scale was not recognized and whole sections have collapsed due to lack of structural integrity.

The list goes on, but it is obvious that the mist eliminator designer and the FGD process designer have to take most of the "credit" for the mist eliminator's poor performance record at many FGD installations.

From this hard earned and costly experience emerge a design philosophy that there should be little debate over today:

- Strong and rugged blades and blade alignment mechanisms that will not be destroyed during maintenance work such as stepping on them, manual cleaning, installation or removal.

- Smooth and strong blades, with no or few hooks, troughs or ridges, that will wash easily and can be washed down manually in a relative short time.

- Smooth blades that will drain quickly so that there is a very small hold-up or residence time of the collected slurry and washing liquid on the blades where residual S02 will be absorbed and converted to calcium sulfite and sulfate crystals that will build up on the blades.

- Adequate washing rate and spray cone coverage to ensure sustained operation with clean blades.

- Wash water which is not saturated, or even worse, super saturated with calcium sulfate. If such water is used, hard gypsum scaling will form on the blades which will greatly accelerate the slurry solids build-up.

- Two stage mist eliminators, a first stage with an "open" blade configuration for effective and high intensity blade washing and a second stage for effective droplet removal in a more "closed" blade configuration and less intensive washing with the highest quality water available in the FGD system.

- Use of washing spray nozzle that do not easily plug and even distribution of washing droplets across the whole mist eliminator section.

- Use of strainers or filters for the mist eliminator wash water system to minimize nozzle plugging.

- Operation of the absorber modules within the velocity limits of the mist eliminator, i.e., don't exceed the specified gas volume to each module.

- Ensure equal gas distribution between each absorber module and equal gas velocity distribution of the gas entering the mist eliminator section. This should be accomplished by careful model studies during the design phase and field confirmation and adjustments after start-up.

- Easy and quick access to the area above and below the mist eliminator section and frequent inspections of the conditions of the blades with respect to solids build-up. Once build-up starts, the rate of build-up increases exponentially.

- As the water loop is closed more and more, the concentration of dissolved solids in the scrubber loop increases and as the SO2 concentration in the flue gas increases, i.e., when firing high sulfur coal and oil, the above stated principles become more and more important to ensure reliable mist eliminator operation with minimal maintenance.

- With closed water loop operation, especially at low loads, the quality and quantity of the available make-up washing water becomes critical in terms of reliable operation. With high dissolved solids in the return water from the slurry dewatering equipment, the calcium sulfate saturation level increases causing an increasing scaling potential if this water is not blended with high quality make-up water.

Hand in hand with a well thought out design philosophy, there must be a sensible operating philosophy such as:

- Frequent inspections of the blades for signs of solids build-up or scaling and plugged wash nozzles

- Cleaning and unplugging on a high priority basis

- Careful monitoring of mist eliminator pressure drop and flow of wash water. Upon changes, high priority correction of the problem

In Germany and Japan, pre-scrubbers are widely used to remove HCl and flyash from the flue gas prior to SO2 absorption. In many cases, this is required for production of high purity gypsum where flyash and chlorides are considered to be contaminants. Mist elimination between the pre-scrubber and the absorber is often required to minimize contamination of the SO2 scrubbing loop with the low pH flyash slurry. With close coupling, i.e., little space between the pre-scrubber and the absorber, high performance mist elimination between the two scrubbing loops becomes a significant design challenge.

The basic performance of the mist eliminator types and shapes must be determined by relatively large scale air and water tests on full size blades. These tests will establish the following basic criteria:

- Maximum gas velocity before significant reentrainment takes place

- Pressure drop versus gas velocity

- Optimum placement and type of spray nozzle for blade washing

- Flow rate and pressure of the washing water

- Drainage characteristics of the blades

In our opinion, the droplet size versus removal efficiency curves published by most eliminator suppliers are useless. The energy level in the spray nozzle cones and gas interaction zones for slurry spray towers is so low that the fraction of droplets smaller than say 20 microns is insignificant. It is in the range below 20 microns that the mist eliminator collection efficiency starts to drop off and it is impossible to confirm these curves under actual operating conditions in the field. Our experience has shown us that is is the velocity at which significant reentrainment or discharge of collected droplets take place that will set the upper velocity limits or capacity of the mist eliminator. The outlet concentration of droplets after mist elimination should be the prime performance criteria.

At this point, a brief discussion of vertical flow versus horizontal flow mist eliminators is appropriate. Table 1 lists some of the pro's and con's of the two different designs. It should be recognized that vertical flow mist eliminator sections often are installed at an angle and horizontal flow elements are typically placed vertical or on a small angle to the vertical position. Figure 1 shows a two stage vertical flow mist eliminator section.

Of the comments listed in Table 1, the most important advantages of the vertical flow units are:

- As the gas exits the SO2 absorption zone, good gas distribution is established without local high velocities which could cause reentrainment and droplet discharge
- Quick, multipoint and "open" drainage of collected slurry droplets, right back to the absorber zone
- Excellent serviceability, manual cleaning and removal from the top of the mist eliminator section

The most important disadvantages are:

- Difficult and expensive to have a separate washing circuit
- Slightly larger cross section is required due to a lower velocity limit before reentrainment of droplets

The most important advantages of the horizontal flow units are:

- Separate washing circuit can easily be made due to the vertical drainage. This might save washing water amounts
- Slightly higher capacity of a cross section due to higher velocity limit before reentrainment
- Savings in scrubber vessel height

The most important disadvantages are:

- Potentially poor gas distribution after the 90o turn into the horizontal flow mist eliminator
- Plugging of drain boxes and pipes due to local scaling. There is

an upper limit of blade length due to drainage amounts toward the bottom of the blade sections

- Manual cleaning is not easy since scaffolding or ladders must be installed to reach the upper sections

As a compromise, some FGD suppliers use a combination of vertical flow for first stage and a horizontal flow section for second stage mist elimination. However, it is our opinion that the advantages of the vertical flow mist eliminator outweighs the advantages of a horizontal flow mist eliminator. The major concern being the gas distribution, plugging of drain boxes and pipes for the horizontal mist eliminator.

OPERATING EXPERIENCE AND TEST RESULTS

Flakt/Peabody's experience with mist eliminator performance over the last 15 years is probably typical among the FGD suppliers, we encountered more or less all of the problems described above. In 1985, after having experienced mist eliminator performance problems in three limestone FGD installations, we decided to investigate the major mist eliminator blades available on the market. After extensive tests in a 7 ft. diameter plexiglas test tower, it was decided none of the blades available satisfied all of the criteria discussed above and we decided to develop our own design. Figure 2 shows a cross section of the first and second stages. The blades are aligned with the help of threaded rods and elastic spacers at one end of the blades and with slots in a bar on the other end. By removing the slotted bar, the FRP blades can be bent aside for full access to the interior of the blades during manual cleaning. The blades come in preassembled sections which can be carried in by two men and quickly be installed or replaced. The design has been granted a U.S. Patent and foreign patents have been filed for.

The second stage blade configuration has a local, free velocity limit of about 14 ft/sec before significant reentrainment will start. Typical design velocities are 10 to 12 ft/sec. As indicated in Table 2, we have tested several of these installations and find that all of them have an outlet droplet concentration of less than 0.01 gr/acf (23 mg/m3) and that the two stage section has a pressure drop of about 0.3 in. W.G. (8 mm W.G.) at 10 ft/sec (3 m/sec) superficial free velocity (excluding support obstructions). Outlet concentrations as low as 0.001 gr/acf (2 mg/m3) have been measured. Very significant increase in time between manual cleaning has been experienced after installation of these new mist eliminators, e.g., from a frequency of every 2 to 3 weeks to every 3 to 4 months or longer on high sulfur coal applications operating with a closed water loop.

The droplets escaping the mist eliminator contains both suspended and dissolved solids. When the gas is reheated, the water will evaporate, and the dissolved and suspended solids will become part of the solids particulate emissions from the system. The impact of these particulates can be significant. If we assume a droplet emission of 0.01 gr/scfd with 10% suspended solids and 5% dissolved solids, this represents 0.0015 gr/scfd or about 10% of a typical NSPS requirement of 0.015 gr/scfd (0.03 lbs/mm Btu). However, if the mist eliminator should emit 0.1 gr/scfd due to poor performance overloading, broken blades or poor installation resulting in openings between sections, with 15% dissolved and suspended solids in the slurry droplets, the plant would emit at NSPS levels just from the droplet emission, leaving no room for residual flyash.

The same argument obviously applies to the impact on the stack opacity. If the flue gas is reheated, the entrained droplets will evaporate and the dissolved solids portion can form a submicron fume which can increase the stack opacity significantly.

On high sulfur coal and oil firing, the impact of droplet caused solids become even more important because of the presence of S03 aerosol. These fines form in the scrubber as the temperature drops below the acid dew point. The S02 absorber is not very effective in collecting the resulting S03 aerosol; only 30% to 40% is collected and the rest will escape. A boiler generating 20 ppm of S03 (0.031 gr/scfd or 71 mg/Nm3) leaves 12 to 14 ppm exiting or about 0.02 gr/scfd. If this is counted as solids in the stack sampling procedure, the plant will be in violation of NSPS just on the S03 portion. 12 to 14 ppm of S03 will also have a very severe impact on the stack opacity (more than 30% in a 20 ft. diameter stack). In this case, it is very important that the mist eliminator contribution to particulate emission is kept at an absolute minimum. The mist eliminator itself is incapable of collecting the submicron S03 fine; it will travel straight through.

From the above discussion, it is obvious that overloading the mist eliminator or allowing operation with plugged sections can severely impact the stack emissions and cause boiler load reduction or, in the worst case, shutdown and manual cleaning.

VERY HIGH PERFORMANCE MIST ELIMINATOR WITH WESP's

In cases where stack opacity and stack emissions have to be reduced significantly, for example, where there is significant concentrations of S03 or submicron flyash particles in the gas exiting from the electrostatic precipitator (ESP), a wet electrostatic precipitator (WESP) installed downstream of the scrubber can be effective. The WESP can, dependent upon the removal efficiency required, be installed on top of the S02 absorption zone as shown in Figure 3 or be a separate stand-alone unit downstream of the absorber. The former case would be a single field unit with 70% to 90% removal efficiency, the latter a multi-field high efficiency unit. In either case, the entrained water droplets will also be collected electrostatically and a high efficiency mist eliminator section would not be required.

A WESP is very effective in removing S03 aerosol which, if uncontrolled, can cause very high stack opacities and corrosion potential downstream of the scrubber. S03 is particularly a problem when firing high sulfur oil with high vanadium content. The vanadium is a catalyst in the oxidation of S02 to S03. Combined S03 and flyash emissions of less than 0.005 gr/scfd (11.4 mg/Nm3) have been demonstrated in a WESP pilot plant operating on flue gas from a high sulfur (5%) coal boiler.

MIST ELIMINATOR PERFORMANCE AND REHEAT REQUIREMENTS

The flue gas is reheated to increase plume buoyancy, operate the stack at high velocity (reduced diameter) and minimize "spitting" caused by entrained droplets exiting the stack. If a fan is installed downstream of the S02 absorber, some reheat might be required to reduce solids build-up on the fan blades causing unbalancing.

There are four typical reheat methods:

- Regenerative reheat, gas to gas or gas to liquid
- Direct reheat by a steam to gas reheat exchanger
- Indirect reheat by blending hot air with flue gas
- Flue gas bypass reheat which requires higher SO2 removal in the absorber

There is also the option of no reheat, i.e., operate a "wet" stack.

In all cases, the performance of the mist eliminator is important for the reheat operation, the major impact being the heat load required to evaporate the escaping water or slurry droplets. The higher the droplet concentration, the lower the resulting reheat temperature due to the required heat of evaporation. If there are heat exchanger surfaces involved in the reheat, i.e. for regenerative and direct reheat, the droplet concentration and the contained dissolved and suspended solids will cause build-up and fouling of the heat exchanger surfaces.

If the no reheat, i.e., the "wet" stack option is selected, efficient mist eliminator operation is important to reduce the "spitting" from the stack. Also, to minimize reentrainment, water drainage point in the ductwork and the stack must be controlled with liquid drainage to the outside.

COSTS

A high quality, two stage mist eliminator costs about $100 per square foot on an installed basis. With 10 ft/sec design velocity and when firing high heating value coal (e.g., 11,000 Btu/lb), this is equivalent to about $0.50/kw, i.e., a very modest cost compared to the cost of the whole FGD system (say $75 to $120/kw for typical FGD vendor scope installed cost). However, as pointed out above, the potential for operational problems with the mist eliminator makes the investment in a high quality, rugged, and well designed mist eliminator extremely cost effective and worthwhile. It does not make sense to save a few dollars in purchasing a fragile, thin blade design that would need replacements after a short time.

Operating costs are minimal due to low pressure drop as long as frequent manual cleaning is not required. Again, careful attention to blade design and washing water quality will ensure reliable operation with minimal maintenance costs.

On the other hand, if a WESP is required for significant reduction in stack emissions, the capital costs will be much higher. Typically, a one field WESP will cost $15 to $25/kw on an installed basis. This investment should be considered as an option to significantly upgrade the particulate removal efficiency of the air pollution control system, or as a method for a drastic reduction on stack opacity caused by SO3 fumes and submicron particles.

CONCLUSIONS

The mist eliminator and its washing must be considered as an integral part of the FGD system. Careful attention to design and operation details will result in reliable low cost operation. If these details are overlooked or ignored, the mist eliminator operation can be very expensive due to potentially high maintenance work in terms of manual cleaning and in the worst case limit the operation of the FGD system and the boiler.

If the mist eliminators are overloaded due to excessive gas flow or poor gas distribution, its lack of performance can severely impact the plant emission to a point where boiler load will have to be limited.

High performance mist eliminators are today available and can, in many cases, be retrofitted into existing FGD systems without excessive capital costs, but with significant maintenance cost reductions in terms of much longer time spans between required maintenance such as manual cleaning.

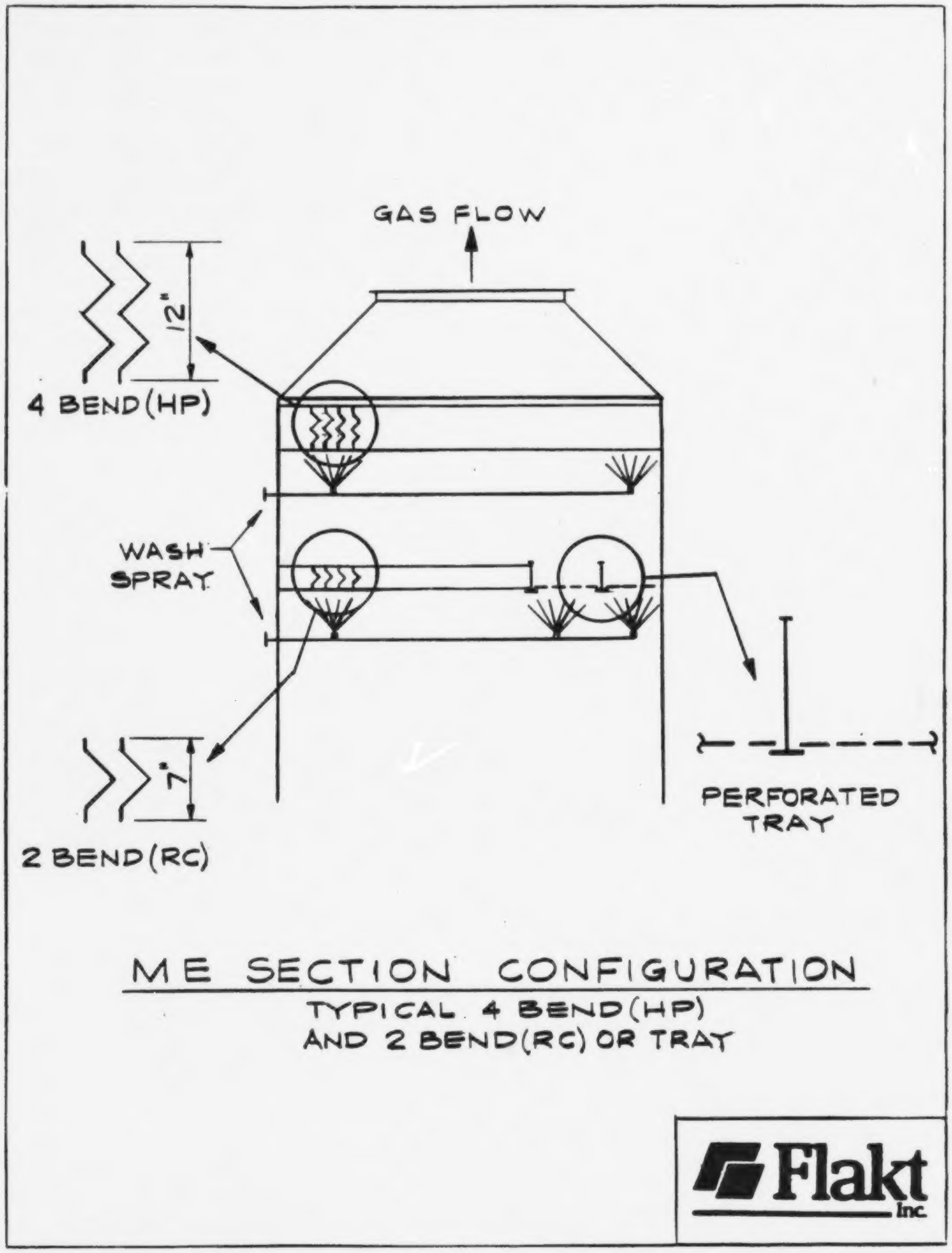
GAS FLOW
12"
4 BEND (HP)
WASH SPRAY
7"
2 BEND (RC)
PERFORATED TRAY
ME SECTION CONFIGURATION
TYPICAL 4 BEND (HP)
AND 2 BEND (RC) OR TRAY
Flakt Inc.

Figure 1: Two Stage Vertical Flow Mist Eliminator Section

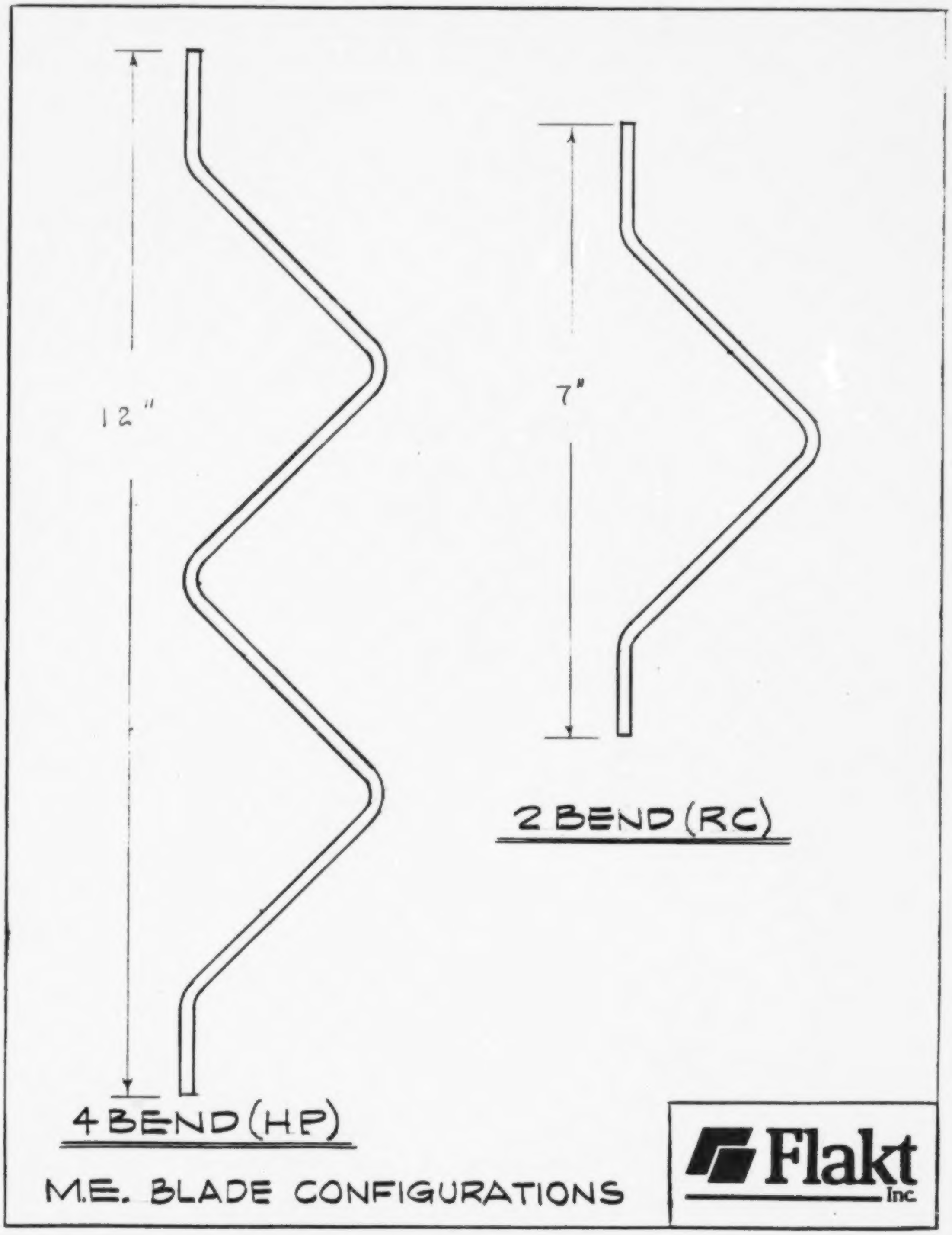
12"
7"
2 BEND (RC)
4 BEND (HP)
M.E. BLADE CONFIGURATIONS
Flakt Inc.

Figure 2: Cross Section of First and Second Stage Mist Eliminator Blades

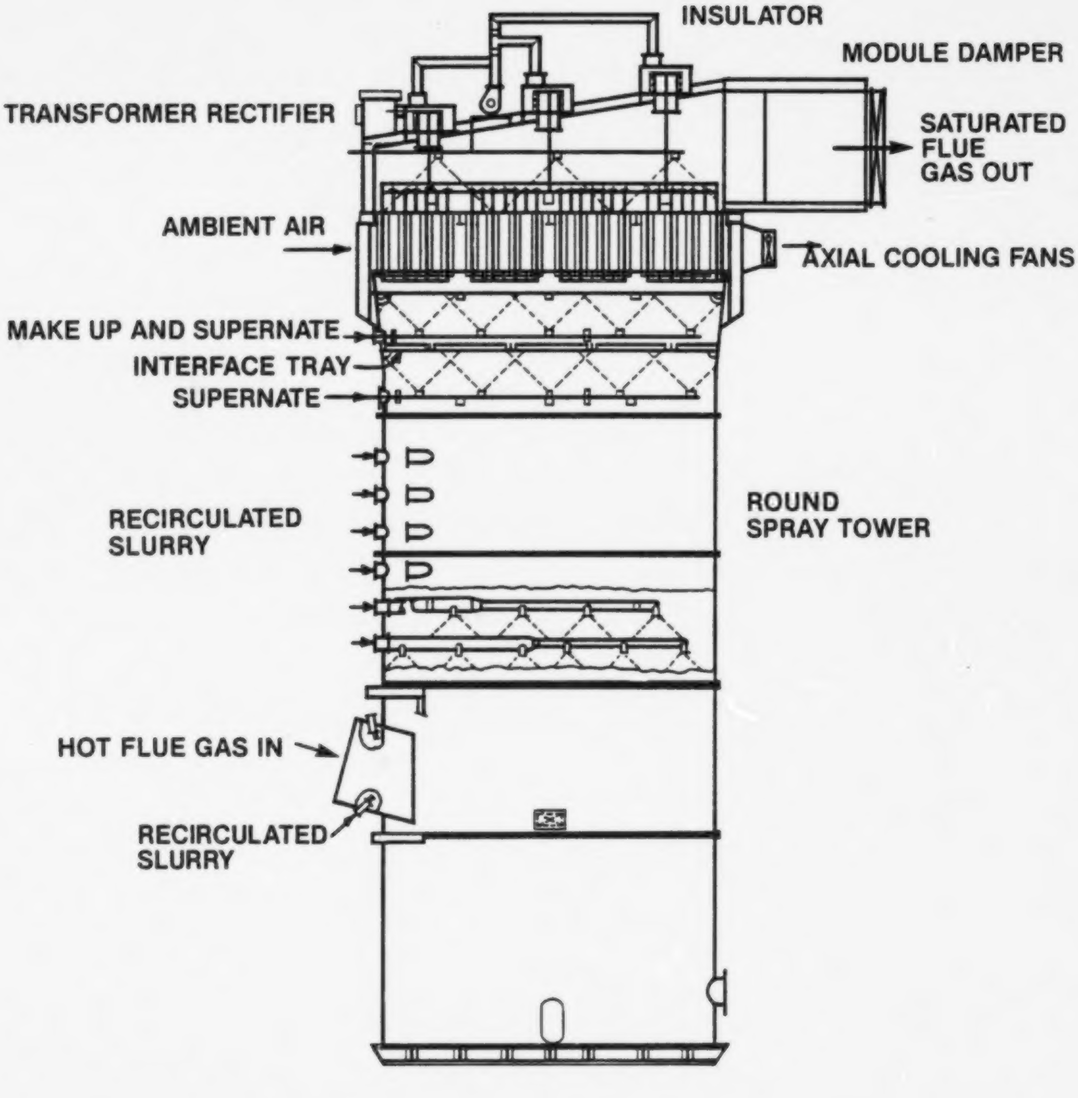
INSULATOR
MODULE DAMPER
TRANSFORMER RECTIFIER
SATURATED FLUE GAS OUT
AMBIENT AIR
AXIAL COOLING FANS
MAKE UP AND SUPERNATE
INTERFACE TRAY
SUPERNATE
RECIRCULATED SLURRY
ROUND SPRAY TOWER
HOT FLUE GAS IN
RECIRCULATED SLURRY

Figure 3: Spray Tower/WESP Combination

TABLE 1. VERTICAL VS. HORIZONTAL FLOW MIST ELIMINATORS

	Vertical Flow	Horizontal Flow
Theoretical Upper Velocity	Lower	Higher
Capacity of a Free Cross Section	Base	Slightly Higher
Separate Washing Circuit	Difficult	Easy
Drainage	Easy	Difficult
Structural Support	More Expensive	Less Expensive
Gas Distribution	Potentially Good	Potentially Poor
Absorber Height	Higher	Lower
Manual Cleaning Upstream	Good	Fair
Manual Cleaning Downstream	Excellent	Fair
Replacement	Potentially Easy	Potentially Harder
Pressure Drop	Lower	Higher
Slurry Application	Good	Fair

TABLE 2: MIST ELIMINATOR TEST RESULTS

Installation Size	P (In. W.G.)	Droplet Emission (qgr/acf & mg/m3)
Minnesota Power 550 MW, 4 Modules	0.3	0.0008 & 1.8
South Illinois Power Corp. 184 MW, 2 Modules	0.2	0.0047 & 10.8
Seminole Electric 2 x 620 MW, 10 Modules	0.3	0.0126 & 28.8 (1)

(1) Particulates plus droplets, 60% reduction in total emission after installation of new mist eliminator

VIDEO BASED IN-SITU DROPLET CONCENTRATION AND SIZE ANALYZER

By: Joseph D. McCain
Southern Research Institute
Birmingham, AL 35255

ABSTRACT

Data concerning the droplet size distribution of liquid sprays is often needed in reserch and diagnostic explorations of scrubbers and mist eliminators. In addition, informtion concerning the spatial and temporal variability of droplet concentrations and size distribution is often desired. The methods that have been available in the past for making such measurements have been generally less thann satisfactory because of problems relating to various combinations of time resolution, traverse capability, representative sampling, sizing range, size resolution, survivability of equipment in the scrubber environment, and cost. A video based droplet size and concentration measurement system has been constructed which provides a solution to most of the above problems. A description of the droplet analyzer and how it functions is provided together with exemplary dta from field applications.

INTRODUCTION

One of the most difficult aspects of scrubber research and problem solving over the years has been associated with obtaining data on spatial and temporal distributions of droplet size and concentration. The sizes of the droplets in a scrubber play an important role in the performance (efficiency) of the scrubber collecting either particles or gases. The spatial distribution of the liquid similarly plays an important role. These factors, together with the gas velocity distribution, not only are major factors in determining the collection efficiency provided by a scrubber, but also in mist eliminator (ME) performance (and malperformance). Thus knowledge of spatial and temporal variations in droplet concentrations and size distributions is potentially of great value in diagnosing the causes of problems in scrubber/mist eliminator operation which in turn are needed if solutions to the problems are to be found in the most expeditious way.

Several methods have been applied in the past, with varying degrees of success, for measuring or estimating droplet size distributions and concentrations. Methods for size measurement have included droplet impingement on coated slides or sensitized paper (1,2), hot wire devices (3), high speed photomicroscopy (4,5), and the use of inertial separators such as impactors or cyclones (6). Each of these has operational limits which restrict its utility. The coated slide/sensitive paper techniques are difficult to apply in high concentration streams and typically provide single point "snapshots" of the size distribution. Sampling and analysis techniques for these two methods are too labor intensive to make wide area traverses for spatial distribution or long term measurements for time resolution feasible. Inertial separators provide data only for sizes smaller than about 15 micrometers while most of the droplet spectrum of interest is in substantially larger sizes. Further, it is difficult or impossible to obtain time resolved data using the inertial devices. The photographic technique offers the possibility of spatial and time resolution but unless applied with motion picture technology has a low data rate; it also has a long analysis time, even if automated image analysers are used to examine the resulting photomicrographs.

Automated video based droplet analysers have been used for at least 20 years; some with online real time data analysis (7) and others with much slower offline analysis (8). Because of equipment size these techniques have generally been limited to laboratory application. However, with the advent of small light-weight solid state video cameras, it became practical to construct a real time video based droplet analyser for field application. Such a system was expected to be of great use in diagnosing problems related to mist eliminator carryover in scrubbers at electric utility power stations. Hence the Electric Power Research Institute contracted with Southern Research Institute through the Stearns-Roger Division of United Engineers and Constructors to construct such a system and provide data from it for several sites which were experiencing ME problems. This paper provides a description of the system which was constructed and some results typical of the data that has been obtained using it.

DESCRIPTION OF THE VIDEO DROPLET ANALYZER (VDA)

The droplet analyzer system consists of a sectionalized probe which provides a working length of up to 6 m (20 feet), a probe operator's console and monitor, analyzer console, and a microcomputer for data collection, storage, and analysis. The probe is designed to work through a 10 cm (four inch) or larger access port. The principal components of the system are shown in Figure 1. The probe is connected to the analyzer console by 75 meters (250 feet) of cable permitting the analyzer and computer to be located well away from the sampling area.

The probe carries an illuminator, a small solid-state video camera, and its associated "macro" lens. A choice of lenses and extension tubes are available to provide particle sizing ranges from 3-450 micrometers to 45-6500 micrometers diameter with corresponding active fields of view ranging from 0.75mm x 1.0mm to 12mm x 15mm. The size resolution at any magnification is equal to the minimum measurable size for the magnification. Data are obtained in 220 equal interval size channels, although usually only the first 150 channels are retained. Back lighting is used to produce dark droplet images on a bright background. The illuminator and camera unit is shown partially disassembled in Figure 2. The illuminator is suspended from and held directly opposite the camera housing on four small tubes. The view volume is located in the center of the large open area between the camera and illuminator housings. Illumination is provided by a high intensity strobe lamp with a flash duration of 250 nanoseconds. The flash lamp is synchronized to fire during alternate vertical retrace periods of the video camera. The short flash duration effectively eliminates blur from droplet motion. The illuminator and camera lenses are protected from fouling due to entrained liquids and solids by baffled shrouds and a purge air system. The purge air is supplied via a hose from a small compressor located adjacent to the operator's console.

Data acquisition and preliminary analysis take place in real time at a rate of 30 data frames per second. Objects in the field of view are detected by analysis of the video signal level during each scan line. On detection of an object, a timing loop is started which results in the analyzer's looking for a recurrence of an object in a similar horizontal location on succeeding scan lines until it is no longer found. During this process the number of scan lines on which the object was detected is counted. The vertical height of the object is directly proportional to the number of scan lines which it intercepts. Thus the intercepted line count is a direct measure of its height (or diameter if the object is spherical as is the case with small droplets). Focus information is obtained from the shape of the video signal of the image. When a particular image is no longer detected, its intercepted line count and focus information are transmitted to a microcomputer for processing. Four parallel counting (timing loop) circuits are incorporated in the analyzer, permitting simultaneous analysis of up to four particles whose images fall on a common video scan line. After the data for an object has been transmitted to the computer the counting circuit which handled the object is cleared and freed to handle another object. Thus a large number of droplets can be measured in a single video frame. Output of data from the image analyzer to the computer is suppressed if any part of the image falls outside the active field of view. This eliminates incorrectly sizing any droplet whose entire image is not available for measurement but makes the effective field of view dependent on the drop size. Major details of the image analysis are depicted in Figure 3.

Upon receiving the image height and focus data from the analyzer the computer clears the analyzer timing loop which generated the data, freeing it for another image, determines whether or not predetermined focus criteria were met, and if so increments the number counted in the appropriate size bin. Partial data are updated once each second on the computer's video display and full data in tabular and graphical forms are available at the end of an operator selected sampling period which can range from 1 to 255 seconds. The data are also stored on floppy disk for further analysis at a later time.

Video monitors in the probe operator's console and at the image analyzer/computer location provide direct views of the camera's video output and diagnostic information on the performance of the image analyzer circuitry. The video signal from the camera can also be recorded for later inspection and analysis.

The dimensions of the active sensing volume are determined by the height and width of the field of view and the depth of field. The field height and width are fixed by the geometries of the lens and camera. However, the depth of field varies with illumination intensity and particle diameter and must be measured empirically. The dimensions of the sensing zone are small enough for all usable magnifications that, at the velocities encountered in scrubbers and ducts, the sensing zone is swept clear and a new sample is introduced between flashes. The total gas volume sampled at a point can thus be calculated from the sensing zone dimensions and the number of video scans (flashes) which were analyzed. Assuming spherical droplets, their volumes can be calculated from their measured heights (diameters). These volumes can then be summed to obtain the total volume of the particles measured, thus permitting the liquid loading (concentration) in the size range spanned by the instrument to be calculated. Assuming that no significant contribution to the liquid loading is due to droplets having diameters outside the instrument range, the calculated loading can be taken to be the actual liquid concentration in the gas stream. The shapes of plots of measured liquid volumes by size channel can be used to assess the validity of the assumption that no significant droplet volume fell outside the measurement range in any given data set.

ANALYSER CALIBRATION AND PERFORMANCE VERIFICATION

Primary calibration of the system is based on glass beads of known sizes mounted on microscope slides. These beads are placed in the view volume and the line count is noted for calibration of diameter versus number of intercepted lines. The slide is then traversed through the depth of the sensing zone by means of a micrometer stage to determine the depth of focus for the size in question. The acceptable focus criteria are adjusted so that the image is considered out of focus if the indicated size differs from the true size by more than ten percent or one line count, whichever results in the greater relative error (ie. one line count for small objects and ten percent in size for large objects). This primary calibration need only be done once in the laboratory for each lens/illuminator setup. Thereafter, depth of field checks at one or two sizes suffice for obtaining corrections for any immediate application.

The measured size spectrum for a mixture of two sizes of glass beads, 450 to 550 μm and 900 to 1250 μm diameter, is shown in Figure 3. The mixture was made up to be approximately 50/50 on a weight basis. This mixture was slowly poured through the sensing zone of the analyzer as part of the verification of the system performance.

Further verification of the performance of the system was obtained by measuring droplet transport rates in the laboratory both directly and by means of the VDA. Two such trials were performed on aerosols which had mass median diameters of about 100 micrometers. The VDA was configured for measurement in the range from 3 to 450 micrometers for these tests. The VDA results showed 80% to 94% of the liquid transport rate measured by direct collection of the liquid that passed through the sensing zone. Comparisons have also been made of the size distributions of liquid sprays from nozzle types for which data were available from other techniques - Malvern optical particle size analysers and KLD hot wire devices. In each case, the results from the VDA were similar to those from the other technique in the size ranges which they had in common.

CALCULATION OF LIQUID TRANSPORT RATES

If the gas flow is horizontal at the measurement plane and the gas velocity is known, the system also provides a direct measurement of droplet flux (or liquid transport rate). In this case, the velocities of the droplets in the direction of the gas flow can be taken to be equal to the gas velocity. However, if the gas flow is vertical the situation becomes more complex. In the latter case, the droplet flux (in the size range measured) is given by the equation:

$$\text{Flux} = \int_{Dmin}^{Dmax} c(D) \times (Vgas - Vs(D))\,dD$$

where Dmin = minimum measurement diameter
Dmax = maximum measurement diameter
c(D) = concentration of drops having diameter, D
Vgas = local gas velocity (positive for flow upward)
and Vs(D) = settling velocity for drops of diameter, D.

For vertical gas flow in the upward direction, small droplets will be moving upward at approximately the velocity of the gas. As the drop size increases the upward velocity of the drops will decrease until the size of the droplets becomes large enough that the settling velocity equals the gas velocity. Droplets having this size, defined as the limiting droplet diameter, will remain virtually suspended until they either decrease in diameter from evaporation or grow by agglomeration. Droplets having diameters greater than the limiting diameter will fall back against the gas flow. The instantaneous values of the limiting diameters will vary with time because of moment to moment velocity fluctuations but values based on local average velocities should be representative. The calculation of liquid fluxes for the case of vertical gas flow thus requires information on the droplet concentration by size, the local gas velocity at each sampling location, and the settling velocities of the droplets by droplet size. The droplet settling velocities can be calculated but the local gas velocities must be separately measured.

Traverses of a sampling plane can be made in two ways. In the first, the probe is inserted through conventional 10 cm (four inch or larger) sampling ports and data is obtained at points along horizontal lines whose spacing is set by the port locations. Because mist eliminator entrainment problems may be associated with highly localized areas across their faces, it was deemed desirable to have the ability to perform a continuous scan over large areas in order to locate trouble spots. Consequently a swiveling probe mount was constructed to provide such a capability. The swiveling mount permits the probe to be swung through an arc slightly greater than 90 degrees while moving in or out over its full 20 foot length. Thus a continuous survey of an area having a 20 foot radius and a slightly more than 90 degree included angle can be obtained. Potentiometers installed in the mount provide information on the position of the particle sensing zone to the computer; this data is logged with the droplet data. This permits accurate repositioning of the probe to obtain more detailed data after identifying areas of special interest. Operation with the swiveling mount does require a large amount of free space around the sampling area and an access port much larger than is commonly used (12 inch or greater in diameter in order to use the full angular swing capability of the mount). The probe is sectionalized in lengths of about 60 cm (22 inches) to minimize free space requirements and access problems in the sampling area. Because of problems in keeping the optical surfaces clean and dry, the probe must be kept horizontal during operation.

By removing the illuminator from the probe, replacing it with a flood light type illumination system, and replacing the "macro" lens with a conventional lens, the probe can be used to examine interior surfaces, etc. within the duct while the scrubber is in operation.

FIELD RESULTS

To date the system has been used at five sites, making measurements around mist eliminators on seven scrubbers and characterizing the spatial distribution of droplets under a variety of conditions in a spray dryer application. It has also been used to measure the droplet size distribution produced by several nozzles being used for spray dry applications.

Figure 5 shows a typical data set taken at the inlet to a mist eliminator on a scrubber installation at a large utility pulverized coal boiler. Measured droplet concentrations by size are shown on the left in the figure. The volumes are in terms of the volume of the droplets in liters per cubic meter found in each of the measured size intervals. In this instance, the droplet size distribution appears to be multimodal with much of the volume in droplets in the one to three millimeter size range. Even larger droplets were present but not shown in the limited size span of the illustration. At the time these data were taken the gas velocity in the sampling zone was such that the limiting droplet diameter was about 1300 micrometers. That is, droplets smaller than 1300 micrometers (1.3 mm) would be carried upward by the gas flow while those larger than this were either falling back against the gas flow or would eventually do so. The liquid transport rate at the measurement plane is shown on the right side of the figure. The transport rate is given as cubic centimeters of droplets per second per square meter of tower cross-section. As droplet sizes increase the net upward velocity of the droplets decreases with small droplets moving at the gas velocity while those near the limiting diameter have near zero velocity. Thus although in terms of concentration, the distribution is dominated by droplets larger than 1000 micrometers, the actual carryover to the mist eliminator is dominated by droplets in the 200 to 900 micrometer size range. If there were no sources injecting large droplets upward into the gas stream below the mist eliminator and no sources above the mist eliminator, the total negative flux, or fallback, should equal the total positive flux, or carryover, if the mist eliminator operated at 100% efficiency.

Figures 6 and 7 show results obtained at the outlet of a ME under two load conditions (40% of full load and full load). As would be expected, the carryover rate was much larger at high load than at low load. The liquid influx to the ME was lower at low load and the mechanisms that cause entrainment from the ME are not as effective at the lower velocities that result from the reduced gas flow. At the high load condition the total carryover from this module was about two liters per minute (0.5 gallons per minute). A companion module to the one from which the data in Figures 6 and 7 were taken had a measured total carryover rate of 12 liters per minute (3 gallons per minute) when the unit was operating at 85% of full load. In terms of detailed spatial distributions, the carryover rates varied by more than a factor of 100 over the zones mapped in each of these two scrubbers and the zones with high carryover rates tended to be zones of much greater than average superficial velocity. Thus improvements in the uniformity of flow distribution might be expected to result in reduced carryover rates. In addition, inspection of the ME structure in regions of high carryover can reveal mechanical causes for high entrainment rates in some instances.

In some instances temporal variations can reveal important information as illustrated in Figure 8. This figure shows the variation in concentration at a single location above the exit of a ME through three ME underspray wash cycles. As can be seen, the droplet concentrations increased dramatically when one specific zone of the ME was being washed. That zone in this instance was located approximately 8 m (25 feet) from the measurement location which was itself less than 50 cm (2 feet) above the ME face. Because the area producing the carryover was located so far from the measurement point, only a small part of the actual carryover would have been seen. It was in fact surprising that any was seen, and the true carryover must have been many fold greater than that measured at the selected location. Conservative estimates of the average droplet carryover from this and another similar scrubber tower were of the order of 150 liters per minute (40 gallons per minute) each.

CONCLUSIONS

The Video Droplet Analyser has proven to be a field useable system capable of providing data that is virtually unobtainable in any other fashion regarding droplet size distributions, concentrations, and transport rates. Useful information has been obtained to date for purposes of mist eliminator problem diagnostics and in quantifying processes in spray dry SO_2 control applications. Other applications might include fundamental research on scrubber performance, verification of design predictions for scrubber spray distributions, and verification of mist eliminator performance.

ACKNOWLEDGEMENTS

The work described in this paper was done under the sponsorship of the Electric Power Research Institute as part of an ongoing program of Mist Eliminator Field Studies. The prime contractor for the work was the Stearns-Roger Division of United Engineers & Constructors, Inc. under EPRI contract RP 2250-3. The EPRI project manager was Mr. Richard G. Rhudy and the Stearns-Roger project manager was Mr. Robert J. Keeth.

The work described in this paper was not funded by the U.S. Environmental Protection Agency and therefore the contents do not necessarily reflect the views of the Agency and no official endorsement should be inferred.

REFERENCES

1. Green, H. L. and W. R. Lane. Particulate clouds: dusts, smokes and mists. pp 230-231.

2. A.P.T., Incorporated. Entrainment separators for scrubbers. Initial Report, October 1974. EPA-650/2-74-119-a. (PB 241 189).

3. Magnus, Daniel E. and David S. Mahler. Paper 17. An in-situ liquid droplet sizing system. In: Proceedings; advances in particle sampling and measurement (Daytona Beach, FL, October 1979). Interagency Energy/Environment R&D Program Report. pp 302-315.

4. Yule, A. J., N. A. Chigier and N. W. Cox. Measurement of particle sizes in sprays by the automated analysis of spark photographs. In: Particle size analysis. M. J. Groves, Editor. Heyden & Son, Ltd. 1978. pp 51-60.

5. Smith, E. O., W. E. Morgan, A. W. Ferguson, and J. B. Galeski of Black & Veatch Consulting Engineers. Research Project 1410-3. Full-scale scrubber characterization of Conesville Unit 5. EPRI CS-2525, Project 1410-3, Final Report, August 1982.

6. Smith, W. B. and J. D. McCain. Particle size measurement in industrial flue gases. In: Air Pollution Control Part III: Measuring and monitoring air pollutants. Edited by Werner Strauss.

7. Simmons, H. C. and D. J. Lapera. A High-speed spray analyzer for gas turbine fuel nozzles. presented at ASME Gas Turbine Conference, Cleveland, March 12, 1969. In: Particle size measurement in industrial flue gases. W. B. Smith and J. D. McCain. pp 96.

8. Hotham, G. A. Sizing aerosols in real time by pulsing UV laser machine. In: Aerosol Measurements. NBS Publication 412, 1974. In: Particle size measurement in industrial flue gases. W. B. Smith and J. D. McCain. pp 95.

Reproduced from best available copy.

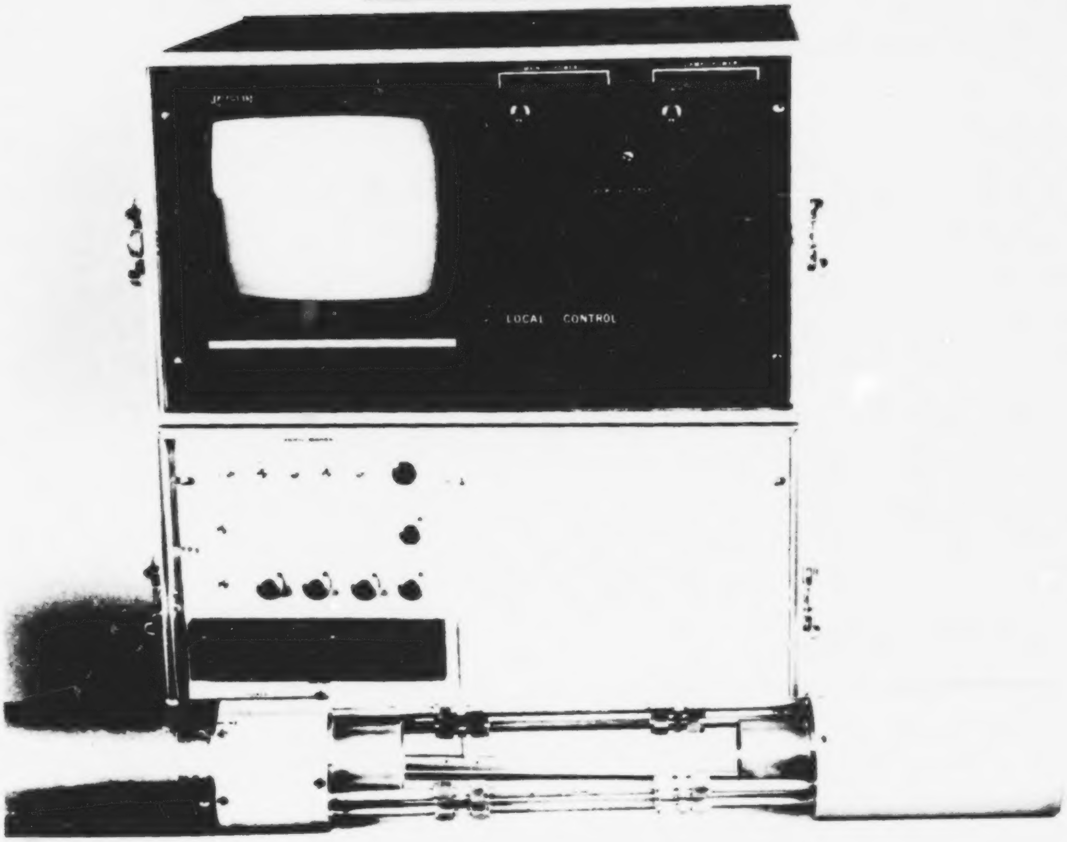
LOCAL CONTROL

Figure 1. Video droplet analyzer electronics and probe end.

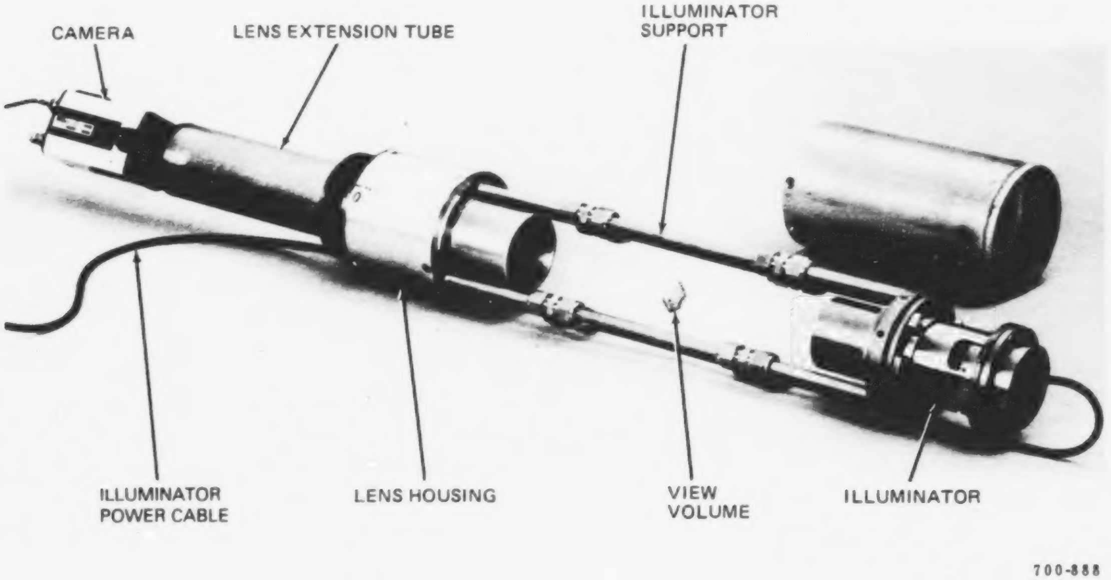
CAMERA
LENS EXTENSION TUBE
ILLUMINATOR SUPPORT
ILLUMINATOR POWER CABLE
LENS HOUSING
VIEW VOLUME
ILLUMINATOR
700-888

Figure 2. Video Droplet Analyzer Probe end partially disassembled showing camera, lens extension, illuminator and illuminator power cable.

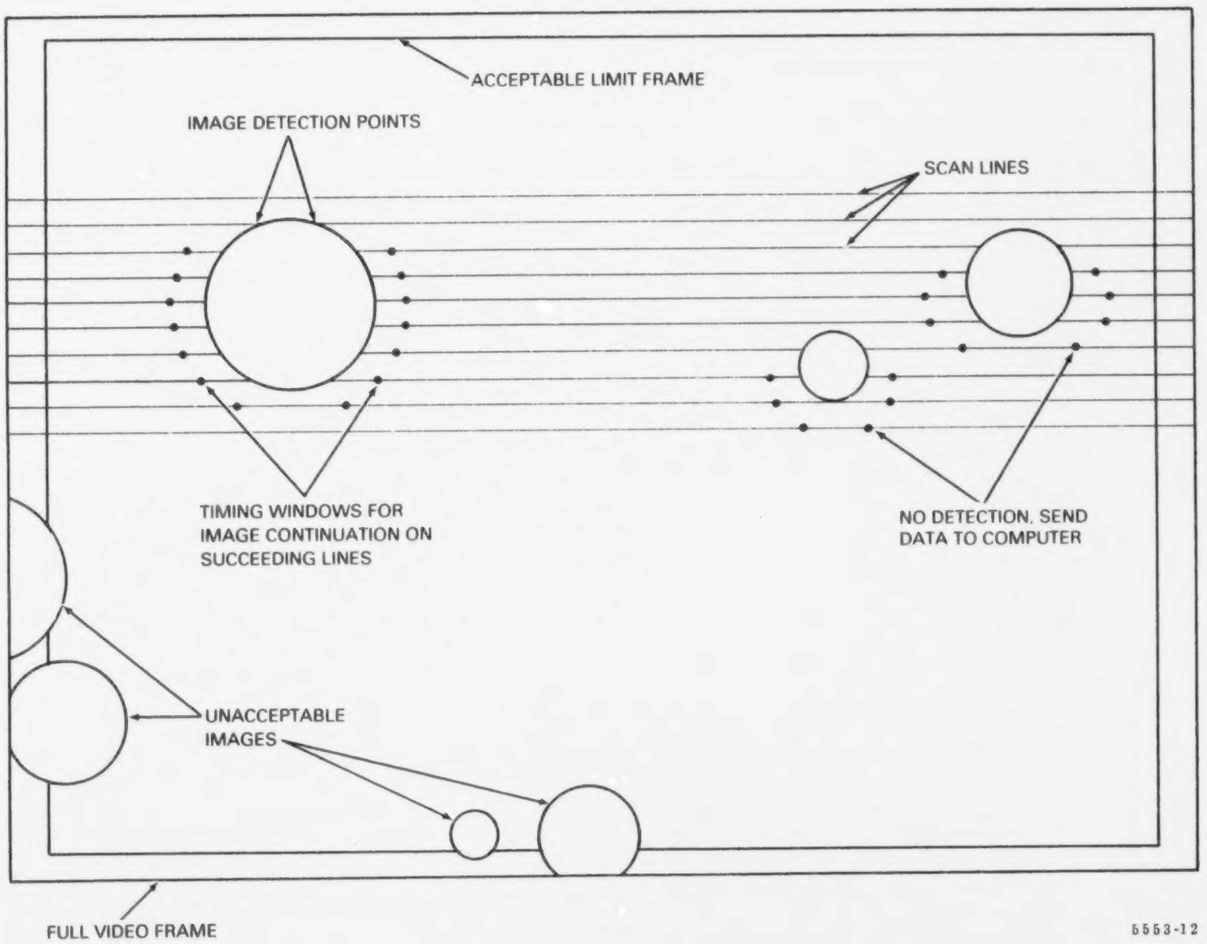
ACCEPTABLE LIMIT FRAME
IMAGE DETECTION POINTS
SCAN LINES
TIMING WINDOWS FOR IMAGE CONTINUATION ON SUCCEEDING LINES
NO DETECTION, SEND DATA TO COMPUTER
UNACCEPTABLE IMAGES
FULL VIDEO FRAME
5553-12

Figure 3. Depiction of image analysis details for the SRI Video Droplet Analyzer.

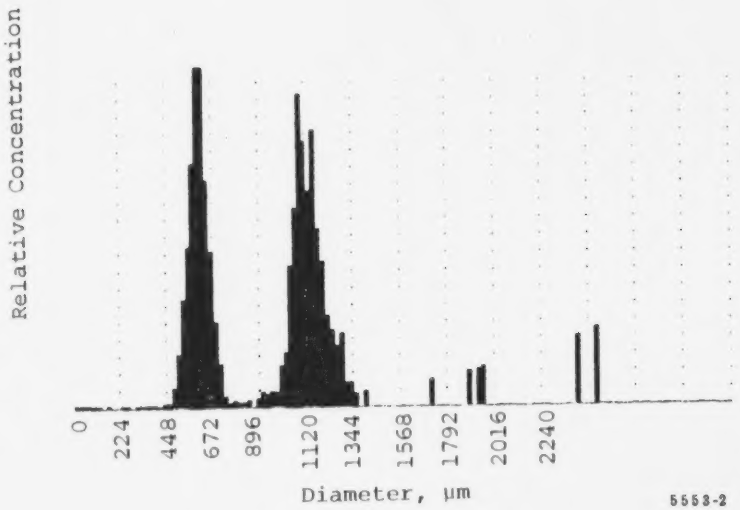

Figure 4. Size spectrum of a mixture of glass beads of two size classes, 450 to 550 µm and 900 to 1250 µm, as measured with the Video Droplet Analyzer.

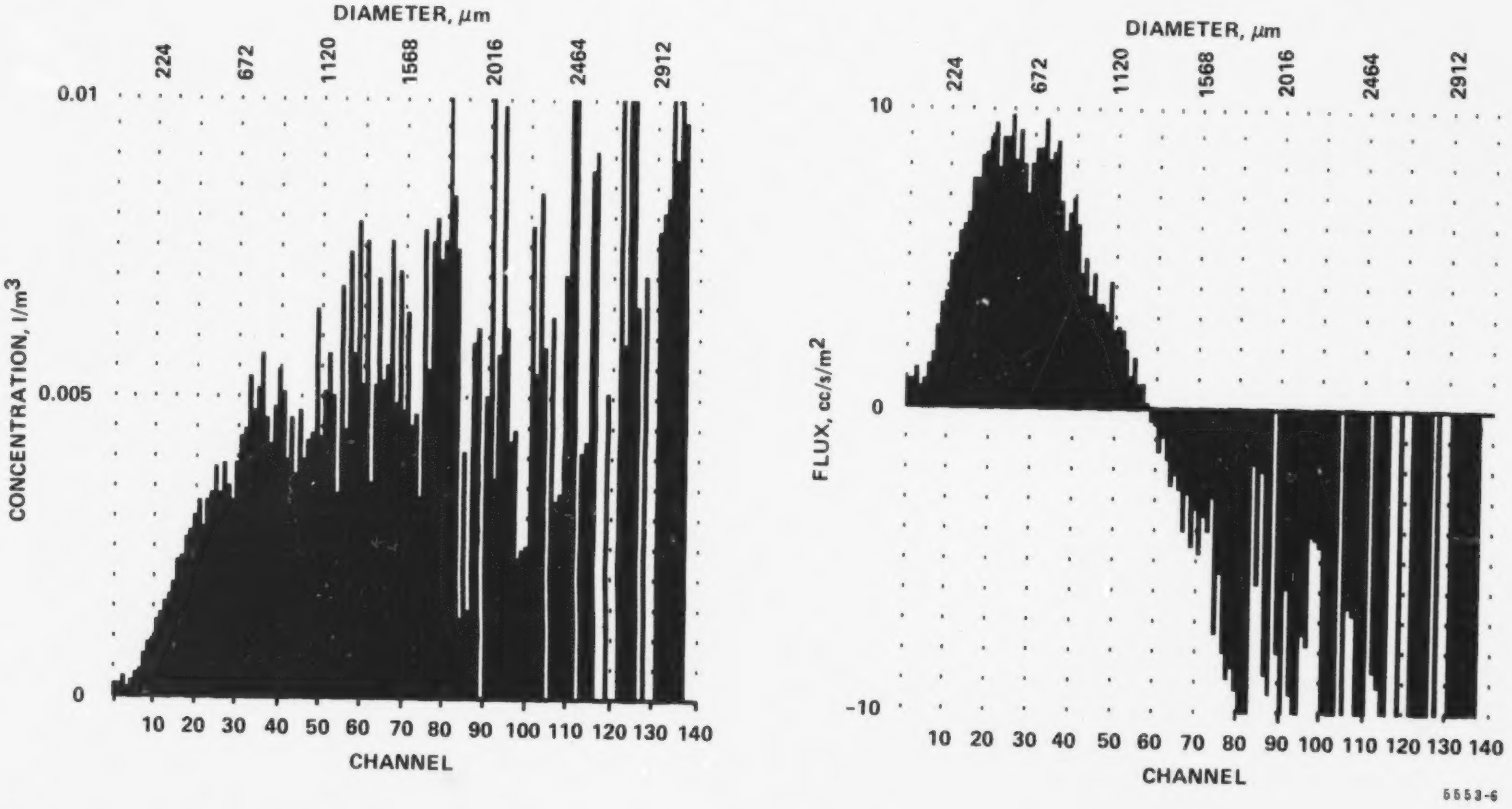

Figure 5. *Concentrations and liquid fluxes by channel for a twelve minute sampling period at a ME inlet. Channel width is 22.4 μm. Positive fluxes represent carryover and negative fluxes represent fallback.*

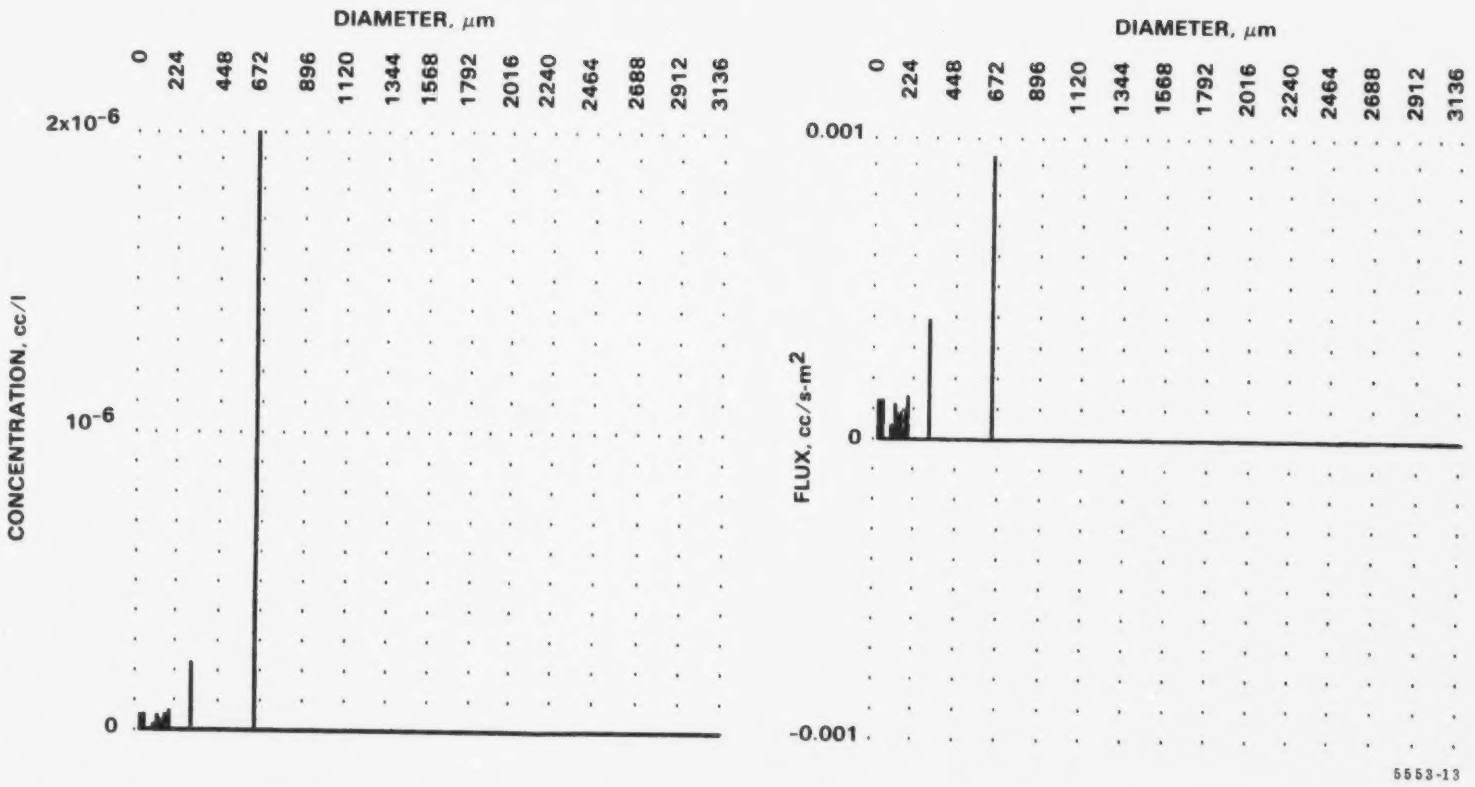

Figure 6. VDA results on a channel by channel basis for the carryover from a scrubber module outlet at a low load test condition.

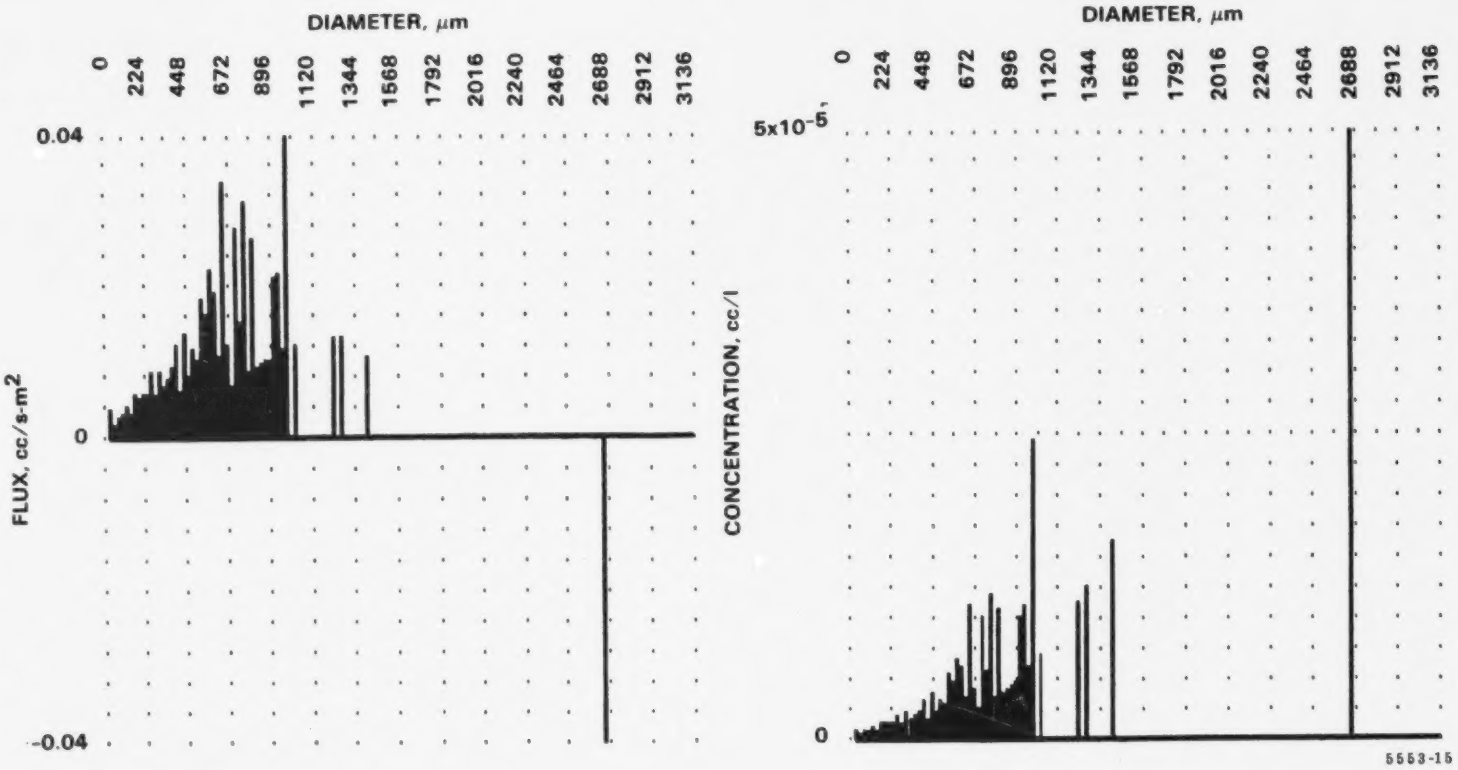

Figure 7. VDA data on a channel by channel basis for the ME outlet of the same module as in Figure 6 at the high load test condition.

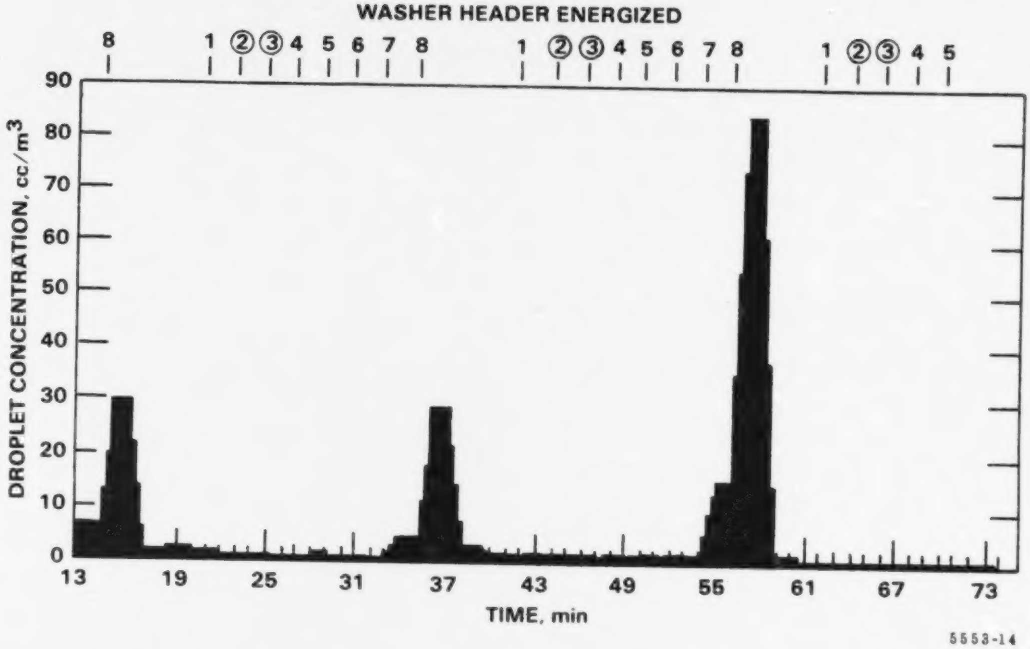

Figure 8. Variation of droplet concentration with time at a single location above a mist eliminator outlet. Timings of ME washes are shown by wash header. The sampling location was above an area washed by headers 2 and 3.

GUIDELINES FOR TROUBLESHOOTING UTILITY MIST ELIMINATION SYSTEMS

by: A. Frank Jones
J. David Colley
W. David Balfour
Radian Corporation
Austin, Texas 78720-1088

Richard G. Rhudy
Electric Power Research Institute
Palo Alto, California 94303

R. J. Keeth
Stearns-Roger Division
Denver, Colorado 80217

ABSTRACT

Flue gas desulfurization system availability studies have indicated that mist elimination system (MES) failures are the second most common cause of unavailability for utilities. The major MES problems are pluggage/scaling, carryover/re-entrainment, and materials failure. Effective solutions to these problems require that the underlying cause of the MES problems be identified. EPRI has sponsored a research program aimed at determining the causes of MES problems and evaluating potential solutions. Based on the knowledge which has been gained in this program, a troubleshooting methodology has been developed to assist utility personnel in their efforts to identify the cause of their MES operating problems. The key to this methodology is the development and conduct of a test program to determine the cause of the MES problem. This paper presents the methodology, and describes appropriate chemical and physical tests that will assist utility personnel in identifying the cause of the MES problems due to pluggage/scaling and carryover/re-entrainment. A case study of the MES problems experienced at a utility site is discussed to demonstrate application of the troubleshooting methodology to identify potential problem causes.

INTRODUCTION

Problems with the mist elimination system (MES) in flue gas desulfurization (FGD) systems have occurred since the application of FGD technology to utility boilers in the late 1960s. Availability studies have found that failures of the MES have been the second most common cause of FGD system outages. The major MES problems--plugging/scaling, carryover/re-entrainment, and materials failure--frequently result in additional operating and maintenance costs and can cause particulate emission problems. Effective solutions to these problems require identification of the underlying cause(s).

EPRI is sponsoring an ongoing program to determine the causes of MES problems and to evaluate potential solutions. This has involved the characterization of MES problems and development of potential solutions at four utility FGD systems. Further work at utility FGD systems is planned in the future along with evaluation of various MES designs in a pilot facility under both clean and dirty (scaled and/or plugged) conditions.

Based on the information which has been gathered to date, a troubleshooting methodology has been outlined to assist utility personnel in their efforts to identify the cause(s) of MES problems. This paper presents the troubleshooting methodology; discusses MES problems, symptoms, and causes; and identifies tests which can assist in determining the cause of the problems. Some of the potential solutions to the causes of MES problems are listed, and a case study which demonstrates application of the troubleshooting methodology is presented. The troubleshooting methodology and potential solutions will be covered in more detail in a troubleshooting manual currently being prepared under EPRI sponsorship. It should be recognized that this is a first attempt at documenting the potential problem causes and solutions and that further research in the area is planned.

TECHNICAL BACKGROUND

The FGD system presents a difficult environment for the MES because of the small droplets and high inlet mist loadings generated by spray towers; low desired outlet mist loadings; the reactive nature of the FGD system chemistry; and tight water balances which prevent liberal washing with fresh water. It is important to understand this environment when troubleshooting MES problems.

The purpose of the FGD system is to remove sulfur dioxide (SO_2) from the flue gas. This requires intimate contact between the gas and scrubbing slurry. In a spray tower FGD system, this is achieved by providing a large number of small droplets which result in a relatively large liquid surface area available for gas contact. However, the small droplets are also prone to entrainment in the gas stream where they are transported to the mist eliminators. High ratios of liquid to gas are also used to increase the gas-liquid contact. The high liquid-to-gas ratios combined with the small droplets can result in high liquid loadings to the mist eliminators.

Low outlet mist loadings are desired to prevent accumulation of liquid and solids downstream of the FGD system and to prevent problems with particulate emissions from the stack. This requires a MES design which is effective at removing the small droplets from the gas stream and is capable of draining the high liquid loadings to prevent re-entrainment.

In a lime or limestone FGD system, the SO_2 removed by the scrubbing slurry is precipitated as the sulfite and/or sulfate salt of calcium, depending on the amount of oxidation occurring. Therefore, the slurry includes both dissolution (reagent) and precipitation (calcium salts) reactions, resulting in a chemically reactive slurry.

The precipitation of gypsum (calcium sulfate) from the slurry provides the most problems due to the hard scale which can form on the mist eliminators. Gypsum is formed when slurry on the mist eliminator surfaces removes SO_2 from the flue gas. This causes the pH of the slurry to drop which will dissolve excess reagent and lead to additional SO_2 removal. Oxidation of the absorbed SO_2 increases the sulfate concentration and the gypsum relative saturation. Scaling results when the gypsum relative saturation reaches the point where precipitation occurs on the mist eliminator surfaces. The amount of gypsum which can precipitate is limited to the calcium available in solution and the excess lime or limestone in the slurry. Therefore, the reagent utilization in the FGD system can affect the tendency for scaling to occur in the MES. Poor reagent utilizations provide more calcium for gypsum precipitation, thereby increasing the scaling tendency. Reagent utilization can be calculated from the results of chemical analysis of the solids in the absorber recirculating slurry for carbonate, sulfite, and sulfate (1).

The high mist loadings to the MES and the reactive nature of the FGD system chemistry make it necessary to wash the mist eliminators periodically to prevent solids accumulation and scaling which could result in subsequent degradation of MES performance. It is desirable to use water with a low gypsum relative saturation that is free of suspended solids; this usually requires fresh water or water from outside the FGD system (not thickener overflow). However, in zero discharge FGD systems, the water which can be brought into the FGD system is limited to the amount of water consumed by the system. Therefore, the amount of fresh water available for mist eliminator washing may be limited, especially when other fresh water requirements are taken into account (i.e., pump seals).

As described above, an effective MES design for the utility application must be capable of removing small droplets from the flue gas and draining the collected liquid to prevent re-entrainment and must be washed in a manner which prevents the buildup of scrubber solids and scale on the internal surfaces. To meet these needs, the typical MES consists of multiple-pass chevrons with close blade spacing. Wash systems must provide adequate coverage and force and must be of a frequency to keep these systems clean.

MAJOR PROBLEM AREAS

The major problem areas experienced by utility MES can be categorized as plugging/scaling, carryover, re-entrainment, and materials failure. These problem areas are reviewed below. In many cases, troubleshooting and solving the problems can be difficult because the problems may be interrelated.

Pluggage/scaling results in the buildup of solid material on the MES and is the MES problem most frequently observed. Pluggage refers to buildup occurring due to settling of suspended solids from the removed slurry or wash water. Scaling refers to the buildup of solids by the precipitation of dissolved solid species from liquor present on the mist eliminator surfaces. While pluggage (soft deposits) is generally easier to remove from the mist eliminators than scale (hard deposits), both mechanisms can result in reduced MES efficiency as explained below. Also, the buildup of solids material from one mechanism often results in subsequent buildup from the other mechanism. For example, scaling can change the surface of the mist eliminator and provide sites for solids deposition, resulting in pluggage.

Pluggage/scaling affects the MES performance by altering the shape and surface characteristics of the mist eliminator blades. Changing the shape of the blades can reduce MES efficiency by altering the path the gas takes through the blades. Changing the surface characteristics may affect drainage and increase the potential for re-entrainment of collected liquid. Pluggage/scaling can also affect MES performance by reducing the open path available for gas flow. This results in higher gas velocities through the MES which can cause re-entrainment. Symptoms which indicate pluggage/scaling include high mist eliminator pressure drop and the symptoms for carryover/re-entrainment which are described below.

Carryover and re-entrainment result in liquid/slurry downstream of the MES. However, the mechanisms for each of these problems is different. Carryover is caused by mist which penetrates (passes through) the MES; re-entrainment occurs when liquid/slurry which has collected on the mist eliminator blades is swept off by the gas flow and resuspended in the gas stream. Both mechanisms result in material downstream of the MES, and the composition of the material generally does not depend on the mechanism. This results in the same observed symptoms for carryover and re-entrainment. Also, most of the potential causes for carryover can cause re-entrainment (although the reverse is generally not true). Because of this, the two problems have been combined into one major problem area for this discussion.

Symptoms caused by carryover and re-entrainment can include solids accumulation in the downstream ductwork and on reheater surfaces; an increase in stack opacity and particulate emissions; liquid/solids fallout from the plume (stack rain); and, if the carryover or re-entrainment is severe, a drop in stack temperature for FGD systems which reheat the flue gas.

Materials failure can refer to several problems including breakage of the individual blades or blade spacers, warpage of the blades, and failure of the blade support structure. Materials failure generally results in carryover through the MES due to mist passing through the gaps. However, materials failure can also promote pluggage/scaling because of surface irregularities from breakage or reduced clearance between blades. Symptoms which can indicate materials failure include missing or damaged mist eliminators, spray nozzles plugged with mist eliminator blade material (possibly indicated by a higher spray header pressure), a drop in stack temperature on FGD systems with reheat (particularly when the mist eliminators are being washed), and the symptoms associated with carryover/re-entrainment. If a sufficient amount of mist eliminator surface area is missing, there may also be a drop in mist eliminator pressure drop.

One of the factors which can make troubleshooting MES problems difficult is that problems are often interrelated. For example, pluggage/scaling can initiate re-entrainment because of localized high gas velocities. Pluggage/scaling can also result in materials failure if mist eliminators or the support structure can not handle the added weight. Therefore, it is important that the symptoms for all three problem areas be reviewed to ensure that the root cause(s) of the MES problems is identified. It is also important to examine the effect of potential solutions to MES problems on the operation of the FGD system to ensure that the solution to one problem does not create another problem.

TROUBLESHOOTING METHODOLOGY

A general troubleshooting approach which will assist in determining the cause of MES problems includes: 1) observing symptoms, 2) identifying possible causes of the observed symptoms, and 3) confirming the cause through one or more tests. A troubleshooting outline for MES's is presented in Table 1; this table lists the observed symptoms, potential causes, and confirming tests for each of the three major problem areas.

The first step in identifying the MES problem is to compile a list of the symptoms which are observed. Some symptoms such as stack "rain" (fallout of liquid/solids from the plume) may be apparent. However, this could be a symptom of all three of the major problem areas. Comparing the list of symptoms to actual operation may help identify the problem. For example, a significant increase in mist eliminator pressure drop accompanied by stack rain may indicate pluggage and/or scaling of the mist eliminators. However, a significant drop in the mist eliminator pressure drop accompanied by stack rain may indicate that a section of the mist eliminator is missing; this points to a potential materials failure problem. This example uses the mist eliminator pressure drop and the presence of stack rain which are determined while the FGD system is in service. Identifying other symptoms may require an inspection while the system is off line.

After the symptoms are identified, a list of potential causes can be assembled. This can be a fairly extensive list, especially if two or all three of the major problem areas are suspected. The confirming tests can be used to narrow down the list of potential causes and assist with developing a solution to the MES problem. Some of the tests can be performed easily (e.g., mist eliminator inspection, wash water analysis, etc.), while others require a test crew and/or specialized equipment (e.g., particulate measurements, spray nozzle droplet size distribution, etc.). In Table 1, the confirming tests for each problem are listed in order of increasing difficulty (i.e., increasing cost and effort). Information from the confirming tests can be used to develop solutions to the MES problem. However, other information and site-specific factors are generally required to obtain the most effective and economical solution.

Each of the potential causes and the tests that may assist in confirming the cause are discussed below.

POTENTIAL CAUSES AND CONFIRMING TESTS

MES problems can be the result of one or a combination of the causes outlined in Table 1. The potential causes for pluggage/scaling and carryover/re-entrainment, which are the most probable causes of MES problems, are discussed below along with the tests (also presented in Table 1) that can be used to assist in confirming or eliminating the cause as a source of the MES problems. Detailed discussions of the potential causes and confirming tests for MES problems due to materials failure have been omitted from this paper due to space limitations.

LIMESTONE UTILIZATION

Poor limestone utilization has been found to be a major cause of mist eliminator pluggage and scaling (2). (The reagent utilization in lime FGD systems is usually high.) The tendency for scaling increases as the utilization goes down. Reasons for poor limestone utilization include high reaction tank pH, poor (coarse) limestone particle size distribution, and, in some instances, limestone blinding (chemical blocking of the limestone surface which prevents dissolution). Limestone utilization can be determined by chemical analysis of the solids in the absorber slurry (1).

MIST ELIMINATOR WASH SYSTEM

Pluggage/scaling problems are frequently a result of the wash system which is responsible for removing slurry collected by the mist eliminators. Important components of the wash system include wash water quality, coverage, intensity, frequency, and duration. Correct design with respect to all of these components is necessary to maintain a clean MES.

The mist eliminator wash water can cause pluggage if it contains suspended solids and scaling if the gypsum relative saturation is too high. The wash water should be essentially free of suspended solids or have a very low concentration. Suspended solids concentration can be easily determined by collecting a sample of the wash water and determining the weight percent solids gravimetrically (1).

The wash water should be subsaturated with respect to gypsum. Wash water with a high gypsum relative saturation can quickly become supersaturated in the absorber and does not sufficiently dilute water/slurry present on the mist eliminators to prevent scaling. A maximum gypsum relative saturation of 0.5 is generally recommended as a guideline for wash water quality. The gypsum relative saturation will usually only be a problem if thickener overflow supplies part or all of the mist eliminator wash water. However, high gypsum relative saturations can also be encountered if cooling tower blowdown or ash sluice water is used for washing the mist eliminators.

Determining the gypsum relative saturation requires analysis of the wash water for calcium, magnesium, sodium, carbonate, chloride, sulfite, and sulfate. The pH and temperature of the wash water must also be determined. Special sample collection and analytical methods have been developed under EPRI sponsorship (1) for samples associated with FGD systems because of the reactive chemistry of the samples. To determine the gypsum relative saturation, the chemical analysis of the wash water should be input to the EPRI liquid equilibrium model FGDLIQEQ (3).

Incomplete coverage of the mist eliminators by the wash system can also cause scaling and pluggage. Reasons for incomplete coverage can include plugged or missing wash nozzles, plugged wash headers, incorrectly installed wash nozzles (nozzles spraying at an angle), and wash system design. A visual inspection of the wash system during a tower outage can be used to identify plugged or missing nozzles. It is recommended that the wash system be observed in operation (i.e., wash the MES when the tower is out of service) since nozzles may be plugged even though no sign of pluggage is visible. Observation of the coverage pattern can also identify nozzles which may be misaligned, resulting in an unwashed area of the mist eliminators. A record of the inspection which notes the location of any plugged nozzles should be kept and compared to other inspection records. This will help determine if a particular nozzle or set of nozzles regularly plugs. The material which caused the nozzle pluggage should also be identified if possible since it would provide a clue to the source of the problem.

Design problems with the wash coverage in fixed grid wash systems can be identified by drawing each nozzle's spray pattern on a scale drawing of the wash system nozzle layout. The spray pattern can be determined from the wash nozzle's spray angle and the distance from the nozzle to the mist eliminator surface. The spray patterns should overlap so that no area is left unwashed. General designs experience recommends that the total area covered by the spray patterns be at least 150% (overlapping sprays) of the mist eliminator surface area. Particular attention should be paid to the edges of the tower since this is where coverage may be lacking. Records of mist eliminator inspections which note the locations of scaling and pluggage can also be used to identify where coverage is a problem. Repeat pluggage/scaling in a particular location may indicate coverage problems caused by factors such as a damaged wash nozzle or a nozzle which has been bent so that it is spraying at an angle.

Coverage problems could also be caused by nozzles which have an uneven distribution of liquid across the spray pattern. Full-cone spray nozzles should be used for MES washing. An uneven spray distribution for a full-cone spray nozzle is rarely a problem. However, a spray distribution test can be performed by many of the nozzle vendors to determine if the distribution is a problem.

The wash intensity is defined as the instantaneous wash water flow rate per unit of mist eliminator surface, generally expressed in units of gallons per minute per square foot of mist eliminator surface. A low wash intensity can result in pluggage/scaling by not providing sufficient water and energy to dilute and dislodge slurry which has accumulated on the mist eliminators since the last wash. A low wash intensity also may not penetrate very deeply into three- or four-pass chevrons to remove slurry from the inner passes. The wash intensity can be determined by dividing the flow rate during washing for the entire tower by the cross-sectional area of the tower at the mist eliminators. If possible, the flow rate should be measured. The flow rate can also be estimated from the pressure at the wash headers and nozzle flow/pressure data. Most nozzle vendors have the flow data available as a function of pressure. The flow data can be used with the number of nozzles to determine the instantaneous wash water flow rate for the entire tower. Research performed at the Shawnee test facility (2) found that wash intensities of 1.5 gpm/ft^2 for the front side of the first mist eliminator and 0.55 gpm/ft^2 for the back side of the first mist eliminator and the front side of the second mist eliminator were capable of maintaining clean mist eliminators (with wash water having a low gypsum relative saturation). Not all MES designs consist of two mist eliminator banks. However, these guidelines can be adapted for other configurations.

The wash frequency and duration are just as important as the wash intensity. Pluggage/scaling can occur if the mist eliminators are not washed often enough or long enough to remove accumulated slurry. The wash frequency and duration should be checked during actual operation of the mist eliminator wash system. Operating records regarding the frequency, duration, and wash water flow rate should also be reviewed if they are available to ensure that the wash system is operating as intended. If the wash system is initiated manually, the FGD system operators should be interviewed to determine frequency and duration of operation. The wash duration and frequency recommendations developed during the Shawnee test work (corresponding to the wash intensities discussed above) are 45 seconds every 30 minutes (2.5% of the time) for the front of the first mist eliminator and 3 minutes every 60 minutes (5% of the time) for the back side of the first mist eliminator and the front side of the second mist eliminator.

HIGH GAS VELOCITY

High gas velocity can cause MES problems by significantly increasing the slurry loading to the MES. The increased loading may result in solids accumulation between washings which the mist eliminator wash system is not capable of removing; this could lead to pluggage/scaling. If the gas velocity exceeds the MES design velocity, it may also cause re-entrainment. High gas velocity can be caused by operating at higher-than-design unit loads, poor distribution of gas between the towers (due to plugged trays/packing or partially shut isolation dampers), high excess air in the flue gas, or problems with the flue gas ductwork design. The gas velocity can be determined by performing velocity traverses at the outlet of a tower, preferably during full-load operation (worst-case condition). Velocity traverses should be done for all operating towers as well as the bypass duct, if possible. This will help determine if the gas velocity for all towers is too high or if poor gas distribution between towers is causing a high velocity in a single tower.

Gas velocity can be determined with a pitot tube using EPA Methods 1 and 2. However, this method is not suitable for wet environments (moisture collects in the tubes and causes measurement problems). Also, the relatively low velocities at which the mist eliminators typically operate (less than 12 to 15 ft/sec) make accurate measurements with pitot tubes difficult. Pitot tubes are best suited for the bypass gas flow and, if the tower outlet flow cannot be measured, the tower inlet gas flow. The procedure for determining the flue gas velocity and volumetric flow rate can be found in EPA Methods 1 and 2. An instrument such as a Fluidics velocity sensor (4) can operate better in a wet environment and would be more suitable for measuring velocity at the MES outlet.

POOR GAS DISTRIBUTION WITHIN A TOWER

Localized high gas velocity caused by poor gas distribution within an individual tower can also result in pluggage/scaling and re-entrainment. With localized high gas velocity, pluggage/scaling generally starts in the high velocity area and eventually spreads to other areas of the MES. Gas maldistribution within a tower may be the result of plugged or missing spray nozzles; partially plugged trays or packing; or poor design of the absorber or inlet duct. A Fluidics velocity sensor (or other such instruments) can be used to identify gas maldistribution within a tower by examining the velocity at each of the points measured. The velocity traverse should be performed in a clean tower (MES free of scaling/pluggage) to determine if gas maldistribution is the cause of the problem or if it occurs as a result of scaling/pluggage.

HIGH MIST LOADING

A high mist loading to the MES could be the result of a high gas velocity as discussed above. It could also be due to excessive mist eliminator washing which does not allow time for liquid to drain from the mist eliminator blades. Particulate or droplet measurements at the MES inlet and outlet, both with and without the wash system in operation, will assist in determining if the wash system is contributing to carryover/re-entrainment. Particulate measurements are described in EPA Method 17. Droplet loading measurements can also be made at the outlet with a device such as the video droplet analyzer developed under EPRI sponsorship (4).

A high mist loading may also be the result of the absorber spray nozzles producing a large number of very fine droplets (less than 600 microns). The number of droplets which get carried up to the mist eliminators is determined by the droplet size distribution and liquid flow rate of the spray nozzles. Since the liquid flow rate is generally set (number and flow rate of the spray pumps required to obtain the necessary SO_2 removal), a spray nozzle which is producing an excessive number of small droplets will result in a high mist loading. This could cause re-entrainment or possibly lead to pluggage/scaling. The small droplets could also increase the chances for carryover from droplets which pass through the mist eliminator. Some of the nozzle vendors can perform a nozzle droplet size distribution test to determine if an excessive number of small droplets are produced by a particular type of spray nozzle.

As mentioned earlier, re-entrainment can be caused by pluggage/scaling. If the initiation of re-entrainment can be identified easily (e.g., stack opacity increase), an inspection of the MES for pluggage/scaling when the re-entrainment starts may indicate it is causing the problem. Particulate or droplet measurements (EPA Method 17 or video droplet analyzer, respectively) at the MES outlet at different degrees of scaling would more accurately assess the effect of scaling on re-entrainment. However, particulate and droplet measurements are difficult and expensive to perform. If pluggage/scaling is resulting in re-entrainment, the cause of pluggage/scaling should be identified before addressing other potential causes for re-entrainment.

MIST ELIMINATOR DESIGN

The mist eliminator design may also contribute to pluggage and scaling. This may be a result of the design preventing adequate washing or because the design provides areas which tend to accumulate solids. For example, a four-pass chevron with close blade spacing that is only washed from the bottom side may plug and scale because the wash water does not reach the last pass. A mist eliminator blade design with a hook-shaped channel on the surface of the blade (intended to prevent droplets from re-entraining) may provide a place for solids to collect which can initiate pluggage and scaling.

Symptoms which may indicate that the design is contributing to pluggage and scaling are difficult to identify and can be different for the various mist eliminator designs. The wash system and its ability to adequately wash the mist eliminators must also be taken into account. Performing frequent inspections at various stages of pluggage/scaling and keeping records of the locations where pluggage and scaling start can help identify if the mist eliminator design is contributing to reliability problems.

The mist eliminator design should also be reviewed with respect to actual operating conditions to determine if the design (e.g., blade spacing, type of chevron, etc.) needs to be modified to avoid problems. Operation outside of design conditions (e.g., high gas velocity or mist loading) could result in carryover/re-entrainment.

MATERIALS FAILURE

Carryover can be caused by materials failure. The best confirming test for the cause of this potential MES problem is a mist eliminator inspection at the initiation of carryover. The inspection can identify if any sections of the MES are missing or damaged. It is important to inspect the top and bottom of each section of the MES, if possible, to locate damage which may be visible from only one side. If carryover resulted from materials failure, then the cause of the materials failure must be identified.

POTENTIAL SOLUTIONS TO THE MES PROBLEM CAUSES

A list of potential solutions to the causes of MES problems is presented in Table 2. This list is not complete by any means because of site-specific factors related to the design and operation of the mist eliminator and FGD system. It is important to stress that the operation of the entire FGD system should be evaluated before developing solutions to MES problems. The solution to one problem may create a problem in another area. For example, lowering the pH can increase limestone utilization, thereby improving MES reliability, but reduce the SO_2 removal to the point where emission regulations are exceeded. An alternate solution to this problem would be to use an additive to enhance SO_2 removal. However, the cost of the additive would have to be compared to the cost of the current operation.

The guidelines listed in Table 2 should be used as good starting points and not considered absolute. They can be adjusted as necessary based on actual operating experience, taking into account the mist eliminator system design and other factors related to the specific FGD system. For example, the potential solution for a wash water with a high gypsum relative saturation is to switch to an all fresh water wash. However, this could cause or increase the discharge of water from the FGD system. The solution here might be to use a blend of thickener overflow and fresh water which has a gypsum relative saturation of 0.5. If this proves successful, the thickener overflow portion of the wash water could be increased to provide a gypsum relative saturation of 0.6. The system could be operated with this blend for a period of time to determine if the mist eliminators stay clean. Future research by EPRI on mist eliminator systems will be aimed at better defining MES operating guidelines such as those listed in Table 2 and developing solutions to MES problems.

CASE STUDY

The original MES design on a utility FGD system that was investigated as part of the EPRI MES program resulted in essentially complete pluggage of the mist eliminators after about 250 hours of operation. An increase in the mist eliminator blade spacing and the addition of thiosulfate to the FGD system to inhibit oxidation increased the operating time before plugging to about 1,000 to 2,000 hours. However, carryover/re-entrainment of slurry to the downstream ductwork started to occur with the wider blade spacing.

The plant and FGD system are briefly described below along with a more detailed description of the MES design. This is followed by a description of the troubleshooting methodology as it was applied at the utility and the recommended solutions to the MES problems.

PLANT DESCRIPTION

The two units at the plant with FGD systems are identical coal-fired boilers (nominally 600 MW) which cycle with load demand. The current fuel source is a washed bituminous coal with a heating value of approximately 12,300 Btu/lb and a sulfur content ranging from 2.5% to 3.1% (as-fired basis with approximately 8% moisture). Fly ash in the flue gas from the boiler is removed in electrostatic precipitators designed to provide 99.6% removal, which would limit particulate emissions to less than 0.029 lb/MMBtu.

The limestone FGD system was designed to remove 90% of the inlet SO_2 (inlet concentration of approximately 2,400 ppm wet). The FGD system for each unit consists of five open spray towers; each tower was designed to treat 25% of the flue gas, leaving one tower available as a spare. The FGD systems for the two units are slightly different in that one system can be operated with forced oxidation, whereas the other system was designed for natural oxidation. However, the FGD system capable of forced oxidation typically operates with natural oxidation. A flow diagram for the natural oxidation FGD system is presented in Figure 1. The MES design was the same for both systems.

The original MES design, presented in Figure 2, included an interface tray followed by a chevron mist eliminator. The interface tray, made from perforated plate, acts as a bulk entrainment separator by direct impaction of mist on the tray. The chevron mist eliminator, presented in Figure 3, is a four-pass design with hooks protruding from the surface of the first three passes. The hooks were designed to collect the removed mist and channel it away to prevent re-entrainment. Gas flow is from the bottom upward through the mist eliminator as viewed in Figure 3.

The mist eliminator blades were originally laid down horizontally and spaced at 1-inch intervals. Because of the severe scaling/pluggage problems which occurred, the blade spacing was increased to 1-3/4 inches. Also, one side of the mist eliminator blades was raised slightly which resulted in an angle of about 2.4 degrees from horizontal. This was intended to improve drainage of liquid from the blades. The changes in blade spacing and elevation along with the addition of thiosulfate to the FGD system increased the operating time before pluggage/scaling, but carryover/re-entrainment of solid material became a problem.

TROUBLESHOOTING METHODOLOGY

The troubleshooting methodology as it was executed at the site is presented in Table 3. This involved first collecting and reviewing all of the observed symptoms which identified carryover/re-entrainment and pluggage/scaling as the potential problems. The potential causes for these problems were identified and confirming tests were selected. The results of these tests are presented below.

RESULTS OF CONFIRMING TESTS

A mist eliminator inspection performed on a tower just taken out of service found that pluggage/scaling appeared to be fairly evenly spread out over the mist eliminator surface, with slightly heavier buildup around some of the edges of the tower. All of the mist eliminator sections were present and did not appear to be damaged, eliminating materials failure as a possible cause for the carryover. No scaling or pluggage was found on the interface tray.

The wash system inspection, performed at the same time as the mist eliminator inspection, did not show any problems. However, a thorough inspection with examination of each of the wash nozzles was not possible because of a high SO_2 concentration in the tower. All of the wash nozzles were in place and did not appear to be misaligned. Because of this and the fairly even distribution of solids on the mist eliminator, it did not appear that the wash system coverage was a problem.

A review of the wash system design for the mist eliminator indicated that the system provided about 200% coverage and full-cone spray nozzles were being used. The wash duration and frequency (2 minutes every 6 minutes) appeared more than adequate. However, based on the wash water flow rate, the wash intensity was only 0.2 to 0.3 gpm/ft^2. This is considered relatively low, especially since the mist eliminator is a four-pass chevron design. The low wash intensity may not have been able to adequately penetrate and wash the last passes. Therefore, the wash intensity was suspected of contributing to mist eliminator scaling and pluggage.

Samples were taken of both the thickener overflow and water from the supernate tank. The chemical analysis of the thickener overflow indicated that the gypsum relative saturation was over 1.0. Two samples of the supernate tank water had gypsum relative saturations of 0.54 and 0.24. Service water was observed being added to the supernate tank during collection of the latter sample. Because of the relative saturation of the former sample (0.54), it was apparent that service water was also being added or had just been added to the supernate tank. Based on information supplied by the plant, the main time that service water was added to the supernate tank was during limestone grinding which occurred for only a few hours each day. Therefore, the majority of the time the mist eliminators were being washed with water having a high gypsum relative saturation. This was suspected of contributing to the scaling problem.

Chemical analysis of the absorber solids found that the limestone utilization in the recycle slurry ranged from 90% to 95%. This was above the guideline of 85% and indicated that limestone utilization should not have been causing problems. However, samples of the filter cake collected and analyzed by the operators of the FGD sludge disposal system indicated that the utilization had dropped to 70% to

80% on several occasions. This indicated that poor limestone utilization could periodically contribute to mist eliminator scaling.

Gas velocity measurements were performed at full load for all four operating towers. The velocity ranged from 11.3 to 15.4 ft/sec, indicating maldistribution of flue gas between the operating towers. This was expected based on the mist eliminator pressure drop data. The design full-load gas velocity for the MES was 11.4 ft/sec with a maximum velocity of 12.3 ft/sec. Therefore, all of the measured velocities were equal to or greater than the design velocity, and the maximum velocity was 35% over the design velocity. As a result, high gas velocity was also contributing to re-entrainment and pluggage/scaling.

Examination of the interface tray open area in combination with the flue gas flow rates through the MES indicated that the gas velocity through the interface tray holes could be up to 50 ft/sec. The high gas velocity through the holes and the fact that some portions of the mist eliminators were washed continuously make it probable that a layer of dilute slurry remained on top of the interface tray. A portion of this slurry could be re-entrained in the flue gas and carried to the mist eliminator. This may also have contributed to the mist eliminator pluggage/scaling.

Particulate measurements were made at the inlet to the FGD system and the stack. The collected solids were analyzed, and the results were used in a chemical element balance (5) to identify the source of the material exiting the stack. Based on the measurements, the total mass exiting the stack was about 10 times greater than the mass entering the FGD system. Measurements of the sulfuric acid mist indicated that sulfuric acid could account for a portion, but not all, of the increase. The chemical element balance indicated that about 15% to 20% of the mass was due to solids from the FGD system. However, the solids present in the ductwork downstream of the FGD system, which were primarily scrubber solids, indicated that a substantial amount of slurry was exiting the FGD system (from 0.5 to 4 gpm per module under full-load gas flow conditions).

MES PROBLEM CAUSES AND POTENTIAL SOLUTIONS

Based on the confirming tests, it was felt that the primary causes of the carryover/re-entrainment were the pluggage/scaling and the high gas velocity. The high gas velocity was due to total gas volume in excess of the design values and to poor distribution of flue gas between towers as a result of mist eliminator pluggage and scaling. The amount of air inleakage to the flue gas could not be easily reduced. The scaling and pluggage were believed to be caused primarily by the poor wash water quality and the low wash intensity. Periodic poor limestone utilization was also considered to contribute to the pluggage/scaling.

Combined with the fact that flue gas could not be bypassed around the FGD system, it was concluded that reducing the overall gas flow to the FGD system was not readily achievable. Therefore, the best solution to the MES problems appeared to be to stop the mist eliminator scaling and pluggage. This would help evenly distribute the gas flow between towers and reduce the potential sites for re-entrainment from the chevrons. If re-entrainment continued after elimination of the scaling and pluggage, a different mist eliminator design may be needed to handle the higher gas flows.

Recommendations to maintain clean mist eliminators included switching to a fresh water mist eliminator wash, increasing the wash intensity, and reducing the wash frequency and duration. Other changes to ensure high limestone utilization (e.g., improve limestone grind, eliminate process hydroclones, etc.) were also suggested. Implementation and testing of these recommendations was seen as a first step in solving the MES problems. If these changes were not successful or only provided limited improvement, then it was recommended that a new MES design be considered.

SUMMARY

The troubleshooting methodology includes identifying the symptoms of the problem, determining potential causes, and performing tests to assist with confirming the cause. An outline of the methodology as it applies to troubleshooting MES problems is presented in Table 1 and includes a listing of the potential problems, symptoms which may be observed, potential causes, and confirming tests. The three major MES problem areas are carryover/re-entrainment, pluggage/scaling, and materials failure; these problems are often interrelated which can make troubleshooting MES difficult. The potential causes for these problems range from mechanical problems such as materials failure to chemistry problems such as gypsum relative saturation of the mist eliminator wash water. The tests which should be selected to confirm the MES problem will depend on the suspected cause and should take into account the cost and effort required to perform the test.

Potential solutions to the problems are presented in Table 2 and include both operating guidelines and equipment modifications. The guidelines were based on past experience at other utility FGD systems and should be considered a starting point for other systems. It should be recognized that the potential solutions to MES problems at a particular location can be very site-specific; they can depend on factors such as the type of FGD system, water balance limitations, SO_2 removal required, and economics to name a few. Future research by EPRI on mist eliminator systems will be aimed at better defining MES operating guidelines and developing solutions to MES problems.

The case study of the MES problems experienced at a utility site demonstrated application of the troubleshooting methodology to identify potential problem causes.

ACKNOWLEDGMENTS

This work was funded and performed as part of the Electric Power Research Institute's Research Project 2250-3.

The work described in this paper was not funded by the U.S. Environmental Protection Agency and therefore the contents do not necessarily reflect the view of the Agency and no official endorsement should be inferred.

REFERENCES

1. Smith, T.P. FGD Chemistry and Analytical Methods Handbook, Volume 2: Chemical and Physical Test Methods. Electric Power Research, CS-3612, Palo Alto, California, July 1984.

2. Burbank, D.A. and Wang, S.C. EPA Alkali Scrubbing Test Facility: Advanced Program - Final Report (October 1974 - June 1978). U.S. Environmental Protection Agency, EPA-600/7-80-115, May 1980.

3. Radian Corporation. FGD Chemistry and Analytical Methods Handbook. Volume 3: FGD Liquid Equilibrium Program - FGDLIQEQ. Electric Power Research Institute. CS-3612. Palo Alto. California. July 1984.

4. McCain. J.D. Video-Based In-Situ Droplet Concentration and Size Analyzer. Paper presented at the First Combined FGD and Dry SO_2 Control Symposium. October 25-28. 1988.

5. Balfour. W.D.. Edwards. L.O.. and Williamson. H.J. Evaluation of Entrained Liquor Contributions to Total Mass Emissions Downstream of a Wet Scrubber. Paper presented at the 1981 Third Symposium on the Transfer and Utilization of Particulate Control Technology. EPA-600/9-82-005. March 1981.

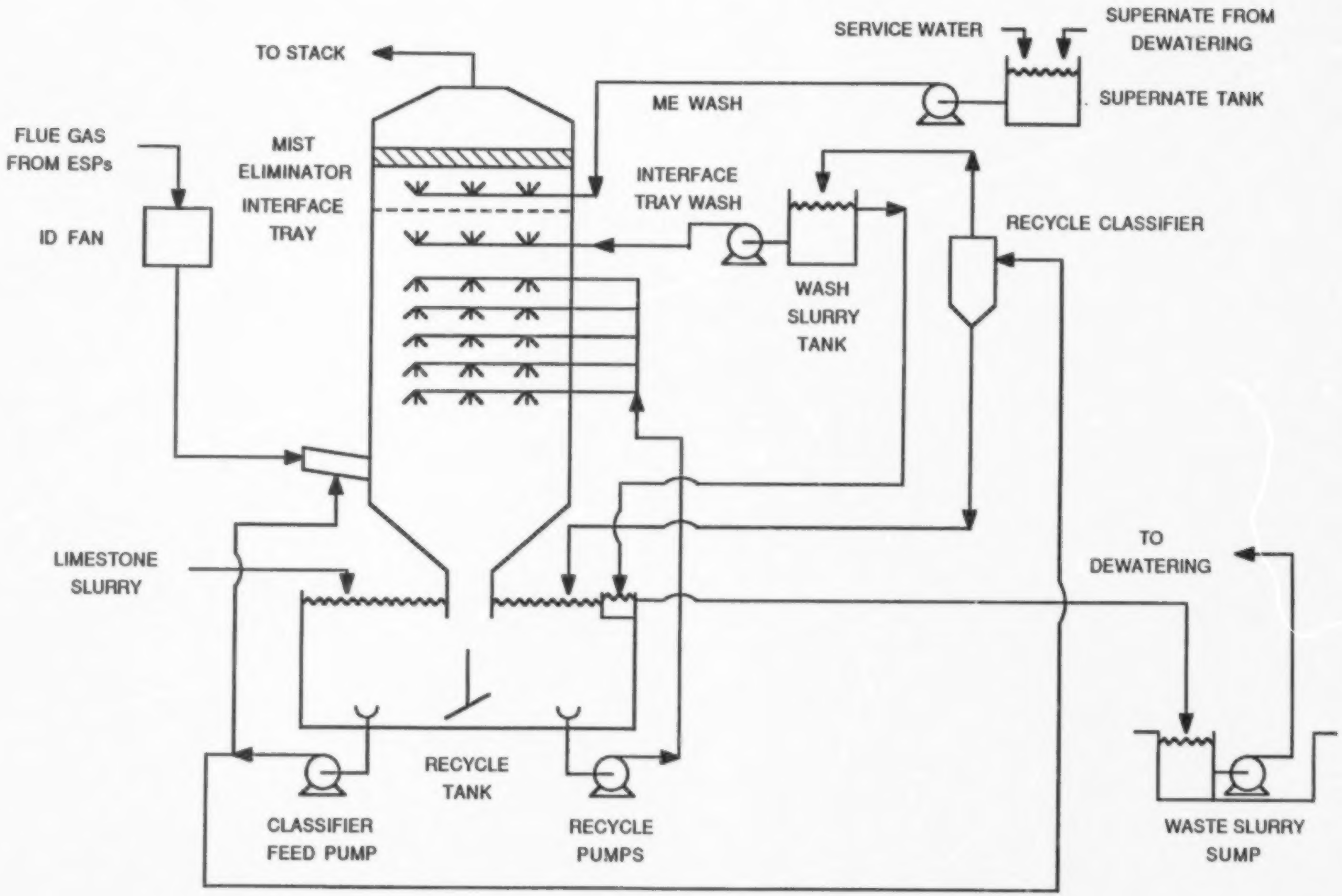
TO STACK
SERVICE WATER
SUPERNATE FROM DEWATERING
SUPERNATE TANK
ME WASH
FLUE GAS FROM ESPs
MIST ELIMINATOR
INTERFACE TRAY
ID FAN
INTERFACE TRAY WASH
RECYCLE CLASSIFIER
WASH SLURRY TANK
LIMESTONE SLURRY
TO DEWATERING
RECYCLE TANK
CLASSIFIER FEED PUMP
RECYCLE PUMPS
WASTE SLURRY SUMP

Figure 1. Flow diagram.

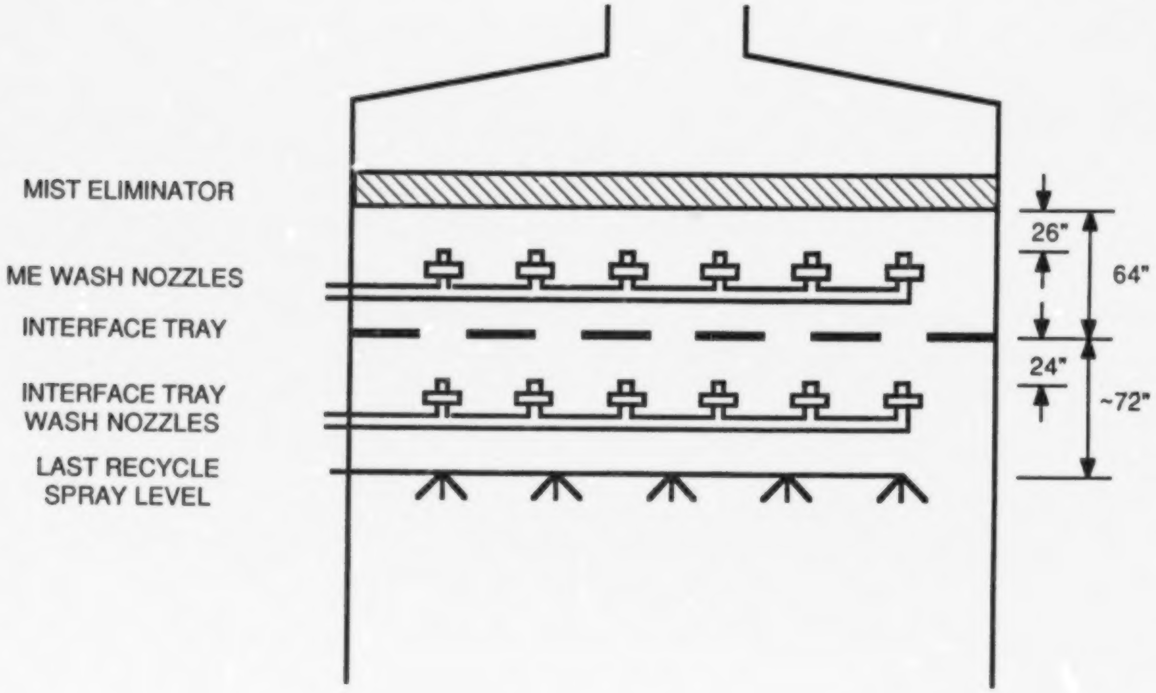
MIST ELIMINATOR
ME WASH NOZZLES
INTERFACE TRAY
INTERFACE TRAY WASH NOZZLES
LAST RECYCLE SPRAY LEVEL
26"
64"
24"
~72"

Figure 2. Mist eliminator system design.

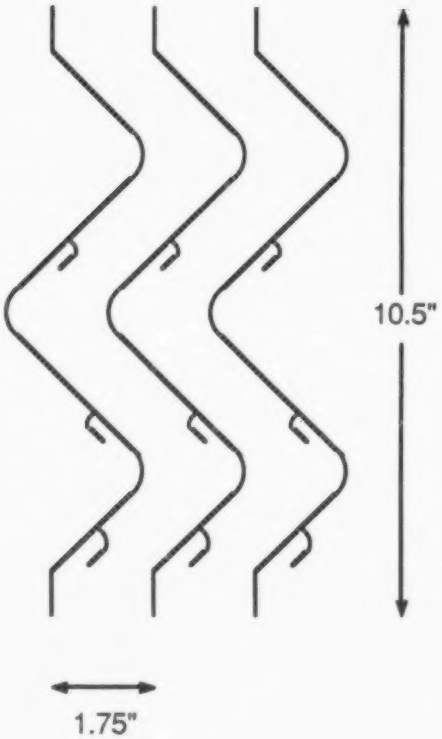

Figure 3. Cross-section of mist eliminator chevrons.

TABLE 1. MES TROUBLESHOOTING GUIDE

Observed Symptoms	Major Problem Areas	Potential Causes[a]	Confirming Tests[b]
High Mist Eliminator Pressure Drop Solids Accumulation on Mist Eliminator Surfaces Also Carryover/Reentrainment Symptoms	Pluggage/Scaling	Poor Limestone Utilization Wash System -- Water Quality -- Coverage -- Intensity -- Frequency -- Duration Poor Gas Distribution High Mist Loading Mist Eliminator Design	Wash System Inspection Mist Elimator Inspection Review Wash System Design Review Operating Records Wash Water Analysis Absorber Solids Analysis Velocity Traverse Spray Nozzle Droplet Size Distribution
Solids Buildup on Downstream Ducts/Reheater Surfaces Stack "Rain" Increased Stack Opacity/Particulates Drop in Stack Temperature	Carryover/Reentrainment	Pluggage/Scaling High Gas Velocity Poor Gas Distribution High Mist Loading Mist Eliminator Design Materials Failure	Mist Eliminator Inspection Review Mist Eliminator Design Velocity Traverse Particulate/Droplet Measurements Spray Nozzle Droplet Size Distribution
Missing/Damaged Mist Eliminators Drop in Mist Eliminator Pressure Drop Plugged Spray Nozzles from ME Material (Higher Spray Header Pressure) Drop in Stack Temperature (Particularly during Mist Eliminator Washing) Also Carryover/Reentrainment Symptoms	Materials Failure	Pluggage/Scaling Installation Procedure Manual Cleaning Procedure Temperature Excursion	Mist Eliminator Inspection Review Operating Temperature Records Review Installation Procedures Review Manual Cleaning Procedure Test Mist Eliminator Material Strength

[a] There may be more than one potential cause for a particular problem and the potential causes can be very site specific. The potential causes are listed here in order of probability (i.e., the most likely cause is listed first). The potential causes can be confirmed by proper selection and execution of one or more confirming tests.

[b] The confirming tests are listed in order of increasing cost and effort for each major problem area.

TABLE 2. POTENTIAL SOLUTIONS TO MES PROBLEM CAUSES

Cause of MES Problem	Potential Solution[a]
High Gas Velocity	Guideline: Less than 12 ft/sec. Reduce air inleakage to flue gas. Bypass flue gas around scrubbers.
Poor Gas Distribution	
- Between Towers	Balance flue gas flow with dampers and other restrictive devices.
- Within a Single Tower	Prevent scaling of tray/packing. Add baffles to evenly distribute gas. Ensure that spray nozzles are not plugged.
High Mist Loading	Change wash system operation. Replace spray nozzles. Lower gas velocity.
Mist Eliminator Design	Install different type of chevron. Install bulk entrainment separator.
Wash System	
- Water Quality	Guideline: Gypsum relative saturation less than 0.5. Use all fresh water for wash. Use blend of water to maintain gypsum relative saturation below 0.5. Use thiosulfate in FGD system.
- Coverage	Guideline: Greater than 150% coverage of mist eliminator surface. Wash nozzles with full cone spray pattern. Increase number of wash nozzles/headers. Replace hollow cone spray pattern nozzles with nozzles having full cone spray pattern.
Wash System	
- Intensity/Frequency/Duration	Guideline: Front side of first mist eliminator - 1.5 gpm/ft^2 for 45 seconds/30 minutes. Back side of first mist eliminator - 0.55 gpm/ft^2 for 3 minutes/1 hour. Front side of second mist eliminator - 0.55 gpm/ft^2. for 3 minutes/1 hour. Increase wash water flow rate. Replace wash nozzles/headers. Revise wash frequency and duration.
Poor Limestone Utilization	Guideline: Limestone utilization greater than 85%. Lower reaction tank pH. Enhance SO_2 removal with organic acid or magnesium if necessary so that reaction tank pH can be lowered. Improve limestone particle size distribution. Remove/prevent pluggage of spray nozzles.
Installation Procedures	Revise installation procedures as necessary.
Temperature Excursion	Install/maintain emergency quench system.
Manual Cleaning Procedure	Prevent pluggage/scaling. Revise manual cleaning procedure as necessary.

---

[a] The guidelines presented under Potential Solutions are based on experience at other FGD systems and should be considered a starting point. The values and the other potential solutions for MES problems at a particular location are very site specific.

TABLE 3. TROUBLESHOOTING METHODOLOGY APPLIED TO A CASE STUDY

Observed Symptoms	Potential Problems	Potential Causes	Confirming Tests Performed
Carryover/re-entrainment to downstream duct-work (solids deposition on duct surfaces) Fallout of solid material from stack (solids noticed on exterior car surfaces) Mist eliminator pressure drop increased and varied between towers (0.3 to >1.0 in. H_2O)	Carryover/ re-entrainment Pluggage/ scaling	Low limestone utilization in absorber loop Inadequate MES wash (wash water chemistry and low wash intensity) Gas maldistribution between towers High gas flow Increase in mist eliminator blade spacing	MES inspection Review of MES wash system design and operation MES wash system inspection Chemical analysis of absorber solids and MES wash water Gas velocity measurements at absorber outlet Particulate loading measurements at FGD system inlet and stack outlet

GUIDELINES FOR TROUBLESHOOTING UTILITY STACK OPACITY

by: W. David Balfour
Radian Corporation
Austin, Texas 78720-1088

R. G. Rhudy
Electric Power Research Institute
Palo Alto, California 94304

R. J. Keeth
Stearns-Roger Division
United Engineers & Constructors, Inc.
Denver, Colorado 80222

ABSTRACT

Stack plume visibility, otherwise defined as plume opacity, has become a concern to the utility industry. This is because some coal-fired stations with operating FGD systems have been cited for opacity in excess of the New Source Performance Standards (NSPS) even though the particulate mass emissions are within regulated limits. Postulated causes for the unacceptable opacities include scrubber-generated particulate matter, condensible particulate matter such as sulfuric acid mist, large amounts of fine particles penetrating the particulate control device, and/or colored gases such as nitrogen dioxide in the flue gas. To develop control strategies to reduce plume opacity, it is important that the underlying cause of the plume opacity be identified. This paper presents a troubleshooting methodology developed during field tests at three utilities experiencing high stack opacities. Results from one of the field tests are presented as a case study to demonstrate how this methodology can be applied by a utility to determine the cause of their plume opacity.

INTRODUCTION

Stack-plume visibility, otherwise defined as plume opacity, has become a concern to the utility industry because some stations have been cited for opacity in excess of the New Source Performance Standards (NSPS) when the particulate mass emissions are within regulated limits. At other utilities, the visible emissions have been higher than anticipated, and there is concern by the utility over the visibility reduction in the local environment. Postulated causes for the unacceptable opacity include scrubber generated particulate matter, condensible particulate matter such as sulfuric acid in the flue gas, large amounts of fine particles penetrating the particulate control device, and/or colored gases such as nitrogen dioxide (NO_2) in the flue gas.

Existing and proposed regulations may make it necessary to develop control strategies to reduce plume opacity. To provide effective control, it is necessary that the underlying cause of the plume opacity be understood. This paper presents a methodology for troubleshooting the cause of plume opacity which may assist utilities experiencing such problems. This method was developed based on experience gained during field programs sponsored by the Electric Power Research Institute (EPRI) to assist utilities in identifying the cause of their stack opacity. Included in the paper are tests for confirming potential causes of plume opacity, possible solutions for these causes and an example of how this methodology was used at a utility.

TECHNICAL BACKGROUND

An understanding of the optical properties which may cause plume opacity is important in order to identify the process operation which results in the observed opacity. The ratio of the intensity of light which reaches an observer from a given source (I/I_o) can be related to the percent opacity as:

$$\%\ \text{Opacity} = (1 - I/I_o) * 100 \qquad (1)$$

The Beer-Lambert Law defines the ratio of transmitted light as:

$$I/I_o = \exp(-b_{ext}L) \qquad (2)$$

where: b_{ext} is the extinction coefficient, and
L is the optical path length.

The extinction coefficient is a measure of the optical properties of the plume (flue gas), while the optical path length is defined by the stack diameter in the case of an in-stack transmissometer measurement or the plume cross-section (depth) in the case of visible emissions observations. This assumes that the background air is clean, and thus the optical properties and path length are the result of the plume, and not significantly affected by the intervening atmosphere.

The extinction coefficient includes the effects of light scattered by particulate matter, light absorbed by particulate matter, and light which is absorbed by gaseous pollutants. Light absorption by particulate matter is typically attributed to soot or the carbonaceous fraction of fly ash and results in black plumes. While black plumes were the primary impetus for visible emission standards, improved burner operation has minimized the contribution of light absorbing particulate matter to current coal-fired utility plumes. Today, visible plumes tend to be white, blue, and/or brown as opposed to black.

Light scattered by particulate matter is influenced by the particle number (as opposed to mass) concentration, the particle size distribution, the refractive index of the particulate matter, and the sun-observer-plume angles. To illustrate the strong dependence of scattered light on particle size, the extinction coefficients for particulate matter typical of emissions from a coal-fired utility boiler with an FGD system were calculated and plotted as a function of particle size. Figure 1 shows the differential plot of the extinction coefficient normalized per unit of particle size versus the aerodynamic particle size. For purposes of comparison, the particle size distribution is also plotted as a differential plot of mass concentration normalized per unit of particle size. The area under the extinction curve (dashed line) is representative of the opacity, and the area under the particle size distribution curve (solid line) is representative of the total particulate mass concentration. From this illustration, it is obvious that the most effective particles at scattering light are in the 0.5 to 1.5 um size range.

A plume dominated by light scattered by fine particles may appear white or blue, with little contrast when the sun is in front of the observer, while the same plume may appear brown with higher contrast when the sun is behind the observer. It should be noted that changes in background color can cause apparent changes in the observed plume color and contrast. Procedures for making visible emission observations (EPA Method 9) attempt to minimize the effect of the viewing angle on the light scattered by particulate matter by specifying the appropriate position of the sun, plume, and observer.

Nitrogen dioxide (NO_2) is the gaseous pollutant most responsible for light absorption. Since NO_2 absorbs shorter wavelength light, a plume dominated by NO_2 light absorption will appear reddish brown, and is not affected by the viewing angle.

It is difficult to distinguish between the combined effects of fine particle light scattering and NO_2 light absorption on plume opacity. However, the ratios of either fine particle mass and NO_2 mass, or extinction due to fine particles and extinction due to NO_2, can be used to qualitatively determine the dominant contributor to plume contrast and color. Data presented by White and Patterson (1) indicate that when the particle size distribution is mostly fine particle mass, the contrast and color of a power plant plume tends to be dominated by the particulate matter rather than NO_2.

TROUBLESHOOTING METHODOLOGY

The intent of any troubleshooting guide is to identify the cause of a problem from observed symptoms so that a solution may be implemented. Such a guide has been developed for troubleshooting plume opacities, as shown in Table 1. The methodology established presents specific symptoms which can be observed to identify the major optical properties contributing to the opacity, as discussed above. Probable causes are associated with each of these properties, and confirming tests are presented which can identify the specific cause.

To use this guide, plume observations would be made and compared to the listed "observed symptoms," in order to identify the probable optical property (or properties) contributing to the observed opacity. This would require observations to be made over a period of time, at various times during the day, and/or from a variety of sun, plume, observer viewing angles. It is possible that the plume observations would not be sufficient to allow determination of a single optical property contributing to the opacity. However, with additional specific observations, it should be possible to identify a primary contributor to the opacity. The confirming tests can then be selected to focus on the causes of the primary optical property affecting the opacity, and if needed, additional confirming tests performed which addresses the cause of the other possible optical property. This approach is suggested because of the effort and expense required to perform each of the confirming test programs. Note that it is not necessarily required to perform each test listed for a given optical property affecting the opacity. However, each of the tests should be considered based on the site-specific factors for the individual utility.

This troubleshooting approach is intended to allow utility personnel to identify the optical property most likely responsible for the observed opacity. They may then design a program of confirming tests for the possible causes of the opacity appropriate to their site. For example, if a low sulfur coal is burned, sulfuric acid is not likely to be of concern. Or, if an FGD system is not used, scrubber generated particulate matter would not be addressed. In most cases, utilities will require the services of a test contractor to perform the confirming tests. The tests are, for the most part, not EPA compliance test methods. The examples presented here should assist the utility personnel to interpret the results of such testing and identify the probable cause of the opacity.

DISCUSSION OF POTENTIAL CAUSES AND CONFIRMING TESTS

As discussed above, plume opacity may be the result of light scattered by fine particles, light absorbed by the particulate matter, and/or light absorbed by gaseous species. The utility and/or environmental processes which can cause each of these effects are discussed below, along with specific tests which may be performed to identify the cause. In general, confirming tests are performed to first assure that the suspected optical property can be responsible for the observed opacity. Additional tests are then performed as needed to identify the probable cause.

LIGHT SCATTERING BY FINE PARTICLES

If it is suspected that the observed opacity is primarily the result of light scattering by fine particles, then the source of the fine particles must be determined. The fine particles may be present in the flue gas and be emitted directly from the power plant stack, or they may form in the plume downwind of the stack as the result of condensation (i.e., sulfuric acid) or atmospheric reactions (i.e., sulfates or nitrates). If the visible plume is not observed until some distance downwind of the stack (i.e., detached), then it is likely that the fine particles did not exist in the process gas stream and are being formed in the plume.

This can be confirmed by measuring the total particulate emission rate and associated particle size distribution in the flue gas at the stack. These measurements must be made at the stack temperature in order to provide data representative of the particulate matter affecting opacity at that location in the gas stream. For this reason, the total particulate mass measurement should be performed using EPA Method 17 or equivalent, and the particle size distribution measurement should be made with an in-stack impactor operated to provide submicron segregation of particles. The extinction coefficient (b_{ext}) can be calculated from the sum of extinction coefficients for discrete particle size intervals ($b_{ext\ i}$) where $b_{ext\ i}$ is defined as:

$$b_{ext\ i} = N_i * Q_{ext\ i} * A_i \qquad (3)$$

where: N_i is the number concentration of particles in size interval i,
$Q_{ext\ i}$ is the extinction efficiency factor for size interval i computed from the Mie equations (2), and
A_i is the cross-sectional area of the geometric mean particle size in size interval i.

The extinction efficiency factor is a function of the particle size, the wavelength of light, and the refractive index of the particulate matter. As presented above, the opacity can then be calculated (Equations 1 and 2) from the extinction coefficient developed from the measured particle size distribution (see Figure 1). Fine particle (<1 um) mass concentrations greater than 0.01 gr/dscf have the potential for causing 20% opacity or greater. Alternatively, an in-stack transmissometer can be used to directly measure the opacity in the stack if conditions allow such measurement (i.e., no entrained moisture).

If the calculated or measured in-stack opacity is of a similar magnitude to the observed plume opacity, then the fine particle concentration present in the gas stream is likely causing the observed opacity. When reheat has been used to raise the stack gas temperature above the water saturation temperature at the exit of an FGD system, the plume opacity may be greater than the in-stack opacity if the ambient relative humidity is high. This is due to the condensation of water on the particles, and is dependent on the chemical nature of the particles. The amount of water associated with the particles can change the particle size and as such, change the observed opacity. If the fine particle concentration in the gas stream or the measured opacity cannot account for the observed plume opacity, then it can be reasoned that the fine particles are being formed outside of the stack, downwind in the plume.

One potential cause of particle formation downwind in the plume resulting in a detached plume is condensation of sulfur trioxide to form sulfuric acid mist. When the temperature of the stack gas is above the sulfuric acid dewpoint (nominally 250°F) and the concentration of sulfur trioxide is 5 ppmv or greater, the potential exists for a detached plume with opacities in excess of 20%. These conditions are typical of high-sulfur coal-fired boilers or oil-fired boilers not equipped with scrubbers. The condensation of sulfur trioxide occurs as the stack gas cools in the ambient air. The particle size and thus the opacity resulting from the condensation of sulfuric acid mist can be influenced by ambient factors such as the air temperature and relative humidity. Stack temperatures are routinely measured, so it is relatively simple to compare the stack exit temperature to the acid dewpoint temperature. Sulfur trioxide/sulfuric acid mist measurements should be made using a controlled condensation sampling system, preferably at a location where the flue gas temperature is above the sulfuric acid dewpoint. For utilities with FGD systems, this would be at a point upstream of the scrubber. The measured value is representative of the total sulfur trioxide/sulfuric acid present in the gas stream, but does not provide information on the fraction present as a vapor or as a mist.

Atmospheric reactions can result in the formation of fine particles (secondary aerosols) downwind in the plume and cause a detached plume. These reactions can include the transformation of gaseous sulfur dioxide to sulfate and/or nitrogen oxides to nitrate. Typical rates for these reactions are such that the visible plume would appear well downwind (miles) of the stack. However, ambient conditions including moisture, sunlight, and the presence of reactive radicals, and/or oxidizing species such as ozone can increase these rates of reaction. Confirmation test for such reactions require plume sampling from an airborne platform such as a helicopter or airplane. Measurements include collecting size fractionated particulate samples to determine the concentration and chemical composition of the particulate matter responsible for the visible plume. Additionally, measurements of the gaseous precursors in the plume and other reactive species in the ambient air are helpful in understanding the atmospheric reactions which are taking place in the plume. Because of the effort and expense associated with such measurements, it is recommended that reactive plume modeling be conducted prior to such a test program. The modeling would be based on the known stack emissions, to determine if and under what ambient conditions sufficient particles could form downwind in the plume to cause the observed opacity. Computer models such as the RPM II (3) developed for the Environmental Protection Agency can be used for such simulations.

If the measured fine particle concentration in the stack gas is capable of causing the observed plume opacity, the source of the fine particles must be identified. Possible sources include the penetration of combusted particulate matter (fly ash) through the particulate control device; generation of particulate matter from the flue gas desulfurization (FGD) system as the result of carryover/reentrainment from the mist eliminator; or sulfuric acid mist which has condensed because the flue gas temperature has dropped below the acid dewpoint.

If sulfuric acid particles are causing the observed opacity in the stack, the flue gas temperature must be below the acid dewpoint. This condition exists when high-sulfur fired boilers are equipped with FGD systems. As shown in Figure 2, sulfur trioxide/sulfuric acid concentrations greater than 5 ppmv have the potential for causing opacities greater than 20%. A pH test of the total and size fractionated particulate samples may be used to indicate the presence of significant sulfuric acid in the collected particulate matter. The concentration of sulfuric acid mist in the flue gas can be quantified using the controlled condensation sampling system as described above. The mass of sulfuric acid (as the acid dihydrate) can then be compared to the fine particle (<1 um) mass fraction calculated from the particle size distribution to confirm that it accounts for a significant fraction of the fine particle mass causing the opacity.

By comparing the results of total and size fractionated particulate measurements obtained from a location downstream of the FGD system (stack) and a location upstream of the FGD system (downstream of the particulate control device), it is possible to determine if the FGD system or a drop in flue gas temperature is introducing fine particles to the stack gas. If there is no significant change in the fine particle mass measured at these two locations, the opacity can be attributed to fly ash penetrating the particulate control device. If there is a significant change in fine particle mass, the mass contributed by sulfuric acid may account for the observed change. If it does not, the contribution of mass can be attributed to the carryover or reentrainment of FGD liquor through the mist eliminator. This can be confirmed by analysis of the collected particulate matter for scrubber solids (i.e., gypsum crystals) using scanning electron microscopy and/or chemical analyses.

LIGHT ABSORPTION BY PARTICULATE MATTER

When it is suspected that the plume opacity is due to light absorption by particulate matter, the cause can typically be attributed to poor combustion conditions resulting in large quantities of soot (unburned carbon). While this used to be the predominant type of visible plume, today's improved combustion processes typically prevent such events except during periods of faulty burner operation. These conditions can be confirmed by analyzing total particulate matter samples for unburned carbon.

LIGHT ABSORPTION BY NO_2

If the the visible plume is thought to be due to light absorption by gaseous species, then the source of the gaseous species must be determined. Typically, NO_2 is the gaseous species responsible for the light absorption resulting in visible plumes from utilities. The NO_2 may be present in the flue gas and emitted directly from the stack, or it may be formed downwind from the stack (detached) in the plume as a result of reactions in the atmosphere. The gaseous precursor to NO_2 is nitrogen oxide (NO), which forms in the flue gas as a result of the nitrogen present both in the fuel and in the air during the combustion process. Measurements may be made at the stack location of the NO, NO_2, and/or NO_x in the flue gas. Researchers have reported that values of NO_2 concentration (ppmv) * path length (meters) in excess of 60 ppmv-meters can result in visible plumes (4). For example, 10 ppmv of NO_2 in a 6 meter plume (pathlength) may result in a visible plume.

As with visible plumes caused by fine particle scattering, when the plume becomes visible downwind of the stack and it is suspected that the primary optical property causing the visible plume is light absorption by gaseous species (NO_2), plume sampling is required for confirmation. This can be done from airborne platforms or with remote sensing instrumentation such as LIDAR. Measurements of the ambient conditions promoting the formation of the NO_2 downwind in the plume are also recommended. These can include ozone concentration, ambient temperature, and sunlight. Because of the effort and expense associated with such measurements, it is recommended that reactive plume modeling (3) be conducted prior to such tests. The modeling would be based on the known stack emissions of NO_2 and NO, to determine if and under what ambient conditions sufficient NO_2 could be formed in the plume to cause the observed opacity.

POSSIBLE SOLUTIONS

As discussed above, the source of a visible plume may originate from a variety of utility operating conditions. The ultimate solution to the visible plume problem must address the combustion process generating the particulate matter or gaseous species causing the plume opacity, and/or the control systems in place to limit their emissions to the environment. These options are reviewed in Table 2. The intent of this information is to provide an initial identification of options available when the cause of the opacity problem has been confirmed. The selection of the most appropriate option will be based on site-specific and economic factors, and is not discussed in this paper.

CASE STUDY

To date, EPRI has assisted three utilities in determining the cause of their plume opacity. In all cases, the utilities have fired high-sulfur coal and been equipped with FGD systems having varying amounts of reheat. The following case study was developed from one of these studies.

Utility personnel had reported that when visual emissions from their unit were noticeable, they were significant (exceeding 30% opacity). Prior particulate emission test results indicated that the unit was meeting the current New Source Performance Standards (NSPS). An initial evaluation of the problem by plant personnel had concluded that the opacity was due to entrained scrubber liquor. This was based in part on the fact that significant amounts of scrubber solids had been deposited in the duct work downstream of the FGD system, prior to the stack exit.

The unit is a nominal 500 MW base-loaded pulverized coal boiler. The boiler fires a bituminous coal with a heating value of 12,000 Btu/lb, and a sulfur content which varies from 2.0% to 3.5%. Particulate emissions are controlled by two cold-side electrostatic precipitators (ESPs). The FGD system consists of four 25% capacity towers with sieve trays. Limestone is used for reaction with the absorbed SO_2, and enhanced with the addition of either dibasic acid, or adipic acid. The mist elimination system consists of a trap-out tray followed by two chevron-type mist eliminators. The stack gas is reheated to nominally 180°F using both bypassed flue gas and indirect (steam) reheat.

A summary of the observed symptoms and postulated causes for the visible plume from the unit is shown in Table 3. The fact that the observed plume color and contrast varied with viewing angle suggested that the plume opacity was the result of light scattering from fine particles. The plume did not appear to be detached, but did show white moisture plumes under certain ambient temperature conditions. The potential causes of the plume opacity were then postulated to include entrained FGD scrubber liquor (as previously identified by the plant personnel), as well as sulfuric acid mist, and/or poor ESP performance. Sulfuric acid mist was considered a potential cause since the sulfur in the coal was 2% to 3.5%. The fact that the unit met NSPS particulate emission standards suggested that the ESPs were performing as designed, and were not the problem.

Total mass and size fractionated particulate samples were collected at the stack location and a location upstream of the FGD system (downstream of the ESP). The measured particle size distributions are shown in Figure 3. The data are presented as differential particle size distributions, representing the mass of particulate matter normalized per unit of particle size as a function of the aerodynamic particle diameter (unit density sphere). This presentation allows the total area under the curve to represent the total particulate mass concentration. The total particulate mass concentration prior to the FGD system was less than 0.008 gr/dscf, while the total particulate mass concentration at the stack location was nominally 0.032 gr/dscf. As shown by the particle size distribution, the increase in particulate mass (nominally 0.024 gr/dscf) from the location upstream of the FGD system to the location at the stack can be attributed primarily to fine particulate mass.

The flue gas opacity was calculated from the particle size distribution measured at the stack location. Extinction coefficients were calculated (Equation 3) for discrete particle size intervals (physical diameters, assuming a density of 2.5 gm/cc) using light extinction efficiency factors for a refractive index of 1.5 and a wavelength of 550 nm (2). The extinction distribution is shown in Figure 4 as a differential plot for aerodynamic particle diameter to allow comparison with the measured particle size distribution. The total area under the curve represents the total extinction (Equation 2). The stack opacity was then calculated as 30%, from the total extinction and using an optical path length equal to the stack diameter (Equation 1). The measured stack opacity was nominally 31%. The plume opacity measured by a trained observer (EPA Method 9) was nominally 35%. The calculated opacity of the flue gas upstream of the FGD system (downstream of the ESP) was nominally 5%. The extinction distribution shows the strong dependence of light scattering on particle size. These data confirm the fact that a source of fine particles downstream of the ESP is responsible for the observed opacity.

Sulfuric acid (H_2SO_4 mist/SO_3) was measured at each of the sampling locations mentioned previously. The measured concentration of sulfuric acid ranged from 6 to 9 ppmv. This value corresponds to a mass concentration of nominally 0.02 gr/dscf. Upstream of the FGD system, the flue gas temperature (280°F) is above the sulfuric acid dewpoint. At temperatures greater than the sulfuric acid dewpoint, sulfur trioxide exists in a gaseous form. The FGD system drops the flue gas temperature to nominally 125°F. At the stack location the flue gas has been reheated to a temperature of nominally 180°F. At these temperatures, the stack gas is well below the acid dewpoint, and the sulfuric acid will exist as fine particles, contributing to the particulate mass concentration. The measured sulfuric acid mass concentration (0.02 gr/dscf) can account for the majority (80%) of the increase in fine particulate mass observed at the stack location (Figure 3). Additionally, the pH of the fine particle fraction was determined, and analyses performed for sulfate. Results showed that the particulate matter was largely sulfate with a pH less than 2, indicating sulfuric acid.

An analysis of the particulate matter collected at the stack location using a scanning electron microscope could not identify any appreciable amount of solids indicative of scrubber carryover/reentrainment. The quantity of scrubber generated solids contributing to the stack emissions was estimated using a chemical element balance technique (5). The chemical element balance is based upon the chemical composition of the fly ash going into the FGD system, the scrubber liquor, and the particulate emissions exiting the FGD system. The mass concentration of scrubber generated solids was calculated to be nominally 0.001 gr/dscf, or less than 5% of the total particulate emissions from the stack. This information supports the fact that the fine particulate mass responsible for the observed stack opacity is caused by sulfuric acid mist, and not scrubber carryover/reentrainment.

The above information confirmed that the excessive plume opacity is the result of light scattering by the significant fine particle fraction of total particulate mass exiting the stack. The source of the fine particulate mass appears to be predominantly sulfuric acid mist. Any attempt to mitigate the plume opacity will have to focus on the sulfuric acid mist (fine particulate mass fraction).

SUMMARY

The major optical properties contributing to plume opacity include light scattering by fine particles, light absorption by particulate matter, and light absorption by gaseous species, primarily NO_2. By observing the optical characteristics of the plume, the probable optical property contributing to the plume opacity can be determined. Using this knowledge, possible sources (causes) of the particulate matter or gaseous species contributing to the plume opacity can be identified by the utility. Performance of the test program for the confirmation of the suspected cause(s) typically will require that the utility contract the work to an experienced test firm.

The information presented in this paper has been based primarily on experiences gained at utilities operating with high-sulfur coal and wet FGD systems. A plume opacity troubleshooting manual is being prepared by EPRI, which will provide additional details with regards to the test methods, calculations used for data interpretation, case studies, etc. The intent is to update this manual as additional experience is gained with other utilities.

ACKNOWLEDGMENTS

This work was funded and performed as part of EPRI Research Project 2250-3. A number of individuals within Radian Corporation's Chemistry and Engineering Divisions contributed to the collection and interpretation of the field data supporting this project including Larry Rohlack, Michael Krall, Juan Martinez, Tim DeFries, Larry Edwards and AJ Jones.

The work described in this paper was not funded by the U.S. Environmental Protection Agency and therefore the contents do not necessarily reflect the views of the Agency and no official endorsement should be inferred.

REFERENCES

1. White, W. H. and D. E. Patterson. On the relative contributions of NO_2 and particles to the color of smoke plumes. Paper presented at 1980 Symposium on Plumes and Visibility: Measurements and Model Components, Grand Canyon, Arizona, November 10-14, 1980.

2. Van de Hulst, H. C. Light scattering by small particles. Wiley, New York, 1957. p. 127.

3. Stewart, D. A. and M. K. Liv. Development and application of a reactive plume model. Atmospheric Environment, Vol. 15, p. 2377-2393, 1981.

4. 1987 Coal Preparation, Utilization, and Environmental Control Contractors Review, Department of Energy, Pittsburgh Environmental Technology Center, July 1987.

5. Balfour, W. D., L. O. Edwards, H. J. Williamson. Evaluation of entrained liquor contribution to total mass emissions downstream of a wet scrubber. Paper presented at 1981 Third Symposium on the Transfer and Utilization of Particulate Control Technology, EPA-600/9-82-005, March 1981.

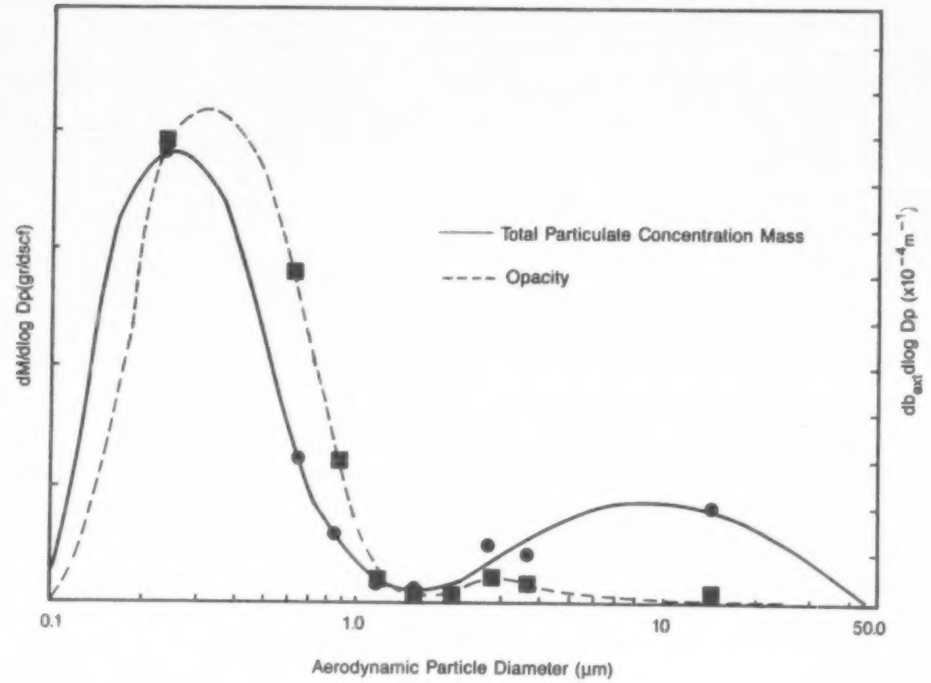

Figure 1. Contribution of particle size to opacity.

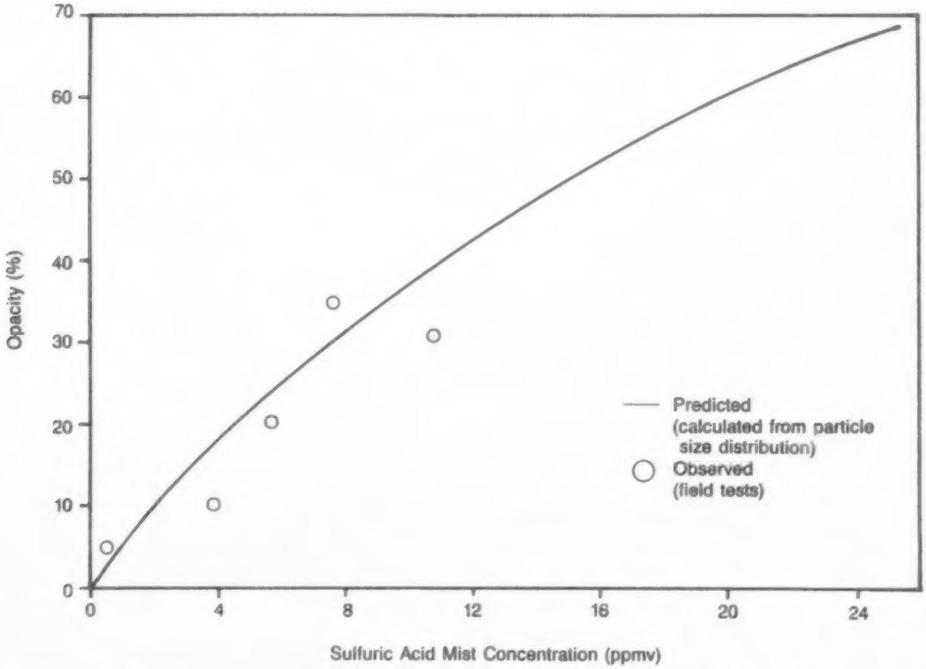

Figure 2. Relationship between opacity and sulfuric acid mist concentrations.

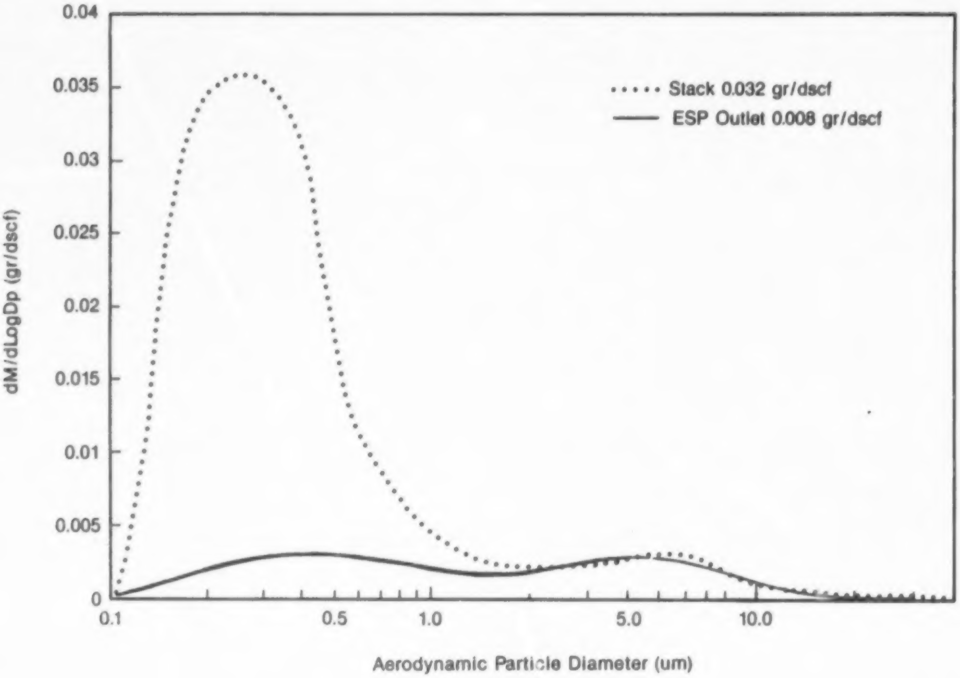

Figure 3. Differential particle size distributions at the stack and ESP outlet sampling locations.

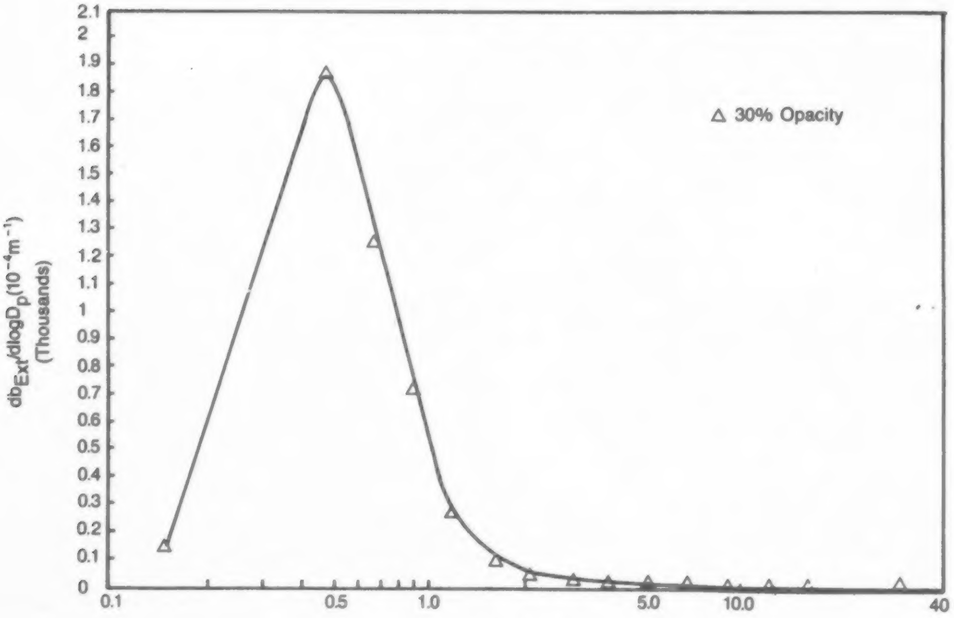

Figure 4. Differential light extinction distribution for stack particulate emissions.

TABLE 1. OPACITY TROUBLESHOOTING GUIDE

Optical Properties Contributing to Opacity	Observed Symptoms*	Potential Causes†	Confirming Tests‡
Scattering of light by fine particles	Blue/white or brown color Color and contrast changes with change in sun angle or position of observer (viewing angle) May be detached from stack May be correlated to ambient conditions	FGD generated particulate matter Sulfuric acid Poor particulate control device performance Secondary aerosols Condensation of sulfuric acid	Stack transmissometer Total & size fractionated particulate matter Stack Temperature SO_3/H_2SO_4 testing SEM Chemical analysis of particulate matter Reactive plume modeling Plume sampling
Absorption of light by particulate matter	Black color Consistent color and contrast with different viewing angles	Poor boiler performance	Total and size fractionated particulate matter Analysis of particulate matter for unburned carbon
Absorption of light by gaseous species	Reddish or brown color Consistent color and contrast with different viewing angles May be detached from stack May be correlated to ambient conditions/concentrations of other pollutants	NO_2 Atmospheric reactions	$NO/NO_2/NO_x$ testing Reactive plume modeling LIDAR Plume sampling

*The observed symptoms are used to identify a probable optical property responsible for the observed opacity.

†The potential causes listed are for the stated optical property. Unit configuration and operation may eliminate consideration of a potential cause.

‡Confirming tests are used to confirm both the probable optical property and the potential causes. The confirming tests performed are based on the potential cause(s) considered for a given unit.

TABLE 2. OPTIONS FOR EVALUATION IN SOLVING OPACITY PROBLEMS*

Potential Cause	Possible Solution
FGD generated particulate matter	Improve MES performance
Sulfuric Acid Mist/Condensation of Sulfur Trioxide	Switch to a low sulfur coal
	Reagents to react with H_2SO_4/SO_3, such as NH_3, MgO, Amines, etc. added prior to ESP
	Wet electrostatic precipitator
Poor particulate control device performance	Review maintenance procedures such as bag failure, hopper operations, etc.
	Review design vs. actual operation
	Modify ash resistivity to improve performance
Poor boiler performance	Adjust combustion parameters
NO_2	Evaluate low NO_x combustion technology
	Evaluate low NO_x control alternatives
	Switch fuels
Atmospheric reactions	Improve plume rise via reheat for better dispersion
	Taller stack
	Temporary load reduction
	Fuel switching/blending
	Evaluate SO_2 controls
	Evaluate NO_x controls
	Evaluate low NO_x combustion technology

*Options are presented here without consideration of site-specific or economic factors. Selection of an ultimate solution by the utility must address such factors.

TABLE 3. CASE STUDY

Observed Symptoms	Optical Property Contributing to Opacity	Potential Causes	Confirming Tests
Plume which appears bluish/white or brown Color and contrast can change with different viewing angles Not detached from stack	Scattering of light by fine particles	FGD generated particulate matter Sulfuric acid Poor particulate control device performance	Stack Temperature Total and size fractionated particulate matter SO_3/H_2SO_4 SEM Chemical composition

SESSION 5B: WET FGD OPERATION
(Continued)

Chairman, Charles Dene, EPRI

PERFORMANCE AND OPERATING COSTS OF THE SOMERSET WET LIMESTONE FGD SYSTEM

by: Duane C. McCoy, Bernard J. Koch
Consolidation Coal Co. R&D
Library, Pennsylvania 15129

Walter A. Rogers, Jr.
Conoco Inc.
Ponca City, Oklahoma 74603

Hoxsie L. Crosby, John E. Smigelski
New York State Electric & Gas Corporation
Binghamton, New York 13902

ABSTRACT

In the first three and one-half years of operation, the 643 MW Somerset Station of New York State Electric and Gas Corporation (NYSEG) has demonstrated that a wet limestone slurry FGD system can be operated reliably and with lower than predicted O&M costs. The FGD operating and maintenance costs are monitored using an in-house data base management system. The actual costs are presented and compared with expected costs based on an EPRI prediction method. The process improvements made by NYSEG to reduce O&M costs of the scrubbing system are described. Further cost reductions for wet limestone scrubbing are possible by developing by-product solid waste utilization options and demonstrating advanced FGD processes which eliminate the need for expensive spare equipment.

INTRODUCTION

To insure that a flue gas desulfurization unit (FGD) is operated reliably and in a cost-effective manner, a utility should develop a performance monitoring system. The monitoring system should record both the operation performance and costs of the FGD system. The New York State Electric & Gas Corporation (NYSEG) in cooperation with Consolidation Coal Company, R&D, developed a data base management system to monitor the performance of the Somerset Station. A description of the data base management system was discussed in an earlier paper (1). This report summarizes the results of data collection for the first three and one-half years of FGD operation.

The Somerset Station is a 643 MW utility power station located on the Lake Ontario shoreline about half way between Niagara Falls and Rochester, N.Y. The unit, which was declared commercial on August 17, 1984, is the first station in the NYSEG system to include an FGD system. The FGD unit is a wet limestone slurry process with natural oxidation. The station currently uses a nominal 2.5 wt% sulfur Northern West Virginia coal supplied by Consolidation Coal Company (Consol). The Somerset Station is also the host site for EPRI's High Sulfur Test Center (HSTC) which began operation in April 1987.

SOMERSET STATION PERFORMANCE AND FGD OPERATING COSTS

To provide its customers with low cost, reliable electrical service, NYSEG designed the Somerset Station for maximum plant availability. Furthermore, to help preserve the low costs and high availability, the NYSEG Performance & Fuel Engineering Department (P&FE) maintains a data base of monthly operating and performance parameters. Identifying deviations or trends in such operating information is an important management tool toward maintaining peak performance of the utility station.

SOMERSET STATION PERFORMANCE

The performance of both the Somerset Station power block and the FGD has exceeded NYSEG expectations. The Utility Data Institute rated Somerset Station the 14th most efficient unit in the nation in 1985 and 20th in 1986 (2,3). Net Heat Rates for these years were 9,473 and 9,518 Btu/kWh, respectively (refer to Table 1). The Somerset Station was the highest rated station which included an FGD system. The average monthly availability from startup through June 1988 was 93.7%, which includes a total of 44 days of scheduled outages for normal inspections and maintenance during three separate outages. For this same period, the Net Heat Rate averaged 9,449 Btu/kWh while the capacity factor averaged 80.0%.

SOMERSET FGD PERFORMANCE

FGD system performance at Somerset has also been exceptional with essentially 100% availability to date. The FGD system has never caused a unit load reduction to maintain environmental compliance. NYSEG feels that the success of the FGD unit is a result of several factors:

1. A high level of primary equipment redundancy.
2. Full time FGD superintendent and instrumentation and control technician supervisor.
3. Stringent cleaning, inspection and maintenance programs.
4. Constant re-evaluation of operating parameters to maintain the best balance of efficiency and economy.
5. Dedication to a preventive maintenance program and quick maintenance response.
6. Continuous monitoring of process operating parameters and operating costs by the operating department.

The FGD system was designed for a coal with a sulfur content ranging from 1.0 to 3.6 wt%. The Somerset Station has a typical 1979 NSPS PSD permit which requires 70 to 90% removal of the SO_2 in the boiler flue gas based on the fuel sulfur content. The permit also limits the maximum sulfur content of the coal burned to 3.5 lbs S/MMBtu. Typical coals purchased for the Somerset Station have contained 1.5 to 2.5 wt% sulfur. Burning these coals limits the SO_2 emissions to 0.6 lbs SO_2/MMBtu on a 30-day rolling average.

The emission results shown in Figure 1 illustrate that NYSEG's goal of compliance to environmental regulations is being met. The monthly average SO_2 emission for the 1985 to mid-1988 operating period has been 0.50 lb SO_2/MMBtu which corresponds to 87.6% SO_2 removal. To insure greater operator awareness and permit compliance, SO_2 emission calculations were added to the process computer program using input from SO_2 analyzers on the flue gas stream before and after the FGD system. The control board operator now has current, hourly, daily and 30-day average emission values continuously displayed on the control room computer CRT screen.

The Somerset Station has normally burned a Northern West Virginia coal since the unit began commercial operation. The as-fired coal has averaged approximately 12,900 Btu/lb, 9.0% ash, and 2.5% sulfur. This analysis represents the actual coal fed to the boiler, including any coal used for test run purposes. The monthly as-fired coal composition has been very consistent (Figure 2). This helps to prevent large fluctuations in the amount of SO_2 sent to the FGD system.

The ash content of the coal burned at Somerset has proven to be an optimum compromise between the low ash coal preference of the boiler versus the high ash coal preference of the sludge stabilization process (1). Fly ash and lime are mixed with the FGD sludge to achieve the desired permeability and compression strength of the stabilized product which is landfilled. Based on a nominal 85% ash carryover from the boiler, the flyash-to-filter cake ratio (FA/FC) available from the as-fired coal has been 0.79 lb/lb at the required SO_2 removal rate for SO_2 permit compliance. This is sufficient ash to achieve satisfactory product characteristics for disposal.

SOMERSET FGD O&M COSTS

The FGD operating department utilizes a Lotus 1-2-3® spreadsheet program on a personal computer to tabulate monthly station summary data, O&M costs, as-fired coal analysis and FGD lab results. In addition to data consolidation, various performance ratios can be calculated to aid in an analysis of the operating and maintenance cost information for the FGD system. Table 2 is a summary of the information developed from the annual O&M spreadsheets for 1985 to June 1988. The O&M spreadsheets are circulated monthly for internal reporting and to P&FE for incorporation into the overall Somerset Station data base.

Using the data in Table 2, the average annual operating and maintenance costs can be calculated.

Calculated Average Annual FGD Costs

Operating Cost	
FGD Supervision and Engineering	$ 373,700
Lime and Limestone	2,586,200
FGD Labor and Miscellaneous Materials	863,700
Sludge Landfilling	787,600
Power	1,153,800
Subtotal	$5,765,000

Maintenance Cost

FGD Supervision and Engineering	$ 177,200
FGD Equipment	747,800
Limestone Handling and Storage	40,200
Limestone Preparation System	45,000
Solid Waste and Sludge	253,900
Subtotal	1,264,100
Total O&M Cost	$7,029,100

A graph of the monthly maintenance and operating costs is shown as Figure 3. Although the monthly costs appear to fluctuate widely over the three and one-half year span of the graph, the annual costs (Table 2) vary only slightly from the average costs (above). For the foreseeable future, the Somerset Station personnel expect the FGD costs to remain at the current average level.

The spreadsheet program also calculates the O&M costs in terms of dollars per ton of SO_2 removed and mills/kWh as shown in Table 2. To date, the O&M costs have averaged $95.65/ton of SO_2 removed or 1.51 mills/kWh. Of these costs, the largest item is for lime and limestone (approximately 37%). Power is about 16% of the O&M costs. Monthly O&M costs expressed in $/ton SO_2 removed and mills/kWh are shown in Figures 4 and 5, respectively.

The FGD power, excluding any associated ID fan power due to the FGD system, is measured and reported monthly on the O&M spreadsheet. We have included, however, the incremental fan power in the power costs shown above and in Table 2. At full load, the FGD system (with incremental fan pressure drop) consumes approximately 7.2 MW, which represents about 1.1% of the station net generating capacity. Since the FGD was designed without flue gas reheat, steam costs for this purpose are not incurred.

A total of 34 operating, instrumentation, maintenance and laboratory personnel are currently dedicated to the FGD system. The personnel breakdown is:

FGD Operations	No. Assigned
FGD Superintendent	1
Shift Supervisors	5
Scrubber Operators	6
Sludge Operators	4
Equipment Operators	4
Laborers	8
Subtotal	28
Maintenance Staff	
Instrument and Control Supervisors	1
Instrument Technicians	4
Subtotal	5
Lab Technicians	1
Total	34

Approximately 250 mechanical and 30 electrical maintenance man-hours are required weekly to support the FGD and sludge fixation operations. However, no mechanical and electrical maintenance personnel are dedicated to the FGD system.

PREDICTED CAPITAL AND O&M COSTS USING THE EPRI CS-3696 METHOD

The total installed capital cost for the Somerset Station FGD system including landfill is about $152.5 MM or $237/KW. This cost, which is for a conservatively designed system, compares within approximately 8% of the predicted cost of $221/KW based on the EPRI CS-3696 Simplified Retrofit Estimating Procedure (4, 5). The EPRI predicted costs are exclusive of preproduction cost and inventory capital.

To compare capital costs, the EPRI estimate was adjusted for the scope and characteristics of the Somerset Station. Since the Somerset Station is a "green field" construction, retrofit factors of 1.0 were assumed for soils, site accessibility and congestion, underground obstruction and duct length. Since inflation was very low during the plant construction period, the EPRI escalation adjustment was not used. An escalation adjustment of 1.024 was assumed based on the Chemical Engineering (CE) plant cost index between December 1982 (EPRI base period) and August 1984 (plant start-up). If standard EPRI escalation factors were used, the predicted capital costs for Somerset would have been higher. Adjustments to the EPRI procedure were made in the SO_2 Removal and Flue Gas Handling sections to accommodate the Somerset Station sparing philosophy of six absorber trains (four operating, two spares) versus the EPRI assumption of four absorber trains (three operating, one spare) and the no reheat design of Somerset.

Although the actual and predicted capital costs agree closely, the actual O&M costs are much lower than predicted. Over the first three and one-half years of Somerset Station operation, the average yearly total O&M costs ranged from 1.42 to 1.58 mills/kWh. These costs are low compared with the EPRI predicted first year O&M costs of 3.08 to 3.84 mills/kWh. The predicted costs shown in Table 3 were also calculated using the EPRI Simplified Retrofit Cost Estimate procedure. The first column shows the expected costs based on EPRI cost assumptions for labor, lime, limestone, power and waste disposal. Adjustments were made for plant capacity factor and coal sulfur content.

To obtain a more common basis between the EPRI calculation procedure and actual costs, the variable costs shown in the second column of Table 3 are based on the 1985 unit costs for the Somerset Station. EPRI labor rates were again used, but the 35% overhead burden was eliminated since the Somerset Station data base costs are reported unburdened. Although reduced somewhat, these adjusted EPRI predicted costs are still much higher than the actual costs incurred at Somerset.

The low O&M costs at Somerset are attributable to the following factors. First, maintenance costs have been very low, because of the quality of the original plant design and the dedication of the plant operations personnel to maintain peak performance from the unit. Also, the equipment is still relatively new, with some costs being covered by warranty. Second, power costs are less than for most conventional limestone scrubbers because the absorber section was designed for low pressure drop (4.8 in. w.c.) and reheat is not used. The third factor which significantly impacts the O&M costs is coal quality. The use of a moderate ash content, high Btu coal versus the use of the EPRI design coal reduced power demand for limestone grinding, limestone slurry circulation and sludge handling. Additionally, the coal quality favorably impacts costs by reducing the consumption of limestone and fixation lime and reducing the quantity of sludge for disposal.

FGD EQUIPMENT AND PROCESS IMPROVEMENTS

FGD EQUIPMENT RELIABILITY IMPROVEMENTS

Efforts to improve the FGD process mechanical equipment reliability have been focused on the corrosive and erosive nature of the liquid or gaseous process streams. The operating and maintenance departments at Somerset have both played an active role in analyzing equipment failures. The goal has been to obtain long-term least-cost solutions for problems. Initial cost versus operating and maintenance costs are calculated for each case. Preventive maintenance procedures are constantly being developed and revised as operating experience is gained. The goal of the preventive maintenance program is to insure that wear components are repaired and replaced before permanent damage of the equipment results or operational difficulties are incurred. A common goal for equipment selection has been solutions which provide a minimum five year life.

A listing of major equipment modifications is summarized as follows:

1. Corrosion and degradation of absorber and ductwork materials. The lower sections of the absorber linings have been successfully changed from Ceilcote Flakeline 103 to Ceilcote 2500AR. This cost was covered by warranty. Since the Somerset Station has two spare absorber modules, the work was easily done without affecting the FGD operation. Several linings and Hastelloy metal clads are still being evaluated for a blistering problem in the absorber outlet ductwork.

2. Erosion problems caused by the coarse limestone grind (63% minus 325 mesh). Changes in the materials of construction of the pumps and piping in the entire limestone slurry system have been required to withstand the erosive characteristics of the slurry. The slurry pump impellers and throat bushings have been successfully changed to hi-chrome or Ni-Hard materials in lieu of rubber lining. Ceramic liners were found to be acceptable for the ball mill classifier overflow piping and in the absorber hydroclones. Concrete-lined carbon steel piping is being evaluated for the limestone reagent transfer lines.

3. Sludge fixation system problems. The oversized ash rotary valves which prevented adequate control of the flyash-to-filter cake ratio were replaced with smaller valves. Preshrunk filtercloth for the rotary drum filters extended the cloth life by a factor of four and reduced significantly the expense of reclothing.

FGD PROCESS RELIABILITY IMPROVEMENTS

In a continuing effort to find ways to cut O&M costs, NYSEG personnel constantly evaluate FGD operating guidelines and other process variables in light of day-to-day operating problems. Maintaining a scale-free process system and reducing the waste water discharge have been the most significant process challenges experienced to date.

Sodium Thiosulfate Usage

Beginning with the October 1985 station outage, significant amounts of gypsum scale were found in the thickeners and the entire supernate system. Based on tests by the Somerset Lab and other utility experience, a decision was made to chemically clean the system with sodium thiosulfate. After maintaining residual levels of approximately 1000 ppm in the supernate system for several weeks, essentially all scale was dissolved. Thiosulfate was used intermittently in 1986 while the benefits from its use were evaluated (6). Beginning in 1987, thiosulfate was used continuously.

Seven tons of thiosulfate are currently added each week to the limestone reagent tank. Thiosulfate costs are approximately $200,000 per year. The thiosulfate usage is based on maintaining residual levels of approximately 50 ppm in the supernate system and a gypsum relative saturation level below 1.0. The gypsum relative saturation is calculated weekly using the EPRI FGD liquid equilibrium computer program (FGDLIQEQ) with data from the Somerset lab.

The benefits from the use of thiosulfate have been:

- Elimination of the gypsum scale which extended the absorber run time from 6 weeks to 20 weeks between cleanings and reduced maintenance on the magnetic flow meters and control valves by 90%.
- Improvement in the solids settling rate in the thickeners and dewatering properties of the FGD sludge.

Mist Eliminator Improvements

Although the use of thiosulfate has also reduced mist eliminator plugging, two other improvements in the mist eliminator section have been made. After evaluating several alternate designs, the first change was to switch to different mist eliminator panels in one absorber. The mist eliminator chosen was an enhanced design supplied by the FGD vendor. The new panels allowed better on-line and off-line cleaning and were more durable than the original design. These new mist eliminator panels will be installed in the remaining absorbers over the next two years.

The second change was an upgrade of the mist eliminator wash system in one absorber based on work sponsored by EPRI at other FGD sites (7). The new system doubled the number of wash nozzles, switched from a 120° to a 90° spray nozzle, doubled the wash water flow rates during washing, but decreased the time spent washing the mist eliminators. The new system provides better mist eliminator cleaning while cutting the fresh water usage by about 50 percent. Upgrading the remaining absorbers with the new mist eliminator wash system is now budgeted for 1990.

Overall Water Balance

A major process problem was finding ways to balance the overall station water usage to achieve zero flow discharge. Various miscellaneous FGD wash water streams were converted to use process water or supernate. Trench wash water, which eliminates solids build-up in the absorber blowdown trenches, was also converted to use supernate. A 3/4 inch orifice was installed in each absorber drain line to allow continuous blowdown of the absorbers. This, in combination with normal overflow, was shown to produce a sludge with better settling and filtering characteristics. To reduce further the station raw water requirements, the absorber slurry circulation pump seal water was switched to treated waste water from the station waste water treatment plant.

With these changes and a steady load, the station has experienced no waste water discharge for several months. When the mist eliminator wash system revisions discussed earlier are completed, reliable maintenance of station water balance should not be a problem. Then, new water balance studies can begin to determine the optimum raw water addition points in the FGD system and perhaps reduce the need for thiosulfate addition.

Future Process Improvements

NYSEG is pursuing several additional process changes to reduce Somerset FGD O&M costs. In-situ production of thiosulfate in the absorbers from the addition of an emulsified sulfur solution has been studied and proven feasible by EPRI at several FGD sites. NYSEG is applying to their Public Service Commission for permission to implement a sulfur addition project at the Somerset Station. The project should begin before the end of the year. The in-situ production of thiosulfate should reduce the cost of thiosulfate addition to less than $50,000 per year.

A proposed project under consideration involves the production of wallboard grade gypsum. The economic production and sale of wallboard grade gypsum is quite site-specific because the FGD must be located near an adequate market to minimize the transportation costs. Although a significant capital investment would be required to convert the FGD to forced oxidation, sale of the gypsum would also open the possibility for sale of the flyash and the elimination of stabilization and landfilling costs. The first phase of this project will be investigating design optimization of gypsum production in FGD systems. NYSEG plans to pursue this project over the next few years with the assistance of other interested parties.

NYSEG has taken advantage of the ongoing research work sponsored by EPRI in their continuing efforts to improve the FGD reliability and reduce operating costs. The reports on corrosion and additives research have been very timely in providing needed information for NYSEG in-house improvement projects.

INDUSTRY NEEDS OF FUTURE FGD SYSTEMS

The NYSEG Somerset Station is an excellent example of current FGD technology. It documents that the costs of FGD operation can be lower than predicted and demonstrates that high reliability can be achieved. Future FGD units must have these same characteristics along with reduced capital cost. To achieve a capital cost reduction, the reliability of FGD equipment must be demonstrated so that expensive spare equipment can be minimized or even eliminated.

Several "advanced" FGD processes have been operated commercially in Europe and Japan without spare absorbers. Most of these FGD installations have achieved near 100% availability while producing a salable gypsum by-product for wallboard use. The commercial viability of the "advanced" FGD processes needs to be demonstrated in the U.S. utility environment while scrubbing flue gas from U.S. high-sulfur coals.

Alternate uses and markets must be developed to utilize the FGD solid by-products which are currently being treated as waste. This ambitious goal can only be achieved in the near future by a close cooperation among the interested parties including utilities, EPRI, solid-waste marketers, coal companies, FGD vendors, and government agencies.

REFERENCES

1. Rogers, W. A., Koch, B. J., McCoy, D. C., Smith, D. B., and Crosby, H. L. FGD data base management system. Paper presented at Coal Technology '86, Pittsburgh, November 19, 1986.

2. Electric Light and Power, 64: No. 12, p. 3, December 1986

3. Electric Light and Power, 66: No. 1, p. 24, January 1988.

4. Shattuck, D.M. et al. Retrofit FGD cost-estimating guidelines. EPRI CS-3696. Research Project 1610-1. Final Report. Electric Power Research Institute, Palo Alto, California, 1984.

5. Keeth, R.J., Miranda, J.E., Reisdorf, J.B., and Scheck, R.W. Economic evaluation of FGD systems. EPRI CS-3342, Vol. 1, Research Project 1610-1. Final Report. Electric Power Research Institute, Palo Alto, California, 1983.

6. Jones, A. F. and Colley, J. D. NYSEG Somerset Station FGD system optimization. Radian Report to NYSEG. Work co-funded by NYSEG and EPRI Research Project 2248-1, FGD Chemical Process Problem Study, 1987.

7. Jones, A. F. and Colley, J. D. Recommendations for mist eliminator wash modifications. Radian Report to NYSEG. Work co-funded by NYSEG and EPRI Research Project 1877-1, FGD Reagent Preparation, 1986.

The work described in this paper was not funded by the U.S. Environmental Protection Agency and therefore the contents do not necessarily reflect the views of the Agency and no official endorsement should be inferred.

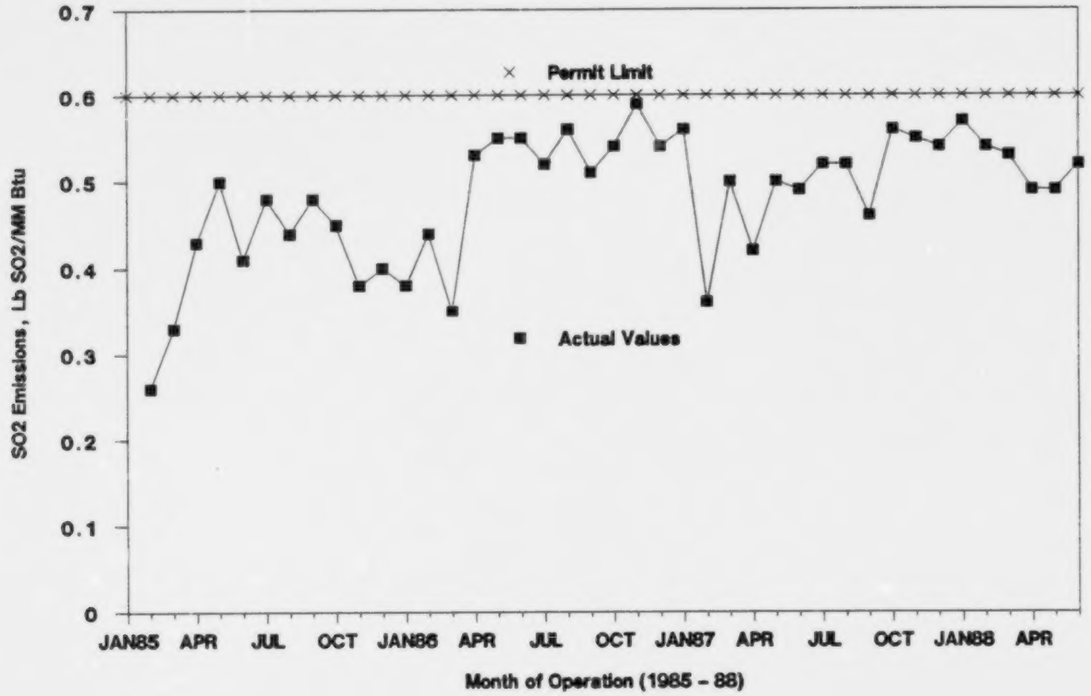

FIGURE 1. FGD MONTHLY SO2 EMISSIONS
NYSEG SOMERSET STATION

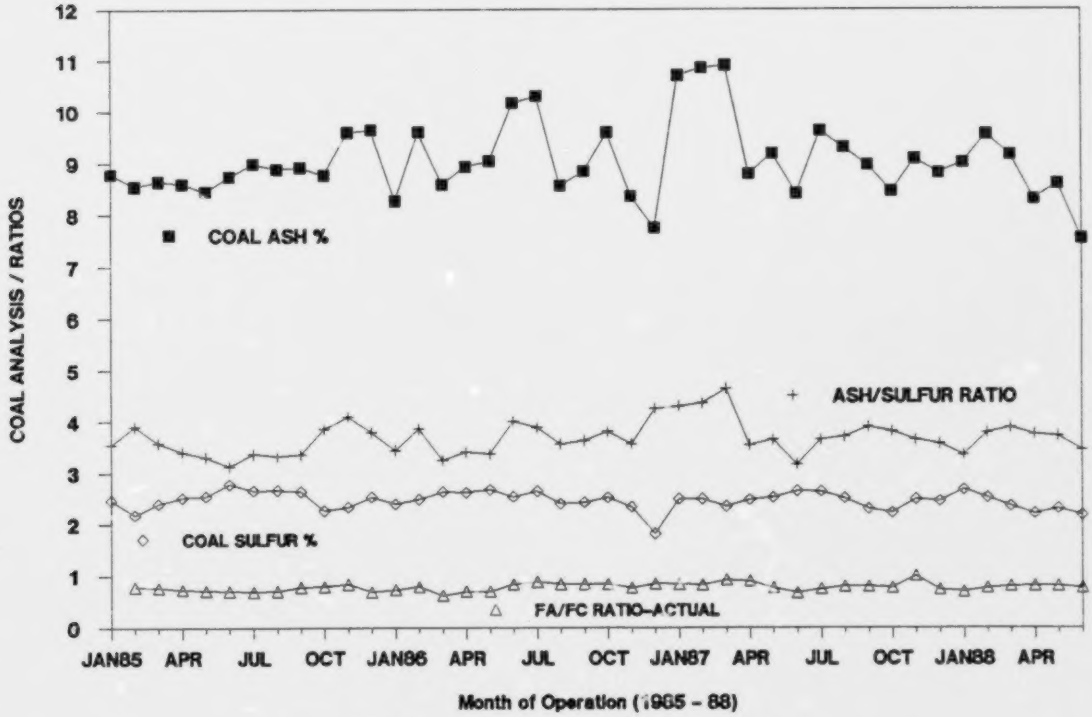

FIGURE 2. NYSEG COAL ANALYSIS / RATIOS
(based on as-burned coal analysis)

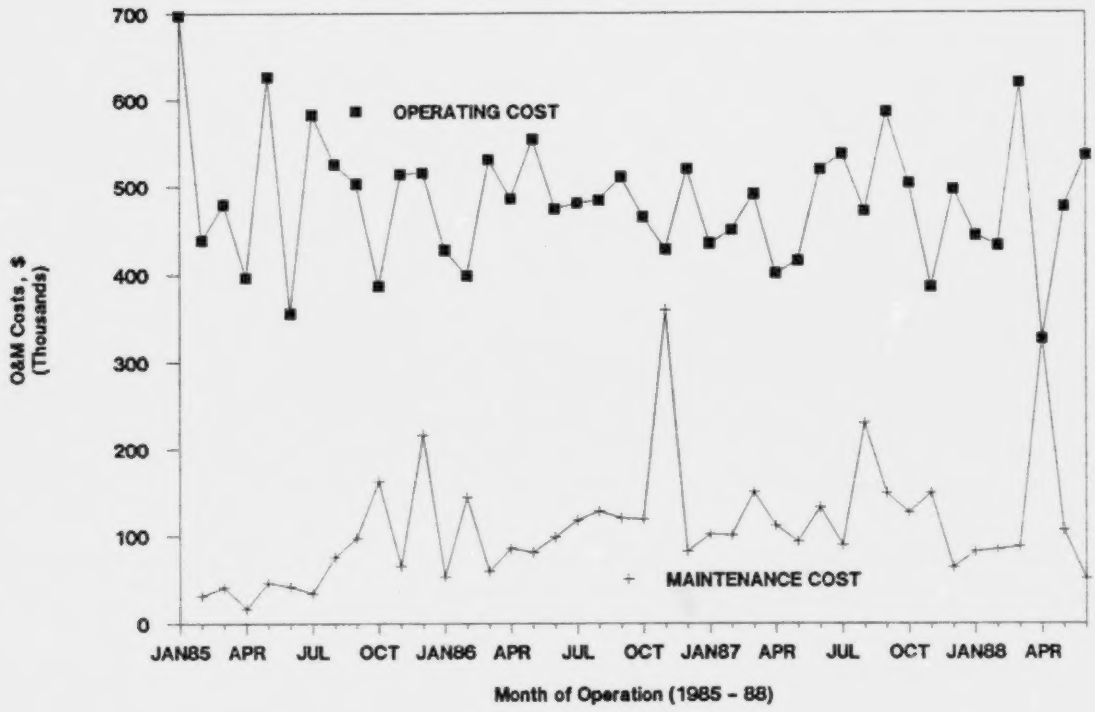

FIGURE 3. FGD MONTHLY O&M COSTS
NYSEG SOMERSET STATION

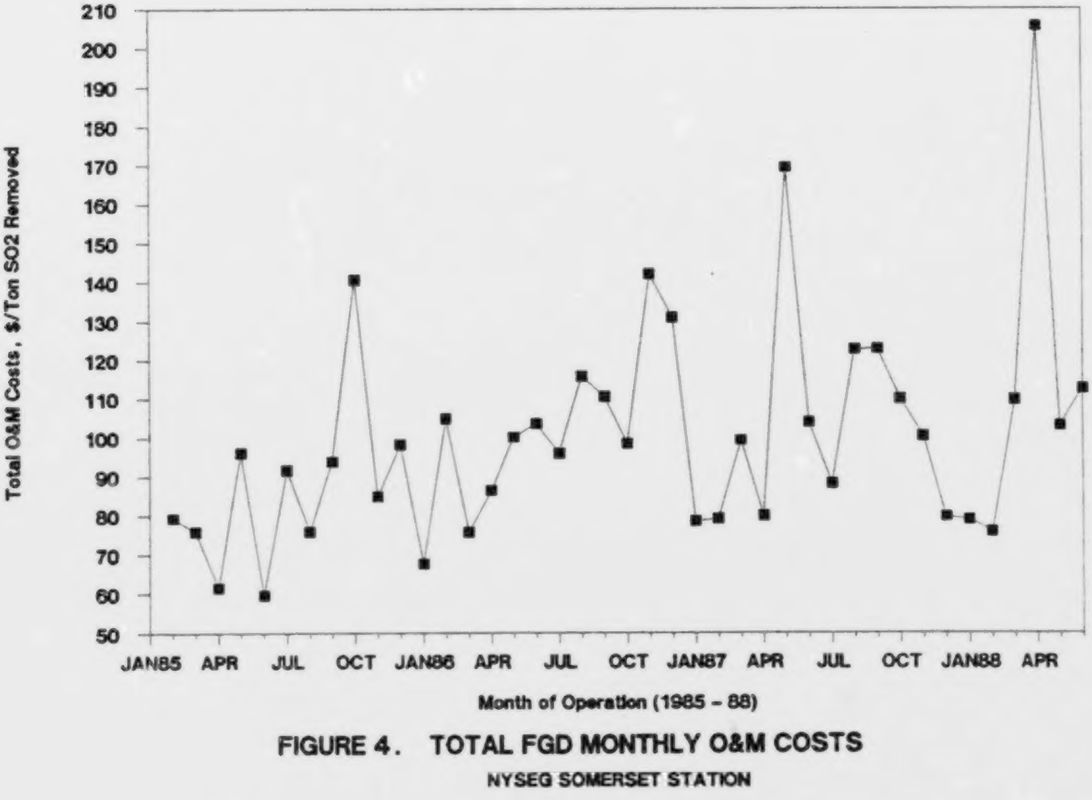

FIGURE 4. TOTAL FGD MONTHLY O&M COSTS
NYSEG SOMERSET STATION

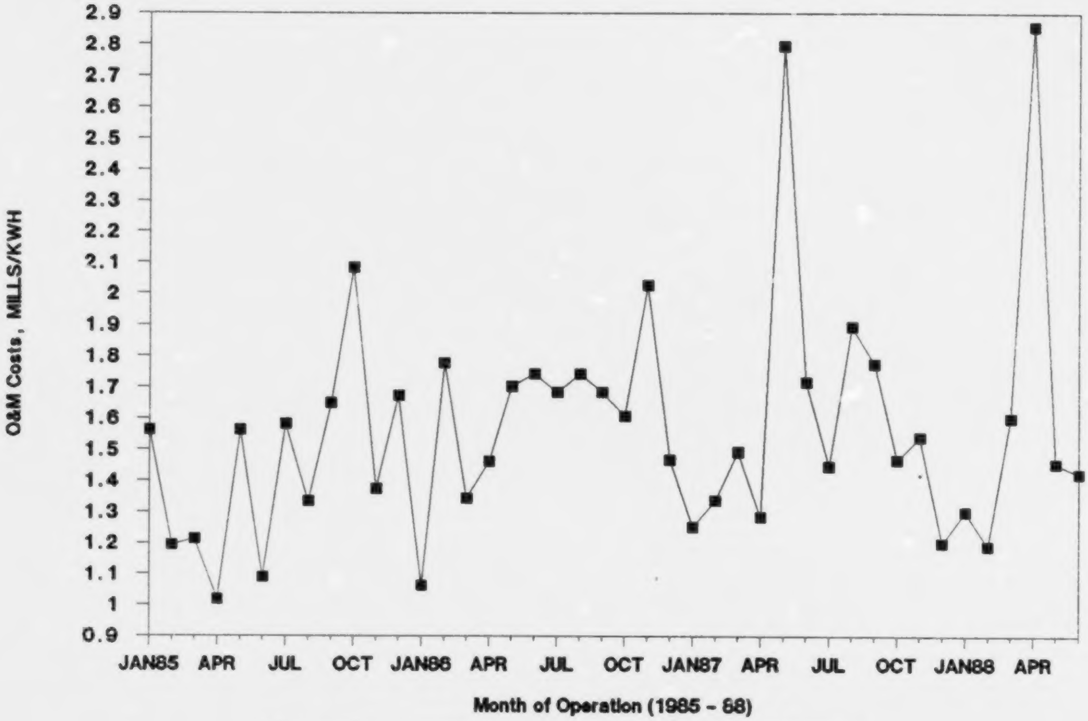

FIGURE 5. TOTAL FGD MONTHLY O&M COSTS

NYSEG SOMERSET STATION

TABLE 1. STATION & FGD SUMMARY DATA
NYSEG SOMERSET STATION

AVERAGE MONTHLY VALUES

	1985	1986	1987	1988 Thru June	1985-88
STATION SUMMARY DATA					
Gross Generation MWH	418,829	401,212	414,246	409,033	411,087
Station Service MWH	24,145	23,229	23,239	22,072	23,328
Station Service %	5.765	5.790	5.610	5.396	5.675
Net Generation MWH	394,684	377,983	391,006	386,960	387,758
Availability %	92.70	96.74	92.63	91.62	93.68
Capacity Factor %	82.45	78.22	80.50	77.88	80.02
Net Heat Rate Btu/KWH	9,473	9,518	9,416	9,331	9,449
Emissions NOx lb/MBtu	0.54	0.48	0.51	0.48	0.50
FGD Inlet Conc SO2 lb/MBtu	4.56	4.16	3.53	3.59	4.00
FGD SO2 Removal %	90.68	87.64	85.84	85.40	87.60
Emissions SO2 lb/MBtu *	0.42	0.51	0.50	0.52	0.50
COAL ANALYSIS (AS-FIRED)					
Ash %	8.90	8.96	9.46	8.75	9.06
HHV Btu/lb	12,873	12,901	12,776	12,969	12,869
Sulfur %	2.51	2.46	2.46	2.39	2.46
FGD LAB RESULTS					
Ca/S Ratio (Measured)	NA	NA	1.13	1.16	1.14
% Sldg Oxidation	NA	17.58	17.91	16.88	17.57
Supernate Values					
Thiosulfate, ppm	--	--	67	27	48
Chlorides, ppm	NA	NA	8,629	9,071	8,833
Rel. Gypsum Sat.	NA	NA	0.93	0.93	0.93
LS Grind, % > 325 Mesh	NA	NA	37.04	36.28	36.66
MAT'L USED,Tons					
Lime	708	600	639	640	648
Limestone	11,529	11,430	11,820	10,825	11,483
Coal	144,783	139,160	143,834	138,890	142,064
SLUDGE VOLUME cu yds	38,437	34,624	34,850	30,525	35,193
FGD PROCESS CALCULATIONS +					
Coal S lb/MBtu	1.95	1.90	1.93	1.84	1.92
Req'd SO2 Removal %	84.60	84.25	84.44	83.73	84.34
Ca/S Ratio (Calculated)	1.08	1.17	1.20	1.17	1.15
FA/FC Ratio-Actual	0.77	0.75	0.79	0.77	0.76
FA/FC @ Req'd SO2 Removal	0.82	0.78	0.80	0.78	0.79

* Emissions based on 30 day running average on last day of month.
+ Based on as-fired coal analysis.

TABLE 2. FGD O&M COST
NYSEG SOMERSET STATION

	1985 TOTAL	1986 TOTAL	1987 TOTAL	1988 Jan. thru June	1985-88 Monthly Ave.
OPER COST, $					
SUPERV & ENG	234,047	400,202	447,807	225,775	31,139
LIME & LIMSTN	3,049,957	2,433,660	2,406,131	1,161,818	215,513
FGD PLANT - OPER. & MISC.	698,090	864,776	961,290	498,705	71,973
SLUDGE REMOVAL	828,659	899,135	674,884	353,984	65,635
POWER COST (EST) *	1,188,881	1,127,887	1,160,763	561,492	96,153
Sub Total	5,999,634	5,725,660	5,650,875	2,801,774	480,413
MAINT COST, $					
SUPERV & ENG	86,058	176,519	221,910	135,770	14,768
FGD EQUIP	413,545	870,610	886,266	447,026	62,320
LS HNDLG & STG	50,097	47,828	26,825	16,130	3,354
LS PREP SYSTEM	37,665	62,436	42,782	14,539	3,748
SLUDGE WASTE PLANT	143,251	292,401	323,417	129,498	21,156
Sub Total	730,616	1,449,794	1,501,200	742,963	105,346
TOTAL O&M COST	$6,730,250	$7,175,454	$7,152,075	$3,544,737	585,759
FGD AVERAGE REAGENT COST					
LIME, $/Ton	73.55	56.06	58.83	61.38	63.05
LIMESTONE (TOTAL), $/Ton	17.51	14.78	13.77	14.23	15.19
FGD O&M COST CALCULATIONS					
FGD O&M COST, mills/KWH	1.42	1.58	1.52	1.53	1.51
FGD O&M COST, $/Ton SO2	85.24	99.89	98.19	104.24	95.65

* Power cost calculation based on 7.2 MW required by the FGD at full load. Includes any related FGD ID fan power costs at 22.9 mills/KWH.

TABLE 3. PREDICTED AND ACTUAL FIRST YEAR O&M COSTS COMPARISON
SOMERSET STATION
1985

		Predicted Costs, $/kW-Year	
Fixed Costs		EPRI Basis*	Adjusted[+]
Operating Labor		1.38	1.02
Maintenance Labor		2.75	2.04
Maintenance Material		4.22	4.22
Administration and Support Labor		1.29	0.96
	Subtotal	9.64	8.24
Variable Operating Costs			
Lime		1.40	1.72
Limestone		4.44	5.55
Power (excluding ESP)		7.82	3.98
Waste Disposal		5.02	3.23
	Subtotal	18.68	14.48
	Total	28.32	22.72
Predicted O&M, mills/kWh[#]		3.84	3.08
Actual O&M, mills/kWh[#]		1.42	

BASIS: As-fired coal sulfur 2.51%, 90.68% SO_2 removal, 82.45% plant capacity factor, 1.0275 escalation adjustment (December 1982 to June 1985).

* EPRI Cost Basis: $60/ton lime, $14/ton limestone, $4.80/ton dry waste disposal charge, 45 mills/kWh.

[+] Adjusted for the 1985 Somerset Station operating charges: $73.55/ton lime, $17.51/ton limestone, $3.09/ton dry waste disposal charge, 22.9 mills/kWh, labor ex. 35% burden.

[#] For a yearly net generation of 4,736,214 MW.

FGD RELIABILITY IMPROVEMENT AT LG&E:
CANE RUN 6 CASE STUDY AND OVERALL PROJECT STATUS

by: Carl V. Weilert and Daniel A. Froelich
Burns & McDonnell Engineering Company
Kansas City, Missouri 64130

Mark A. Schmitt and Michael L. McInnis
Louisville Gas & Electric Company
Louisville, Kentucky 40232

ABSTRACT

This paper has been written in two parts. Both parts present information on results of the Sulfur Dioxide Removal Systems (SDRS) Renovation Program recently completed by LG&E. The five-year renovation program included upgrades of sulfur dioxide removal systems for seven coal-fired boilers at two generating stations. The goal of the project was to improve SDRS operability to 90 percent while reducing O&M costs.

Part I presents a case study of the SDRS renovation at Cane Run 6, a 260-MW unit which had been retrofitted with a dual alkali SDRS in 1979. The paper describes the problems which had resulted in reduced operability and high O&M costs, the process changes and modifications made, and the effect of those modifications on SDRS operability and O&M costs.

Part II presents a summary of the overall results of LG&E's SDRS Renovation Program with regard to system-wide SDRS operability and O&M costs.

PART I: CANE RUN 6 CASE STUDY

INTRODUCTION

In mid-1983 Louisville Gas & Electric retained Burns & McDonnell to perform engineering services for the renovation of all seven of its operating SDRS units. This paper presents, as a case study, the results of the renovation program for the Cane Run 6 dual alkali SDRS. It includes a description of the problems which had resulted in reduced SDRS operability, the process and equipment modifications made to resolve those problems and the effect of the modifications on system operability and performance parameters.

BACKGROUND

The sulfur dioxide removal system (SDRS) for Louisville Gas & Electric's Cane Run Unit 6 was designed in the late 1970s as part of EPA's full-scale demonstration of the dual alkali SO_2 removal process (1). The SDRS was installed as a retrofit to the 260-MW unit and began operation in 1979. Table 1 provides information on the original system design and equipment configuration. The flow diagram in Figure 1 represents the complete Cane Run 6 SDRS process as it existed prior to the modifications discussed in this paper.

For the EPA's one-year demonstration period (May 1980-May 1981), during which system operation was closely monitored and controlled, the SDRS achieved 94 percent operability. However, a variety of problems with mechanical equipment and chemical and physical process control were already evident (2).

In the years following the completion of the demonstration period, the frequency and severity of equipment malfunctions and process upsets increased. This resulted in a decline in SDRS operability and an increase in operation and maintenance costs. Operability of the Cane Run 6 SDRS for the 12 months prior to the start of the renovation program (July 1982 through June 1983) was 67 percent.

PROBLEM DEFINITION

The goal of the SDRS renovation program was to achieve a minimum 90 percent SDRS operability while reducing excessive operating and maintenance costs. To obtain the maximum benefit from the renovation activities, records of unplanned Cane Run 6 SDRS outages were reviewed to determine the most frequently cited outage causes. The data reviewed for this purpose was the Generation Availability Data System (GADS) records for Cane Run 6 compiled by the North American Electric Reliability Council (NERC). This data was supplemented by information obtained during inspections of the SDRS and by interviews with plant operations and engineering personnel.

The following problem areas were identified as the sources of the majority of the unplanned SDRS outage hours.

- Pluggage and scaling of the absorber sieve trays.
- Piping failures, especially in the absorber bleed piping.
- Inadequate thickener performance, including low underflow density and excessive levels of suspended solids in the overflow. (When the solids inventory in the thickener became excessive, SDRS outages were necessary to prevent further overloading of the system.)
- Inadequate vacuum filter performance, including excessive filter cake moisture and low cake production rates. (Inability of the vacuum filters to keep up with the rate of SO_2 removal and sludge production necessitated SDRS outages.)
- Mechanical problems with the oil-fired flue gas reheaters.

Several of these leading causes of SDRS downtime also contributed to excessive operating costs. The annual fuel costs alone for the oil-fired reheaters approached $1.0 million. The pluggage of the sieve trays caused the tray differential pressure to run up to two times the design value, effectively imposing various load limitations on the Cane Run Unit 6 boiler. The excessive moisture content in the filter cake caused soda ash consumption to be significantly above the original contract guarantee. Even under the closely monitored one year demonstration period soda ash usage was nearly 60 percent above the guarantee value, due mainly to the inability of the filters to produce design cake quality.

INVESTIGATIVE STUDIES

Burns & McDonnell worked closely with LG&E staff engineers and plant personnel to obtain the information needed to determine the root causes of the various problems and to identify and evaluate potential solutions. In some cases specialized studies were conducted.

Previous evaluations of process problems at Cane Run 6 and other dual alkali systems indicated that subtle changes in the system chemistry and regeneration reactor dynamics might be affecting performance of the thickener and vacuum filters and contributing to sieve tray pluggage. To investigate these interactions, consultants from P.S. Lowell & Company and CODAN Associates were retained to conduct field tests, laboratory studies and computerized process simulations. Lowell & Company also performed sieve tray differential pressure modeling.

Economic evaluation of alternatives to the continued use of the oil-fired reheaters showed that conversion to wet stack operation would be cost effective. Dynatech R/D Company was contracted to perform two-phase flow modeling of the outlet ductwork and stack to identify the potential for droplet entrainment and the countermeasures needed to minimize droplet formation and subsequent fallout.

Based on the results of on-site inspections and testing, review of operating data and maintenance records, consultation with plant personnel and consideration of the recommendations of the specialized study consultants, the project team formulated alternative solutions to each of the previously defined problems. The alternatives were then evaluated with regard to capital cost, operating costs, requirements for system outages during installation and potential for improvements in SDRS operability. Preferred alternatives were selected and submitted to LG&E for approval.

SYSTEM MODIFICATIONS

The process changes and equipment modifications made to the Cane Run 6 SDRS during the renovation project are summarized below. Additional detail is provided to explain the rationale for the process changes. The flow diagram in Figure 2 shows the system as modified.

Reheaters and Stack

The oil-fired reheaters were eliminated and the system was converted to wet-stack operation. The existing carbon steel chimney liner and breeching were lined with Alloy C-276 sheet for protection against corrosion in the severe environment created by the mixture of scrubbed and unscrubbed flue gases. The absorber module outlet ducts upstream of the former reheat addition point, which had been flake-glass lined, were lined with 317L stainless sheet. A stack flush system was installed to remove accumulated ash and condensate and keep the stack drain line clean.

Flue Gas Dampers

The original inlet, outlet and bypass dampers were replaced with new dampers. The new inlet and outlet guillotine dampers are equipped with individual seal air systems to provide the capability for safely isolating one or both modules from the flue gas to allow on-line maintenance if needed.

Absorber Sieve Trays

All absorber sieve tray panels were replaced with new 317L stainless steel sieve trays. The new trays have the same open area as the original trays, but the diameter of the perforations is now 5/8 inch. The original trays had perforations which were 3/16 inch and 13/64 inch, respectively, for the top and bottom levels. The larger perforations in the new trays were designed to minimize the possibility for, and the effects of, pluggage with scale or flyash carryover.

Thickener

The recirculation loop on the thickener underflow piping system was eliminated to minimize the physical degradation of the sludge particles due to repeated recirculation through the underflow pumps. The investigative studies proved that this phenomenon had been the leading cause of the poor performance of the thickener and vacuum filters which had plagued the SDRS since startup. To allow controlled withdrawal of sludge from the thickener, the original constant speed underflow pumps were replaced with smaller centrifugal pumps with variable frequency drives. The underflow piping was routed to newly created filter feed tanks described below.

Vacuum Filters

Although only very minor modifications were made to the vacuum filters themselves, the feed system was completely revised. The rotary lobe vacuum pumps were replaced with new liquid ring vacuum pumps to eliminate excessive maintenance requirements associated with the old pumps.

The new vacuum filter feed system was created by converting the original secondary regeneration reactor tanks to filter feed tanks. The investigative studies indicated that the secondary reactor tanks were not necessary for the regeneration process. New centrifugal filter feed pumps with variable frequency drives were added to provide for control of slurry feed rate to the vacuum filters.

The addition of the filter feed tanks to the process ensured that a consistent quality of feed slurry was supplied to the vacuum filters during their operation. The filter feed tanks benefited the thickener operation by eliminating the need to recirculate the sludge when the vacuum filters were not running, as was the case in the original process design. Both these factors support LG&E's preference for shift operation of the filters as opposed to the continuous operation on which the original process design was predicated.

Regeneration Reactors

As noted above, the regeneration reactor systems were revised to eliminate the secondary reactor tanks from the process. Investigative studies indicated that the secondary reactors added no net benefit to the process, since the additional reaction time was not necessary and the extra agitation time tended to cause degradation of the crystalline sludge particles. A new overflow trough was installed to route the primary reactor overflow directly to the thickener feedwell. This trough was fabricated from high density polyethylene pipe to minimize the problems of scale buildup which had occurred in the stainless steel overflow chute used in the original system design. The reactors were also provided with new low-shear agitators to minimize degradation of the sludge crystals.

Absorber Bleed Piping

Investigation of piping failure events revealed that the majority of the failures were caused, directly or indirectly, by cavitation and water hammer effects associated with excessive pressure drop across the bleed control valves. To solve this problem a riser loop equipped with a vacuum breaker at the high point of the loop was installed downstream of each bleed valve. The piping layout in the recycle pumphouses was completely redesigned to improve maintenance access. The original

FRP piping material was replaced with polypropylene-lined steel. Subsequent redesign of the riser loop has reduced the height of the loop and eliminated several fittings, thus aiding maintenance.

Ash Silo

The original mass flow hopper and ash screw feeder were replaced with a new conical, air-fluidized hopper and a variable speed rotary vane feeder. This design change was implemented to prevent recurrence of the uncontrollable floods of fly ash which had occurred periodically for years. These floods occurred when the silo became pressurized during pneumatic ash transfer into the silo while the screw feeder was operating and the ash level in the silo was low.

RESULTS

Schedule

The investigative study phase of the renovation for the Cane Run 6 SDRS was completed in March 1985. Design and procurement activities continued through the end of 1985. System modifications were completed during a boiler outage from September 1985 through February 1986. The extended outage was necessary due to the alloy cladding work on the stack liner. The modified SDRS resumed operation in March 1986.

Operability Improvement

The improved operability resulting from the SDRS renovation program at Cane Run 6 is displayed in Table 2. Data from the demonstration period and the last year before the renovation program began are included for comparison.

The operability of the Cane Run 6 SDRS since the renovation has contributed to help meet the overall program goal of 90 percent, and has been better than during the EPA's demonstration program when the entire system was new.

Performance Improvement

Prior to the renovation program the poor performance of the thickener and vacuum filters were the cause of numerous operating problems and much frustration for the operators of the Cane Run 6 SDRS. As a result of the renovation program the performance of this equipment is greatly improved. Before the renovation program it was frequently necessary to operate two vacuum filters to obtain the necessary cake production rate. Since the elimination of the thickener recirculation mode and the installation of the filter feed system, the normal mode of operation is to run only one vacuum filter. In addition to filtration rate, percent solids in the filter cake have also improved significantly as shown in Table 3. Again, the performance of the modified system represents a significant improvement over that experienced during the one year demonstration program by EPA on the original system.

Reductions in Operating and Maintenance Costs

At the outset of the SDRS renovation program some of the most frequent complaints regarding excessive operating and maintenance costs on the Cane Run 6 SDRS involved the oil-fired reheaters, the high absorber pressure drop and the soda ash consumption rate. The renovation program has succeeded in reducing costs significantly in all these areas. The oil-fired reheaters have been eliminated. The new sieve trays have been virtually free from pluggage and the soda ash consumption has been reduced.

With the use of perforations which are more than three times the diameter of those used in the original design, the new sieve trays have never become plugged with ash or scale. In fact, the ability of the new trays to remain clean has even allowed LG&E to discontinue the use of the under-tray spray headers. The elimination of pluggage on the sieve trays has provided the benefits of reduced maintenance (the new trays have not required cleaning) and reduced operating costs. The savings in operating cost is due to the reduced absorber pressure drop as shown in Figure 3. This reduced pressure drop has effectively eliminated the load limitation previously encountered with the original tray design.

The original contract guarantee for soda ash consumption by the Cane Run 6 SDRS was 0.045 moles Na_2CO_3 per mole of SO_2 removed. Although compliance with this guarantee could be achieved on a short-term basis, the long-term soda ash consumption during the EPA-sponsored one-year demonstration program was 0.071 moles Na_2CO_3 per mole SO_2 removed (2). Following the renovation program modifications the long-term soda ash consumption rate has decreased and is trending downward. Soda ash consumption for 1987 was 0.054 moles Na_2CO_3 per mole SO_2 removed. This reduction was achieved despite the switch to the single vacuum filter operating mode, which effectively cuts the wash ratio in half.

Ongoing Studies

LG&E and Burns & McDonnell are currently working to further optimize the Unit 6 SDRS process. The optimization study will concentrate on improving the control of lime feed to the reactors by determining the relationship among bleed flow, lime feed rate and reactor pH with the goal being further reductions in operation and maintenance costs. Inherent problems with pH probe scaling in the regeneration reactors have been alleviated somewhat by moving the pH control measurement point to the thickener feedwell. Evaluation of mechanical changes to the vacuum filters to improve cake wash efficiency is now underway.

PART II: OVERALL PROJECT STATUS

BACKGROUND

In 1973, Louisville Gas and Electric initiated an ambitious and capital intensive program to control the sulfur dioxide emissions from its electric generating units. The program was premised upon continued use of local, high-sulfur Kentucky coal. By 1982, seven (7) sulfur dioxide removal systems were in operation treating flue gas generated by 2178 megawatts of generating capacity. This represents all of LG&E's coal fired generation.

The original design for all seven units was performed during the early years of sulfur dioxide removal system (SDRS) technology. Many of the inherent problems of first generation technology were prevalent on these units. Major system problems included corrosion, abrasion, and plugging of absorber internals and piping systems. Mechanical difficulties were incurred with pumps, dampers, and valves. Original materials of construction were found to be inadequate and inappropriate given the application. Freezing problems were also prevalent. The instrumentation and controls were so overly complex that in many cases reliable SDRS operation was difficult to achieve. Additionally, each of these scrubbers was retrofitted to the existing generating station and built within existing space constraints.

During the early part of 1983, Louisville Gas & Electric implemented a renovation program to upgrade these mid-1970 vintage sulfur dioxide removal systems (SDRS) to current design standards. The goal of the project was to improve SDRS system operability to a minimum level of 90 percent while reducing excessive operating and maintenance expenses.

To achieve 90 percent SDRS operability (operability being the number of hours the SDRS is operating divided by the number of hours it is called upon to operate), the scope of the improvement program included all equipment from the ID fan outlet to the top of the chimney, all carbide lime (additive) handling systems, make-up water supply, process return water, and sludge thickening. Support systems evaluated included stack plume reheat, mist eliminator wash, slurry recirculation, thickeners, and instrument air. Electrical supply and control modifications were also an integral part of the program.

SUMMARY OF RESULTS

The SDRS Renovation Program was completed in June, 1988. All seven (7) units were substantially modified as demonstrated in Table 4. Results experienced to date indicate that the Renovation Program has successfully addressed both of our original project goals.

LG&E System SDRS operability from 1983 through mid 1988 is depicted in Figure 4. This data indicates a system wide improvement in operability of twenty-three percent (23%); with 1988 operability levels reaching eighty-six percent (86%). It's noteworthy that these operability levels have been achieved without the benefit of spare scrubbing capacity on any of the seven (7) units. While this data has been adjusted for outages precipitated by vendor reagent delivery problems, as well as sludge process plant problems, no effort has been made to reflect planned outages that were necessary to complete the renovation project. Identification and removal of these renovation outages would result in additional operability improvement. We anticipate further improvement in the future as a result of this years' conversion of the Mill Creek units to limestone (elimination of reagent delivery problems) and completion of the Renovation Program (elimination of lengthy renovation outages.)

Project operating and maintenance expense results are equally encouraging. Figure 5 delineates total operating and maintenance expenses attributable to the seven (7) SDRS's from 1983 through 1988. Operating and maintenance expenses have decreased from a high of \$136.41/ton SO_2 removal in 1985 to a low of \$112.27/ton SO_2 removal through mid 1988. It is important to note that this decrease has occurred despite a 48% increase in the lime reagent use and additional cost necessary to support the 23% operability increase described above. Figure 6 depicts only the maintenance expenses incurred from 1983 through mid 1988. This data, uninfluenced by increased lime consumption, more demonstrably illustrates the dramatic effect of the Renovation Program. Maintenance expenses peaked in 1984 at \$42.27/ton SO_2 removal and have been decreased to \$31.72/ton SO_2 removal in 1987. Further improvement is expected in 1988 with the completion of the project.

The most significant and beneficial aspect of the Louisville Gas and Electric SDRS Renovation Project is the effect on air quality in Jefferson County, Kentucky. Figure 7 illustrates the tons of sulfur dioxide that have been removed by LG&E's scrubbers from 1983-1988. As is readily apparent, the Renovation Project has resulted in a 48,000 ton per year decrease of sulfur dioxide emissions which represents a reduction of 36%. Due in large part to LG&E's SDRS Renovation Program, Jefferson County, Kentucky achieved attainment status for sulfur dioxide on August 11, 1986.

The work described in this paper was not funded by the U.S. Environmental Protection Agency and therefore the contents do not necessarily reflect the views of the Agency and no official endorsement should be inferred.

REFERENCES

1. VanNess, R. P., et al. Full-Scale Dual-Alkali Demonstration System at Louisville Gas & Electric Co. - Final Design and System Cost. EPA-600/7-79-221b, (NTIS: PB80-146715). U.S. Environmental Protection Agency, Washington, D.C., 1979.

2. VanNess, R. P., Woodland, L. R., and Gibson, E. D. Full-Scale Dual Alkali FGD Demonstration at Louisville Gas and Electric Company. EPA-600/7-83-039, (NTIS: PB83-241364). U.S. Environmental Protection Agency, Washington, D.C., 1983.

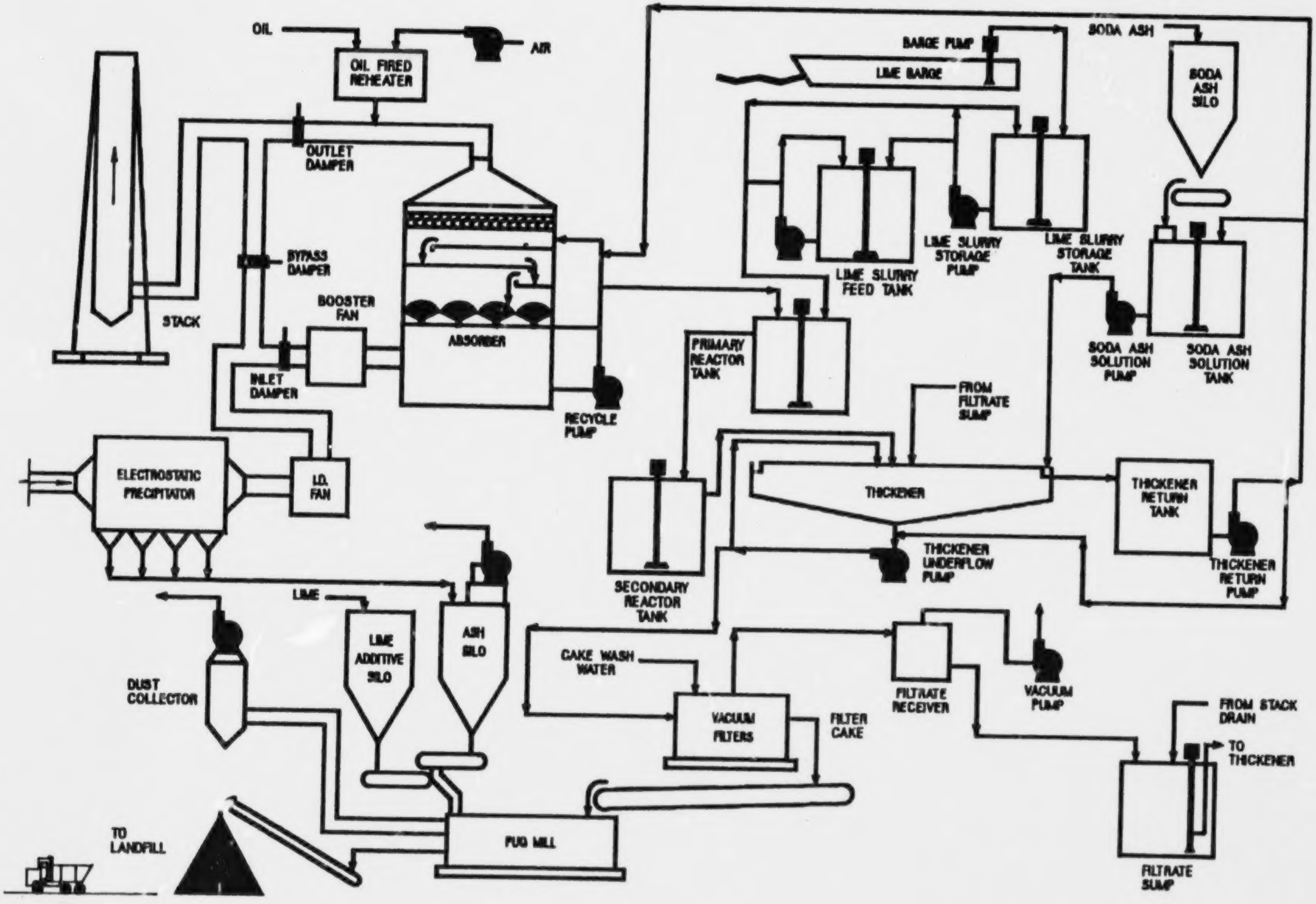
OIL
AIR
OIL FIRED REHEATER
OUTLET DAMPER
BYPASS DAMPER
STACK
BOOSTER FAN
ABSORBER
INLET DAMPER
RECYCLE PUMP
ELECTROSTATIC PRECIPITATOR
I.D. FAN
BARGE PUMP
LIME BARGE
SODA ASH
SODA ASH SILO
LIME SLURRY FEED TANK
LIME SLURRY STORAGE PUMP
LIME SLURRY STORAGE TANK
SODA ASH SOLUTION PUMP
SODA ASH SOLUTION TANK
PRIMARY REACTOR TANK
FROM FILTRATE SUMP
THICKENER
THICKENER RETURN TANK
SECONDARY REACTOR TANK
THICKENER UNDERFLOW PUMP
THICKENER RETURN PUMP
LIME
DUST COLLECTOR
LIME ADDITIVE SILO
ASH SILO
CAKE WASH WATER
VACUUM FILTERS
FILTER CAKE
FILTRATE RECEIVER
VACUUM PUMP
FROM STACK DRAIN
TO THICKENER
FILTRATE SUMP
TO LANDFILL
PUG MILL

Figure 1. Cane Run 6 SDRS flow diagram - original.

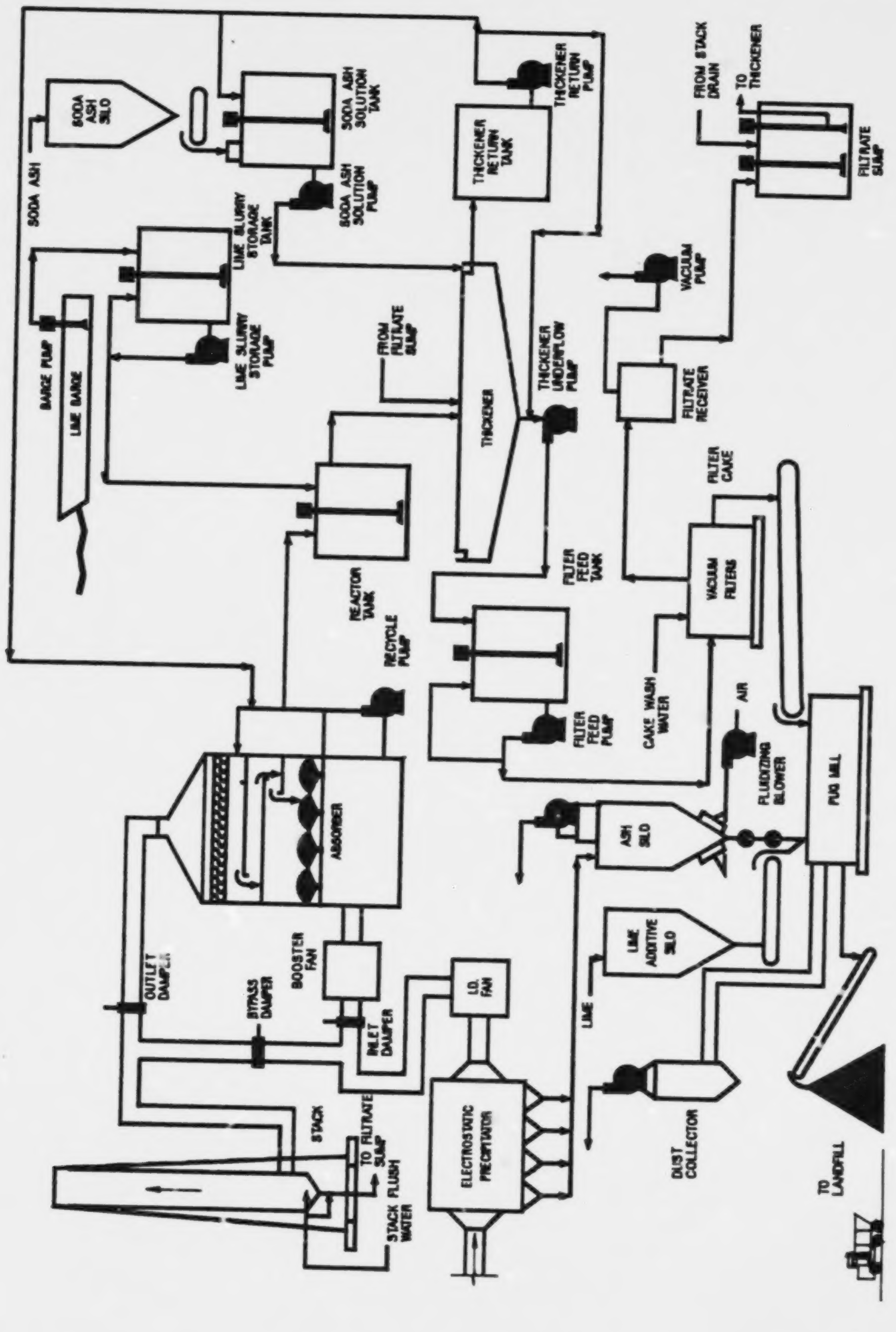
SODA ASH
SODA ASH SILO
SODA ASH SOLUTION TANK
SODA ASH SOLUTION PUMP
THICKENER RETURN TANK
THICKENER RETURN PUMP
FROM STACK DRAIN
TO THICKENER
FILTRATE SUMP
LIME SLURRY STORAGE TANK
BARGE PUMP
LIME BARGE
LIME SLURRY STORAGE PUMP
FROM FILTRATE SUMP
THICKENER
THICKENER UNDERFLOW PUMP
VACUUM PUMP
FILTRATE RECEIVER
FILTER CAKE
VACUUM FILTERS
REACTOR TANK
RECYCLE PUMP
FILTER FEED TANK
FILTER FEED PUMP
CAKE WASH WATER
AIR
FLUIDIZING BLOWER
PUG MILL
ABSORBER
ASH SILO
LIME ADDITIVE SILO
LIME
OUTLET DAMPER
BYPASS DAMPER
BOOSTER FAN
INLET DAMPER
I.D. FAN
ELECTROSTATIC PRECIPITATOR
DUST COLLECTOR
STACK
TO FILTRATE SUMP
STACK FLUSH WATER
TO LANDFILL

Figure 2. Cane Run 6 SDRS flow diagram - modified.

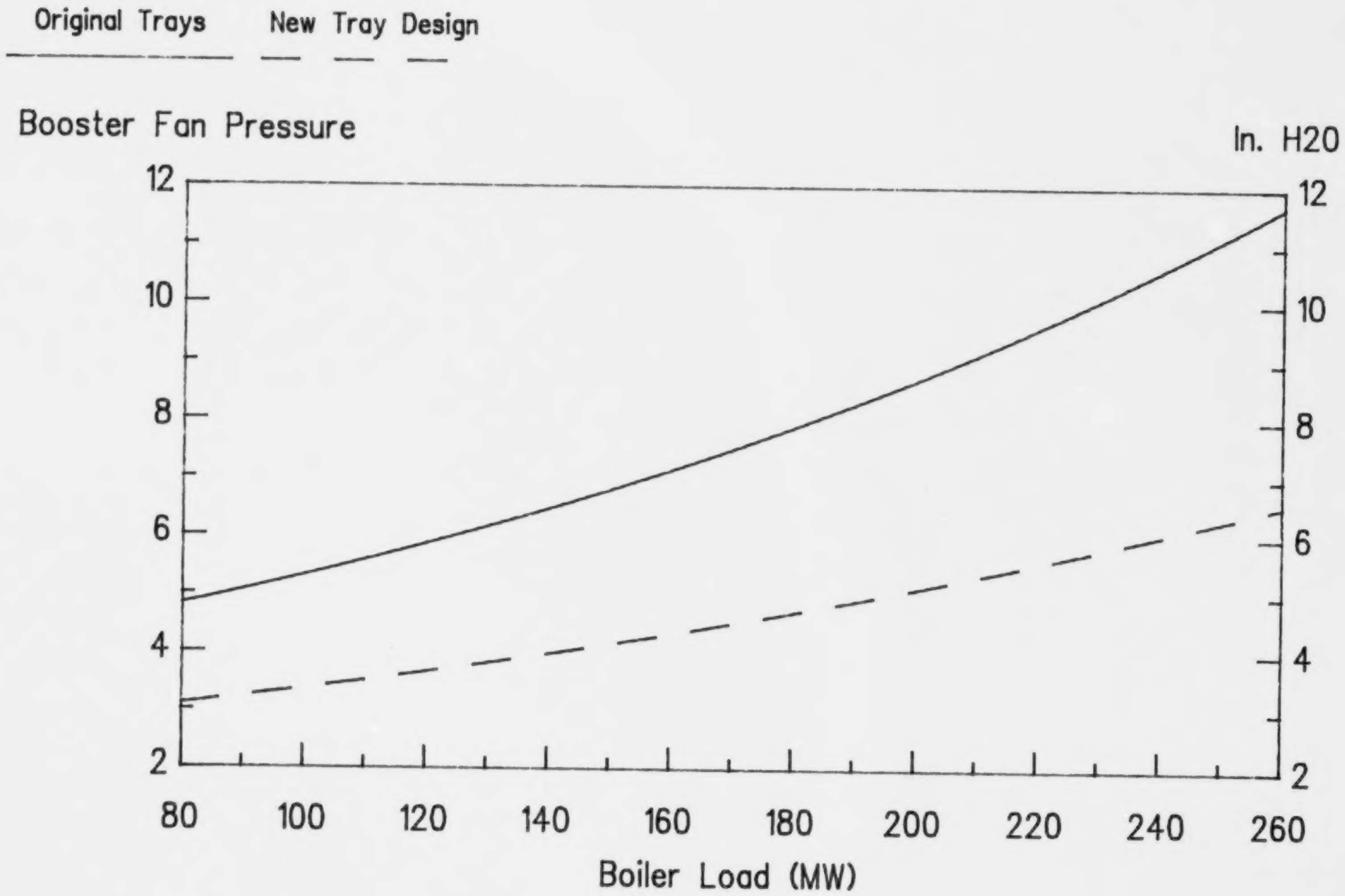

Figure 3. Effect of tray redesign on pressure drop.

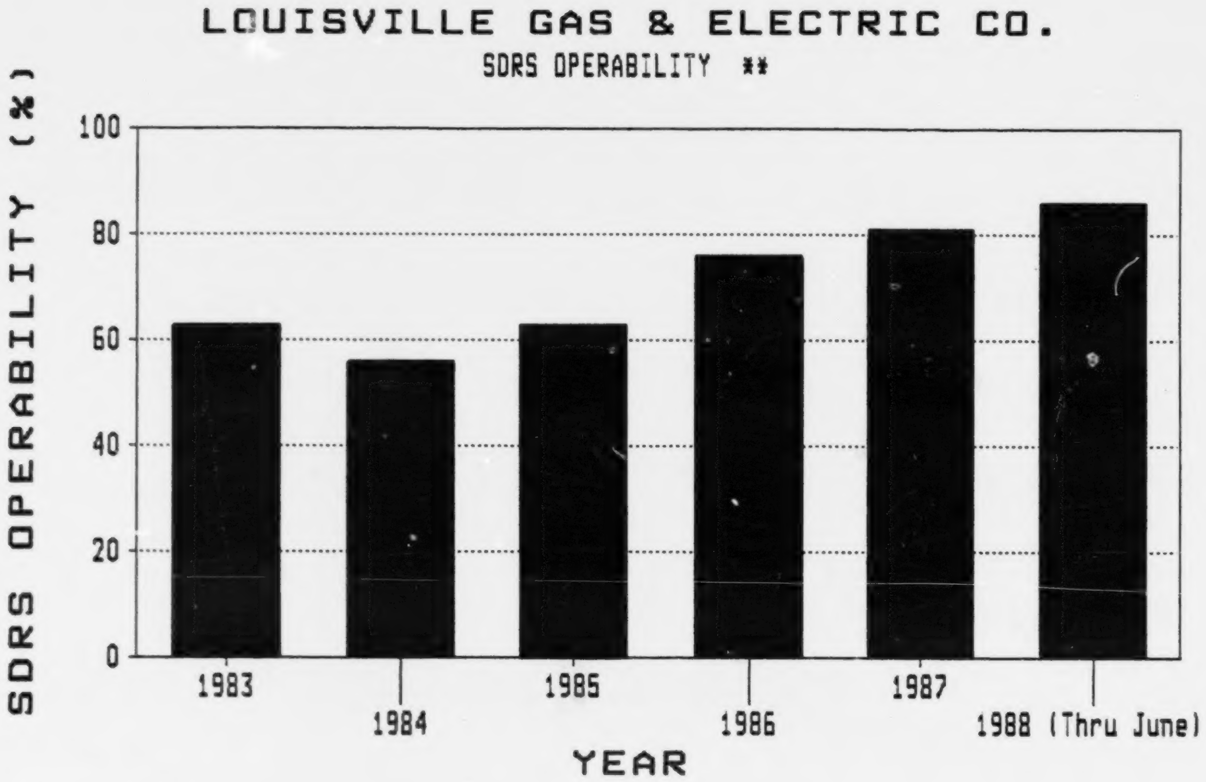

Year	Operating Hours	SDRS Operating Hours **	SDRS Operability **
1983	38376.90	24468.53	63%
1984	39486.60	22335.66	56%
1985	39509.38	25266.87	63%
1986	38144.94	29206.35	76%
1987	38843.14	31471.43	81%
1988 (June)	19255.83	16675.65	86%

** Adjusted for reagent and sludge process plant problems.

Figure 4. LG&E SDRS operability - 1983 thru June 1988.

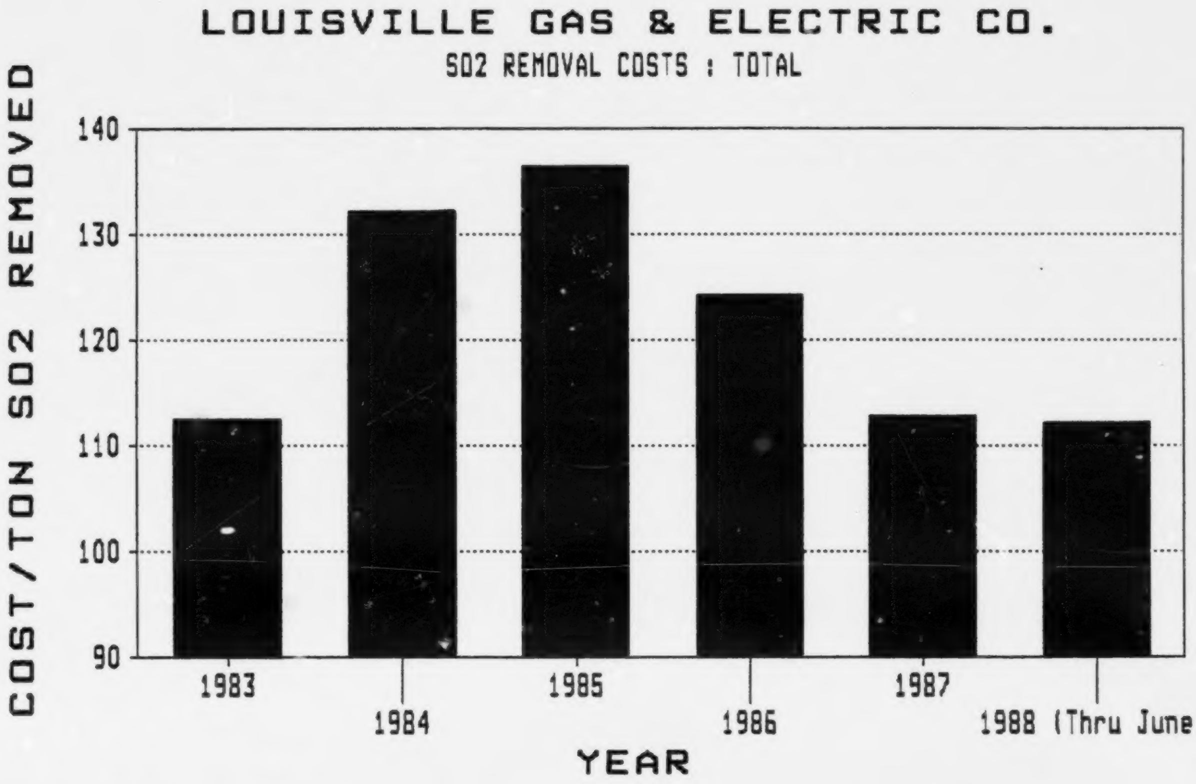

YEAR	SDRS COST	TONS SO2 REMOVED	COST PER TON SO2 REMOVED
1983	$ 14,938,059	132,790.71	$ 112.50
1984	15,128,163	114,332.50	132.32
1985	18,010,002	132,037.14	136.41
1986	20,912,406	168,248.95	124.30
1987	20,189,704	178,802.09	112.92
1988 (June)	10,143,842	90,357.54	112.27

Figure 5. LG&E SO_2 removal cost (total) - 1983 thru June 1988.

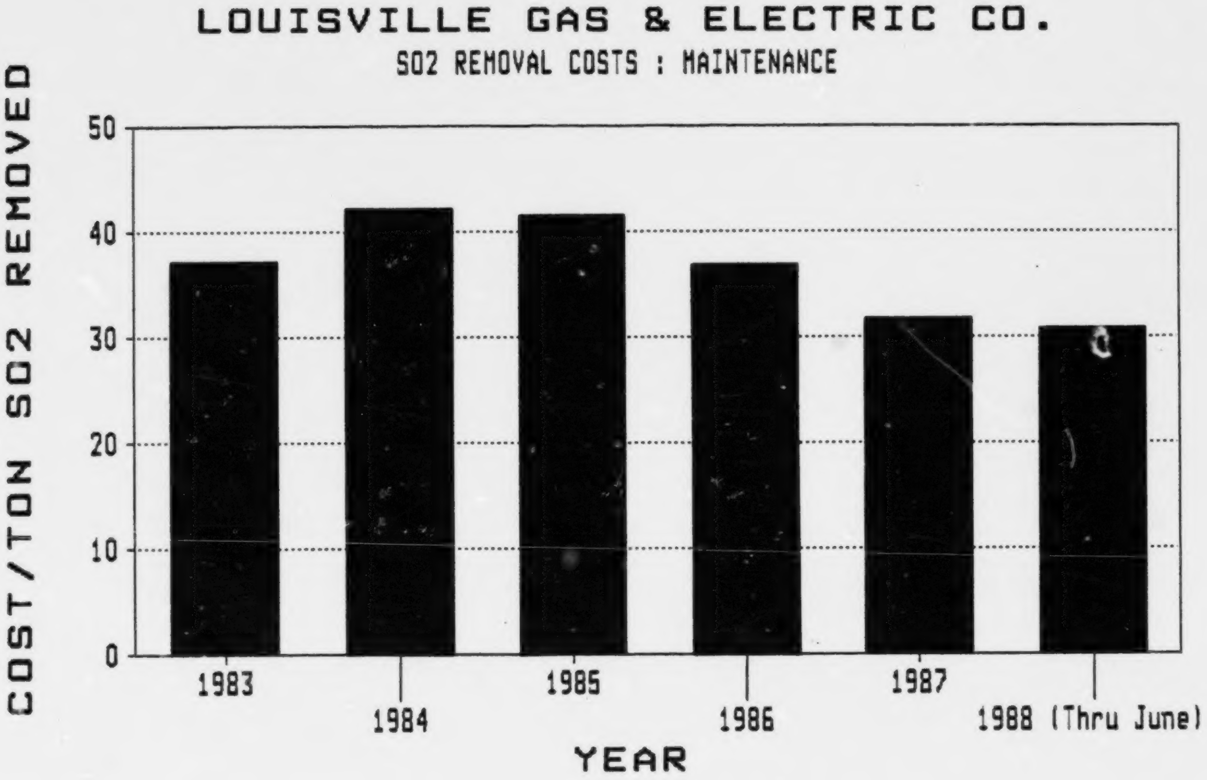

YEAR	MAINTENANCE COST	TONS SO2 REMOVED	MAINTENANCE COST PER TON SO2 REMOVED
1983	$ 4,939,648	132,790.71	$ 37.20
1984	4,832,591	114,332.50	42.27
1985	5,502,224	132,037.14	41.67
1986	6,205,232	168,248.95	36.88
1987	5,671,868	178,802.09	31.72
1988 (June)	2,793,239	90,357.54	30.91

Figure 6. LG&E SO_2 removal cost (maintenance) - 1983 thru June 1988.

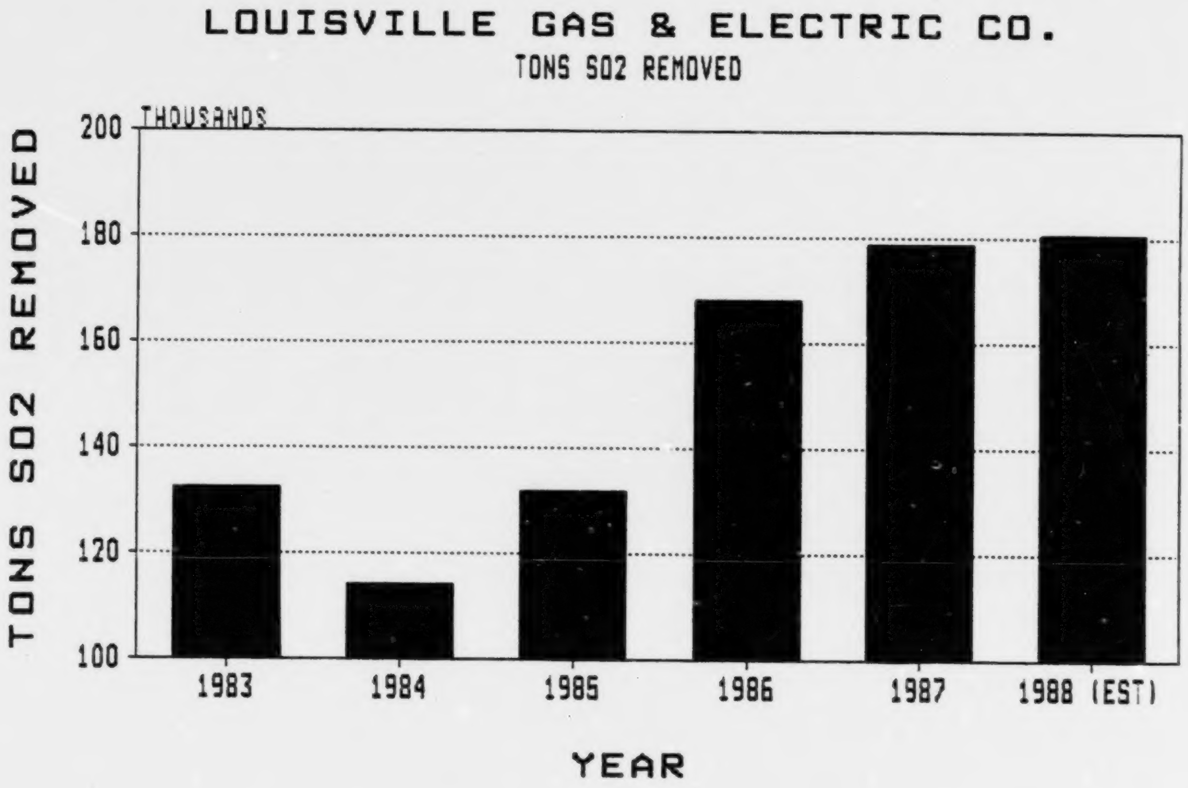

YEAR	TONS SO2 REMOVED
1983	132,790.71
1984	114,332.50
1985	132,037.14
1986	168,248.95
1987	178,802.09
1988 (EST)	180,715.07

Figure 7. LG&E total tons SO_2 removed - 1983 thru 1988(est).

TABLE 1. DUAL ALKALI SYSTEM AT CANE RUN 6 - SYSTEM DESIGN AND EQUIPMENT CONFIGURATION

System Supplier	CEA/ADL
Reagents	Soda Ash/Carbide Lime
Process Mode	Concentrated
Gas Flow at System Inlet, acfm	1,065,000
Gas Temperature at Inlet, ^{o}F	300
SO_2 at Inlet, lb/MBtu	8.55 (maximum)
SO_2 removal, %	94.2 (90 minimum)
Number/Type of Absorber Modules	2/Dual-Tray
Number of Reactor Tanks	2/Absorber
Number/Diameter/Type of Thickener	1/125'/Bridge supported
Number/Type of Vacuum Filters	3/Drum (one spare)
Reheater	Direct Oil-Fired

TABLE 2. CANE RUN 6 SDRS OPERABILITY

Condition	Time Period	Operability
Original System when New	May 1980-May 1981	94.0%
Before Renovation Program	July 1982-June 1983	67.4%
After Renovation Program	March 1986-December 1986	97.6%
	January 1987-December 1987	96.9%

TABLE 3. VACUUM FILTER PERFORMANCE

Condition	Time Period	Avg. Cake % Solids
Original System when New	May 1980-May 1981	48.8
After Renovation	January 1987-December 1987	54.7

TABLE 4. LOUISVILLE GAS & ELECTRIC CO. SDRS RENOVATION PROJECT SYSTEM DATA

UNIT	UNIT RATING	UNIT START-UP	SDRS START-UP	SDRS MANUFACTURER	ORIGINAL ABSORBER TYPE	ORIGINAL REAGENT	MODIFICATION
Mill Creek 1	321	1972	1981	Combustion Engineering	Spray Tower	Lime or Limestone	Components Only
Mill Creek 2	338	1974	1982	Combustion Engineering	Spray Tower	Lime or Limestone	Components Only
Mill Creek 3	412	1978	1978	American Air Filter	Mobile Bed	Lime	Spray Tower - Lime or Limestone
Mill Creek 4	496	1982	1982	American Air Filter	Mobile Bed	Lime	Spray Tower - Lime or Limestone
Cane Run 4	170	1964	1976	American Air Filter	Mobile Bed	Lime	Spray Tower Wet Stack
Cane Run 5	181	1966	1977	Combustion Engineering	Spray Tower	Lime	Wet Stack, Draft Fans & Other Components
Cane Run 6	260	1969	1979	Combustion Equipment Associates	Tray Tower	Soda Ash/ Lime	Wet Stack & Other Components

INHIBITED SULFITE OXIDATION BY THIOSULFATE IN WET LIME/LIMESTONE FGD PROCESSES: RESULTS OF LABORATORY STUDIES AND TESTING AT EPRI'S HIGH SULFUR TEST CENTER MINI-PILOT

by: Gordon Maller
David R. Owens
Frank B. Meserole
Robert C. Chin
Radian Corporation
Austin, Texas 78720-1088

Gary T. Rochelle
The University of Texas at Austin
Austin, Texas 78712

and

Robert E. Moser
Electric Power Research Institute
Palo Alto, California 94303

ABSTRACT

Thiosulfate was studied in a batch laboratory reactor and at the EPRI High Sulfur Test Center Mini-Pilot FGD system to quantify the effects of important FGD system operating variables, such as pH, sulfite concentration, thiosulfate concentration, temperature, inlet SO_2 concentration and L/G, on thiosulfate consumption rates and inhibited sulfite oxidation rates. The laboratory data showed that the thiosulfate degradation rates could be correlated by the square root of the product of the oxidation rate and thiosulfate concentration. Both the mini-pilot and laboratory test results showed strong evidence for a threshold thiosulfate concentration below which sulfite oxidation rates and thiosulfate degradation rates increase dramatically. Thiosulfate degradation by-products were measured in both the laboratory and mini-pilot test solutions. Only trithionate was detected in any significant concentration.

INTRODUCTION

Sulfite oxidation is an important side reaction in flue gas desulfurization processes scrubbing with limestone or lime slurries. At oxidation rates above 15% to 20%, the resulting sulfate concentrations can cause the solutions to become supersaturated with respect to calcium sulfate. These solutions display a scaling tendency. Gypsum ($CaSO_4 \cdot 2H_2O$) scaling on mist eliminators and scrubber internals can be a severe and costly operational problem in these systems. The scaling can result in poor system reliability, poor system performance, and high system maintenance costs.

Thiosulfate has been shown, in pilot- and full-scale applications and studies, to be an effective oxidation inhibitor. It reduces the oxidation rate of absorbed SO_2 to sulfate and thereby reduces gypsum relative saturation, resulting in a reduced tendency for gypsum scaling to occur. It has also been shown to enhance the dewatering characteristics of calcium sulfite scrubber solids and, in some instances, its use has resulted in improved limestone utilization and improved SO_2 removal.

Thiosulfate was recognized as an oxidation inhibitor in early work by the Tennessee Valley Authority (TVA) (1) and Fuji Electric Company (2). In 1978, Radian Corporation identified thiosulfate as the oxidation inhibitor present with carbide lime that was responsible for the scale-free operation of a scrubber operated by Louisville Gas and Electric (3). Further development was slowed by negative results with lime scrubbing in the Environmental Protection Agency (EPA) pilot plant at Research Triangle Park (4). Nevertheless, in 1979, Duquesne Light successfully started adding sodium thiosulfate to eliminate gypsum scaling and enhance SO_2 removal in a 387-MW magnesium-promoted lime scrubbing system (5).

Laboratory studies of thiosulfate were begun at the University of Texas in 1981. The initial studies demonstrated that as little as 1 millimole (mM) of thiosulfate would practically stop sulfite oxidation and adipic acid degradation at pH 5 (6). Extensive testing of thiosulfate at Shawnee was begun in 1982. That work showed that 1 mM of thiosulfate was effective in reducing gypsum saturation and 3 mM was effective in enhancing the dewatering properties of the waste solids (7). Also during that study, trithionate was identified as the primary thiosulfate degradation product.

Additional laboratory testing was begun at the University of Texas in 1983-84 (8). The objective of that study was to quantify sulfite oxidation and thiosulfate degradation as a function of solution composition. Also in 1983-84, extensive pilot testing was performed in a turbulent contact absorber at the EPA-RTP test facility. The results of this testing quantified the effect of thiosulfate on gypsum saturation and solids dewatering and demonstrated that thiosulfate is generally useful in any slurry scrubbing process not using forced oxidation (9).

Testing of thiosulfate conducted by Radian Corporation and funded by the Electric Power Research Institute (EPRI) was begun in late 1987. The objective of this study was to quantify the effects of important chemical variables, such as pH, solution sulfite concentration, solution thiosulfate concentration and temperature, on thiosulfate degradation and inhibited sulfite oxidation rates. A second objective was to develop analytical methods to measure the degradation byproducts which result from the reaction of thiosulfate and sulfite, and to measure the rates of reaction of these products to regenerate thiosulfate. The results of that study are presented in this paper along with some preliminary results of thiosulfate testing currently being performed at EPRI's High Sulfur Test Center (HSTC) mini wet pilot flue gas desulfurization (FGD) system. The objective of the testing being performed at the HSTC is to determine how the effectiveness and consumption rate of thiosulfate are affected by basic FGD system operating variables such as pH, thiosulfate concentration, inlet SO_2 concentration, L/G, and solution composition (e.g., dissolved sulfite concentration). Key process performance indicators which are determined include gypsum relative saturation, limestone utilization, sulfite oxidation, and the concentration of thiosulfate degradation by-products such as trithionate ion ($S_3O_6^{=}$).

To date, in addition to the laboratory and pilot-scale evaluation of thiosulfate, many utilities have evaluated thiosulfate in full-scale FGD systems and have been successful in reducing or eliminating gypsum scaling. Several utilities have also observed a significant enhancement in the settling and dewatering characteristics of waste scrubber solids. The results of some of the full-scale evaluations are presented in a separate paper (10).

However, the amount of thiosulfate required to reduce sulfite to a given level varies among the systems using thiosulfate. The laboratory and HSTC studies are aimed at developing sufficient information about the effects of solution composition on the inhibiting properties of thiosulfate to understand and predict these differences.

THEORY

Oxidation of sulfite in aqueous solutions proceeds according to the following simple stoichiometry:

$$SO_3 + 1/2\ O_2 \text{ ----> } SO_4$$

Previous investigations have studied sulfite oxidation reactions and have postulated a free radical chain reaction mechanism involving a sequence of one-electron transfer steps (11). In the postulated mechanism, the chain reactions are initiated by the reaction of sulfite with a transition metal ion in the appropriate oxidation state.

$$\text{Initiation:}\quad M^{+n} + SO_3^{=} \text{ ----> } M^{+(n-1)} + SO_3^{\dot{-}\,*} \qquad (1)$$

An example initiation transition metal ion is iron (III).

$$Fe^{+3} + SO_3^{=} \text{ ----> } Fe^{+2} + SO_3^{\dot{-}} \qquad (2)$$

The propagation steps of the chain reaction involve $SO_3^{\dot{-}}$, $SO_5^{\dot{-}}$, $SO_4^{\dot{-}}$, and $SO_5^{=}$ (peroxymonosulfite) as reactive intermediates.

$$\text{Propagation:}\quad SO_3^{\dot{-}} + O_2 \text{ ----> } SO_5^{\dot{-}} \qquad (3)$$

$$\text{Propagation:}\quad SO_5^{\dot{-}} + SO_3^{=} \text{ ----> } SO_5^{=} + SO_3^{\dot{-}} \qquad (4)$$

$$\text{Propagation:}\quad SO_3^{=} + SO_5^{\dot{-}} \text{ ----> } SO_4^{\dot{-}} + SO_4^{=} \qquad (5)$$

---

*$SO_3^{\dot{-}}$ denotes a free radical, an ion that has given up one of an original pair of electrons.

Propagation: $SO_3^= + SO_4^{\cdot -}$ ----> $SO_3^{\cdot -} + SO_4^=$ (6)

Oxidation: $SO_3^= + SO_5^=$ ----> $2SO_4^=$ (7)

The termination steps result in the production of $S_2O_6^=$ (dithionate) and $S_2O_8^=$ (persulfate), both of which were observed in the laboratory studies in very low-yield concentrations.

Termination: $SO_3^{\cdot -} + SO_3^{\cdot -}$ ----> $S_2O_6^=$ (8)

Termination: $SO_3^{\cdot -} + SO_5^{\cdot -}$ ----> $S_2O_6^= + O_2$ (9)

Termination: $SO_4^{\cdot -} + SO_4^{\cdot -}$ ----> $S_2O_8^=$ (10)

Termination: $SO_5^{\cdot -} + SO_5^{\cdot -}$ ----> $S_2O_8^= + O_2$ (11)

In a closed catalytic sequence, additional reactions must occur to regenerate the transition metal catalyst. For example:

$Fe^{+2} + SO_5^{\cdot -}$ ----> $Fe^{+3} + SO_5^=$ (12)

Branching reactions can also occur in which both a free radical and an active transition metal catalyst are generated. For example:

$Fe^{+2} + SO_5^= + H_2O$ ----> $Fe^{+3} + SO_4^{\cdot -} + 2OH^-$ (13)

Thiosulfate acts to inhibit oxidation by reacting with the free radicals generated in the initiation and propagation reactions.

$SO_3^{\cdot -} + S_2O_3^=$ ----> $SO_3^= + S_2O_3^{\cdot -}$ (14)

$SO_4^{\cdot -} + S_2O_3^=$ ----> $SO_4^= + S_2O_3^{\cdot -}$ (15)

$SO_5^{\cdot -} + S_2O_3^=$ ----> $SO_5^= + S_2O_3^{\cdot -}$ (16)

The final termination products of these reactions are $S_3O_6^=$ (trithionate) and $S_4O_6^=$ (tetrathionate).

$SO_3^{\cdot -} + S_2O_3^{\cdot -}$ ----> $S_3O_6^=$ (17)

$S_2O_3^{\cdot -} + S_2O_3^{\cdot -}$ ----> $S_4O_6^=$ (18)

In the presence of sulfite, however, $S_4O_6^=$ is rapidly converted to trithionate by the reversible reaction:

$$S_4O_6^= + SO_3^= \underset{k_2}{\overset{k_1}{<\!\!=\!\!=\!\!=\!\!=\!\!>}} S_3O_6^= + S_2O_3^=, \text{ with } k_1 >> k_2 \qquad (19)$$

The net stoichiometry for the inhibition and degradation reactions is:

$S_2O_3^= + SO_3^= + 1/2\ O_2 + H_2O$ ----> $S_3O_6^= + 2OH^-$ (20)

Trithionate will react slowly with water to regenerate thiosulfate:

$S_3O_6^= + H_2O$ ----> $S_2O_3^= + SO_4^= + 2H^+$ (21)

The first order rate constant for this reaction has been measured (12) as a function of temperature and is best calculated by the equation:

$$k_h\ (hr^{-1}) = 1.5 \times 10^{12} \exp(-10.166/T) \qquad (22)$$

$$k_h\ (T = 50°C) = 0.032\ hr^{-1} \qquad (23)$$

At sufficiently high levels of thiosulfate, the rate at which thiosulfate reacts with free radicals will be limited by their production in the initiation step (Eq. 1). Researchers have shown that this primary initiation reaction occurs primarily with sulfite rather than with bisulfite (13) so there will be a pH, as well as a total S(IV), dependence on the rate of this reaction. In addition, the rate will be somewhat dependent on the solubility of the transition metal catalyst in the appropriate oxidation state, for example Fe(III). The metal solubility implies a pH dependence which is the inverse of the pH dependency due to the sulfite-bisulfite ratio.

If sufficient thiosulfate is present to react with all of the sulfite free radicals produced in the initiation step, the autocatalytic branching propagation reactions cannot occur, and the oxidation rate, as well as the thiosulfate degradation rate, will be limited by the rate of the sulfite free radical initiation reaction (Eq. 1). In addition, there will be a limited concentration of free radicals to regenerate the metal catalyst (Eq. 12) which will also tend to limit the oxidation and thiosulfate degradation rates. Rochelle estimated that in this oxidation regime, oxidation in a full-scale system should be 1.5% (13).

If, however, the rate of the sulfite free radical initiation reaction is high because of high soluble sulfite concentration, high metal catalyst concentration, and/or high temperature, and if there is insufficient thiosulfate to react with all of the generated sulfite free radicals, then the rates of the multi-branching propagation reactions become significant and the oxidation and thiosulfate degradation rates rise dramatically. Also, the availability of free radicals increases the rate of the reactions to regenerate the metal catalyst (Eq. 12) which in turn increases the rate of the initiation reaction (autocatalytic effect).

There are two implications from these facts. First, there is a critical threshold concentration of thiosulfate to effectively reduce or inhibit oxidation rates. This concentration is specific for a particular set of operating conditions and is based on the rate of the primary propagation or initiation reactions to generate the sulfite free radical. If the level of thiosulfate drops below this critical concentration, there are sufficient free radicals to feed the multi-branching propagation reactions and the oxidation rate and thiosulfate degradation rate rise significantly. A critical or threshold concentration for thiosulfate was first observed in research performed at the University of Texas (8) and has since been observed in both the laboratory and mini-pilot studies reported here.

The second implication is that the rate of reaction of thiosulfate with the free radicals is strongly tied to the rate at which the free radicals are being generated. Factors which determine the concentration of free radicals (e.g., total soluble sulfite, total soluble metal catalyst, temperature) will increase the "demand" for thiosulfate or diminish its effectiveness. At high rates of oxidation (high concentrations of free radicals), there will be a dependency of thiosulfate concentration on the thiosulfate degradation rate. At low rates of oxidation, the rate of thiosulfate degradation may or may not be independent of thiosulfate concentration.

EXPERIMENTAL METHODS

LABORATORY STUDIES

The pH-stat method was used to measure the rate of sulfite oxidation in the laboratory studies. The experimental approach of this method is to control the pH by titrating with a solution of 1.75 M Na_2SO_3. In the absence of other reactions involving pH changes, the rate of sulfite oxidation is equal to the titration rate of Na_2SO_3, and the pH and SO_3 concentration should be constant.

Oxidation was carried out in a 2-liter reactor agitated at 835 rpm and sparged with 1.8 liter per minute of air. The reactor was held in a temperature-controlled water bath to maintain experimental temperature within ±2°C. Na_2SO_3 titrant was fed to the reactor with a peristaltic pump in response to a pH feedback signal. The weight of titrant added to the reactor was recorded as a function of time throughout an experiment.

All experiments were performed with an initial background electrolyte of 0.1 M Na_2SO_4, 1 mg/L Fe, and 5 mg/L Mn. Fe, Mn, and thiosulfate were added as solutions of $FeSO_4$, $MnSO_4$ and $Na_2S_2O_3$, respectively.

During an experiment, samples were withdrawn from the reactor at regular intervals to be analyzed for thiosulfate, sulfite, and other complex sulfur species including trithionate ($S_3O_6^{=}$), dithionate ($S_2O_6^{=}$), tetrathionate ($S_4O_6^{=}$), and persulfate ($S_2O_8^{=}$). Iodometric titration, in the presence or absence of formaldehyde, was used to measure the concentration of sulfite and thiosulfate. The other sulfur species were determined employing an ion-pair chromatography technique.

The experiments were begun with air oxidation and no thiosulfate to allow the free radical intermediate concentrations to reach a steady state. The measured oxidation rates during this uninhibited oxidation period ranged from 70 to 245 mM/hr and probably represented the limit of oxygen mass transfer in the solution. Following this induction period, thiosulfate was added and the apparent oxidation rate decreased to values as low as 0.6 mM/hr, then increased to the oxygen mass transfer limit as the thiosulfate degraded over a period of 10 to 300 minutes.

Because thiosulfate degradation results in the generation of some hydroxyl ion (Eq. 20), the measured oxidation rate must be corrected by the equation:

$$R_{oxidation} = R_{titration} + R_{degradation} (1 + 2f) \tag{24}$$

where: $f = K_a \, 10^{pH}$

$$K_a = \frac{[SO_3^{=}][H^+]}{[HSO_3^-]}$$

MINI-PILOT STUDIES

Figure 1 is a flow schematic of the mini-pilot unit at the HSTC. The mini-pilot is a combination of a single-nozzle spray tower and a single-tray tower. The spray nozzles are located above a 27%-open perforated tray. Solids dewatering is accomplished using a horizontal centrifuge.

Baseline operating conditions for the thiosulfate testing were:

750 scfm Inlet Gas Flow Rate;
300°F Inlet Gas Temperature;
5% to 7% Inlet O_2, Wet;
460 gal Reaction Tank Volume;
550 gal Total System Volume;
140 mM Ca++, maintained by calcium chloride addition;
130 mM Mg++, maintained by magnesium chloride or hydroxide addition;
120°F Slurry Adiabatic Saturation Temperature; and
12 weight percent Solids in the Reaction Tank.

The specific range of parameters tested include reaction tank pHs of 5.0, 5.5, and 5.8; L/G of 83 and 46 gal/1000 acf measured at outlet gas conditions; and inlet SO_2 levels of 2500 and 1800 ppm, wet.

The test procedure used to measure the thiosulfate consumption rate was identical for each test. Upon establishment of the appropriate test conditions, a spike of anhydrous sodium thiosulfate was added to the reaction tank. From that point on, the thiosulfate and trithionate concentrations were monitored with time. Liquid-phase samples were collected daily to document system chemistry (e.g., sulfite, gypsum relative saturation, iron, and manganese levels) and to provide a basis for daily addition of calcium and magnesium chlorides. Solid-phase samples were collected on alternate days to document process performance parameters such as sulfite oxidation and limestone utilization. Also, process operating conditions such as SO_2 removal, reaction tank level, and gas and slurry flow rates were continuously monitored. Each test was continued until the thiosulfate concentration decreased to below 100 ppm, at which point the operating conditions were changed for the start of the next test.

RESULTS AND DISCUSSION

LABORATORY STUDIES

Results of typical experiments run at pHs 4.5, 5.2, and 6.2 are shown in Figures 2 and 3. The sulfite and thiosulfate concentrations for these experiments were 20 and 2 mM, respectively. Figure 2 shows the cumulative mM of Na_2SO_3 titrant added which is a measure of the apparent sulfite oxidation rate as a function of time. Prior to thiosulfate addition, which occurs at 40 minutes, this oxidation rate is fast and is controlled by the mass transfer absorption of oxygen in the solution. During the uninhibited oxidation period, sulfite oxidation by-products, such as dithionate ($S_2O_6^=$) and persulfate ($S_2O_8^=$), are allowed to accumulate in the solution. Measurements of the concentrations of these by-products showed a significant concentration (0.15 to 0.24 mM) of persulfate in many of the pH 4.5 experiments. This ion was not detected in any of the other pH ranges tested.

At 40 minutes, thiosulfate is added to the solution and the apparent oxidation rate decreases. The rate of oxidation during this time period no longer depends on the rate of oxygen absorption in the solution, but is instead controlled by the rate of the sulfite free radical initiation and propagation reactions. The apparent inhibited oxidation rate remains fairly constant until the thiosulfate is degraded, at which point it returns to its initial mass transfer controlled value.

Figure 3 shows the measured thiosulfate concentrations as a function of time for the same three experiments. Several interesting results can be observed in these figures. First, there appears to be a strong relationship between increasing pH and increasing rates of inhibited oxidation and thiosulfate degradation.

This pH dependence must be due to the increasing sulfite-to-bisulfite ratio at the higher pHs since the metal catalyst concentration is constant for all three pH ranges. This is a reasonable assumption since the concentrations of iron and manganese added were always the same, and in the low inhibited oxidation regime, most of the iron is in the more soluble Fe^{+2} oxidation state.

A second interesting result which can be observed in these figures is the behavior of the pH 4.5 thiosulfate degradation curve. This curve shows an initial higher degradation rate which would indicate that some free radical by-product has accumulated during the uninhibited induction period and initially reacts with thiosulfate. One possible reaction which could account for this behavior would be the reaction of persulfate, which was observed in many of the pH 4.5 experiments, and thiosulfate:

$$S_2O_8^= + 2S_2O_3^= \text{ ----> } S_4O_6^= + 2SO_4^= \qquad (25)$$

Since this reaction does not involve sulfite, it represents a direct thiosulfate degradation route unrelated to sulfite oxidation inhibition. A higher initial thiosulfate degradation rate was observed in most of the pH 4.5 experiments but was not observed in the other pH ranges tested.

A final interesting observation which can be made for the pH 5.2 data is the increase in both the inhibited oxidation rate and thiosulfate degradation rate that occurs at 80 minutes. For this test condition, this may represent the point where there is no longer sufficient thiosulfate to react with the sulfite free radical generated in the initiation reaction and an autocatalytic oxidation mechanism begins. The concentration of thiosulfate at this point was about 1 mM.

An attempt was made to develop a correlation between the measured inhibited sulfite oxidation rates and the measured thiosulfate degradation rates. In developing this correlation, experiments were not considered where little or no inhibition occurred when thiosulfate was added, since it was felt that for these experiments sulfite oxidation rates were limited by the absorption of oxygen in the solution. The excluded experiments were predominantly the high sulfite, pH 5.8 runs.

A tabulation of the average inhibited sulfite oxidation rate and thiosulfate degradation rate is presented in Table 1 along with the sulfite oxdiation rate just prior to thiosulfate addition, the average sulfite concentration, the activity of the free sulfite, the average thiosulfate concentration, and average trithionate concentration. Trithionate is the only degradation by-product reported in this table because, in almost all experiments, it was the only by-product detected and accounted for all of the thiosulfate that had degraded.

The thiosulfate degradation rate was found to be a function of both the sulfite oxidation rate and the thiosulfate concentration. The data for the 50°C tests are shown in Figure 4. As can be seen, a strong correlation was found between the degradation rate and the square root of the product of the oxidation rate and the thiosulfate concentration. A best fit of these data was used to develop the following relationship:

$$R_{deg} = 0.6\ (R_{ox} \times [S_2O_3^=])^{1/2} \qquad (26)$$

where: R_{deg} = the degradation rate of thiosulfate (mM/hr);
R_{ox} = the inhibited sulfite oxidation rate (mM/hr);
$[S_2O_3^=]$ = the thiosulfate concentration.

INHIBITED SULFITE OXIDATION

As previously discussed, during periods when sulfite oxidation is inhibited by thiosulfate, the rate of oxidation will be limited by the reaction of thiosulfate with the sulfite free radical reactants. This suggests that, for the experimental data, the inhibited sulfite oxidation rate should be a function of the sulfite and thiosulfate concentrations since the temperature and trace metal concentrations were constant. If free sulfite is used to develop this relationship, it should apply for all the pH ranges tested.

A relationship between the sulfite oxidation rate and free sulfite and thiosulfate was derived using the 50°C experimental data and is presented in Figure 5. This figure shows the log of the oxidation rate as a function of the log of the free sulfite-thiosulfate ratio. Although there is considerable scatter in the data, a best fit correlation was calculated. The resulting equation is given below:

$$R_{ox} = 125\ ([SO_3^=]\ /\ [S_2O_3^=]) \tag{27}$$

The scatter in the data may be a reflection on the assumption that the metal catalyst concentration is constant over all pH ranges tested. Substituting the relationship for the oxidation rate into Eq. 26 for the thiosulfate degradation rate gives the following expression:

$$R_{deg} = 6.7\ (SO_3^=)^{1/2} \tag{28}$$

This equation should only be taken as a first approximation of the thiosulfate loss rate due to chemical reaction and holds only under inhibited oxidation conditions. However, Eq. 28 does suggest that the chemical consumption of thiosulfate will vary as the square root of the sulfite activity of a solution.

TEMPERATURE EFFECT

While the majority of the experiments were run at 50°C, several were made at about 37 and 63°C. The thiosulfate degradation rate constants derived from the three different temperature data were used to calculate an Arrhenius-type temperature effect. The logarithms of the rate constants were graphed against the reciprocal of the solution temperature expressed in degrees Kelvin (Figure 6). The slope of a straight-line fit of these data was used to calculate an activation energy, E*, and the numerical coefficient.

The Arrhenius plot is shown in Figure 6. The temperature dependence of the rate constant was found to be given by the following equation:

$$k(T) = 10{,}000e^{-6300/RT} \tag{29}$$

TRITHIONATE HYDROLYSIS

The hydrolysis rate of trithionate to regenerate thiosulfate was measured directly at three different pHs. These experiments were performed at 50°C in the presence of metal catalyst but without sulfite. The disappearance of trithionate and the appearance of thiosulfate were measured and are plotted as a function of time (Figure 7). The slope of a linear regression fit of these data was used to determine the reaction rate constant, and a value of .034 hr^{-1} was obtained. This value agrees quite well with the literature rate constant (Eq. 22) for 50°C which is .032 hr^{-1}. Also, the data show that the rate of the trithionate reaction was independent of pH between pH 4.5 and 5.8.

A second approach was used to determine the hydrolysis rate of trithionate. A series of experiments was performed in which several spikes of thiosulfate were added and allowed to degrade. Another experiment was performed in which a large spike of trithionate was added prior to the addition of thiosulfate. In both cases, the thiosulfate degradation rate was measured in the presence of a significantly higher concentration of trithionate than in the other experiments. A comparison of the measured thiosulfate degradation rates for these experiments with the degradation rate calculated using the correlation developed in Eq. 26 would then allow an apparent trithionate hydrolysis rate constant to be determined.

The experimental approach used to determine this apparent rate constant is illustrated in Figure 8, which shows the sulfite oxidation and thiosulfate data for one of the multi-addition experiments. The data show a significant decrease in the loss rate of thiosulfate with each subsequent addition of thiosulfate. This occurs even though the inhibited sulfite oxidation rate remains fairly constant throughout the experiment.

Data used to calculate the apparent trithionate rate constant are tabulated in Table 2. The rate constant values determined are about a factor of 5 higher than the hydrolysis rate constant measured directly (.034 hr^{-1}).

Measurement of a rate constant for the hydrolysis reaction of trithionate to regenerate thiosulfate was also attempted in the mini-pilot system. This was done by measuring the disappearance of trithionate and the appearance of thiosulfate over time when the system was off-line. During the time that measurements were made, the solution temperature was not constant but instead was cooling from the normal solution process temperature of 50°C. A value of .039 hr^{-1} was determined for the trithionate hydrolysis rate constant from the trithionate measurements. This value compares to a calculated value at 45°C of .020 hr^{-1} (Eq. 22)*. Even taking into account the uncertainty of the temperature, this seems to indicate that trithionate hydrolysis is faster in a scrubber solution matrix.

MINI-PILOT TESTS

The HSTC mini-pilot FGD system afforded an opportunity to study thiosulfate under actual scrubber conditions where precipitation of calcium-sulfur solids occurs and the system, at times, operates under non-steady-state conditions. This is contrasted to the batch laboratory experiments where no precipitation can occur and steady-state conditions are reached very quickly. Three different mechanisms for consumption of thiosulfate can be identified during a mini-pilot experiment:

- Reaction of thiosulfate with sulfite free radicals to generate trithionate;
- Solution losses of thiosulfate in the waste solids; and
- Coprecipitation of thiosulfate with the calcium sulfite waste solids.

The loss of thiosulfate due to coprecipitation was a somewhat unexpected finding as this phenomenon had not been previously reported. The presence of thiosulfate in the waste solids was confirmed by a semi-quantitative analytical technique. Work is currently underway to refine this technique to make it more quantitative.

---

*The average solution temperature was 45°C during the time that trithionate measurements were made.

Tests that are reported measured the effects of three different pHs, two different inlet SO_2 concentrations, and two different liquid-to-gas ratios on the thiosulfate consumption rate.

The data collected from the mini-pilot thiosulfate tests--primarily the measured thiosulfate and trithionate concentrations--were used to determine the rate of thiosulfate reaction to trithionate and the coprecipitation rate constant. These values were calculated using a material balance equation for thiosulfate. This equation includes the consumption mechanisms previously discussed and the hydrolysis reaction of trithionate to thiosulfate, which are expressed mathematically as:

Rate of chemical reaction of thiosulfate to trithionate:

K_{deg} [mM/hr]

Rate of coprecipitation of thiosulfate:

$K_{cp}\,[S_2O_3^=]$, where $K_{cp} = hr^{-1}$

Solution losses:

$B[S_2O_3^=]$, where B = liquid blowdown rate of solution entrained in the waste solids (L/hr)

Trithionate hydrolysis to thiosulfate:

$K_h[S_3O_6^=]$, where $K_h = .032\ hr^{-1}$ at $T = 50°C$

The total material balance equation then being:

$$\frac{d\,[S_2O_3^=]\,V}{dt} = VK_h\,[S_3O_6^=] - VK_{deg} - VK_{cp}\,[S_2O_3^=] - B\,[S_2O_3^=].$$

The model uses this equation to iterate on the thiosulfate degradation rate and coprecipitation rate constant until the best fit of the thiosulfate and trithionate analyses are obtained using a least squares analysis. It should be noted that only the data collected during constant thiosulfate degradation were used in this analysis. Therefore, the data collected where the thiosulfate consumption rate increased dramatically, due to increased propagation of free radicals, were not used. However, documentation of the thiosulfate concentration at which its consumption increases rapidly is useful for determining the minimum level of thiosulfate concentration necessary for practical use.

If the rate expressions are correct, the rate constants calculated by the model should be independent of the test conditions; however, the rate expressions used--zero order in thiosulfate for reaction to degradation and first order in thiosulfate for coprecipitation--are not completely accurate. Therefore, some variation does occur, but this information can be used to improve the rate expressions or to develop an empirical expression.

Table 3 presents the calculated thiosulfate degradation rates, coprecipitation rate constants, and measured $CaSO_3$ precipitation rates for the tests conducted on the mini-pilot to date. Also given in Table 3 are the operating conditions for the tests. It can be observed from these data that the coprecipitation rate constant does not vary significantly with pH, which indicates that the assumed rate form may be accurate. The average value of the coprecipitation rate constant at 50°C is 0.0046 hr^{-1}. There does appear to be a correlation between the $CaSO_3$ precipitation rate and the coprecipitation rate constant. This seems to indicate a dependence of both the thiosulfate concentration and the precipitation rate on the rate of coprecipitation.

The data do show a significant decrease in the degradation rate of thiosulfate with pH. This was expected since pH significantly affects the rate of sulfite oxidation, and therefore, the thiosulfate reaction rate of trithionate. The relationship between this reaction rate and pH is linear, and therefore a pH term could easily be incorporated into the rate expression for the reaction of thiosulfate to trithionate. However, because a change in pH affects several variables (e.g., catalyst and total sulfite concentrations), inclusion of a pH term in the degradation rate may be too gross of an approximation and may not accurately predict the effect of pH changes for different solution compositions.

A lower inlet SO_2 only slightly reduces the rate of reaction of thiosulfate to trithionate, while a lower L/G significantly reduces this rate. The L/G was reduced by 45% and this effected a 52% decrease in the rate, indicating that, for these conditions, this rate is about proportional to the L/G. These results indicate that the sulfite oxidation rate--and thiosulfate reaction to trithionate --is not dependent upon the O_2/SO_2 ratio, but is dependent upon the pickup of O_2. Lowering the inlet SO_2 concentration has no effect on O_2 mass transfer. Therefore the percentage of SO_2 that is oxidized may increase, but the oxidation rate and thiosulfate reaction rate to trithionate do not. Reducing the L/G does reduce the amount of O_2 absorbed, and therefore, reduces the oxidation and thiosulfate reaction rates.

THIOSULFATE THRESHOLD CONCENTRATION

Many of the mini-pilot tests that have been run to date have shown indications of a threshold concentration. Above this concentration, both the sulfite oxidation rate and thiosulfate degradation rate are slow and any increase in the thiosulfate concentration has little effect on these rates. If, however, the thiosulfate concentration drops below this threshold, both the oxidation rate and degradation rate increase dramatically. The explanation for this phenomenon, discussed previously in more detail, is that the threshold concentration represents the point where sufficient thiosulfate is no longer present to quench all of the sulfite free radicals. These free radicals are therefore available to drive the autocatalytic branching free radical reactions, thereby significantly increasing the sulfite oxidation rate.

Figure 9 presents the measured thiosulfate concentrations as a function of time for tests at pHs 5.2 and 5.5. There is a clear indication that about 300 ppm is the threshold concentration for the pH 5.2 test. On the other hand, at pH 5.5, there does not appear to be a threshold concentration as the thiosulfate concentration decreases gradually from 400 ppm to about 100 ppm. Tests conducted at pH 5.0 (not shown in Figure 9) indicate that the threshold concentration is closer to 500 ppm.

The threshold concentrations determined for the mini-pilot tests show a strong pH dependence with the concentration tending to increase at lower pH. This is probably related to increased solubility of trace metals in the appropriate oxidation state necessary to act as catalysts. The laboratory study data indicated that the threshold concentration tended to increase at higher pH. For example, at pH 5.8 and a sulfate concentration of 35 mM, 550 ppm of thiosulfate could not slow oxidation, while at pH 4.5 and a similar sulfite level, a thiosulfate concentration as low as 180 ppm completely stopped oxidation. The explanation for this apparent contradiction between the mini-pilot and laboratory data is that in the laboratory studies, the metal catalyst was held constant. The oxidation rate is therefore proportional to the free sulfite concentration which tends to increase at higher pH.

EFFECT OF THIOSULFATE ON WASTE SOLIDS

Previous research has shown that the use of thiosulfate can have a significant impact on the characteristics of calcium sulfite waste solids produced in a limestone FGD system. Under conditions where the sulfite oxidation rate is reduced to very low levels and a very pure calcium sulfite crystal is produced, the calcium sulfite crystals grow larger and have a more regular shape. These crystals settle much more rapidly and actually seem to have dewatering properties similar to gypsum. Pilot tests which documented this phenomenon were conducted by TVA, and TVA researchers hold a patent on the use of thiosulfate for the purpose of improving the FGD waste dewatering properties.

This phenomenon has also been observed during testing at the HSTC. Prior to thiosulfate testing, the centrifuge product typically ran 55 to 60 weight percent solids. At the low oxidations obtained with thiosulfate, however, the waste solids have been measured as high as 78 weight percent solids. There has also been as much as a tenfold increase in the settling rate of the recycle slurry as measured by a batch settling test. One implication of these results is the possibility that thiosulfate could produce crystals which would cause problems in existing dewatering equipment. In particular, problems could be encountered in thickeners sized to settle a slower settling solid solution waste product.

EFFECT OF THIOSULFATE ON IRON AND MANGANESE

The effect of thiosulfate on iron concentration was evaluated for the mini-pilot experimental data. These data are presented in Figure 10. At pHs below 5.80, higher thiosulfate levels resulted in higher iron concentrations. This may indicate that thiosulfate is complexing with iron, and this may render it inactive and unable to catalyze sulfite oxidation. Manganese was also evaluated to see how it varied as a function of thiosulfate. In contrast to iron, the measured manganese concentration does not vary with changes in the thiosulfate level. This may indicate that manganese is free to aid in generating free radicals, which may be the free radicals that thiosulfate reacts with.

COMPARISON OF LABORATORY AND MINI-PILOT DATA

A comparison was made of the thiosulfate degradation rates calculated from the mini-pilot data to the rates predicted from the correlation developed from the laboratory testing (Table 4). To make the comparison, the thiosulfate degradation rates obtained from the field data were recalculated using the rate constant for the conversion of trithionate to thiosulfate which was calculated from the multi-addition tests conducted in the laboratory program. The new value of 0.2 hr^{-1} compares to 0.032 hr^{-1}, which is the hydrolysis rate of trithionate. The laboratory results suggest that this rate is considerably faster under oxidizing conditions.

The differences between the rates obtained from the mini-pilot tests and the predicted rates based on the laboratory correlation may be due to a number of possibilities, including:

- Uncertainties in the measurement of the sulfite oxidation rates at the very low oxidation levels attained in the mini-pilot;

- The possibility of tetrathionate as a reaction-regeneration intermediate;

- The presence of other sulfite oxidation modifiers in the mini-pilot solutions that are not included in the laboratory solutions, e.g., organic oxidation inhibitors and other trace elements; and

- Other sulfite oxidation pathways than the trace element-catalyzed mechanism.

CONCLUSIONS

The major conclusions of this study are listed below:

- Data for both the laboratory experiments and mini-pilot experiments were consistent with an autocatalytic branching free radical mechanism for sulfite oxidation. In this proposed mechanism, when sufficient thiosulfate is present to react with all sulfite free radicals generated in the initiation reaction, the branching propagation reaction cannot occur and the oxidation rate, as well as the thiosulfate degradation rate, will be limited by the rate of the sulfite free radical initiation reaction. This implies that there is a threshold concentration of thiosulfate which is specific for a particular operating condition. Below this threshold concentration, the autocatalytic branching propagation reaction dominates and sulfite oxidation rates and thiosulfate degradation rates rise significantly. Clear indications of a threshold concentration for thiosulfate were observed in the mini-pilot and laboratory experimental results.

- A strong correlation was found between the thiosulfate degradation rates for the laboratory experiments and the square root of the product of the oxidation rate and the thiosulfate concentration. A best fit of these data was used to develop the following relationship:

  $$R_{deg} = 0.6 \ (R_{ox} \times [S_2O_3^{=}])^{1/2}.$$

- A relationship between inhibited sulfite oxidation and free sulfite and thiosulfate was developed for the laboratory experimental data. It was best fit by the equation:

  $$R_{ox} = 125 \ ([SO_3^{=}] \ / \ [S_2O_3^{=}]).$$

- Laboratory experimental data were used to approximate a trithionate hydrolysis rate constant under sulfite oxidation conditions. The value obtained was a factor of 5 greater than the literature value. Measurement of the rate of the hydrolysis reaction was also performed during a mini-pilot experiment and a value 2 times greater than the literature value was obtained. This may mean that under scrubber conditions, the trithionate hydrolysis reaction is more significant than literature values would suggest.

- An activation energy of 6.3 kcal/mole was determined from the temperature dependence on the thiosulfate degradation rate. The temperature dependence of the rate constant is:

  $$k(T) = 10{,}000e^{-6300/RT}.$$

- Analysis of the test solutions from both the mini-pilot and laboratory experiments showed that trithionate was the only significant degradation by-product generated in the reaction of thiosulfate and the sulfite free radicals. For the laboratory tests, the concentration of trithionate accounted for all of the thiosulfate that had degraded.

- There appears to be a pH dependence for sulfite oxidation rates and thiosulfate degradation rates for both the laboratory and mini-pilot data. For the mini-pilot data, the rates tended to increase at lower pH, indicating that the dependence was probably due to a solubility effect of metal catalysts. The laboratory test data showed higher oxidation and degradation rates at higher pHs, indicating that, with the metal catalyst concentration constant, the dependence is due to higher free sulfite radical concentrations at the higher pHs.

- Thiosulfate degradation rates measured in mini-pilot tests differed by a factor of 5 to 10 from the predicted rates calculated from the correlation developed for the laboratory test data. Although there appears to be a strong correlation between sulfite oxidation rates and thiosulfate degradation rates for both the laboratory and mini-pilot test data, the correlation may be different for the two experimental approaches. Differences may lie in the formation of different free radicals or formation of other sulfite oxidation modifiers. In addition, there is a good deal of uncertainty in the measurement of the sulfite oxidation rates at the very low oxidation levels in the mini-pilot. These uncertainties also contribute to the apparent differences in thiosulfate degradation rates between the mini-pilot and laboratory data.

REFERENCES

1. Potts, J.M., Jordan, J.E., et al. Removal of sulfur oxides from waste gases. Monthly progress report, Applied Research Branch, Division of Fertilizer Development, Tennessee Valley Authority, October 1972.

2. Inoue, J, Ueda, K., and Komatsu, T. Antioxidation of sulfite aqueous solutions. Japan, Kokai, 75, 125, 993, 1974 (Chem. Abstr., 84:107943).

3. Holcombe, L.J. and Luke, K.W. Characterization of carbide lime to identify sulfite oxidation inhibitors. EPA-600/7-78-176 (NTIS No. PB286-646), September 1978.

4. Borgwardt, R.H. Limestone scrubbing of SO_2 at EPA/RTP pilot plant. Progress report no. 36, October 1978.

5. Miller, J.F., et al. Lime/limestone scrubber modifications: investigation of thiosulfate as an oxidation/scaling inhibitor. DOE/TIC-2005972, December 1981.

6. Rochelle, G.T., et al. Buffer additives for lime/limestone slurry scrubbing. ASC Symp. Ser., 188:243-266, 1982.

7. Barkley, J.B., et al. Evaluation of sodium thiosulfate additive on the performance of a spray tower scrubber system using limestone slurry. TVA/OP/EDT-84-7, November 1983.

8. Owens, D.R. and Rochelle, G.T. Sulfite oxidation inhibited by thiosulfate. MS Thesis, University of Texas at Austin, 1984.

9. Chang, J.C.S. and Brna, T.G. Pilot testing of sodium thiosulfate for oxidation/scaling inhibition in lime/limestone flue gas desulfurization systems. Presented at the AIChE Annual Meeting, Chicago, IL, November 1985.

10. Colley, J.D., et al. Control and reduction of gypsum scale in wet lime/limestone FGD systems by addition of thiosulfate: summary of field experience. Presented at the First Combined FGD and Dry SO_2 Control Symposium, St. Louis, MO, October 1988.

11. Ross, A.B. and Neta, P. Rates of free radical reactions in aqueous solution. National Bureau of Standards, June 1979.

12. Naito, K., Hayata, H., and Mochizuki, M. The reactions of polythionates: kinetics of the cleavage of trithionate ion in aqueous solutions. J. Inorg. Nucl. Chem., 37:1453-1457, 1975.

13. Rochelle, G.T. and Owens, D.R. Sulfite oxidation inhibited by thiosulfate. In Processing and Utilization of High Sulfur Coals. Ed. by Y.A. Attia. Elsevier, NY, pp. 611-624, 1985.

DISCLAIMER

The work described in this paper was not funded by the U.S. Environmental Protection Agency and therefore the contents do not necessarily reflect the views of the Agency and no official endorsement should be inferred.

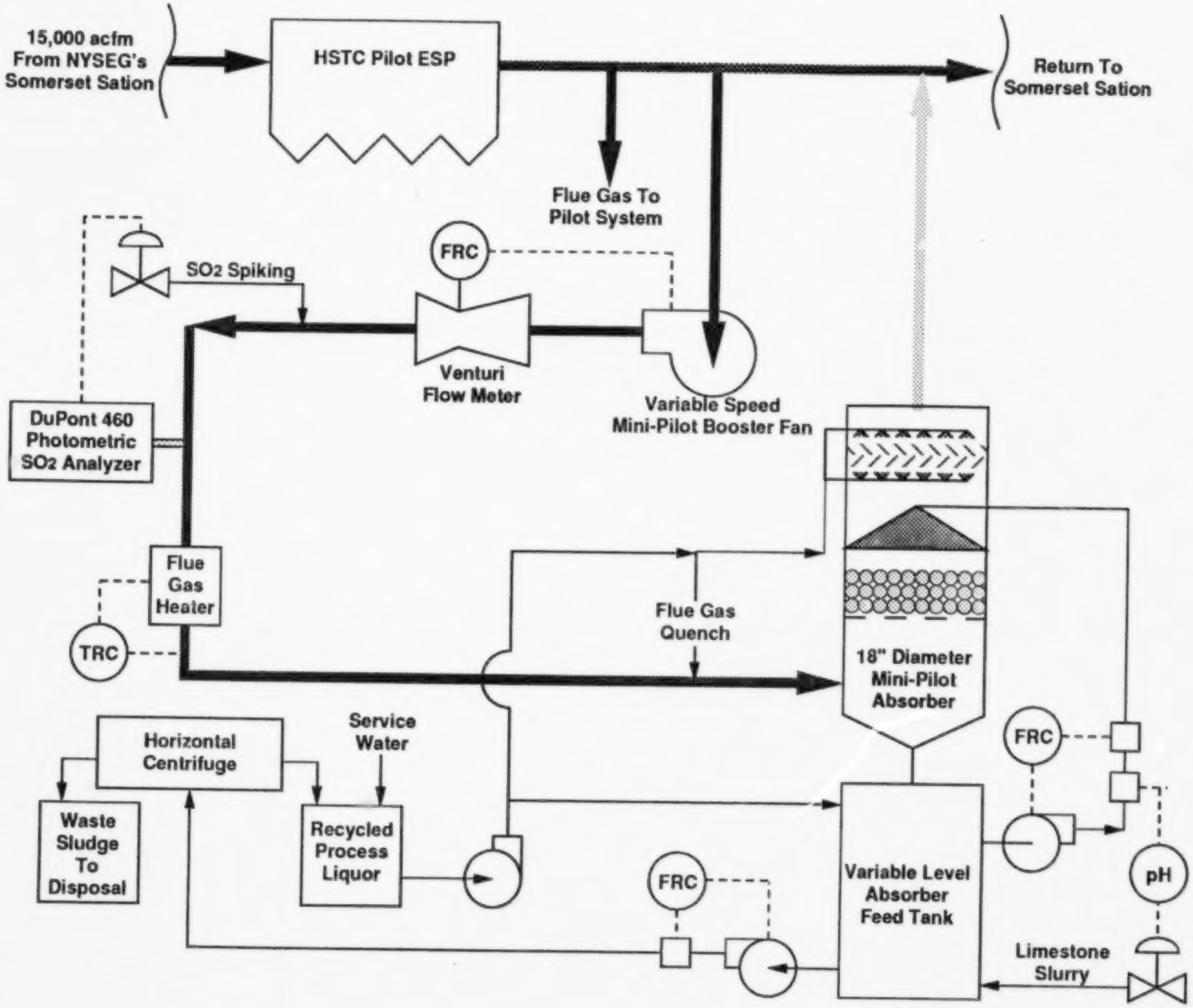
15,000 acfm
From NYSEG's
Somerset Sation
HSTC Pilot ESP
Return To
Somerset Sation
Flue Gas To
Pilot System
FRC
SO_2 Spiking
Venturi
Flow Meter
Variable Speed
Mini-Pilot Booster Fan
DuPont 460
Photometric
SO_2 Analyzer
Flue
Gas
Heater
TRC
Flue Gas
Quench
18" Diameter
Mini-Pilot
Absorber
FRC
Horizontal
Centrifuge
Service
Water
Waste
Sludge
To
Disposal
Recycled
Process
Liquor
FRC
Variable Level
Absorber
Feed Tank
pH
Limestone
Slurry

Figure 1. HSTC mini-pilot FGD system flow schematic.

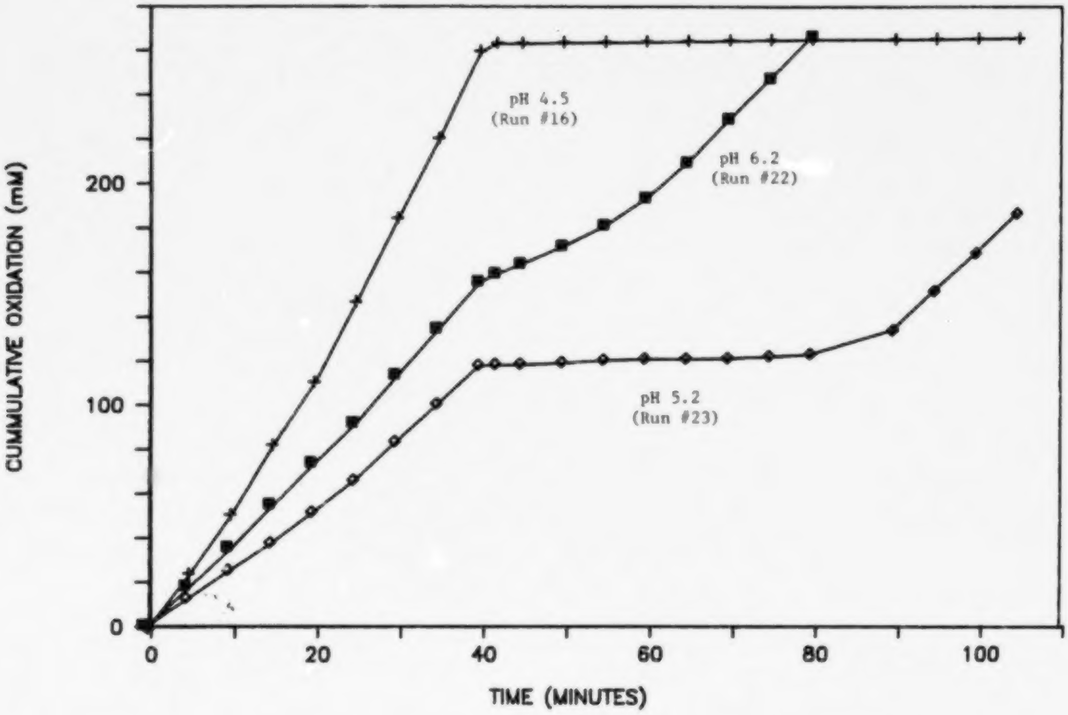

Figure 2. Example sulfite oxidation trends at different pH values.

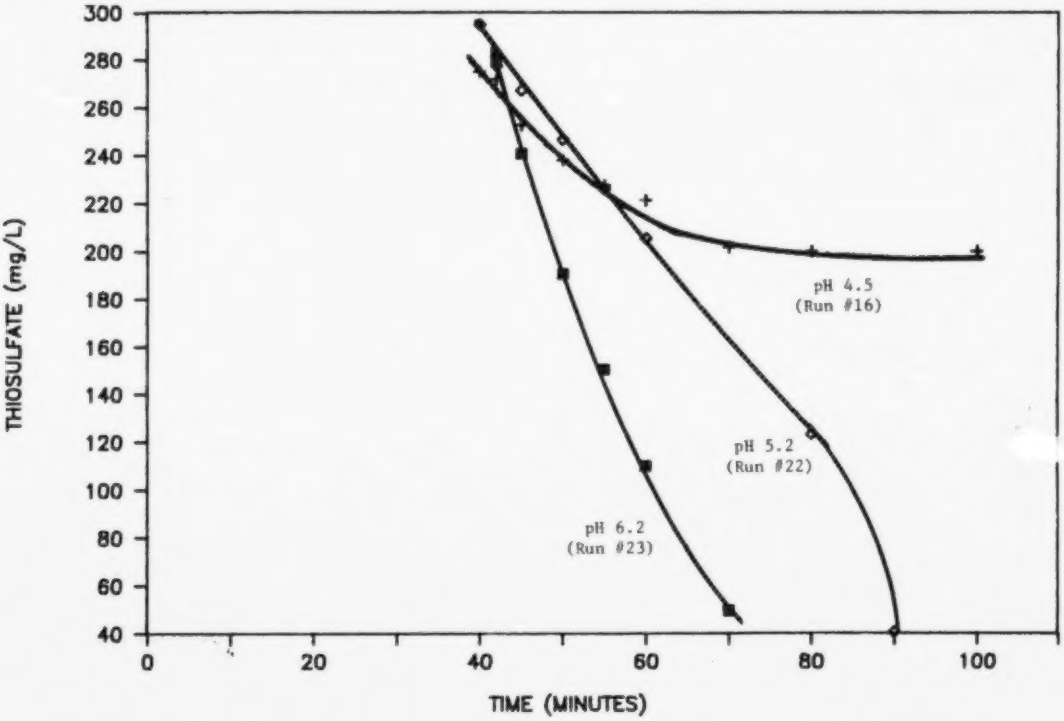

Figure 3. Example thiosulfate concentration profiles at different pH values.

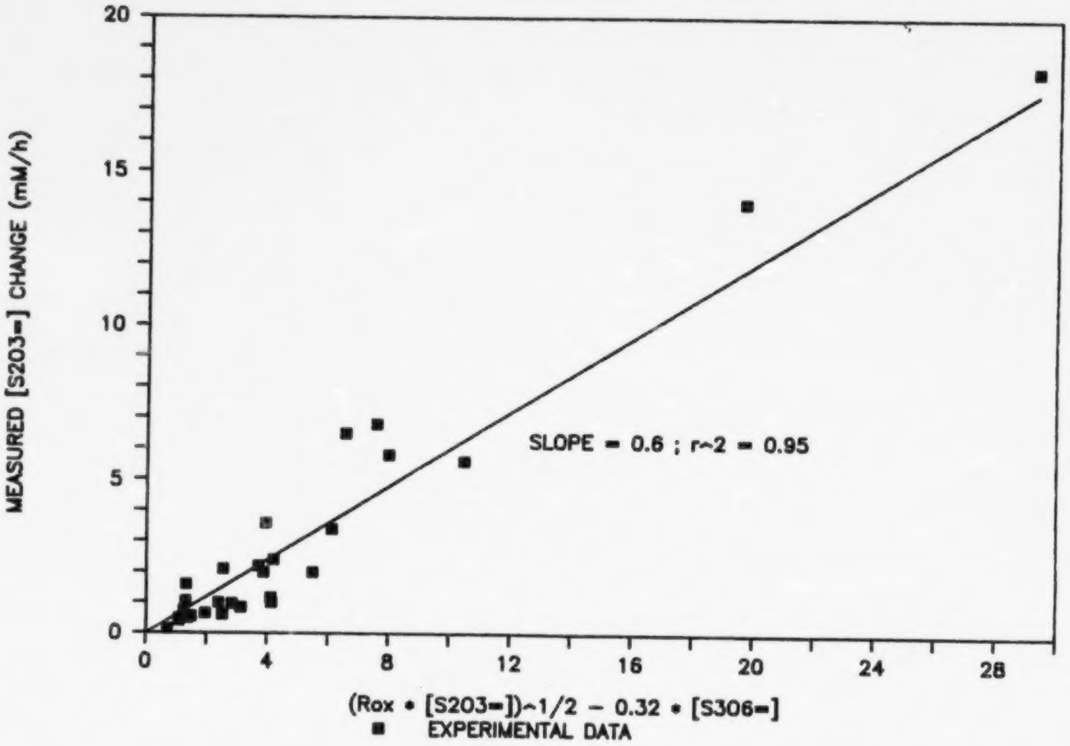

Figure 4. Thiosulfate degradation as a function of oxidation and thiosulfate.

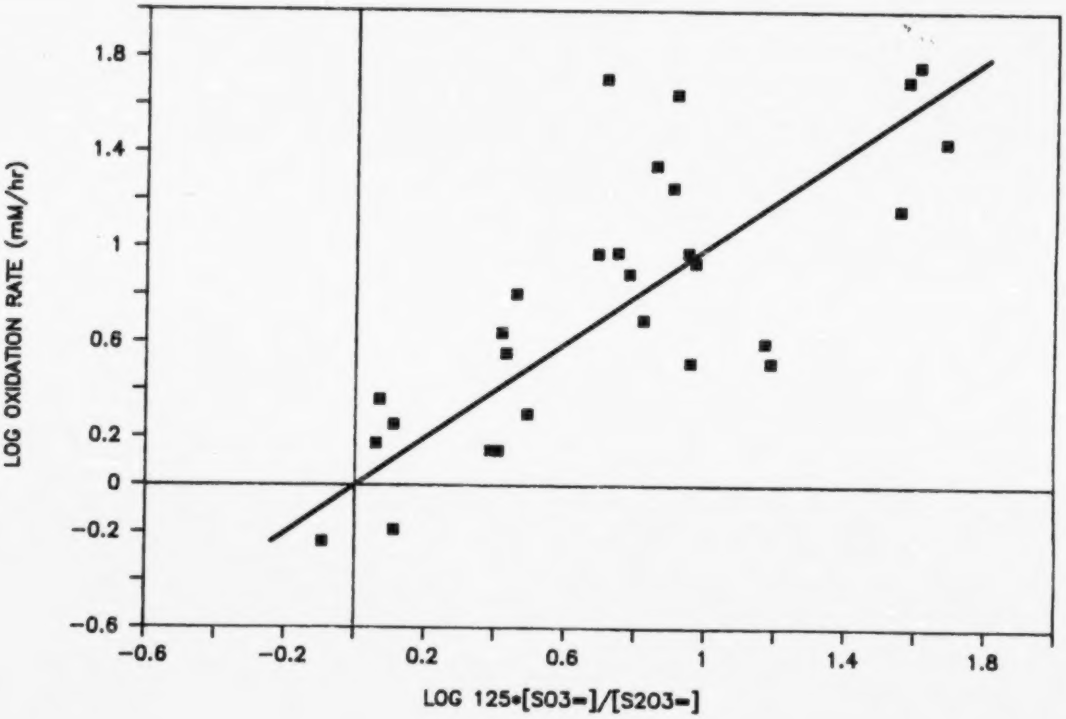

Figure 5. Sulfite oxidation as a function of sulfite and thiosulfate.

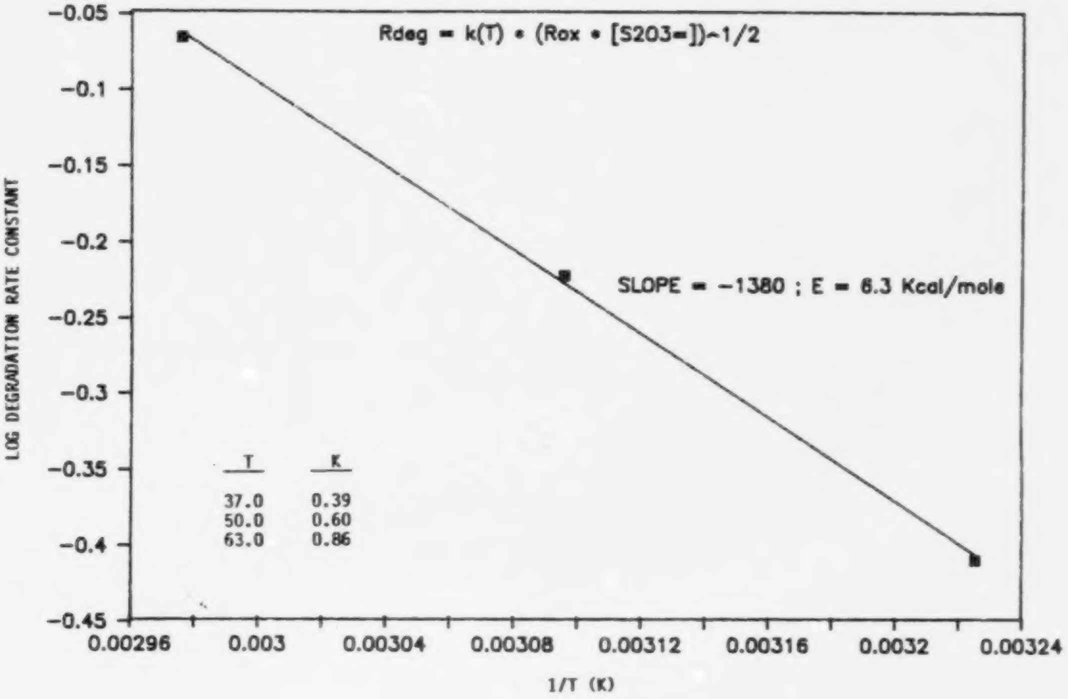

Figure 6. Arrhenius plot of thiosulfate degradation rate constant.

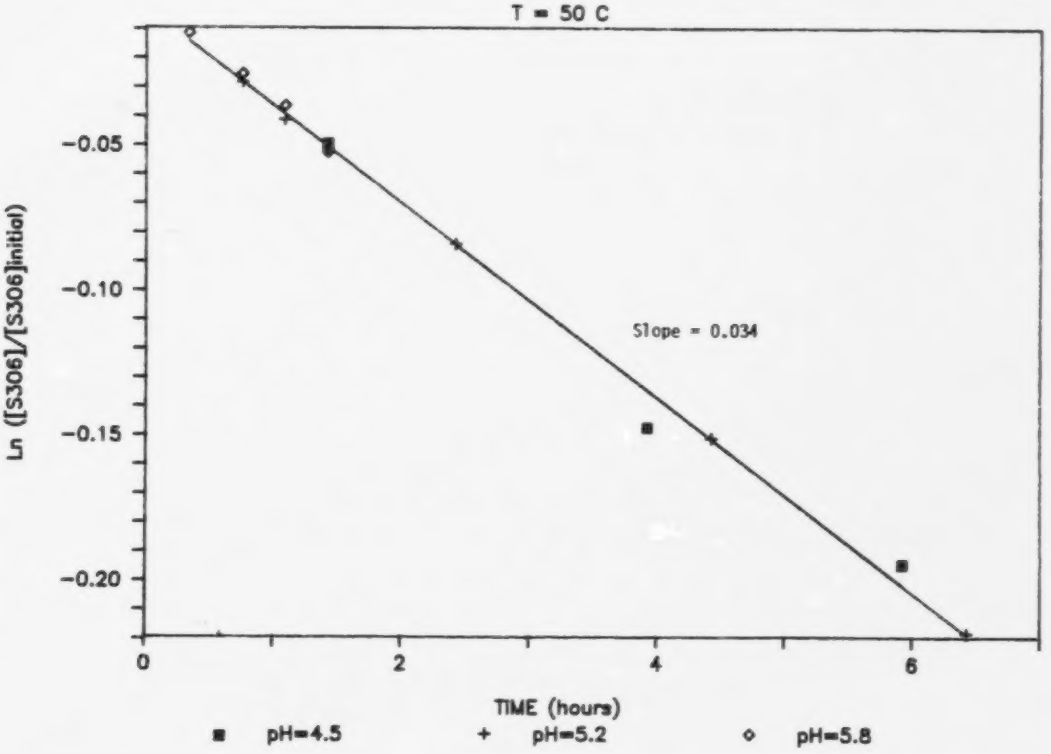

Figure 7. Trithionate hydrolysis rate data.

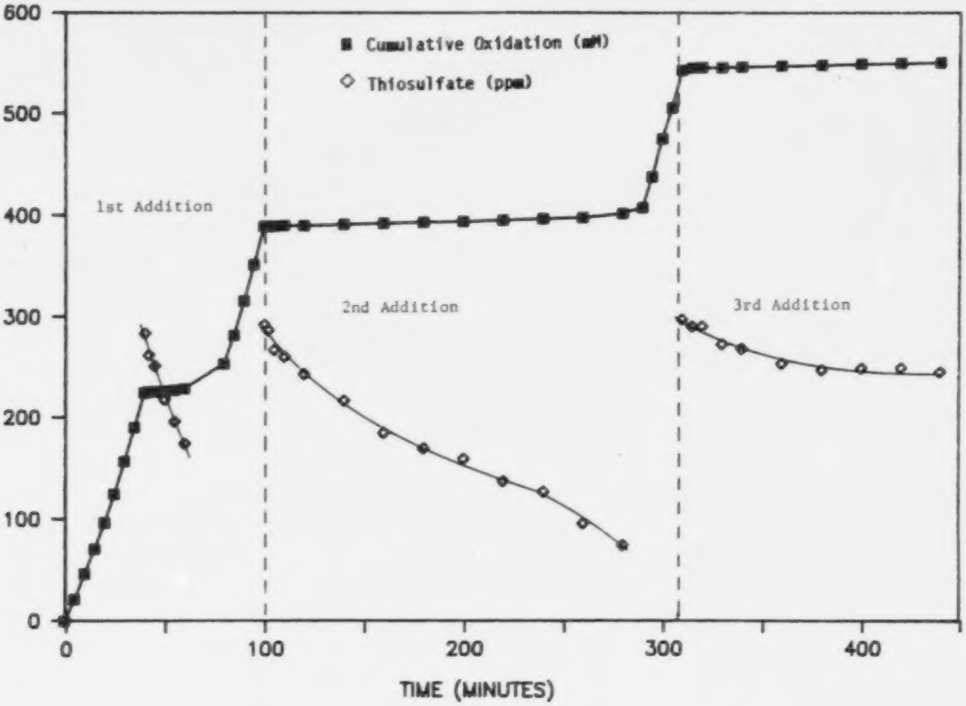

Figure 8. Oxidation and thiosulfate profiles for multi-addition test.

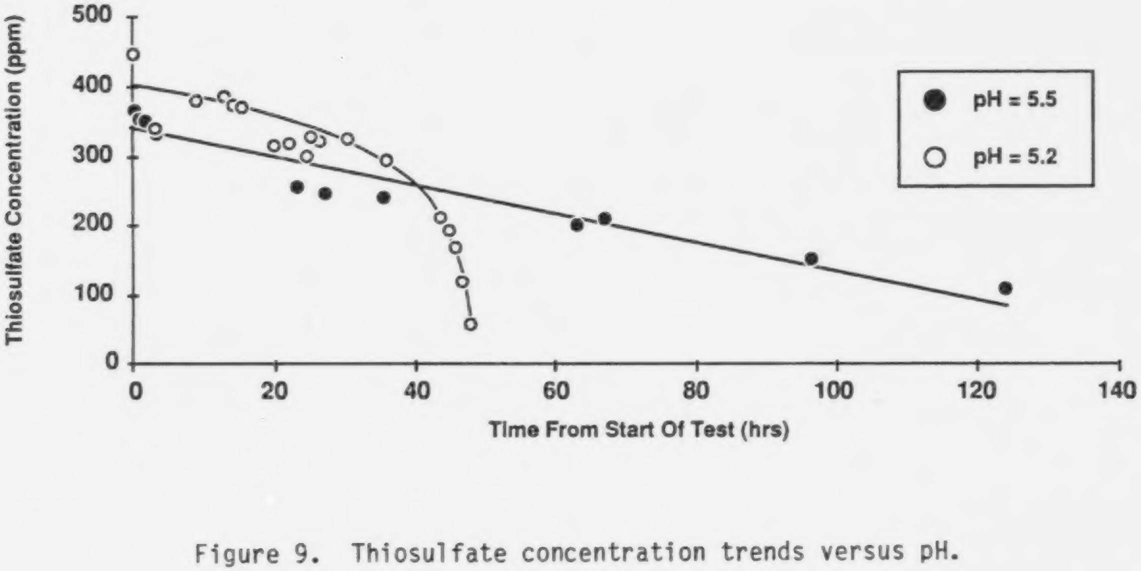

Figure 9. Thiosulfate concentration trends versus pH.

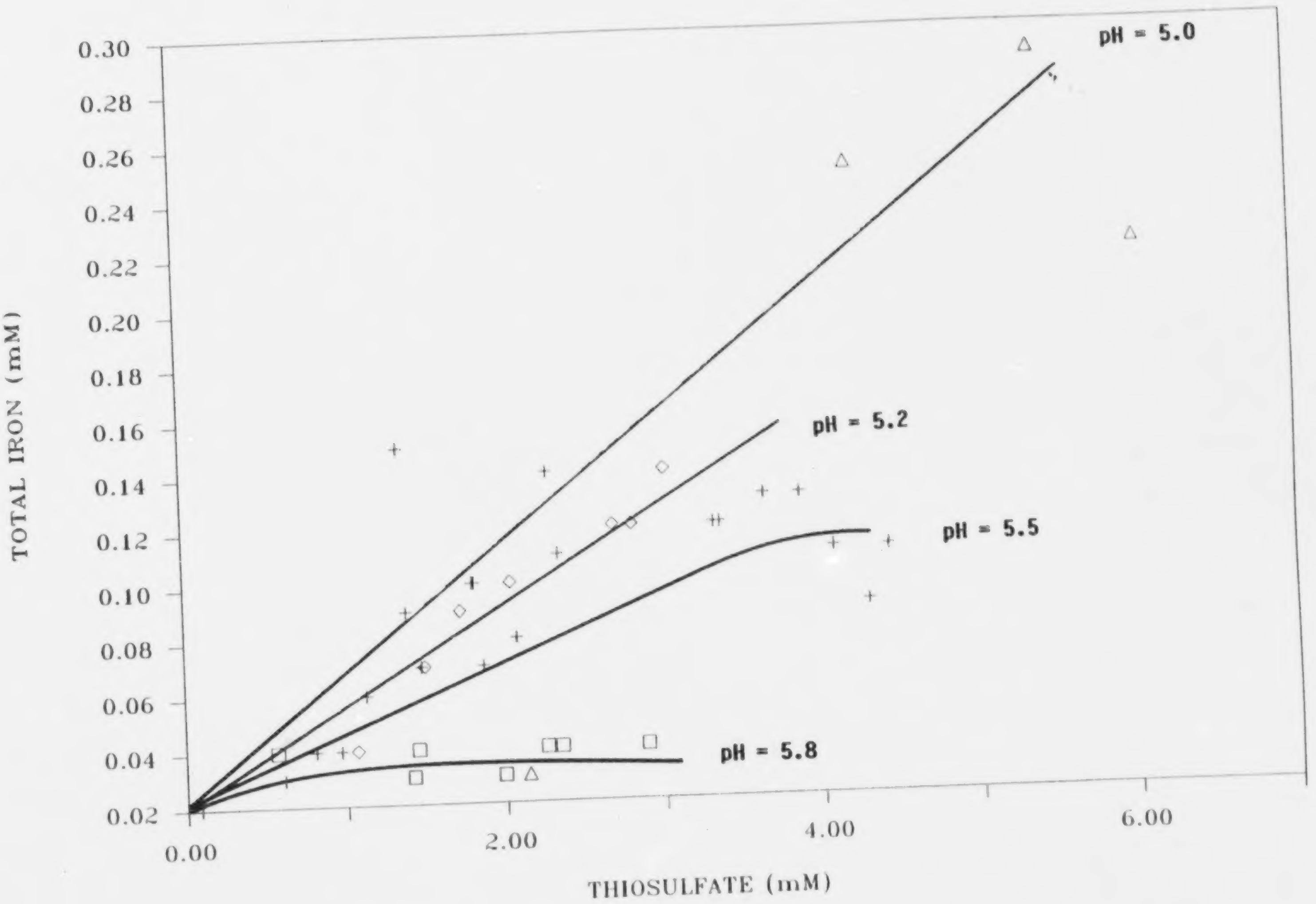

Figure 10. Effect of thiosulfate concentration on total iron.

TABLE 1. THIOSULFATE DEGRADATION DATA SUMMARY*

Run No.	Temperature (°C)	pH	Uninhibited Oxidation Rate (mM/hr)	Inhibited Oxidation Rate (mM/hr)	$S_2O_3^=$ Degradation Rate (mM/hr)	Total S(IV) (mM)	$[SO_3^=]$ Activity (mM)	$[S_2O_3^=]$ (mM)	$[S_3O_6^=]$ (mM)
1	50	5.2	97	2.0	1.06	7.7	0.0093	1.44	1.23
2	50	5.2	70	5.0	2.10	18.1	0.0233	1.59	0.89
3	50	5.2	210	0.6	0.14	2.5	0.0027	1.80	1.01
4	50	4.5	182	6.4	1.60	8.4	0.0063	0.36	0.64
5	50	4.5	232	1.5	0.75	13.8	0.0015	1.48	0.78
6	50	4.5	245	0.7	0.40	34.0	0.0006	3.24	1.14
7	50	4.5	182	3.6	0.50	10.5	0.0036	0.48	0.73
8	50	4.5	187	1.4	0.50	35.0	0.0014	1.77	0.63
9	50	5.2	220	9.5	3.60	15.2	0.0442	1.80	0.63
10	50	5.2	210	4.4	2.00	18.0	0.0205	4.00	1.04
11	50	5.2	225	22.3	6.80	36.0	0.1037	2.92	1.57
12	50	5.8	240	9.6	3.40	19.0	0.1477	7.80	0.58
13	50	5.8	240	8.7	2.00	18.5	0.1338	3.81	0.88
14	50	5.8	280	3.3	1.00	9.1	0.0508	1.93	0.43
15	50	5.8	260	51.0	6.50	17.0	0.7846	0.87	0.38
16	50	4.5	208	2.3	0.65	18.5	0.0023	1.94	0.52
17	50	4.5	169	1.4	0.55	40.0	0.0014	1.92	0.49
18	50	5.2	220	18.0	5.80	52.0	0.0837	3.78	0.87
19	50	4.5	138	1.8	0.97	50.0	0.0018	4.78	0.35
20	50	5.8	132	44.4	14.00	49.0	0.6831	11.50	9.20
21	50	5.8	132	51.6	18.30	47.5	0.7938	17.71	2.99
22	50	5.2	98	7.8	2.20	20.3	0.0363	1.96	0.68
23	50	6.2	120	58.9	5.60	20.0	1.8406	1.93	0.62
24	50	6.2	132	4.0	0.84	9.5	0.1250	2.51	0.14
25	50	6.2	132	3.3	0.61	8.5	0.1031	2.16	0.49
26	50	6.2	122	14.6	1.16	11.0	0.4563	1.20	0.25
27	50	6.2	122	28.1	1.00	8.4	0.8781	0.68	0.77
28	37	5.2	110	5.6	1.90	19.6	0.0260	2.19	0.42
29	37	4.5	77	0.6	0.35	20.5	0.0006	2.26	0.43
30	37	5.8	100	7.5	1.16	20.0	0.1154	2.26	0.25
31	64	5.8	190	60.0	9.20	19.5	0.9231	2.00	0.65
32	62	5.2	175	13.3	4.50	19.0	0.0619	2.04	0.41
33	62	4.5	162	1.1	2.70	17.5	0.0011	2.14	0.46
34	50	5.2	140	9.6	2.40	19.2	0.0447	2.00	0.61

*Experimental conditions: Fe = 1 mg/L. Mn = 5 mg/L. air sparged at 1.8 L/min.

TABLE 2. EXPERIMENTAL DATA FOR TRITHIONATE HYDROLYSIS RATE MEASUREMENT EXPERIMENT

Test Identification	pH	Temp (°C)	SO_3 (mM)	S_2O_3 (mM)	S_3O_6 (mM)	Rate of SO_3 Oxidation (mM/hr)	Calculated Rate of S_2O_3 Degradation (mM/hr)	Measured Rate of S_2O_3 Degradation (mM/hr)	S_3O_6 Hydrolysis Rate Constant (hr^{-1})
Multi-addition 1	5.2	50	12.9	1.59	3.51	2.15	-1.16	-0.61	0.16
Multi-addition 2	5.2	50	8.9	2.29	5.41	1.40	-1.12	-0.16	0.18
Multi-addition 3	5.2	50	12.6	2.03	3.09	1.23	-0.99	-0.27	0.23
Multi-addition 4	5.2	50	16.5	1.93	12.6	3.15	-1.55	-0.23	0.11

TABLE 3. MINI-PILOT TEST CONDITIONS AND RESULTS

Test ID	Initial $[S_2O_3^=]$ (ppm)	Inlet $[SO_2]_g$ (ppm wet)	Inlet $[O_2]_g$ (% wet)	L/G ($gal/MACF_{out}$)	Reaction Tank Volume (gal)	Reaction Tank pH	$[Ca^{++}]$ (mM)	$[Mg^{++}]$ (mM)	K_{cp} (hr^{-1})	K_{deg} (mM/hr)	$CaSO_3$ Precipitation Rate (mM/hr)
MTVT-4	400	2500	7	83	490	5.50	140	130	0.0044	0.027	47.3
MTVT-5	400	2500	7	83	490	5.80	140	130	0.0055	0.012	57.5
MTVT-8	800	2500	7	83	490	5.00	140	130	0.0047	0.052	45.2
MTVT-10	400	2500	7	46	490	5.50	140	130	0.0041	0.013	36.4
MTVT-12	400	1800	7	83	490	5.50	140	130	0.0044	0.023	38.1

TABLE 4. COMPARISON OF LABORATORY AND MINI-PILOT THIOSULFATE DEGRADATION RESULTS

Test ID	Adjusted Mini-Pilot Degradation Rate* (mM/hr)	Degradation Rate From Laboratory Correlation** (mM/hr)	R_{ox} (mM/hr)	$[S_2O_3^=]$ (mM)
MTVT 4	0.14	0.51	0.66	1.4
MTVT 5	0.06	0.62	0.58	2.0
MTVT 8	0.32	2.4	2.87	6.0
MTVT 10	0.06	0.70	0.79	1.9
MTVT 12	0.11	0.75	0.80	2.4

*The mini-pilot data were recalculated using the trithionate conversion rate determined from the laboratory results.

**$R_{deg} = 0.6[R_{ox}]^{1/2} [S_2O_3^=]^{1/2}$.

CONTROL AND REDUCTION OF GYPSUM SCALE IN WET LIME/LIMESTONE FGD SYSTEMS BY ADDITION OF THIOSULFATE: SUMMARY OF FIELD EXPERIENCES

by: Robert E. Moser
Electric Power Research Institute
Palo Alto, California 94304

J. David Colley
James G. Noblett
A. Frank Jones
Radian Corporation
Austin, Texas 78720-1088

ABSTRACT

This paper presents the results of the application of thiosulfate to eight wet FGD systems--three of which were using lime as the reagent at the time of the testing and five which were using limestone. The primary purpose of the addition of thiosulfate was to improve the reliability of the scrubbers by reducing or avoiding the deposition of gypsum scale on the internals of the scrubber towers. Information is presented on the effects of different levels of thiosulfate on the sulfite oxidation fraction and the gypsum relative saturation in the scrubber reaction tanks. Differences from system to system which affect the amount of thiosulfate required to reduce the oxidation rate of sulfite are discussed. These variables include liquid-phase magnesium, chloride, and sulfite; inlet SO_2; flue gas saturation temperature; unit load; and scrubber pH. The mechanism by which thiosulfate can enhance limestone dissolution is presented along with observations from two limestone FGD systems where the dissolution rates increased due to the presence of thiosulfate. Also, the effect of thiosulfate on the dewatering characteristics of calcium sulfite sludges is discussed. Finally, the annual costs for thiosulfate for each of the eight scrubber systems tested are presented. The differences in costs between sodium thiosulfate and sulfur as the raw material sources for thiosulfate in an FGD system is pointed out in this discussion.

INTRODUCTION

The use of thiosulfate in lime/limestone FGD systems has accelerated over the past few years. The acceptance of this additive has grown because it has proven successful at decreasing scrubber O&M costs while improving scrubber reliability, and the use of elemental sulfur to generate thiosulfate in situ has substantially reduced the annual costs for the additive. Furthermore, there have been few adverse side effects observed from the use of thiosulfate. There have been, in fact, several beneficial side effects which can be attributed to the presence of this compound.

This paper presents results from eight test programs at utility lime/limestone FGD systems to evaluate the costs and benefits of thiosulfate. EPRI participated in the tests by providing the various utilities with chemistry and engineering assistance. This work was part of the FGD Chemical Process Problems Program, RP 2248-1.

Information is presented on the effect of thiosulfate on the chemistry of each scrubber. This includes sulfite oxidation, gypsum relative saturation, liquid-phase alkalinity, limestone utilization, and crystal morphology. In addition, the relative effects of unit load, scrubber temperature, sulfite concentration, scrubber pH, and inlet SO_2 concentration on the effectiveness of thiosulfate are discussed. The reduction in the gypsum scale formation rates within the absorbers is also discussed. Finally, available data on the annual costs for sulfur and thiosulfate addition are presented along with the cost differential between sodium thiosulfate and sulfur.

The following section presents background information on the various plants at which the thiosulfate test work was performed. Brief descriptions of the objectives of the testing and of basic plant and FGD system designs are included. The next section describes the effects of thiosulfate on the FGD system chemistry and gypsum scaling rate. The last section contains information on the annual costs for addition of sodium thiosulfate and sulfur to FGD systems.

PLANT DESCRIPTIONS AND TEST OBJECTIVES

The following contains a brief description of each of the sites at which thiosulfate testing has been conducted under RP 2248-1. Also included with the descriptions are the reasons for which the utilities were testing thiosulfate.

DUQUESNE LIGHT'S PHILLIPS STATION

The Phillips Station consists of six Foster Wheeler boilers, four main unit generators with a combined capacity of 400 MW (387 MW net), and four parallel scrubber trains designed to process a total of 2,190,000 acfm of flue gas. The appplicable regulation limits SO_2 emissions to 0.6 lb/MMBtu of heat input.

The FGD system was designed to achieve 83% SO_2 removal with a design coal sulfur content of 2.0%. The system consists of four single-stage variable-throat venturi scrubbers. Each of the four absorbers has a design liquid-to-gas ratio (L/G) of 30 gallons per 1000 acf. Initial dewatering of the solids produced in the FGD system occurs in a thickener, and a vacuum filter is used for final solids dewatering.

In the one-stage scrubber train, flue gas passes through a venturi scrubber followed by the ID fan. The gas then passes through a mist eliminator and is reheated before going to the stack.

Thiosulfate was added to the FGD system at Phillips to reduce sulfite oxidation and reduce/eliminate the gypsum scaling occurring in the mist eliminators and outlet ductwork (wet ID fan, duct walls, and external mist eliminator on single-stage scrubber trains).

DUQUESNE LIGHT'S ELRAMA STATION

The Elrama Station consists of four pulverized-coal units with a gross generating capacity of 510 MW (494 MW net). The plant must meet an SO_2 emission limit of 0.6 lb/MMBtu of heat input while burning 2.1% sulfur coal. Pollution control equipment includes mechanical and electrostatic precipitators for particulate matter removal, followed by a lime FGD system for SO_2 control.

The FGD system consists of five single-stage variable-throat venturi scrubbers similar to the scrubbers at Phillips. The five Elrama venturis operate at an L/G of 30 gal/macf and treat 2,040,000 acfm of flue gas. As in the case of the Phillips Station, the Elrama system uses magnesium-augmented lime as the reagent. Initial dewatering of the solids produced in the FGD system occurs in a thickener, and a rotary vacuum filter is used for final solids dewatering.

As at Phillips, thiosulfate was added to the FGD system at Elrama to reduce sulfite oxidation and reduce/eliminate the gypsum scaling occurring in the mist eliminators and outlet ductwork (wet ID fan, duct walls, and external mist eliminator).

NEW YORK STATE ELECTRIC AND GAS' SOMERSET STATION

New York State Electric and Gas' (NYSEG) Somerset Station consists of one 650-MW (gross) boiler which began commercial operation in August 1984. The boiler fires a bituminous coal with a heating value of about 12,800 Btu/lb (as-fired) and a sulfur content which varies between 2.1% and 2.4%.

The FGD system was designed to remove 90% of the inlet SO_2. The inlet SO_2 concentration varies between 1400 ppm and 2100 ppm, depending on load and fuel sulfur content. There are six absorber modules; four modules are used during normal full-load operation. The modules are open vertical spray towers with five spray levels in each tower; four spray levels are normally used. The mist elimination section, contained in the towers above the upper spray level, consists of an interface tray (perforated plate) followed by a four-pass chevron mist eliminator. Total design gas flow for the four operating modules is 1,880,000 acfm (120°F). The liquid-to-gas ratio is 93 gal/macf. Limestone is used as the reagent. Solids produced in the FGD system are dewatered initially in a thickener, with final dewatering by rotary vacuum filters. The filter cake is blended with fly ash and lime and landfilled on site.

Thiosulfate was first added to the Somerset FGD system in October 1985 to remove gypsum scale which had formed in the thickener overflow return lines. Significant scale formation was also occurring in the mist eliminators and the interface tray wash system (wash tank, headers, and nozzles).

INDIANAPOLIS POWER AND LIGHT'S PETERSBURG GENERATING STATION UNIT 4

Unit 4 at Indianapolis Power and Light's (IP&L) Petersburg Generating Station is a 500-MW base-loaded boiler with began commercial operation in April 1986. The boiler fires a bituminous coal with a heating value of approximately 12,000 Btu/lb and a sulfur content which varies from 2.0% to 4.0%. Cold-side electrostatic precipitators (ESPs) provided by Environmental Elements Corporation limit particulate emissions to less than 0.10 lb/MMBtu. Fly ash from the ESPs is mixed with dewatered FGD solids and landfilled on site.

The FGD system was designed to remove 90% of the inlet SO_2 and limit stack SO_2 emissions to 1.20 lb/MMBtu. The system consists of three absorber trains, with all three trains required during full-load operation. The gas flow for each tower during full-load operation is approximately 567,000 acfm (120°F).

Each absorber train is a dual-loop system consisting of a quencher section followed by the absorber section. Both sections are contained in a single tower for each train. The quencher is an open spray section located at the bottom of the tower and has a liquid-to-gas ratio (L/G) of about 20 gal/macf. The absorber section is located in the tower above a bowl which separates the two sections. Flue gas from the quench section passes around the outside of the bowl. Liquid from the absorber section collects in the bowl and is sent to an external tank. The absorber section consists of two spray levels followed by a wetted film contactor (packing). The L/G for the absorber section (combined packing and spray section) is about 71 gal/macf.

Mist elimination is performed by two levels of chevron mist eliminators located in the tower above the absorber section. Limestone is used as the reagent. Solids produced by the FGD system are sent to a thickener for initial dewatering, followed by a rotary vacuum filter for final dewatering.

Thiosulfate was added to the Petersburg Unit 4 FGD system to determine if it could prevent gypsum scaling and solids accumulation on the scrubber internals. Scaling was occurring on the walls and internal support structure (nozzle headers and bowl supports) of the quench section, in the wetted film contactor, and in the mist eliminator.

SOUTHWESTERN ELECTRIC POWER COMPANY'S PIRKEY GENERATING STATION

Southwestern Electric Power Company's (SWEPCo) Pirkey Station consists of one 720-MW (gross) boiler which fires lignite with an average heating value of about 7,000 Btu/lb and sulfur content of about 1.5%. Commercial operation of the unit began in January 1985.

The FGD system consists of four absorber modules, three of which are normally required for full-load operation. The FGD system was designed to provide 90% SO_2 removal while treating 660,000 acfm of flue gas per tower with an inlet SO_2 of 5.0 lb/MMBtu. The individual absorbers are dual-loop towers with a trapout tray separating the upper and lower loop sections of each tower. The upper and lower loops have liquid-to-gas ratios of 35 gal/macf and 17 gal/macf, respectively. A single tray is installed in the upper loop to promote SO_2 absorption. The mist elimination section, which is located in the tower above the upper loop, consists of a three-pass chevron mist eliminator followed by a two-pass chevron mist eliminator. Solids produced in the absorbers are initially dewatered in a thickener, with a rotary vacuum filter used for final dewatering. The filter cake is mixed with fly ash and landfilled. Limestone is used as the reagent for the FGD system.

Thiosulfate was added to the Pirkey FGD system to solve scaling problems which were hindering system performance and reliability. The scaling was primarily occurring at the mist eliminators, lower locp reaction tank walls, lower loop recycle pump suction screens, and at the trapout trays which separate the upper and lower loops.

PUBLIC SERVICE OF INDIANA'S GIBSON STATION UNIT 5

Public Service of Indiana's (PSI) Gibson Station Unit 5 is a 670-MW (gross) boiler that began commercial operation in October 1982. The unit fires a 3.1% sulfur coal, resulting in a flue gas SO_2 level in the range of 5 to 6 lb/MMBtu.

The FGD system consists of four rectangular-shaped, horizontal open spray towers which provide cross-current scrubbing of the flue gas. Three towers are required during normal full-load operation. The mist elimination section is located at the end of each of the horizontal spray towers and consists of two chevron-type mist eliminators. Solids produced in the FGD system undergo initial and final dewatering in a thickener and rotary vacuum filters, respectively.

Thiosulfate was added to the Gibson FGD system to prevent gypsum scaling problems in the FGD system. From a clean state, the mist eliminators would take about 11 days to scale with the pressure drop increasing from 1 inch W.G. (clean) to about 4 inches W.G. (scaled). Removing scale from the mist eliminators required the absorber to be taken out of service; high pressure water was required to clean the mist eliminators.

CENTRAL LOUISIANA ELECTRIC COMPANY'S DOLET HILLS STATION

The Central Louisiana Electric Company's (CLECo) Dolet Hills Station, a duplicate of SWEPCo's Pirkey plant, is a 720-MW (gross) boiler which fires lignite with an average heating value of 7000 Btu/lb and sulfur content of about 0.6%. The sulfur content is expected to increase to about 0.9% over the life of the plant.

The FGD system is designed identical to the SWEPCo Pirkey FGD system. The only real difference between the two is that the Dolet Hills fuel sulfur content is less than half that at Pirkey. As a result, the amount of flue gas bypassed for reheat around the Dolet Hills FGD system is much greater. Also, the FGD thickener was designed for a higher fraction of sulfate in the scrubber blowdown due to the higher expected oxidation fraction caused by the lower inlet SO_2.

Thiosulfate was tested at Dolet Hills to attempt to change the settling characteristics of solids sent to the thickener by changing the composition of those solids from predominantly gypsum to a calcium sulfite/sulfate mixture. The high gypsum settling rate was causing problems with the thickener rake and thickener underflow storage tank agitators. Some pluggage was also occurring in the thickener underflow recycle lines and the lines feeding the vacuum filters.

ARIZONA PUBLIC SERVICE COMPANY'S CHOLLA UNIT 2

Arizona Public Service Company's (APS) Cholla Unit 2 is a 250-MW boiler burning coal with an average heating value of about 10,000 Btu/lb and a sulfur content of 0.5%. Mechanical collectors are used upstream of the FGD system to remove the majority of the fly ash from the flue gas. However, the FGD system also provides a significant amount of fly ash removal.

The FGD system is a dual-loop system. The first, or lower, loop is designed primarily for particulate removal, and the second, or upper, loop is designed for SO_2 removal. The system has four modules, but only three modules are needed for full-load operation. The first loop in each module is a "flooded disc" scrubber which acts as a venturi-like device. The flue gas enters the top of the flooded disc scrubber, makes a 180-degree turn at the bottom of the scrubber, and then heads upward through the second loop. The second loop is a vertical, open spray tower. Mist elimination is provided by two stages of chevron-type mist eliminators located in the absorber above the second loop. Waste slurry from the FGD system is sent to an evaporation pond for final disposal. Limestone is used as the reagent for the Cholla Unit 2 FGD system.

Severe gypsum scaling was occurring on the walls of the absorber modules just below the second loop. Deposits of over 1 foot in thickness have been reported after 12 months of operation. Thiosulfate addition to the FGD system was tested in an attempt to lower the sulfite oxidation and prevent gypsum scaling. The test also involved the addition of lime in conjunction with the thiosulfate to raise the pH of the recycle slurry. Raising the pH was necessary because of the trace metals leached from the fly ash that was removed from the flue gas by the scrubber. This is discussed in more detail in the results section.

EFFECTS OF THIOSULFATE ON SULFITE OXIDATION AND GYPSUM RELATIVE SATURATION

Thiosulfate reduces or eliminates gypsum scaling by reducing the rate of oxidation of absorbed SO_2 to sulfate. It has been well documented that when oxidation is less than about 15% of the absorbed SO_2, the sulfate which is formed precipitates as a solid solution of calcium sulfite hemihydrate ($CaSO_3 \cdot 1/2H_2O$) and calcium sulfate hemihydrate ($CaSO_4 \cdot 1/2H_2O$). Gypsum (calcium sulfate dihydrate, $CaSO_4 \cdot 2H_2O$) solids only form when the sulfite oxidation fraction is higher than about 15% of the absorbed SO_2. When oxidation is below about 15%, the gypsum relative saturation is below 1.0, which generally eliminates gypsum scaling problems.

Full-scale FGD system experience has shown that gypsum scaling is most likely to be a problem when the natural oxidation is above 15% of the absorbed SO_2. In this range, calcium sulfate will precipitate as both the solid solution and as gypsum. However, there may not be an abundance of gypsum seed crystals to serve as precipitation sites, so the gypsum also precipitates on vessel and pipe walls forming scale deposits. Also, when scrubber slurry is disengaged from the flue gas in the mist eliminators, a localized chemistry phenomenon occurs. In the presence of unreacted calcium carbonate, additional SO_2 absorption and oxidation coupled with additional limestone dissolution raises both the calcium and sulfate concentrations in the liquid phase. This can raise the gypsum relative saturation locally and result in scaling and plugging of the mist eliminators. This same phenomenon can occur on other absorber internals such as packing or trays.

Thiosulfate reduces sulfite oxidation by reacting with free radicals to break the free radical chain reactions involved in the oxidation of sulfite to sulfate. These free radical chain reactions are theorized to be initiated by trace amounts of metal ion catalysts (such as iron or manganese) and dissolved oxygen. The oxidation initiation and to some extent the overall oxidation rates are therefore functions of the liquid-phase sulfite, oxygen, and catalyst concentrations. In addition, the higher saturation temperatures which occur in FGD systems treating flue gas from high moisture lignite fired boilers tend to increase oxidation.

Thiosulfate inhibits oxidation by reacting with the free radicals which are produced in initiation or propagation reactions. The products of these reactions are trithionate ($S_3O_6^{=}$) and tetrathionate ($S_4O_6^{=}$). The effectiveness of thiosulfate (or conversely how much is required to be effective) is determined by the same factors which affect the initiation reactions. For example, FGD systems which have high magnesium or sodium concentrations (and therefore high sulfite concentrations) generally require higher levels of thiosulfate to significantly impact oxidation rates. Conversely, systems with low dissolved sulfite concentrations (due to high chlorides, for example) tend to require much lower thiosulfate concentrations to lower oxidation to less than 15% of the absorbed SO_2.

RESULTS OF FIELD STUDIES

This section of the paper summarizes the impact of thiosulfate on sulfite oxidation and gypsum relative saturation at eight FGD systems which have been studied under EPRI RP 2248-1. These effects are related to the degree of problems encountered before and after thiosulfate use with respect to gypsum scale formation. Information on limestone utilization, solids dewatering, and required thiosulfate addition rates for these plants is presented in later sections.

DUQUESNE LIGHT'S PHILLIPS AND ELRAMA STATIONS

Both of these stations had experienced severe gypsum scaling problems on FGD absorber internals and in the internal mist eliminators, outlet ductwork walls, fans, and external mist eliminators. Most of the gypsum scaling problems on the absorber internals were eliminated when the thiosorbic lime reagent was augmented with dolomitic lime. The high magnesium concentrations which resulted apparently helped reduce the formation of hard gypsum deposits within the absorber. Sodium thiosulfate addition was implemented to control gypsum relative saturation and to eliminate scale formation in the other parts of the system.

Figures 1 and 2 show the effects of thiosulfate on gypsum relative saturation in the Elrama and Phillips Stations' FGD systems, respectively. These measurements were made in August 1983. Figure 1 shows that a little over 70 ppm of thiosulfate is needed at Elrama to reduce the gypsum relative saturation to 0.9 to 1.0. However, 100 to 150 ppm of thiosulfate is needed to reduce the gypsum relative saturation to the safer operating level of 0.5. At the Phillips Station (see Figure 2), as little as 70 ppm of thiosulfate is capable of reducing the gypsum relative saturation to about 0.1 to 0.4. An examination of measured sulfite oxidation versus flue gas oxygen content showed no trends. That is, the oxidation remained constant even though the flue gas oxygen content was higher at lower loads.

The thiosulfate test data can be used to identify the optimum thiosulfate concentrations which should be maintained in both the Phillips and Elrama FGD systems. For the Phillips Station, no more than 70 ppm of thiosulfate is needed to keep the gypsum relative saturation in a safe region--below 0.5. Therefore, controlling the addition rate of thiosulfate to the scrubbers to maintain the concentration in the reaction tanks as close to 70 ppm as possible will ensure maximum benefit at minimum cost for the reagent. Similarly, controlling the addition rate of thiosulfate at the Elrama scrubbers to maintain a concentration of thiosulfate in the range of 100 to 150 ppm is needed to keep the gypsum relative saturation below 0.5. The minimum cost for raw material and the maximum benefit will be seen by controlling the concentration in this range.

The reason for the difference in the thiosulfate concentrations needed to obtain a gypsum relative saturation of 0.5 or below is thought to be due to the different liquid-phase sulfite concentrations at the two plants. The measured liquid-phase sulfite concentration at Phillips was 6 mm/L (480 ppm), while at the Elrama, it averaged 19 mm/L (1500 ppm). As has been seen during the limestone FGD thiosulfate testing which is covered in the rest of this section, higher sulfite concentrations require greater thiosulfate concentrations to achieve equivalent reductions in oxidation. This can be seen by comparing the results of the Somerset and Petersburg (low sulfite) testing to those of the Gibson and Pirkey (high sulfite) testing.

NEW YORK STATE ELECTRIC AND GAS' SOMERSET STATION

The Somerset Station had experienced gypsum scaling in its thickener overflow lines and in the mist eliminators and sieve tray wash system. This scale formation required cleaning after about six weeks of operation. Thiosulfate was originally added to the Somerset FGD system in 1985 as solid sodium thiosulfate (anhydrous). The sodium thiosulfate was added to the waste slurry sump batchwise about every three or four days. In 1988, Somerset switched to addition of sodium thiosulfate as an aqueous solution. It is now added on a daily basis to the limestone storage tank. The original method resulted in higher thiosulfate concentrations in the thickener overflow than in the absorber. The newer method results in roughly equivalent concentrations throughout the system.

Figure 3 shows the effect of thiosulfate concentration on gypsum relative saturation at the Somerset Station FGD system. Two curves are shown. One is for operation at a pH of 5.4 to 5.5 (low pH) and one is for higher pH operation (about 5.8). The thiosulfate was much more effective at high pH, requiring only 50 ppm thiosulfate to reduce the gypsum relative saturation to a value of about 0.2. With the same addition rate of thiosulfate but a lower reaction tank pH, the gypsum relative saturation was not significantly reduced below 1.0, but thiosulfate concentrations above 60 ppm were not tried because of the high costs for the required addition rate. The reason for this difference in thiosulfate effectiveness at different pH levels could be due to higher dissolved sulfite levels at lower pHs (calcium sulfite solubility is higher at lower pHs). Also, at lower pHs, trace metal catalysts' solubilities (particularly iron) are increased. Both of these effects could result in higher oxidation rates and an increased requirement for thiosulfate to "quench" the free radical chain reactions when the system is operated at the lower pH range.

Another important observation at the Somerset Station was that reduction of the gypsum relative saturation to slightly below 1.0 in the reaction tank was not sufficient to prevent scaling in the thickener overflow lines. This was due to additional oxidation occurring in the thickener, which resulted in increased sulfate concentration and, therefore, increased gypsum relative saturation in the thickener overflow liquor. It was determined that the gypsum relative saturation in the reaction tank had to be reduced to at least 0.7 in order to prevent scaling in the thickener overflow lines. Significant reduction in the mist eliminator scaling rate was seen under these conditions as well. The addition rate of thiosulfate is now controlled to maintain a gypsum relative saturation of 0.7 in the reaction tank.

INDIANAPOLIS POWER AND LIGHT'S PETERSBURG GENERATING STATION UNIT 4

The Petersburg Unit 4 FGD system had been experiencing gypsum scaling problems and solids accumulation on the absorber internals since start-up. The scaling problems occurred on the walls and internals of the first (quencher) loop, in the packing of the second loop, and in the mist eliminators. In June 1987, testing was conducted with sodium thiosulfate to determine if the gypsum scaling problems could be eliminated by lowering the oxidation rate.

The testing conducted at Petersburg showed that with thiosulfate concentrations of 30 to 200 ppm, the gypsum relative saturation in the second loop reaction tank (absorber feed tanks or AFTs) was reduced to 0.1 to 0.5. However, the gypsum relative saturations in the quencher remained at or above 1.0, except for short periods of operation at high pH (at or above 6.0) and high thiosulfate concentrations (>300 ppm). In fact, the average quencher gypsum relative saturation actually increased slightly from about 1.1 to about 1.3 when thiosulfate was present in the system.

The gypsum relative saturation in the quenchers probably increased due to a reduction in the amount of gypsum seed crystals entering from the AFT. Since the second loop oxidation was below 15%, no gypsum seed crystals were discharged to the quenchers from the AFTs in the normal overflow stream. When the amount of gypsum seed crystals in the quencher decreased, the gypsum relative saturation had to increase to maintain the same sulfate precipitation rate since oxidation in this loop was not changed by thiosulfate.

The inability of thiosulfate to reduce oxidation (and therefore gypsum relative saturation) in the quenchers can be attributed to the low pH. Figure 4 shows the relationship between pH and gypsum relative saturation measured in the quenchers with thiosulfate present. These data indicate that a pH value of about 5.3 to 5.4 is required to reduce the gypsum relative saturation below 1.0 at the thiosulfate concentrations tested (generally less than 200 ppm). Since this testing, the utility has controlled the pH in the quenchers at 5.3. The degree of gypsum scaling has been significantly reduced in this area of the tower as a result.

The reduction in the upper loop gypsum relative saturation observed at Petersburg resulted in a dramatic decrease in gypsum scale formation. Module inspections both before and after the testing showed that no deposits were formed on the packing in the second loop of one of the modules after about 10 weeks of operation. Only a small amount of soft scale was formed on another module. Prior to the use of thiosulfate, the modules were severely scaled after 9 to 12 weeks of operation. There have been two instances in the past year during which the oxidation in the second loop could not be reduced below 15% despite high concentrations of thiosulfate (up to 900 ppm). These episodes occurred during normal plant operation and were not caused by low pH excursions. The gypsum scale rate in the upper loop accelerated rapidly during these periods. No apparent cause has been identified at this time.

SOUTHWESTERN ELECTRIC POWER COMPANY'S PIRKEY GENERATING STATION

The Pirkey Station FGD system had been experiencing performance and reliability problems related to gypsum scale formation in the mist eliminators, lower loop reaction tank walls, lower loop recycle pump suction screens, and on the trapout trays which separate the upper and lower loops. Thiosulfate was first tested at Pirkey in early 1987 and was successful in lowering gypsum relative saturation to about 0.4. In August 1987, a more comprehensive test program was conducted to optimize thiosulfate addition. Since that time, the Pirkey Station has switched to emulsified sulfur to generate thiosulfate within the FGD system.

Figure 5 presents the effects of thiosulfate on gypsum relative saturation in the Pirkey FGD system. It is interesting to note that little effect of pH was observed over the range of 5.4 to 5.8. However, at the time, the plant was recycling about 300 gpm of slurry from the lower loop to the upper loop which would tend to make the liquid- and solid-phase compositions more similar between the two loops. Other plants with similar pH differences between the first and second loops (such as Petersburg) have seen significant differences in thiosulfate effectiveness, presumably due to higher sulfite concentrations and/or higher trace metal catalyst solubilities.

Figure 5 also shows that significantly higher thiosulfate concentrations were necessary to reduce the gypsum relative saturation to about 0.5 than for other plants. This is probably because of the higher dissolved sulfite concentrations at Pirkey, which are a result of high magnesium concentrations (about 100 mm/L). In addition, Pirkey fires a high-moisture lignite which results in a scrubber slurry temperature that is higher by about 10°C compared to units firing bituminous coal. This higher temperature would be expected to increase the oxidation rate of reaction significantly. This in turn might require more thiosulfate to drive the system subsaturated.

The data in Figure 5 show that about 400 ppm of thiosulfate is necessary to lower the gypsum relative saturation to about 0.5. Reduction of the gypsum relative saturation resulted in virtual elimination of the scaling problems. Before thiosulfate addition, the mist eliminators required cleaning every three to four weeks, but now stay in service in excess of seven months. Some scaling still occurs at low loads on the tray which separates the two loops and on the lower loop absorber walls, but it is significantly reduced from operation without thiosulfate.

In fact, during extended periods of operation at reduced load (50% to 75% of rated capacity), thiosulfate is unable to reduce the fraction of sulfite oxidation to below 15%. Using emulsified sulfur to generate thiosulfate has allowed the utility to economically increase the thiosulfate level to 4,000 ppm during these times in an effort to lower the oxidation. However, even at these concentrations, the oxidation cannot be dropped below 15%. Fortunately, the scaling rate in the mist eliminators increases very little during these periods. Evidently, the thiosulfate is able to reduce the formation of gypsum within the mist eliminator by affecting the localized chemical reactions which lead to scaling of this equipment.

PUBLIC SERVICE OF INDIANA'S GIBSON STATION UNIT 5

The Gibson Unit 5 FGD system had experienced gypsum scaling problems in the mist eliminators. Pressure drop across the mist eliminators would increase from about 1 inch W.G. to as high as 4 inches W.G. in about 11 days of operation. In July 1987, addition of sodium thiosulfate was tried successfully, but the cost was roughly equal to the incremental savings from reduced ME cleanings. In the first known full-scale demonstration of in-situ thiosulfate generation from sulfur, testing was conducted in November 1987 at Gibson.

Figure 6 shows the effect of thiosulfate concentration on sulfite oxidation. As shown, the oxidation decreased from about 35% without thiosulfate to about 15% at a thiosulfate concentration of about 300 to 400 ppm. Additional increases in thiosulfate concentration produced little additional decrease in oxidation. However, most of the data were collected shortly after sulfur addition was started, and the system did not have sufficient time to reach steady state. Three samples collected after several months of operation showed gypsum relative saturations of about 0.3 with 1800 to 2500 ppm thiosulfate.

Figure 7 shows the effect the presence of thiosulfate had on mist eliminator operation. The upper line shows that the mist eliminator pressure drop increased rapidly when no thiosulfate was present. Within 11 days the pressure drop had risen from about 1 inch W.G. to over 3 inches W.G. With 200 to 1100 ppm thiosulfate in the system, the pressure drop remained relatively constant over 17 days of operation.

CENTRAL LOUISIANA ELECTRIC COMPANY'S DOLET HILLS STATION

Although Dolet Hills has not experienced gypsum scaling problems within the scrubbers, the ability was tested of thiosulfate to reduce oxidation so that a mixture of calcium sulfite and sulfate solids mixture was produced instead of primarily gypsum. The thickeners at the plant were originally designed for a mixture of sulfite and sulfate, and some plugging problems were encountered because natural oxidation was converting all sulfite to the more rapid settling sulfate solids.

Figure 8 shows the measured sulfite oxidation versus thiosulfate concentration during testing conducted over the first four months of 1988. Although there is significant scatter in the data, at thiosulfate levels greater than 500 ppm, the solids produced from the scrubber will be a mixture of calcium sulfite and sulfate. The solids settling properties were changed under these conditions and thickener underflow plugging problems were stopped.

The high thiosulfate concentrations required to reduce oxidation to around 10% may be a result of the low inlet SO_2 concentration (0.6% S in coal) and/or the higher slurry temperature which results from firing lignite versus bituminous coal. The low inlet SO_2 concentration means a very high ratio of oxygen to SO_2 in the flue gas, which usually results in a high natural oxidation fraction. In addition to low SO_2, the amount of oxygen in the flue gas is increased by serious air heater and ESP in-leakage which is being investigated. The high slurry temperature would also be expected to increase the oxidation rate.

ARIZONA PUBLIC SERVICE COMPANY'S CHOLLA UNIT 2

Severe gypsum scale/deposit problems have been encountered routinely in the lower loop of the APS Cholla Unit 2 FGD system. Buildups of over 1 foot in thickness after one year of operation are typical. These deposits occur on the walls of the lower loop absorber near the bowl which separates the upper and lower loops.

In 1987, APS tested sodium thiosulfate in the system but the gypsum relative saturation could not be reduced below 1.0 in the first loop despite concentrations of over 1000 ppm. This is thought to be due to the low pH (4.5) in this loop which elevated trace metal levels and dissolved sulfite concentrations. In the Cholla Unit 2 system, the first loop is used for removing ash, which contains significant levels of oxidation catalysts (such as iron and manganese). Addition of limestone directly to the first loop to elevate the pH was tried, but it could not be raised above about 5.0. The presence of high concentrations of aluminum and fluoride was probably restricting limestone dissolution and thus preventing the pH from rising into a range in which thiosulfate would be more effective.

In July and August 1988, testing at the Cholla Unit 2 FGD system was performed using dolomitic lime as the reagent. This was tried both without limestone and in conjunction with limestone in an attempt to reduce lime costs. A sulfur emulsion was added to generate thiosulfate in situ. Because of the very low scrubber inlet SO_2 concentrations (less than 400 ppm) and because of the very high measured trace metal concentrations in solution, it was thought that achieving the goal of a gypsum relative saturation in the lower loop of less than 0.5 would be very difficult. Achieving a gypsum relative saturation of less than 0.5 would mean reducing the sulfite oxidation in the solid phase to well below 10%. To accomplish this with a system that absorbs very little SO_2 would mean reducing the rate of oxidation to an extremely low level. Previous testing at APS's Four Corners Station had indicated that very low solids oxidation could be achieved by operating the pH of the reaction tank around 7.0. The presence of magnesium in the liquid phase was also seen to be beneficial in reducing the solids oxidation and the gypsum relative saturation.

The presence of elevated magnesium in the scrubber liquor allows a significant amount of the sulfate formed in the scrubber to leave as magnesium sulfate in the liquor. Since the Cholla Unit 2 scrubber operates with no recycle of disposal pond water back to the scrubber, there is a large amount of liquor blowdown from the scrubbers relative to the amount of solids generated. This allows significant amounts of sulfate to be purged from the system in the liquid phase rather than precipitating as gypsum. The effect is to allow a lower gypsum relative saturation in the scrubber reaction tank at oxidation rates that would result in a relative gypsum saturation of greater than 1.0.

At magnesium concentrations of about 2,400 ppm, slurry pH values of 6.0 to 7.0, and thiosulfate concentrations of 1,000 to 3,000 ppm, the gypsum relative saturation in the first loop of the Cholla Unit 2 FGD system was lowered to the 0.1 to 0.3 range. One test was performed for about four system residence times (36 hours) to be sure the system was at steady state. This test used only lime as the reagent and the slurry pH was controlled at 7.0. Another test was conducted with a mixture of lime and limestone, but excessive amounts of limestone were required to keep the pH at 6.0. Operation at a pH of 7.0 resulted in the lower relative saturation (0.1) and at a pH of 6.0 resulted in the higher relative saturation (0.3). The dissolution rate of the limestone was too slow at pH 6.0 to help offset any of the lime costs.

It was thus demonstrated that it is possible to operate the Cholla Unit 2 FGD system subsaturated with respect to gypsum, which should eliminate or at least reduce the deposit buildup on the lower loop absorber walls. However, this would require conversion of the system to dolomitic lime as the reagent. The economics of savings in operating and maintenance costs versus increased reagent costs are being evaluated. It should be noted that the second loop pumps could be shut off without exceeding SO_2 emission limitations when operating the first loop at either pH 6 or 7. Several tests conducted during the thiosulfate/lime addition testing confirmed this.

EFFECT OF THIOSULFATE ON LIMESTONE UTILIZATION

A potential beneficial side effect of operation with thiosulfate in a wet limestone FGD system is an improvement in limestone utilization. This effect was not seen in all cases, however, and depended on the particular operating and chemical conditions of the scrubber. The improvement in utilization results from a significant percentage reduction in the dissolved calcium. The reduction in calcium comes about as a result of the reduction in the dissolved calcium sulfate concentration which occurs as thiosulfate acts to reduce the formation rate of sulfate in the scrubbers.

As the dissolved calcium level drops, a reduction in the calcium carbonate ($CaCO_3$) relative saturation occurs. The magnitude of the decrease in the $CaCO_3$ relative saturation governs the magnitude of the improvement in limestone utilization. The greatest percentage decrease in calcium is possible in those systems where the dissolved sulfate-to-calcium ratio is equal to or greater than 1.0. In this case, a substantial reduction in the gypsum relative saturation, for example, from 1.2 down to 0.1, will result in a large percentage decrease in the calcium level. When this happens, the dissolution rate of limestone in the reaction tank will increase due to a reduction in the calcium carbonate relative saturation. The increase in dissolution means less limestone surface area is needed in the reaction tank to maintain the pH setpoint. Thus, the excess limestone in the scrubber slurry decreases and the utilization improves. Conversely, the pH of the reaction tank may be increased and the limestone utilization kept constant. This will have the effect of improving the liquid-phase alkalinity of the scrubber and improving the scrubber SO_2 removal efficiency without increasing operating costs.

There are conditions under which the effect of thiosulfate on limestone utilization is minimal. If the dissolved calcium level is very high due to the presence of high concentrations of chloride, the improvement in utilization will be minimal. This is because, as the gypsum relative saturation is reduced after the addition of thiosulfate and the dissolved calcium and sulfate concentrations drop, the relative decrease in calcium is much less than in a low chloride liquor. As a result, the effect on the $CaCO_3$ relative saturation is reduced to the extent that little, if any, improvement is seen in utilization.

In addition, unless a substantial reduction in the calcium sulfate relative saturation is observed from the addition of thiosulfate, the improvement in utilization will be minimal. Two conditions have been observed in which there has been difficulty in lowering the gypsum relative saturation below 1.0. The first is when the coal sulfur level is low (the lower limit has not been identified). With the low SO_2 absorption rates, the fraction of SO_2 which oxidizes is such that gypsum must precipitate, thereby keeping the relative saturation of gypsum above 1.0. Despite large concentrations of thiosulfate, no further reductions in oxidation can be realized. The second condition is high inlet O_2 levels to the scrubber due to low load operation. Apparently in at least one case, the initiation step in the overall sulfite oxidation reaction is fast enough that it results in greater than 15% of the SO_2 absorbed being oxidized. Again, this causes the gypsum relative saturation to be above 1.0.

Of the five limestone FGD systems tested with thiosulfate, significant improvements in utilization were seen at two. Both PSI's Gibson Station and SWEPCo's Pirkey Station reported improvements in limestone utilization as a result of operation with thiosulfate. However, in both cases, certain operating conditions were observed which caused the improvement to go away. At Gibson, switching to a low-sulfur coal (3 lb SO_2 per million Btu) caused the gypsum relative saturation to rise and, along with it, the dissolved calcium level. This situation probably occurred due to the lower amount of SO_2 being absorbed relative to the constant amount which was being oxidized, as discussed above. The improvements in limestone utilization were lost for the period of time that this coal was being burned. At Pirkey, operation at low load caused the gypsum relative saturation to increase and the improvements in utilization to drop off. It is believed that the higher flue gas O_2 concentrations during low load operation caused the higher oxidation rates. The high rate of oxidation could not be reduced despite elevating the thiosulfate concentration to greater than 4,000 ppm.

Under normal operating conditions, and with approximately 2,500 ppm of thiosulfate in the Gibson scrubbers, the limestone utilization has improved from an average of 87% to over 99% (calcium fraction only) at a reaction tank pH setpoint of 5.4.

By controlling the thiosulfate concentration at 1,500 ppm in the Pirkey FGD system, a significant improvement in limestone utilization results when the unit is operating at higher load. Taking advantage of the higher limestone dissolution rates, the Pirkey scrubber pH setpoints have been elevated so that the utilization remains unchanged. The lower loop pH setpoint has been raised from 5.2 to 5.5. The upper loop pH setpoint has been raised from 5.9 to 6.2. The overall limestone utilization is still greater than 90%. The higher pH setpoints have resulted in improved SO_2 removal efficiencies for the scrubbers according to plant personnel. The higher removals allow more flue gas to be bypassed, reducing the system pressure drop and increasing the stack exit temperature. In addition, as the unit load is decreased during off-peak periods of the year, a tower can be taken out of service earlier because of the higher amounts of gas bypassed.

EFFECT OF THIOSULFATE ON SULFITE CRYSTAL MORPHOLOGY AND SOLIDS DEWATERING

Improvements in the dewatering characteristics of some calcium sulfite sludges have been attributed to the use of thiosulfate. This benefit was first observed during tests performed at the TVA 10-MW Shawnee Test Facility and later observed at an EPA-sponsored test program at the Research Triangle Park test facility in North Carolina. The work performed at Shawnee has led to a patent being issued to TVA for the use of thiosulfate to generate improved settling calcium sulfite solids from limestone scrubbers.

The changes that have been observed in the crystal habit of sulfite solids from limestone systems using thiosulfate include: larger mean particle size; increased thickness of individual crystals; and increased tendency for single crystals rather than agglomerates to form. Each of these changes would account for an improvement in the dewatering characteristics of the sulfite solids. In combination, these changes can result in a dramatic improvement in settling and filtering characteristics--approaching that of gypsum.

As in the case with limestone utilization, the presence of thiosulfate itself does not automatically result in improvements in the settling characteristics of the calcium sulfite solids. This is because thiosulfate does not act as a crystal modifier of the precipitating calcium sulfite. The improvements in the sulfite crystal occur as a result of less sulfate being formed in the scrubber. This has the effect of producing a more pure sulfite crystal which has substantially less sulfate present in the sulfite crystal lattice.

The only condition under which a very pure sulfite crystal will precipitate is a very low sulfite oxidation environment. In other words, the inhibition of oxidation due to thiosulfate must be great enough so that the overall fraction of sulfite oxidized is in the range of 1% to 5%. These numbers are not exact owing to the difficulty of quantifying the oxidation fraction when it is in this range. Nonetheless, there have been very few cases documented in the application of thiosulfate to utility scrubbers where this low level of sulfite oxidation has been achieved.

Of the eight plants reported on in this paper, none have been able to produce the dramatically large sulfite crystals. In most cases, this appears to be due to the relatively large amount of sulfite which is oxidizing as a result of the initiation oxidation step which is not strongly affected by the presence of thiosulfate. The possibility of forming the large crystals appears greatest at Somerset since the factors which contribute to achieving low oxidation rates are all present: low dissolved sulfate, high inlet SO_2, and a scrubber temperature in the range of 125 to 130°F. However, at this time, the thiosulfate concentration is being controlled at a level which is sufficient for prevention of scaling, not at the higher level which would lower the oxidation fraction of sulfite into the 1% to 5% range. At Somerset, there is no economic incentive to do this--the dewatering equipment is designed for the slow settling sulfite crystals.

ANNUAL COSTS FOR THIOSULFATE USE

Costs for operation with thiosulfate in the FGD systems of the eight plants reported in this paper are presented in Table 1. The cost numbers reflect the current consumption of sodium thiosulfate or sulfur as of mid-1988 for all but the Duquesne plants. The cost numbers for Duquesne's Phillips and Elrama Stations are based on the feed rates observed during the testing which took place in 1983.

For the Phillips, Elrama, Somerset, and Petersburg Stations, the estimates are based on the material they are currently using (sodium thiosulfate), and for the others, the estimates are based on the material they used during testing (sulfur emulsion). Sulfur emulsion, which is a 70 weight percent suspended sulfur aqueous slurry, represents a lower cost alternative to sodium thiosulfate. Typically, about 50% of the sulfur added to the FGD system reacts to form thiosulfate. At this conversion efficiency, the costs for using this source of thiosulfate are a factor of 7 or 8 less than the costs for using sodium thiosulfate.

There is a wide variation in the addition rates of thiosulfate. The numbers presented in Table 1 for the addition rates have been converted to an equivalent thiosulfate basis for comparison. As discussed previously, the concentration of thiosulfate (and therefore the addition rate) necessary for a reduction in the gypsum relative saturation varies according to the particular design, operating, and chemical conditions of each FGD system. For example, the thiosulfate addition rates for the Somerset and Petersburg FGD systems are relatively low compared to those for the Gibson and Cholla FGD systems. This is because at Gibson, the dissolved sulfite concentration is approximately a factor of 10 higher than that at either Somerset or Petersburg. The consumption at Cholla is high because of the low inlet SO_2 and the once-through water arrangement for the scrubbers. No water is recycled from the disposal pond to the scrubbers.

SUMMARY

The use of thiosulfate in wet lime/limestone scrubbing systems has resulted in a major improvement in the reliability of this type of FGD system. The successes with the application of this material extend to many other FGD installations besides those documented in this paper. The ability to reduce sulfite oxidation in the lime/limestone wet FGD system with relatively little cost and with no known adverse side effects has resulted in significant cost savings to date. For example, the net reduction in the annual FGD O&M costs at PSI's Gibson Station due to the use of thiosulfate has been estimated to be over $500,000. For SWEPCo's Pirkey Station, the net reduction in the annual FGD O&M costs attributed to the use of thiosulfate is estimated to be approximately $350,000. The exact amount of thiosulfate that is required to reduce the sulfite oxidation rate is a function of the particular chemistry and operating conditions which prevail within an FGD system. Variations in the dissolved species, especially calcium, magnesium, chloride, and sulfite, as well as inlet SO_2, flue gas oxygen, reaction tank pH, and the gas saturation temperature all impact the effectiveness of thiosulfate. These variables should all be taken into account to achieve maximum benefit from the use of thiosulfate in lime/limestone scrubbing systems.

ACKNOWLEDGMENTS

The authors of this paper would like to recognize the participation and assistance of the utility staffs of: Duquesne Light Company, New York State Electric and Gas, Indianapolis Power and Light, Southwestern Electric Power Company, Public Service of Indiana, Central Louisiana Electric Company, and Arizona Public Service. Their roles in the testing contributed greatly to the quality and quantity of information which was used in completing this paper. In addition, their work in this area has led to a significant advancement in the reliability of wet lime/limestone FGD technology.

The work described in this paper was not funded by the U.S. Environmental Protection Agency and therefore the contents do not necessarily reflect the views of the Agency and no official endorsement should be inferred.

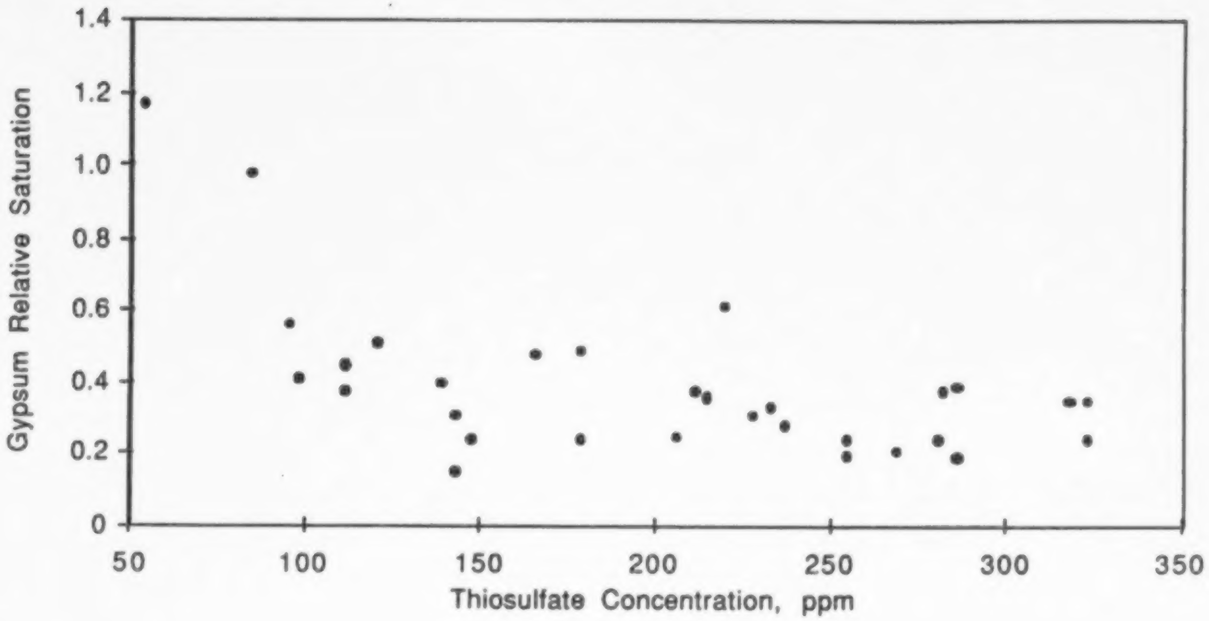

Figure 1. Effect of thiosulfate on gypsum relative saturation - Elrama Station.

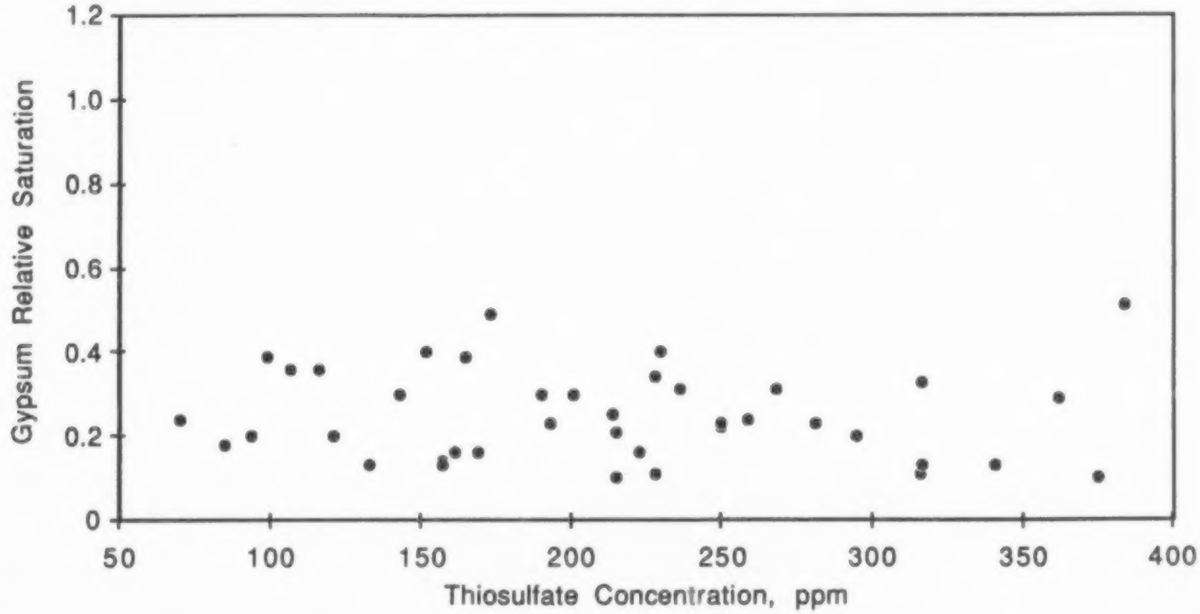

Figure 2. Effect of thiosulfate on gypsum relative saturation - Phillips Station.

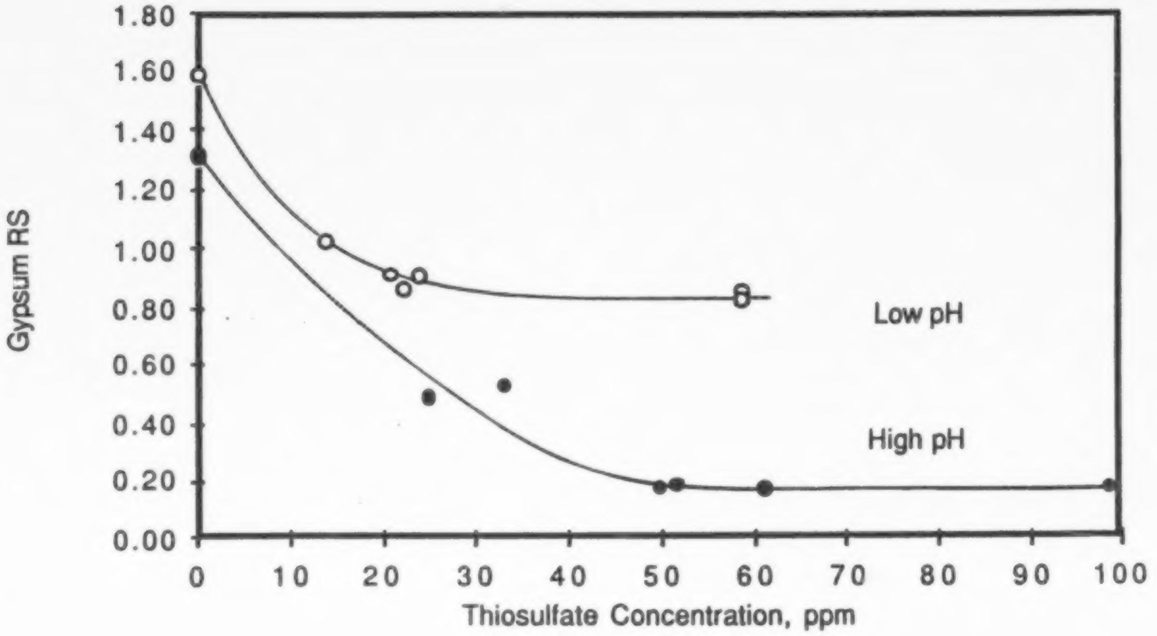

Figure 3. Effect of thiosulfate on reaction tank gypsum relative saturation - Somerset Station.

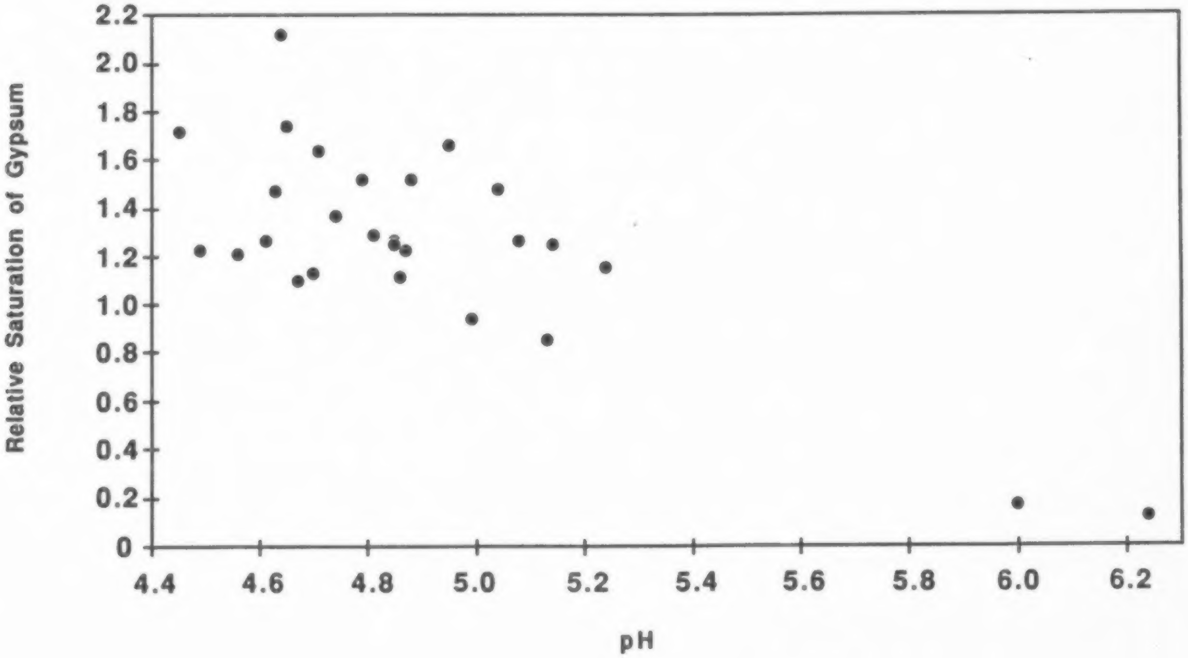

Figure 4. Effect of pH on gypsum relative saturation in the quencher loops at Petersburg Unit 4 (with thiosulfate).

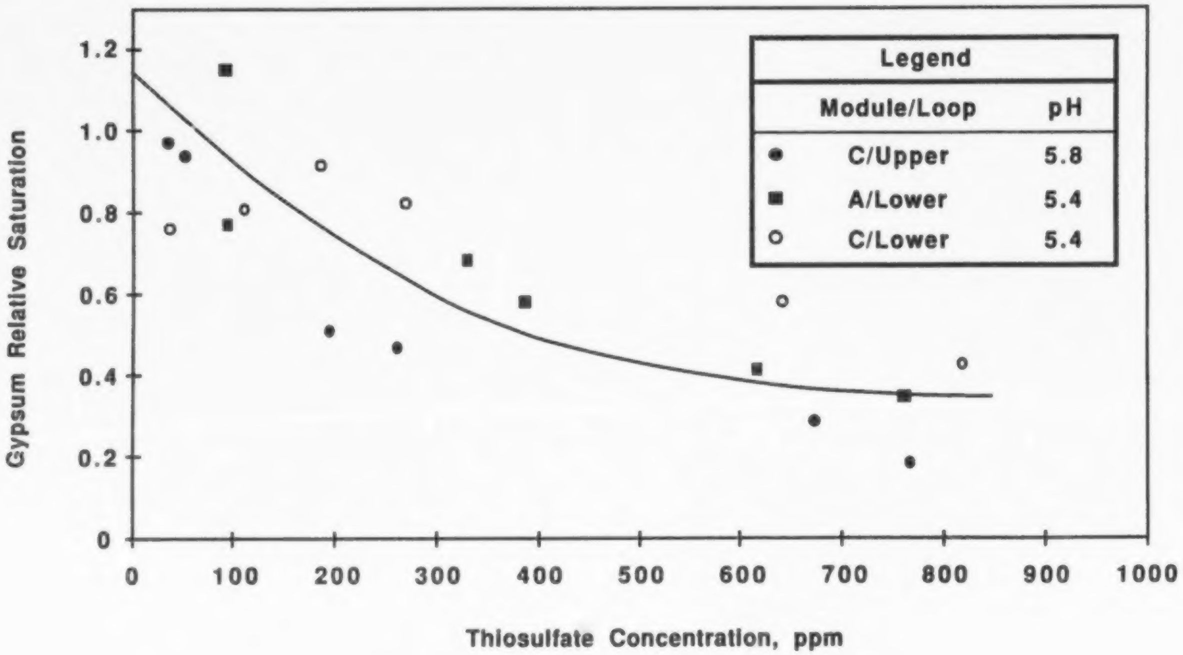

Figure 5. Effect of thiosulfate on gypsum relative saturation - Pirkey Station.

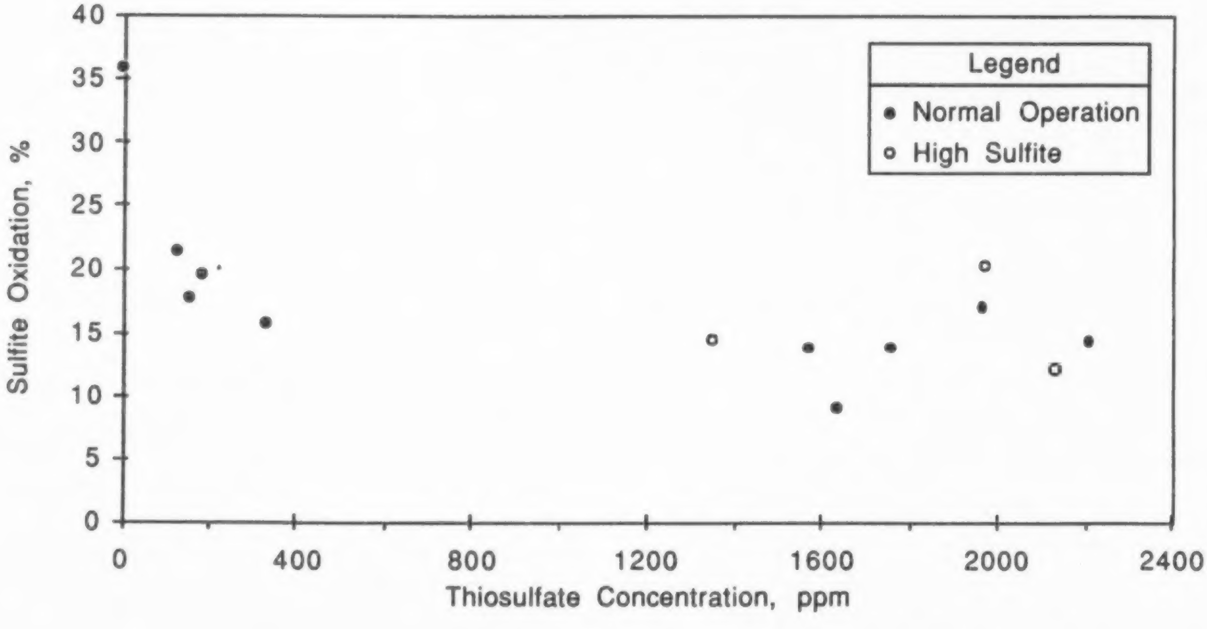

Figure 6. Effect of thiosulfate on sulfite oxidation, pH 5.24 to 5.64 - Gibson Station.

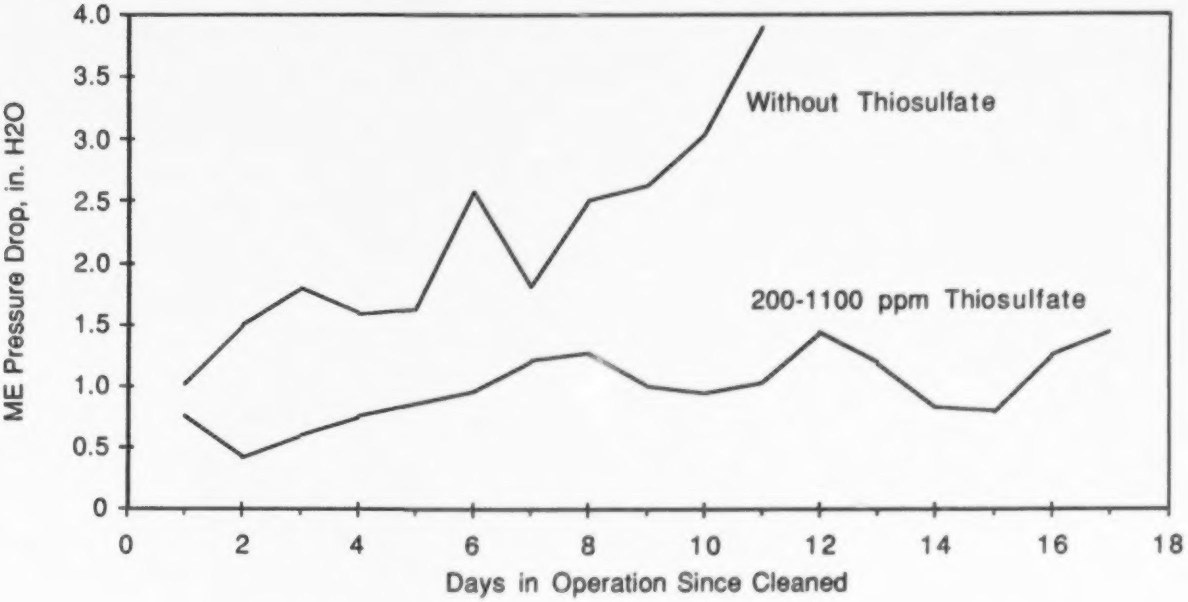

Figure 7. Mist eliminator pressure drop - Gibson Station.

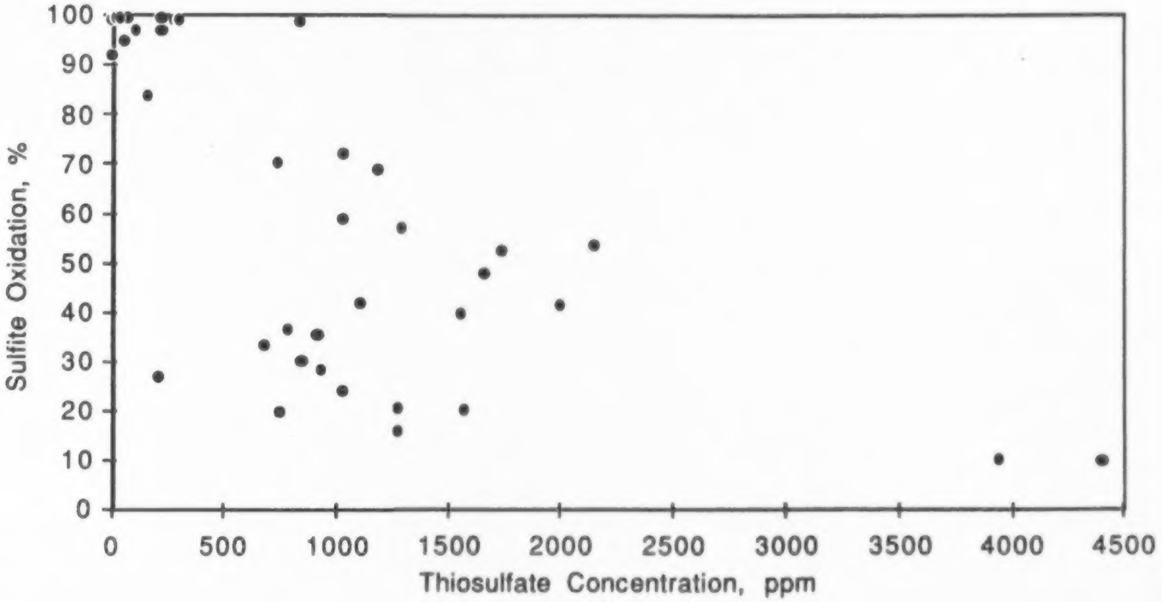

Figure 8. Effect of thiosulfate concentration on sulfite oxidation at Dolet Hills (lower loop).

TABLE 1. PROJECTED ANNUAL COSTS FOR THIOSULFATE USE IN UTILITY FGD SYSTEMS

Plant	Plant Size (MW)	Additive Form	Addition Rate as lb $S_2O_3^{=}$/hr	Concentration (ppm $S_2O_3^{=}$)	Projected Annual Cost[a]
Duquesne Phillips	400	Solid $Na_2S_2O_3\cdot 5H_2O$	8-23[b]	100-525	20,800-61,200
Duquesne Elrama	510	Solid $Na_2S_2O_3\cdot 5H_2O$	23	75-450	61,200
NYSEG Somerset	650	Solid $Na_2S_2O_3$	59	20-100	161,000
IPL Petersburg Unit 4	530	Liquid 30 wt.% $Na_2S_2O_3$	36	230	99,000
SWEPCo Pirkey	720	70 wt.% Sulfur Emulsion	72	1,500	38,400
PSI Gibson Unit 5	670	70 wt.% Sulfur Emulsion	124	2,500	66,500
CLECo Dolet Hills	720	70 wt.% Sulfur Emulsion	128	2,000-4,000	68,300
APS Cholla Unit 2[c]	250	70 wt.% Sulfur Emulsion	150	1,000	80,500

[a] Based on addition rate assuming 300 days of operation per year. Sulfur - \$0.13/lb. $Na_2S_2O_3\cdot 5H_2O$ - \$0.17 lb. $Na_2S_2O_3$ - \$0.27 lb.

[b] 23 lb/hr at loads less than 200 MW. 8 lb/hr at loads greater than 200 MW. Addition rate is greater at low loads because of higher flue gas oxygen content.

[c] Based on test results. Permanent feed system is pending evaluation.

DESIGN, STARTUP AND OPERATING EXPERIENCE OF FGD SYSTEM WITH GYPSUM BYPRODUCT AT RIEDERSBACH NO. 2 IN AUSTRIA.

by Peter J. Kneissl, OKA-Riedersbach, St. Pantaleon, Austria, A-5120
Gernot Staudinger, Univ. of Technology, Graz, Austria, A-8010
Manfred Weitzer, Waagner-Biro, Graz, Austria, A-8010
Ramani Iyer, GE Environmental Services, Inc., Lebanon, Pennsylvania, 17042

ABSTRACT

The Austrian government recently enacted a law introducing strict emission regulations for power plants to control SO_2, NOx, particulate and effluent water quality. As a result, the design of Riedersbach No. 2, 160 MWe unit, which went into commercial operation in the autumn of 1986 (1), incorporated the latest available control technologies. Selection and design of the FGD-System presented a unique challenge as the boiler was designed for multi-fuel firing including lignite, bituminous coal and high sulfur oil (2). Due to solid waste disposal restrictions, production of commercial grade gypsum for use in the wall-board and plaster industry was mandatory.

The FGD-System was selected from fifteen different offers from worldwide suppliers (3). The system chosen consists of a prescrubber (for fluoride, chloride removal), absorber, wet fan (downstream of the absorber), gas/gas reheater, gypsum dewatering system (hydrocyclones and vacuum belt filter), steam heated gypsum dryer and briquetting equipment (4, 5). A limestone grinding mill economises on operation costs and facilitates high efficiency in the removal of SO_2. A system for treating waste water deals with the water flowing from the FGD-System before discharge.

In over 8000 hours of operation more than 50,000 tons of commercial grade gypsum have been produced. Overall reliability of the FGD-system during this period is, according to the results obtained, excellent.

Towards the end of this paper the influence of the quality of limestone and its grinding on high removal of SO_2, plus the production of excellent commercial grade gypsum will be discussed. Particle Size Analysis with the LUMOSED (6) is a low cost and effective means to optimize limestone grinding for achieving both, sulfur removal of more than 95 % and a low sulfite gypsum. Further, the LUMOSED proved to be a powerful tool in detecting the causes of operational problems in relation with the scrubber slurry; it enables the operator to anticipate a runaway of the particle size in the slurry system.

A process, in which limestone particle dissolution and gypsum particle formation are the governing mechanisms should be furnished with particle measuring equipment.

INTRODUCTION

At present the annual consumption of energy in Austria is 1000 Petajoules (approx. 278,000 GWh). About two thirds of the energy required - mainly crude oil and natural gas - has to be imported.

The total annual production of electricity is about 45,000 GWh and a quarter of this electricity comes from thermal power stations. Since the option of nuclear energy has been rejected in Austria and because of the two oil crises, the increased building of power stations fired by local lignite and imported bituminous coal has been encouraged.

At the same time environmental issues have gained major political importance especially those concerning the prevention of air pollution. In addition to the stringent regulations on the environmental effect of pollutants specified by the Austrian Academy of Sciences, extremely severe laws on air pollution control for the protection of forests have been passed. Mainly regulations concerning large steam boiler plants have been put into force and their emission standards have gradually been tightened. Thus it may be said today that the Austrian policy concerning restrictions on power plant emissions is one of the most advanced and stringent in the world.

These altered circumstances presented our company, the Oberoesterreichische Kraftwerke AG (OKA), with the challenge of finding new solutions to the technical problems when building started on the new thermal power plant Riedersbach No. 2 (figure 1: Riedersbach Power Plant).

FUEL SUPPLY

Local lignite with a relatively high sulfur content forms the basis of the fuel supply. To cover the insufficient supply of local lignite, bituminous coal available on the world market and heavy fuel oil has also been considered in the design, as well as domestic and foreign lignite. This means that not only all the equipment for the combustion of the most diverse types of fuel has been installed, but also that the wide range of different flue gas compositions have had to be considered in the design of the downstream flue gas cleaning systems (table 1: Flue gas data).

This range in flue gas compositions caused particular difficulties when a suitable flue gas desulfurization process had to be selected.

EMISSION AND GROUND LEVEL CONCENTRATION REGULATIONS

Very stringent laws on emissions and their environmental effect plus monitoring devices have officially been stipulated for the intended site of Riedersbach which is situated close to the border between Bavaria and Salzburg in a densely forested and agriculturally utilized recreational area. In addition to the environmental protection plan that takes into consideration the on-line connection to the automatic air monitoring stations which record the level of pollutants and the Salzburg weather centre supplying its meteorological data, extensive forestry, agricultural and biological control measures have also been prescribed. The latest version of the "Act on Steam Boiler Emissions" and local government agreements form the basis of the emission limitations for the power plant (table 2: Government Regulations on Emission and Ground Level Concentrations for Riedersbach No. 2). In Austria is it the half-hour mean value which is the decisive evaluation factor for the restriction of pollutants and not the annual or daily mean values. It was not only the high ash content of the lignite (approx. 30 %) but also the considerably varying content of the sulfur dioxide in the flue gas, often changing within a short period of time, that presented a major design problem. Furthermore, the relatively high fluorine content in the local lignite and possibly high chlorine content in the bituminous coal also had to be considered in controlling the emissions. Since the construction of the power plant had already begun in 1982 and the decision to build the FGD-plant was only taken in 1983 and putting the system into operation had to take place in 1985/86 because of the coal supply contracts, there was very little time available to decide on the proper process and the construction of the plant.

DESIGN CRITERIA FOR THE FGD-PLANT AND SELECTION OF THE PROCESS

The following principal requirements formed the basis for the design of the FGD-plant (table 3: Design Criteria for the FGD):

- Treatment of 100 % of the flue gas volume when firing lignite and a mixture of lignite, bituminous coal and fuel oil respectively.
- Desulfurization by at least 95 % of the peak sulfur content in the lignite.
- Complete profitable utilization of the product at the same time avoiding the need for dumping grounds.
- Lowest possible operating costs.
- Maximum operational reliability and the reduction to a minimum of forseeable risks.

Whilst dealing with the international tenders, which led to more than 15 offers, it was realized that the expertise of the USA and the Federal Republic of Germany could not be applied without modifications. In the USA, the residues were virtually all dumped and in the Federal Republic of Germany the operators of lignite fired power stations still followed the "dry" method. It was only in Japan that partially applicable methods were found, although not for lignite.

It was necessary to eliminate the dry-additive process because of its insufficient desulfurization rate and also the spray absorption process, mainly because of the too costly agent used. A single cycle limestone scrubber could not be safely considered with regard to the quality of the gypsum given by the existing range of fuel qualities. A further detailed tender led to six offers, namely: three two-cycle limestone scrubbing processes, one Austrian MgO process, one caustic process and one ammonia process. Eventually the IFO limestone scrubbing process with a prescrubber from General Electric was chosen and in April 1984, Messrs. Waagner-Biro of Graz, a licensee of GE, were awarded the contract.

In order to cope with the requirements of all the load ranges and all fuel conditions the following basic system was chosen (figure 2: Flowsheet of FGD Riedersbach No. 2):

By employing extensive primary measures to reduce the NOx content in the combustion chamber it was possible to keep within the present NOx limits. A sophisticated electrostatic precipitator, with a guaranteed efficiency of 99.85 %, is employed to remove the fly ash from lignites containing a high percentage of ballast substances.

Two I.D. fans transport the flue gas from the boiler into the FGD or, in the case of a breakdown, via the open by-pass into the stack. A regenerative gas/gas reheater (REGAVO) is installed upstream of the FGD, it is followed by a prescrubber with a downstream mist eliminator, and the main scrubber with five spray levels and recycle pumps. The clean gas flows to the wet fan via a two-stage mist eliminator system (horizontal/vertical). On its way into the stack the flue gas is reheated in the REGAVO. Limestone is supplied by means of a limestone grinding mill and an intermediary slurry tank. Gypsum is dewatered using hydrocyclones and vacuum belt filters. The gypsum cake is dried using waste steam from the turbine and finally briquetted. Additional water is supplied by a deep well; the waste water removed from the prescrubber is purified in a multi-stage treatment plant and joins the flow of cooling water, virtually with the quality of drinking water. The sludge from the waste water treatment is recycled via the vacuum belt filter and discharged with the gypsum.

DESIGN CRITERIA

Criterium 1: Treatment of 100 % of the flue gases when firing either lignite or a mixture of lignite - bituminous coal - fuel oil (figure 3: Detailed flow diagram of the FGD).

The I.D. (2) and the wet fan (12) are designed to cope with the highest potential output of flue gas. The principle of the control system permits the operation with an open by-pass attaining recirculation of about 5 - 10 % of the clean gas. This also guarantees a safe operation of the boiler in case of a change in fuel and pressure variations in the combustion chamber. The highly efficient fly-ash removal system prevents the transmission of ash and associated heavy metals in to the FGD even when fuels with a high ballast content are used. The prescrubber (6) guarantees the removal of the residual dusts and ensures constant conditions for the removal of SO_2 in the spray tower regardless of the fuel used. The complete elimination of chlorine and fluorine in the prescrubber and the downstream mist eliminator (10), which is designed to be a chlorine trapping system, provide sufficient desulfurization for the most diverse flue gas compositions.

Criterium 2: Guarantee of at least 95 % efficiency in the removal of SO_2, even with a peak sulfur content in the lignite.

For short periods of time the SO_2 content in the untreated gas may sometimes amount to 8,000 mg/Nm^3 (dry, 6 % O_2) when firing lignite. As the half-hour limit is set at 400 mg/Nm^3, the FGD has to be able to maintain a SO_2 removal rate of at least 95 % even when dealing with maximum flue gas quantities. Due to the design of the spray tower (7), which has a high L/G ratio in the range of 23 and the existing five spray levels, each with a recycling pump, a high degree of SO_2 removal efficiency can be achieved.

The wet fan (12) plays an essential part in the efficiency of desulfurization. Due to the difference in pressure, the wet fan ensures that any leakages of flue gas are always forced from the clean to the untreated gas side. Thus there is no need for sealing measures and the efficiency of the scrubber is virtually equal to the efficiency of the entire FGD-System. A further contribution to the removal of SO_2 is made by the preparation of the limestone in an on-site grinding mill (15). The possibility of selecting highly reactive limestones and the fineness of grinding (80 % with a grain size < 20 µm) plus the presolution in the intermediary slurry tank (16) produces a highly reactive scrubbing solution. The advantages of this will be dealt with in greater detail later in the paper.

Criterium 3: Complete profitable utilization of the product at the same time avoiding the need for dumping grounds.

Fly ash from the electrostatic precipitator (1) is used in the production of cement and concrete which comply with Austrian production standards (Austrian standards B 3319 and B 3320). As the flue gas is treated in the prescrubber (6), the growth of crystals in the main scrubber can take place in optimum conditions without any interference. The finely ground reactive limestone slurry, of optimum limestone quality, ensures good reaction conditions and the IN SITU-FORCED-OXIDATION (11) plus the length of time spent in the spray tower sump create excellent conditions for the growth of gypsum crystals whilst maintaining an extremely low sulfite content in the by-product. The "cut-point" of the hydrocyclone (19) is at about 20 µm and due to the fine grinding of the limestone, the $CaCO_3$ content of the gypsum plus the stochiometry is at an optimum level. In most cases of operation it is also possible to connect the waste water treatment plant (25) in such a way that the produced sludge is deliberately recycled to the gypsum. The lowest possible level of ash in the prescrubber, the quality of the water added and high quality limestone permit this recycling of sludge whilst at the same time maintaining the specified gypsum standards.

Criterium 4: Lowest possible operating costs.

Costs for the initial input of energy are completely avoided by having the regenerative gas heater (REGAVO) (5) to reheat the flue gases. Due to the installation of the fan (12) in the wet zone there is a considerable decrease in the plants electricity requirements and the gypsum (26) is dried by means of steam tapped from the turbine. The use of cheap limestone gravel and the sale of the gypsum by-product also reduce the operating costs. The transport and storage costs of the raw materials and the final product have been minimized by briquetting the gypsum and selecting an appropriate size of limestone pebble. The In Situ-Oxidation (11) avoids the cost of additional chemicals and due to the computerized operation and control the monitoring and operating personnel costs are low.

Criterium 5: Maximum operational reliability and reduction to a minimum of forseeable risks.

By choosing a well tested limestone scrubbing process and adjusting it to the particular requirements of the Riedersbach No. 2 Power Station, the risks have been reduced as far as possible. The open by-pass (4) guarantees a greater degree of safety in the operation of the boiler in case of a malfunction in the FGD and conversly also ensures the safety of the FGD-plant in case of a fault in the boiler. The superfluety of the auxiliary systems and the sufficient dimensions of the flue gas ducts and spray tower considerably contribute to the high efficiency of the plant. A sophisticated mist eliminator system (10) downstream of the spray tower prevents any interference in the running of the wet fan. The necessary cleaning cycles of the regenerative gas heater (REGAVO) are reduced to an absolute minimum while still fulfilling operational requirements.

OPERATING EXPERIENCES

COMMISSIONING

After the boiler plant had successfully been put into operation, the initial operation of the FGD, including its auxiliary systems, such as the waste water treatment plant and the gypsum production plant, could be started on time in the autumn of 1986 after only 28 months of construction time (figure 4: Schedule of trial and commercial operation and availability of FGD).

The open by-pass concept and wet fan design with a variable pitch control has proven particularly successful during the starting up phase of the FGD since even total failures of the FGD-plant did not have any negative effects on the operation of the power plant.

One of the most important reasons for faults during the starting up phase was the failure of the various materials of the fixing bolts for the spray levels in the prescrubber. Unsealed fibreglas, reinforced plastic material plus HASTELOY-C4 bolts, was destroyed by corrosion within a few days. The sealed bolts of fibreglas, reinforced plastic used at present are a suitable solution in the existing circumstance where there is a relatively low amount of chloride entering the system while at the same time the fluoride content is high and the pH-value is about 1. Despite the complex mist elimination system and a sophisticated electrostatic precipitator, the gas reheater is still subject to dirt which displays an uncharacteristic behavioural pattern. This dirt builds up relatively slowly but still cannot be adequately removed by the installed air blowing devices. The problem is dealt with by means of regular high pressure washing with water during normal operation and correction of the fault is underway in corporation with the supplier.

There were also some difficulties with the comprehensive sound protection measures, i.e. the mineral wool of the absorption silencers on the pressure side of the oxidation air fan disintegrated and led to severe pluggages within the oxidation air systems. This problem was overcome by replacing the absorption material. The design of the corrosion resistant reflexion silencer downstream of the FGD fan is a recently developed product. Due to mechanical problems with the plastic supporting structure, foam material was carried along by the flue gas into the duct. The necessary modification to the design has been carried out. In the gypsum treatment plant the necessary modifications to the belt filter cloths for gypsum dewatering and modifications in the steam heated dryer have already been completed. The on going optimization efforts of the briquetting system enabled the by-product to be stored out of doors as early as the first operational phase. More than 93 % (16,300 t) of the gypsum produced during the first period conformed to the standards of the gypsum industry and the remaining 7 % (1,700 t) were used for the production of cement since the sulfite content was marginally too high for plaster production.

OPERATIONAL EXPERIENCES

Up to now the plant has been in operation for more than 8000 hours. The efficiency and reliability of this plant is very satisfactory. From our point of view, the overall concept has proven very successful and in conclusion we can say that the following positive results have been obtained.

The requirement of achieving a high efficiency in the removal of SO_2 with the variety of fuels used and varying limestone quality yet producing a gypsum of constant high quality comes up to expectations. As it can be seen from figure 5 and figure 5a (desulfurization efficiency), SO_2 emissions have always been in compliance with the half-hour limit of 400 mg/Nm^3 (dry, 6 % O_2) despite different operational conditions. Due to the high L/G ratio and the reactive limestone slurry, the pH-optimization in the scrubber had always been possible and this also assured a constant high level of SO_2 removal even during peak loads of SO_2. We believe that this special reactivity is due to the fineness of the limestone at 80 % with a diameter less than 20 µ ground in the wet ball mill on site.

Operational experience to date has shown that the use of considerably finer ground material resulted in important advantages in the process for the following reasons:

- To achieve a maximum SO_2 removal efficiency, high pH-values are required.

- The oxidation of calcium sulfite necessary to meet the required quality of gypsum, however, puts an upper limit on the pH-value.

Using ground limestone of 90 % < 63 µm, a limited sulfite content ($SO_2 \leq 0.25$ %) in the gypsum for a pH-value of up to 5.8 could be assured.

Using ground limestone of 80 % < 20 µm from the ball mill on site, the required limit of sulfite in the gypsum could be achieved for a pH-value of more than 6.0 in the scrubbing slurry. This means that the use of finely ground limestone from the power plants grinding mill led to a considerable improvement in achieving the required gypsum quality and SO_2 removal.

In addition to the above improvements the limestone content in the gypsum could be minimized to about 1 % of the limestone used (table 4: Gypsum quality). Since the chemical parameters of the limestone are of great importance to the desulfurization process, it was necessary to define an optimal composition of limestone. The minimum requirements specified by the supplier to the FGD-plant were used as a basis for selecting a suitable limestone:

- at least 95 % $CaCO_3$ content
- less than 1.5 % MgO content
- particle size specification of 90 % < 63 µm
- reactivity: minimum requirements according to a specified calibration curve

Moreover, the following criteria were also considered when evaluation the quality of the limestone:

- Iron content and compounds not soluble in HCL.
  This requirement had to be considered in view of the whiteness of the gypsum produced by the FGD-plant since the whiteness of this product depends on the whiteness of the limestone used, which shows a good correlation with the content of iron and compounds not soluble in HCL.

- Silicates content.
  In order to avoid erosions, especially in the feed pumps, a minimal silicate content was required.

- The content of other compounds, such as phosphates, chlorine, fluorine, sodium and potassium oxides, which depends on the limits set by the gypsum user, had to be considered.

- Limitation of the limestone to an acceptable grain size between 30 and 90 mm for use in the crusher of the on site grinding mill. This requirement has been specified for the following reasons:

- To avoid difficulties with the conveyor devices in the limestone grinding plant, eg. plugging, scaling, clustering due to frost in winter, etc.
- to assure minimum contamination with soil, organic and clay, found in limestone quarries and thus where possible, to avoid problems with the gypsum whiteness, formation of foam in the slurry and the treatment of waste water, eg. high chemical oxygen demand.

To examine the chemical composition, a great number of samples from possible limestone suppliers were analysed and evaluated according to the above criteria. On the basis of these results and taking into consideration the operational costs of the FGD, a limestone that was as pure as possible was selected. Thus the design criterium of complete utilization of the by-product whilst avoiding the need for dumping grounds was achieved:

- Since putting the FGD-plant into operation, a gypsum that is suitable for the gypsum industry is produced (figure 6: Gypsum crystal).

- From the beginning the excellent quality of the FGD gypsum an optimum operation of all the components of the FGD (eg. excellent dewatering of the gypsum slurry by means of the hydrocyclones and belt filter without any problems due to the favourable structure of the crystals; this also means favourable conditions for drying and briquetting the gypsum).

- No problems with the process due to the formation of foams.

- Extremely low erosion problems of all pumps.

- Low impurities in the waste water and therefore no problems with effluent treatment and discharge of purified waste water and solide from the treatment plant. The solids are recycled into the gypsum without any negative effects on the quality of the gypsum.

The design objective to achieve the lowest possible operating costs has been successfully realized and to date has proven its suitability during operation:

- The use of limestone pebbles and the production of high quality gypsum enables low production costs to be achieved.

- The total energy input is low due to the regenerative gas reheating system and the use of LP steam to dry the gypsum.

The briquetted gypsum can easily be transported and, due to its reaction and resistance to freeze/thaw cycles, can also be stored out of doors. There also exists an optimal solution to the problem of transportation since the overall road transport requirements have been optimized by delivering limestone pebbles and taking gypsum briquettes as return freight.

Comprehensive tests to assess the suitability of outdoor storage of the gypsum pebbles have also been made and possible impacts on the ground water quality due to leaching from the gypsum were examined. The results of these tests show that practically the same requirements for outdoor storage of the FGD gypsum as for natural gypsum exist and, therefore, no special storage measures are necessary.

Other conditions too, especially those that are necessary to the image of a new product, such as the heavy metal content, susceptability to leaching, and particularly the question of radioactivity, which is environmentally important, have been examined and clarified in detail. Since these factors are considered as an important contribution to the future image of FGD gypsum as a structural material, we have taken the liberty of quoting an expert from the University of Salzburg, Institute of Biology, Biochemestry and Biophysics:

"As a summary, it can be said that the use of the examined FGD gypsum is harmless from the radiological point of view. Considering the lowest possible level of radiation exposure caused by natural radioactivity in building materials, the use of this material can be highly recommended."

The reduction of operating costs has successfully been achieved by a decrease in the energy input. The regenerative gas reheater has been proven as successful as the wet fan in continuous operation and up to now the efficiency of the plant has not been influenced in a negative way by these two components.

The steam heated gypsum drying system also offers the possibility of varying the degree of initial calcination. This leads to a considerable improvement in the briquetting conditions and hence the strength and outdoor storage life of the gypsum briquetts.

The demand for maximum efficiency and safety was always satisfied by the careful design, sufficient manual redundancy and good plant management. The only exception is the difficulties experienced with the rubber lining, particularly in the prescrubber zone, which should be mentioned here. The defects in the rubber lining led to a considerable decrease in the plant's efficiency during the last period of operation. Due to the necessary repair measures the availability was reduced to about 92 %.

Conclusion

Despite the considerably varying quality of the fuel and the most diverse of operating conditions during continous running of the plant, the extremely stringent standards specified by the Austrian authorities were already satisfied during the initial period of operation, whilst at the same time maintaining a high plant efficiency. This does not only confirm the fact that the design of the process is particularly suited to firing either lignite, or a combination of lignite and bituminous coal, but also proves that the performance of the plant can be considerably improved by optimizing operation methods.

Good technology is an essential basic requirement for optimizing the process. Thus the next section of this report will deal with the potential of rapid and accurate analysis of particle sizes in further detail.

PARTICLE SIZE MEASUREMENT FOR PROCESS OPTIMIZATION

Knowledge of particle size and particle size distribution of the powders and suspensions used in a FGD helps to operate the plant in a cost-efficient and reliable manner. Two case studies show how operational problems could be identified and solved with the aid of particle size analysis (PSA). In Riedersbach No. 2 PSA has become a routine checking procedure.

OPERATION OF RIEDERSBACH NO. 2 AND PSA

The FGD of Riedersbach No. 2, including the limestone grinding, was fine-tuned to the use of limestone from a quarry called "Bernegger".
When limestone from a different quarry was used the tuning of the grinder had to be revised. Some typical operating data are given in table 5. With limestone Bernegger - the particle size distribution of which can be seen from table 6 - sulfur removal is high at a moderate pH value, while still producing a high sulfate and low sulfite gypsum.

When in August 1987 limestone "Tagger" was introduced the operating data changed. Sulfur removal was less and there was more carbonate in the gypsum. A look at the particle size distribution of the limestone slurry (table 6) made it clear that the coarser limestone particles were the reason. After tuning the limestone grinding circuit, the particle size of the slurry was back (table 6) on Sept. 25 to what it had been with limestone Bernegger and also the operational data were again excellent. A high pH allows a very low SO_2 concentration in the clean gas but there is still a low carbonate content in the gypsum.

Conclusion

The conclusion of this experiment is that the FGD of Riedersbach No. 2 can be operated with different limestones at excellent sulfur removal rates and at the same time produce a high quality gypsum if the operation of the limestone grinding circuit is tuned to the hardness of the limestone. Frequent particle size analysis is a tool to achieve

- high sulfur removal
- high quality gypsum
- save power for grinding at the same time.

In order to have easy, quick and economic access to the particle size and particle size distribution Riedersbach No. 2 bought a LUMOSED as particle sizing equipment. Today the suspensions of the FGD are examined in routine checks in order to monitor the proper operation of the FGD. Figure 7 shows the typical particle size distributions of the limestone slurry (1) the scrubber slurry (2) and the gypsum (3) as sampled from the belt filter.

OPERATION OF MELLACH POWER PLANT AND PSA

Mellach of Steirische Wasserkraft und Elektrizitaets AG (STEWEAG) is a new, 200 MWe unit, fired with low sulfur coal. The plant is faced with tough emission limits for both, SO_2 and NOx. In order to control SO_2 emission a limestone scrubber treats the full flue gas flow. The FGD plant was built by the same contractor as Riedersbach No. 2. In Mellach too, PSA helped to identify the source of problems which arose in the operation of the scrubber.

The relevant part of the flowsheet of the Mellach FGD (figure 8) shows a common set up with a spray tower, cyclones and a vacuum-belt-filter. The gypsum filter cake is processed through a pelletizer and a dryer. Broken pellets and dust from the dryer are returned to the scrubber circuit. A number of sampling points for the relevant suspensions are indicated in the flow sheet.

Diagnostics

The particle size distribution of the suspensions from normal operating FGD as determined with a LUMOSED are given in figure 9. One day, sulfur removal efficiency dropped, while all characteristic parameters were constant but the fraction of broken pellets, which had to be recycled to the scrubber circuit, had increased. The reason for the increase in broken pellets was easily found: there was more water in the filter cake than specified for the production of rigid pellets. The reason for this insufficient dewatering could be found with the aid of the LUMOSED. Figure 10 shows the particle size distribution of the filter cake on 1988 04 15; the mass-fraction of particles smaller than 10 µm is close to 5 %, the mass-fraction of particles smaller than 20 µm is close to 9 % whereas these figures are 1.5 % and 5 % respectively during normal operation (see figure 9). Because of the large fraction of small particles the filter cake could not be dewatered as well as during normal operation.

To find out the key problem, one more particle size measurement was needed, i.e. that of the gypsum crystals, of which the pellets consist. For this, the pellets were suspended in water and this suspension was fed to the LUMOSED. The result of this measurement is shown in figure 10 and labeled PE. It is obvious that the gypsum crystals are reduced in size during pelletizing. These small particles - if recycled to the scrubber - increase the contents of fines in the scrubber suspension even in normal operation as the shape of curve SC in figure 9 shows (if compared with the equivalent of Riedersbach No. 2, which is curve 2 in figure 7).

Conclusion

In the FGD of Mellach the fraction of fines in the scrubber slurry is increased by the recycling of off-spec pellets above the level of other FGD plants. A small disturbance from outside, like a high ash slip through the precipitator or a quick change in load, may bring the plant out of balance and increase the hold-up of small particles to such a degree that, because of poor dewatering, the product gypsum cannot be removed from the FGD. The poor sulfur removal, which occurs at the same time can probably be explained by the higher viscosity which fine-grained slurries show if compared with coarse grained slurries. If the higher viscosity results in larger droplets in the spray tower, then the exchange surface becomes smaller and this would explain the reduced sulfur removal efficiency in connection with a large fraction of small particles in the scrubber slurry. Accurate PSA would have shown from the beginning that the recycling of off-spec pellets from the pelletizer increases the fraction of fines in the scrubber slurry to a possibly dangerous level. Daily inspection of the particle size distribution would allow operation of the FGD close to the borderline and it would indicate, when the off-spec pellets must not be recycled, but must be eliminated from the system so as not to jeopardize safe scrubber operation.

The work described in this paper was not funded by the U.S. Environmental Protection Agency and therefore the contents do not necessarily reflect the views of the Agency and no official endorsement should be inferred.

"REFERENCES,"

1) Power Plant Riedersbach No. 2 in Operation.
Oesterreichische Zeitschrift fuer Elektrizitaetswirtschaft
40th annual series (1987) No. 6/7

2) Praxmarer, G., Gilli, P.G. and Kneissl, P.J.
Mixed Firing of Brown Coal and Bituminous Coal at Riedersbach No. 2 Power Plant and Utilization of Fly Ash and Gypsum from the Flue Gas Desulfurization. Paper presented at VGB-, Technical Association of Large Power Plant Operators-, Congress "Power Plants 1987", Vienna, Austria, September 15 - 18, 1987. In: VGB-"Kraftwerkstechnik", 68th annual series, No. 7, July 1988, 726-735

3) FGD-Riedersbach No. 2. In: Wabiscope - The Waagner-Biró Aktiengesellschaft Customer's Magazine, 43th annual series (1985), Vienna-Graz/Austria.

4) Kneissl, P.J., Praxmarer, G. and Waltl, J.
The Flue Gas Desulfurization at Riedersbach No. 2.
Paper presented at 1987 Specialty Conference, Problems and Perspectives of Energy Conversion Technologies and Environment Protection. Varna/SR. Bulgaria, October 12 - 14, 1987

5) Gebel, K., Kneissl, P.J. and Praxmarer, G.
Flue Gas Desulfurization in the Lignite Fired Riedersbach No. 2 Power Plant, Concept and First Operating Experiences. Paper presented at VGB-, Technical Association of Large Power Plant Operators-, Conference "Power Plant and Environment 1987", Essen, Federal Republic of Germany, March 4 - 5, 1987

6) Staudinger, G., Hangl, M. and Pechtl, P. Quick Optical Measurement of Particle Size Distribution in a Sedimentation Apparatus.
In: Particle Characterization 3(1986) 158-162

Figure 1: **Riedersbach Power Plant (on right, Unit No. 2)**

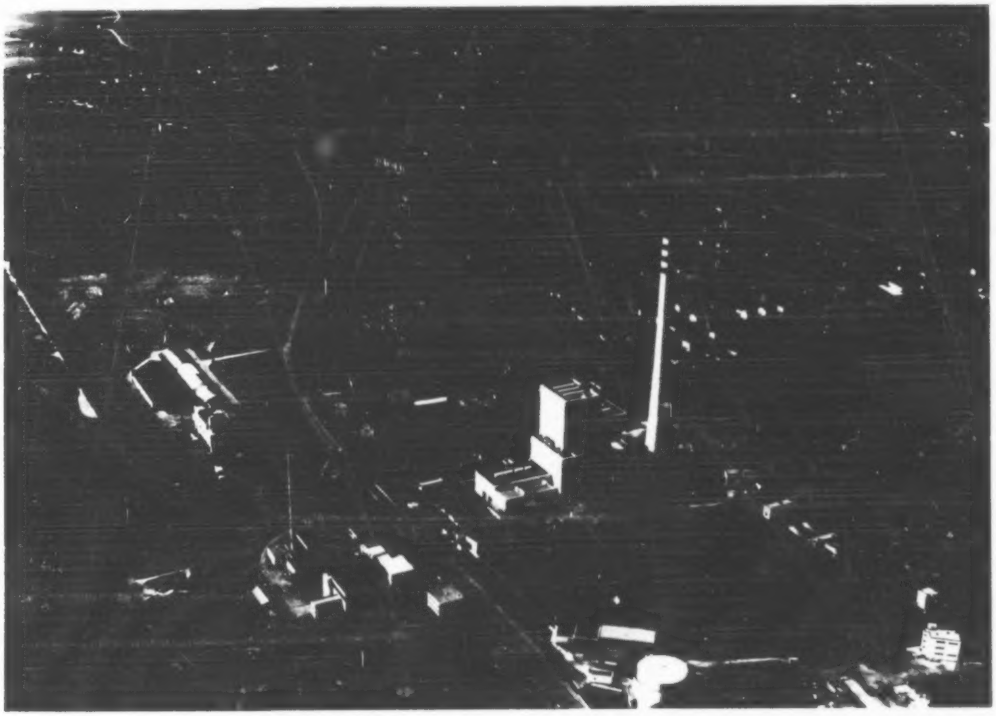

Table 1: **Flue gas data of Riedersbach No. 2**

Fuel Combination	Unity	100 % Lignite-coal	50 % Lignite- 50 % Bituminous-coal	100 % Bituminous-coal	100 % Heavy-Oil
Boiler load	%	100	100	60	40
Flue gas (raw gas)	Nm^3/h (dry)	513480	504110	348650	286000
Calorific value	kJ/kg	10470	L.C 10470 B.C 24285	24285	39710
Flue gas temperature	°C	138	136	122	119
Flue gas saturation temperature (scrubber)	°C	59	54	43	45
H_2O-content	vol.-%	17,6	12,9	6,7	7,7
SO_2-content	mg/Nm^3 (dry, 6 % O_2)	> 6000	> 4000	2000	3600
Cl-content	mg/Nm^3 (dry, 6 % O_2)	< 50	103	174	-
F-content	mg/Nm^3 (dry, 6 % O_2)	38	19	10	-

Table 2: **Government Regulations on Emission and Ground Level Concentrations for Riedersbach No. 2**

Ambient Air Qualitiy Standard

mg/m^3	SO_2	NO_2	Particulate
1/2 h Average	< 0,5	< 0,3	-
24 h Average	< 0,2	< 0,1	< 0,2

Emission Government Regulations

mg/Nm^3 (dry, 6 % O_2)	SO_2	NO_x	Particulate	CO	HCl	HF
1/2 h Average	< 400 < 300**	< 450*	< 50	< 250	< 100	< 5

*local agreement/** legal from January 01, 1989

Forest Protection Government Regulations

mg/m^3 SO_2	April - October	November - March
1/2 h Average	< 0,14 (97,5 % < 0,07)	< 0,30 (97,5 % < 0,15)
24 h Average	< 0,05	< 0,1

Table 3: **Design criteria for the FGD**

- Treatment of 100% of the flue gas volume when firing lignite and a mixture of lignite, bituminous coal and fuel oil respectively.

- Desulfurization by at least 95% of the peak sulfur content in the lignite.

- Complete profitable utilization of the product at the same time avoiding the need for dumping grounds.

- Lowest possible operating costs.

- Maximum operational reliability and the reduction to a minimum of forseeable risks.

Figure 2 : **Flowsheet FGD Riedersbach No. 2**

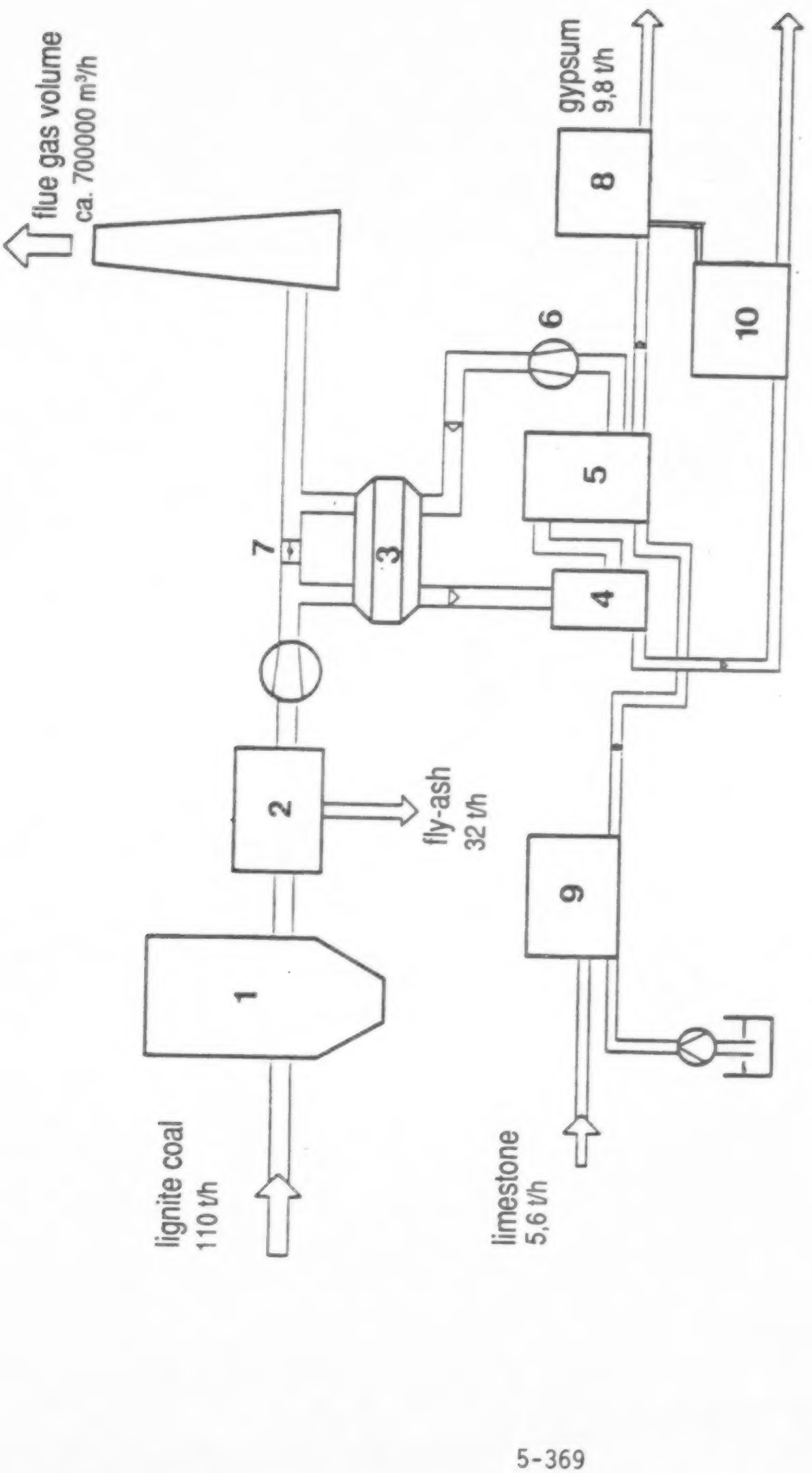
flue gas volume
ca. 700000 m³/h
gypsum
9,8 t/h
lignite coal
110 t/h
limestone
5,6 t/h
fly-ash
32 t/h
1
2
3
4
5
6
7
8
9
10

1	boiler	6	FGD wet fan
2	electro precipitator	7	by pass damper
3	gas-gas reheater	8	gypsum treatment
4	pre scrubber	9	limestone treatment
5	absorber	10	waste water treatment

Figure 3 : **Flowsheet FGD Riedersbach No. 2**

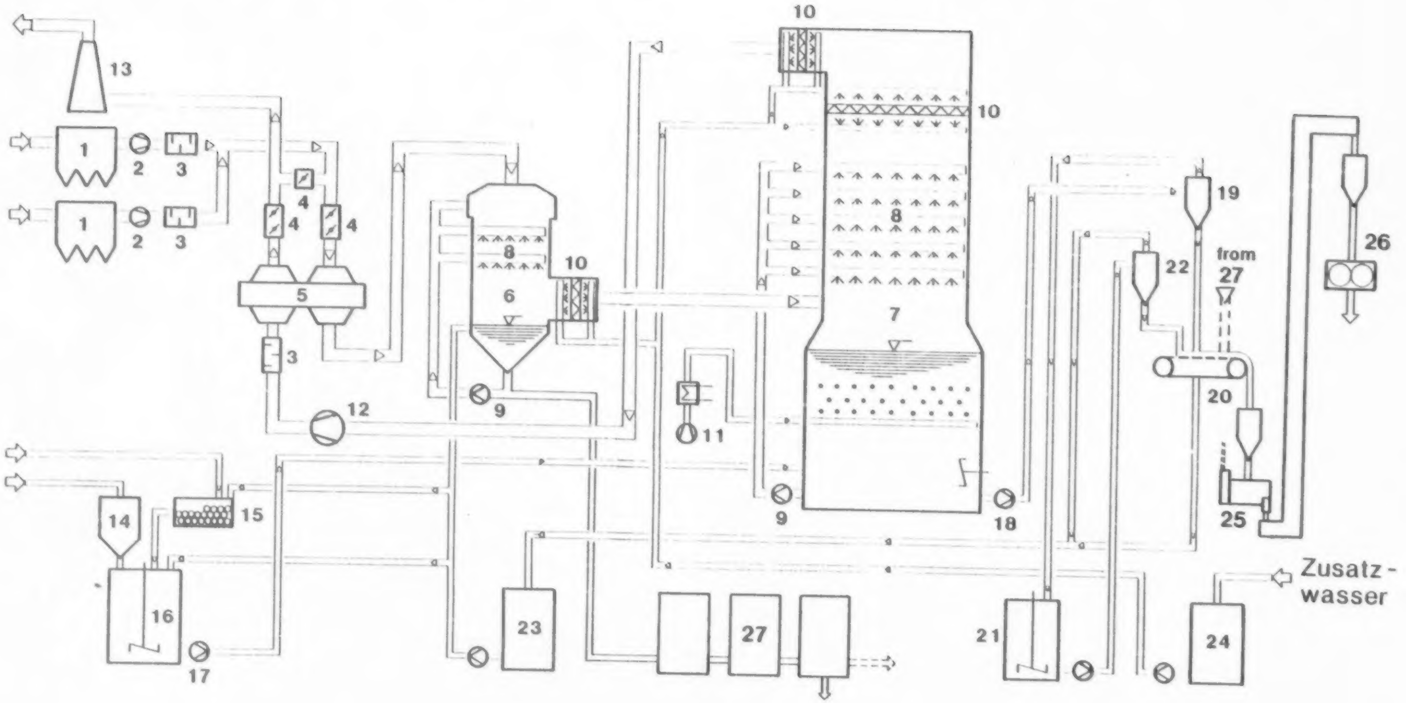

1
2
3
4
5
6
7
8
9
10
11
12
13
14
15
16
17
18
19
20
21
22
23
24
25
26
27
from 27
Zusatz-
wasser

1 electro precipitator
2 exhaust fan
3 silencer
4 flue gas duct dampers
5 gas-gas reheater
6 pre scrubber
7 absorber
8 spray level
9 absorber pumpe

10 mist eliminator
11 oxidation air
12 FGD wet fan
13 stack
14 limestone silo
15 limestone mill
16 limestone slurry tank
17 limestone slurry pump
18 absorger slurry pump

19 product hydrocyclone
20 belt filter
21 overflow tank
22 overflow hydrocyclone
23 filtrate tank
24 water tank
25 gypsum dryer
26 briquetting press
27 waste water treatment

Figure 4: **Scedule of trial and commercial operation and availability of FGD**

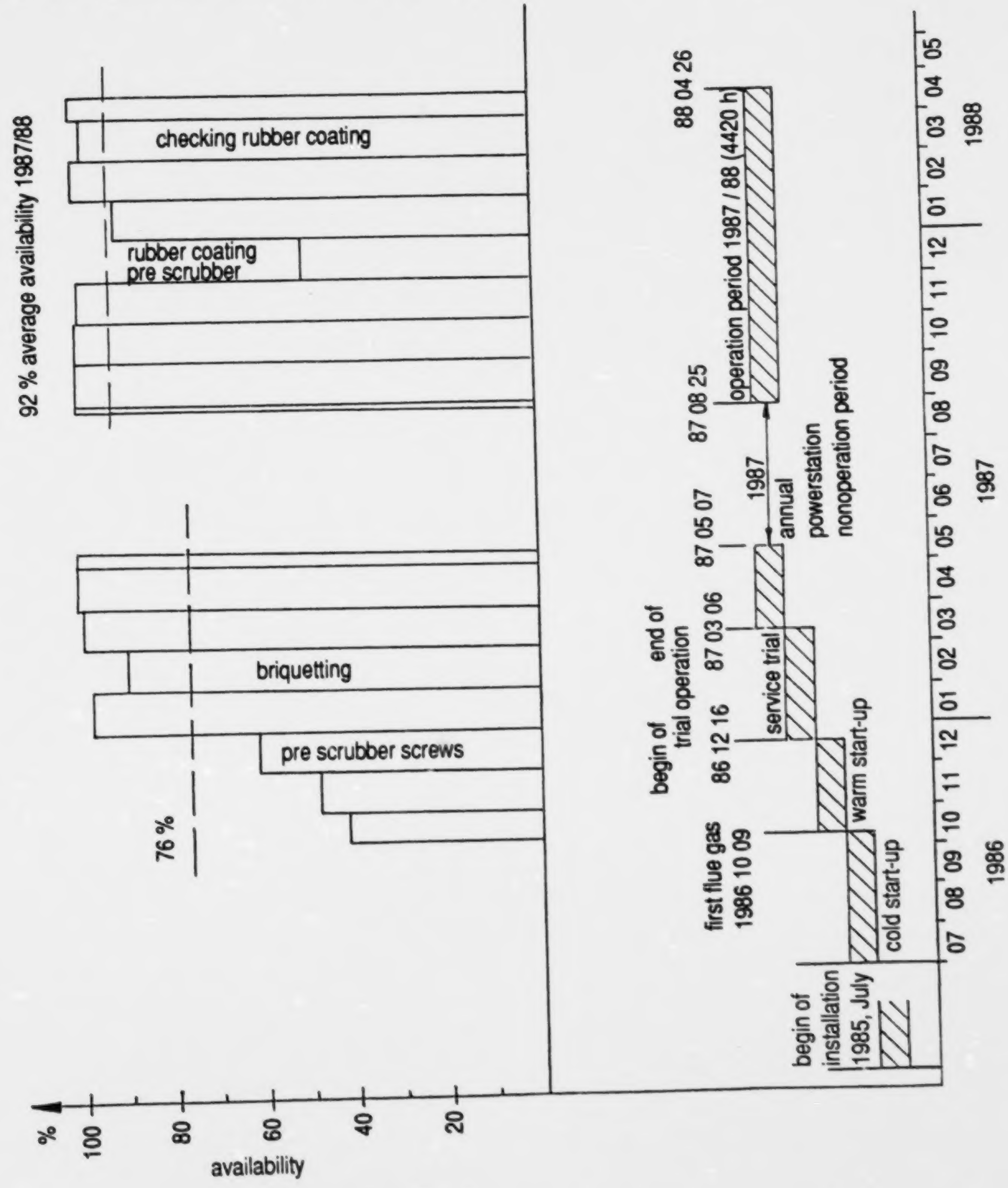

Figure 5: **Desulfurization efficiency**

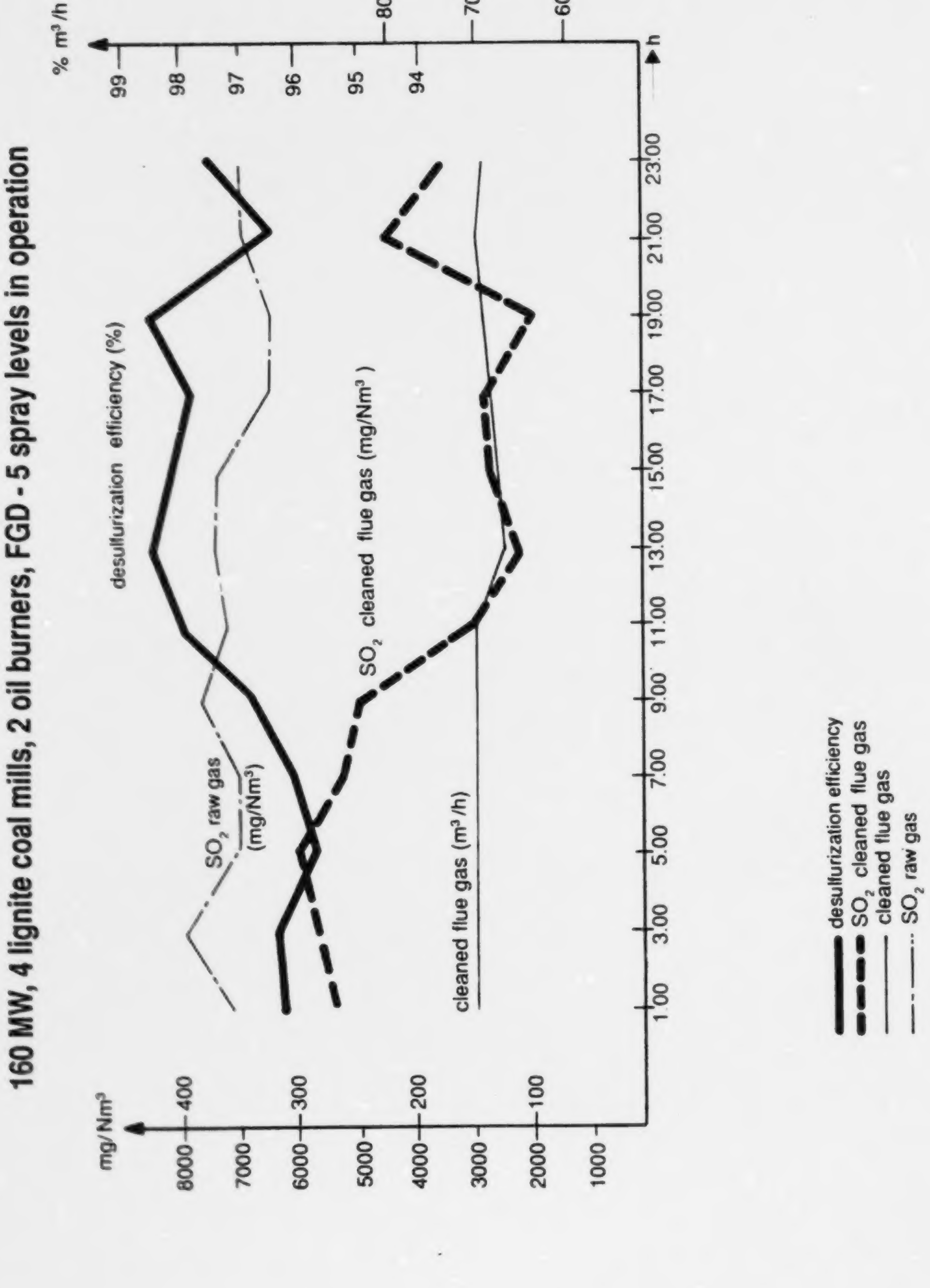

Figure 5a: **Desulfurization efficiency**

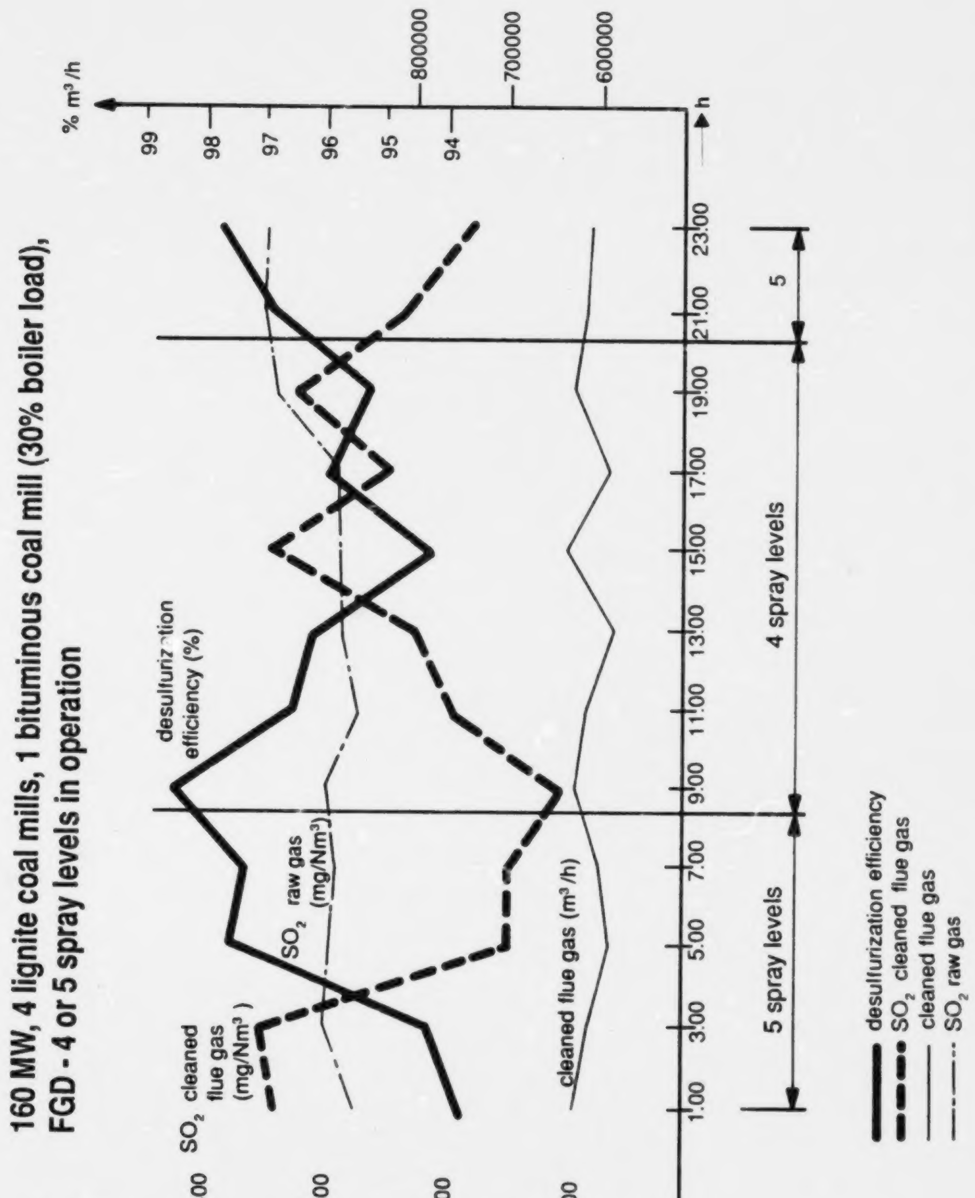

Table 4: **FGD gypsum quality**

	Requirements	Actual Data
free moisture	< 8.0 %	0%
crystal water content	-	16 - 18 %
purity ($CaSO_4 . 2H_2O$)	> 95.0 %	96 - 99,5 %
MgO (soluble)	< 0.10 %	0.01 - 0.06 %
Na_2O (soluble)	< 0.06 %	0.003 - 0.01 %
chlorides	< 0.10 %	0.001 - 0.003 %
sulfite (SO_2)	< 0.25 %	0.001 - 0.2 %
pH-value	5 - 9	6.5 - 9.0
colour	white	white
odour	neutral	neutral
bulk density (briquetts)		approx. 2.1 g/cm^3
compressive strength		> 700 N
compressive strength (24 hrs storage in water)		approx. 500 N
compressive strength after renewed drying		> 1000 N
storage life (particle size larger than 7 mm after 5 alternating freeze/thaw changes)		96.5 %
Fe_2O_3		350 - 500 mg/kg
Al_2O_3		200 - 500 mg/kg
MnO_2		20 - 50 mg/kg
zinc		< 10 mg/kg
copper		< 10 mg/kg

Figure 6: **Gypsum Crystal, FGD Riedersbach No. 2**

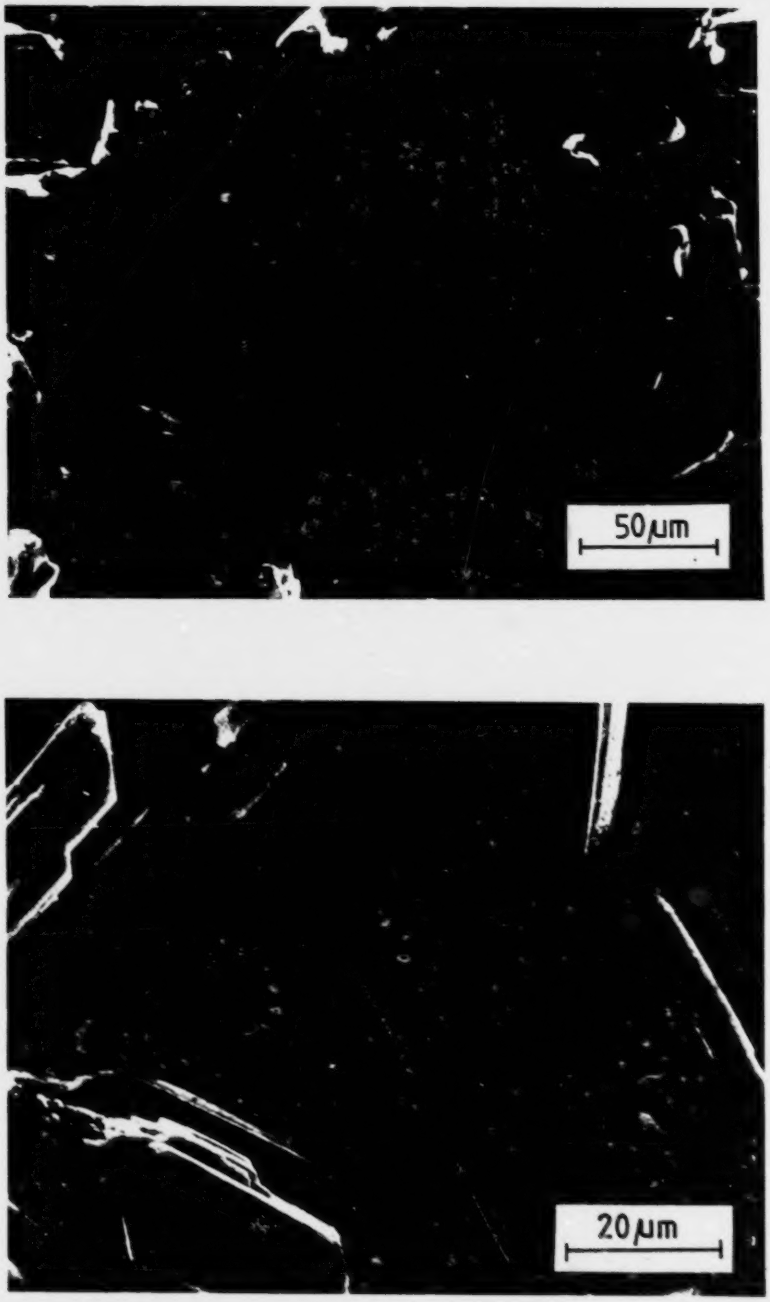

Reproduced from
best available copy.

Table 5: **TYPICAL OPERATING DATA OF THE FGD OF RIEDERSBACH No. 2**

Limestone	Bernegger			Tagger	
Date	870131	870203	870317	870911	870925-29
Gypsum: $CaSO_4.2H_2O$ % wt	99.53	98.3	98.7	97	98.2
$CaSO_3.1/2H_2O$ % wt	0.10	0.18	0.02	0.08 0.2 (3)	0.02
pH	5.7	6.25	5.9 - 6.1	5.7 5.9 (6)	6.0
SO_2 raw gas*	6400	6500	6800	7900	6800
SO_2 clean gas*	325	240	250	460 250	160

*SO_2 concentration in flue gas (mg/Nm³, dry and 6 % O_2)

Table 6: **PARTICLE SIZE DISTRIBUTION OF LIMESTONE SLURRY**

Lime-stone	Date	Particle mass %					
		*90	60-90	45-60	30-45	15-30	15
Bernegger	870129	0.61	1.29	0.09	6.81	14.66	76.54
	870130	0	0.21	0.07	3.76	12.0	83.96
	870203	0.13	0.09	0.20	3.95	16.4	79.23
	870821 +	0.70	4.62	8.76	10.34	11.68	63.9
	870821 §	2.5	4.18	10.16	13.42	13.26	56.48
Tagger	870925	0.9	1.8	2.48	6.51	9.63	78.67
	870929	0.45	0.60	1.58	7.87	14.53	74.97

* Particle diameter determined by ultrasound sieve analysis
+ 1.00 p. m.
§ 3.00 p. m.

Figure 7: **Particle size distributions of the FGD in Riedersbach No. 2**
(1) limestone slurry, (2) scrubber slurry, (3) gypsum sampled from the beltfilter

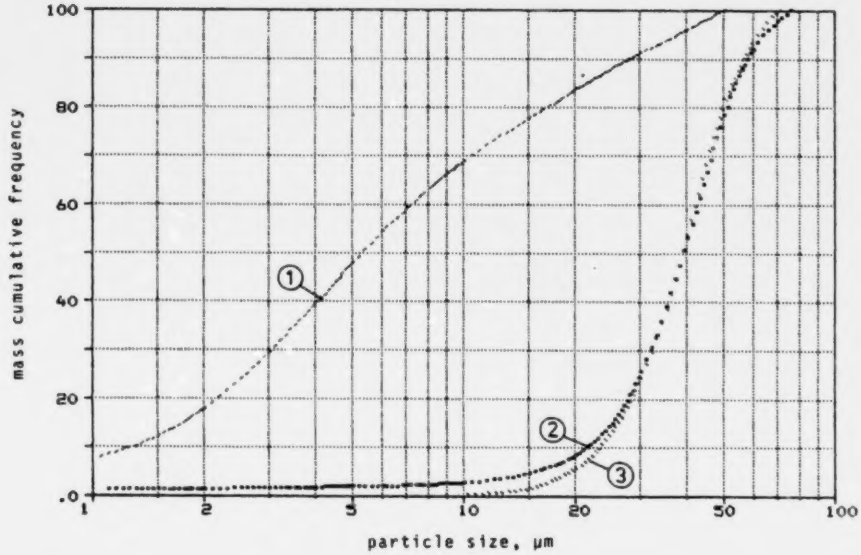

Figure 8: **Flow sheet of Mellach FGD showing sampling points**
(CO cyclone underflow, CU cyclone overflow, VBF vacuum beltfilter cake, PE pellets)

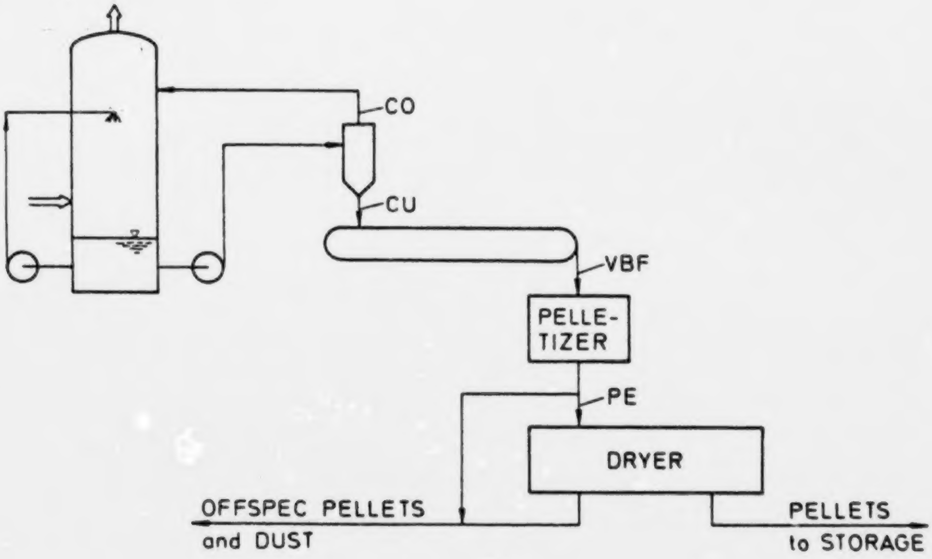

CO
CU
VBF
PELLE-TIZER
PE
DRYER
OFFSPEC PELLETS and DUST
PELLETS to STORAGE

Figure 9: Particle size distributions of scrubber slurry (SC), vacuum belt filter (VBF), hydrocyclone underflow (CU) and hydrocyclone overflow (CO)

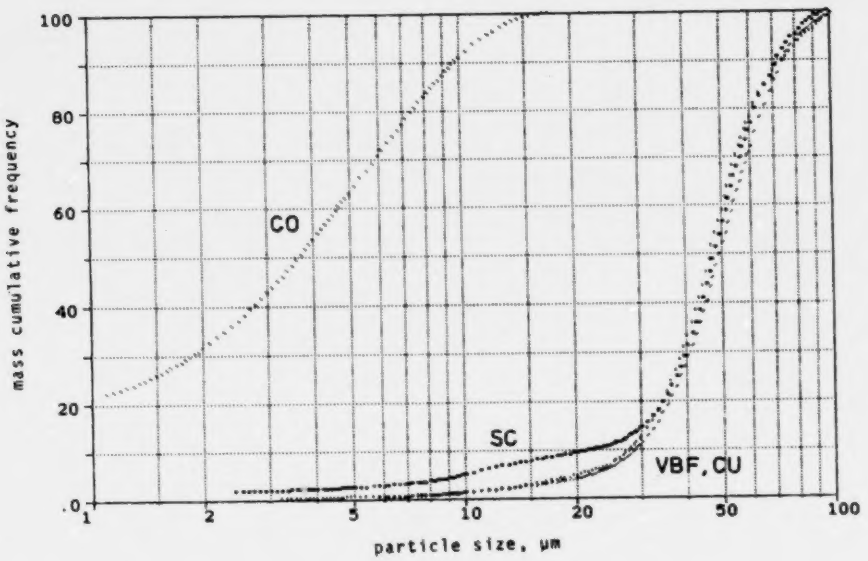

Figure 10: Particle size distribution of filter cake from vacuum belt filter on 1988 04 15 (VBF) and of gypsum crystal of pellets (PE)

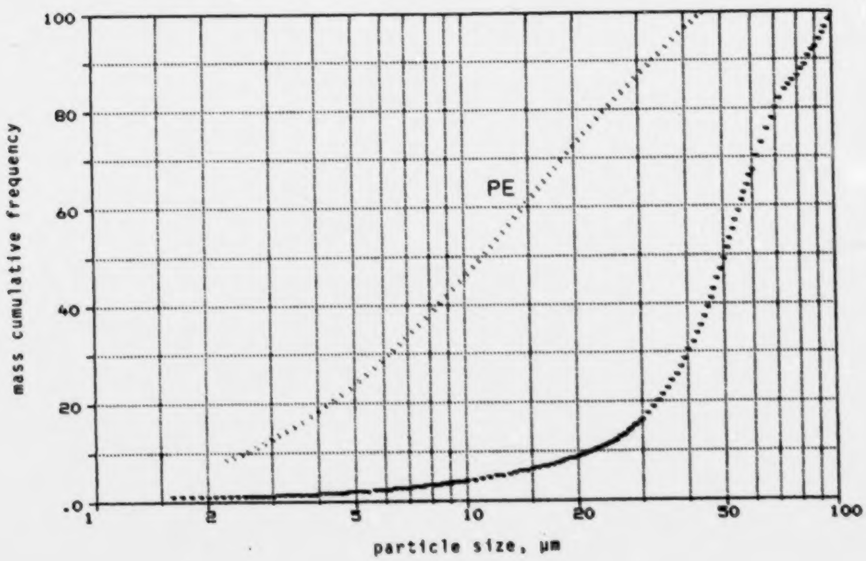

SIMULTANEOUS SO_2 AND PARTICULATE REMOVAL IN A JET BUBBLING REACTOR

B. R. Gilbert and R. M. Sherwin
Bechtel National, Inc.
San Francisco, California 94119

Kensei Kitamoto and Yoshikuni Yamaguchi
Hokuriku Electric Company
Toyama, Japan

Yoshio Ogawa and Hiromi Koshizuka
Chiyoda Corporation
Yokohama, Japan

ABSTRACT

This paper addresses five aspects of CT-121 system design that are of interest to potential users:

1) Absorption without prescrubbing
2) Use of an axial flow fan on the untreated gas side
3) Gas-to-gas heat exchange for reheat, ahead of the fan
4) Simplified instrumentation, using a distributed control system (DCS) in cycling service
5) Use of continuous decanters for dewatering of gypsum

These features are incorporated into the most recent CT-121 installation, a 250 MW system built for Hokuriku Electric Company at Kusajima, Japan. This facility came on line in July 1987, replacing an earlier CT-101 installation built in 1975.

Design philosophy and operating experience during the first year of operation is reviewed, and an update is given on the status of other operating facilities.

The advanced limestone/gypsum CT-121 process incorporates all of the necessary steps for SO_2 removal into a unique gas/liquid/solid reactor, the Jet Bubbling Reactor. Eight units are currently in commercial operation treating flue gas from coal, oil, and asphalt fired boilers.

EPA/EPRI First Combined FGD
and Dry SO_2
Control Symposium

St. Louis, Missouri, U.S.A.
October 25-28, 1988

SIMULTANEOUS SO_2 AND PARTICULATE REMOVAL IN A JET BUBBLING REACTOR

The latest CT-121 installation in Japan began operation in July 1987 and passed its performance test by the end of that same month. This is the eighth commercial unit to have gone on line since CT-121 development began in 1976. Eleven CT-101 units also continue to operate successfully after many years of service. Two original CT-101 units have been replaced with the more advanced CT-121 process.

BACKGROUND

The new 250 MW facility is located at Kusajima in Toyama Prefecture, and is owned by the Hokuriku Electric Power Company. It replaces a CT-101 system installed by Chiyoda in 1975 ([1]). In the daytime the boiler, fired with 2.5 percent sulfur fuel oil, has recently been cycling between 37 and 250 MW. It is shut down nights and weekends.

Electrostatic precipitators limit particulate loading ahead of the scrubber to a level of 10 to 30 mg/Nm^3 (0.004 to 0.012 gr/scf), dry basis.

DESCRIPTION OF THE ORIGINAL CT-101 FACILITY

A simplified flow sheet for the former scrubber process appears in Figure 1. The gas side included two booster fans, two prescrubbers, a single absorber/oxidizer vessel, mist eliminators, and an oil-fired reheater/gas mixer, as shown in Figure 2. The slurry side included a weak acid tank, two crystallizers, and a thickener, with six basket centrifuges for gypsum dewatering.

The original CT-101 installation had an excellent operating record, providing outstanding reliability for more than 10 years. However, the polypropylene packing rings used in the older design were beginning to deteriorate, and Hokuriku Electric considered the fuel oil consumption for reheat, 170 barrels per day, to be excessive. They decided to do away with the two prescrubbers to make room for gas-to-gas heat exchangers. At the same time, they chose to replace the system with a CT-121 arrangement, thereby simplifying the operation.

This decision was strongly influenced by the favorable performance record of the two new CT-121 installations at Toyama Kyodo. As a partner in that venture, Hokuriku Electric was familiar with the low maintenance, power economy, and high reliability of the FGD equipment. The existing Type 316L absorber/oxidizer was converted to a Jet Bubbling Reactor (JBR), and the Tellerette packing replaced with spargers. An up-to-date distributed control system provides the latest in trouble-free operation.

DESCRIPTION OF THE MODIFIED FACILITY

The revised flow sheet appears in Figure 3.

The heart of the CT-121 process is the Jet Bubbling Reactor, where the flue gas is dispersed through crystalline slurry, using spargers. The typical configuration for this arrangement is shown in Figures 4 and 5, and has been described elsewhere (2). The depth of sparger submergence and the pH level within the gently agitated slurry jointly determine the removal efficiency. Sparger submergence creates a steady back pressure at the booster fan discharge, accounting for 60 to 80 percent of the total system energy usage.

The two former centrifugal booster fans were replaced with a single fan of higher efficiency. The original mist eliminator configuration was retained. New and updated coating systems were applied.

---

[1] For a more detailed description of a similar facility, see Reference 1.

The gypsum slurry is maintained in suspension by eight vertically mounted agitators arranged at 45 degree spacing. The weak acid tank and separate crystallizers were removed.

SPECIAL FEATURES

In addition to the JBR, the new system incorporates the latest in state-of-the-art FGD practices, notably with respect to flue gas precooling, fan selection, reheat, simplified control methodology, and gypsum dewatering practice.

Flue Gas Precooling

Flue gas precooling is carried out in steps. The gas is first cooled from 144 C to 90 C in the GGH. It subsequently gains 8 C by the heat of compression in the booster fan. Finally, it is adiabatically cooled from 98 C to about 50 C.

The adiabatic contact is made in two spray zone stages. The first (precooler) is with mother liquor diluted with makeup water. The second is with gypsum slurry. The slurry nozzles stay clean because they are continually exposed to precooler spray carryover. This takes place in a single length of ductwork. The use of mother liquor for presaturation cuts down on the overall plant water consumption.

Fan Selection

The need to maintain high energy efficiencies under cycling conditions led to selection of a horizontal flow axial flow fan with two stages of variable-pitch rotating blades. Power consumption was reduced by locating the fan in the relatively cool untreated flue gas between the GGH and the JBR. This location also minimized short circuiting of untreated gas across the GGH. Because of their small blade size, these fans have low starting torque, which leads to a substantial reduction in the size of motor load controllers.

Inconel 625 is used for the rotor blades. Stator housing and blades are of Type 316 L stainless steel. The inlet and outlet housings are of carbon steel coated with flakeglass reinforced plastic. Ammonia gas has been injected into the flue gas ahead of the precipitator to improve particulate removal. This also reduces the severity of cold side corrosion by lowering the acid dew point.

A year of operating experience has convinced the owners that the axial fan application is a good one in this service. Preventive maintenance has been carefully practiced, with the following monitoring and inspection precautions:

Daily--	Sound Shaft temperature Vibration Blade position Amperage	Lube oil pressure Oil strainer differential pressure Lube oil temperature Oil sump level Seal air temperature and differential pressure
Weekly--	Lube oil cooling water flow	
Monthly--	Flue gas discharge pressure Check for oil leakage Clean and switch oil strainers	
Semi-annually--	Switch lube oil pumps Check for degradation of oil	
Annually--	Remove dust deposits from rotor, casing, and shaft Observe any corrosion or erosion of rotor, casing, shaft, or flexible coupling Measure deflection and wear of bearing and actuator Check for oil leakage	

Reheat

The horizontal-flow gas-to-gas heat exchanger is of the Ljungstrom type, with flakeglass coated carbon steel housings, corrosion resistant low alloy steel baskets, and enameled heating elements. The gas is raised from adiabatic temperature (approximately 50 C) to a level between 94 C and 99 C.

Use of the GGH reduces the saturation temperature and the evaporation load. This, together with the partial use of mother liquor, substantially reduces the amount of water needed for makeup. The total requirement is 500 liters/minute (132 gpm).

Control Methodology

Routine startup and shutdown of the FGD system takes place to satisfy the varying gas flow requirements of a cycling boiler. The boiler has averaged about 46 percent load factor since the new FGD system was installed. The FGD panel is adjacent to the boiler control panel. Monitoring, operation, and control is entirely from that location (Figure 7), using single-loop programmable controllers as backup controllers for the DCS.

The CT-121 has two major control loops: flue gas control and pH control. The flow of flue gas is automatically adjusted by a pressure controller on the suction side of the booster fan, which controls the variable rotating blade orientation on the fan rotor. The pH in the JBR is controlled with the addition of ground limestone, counterbalancing the feed forward signal of the SO_2 load against the feedback signal from the JBR pH.

The system is monitored and controlled remotely from the process, making use of a state-of-the-art distributed control system. This system is functionally configured in a hierarchical manner so as to provide only the information and control features needed by plant and management personnel. However, with the CT-121 process these needs are minimized.

The management functions performed by the system include:

- Database management
- Data reduction
- Data presentation
- Data archival
- Data generation

The supervisory functions performed are:

- Status displays
- Events and alarms
- Process records

The data acquisition and control functions performed are:

- Input
- Output
- Computation

The control system is a microprocessor based system consisting of the following:

- Operator station (man-machine interface)
- Control unit (including communications interfaces)
- Input/output interface devices

System startup and shutdown takes less than 10 minutes, and is handled from a keyboard. Load changes are handled at the rate of 5 percent per minute. The gas flow and SO_2 outlet concentration response to typical load changes over a range of 15 to 100 percent is shown in Figures 8 and 9. These figures, typical strip charts taken from the FGD system control panel, also show the ability of the system to hold steady pH over the wide range of load conditions.

Gypsum Dewatering

Other changes made to the 1975 Hokuriku installation include replacement of the original six basket centrifuges with three continuous screw-type decanters. The decanter system has greater throughput capacity per unit, and is simpler to operate. It does not require the gypsum slurry feed tank, thickener, and complicated start-stop control system needed for the batch-type basket centrifuge. There is much less maintenance. With the large CT-121 gypsum crystals, dryness reaches 90 percent, which is adequate for end use.

PERFORMANCE

A summary of design, guarantee, and performance test results appears in Table 1.

Under typical operating scenarios, the SO_2 outlet concentrations registered in Figures 8 and 9 are equivalent to SO_2 efficiencies ranging from 92 percent at full load up to 94 percent at minimum load. The outlet SO_2 at a given load typically varies by +/-10 ppmv.

Above the 50 percent load point the fan suction pressure is steady at 0 +/- 25 mm of water, and is unaffected by load change. The pH holds at 3.5 +/- 0.2. The system responds well automatically, with typical load changes of 5 percent per minute, down to 15 percent of full load.

Total power consumption for the system, with gypsum dewatering, was 2,990 kW under the following conditions:

Boiler at full load, MW	250
Flue gas flow, Nm^3/hr	732,000
SO_2 concentration, ppmv	1,238
SO_2 removal efficiency, %	91.7

This power usage is 1.2 percent of the power generated. The duct runs at Kusajima are unusually long, accounting for a significant portion of the system pressure drop. Under more favorable layout conditions power usage would be less than 1.1 percent.

At 10.7 mg/Nm^3, the inlet grain loading leaving the precipitator for the FGD system is an order of magnitude lower than for a typical modern day coal fired plant, with a higher proportion of submicron fines. Nevertheless, the JBR does an outstanding job of particulate cleanup, taking out about 75 percent of the fine particulate that gets by the electrostatic precipitator. Figure 10 shows the overall measured particulate balance. Figure 11 shows the effect of size concentration and distribution on the observed grade efficiencies.

A major reduction in operating manpower has also been realized. Whereas two operators per shift were originally dedicated to the FGD system, the job responsibilities are now covered by the boiler operator. The estimated coverage is about 0.2 men per shift. This includes FGD, limestone handling, and gypsum dewatering operations. An added man is brought in for startup and for prolonged shutdown, but no additional coverage is needed for the daily or weekly routine startup and shutdown.

Gypsum from the continuous decanter is sold for wallboard or Portland cement manufacturing. Quality is excellent, running 97.6 to 99.9 percent $CaSO_4 \cdot 2H_2O$, and 89.7 percent solids, with a median crystal size of 69 microns. Figure 12 shows this size to compare favorably with other CT-121 gypsum.

AVAILABILITY

The availability record for CT-121 installations continues to justify the confidence of its owners. An updated description of operating conditions and reliability parameters for the six CT-121 plants in commercial operation appears in Table 2.

ABBOTT

The latest CT-121 installation to go on line is the 45MWe unit for Abbott Station, located on the University of Illinois Champaign-Urbana campus. This facility is converting three boilers from oil/gas service back to coal stoker firing. Two boilers have been converted thus far, and the CT-121 unit started up in early April. The SO_2 removal ranges from 95 to 98 percent, depending on load, weir setting, and SO_2 concentration. The scrubber has been running close to 80 percent of design load and at about 60 percent of the design SO_2 inlet concentration. The inlet SO_2 varies between 1,600 and 1,800 ppmv, and the system pressure drop is about 15 inches of water.

A small (5 ft^2) Bird-Young filter is used for dewatering 90 tons per day of gypsum under design conditions. The coarse JBR gypsum has a dramatic impact on the throughput of this equipment. Under present operating conditions of 40 tons per day it has been necessary to blank off one-third of the filter drum area. The moisture content lies between 8 and 10 percent. The overall gypsum quality exceeds that of wallboard gypsum without washing.

On August 18 a year-long monitoring program was initiated as part of the overall effort sponsored by the Illinois Capital Development Board, the Illinois Department of Energy and Natural Resources, the University of Illinois, and EPRI. The test program contractor is Radian Corporation. The objective is to establish technical viability and economic feasibility. The first phase of this program, a 30-day acceptance test, has been successfully completed, and several weeks of parametric testing are now in progress. When fully operational, the plant will burn 80-90,000 tons of coal per year cleanly and more cheaply than natural gas or oil.

SUMMARY

The CT-121 installation at Kusajima has met or exceeded all performance guarantees and expectations. The system has routinely achieved excellent SO_2 and particulate removal. It has been further shown that, given reliable and efficient particulate removal in the precipitator, a separate prescrubber vessel has been unnecessary.

The Abbott Station represents the first commercial installation of the CT-121 process in the United States. The startup and performance testing initiated in April of this year were highly successful, achieving or exceeding all of its projected goals. With the decanter and the Bird Young filter we now have two commercially demonstrated equipment alternatives for mechanical dewatering of CT-121 gypsum.

The CT-121 process continues to prove effective in all areas, including:

- Operating and maintenance simplicity
- Low power consumption
- High limestone utilization (over 99 percent)

- High gypsum quality
- Low effluent COD

The work described in this paper was not funded by the U. S. Environmental Protection Agency and therefore the contents do not necessarily reflect the views of the Agency and no official endorsement should be inferred.

REFERENCES

1. A. Tamaki. The Thoroughbred 101 Desulfurization Process. Chemical Engineering Progress. Vol. 71, No. 5, May 1975, p. 55

2. M. Sawahata, Y. Kogawa, A. Kumagai, B. R. Gilbert. Commercial Status of the Chiyoda Thoroughbred 121 (CT-121) Flue Gas Desulfurization Process. Paper presented at tthe American Power Conference, Chicago, Illinois, April 27-29, 1987

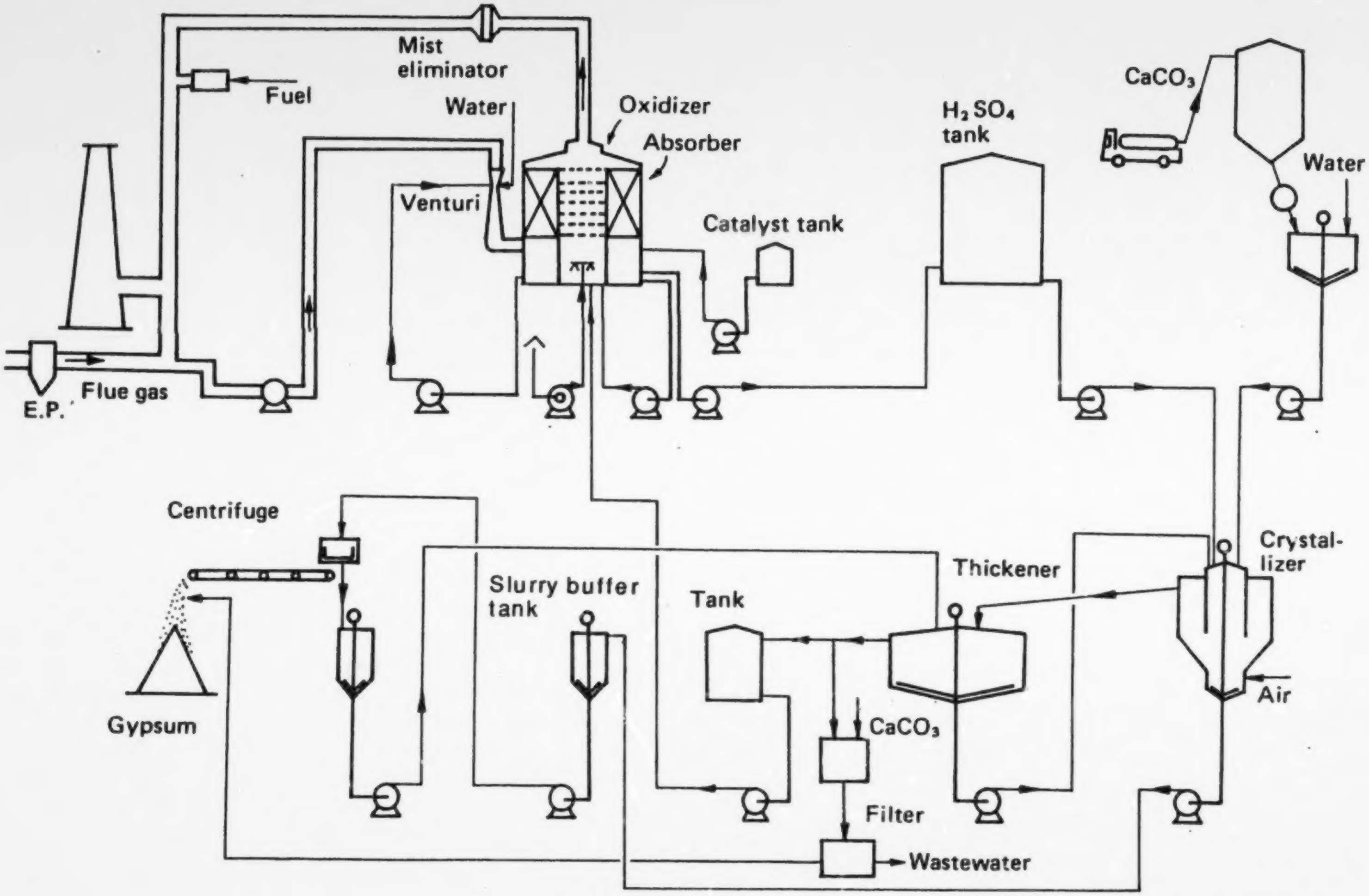
Mist
eliminator
Fuel
Water
Oxidizer
Absorber
Venturi
Catalyst tank
H_2SO_4
tank
$CaCO_3$
Water
E.P.
Flue gas
Centrifuge
Slurry buffer
tank
Tank
Thickener
Crystal-
lizer
Air
$CaCO_3$
Filter
Wastewater
Gypsum

Figure 1 Original CT-101 Process Flow Diagram Before Commission

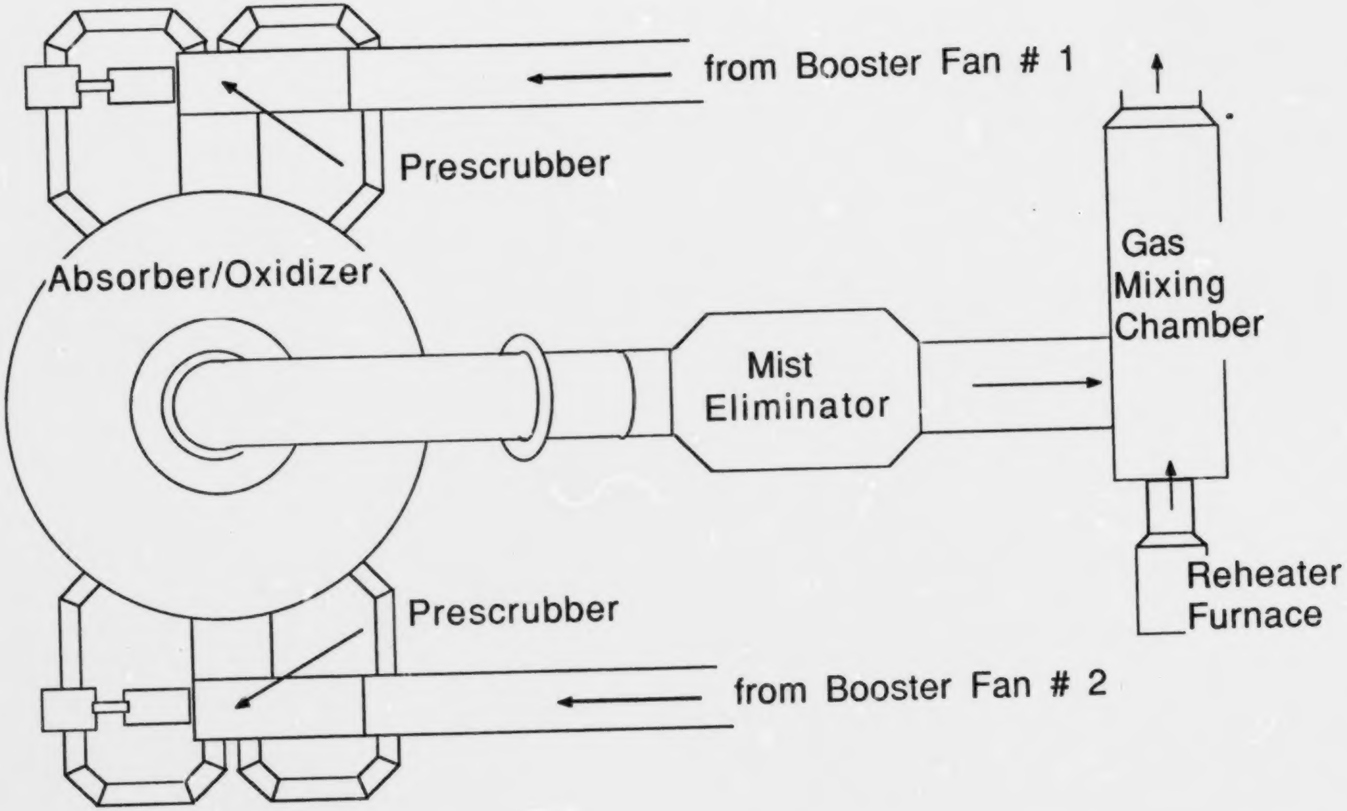
from Booster Fan # 1
Prescrubber
Absorber/Oxidizer
Gas
Mixing
Chamber
Mist
Eliminator
Reheater
Furnace
Prescrubber
from Booster Fan # 2

Figure 2 CT-101 Arrangement Before Conversion

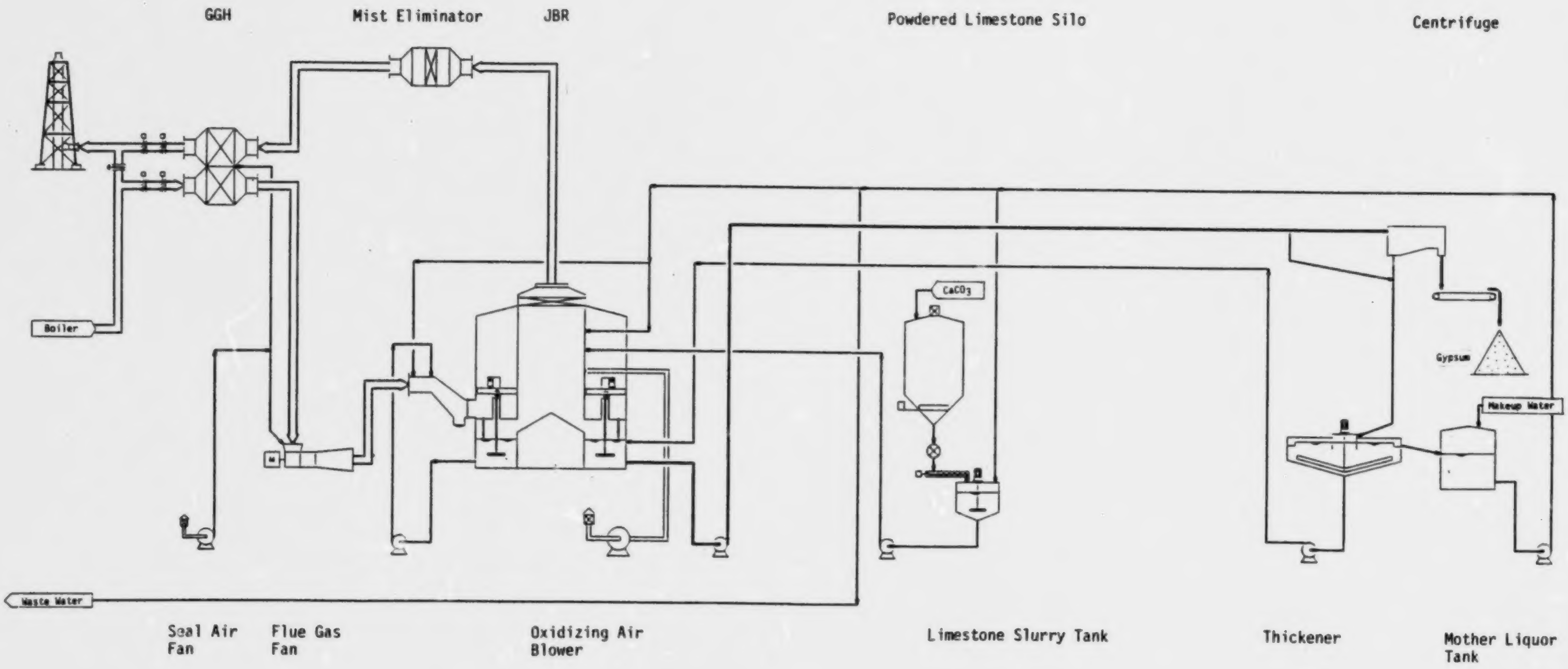
GGH
Mist Eliminator
JBR
Powdered Limestone Silo
Centrifuge
Boiler
CaCO3
Gypsum
Makeup Water
Waste Water
Seal Air Fan
Flue Gas Fan
Oxidizing Air Blower
Limestone Slurry Tank
Thickener
Mother Liquor Tank

Figure 3 CT-121 Process Flow Diagram After Conversion

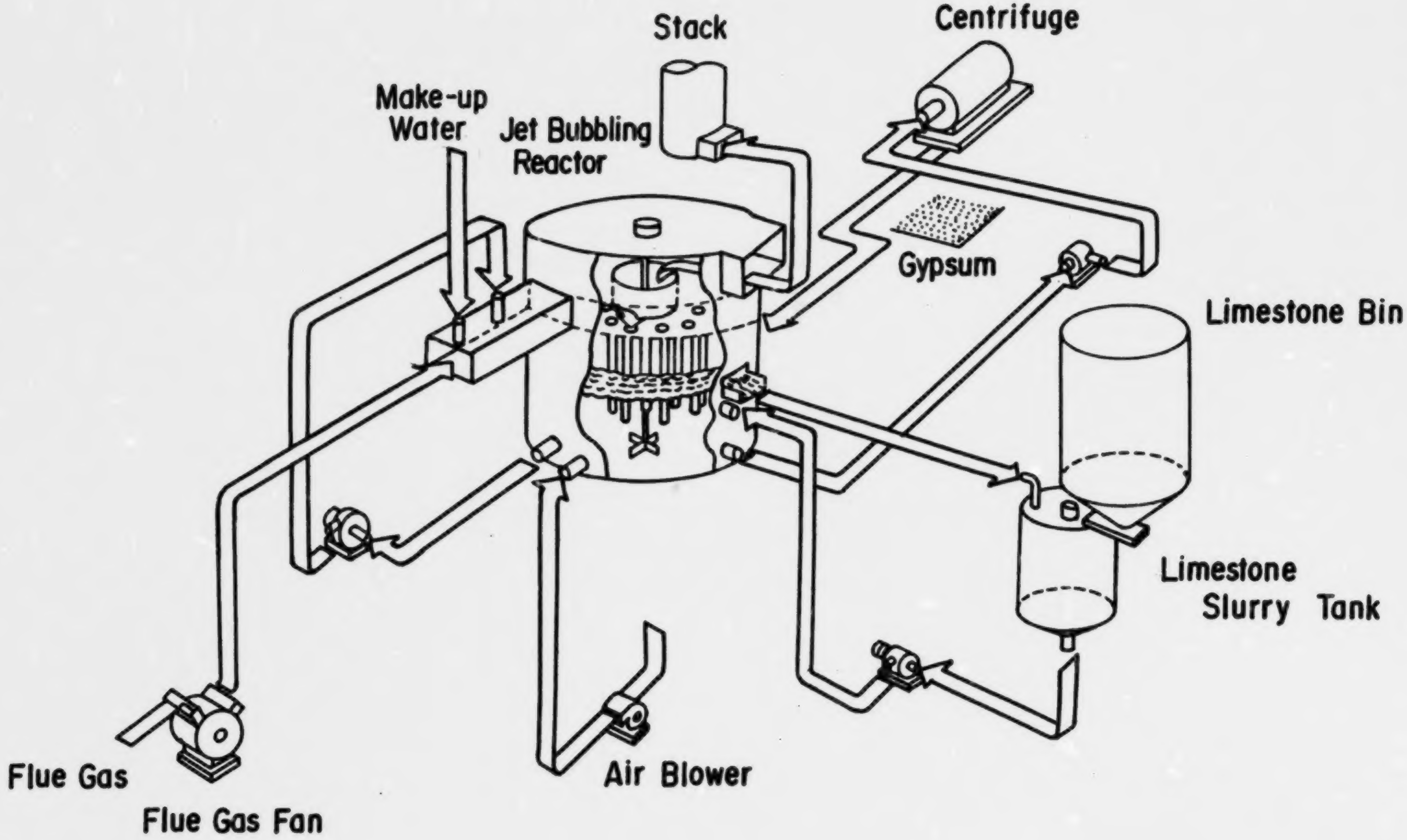
Stack
Centrifuge
Make-up
Water
Jet Bubbling
Reactor
Gypsum
Limestone Bin
Limestone
Slurry Tank
Flue Gas
Flue Gas Fan
Air Blower

Figure 4 Schematic of CT-121 Process

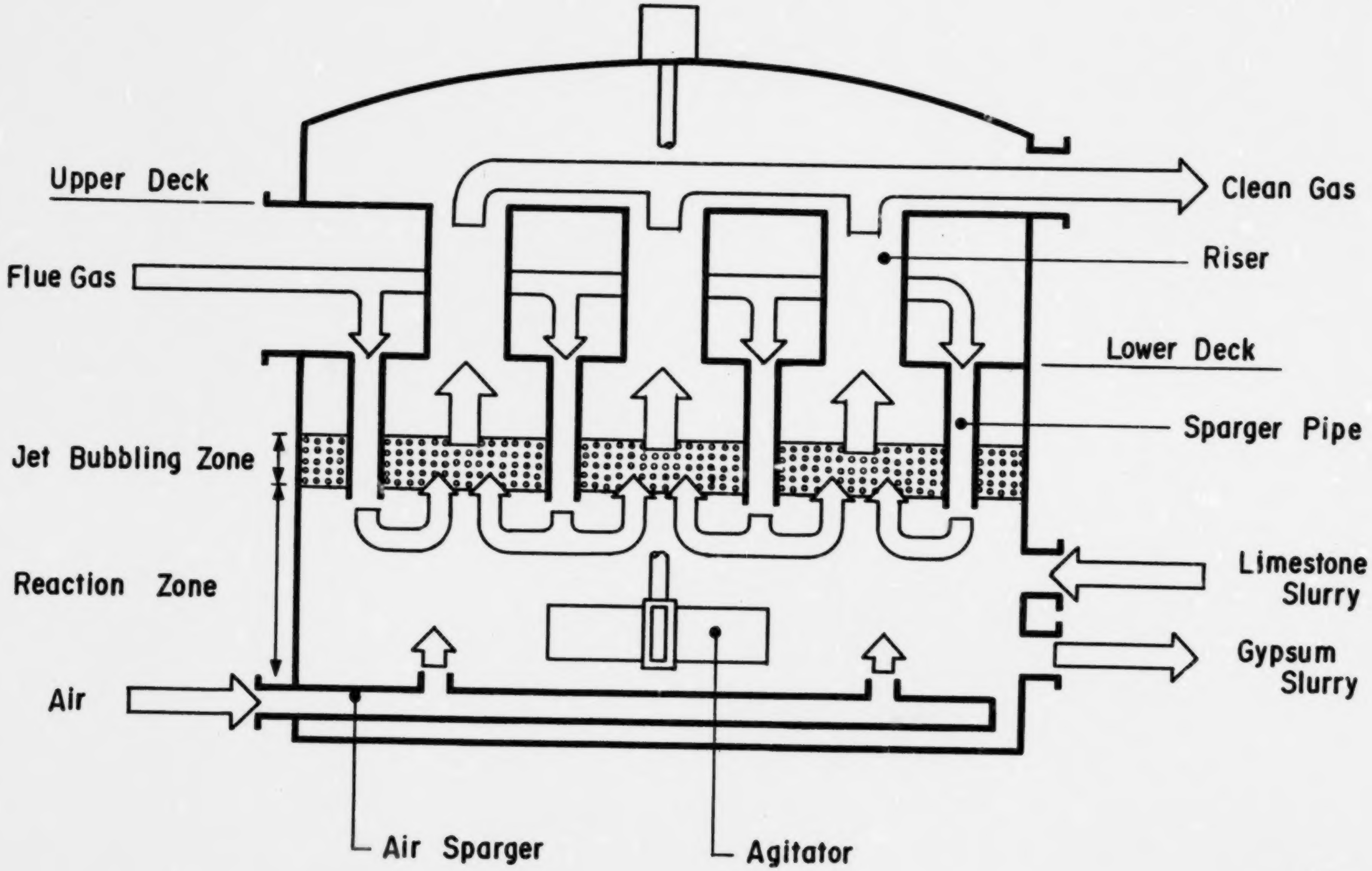
Upper Deck
Flue Gas
Jet Bubbling Zone
Reaction Zone
Air
Clean Gas
Riser
Lower Deck
Sparger Pipe
Limestone Slurry
Gypsum Slurry
Air Sparger
Agitator

Figure 5 Schematic of JBR Internals

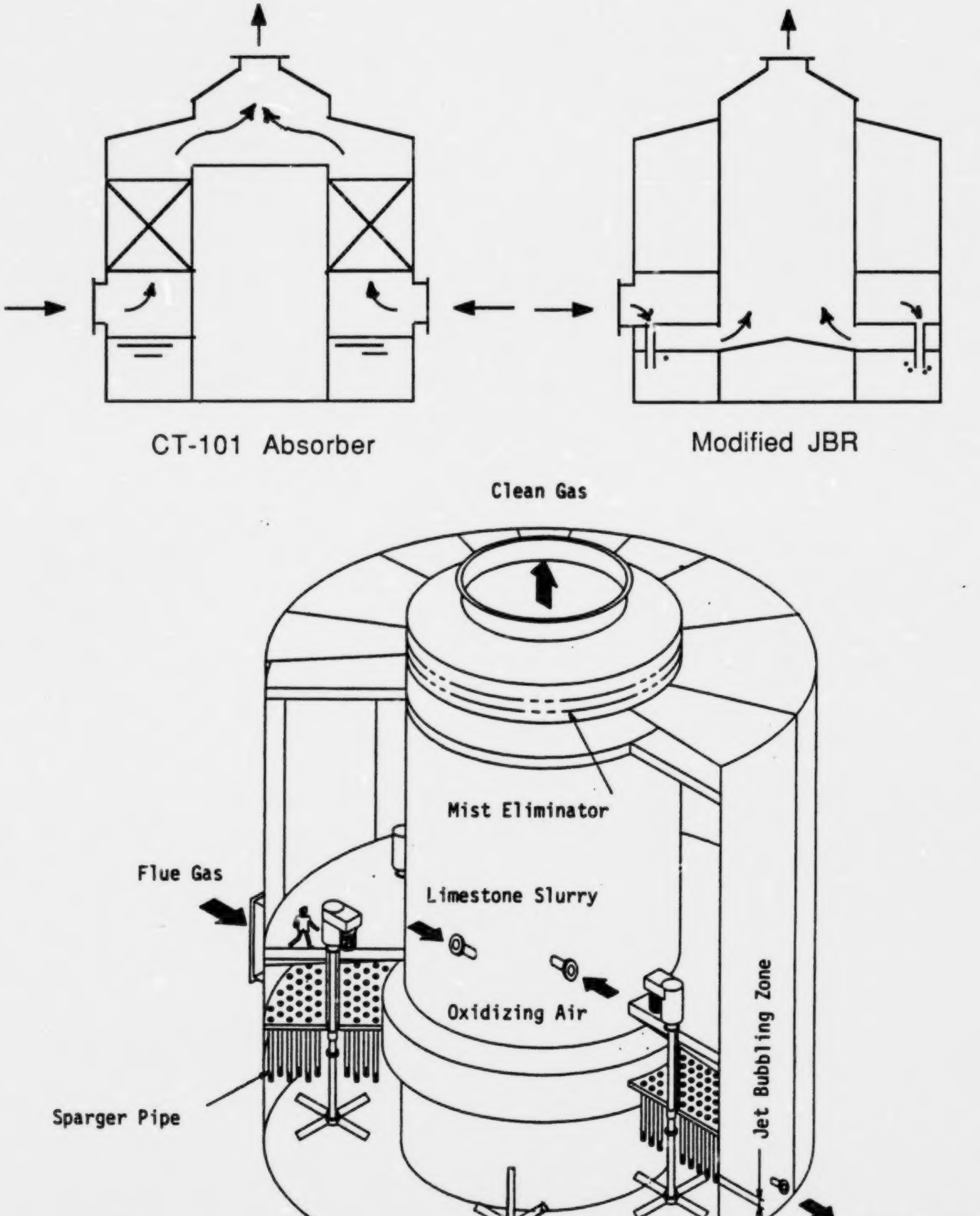
CT-101 Absorber
Modified JBR
Clean Gas
Mist Eliminator
Flue Gas
Limestone Slurry
Oxidizing Air
Sparger Pipe
Jet Bubbling Zone
Gypsum Slurry
Reaction Zone

Figure 6 Kusajima JBR Before and After Conversion

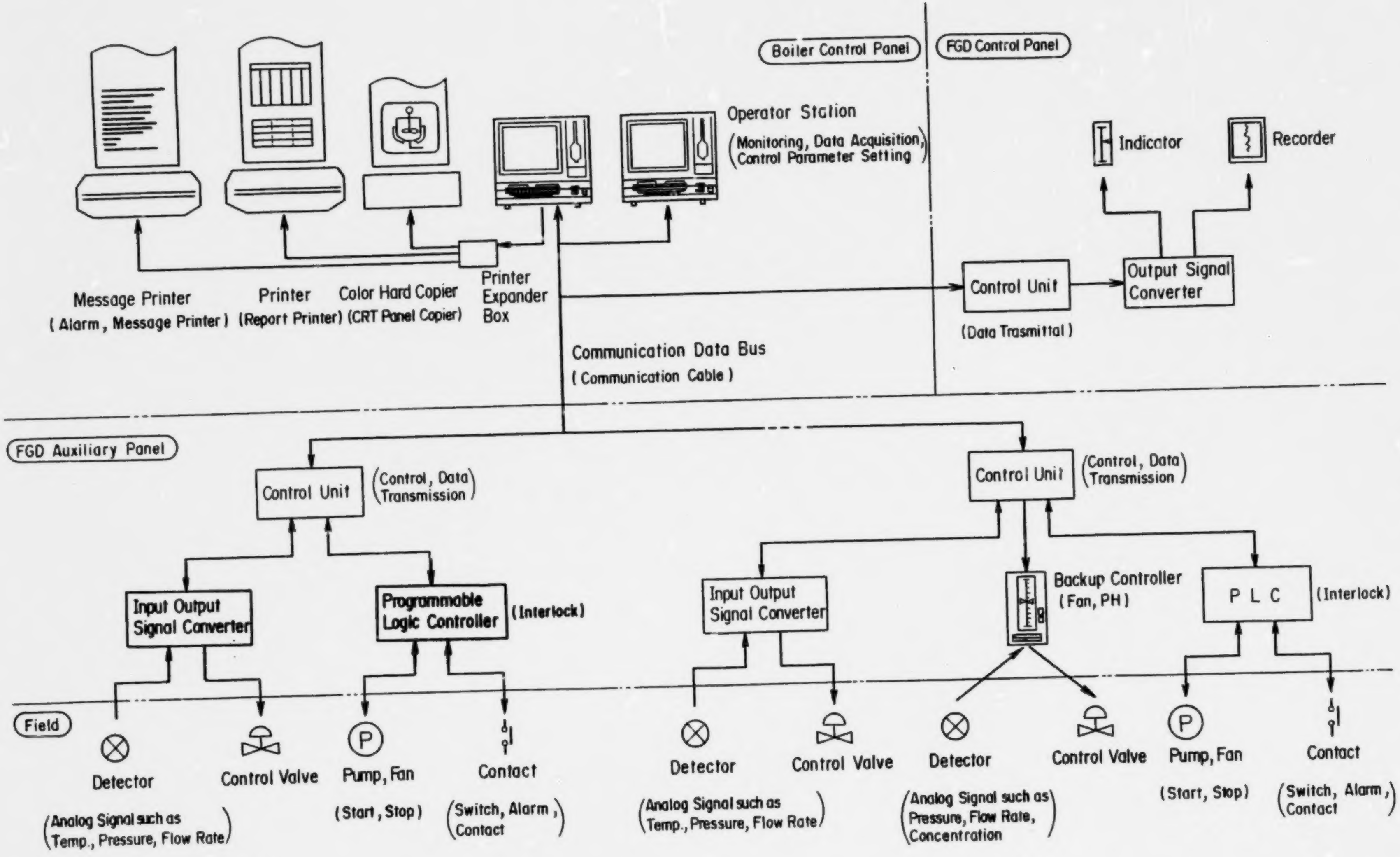
Boiler Control Panel
FGD Control Panel
Message Printer
(Alarm , Message Printer)
Printer
(Report Printer)
Color Hard Copier
(CRT Panel Copier)
Printer Expander Box
Operator Station
(Monitoring, Data Acquisition, Control Parameter Setting)
Indicator
Recorder
Control Unit
(Data Trasmittal)
Output Signal Converter
Communication Data Bus
(Communication Cable)
FGD Auxiliary Panel
Control Unit
(Control, Data Transmission)
Input Output Signal Converter
Programmable Logic Controller
(Interlock)
Control Unit
(Control, Data Transmission)
Input Output Signal Converter
Backup Controller
(Fan, PH)
P L C
(Interlock)
Field
Detector
(Analog Signal such as Temp., Pressure, Flow Rate)
Control Valve
Pump, Fan
(Start, Stop)
Contact
(Switch, Alarm, Contact)
Detector
(Analog Signal such as Temp., Pressure, Flow Rate)
Control Valve
Detector
(Analog Signal such as Pressure, Flow Rate, Concentration)
Control Valve
Pump, Fan
(Start, Stop)
Contact
(Switch, Alarm, Contact)

Figure 7 Control System Configuration After Conversion

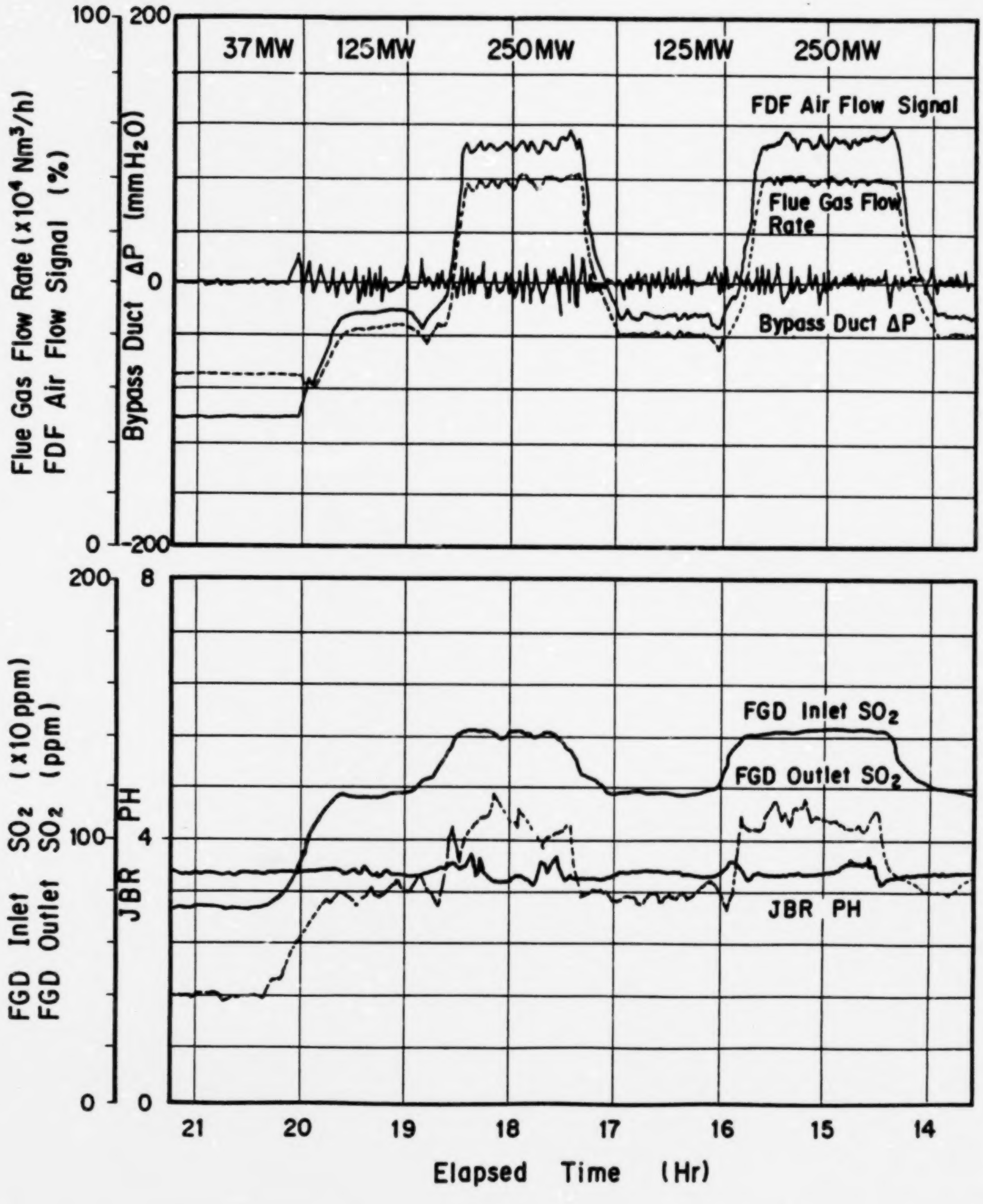

Figure 8 CT-121 System Response to Boiler Load Change (250 MW to 37 MW)

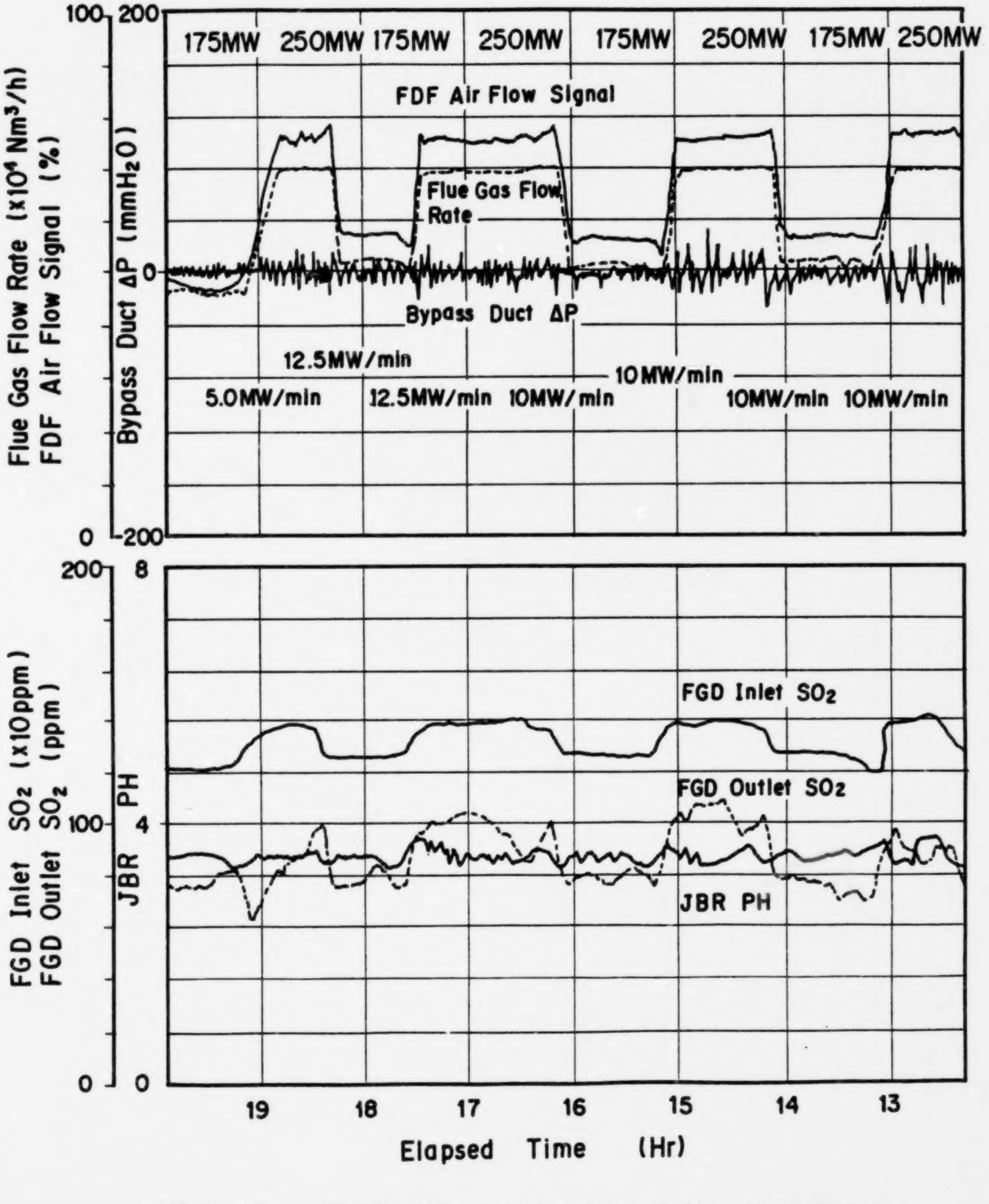

Figure 9 CT-121 System Response to Boiler Load Change (Maximum @ 5% per minute)

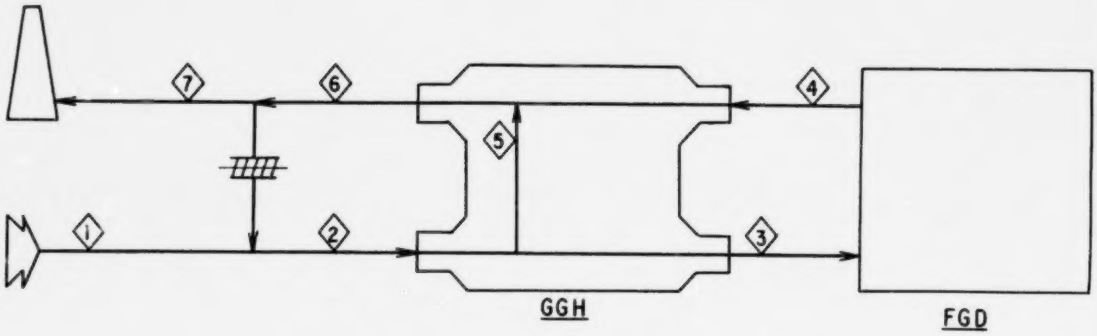

Particulate Balance(mg/Nm3 dry)

	⟨1⟩	⟨2⟩	⟨3⟩	⟨4⟩	⟨5⟩	⟨6⟩	⟨7⟩
Design	29.8	29.8	(28.8)	24.0	MAX.1	25.0	(25.0)
Result	–	10.7	6.0	2.6	–	4.1	–

Figure 10 CT-121 Particulate Balance, Kusajima (Oil Firing)

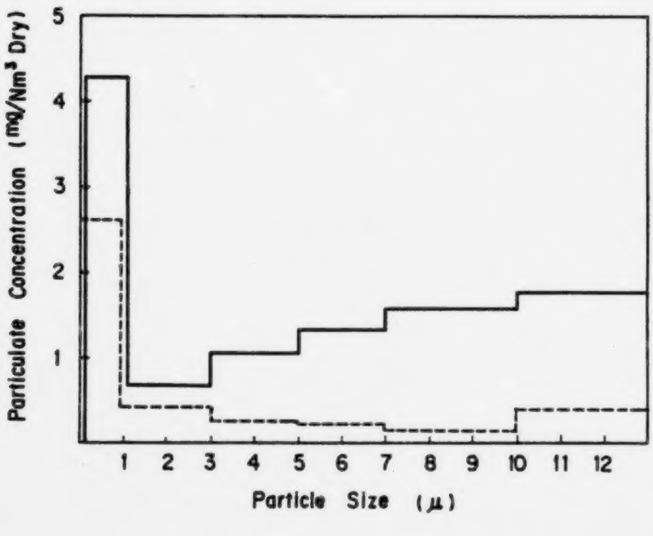

Figure 11 CT-121 Particle Size Distribution at Inlet and Outlet of FGD System, Kusajima (Oil Firing)

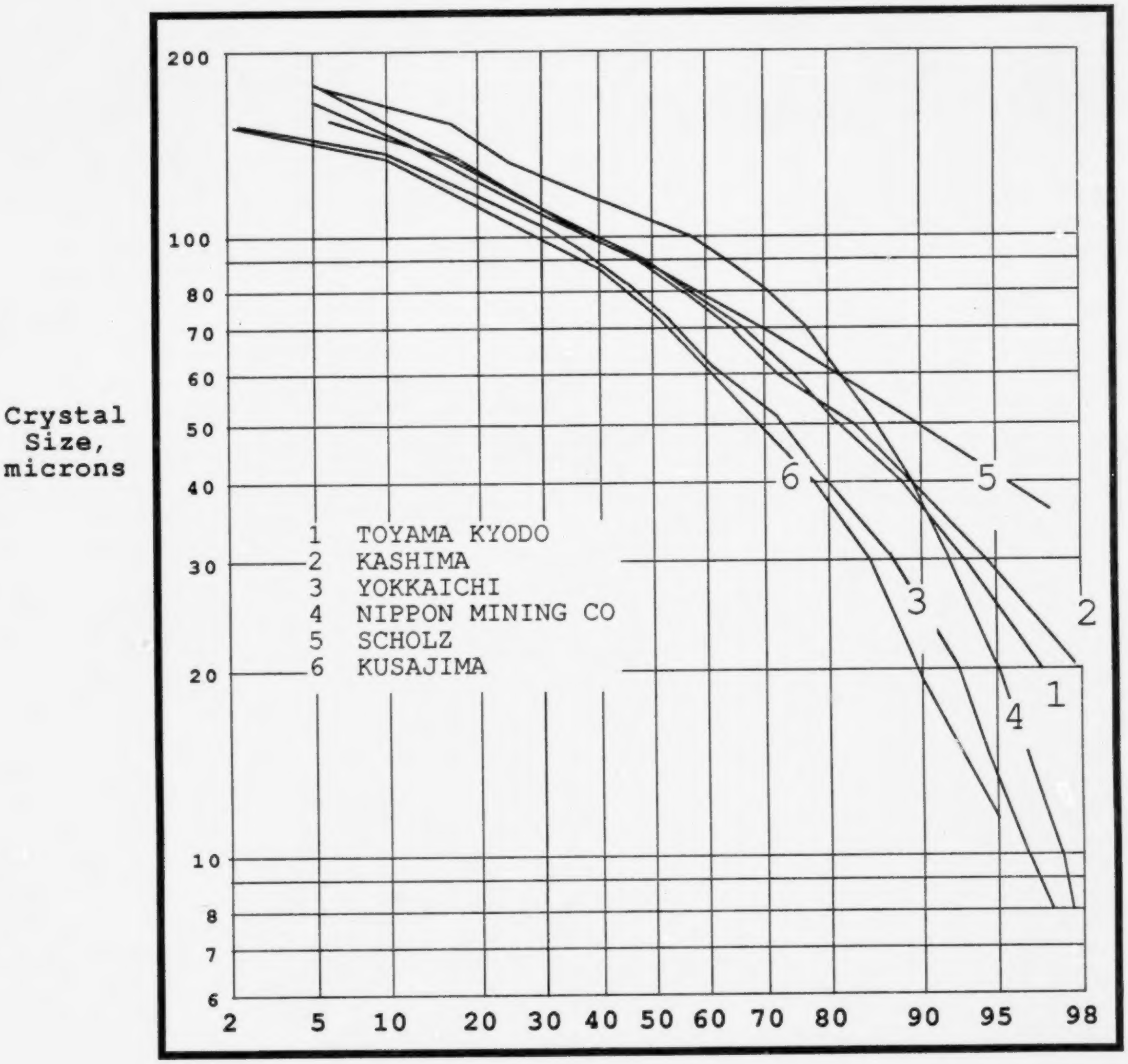

Cumulative Percent

Figure 12 CT-121 Gypsum Grain Size Distribution

Table 1

CT-121 DESIGN FIGURES AND RESULTS OF PERFORMANCE TEST
HOKURIKU ELECTRIC POWER (250 MW)
KUSAJIMA, JAPAN

DESIGN ITEM AND CONDITION	UNITS	DESIGN VALUES	TEST RESULTS
1. *Flue Gas Condition:*			
Flue gas flow rate	Nm^3/h	764,000	732,000
SO_2 concentration	ppm(wet)	1,395	1,238
H_2O concentration	%	10.6	12.0
Particulate loading	mg/Nm^3 (dry)	29.8	10.7
Temperature	°C.	142	144
2. *SO_2 Removal Efficiency at Stack Inlet*	*%*	*91 **	*91.7*
3. *Particulate in Treated Gas*	*mg/Nm^3 (dry)*	*less than the inlet concentration **	*2.3*
4. *Reheat Temperature*	*°C*	*higher than 94 **	*99*
5. *By-product Gypsum Moisture Content*	*wt %*	*less than 15 **	*10.3*
6. *Waste Water:*			
Quantity	m^3/h	4 *	4
pH		4 - 8 *	7.4
Suspended solids	ppm	less than 1,000 *	14
COD (Mn)	ppm	less than 10 *	4.1

* Guaranteed Values

Table 2

CT-121 RELIABILITY PARAMETERS

	Mitsubishi Petrochemical Yokkaichi	Nippon Mining Co Chita	Toyama Kyodo Electric Power Unit 1	Toyama Kyodo Electric Power Unit 2	Kashima Northern Joint Power Co.	Hokuriku Electric Power Toyama
Period:						
From	May 11, 1982	Nov 10, 1983	July 9, 1984	Aug 23, 1984	Nov 15, 1985	July 24, 1987
To	April 30, 1988	April 30, 1988	April 30, 1988	April 30, 1988	April 30, 1988	April 30, 1988
Hours of FGD operation	47,262	35,805	29,296	28,877	19,392	3,132
Hours called upon to operate	48,105	36,168	29,296	28,877	19,728	3,132
Reliability, %	98.2	99.0	100.0	100.0	98.3	100.0
Hours FGD available	47,262	37,053	32,130	31,872	20,616	6,270
Hours in period	50,280	39,216	33,600	32,856	21,528	6,750
Availability, %	94.0	94.5	95.6	97.0	95.8	92.9
Hours of FGD operation	47,262	35,805	29,296	28,877	19,392	3,132
Hours of boiler operation	48,111	36,168	29,296	28,877	19,728	3,132
Operability, %	98.2	99.0	100.0	100.0	98.3	100.0
Hours of FGD operation	47,262	35,805	29,296	28,877	19,392	3,132
Hours in period	50,280	39,216	33,600	32,856	21,528	6,750
Utilization, %	94.0	91.3	87.2	87.9	90.1	46.4

Reliability	-	hours the FGD system was operated divided by the hours the FGD system was called upon to operate.
Availability	-	hours the FGD system was available for operation (whether operated or not), divided by the hours in the period.
Operability	-	hours the FGD system was operated divided by the boiler operating hours in the period.
Utilization Factor	-	hours that the FGD system was operated divided by the hours in the period.

THE BISCHOFF FLUE GAS DESULFURIZATION PROCESS

by: K-R. Hegemann
Managing Director
Bischoff GmbH
Essen, West Germany

P. Kutemeyer
General Manager
Bischoff Environmental Systems
Pittsburgh, PA

ABSTRACT

The wet lime/limestone process by Bischoff, first introduced commercially in 1982, still represents the leading edge in wet FGD technology.

This system, initially tested in the 1960's, has been proven in several large commercial installations. This paper describes the system based on a 770 MW installation.

In 1982 the largest single train installation in Europe started up at the 770 MW Wilhelmshaven plant, treating 933,000 SCFM of the flue gas. All salient process steps, such as SO_2 absorption, oxidation, and mist separation were combined, for the first time, in one scrubber tower. The system employed a regenerative heat exchanger and produced marketable gypsum.

In 1985 a second scrubber treating the remaining 808,000 SCFM at Wilhelmshaven was commissioned, using a wet fan downstream of the scrubber, a first in a plant of this size. The objective was to reduce power and reagent while increasing SO_2 absorption.

Extensive operating results clearly demonstrate this system to be superior in operating reliability and simplicity.

INTRODUCTION

The Bischoff Flue Gas Desulfurization (FGD) System employs a wet lime/limestone process producing industrially marketable gypsum as by-product. The process was developed by Bischoff over a twenty-year period starting in the earily 1960's. The first European FGD demonstration plant was installed by Bischoff in 1977 at the 770 MW Wilhelmshaven Power Generation Plant of the Preussenelectra A.G.. This plant treated 311,000 SCFM (500,000 m_n^3/h) of flue gas, of the plant's total output of 1.74 million SCFM (2.8 million m_n^3/h).

After successfully demonstrating the concepts of its design, Bischoff began construction of a larger plant at Wilhemshaven designed to treat 933,000 SCFM (1.5 million m_n^3/h) of the flue gas in a single scrubber tower. This was the first plant in Europe with an integrated forced oxidation stage and started up in 1982. In 1985 a second scrubber designed to treat the remaining 808,000 SCFM (1.3 million m_n^3/h) was started up. This installation featured Europe's first compact FGD plant, using lime or limestone, with a wet fan located vertically between the scrubber and the heat exchanger on the clean gas side.

Although Bischoff FGD systems are presently treating 7,000 MW of capacity worldwide, it is the Wilhelmshaven plant that has served as the testing ground of this process. This plant has played a major role in demonstrating several FGD related developments that have had a major impact on FGD technology and operational methodology in Europe. Many of these innovations, it is felt, have direct or indirect application potential in North America and can contribute to make FGD plants here cheaper and more reliable.

Wilhelmshaven FGD Plants 1 and 2

After successfully demonstrating the basic concepts of its FGD process in various experiments and pilot plants, Bischoff started up Europe's first FGD demonstration plant at the 770 MW Wilhelmshaven Power Plant of the PreussenElectra A.G., in 1977. This co-current scrubber treated 311,000 SCFM (500,000 m_n^3/h) of flue gas of the plant's total 1.74 million SCFM (2.8 million m_n^3/h).

In 1980, having successfully demonstrated the Bischoff process on a large scale, plans were being developed for the next phase in the process of treating Wilhelmshaven's flue gases. The next step called for treating 933,000 SCFM (1.5 million m_n^3/h) of flue gas in a single scrubber tower.

Based on experience gained with Plant 1, Bischoff designed and built a large scrubber tower which treated 933,000 SCFM (1.5 million m_n^3/h) of flue gas in a countercurrent, instead of co-current, process. All process steps, i.e. absorption, forced oxidation, crystallization and mist elmination are integrated in this single scrubber. Designated Plant 2, it was erected next to Plant 1 which was subsequently shut down and later dismantled when the new FGD Plant 1A was erected. (see figure 1 for Plants 1 & 2).

The use of one single scrubber to treat such a large volume of flue gas, instead of using several smaller units, was a radical departure from the conventional approach and resulted in considerable savings to the power plant operator.

PROCESS DESCRIPTION OF FGD PLANT 2

The Flue Gas Side (an overview)

Let us now take a closer look at the Bischoff FGD process, first looking at the flue gas side. A process flow diagrm is shown in figure 2 with the flue gas side on the left.

After leaving the ESP, the hot raw gas passes through an axial fan from there to a regenerative heat exchanger, where it transmits a part of its heat energy to the cleaned and cool flue gas. The cooled raw gas then enters the side of the scrubber vessel approximately 1/3 of the way up.

In the scrubber's absorber section, pollutants are removed from the flue gas. The gas is treated by streaming upward through various levels of scrubbing slurry sprays. The slurry contains lime or limestone as reagent. At the top the now saturated flue gas passes through a mist separator where most of the free moisture is removed. It then leaves the scrubber on one side and enters a gas mixer where any remaining free moisture is vaporized. Next the gas again passes through the regenerative heat exchanger in the opposite direction, is reheated, and passes to the stack.

The Slurry and By-Product Side (an overview)

The flue gas passage through the FGD-system represents one portion of the FGD-plant; the other important part consists of the slurry/by-product treatment and the reagent preparation, delivery and circulation system. Figure 2 shows that portion of the process on the right hand side.

The scrubbing slurry dropping from the absorber section, and laden with removed pollutants, is collected in the lower portion of the scrubber commonly referred to as the sump. The sump is divided into two main sections. The top section is called the forced oxidation zone, and the lower section the crystallization zone.

In the forced oxidation zone gypsum is formed by a reaction between oxygen from the blown in air and the sulfur dioxide laden slurry. In the crystallization zone the gypsum particles form larger crystals. Also in this section new lime or limestone slurry is added to the system.

Recirculation pumps recirculate the slurry in the sump to the absorber sprays. A small portion of the gypsum slurry in the sump is removed and pumped to a hydrocyclone. The underflow from the cyclone is fed to a screw centrifuge or a vacuum band filter, from which the dewatered gypsum is dumped into a silo.

DETAILS OF FGD PLANT 2

The Flue Gas Side

We shall now take a closer look at some of the more important components that comprise the Bischoff System.

Regenerative Heat Exchanger

As was mentioned above, the hot flue gas, after leaving the axial fan, passes through the regenerative heat exchanger. This is a gas/gas type heat exchanger. The hot flue gas, with a temperature of about 270°F (130°C), passes through the heat exchanger from bottom to top, transmitting a part of its heat energy to rotating heat storage elements. In the process the raw gas is cooled down to about 175°F (80°C).

After passing through the scrubber, the mist eliminator, and the gas mixer, the cleaned flue gas again passes through the heat exchanger in the opposite direction and is reheated to 210°F (100°C) by the hot heat storage elements.

The heat storage elements in the heat exchanger consist of plate bundles arranged parallel to the gas stream. They are fabricated of enameled steel plates on the hot gas side, and thermoplastic material on the cold side (see figure 3).

In this type of heat exchanger, leakages between the raw and clean gas side are unfortunately unavoidable. On the one hand these leakages are caused by the continuous rotation of the heat storage elements, on the other hand gas from the high pressure side leaks into the low pressure side. Due to the fact that the Wilhelmshaven FGD Plant 2 operates with the raw gas side at a higher pressure than the clean gas side, raw gas leaks into the clean gas stream at the heat exchanger. The total leakage amounts to about 4%. To compensate for a resulting reduction of the overall treatment efficiency, the scrubber is designed to achieve a higher degree of pollutant removal. Depending on design, the scrubber efficiency ranges between 95% and 98%.

The decision to employ a regenerative heat exchanger was made after extensive tests with various reheat systems. The regenerative heat exchanger has the distinct advantage that practically no additional energy, such as steam for example, is required. This reduces operating costs significantly. The advantages of a regenerative heat exchanger are as follows:

1. Reheating of the flue gas without additional energy and thus lower operating costs.

2. Reduce thermal loads in the scrubber due to the lower gas inlet temperatures.

Absorption

The next step in the flue gas treatment is the removal of various environmentally undesireable components from the flue gas. This is accomplished in the absorber section located in the top half of the scrubber.

The absorber section, like the rest of the scrubber vessel is a rubber lined steel shell. The absorber consists of several levels of sprays (six in the case of Plant 2). At each level, nozzles protruding from the scrubber wall spray lime or limestone slurry into the upward flowing gas stream.

In this counter current washing process SO_2, HCl and HF, as well as any remaining fly ash particles, are removed from the flue gas. Here the gas is also cooled to a saturation temperature of 113°F (45°C).

Each spraying level is equipped with a number of large, non-clogging nozzles, especially developed by Bischoff. These nozzles, arranged in a circular pattern around the scrubber, spray in both directions, with the exception of the topmost level which only sprays downward. The conical spray patterns of the nozzles overlap producing a solid curtain of fine droplets through which the gas must pass. This curtain of fine droplets provides a large effective surface area for the reactions necessary to remove the pollutants. The slurry sprayed into the flue gas consists of approximately 100,000 ppm of solids, most of which is gypsum. Only 3,000 to 5,000 ppm of the solids content is lime or limestone.

The advantages of this approach can be summarized as follows:

1. Large non clogging nozzles
2. Completely open absorber section
3. Curtains of fine droplets, resulting in a large effective reaction area
4. Easily replaceable nozzles

Mist Separator

In passing through the absorber section, the flue gas inevitably will carry along with it slurry droplets which contain solids and dissolved salts. To prevent a buildup of deposits and corrosion downstream of the scrubber, these droplets must be removed. For this purpose a mist separator is installed at the top of the scrubber tower.

This mist separator is a horizontal flow vane-type eliminator consisting of bundles arranged in a circular manner around the top, with two bundles behind each other (see figure 4). The gas flows horizontally through the mist separator from the inside to the outside.

The circular arrangement selected offers several advantages over mist separators placed at the scrubber exit on one side of the vessel.

For one, given the low pressure drop in the scrubber tower, it is difficult to achieve good gas distribution over the surface of the conventionally placed mist separator. This results in droplets being carried through the mist separator since the uneven gas distribution over the separator results in flow velocities greater than those for which the mist separator was designed. Also, the gas flow in the scrubber tower would not be evenly distributed with a mist separator located at the scrubber exit on one side of the vessel.

The circular, and slightly eccentric, arrangement selected in this design results in an even distribution of gas flow over the entire mist separator and thus avoids the use of gas distribution vanes. This arrangement also has the advantage over the more conventional type in that water draining off the mist separator does not affect the gas flow.

The mist separator bundles are periodically washed to remove any deposits that may have built up. The wash water spray also serves as makeup water for the system. In the Wilhelmshaven plants sea water is used. Operating experience with this design has shown the following advantages:

1. A highly efficient mist separation
2. Even gas flow distribution over the entire mist separator area
3. Axially symmetric gas distribution in the scrubber's absorption section
4. Even weight distribution on the scrubber vessel

Flue Gas Mixer

After exiting the scrubber the flue gas enters a flue gas mixer designed to vaporize any remaining free moisture in the flue gas. In this venturi mixer a small amount of hot untreated flue gas is mixed with the clean gas to effect the vaporization. The reason for this mixer was the concern that any remaining free moisture in the flue gas, after the mist separator, would cause buildups on the surfaces of the regenerative heat exchanger.

Experiments after the startup have shown, however, that in this plant the mixer is not really required. First of all the efficiency of the mist separator is such that very little free moisture remains in the flue gas; and second, the buildups which do occur on the heat exchanger surfaces can be readily removed by means of high pressure air or water sprays during operation. Heat exchanger pressure drop measurements determine when deposits must be removed. Figure 5 shows a chart of pressure drops for the heat exchanger covering a period of almost four years.

The Slurry and By-Product Side

We shall now take a closer look at the slurry and by-product side of the Bischoff FGD process.

The Forced Oxidation Zone

After absorbing various pollutants from the flue gas in the absorber section, the slurry falls to the bottom of the scrubber where it collects in the sump. As we indicated earilier, the sump is divided into two zones, the forced oxidation zone, and the crystallization zone.

In the forced oxidation zone, air is blown into the slurry, which aids in the formation of gypsum particles. The chemical reactions taking place in the absorption and oxidation processes are shown in figure 6, using limestone as the reagent.

The relatively low solubility of limestone, or calcium carbonate, in water is increased in the scrubber by the presence of carbon dioxide. In the solution calcium hydrogen carbonate is formed. This in turn reacts with sulfur dioxide to form a soluble calcium hydrogen sulfite. In cases where the pH value is greater than 5, a not readily soluble calcium sulfite is formed instead. Since dissolved components are oxidized more readily, this reaction is not desired and the pH value in the forced oxidation zone is maintained between 4 and 5.

In the oxidation zone, the calcium hydrogen sulfite reacts with oxygen from the blown in air to form calcium sulfate. The sulfuric acid formed during the oxidation process reacts with limestone in the formation of calcium sulfate and carbon dioxide. The latter in turn aids in the further solution of limestone in water. Calcium sulfate then crystalizes to calcium sulfate dihydrate, or gypsum.

Besides sulfur dioxide, the limestone also reacts with hydrogen chloride and hydrogen fluoride to form dissolved calcium chloride and solid calcuim fluoride.

The addition of air into the forced oxidation zone is accomplished by a specially designed air distribution system. This air distribution system consists of a large central air tunnel which bisects the scrubber at the forced oxidation zone level with hoods radiating out from its side. The U shaped hoods, open to the bottom, have holes drilled in the top which allow the air to percolate up through the slurry. (see figure 7).

The advantage of this system is that during a shut down the air supply can be turned off without having deposits settle out in the hoods and clogging them.

Because of the design of this air distribution system, using large air hoods, the flow of the scrubber slurry between these hoods is increased, and this in turn prevents a back mixing of slurry from the higher pH value crystallization zone. Such a back mixing would increase the pH value in the forced oxidation zone, and this would reduce the efficiency of the oxidation process.

Based on the buildup of gypsum in the system, part of the slurry in the forced oxidation zone is removed and pumped to a gypsum dewatering station.

The Crystallization Zone

The crystallization zone is the lower portion of the sump. The retention time is long enough to decompose the oversaturation of the gypsum. Larger gypsum-crystals are built up. Here, too, the makeup lime or limestone slurry is added to regenerate the scrubbing slurry. The lime or limestone slurry added is evenly distributed in the scrubber sump and causes an increase of the pH value. Recirculation pumps extract the slurry from the conical bottom of this section and deliver it to the various spray nozzles in the absorber section. The recirculated slurry at the Wilhelmshaven FGD Plant 2 is approximately 40,500 gals/min (9,200 m^3/h).

Lime or limestone is stored in a silo and from there transported to a preparation tank where it is mixed with water. The lime or limestone slurry then flows into a feed tank from where it is pumped to the scrubber.

In case of a shut down the entire amount of slurry in the scrubber collects in the sump. Even though about a hundred tons of gypsum settle out at the bottom, in this case, no recirculation pumps or agitators are employed.

During start-up liquid above the solid layer is discharge by the recirculation pumps and pumped into the lower part of the scrubber sump via the discharge pipes. In this way it is possible to re-suspend the settled out gypsum in a few minutes. The pumps are then switched to normal operation, where they again provide slurry to the absorber sprays. Usually within 15 minutes after startup, the system is able to reach its full desulfurization efficiency again. The following advantages can, in summary, be listed for this scrubber sump design philosophy:

1. Non clogging forced air system provides an optimum air distribution

2. Effective separation of forced oxidation and crystallization zone without separator walls or the undersirable back mixing of slurry from the latter to the former.

3. Integration of absorption, oxidation and crystallization in a single scrubber vessel

Gypsum Dewatering and Storage

As gypsum in the scrubber slurry builds up, a portion of the slurry is removed at the oxidation zone level and is pumped to a gypsum dewatering station where the large gypsum crystals are removed, and the rest is returned to the scrubber. The dewatering station consist of several hydrocyclones, operating in parallel, followed by either a screw centrifuge or a vacuum band filter. In Wilhelmshaven the owner decided to install a screw centrifuge.

The hydrocyclones are used to classify the solids, with the larger being removed with the underflow, which is fed to the screw centrifuge. The screw centrifuge consists mainly of a feeder tube, which accepts the underflow from the cyclones and an inclined strainer drum with a concentric screw conveyor. Both rotate in the same direction at slightly different speeds so that the gypsum is transported to the discharge pipe. Water is removed through a screen which comprises the drum, and is added to the hydrocyclone overflow. (see figure 8)

Because of the susceptibility of the centrifuge to clogging the owner at Wilhelmshaven has decided to retrofit this unit with a vacuum belt filter.

Salts, which are not a desirable additive to gypsum used commercially, are washed out by adding water to the dewatering system.

The dewatered gypsum, with a moisture content of about 10%, is dumped into a silo from where it is withdrawn and transported to the end user.

The filrate from the dewatering process and the overflow from the hydrocyclones is returned to the scrubber where the small gypsum particles serve as crystallization nuclei.

A small portion of the hydrocyclone overflow is removed from the system as waste water.

Due to the close proximity of the plant to the end user of the by-product gypsum, the silo at Wilhelmshaven is only large enough to accomodate the gypsum produced during one weekend. At other plants, such as Kiel and Farge, for example, where distances to the end user are greater, the silos are capable of storing 1,200 tons of gypsum. Figure 9 shows a comparision of the two silos both of which incorporate the dewatering station on top.

Waste Water Treatment

As stated earlier, a small portion of the cyclone overflow is removed from the system as waste water. This is required to prevent a build up of chlorides that would adversely affect the desulfurization process.

The waste water treatment plant is designed to remove heavy metals which enter the system primarily via the lime or limestone reagent, in the dust particles not removed by the ESP's, and in the makeup water.

Water treatment consists of a neutralization step using lime milk of a soda-lye solution and a precipitation step using a sodium sulfide solution. In this process heavy metals are precipitated in the form of not readily soluble hydroxides,oxyhydrates and sulfides. They are then removed by floculation and sedimentation. Dewatering is accomplished using a filter press, and final water treatment by means of a sand filter. (see figure 10).

WILHELMSHAVEN FGD PLANT 1A

Goals

As we showed earlier, FGD Plant 2 at Wilhelmshaven treated more than 50% of the flue gas generated by the plant, which satisfied the requirements in existance at that time. In 1983, however, a new law was passed which required that by 1988 all power plants with a capacity greater than 50 MW treat 100% of their flue gas. The law also mandated a maximum allowable SO_2 emission of 0.165 grains/SCFM (400 mg/m^3). As a result the decision was made to build an additional plant at Wilhelmshaven to treat the remaining 808,000 SCFM (1.3 million m^3/h) of flue gas. This plant was designated as FGD Plant 1A (see figure 11).

The goal in designing this plant was to reduce the overall cost of the plant, reduce the energy required to operate it, and to increase the efficiency.

To realize these goals Bischoff and the engineers from the power plant went to work reviewing the operating experience gained with Plants 1 and 2 and to determine where improvements were possible. The results of this effort was Plant 1A, where, in fact, savings were realized and the efficiency was improved. (see figure 12 for a flow diagram of Plant 1A)

Another First At Wilhlemshaven

To its reputation as being a plant where several signficant firsts in FGD technology were tested and proven in Europe, Wilhelmshaven added one more. The FGD-Plant 1A was Europe's first compact FGD plant using lime or limestone to employ a wet fan located vertically between the scrubber and the heat exchanger on the clean gas side. It started up in 1985.

Clearly, this location provided significant advantages both in terms of costs and efficiency. For one, the hot gas mixer initially installed in Plant 2 was no longer necessary since any droplets carried through the mist separator would be evaporated by the heat of compression in the fan.

The location of the fan downstream of the scrubber was possible due to the extremely efficient operation of the mist separator, because an excessive free moisture carryover would have adversely affected the fan. Measurements confirmed that free moisture downstream of the mist separator was well below the guarantee value of 0.08 grains/SCF (200 mg/m_n^3). In fact only 0.012 grains/SCF (30 mg/m_n^3) were measured. Thus a trouble free operation of both the fan and the heat exchanger was anticipated.

Another advantage of locating the flue gas fan on the clean gas side, between the scrubber and the cold side of the heat exchanger, was the fact that in the heat exchanger the pressure leakage, which we talked about earlier, was now from the clean gas side to the raw gas side. This resulted in a greater efficiency for the FGD system.

Additionally, due to a more direct flue gas path, the amount of flue gas was reduced, resulting in a lower pressure drop in the system. Capital costs for flue gas duct, steel structure and fan foundation were reduced due to the compact construction. Finally the wet fan required signficantly less power than a fan located on the hot side due to the fact that the gas volume to be moved is less.

The Fan

The fan used in Plant 1A is an axial fan with the motor located at the fan's hub. Thus the fan wheel is mounted directly on the motor shaft, eliminating the transmission, the fan shaft, and the fan shaft bearing.

The axial fan at the Wilhelmshaven FGD Plant 1A has the following noteworthy characteristics:

1. All starter components are rubberized to protect them against corrosion
2. Fan blades and the fan blade housing are constructed of corrosion resistant materials
3. The fan hub is pressurized to prevent corrosive materials from entering
4. To cool the motor in the hub, a cooling air system is installed

In case the fan must be replaced, provisions are made to install rails on which the entire fan assembly can be rolled out on one side.

In order to determine sound insulation requirements, measurements were made. The results were surprisingly good, with maximum sound levels of only 93 dB (A) measured near the fan.

Results

One aim in arranging the fan on the cold clean gas side was to improve the overall SO_2-removal efficiency. This proved to be totally successful as can be seen by comparing the overall SO_2-removal efficiency of 95% of the FGD-Plant 1A with the greater than 80% efficiency of the FGD-Plant 2. The SO_2 content in the raw gas is 1.25 grains/SCF (3 mg/m_n^3). The SO_2-content in the clean gas is 0.06 grains/SCF (150 mg/m_n^3) far below the legally required limit.

Figure 13 shows the success achieved in Wilhelmshaven in reducing the power requirements starting with Plant 1 and ending with Plant 1A.

We can see for example, that the power requirements of Plant 1A, as compared to Plant 1, were reduced by 20%.

The degree of automation in the operating control system of the FGD plants at Wilhelmshaven is the result of the desire by the plant operator to simplify the operation as much as possible. Optimization of the operation in Plant 2, as compared to Plant 1, resulted in an almost 50% reduction in the number of actuators and measurement points. (see figure 14)

Whereas Plant 1, which employed a relay control system, was operated from a separate control stand, Plant 2, which employed free programable controllers, ended up, after optimization, being controlled directly from the main plant control room.

In optimizing the control system for Plant 2 various functional groups were combined and an overall control scheme was developed. The free programable control system proved to be a good choice, particularly in view of the many changes that had to be made in the control scheme during the optimization process.

The good results obtained with Plant 2 were also used to give Plant 1A a fully automatic control system. Now both Plant 2 and Plant 1A are operated from the main plant control room without the need for additional operating personnel.

The control system of Plant 1A is arranged such that after the boiler comes on line, the various funcational groups actuate one after the other, bringing the FGD plant to full operation.

The first step in this process is to start the regenerative heat exchanger. The second is to start the recirculating pumps. Next, after determining that the heat exchanger has attained the required RPM, the flue gas fan is started. The fourth step activates the lime slurry addition. New lime slurry is automatically mixed when the slurry level in the slurry feed tank drops to a preset level. This insures a continuous supply of reagent to the scrubber.

At this point the plant is in full operation treating the power plant's flue gas.

THE FUTURE

Figure 15 shows Bischoff FGD plant size as a function of time. Given the experience gained at Wilhelmshaven over the years, as well as the technical capabilities available today, Bischoff would have no qualms in designing and building an even larger plant, such as for example one capable of treating 1.74 million SCFM (2.8 million m_n^3/h), of the flue gas, corresponding to a 800 MW power station, in a single scrubber.

Based on the experience gained and the excellent operating results of the plants at Wilhelmshaven, it is our opinion that building larger single scrubber FGD plants is the next logical step in the attempt to simplify the operation of an FGD plant and in reducing both operating and capital costs.

CONCLUSION

The Wilhelmshaven experience has shown that much can be achieved, and many innovations made, if the designer/supplier of the FGD equipment and the power plant operator work closely together in identifying problems, accepting risks and trying new solutions, and in making the commitment to insure that the system works.

That the Bischoff concept works is demonstrated by the fact that the flue gas from a total of 7,000 MW of electric power in Europe is or soon will be cleaned by this process. We feel that many of the lessions learned with these plants are directly applicable in North America, where, as in Europe, they can contribute to significant savings in capital as well as operating costs.

NOTE: The work described in this paper was not funded by the U.S. Environmental Portection Agency and therefore the contents do not necessarily reflect the view of the Agency and no official endorsement should be inferred.

REFERENCES

W. Bosselmann, H. Weiler
Erste Betriebserfhrunge mit der Rauchgasentschwefelungsanlage
im Kraftwerk Wilhelmshaven
(VGB 1978)

W. Bosselmann, K-R. Hegemann, J. Leimkuhler
Weitere Betriebserfhrungen mit einer Rauchgasentschwefelungsanlage
in Wilhelmshaven und deren Ubertragung auf die Anlagenerweiterung
(VGB 1981)

M. Frauenfield
Lhunstrom - Gasvorwarmer zur Wiederaufheizung nassentschwefelter
Reingase
Technische Losungmoglichkeiten zur Verminderung von Leckage,
Verschmutzung und Korrosion
(1982)

J. Leimkuhler, H. Weissert
Erst Betriebserfahrung mit der Rauchgasentschwefelungsanlage 2
im Kraftwerk Wilhelmshaven und Entsorgung der REA=Ruckstandsporduckte
(1982)

B. Stellbrink, H. Weissert, P. Kutemeyer
Operational Experience with FGD Plant 2 at Wilhlemshaven Power Plant
(1983)

DISCLAIMER

The work described in this paper was not funded by the U.S. Environmental Protection Agency and therefore the contents do not necessarily reflect the views of the Agency and no official endorsement should be inferred.

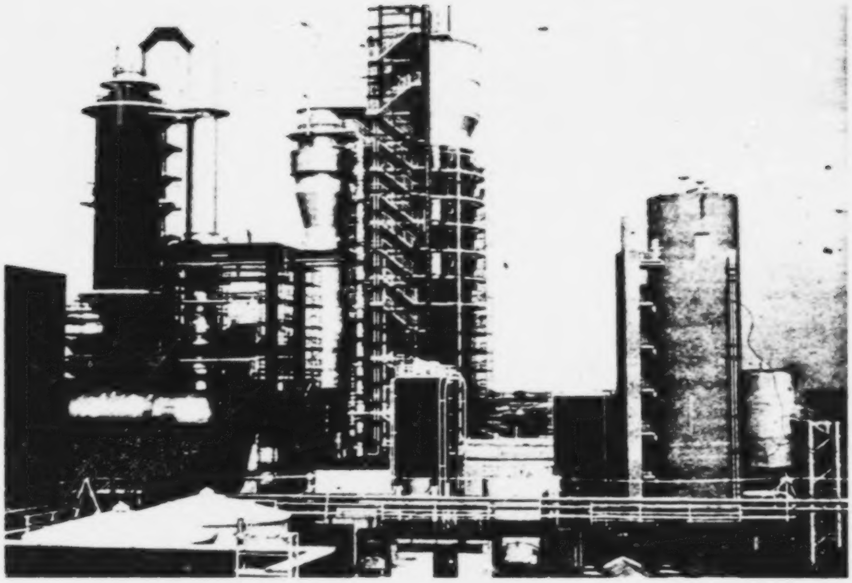

Figure 1 FGD PLANT 1 & 2 WILHELMSHAVEN

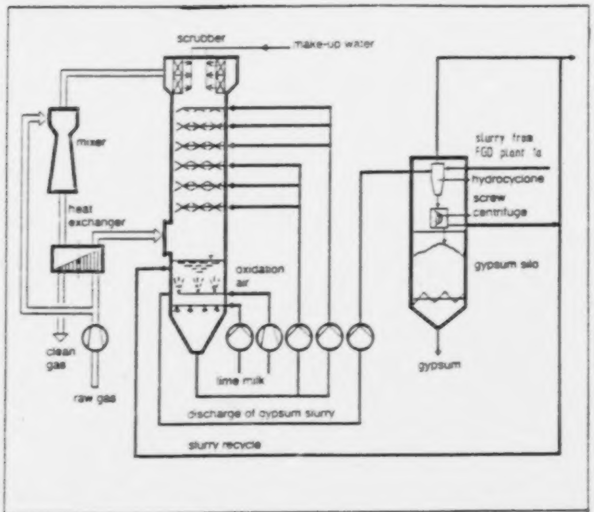
scrubber
make-up water
mixer
heat exchanger
slurry from FGD plant 1a
hydrocyclone
screw centrifuge
gypsum silo
oxidation air
clean gas
raw gas
lime milk
gypsum
discharge of gypsum slurry
slurry recycle

FIGURE 2 Flow Sheet of FGD plant 2 at Wilhelmshaven Power Station

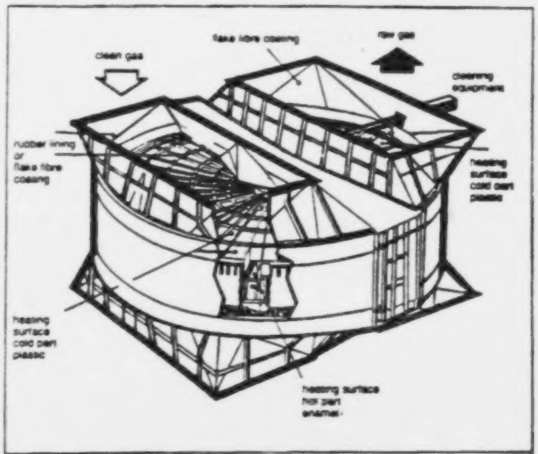
flake fibre coating
raw gas
clean gas
cleaning equipment
rubber lining or flake fibre coating
heating surface cold part plastic
heating surface cold part plastic
heating surface hot part enamel

FIGURE 3 **Regenerative heat exchanger (GAVO)**

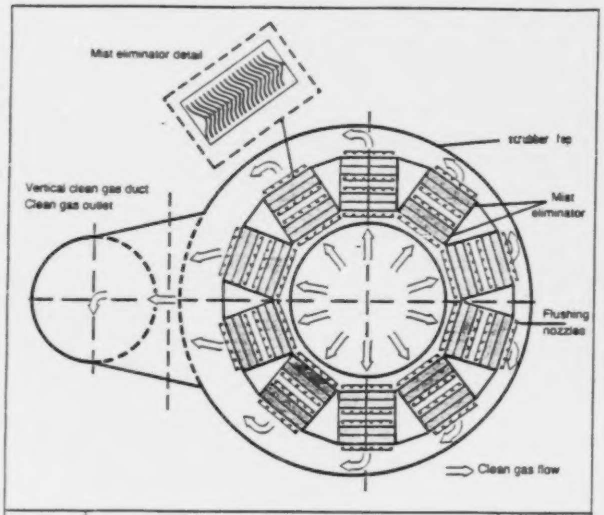
Mist eliminator detail
scrubber top
Vertical clean gas duct
Clean gas outlet
Mist eliminator
Flushing nozzles
Clean gas flow

FIGURE 4 Position of the Mist Eliminators

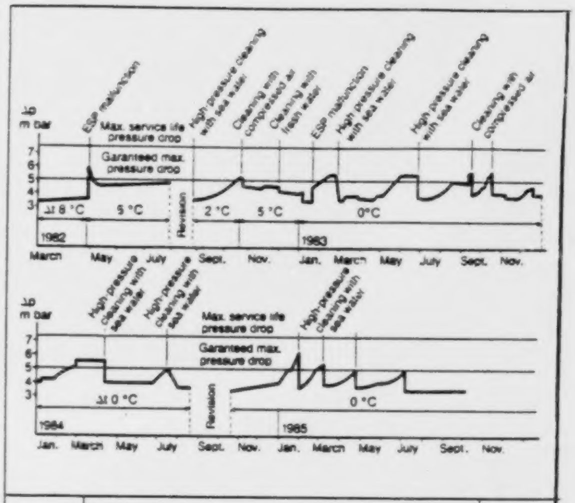

FIGURE 5 Pressure Losses in Heat Exchanger FGD plant 2

Overall Chemical Reactions:

$CaCO_3 + SO_2 + \frac{1}{2}O_2 + 2H_2O \rightarrow CaSO_4 \cdot 2H_2O + CO_2$

$CaCO_3 + 2HCl \rightarrow CaCl_2 + H_2O + CO_2$

$CaCO_3 + 2HF \rightarrow CaF_2 + H_2O + CO_2$

Absorption of SO$_2$:

1) $CaCO_3 + CO_2 + H_2O \rightarrow Ca(HCO_3)_2$
2) $Ca(HCO_3)_2 + 2SO_2 \rightarrow Ca(HSO_3)_2 + 2CO_2$
2a) $Ca(HCO_3)_2 + SO_2 \rightarrow CaSO_3 + 2CO_2 + H_2O$ $pH > 5$
3) $Ca(HSO_3)_2 + O_2 \rightarrow CaSO_4 + H_2SO_4$
4) $H_2SO_4 + CaCO_3 \rightarrow CaSO_4 + CO_2 + H_2O$
5) $CaSO_4 + 2H_2O \rightarrow CaSO_4 \cdot 2H_2O$

FIGURE 6 Basic chemistry of the Limestone-process

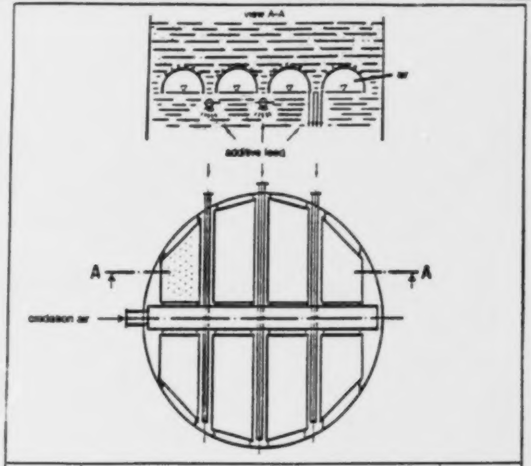
view A-A
air
additive feed
A
A
oxidation air

FIGURE 7 Oxidizer Internals and Additive Feed

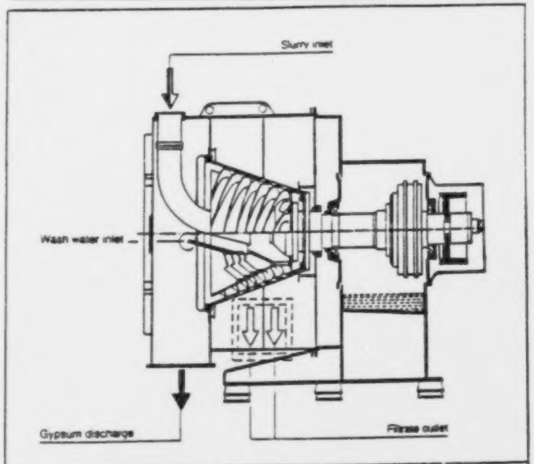
Slurry inlet
Wash water inlet
Gypsum discharge
Filtrate outlet

FIGURE 8 Screw Centrifuge for Dewatering of FGD-Byproduct-Gypsum

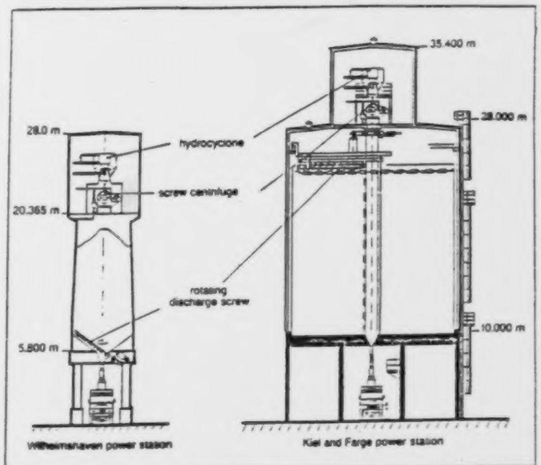
35.400 m
28.000 m
28.0 m
hydrocyclone
screw centrifuge
20.365 m
rotating discharge screw
10.000 m
5.800 m
Wilhelmshaven power station
Kiel and Farge power station

FIGURE 9 Wilhelmshaven, Kiel and Farge Power Stations Gypsum Dewatering and Storage

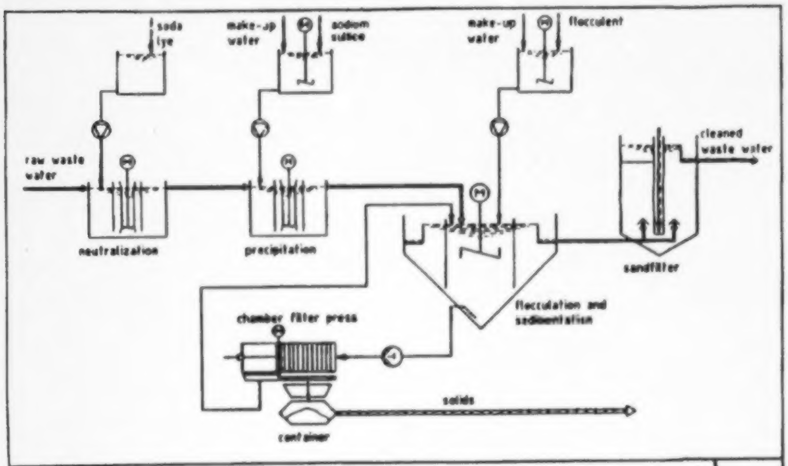
soda
lye
make-up
water
sodium
sulfide
make-up
water
flocculent
raw waste
water
cleaned
waste water
neutralization
precipitation
sandfilter
flocculation and
sedimentation
chamber filter press
solids
container

FIGURE 1

Waste water treatment

FIGURE 11 WILHELMSHAVEN PLANT 1A & 2

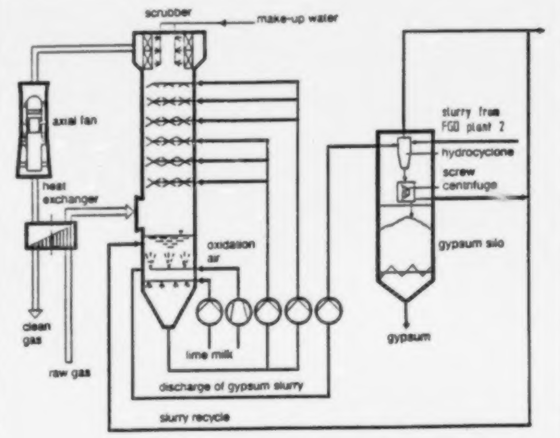
scrubber
make-up water
axial fan
heat exchanger
clean gas
raw gas
oxidation air
lime milk
discharge of gypsum slurry
slurry recycle
slurry from FGD plant 2
hydrocyclone
screw centrifuge
gypsum silo
gypsum

FIGURE 12 Flow Sheet of FGD plant 1a at Wilhelmshaven Power Station

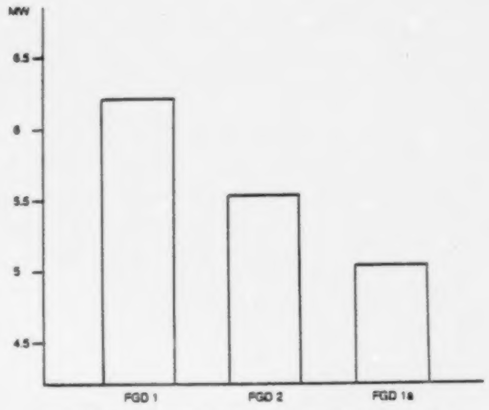

change in power consumption for a flue gas flow rate of 1,300,000 m³ (n)/hr.

FIGURE 13 Wilhelmshaven Power Station Decrease in Power Requirements

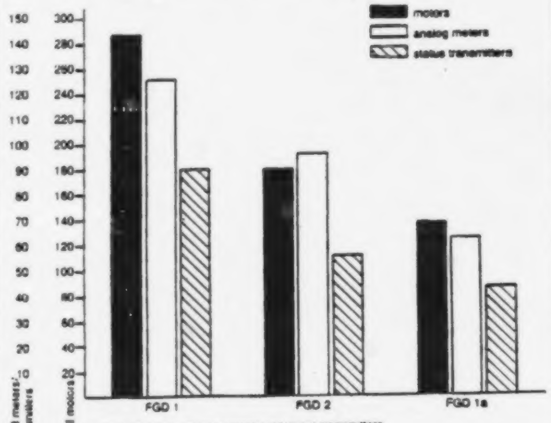

number of motors, analog meters and status transmitters for a flue gas flow of 1,300,000 m³ (standard)/hr.

FIGURE 14 Simplification of the Wilhelmshaven Power Station Layout

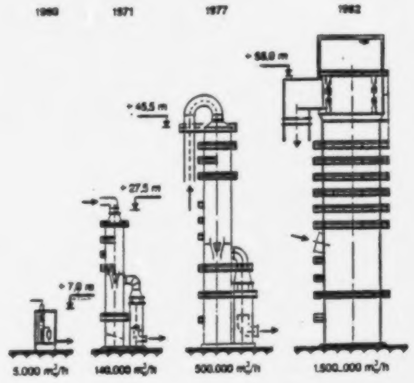
1960
1971
1977
1982
+ 7,0 m
+ 27,5 m
+ 45,5 m
+ 58,0 m
5.000 m³/h
140.000 m³/h
500.000 m³/h
1.500.000 m³/h

FIGURE 15 The Bischoff FGD Process as a function of time

OPERATING EXPERIENCE WITH ADVANCED FGD TECHNOLOGY IN WEST GERMANY

by: Dr. Manfred Schütz
Saarbergwerke AG
Saarbrücken, W. Germany

John Glamser
Lodge-Cottrell/Dresser
Houston, Texas

Michael Eikmeier
Saarberg Hölter Umwelttechnik,
Saarbrücken, W. Germany

ABSTRACT

Due to the stringent acid rain legislation, there has been a great deal of activity in the design and construction of FGD systems in West Germany. This has led to many advances in process design technology in the areas of organic acid enhancement, forced oxidation, and absorber design.

Operating data and experience with organic acid addition gained at the Weiher, Bexbach, and Volkingen Power Stations have resulted in several process advancements.

- Organic Acid Enhanced Absorption . . .

  A cocurrent/countercurrent absorber design has been developed to optimize pressure drop, residence time, liquid to gas ratios, and organic acid concentrations. Commercial plants of this design are operational.

- Forced oxidation . . .

  In situ, forced oxidation in the absorber sump has been implemented to eliminate the necessity for a separate oxidation vessel and results in larger, more uniform crystal sizes. Thickeners have been eliminated.

Saarbergwerke AG operating data and experience for the SHU flue gas desulfurization process are presented.

INTRODUCTION TO SAARBERGWERKE

SaarbergWerke AG is the second largest coal mining company in West Germany with a capacity of about 8 million tons of bituminous coal annually. About 1/3 of the produced capacity of bituminous coal is burned in Saarberg owned power plants at 3 sites: Weiher, Völkingen and Bexbach. About 2500 MW electric power generating capacity is installed and operated in typical medium load regime.

Saarberg also operates 2 coke plants with an output of 1.2 million tons annually. Both plants are equipped with modern gas cleaning equipment. Saarberg is currently involved in research and development in the area of coal technology and power generation including coal gasification.

FGD PROGRAM

Saarberg began to consider the possibilities of removing sulfur dioxide and other harmful gaseous substances from flue gases as long ago as the early 1970's when it was proposing to build a new coal-fired power plant.

Saarberg, along with Holter Engineering, formed an environmental company, Saarberg Hölter Umwelttechnik, to develop an FGD technology.

The technology was developed first using lime as absorbent, later limestone, and utilizes an organic acid additive for SO_2 absorption enhancement.

The first commercial unit, Weiher III/1 entered into service in 1979 using lime as absorbent in the new 707 MW coal-fired power station. Initial desulfurization capacity was 625,000 Nm^3/h of flue gas which was increased shortly afterwards, as a result of optimization to 800,000 Nm^3/h.

The startup of the Völklingen power station in 1982 marked the first time in Germany that the entire flue gas capacity from a power plant had been desulfurized. The combination developed here of a flue gas desulfurization unit and cooling tower, without any stack, triggered a wide range of interdisciplinary research programs and, as far as the discharge of power plant flue gases with the cooling tower plume is concerned, has been taken into account by other power plant operators in the modernization of flue gas desulfurization units. Presently more than 7000 MW are desulfurized and discharged to cooling towers in West Germany.

ACID RAIN LEGISLATION

In 1983, a new environmental regulation was enacted in West Germany. Under this regulation all coal, lignite and oil fired power plants and boilers above approximately 100 MWe had to install equipment to limit SO_2 emission to less than 400 mg/Nm^3 (140 ppmv) and achieve at least 85% desulfurization efficiency. The law specified 400 mg SO_2/Nm^3 and at least 85% efficiency by design to prevent fuel switching. By June 30, 1988, approximately 35,000 MW of power plant capacity has ben retrofitted with FGD to comply with this law.

This legislation initiated a program at Saarberg for retrofitting all units to meet the legislative requirements.

WEIHER

At Weiher a second FGD unit, utilizing limestone, was commissioned in Spring, 1983. A third FGD train for this unit has been in operation since October 1987, desulfurizing the total flue gas from the boiler. Also, the first unit has been converted from lime to limestone. Here at Weiher III, the flue gases coming from the 3 FGD plants are collected in a duct feeding the cleaned gases to the existing cooling tower for discharge.

BEXBACH

The 750 MW boiler in Bexbach was retrofitted with 3 FGD trains as well. All units use limestone as absorbing material. The first train was commissioned in 1982, the second in 1984, and the third in 1987.

The 260 MW power station, Barbara, located on the same site, was decommissioned in July 1988, as retrofitting FGD was not considered to be economical.

VÖLKLINGEN

At Völklingen - mentioned before - we operate a so-called prototype power plant, a 230 MW unit. Prototype, because some very modern ideas for power generation were realized for this plant, including fluidized bed combustion, additional gas turbines, and the stackless power plant.

Adjacent to this plant, we operate the 163 MW Fenne III unit. The FGD plant was put into operation in October 1987.

A 210 MW cogeneration unit for district heating is under construction for commissioning in 1989. Here too, we are applying the cooling tower discharge.

PROCESS FEATURES

GENERAL

The Saarberg-Holter FGD process is a wet scrubbing process based on limestone. The process is designed to desulfurize flue gases to environmentally acceptable levels and to form, in an integrated process step, a high grade gypsum by-product.

The process is unique compared with other wet scrubbing processes and offers the following advantages:

- Two-stage Cocurrent/Countercurrent Absorber
- Organic Acid Buffering
- SO_2 Absorption at relatively low pH levels, in the range 5.0 - 4.0
- 'In Situ' Forced Oxidation
- Commercial Gypsum By-product

These features work together to ensure a efficient, reliable process, avoiding problems of scaling or plugging, low reagent utilization, low SO_2 absorption efficiency, poor turndown and poor load following characteristics that have been experienced with less technically advanced processes.

LOW PH ABSORPTION

Saarberg-Holter experience has shown that in flue gas desulfurization, the sulfite phase of the absorption process should be avoided in preference to the bisulfite phase to achieve high availability and straight-forward gypsum production. As shown, pH determines the sulfur-containing ion formed during the absorption process. For example, at a pH of 5.5, approximately 20% of the SO_2 absorbed is present as sulfite and 80% is present as bisulfite. In the pH range between 4.0 and 5.0, the Saarberg-Holter operating range, virtually all ions formed are bisulfite. Sulfite ions are not formed in this pH range. Therefore, calcium sulfite production is precluded, and susceptibility to sulfite scale is eliminated.

Additionally, this pH range is ideal for 'in situ' forced oxidation to yield a commercial gypsum by-product. A quantity of air, approximately equal to the original stoichiometric demand, is injected into the absorber sump to achieve virtually 100% oxidation.

With this low pH process, the crystals are barrel-shaped, the gypsum is easier to dewater, and is suitable for use in the wallboard industry (a by-product market). At a higher pH absorbtion, the crystals are mainly needle or slab-shaped, are difficult to dewater, and often not suitable for wallboard production.

ORGANIC ACID BUFFERING

These obvious advantages of low pH operation can be effectively exploited if the scrubbing system is stabilized by buffering.

The process utilizes a small concentration of formic acid in the washing fluid to enhance SO_2 absorption efficiency and to buffer and control the pH drop of the washing fluid during absorption.

The formic acid addition permits low pH SO_2 absorption and, in a properly designed system, allows increased flexibility in operation, greatly reducing the operating and maintenance requirements. During the annual outage, a cleaning of the absorber system is not necessary.

Formic acid buffering also greatly increases SO_2 absorption efficiency. All of the Saarberg units desulfurize the flue gas from peak load or medium load generating stations. These units have shown the ability to track the design SO_2 absorption efficiency over sudden changes of from 20 to 100% of load with simultaneous increases of inlet SO_2 concentrations of up to 50%.

ABSORBER DESIGN

Based on the operating experience with using lime as absorbent at plants Weiher III/I, the process was modified to use limestone and the first plants of this kind in Europe were built and commissioned for Weiher III second train and Bexbach first train. Subsequently all lime units have been converted to limestone units. The first absorbers were designed as cocurrent absorbing units with an SO_2 efficiency of 80%.

Following the more stringent 1983 emission requirements. recently built plants have a combined cocurrent/countercurrent absorber designed for a removal efficiency of 95%. The operational results show an efficiency of more than 98%.

The entering pH of the washing fluid in the cocurrent absorption varies due to the SO_2 load between 4.5 and 5.2 pH. The cocurrent absorption allows a more significant pH drop - about 0.3 pH lower - than countercurrent absorption. Along the spray zone, the pH drops to about 4 pH and is in the range to form the intermediate bisulfite, which is at this pH easily oxidized to calcium sulfate.

When the first two limestone units were introduced, they were tested to increase sulfur abatement by an over-stoichiometric addition of limestone. Over a period of several hours, an over-stoichiometric addition does indeed increase marginally the level of desulfurization, but at the same time, sulfite occurs because the pH value is no longer sufficiently reduced. The fine sulfite particles settle on larger particles so that the limestone dissolves progressively less well and the formation of gypsum crystals is impeded so that more and more limestone is removed with the gypsum. The result is a drop in the level of desulfurization. It is normally possible to restore higher efficiency to the unit by reducing the pH of the washing fluid back to the value required for bisulfite formation.

OPTIMIZATION

Since the development of the process, Saarberg has relied on free spray tower absorbers similar to those used in particle removal technology, not least for reasons of operational reliability, although the efficacy of built-in components has been tested from time to time, as well as varying retention time and liquid to gas ratios.

It is remarkable that the same level of sulfur abatement is achieved in the first Bexbach unit with 0.9 sec. as in the second with a residence of 10 sec.

The retention time for the washing fluid in the sump amounts to about 3 minutes based on recirculating pump capacity. Assuming an average density of solid particles of 150 g/l, in the new units the gypsum spends around 15 hours on average in the washing fluid before it is removed for de-watering.
Operating results have shown that the injection of oxidation air is not always necessary over the full load range. Most of the oxidation takes place by boiler excess air.

The above shows that a comparison of existing plants and operational data can yield important conclusion for new plants regarding L/G, retention time, absorber size, oxidation requirements with a view to reducing investment and running cost.

OPERATING MANPOWER

The FGD plants of Saarberg are operated, per shift, by an operator in the main control room and an outside operator in the plant. There is one engineer per day shift who is in charge of all FGD and water treatment activities on site, and who reports to the power plant director. Per day shift, there is also one additional man in the power plant laboratory for taking analysis and quality checks.

EQUIPMENT AND MATERIALS

DEWATERING

We have utilized in our power plants, vacuum drum filters with approximately 20% moisture in the gypsum, vacuum belt filters with 10%-12% and centrifuges with 6%-8% residual moisture.

Each site operates with a central dewatering station. Via a circle pipeline, the suspension is pumped to vertical basket centrifuge system. The feed is controlled by a specified density of the suspension.

All gypsum produced in the power plants is commercial grade. The product is washed to the specified level of chloride and heavy metal during dewatering and is marketed to the wallboard and cement industries.

For achieving reliable dewatering results below 10% residual moisture, all dewatering stations are now equipped with centrifuges.

LININGS

All Saarberg-Holter absorbers are made of carbon steel.

A chlorbutyl type self vulcanizing or pre-vulcanized rubber lining is used as corrosion/erosion protection for the absorber and all piping, vessels, and duct that come in contact with the washing suspension.

The rubber qualities in use are thoroughly suitable for the wash water suspension even at chloride levels of 80,000 ppm chloride. The key for a good performance of lining is a capable application and an experienced quality control program to prove that the application is accomplished as specified. On this basis, we do not see any alternative in plastic linings or exotic materials at this time.

Due to the high temperature in the quenching zone, Hastelloy C-276 is applied in a wall paper type technique about 1 m above and 1 m below the first spray level.

The Hastelloy cannot be considered as corrosion proof as long as chloride levels are above 50,000 ppm. The life expectancy for the Hastelloy is about 7 years before replacement. A test program has been started for investigating the suitability of titanium for this service.

SPRAY NOZZLES

Spray nozzles are of the pig tail or hollow cone type made of ceramic. The earlier use of stainless steel or stellite type nozzles have not given satisfactory equipment life results. This problem has been solved by using ceramic materials, and now, after 16,000 hours, no wear has been recognized.

MIST ELIMINATORS

Mist eliminators require careful design for reducing the liquid entrainment below 150 mg/Nm^3. An optimization of the intermittent washing sequence and proper placement in the vessel allows reliable low absorber maintenance operation. Blocking of this system has not been experienced and additional cleaning during the scheduled outages is not required.

PUMPS

As slurry pumps, we operate hard metal, rubber lined and plastic pumps. The major wash water recirculation pumps are hard metal pumps, except for Bexbach train III, where we operate rubber lined pumps.

Experience has shown that the hard metal type pump is preferable to the rubber lined pump in terms of equipment life, overall size requirements and efficiency.

The plastic type pump manufactured in high molecular polypropylene is used as an auxiliary slurry pump for all services except the main recirculation pumps. This type of pump has shown a very satisfactory performance for these applications.

CONCLUSION

More than 10 years ago, the very first FGD plants suffered a variety of problems, causing significant maintenance and repair work. Now with the third generation of FGD plants, we experience a reliability of this kind of equipment of almost 100%. The investment of a spare absorber was never really considered by Saarberg.

The work described in this paper was not funded by the U.S. Environmental Protection Agency and therefore the contents do not necessarily reflect the views of the Agency and no official endorsement should be inferred.

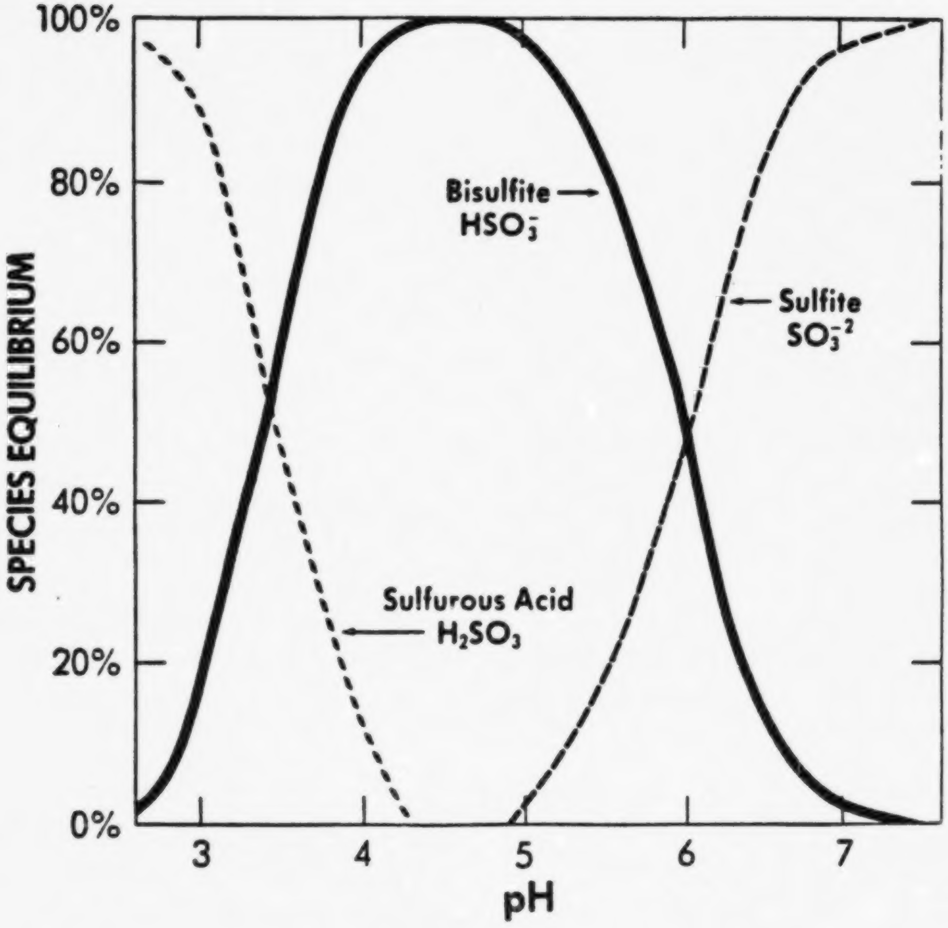

Figure 1: SO_2 absorption species versus pH

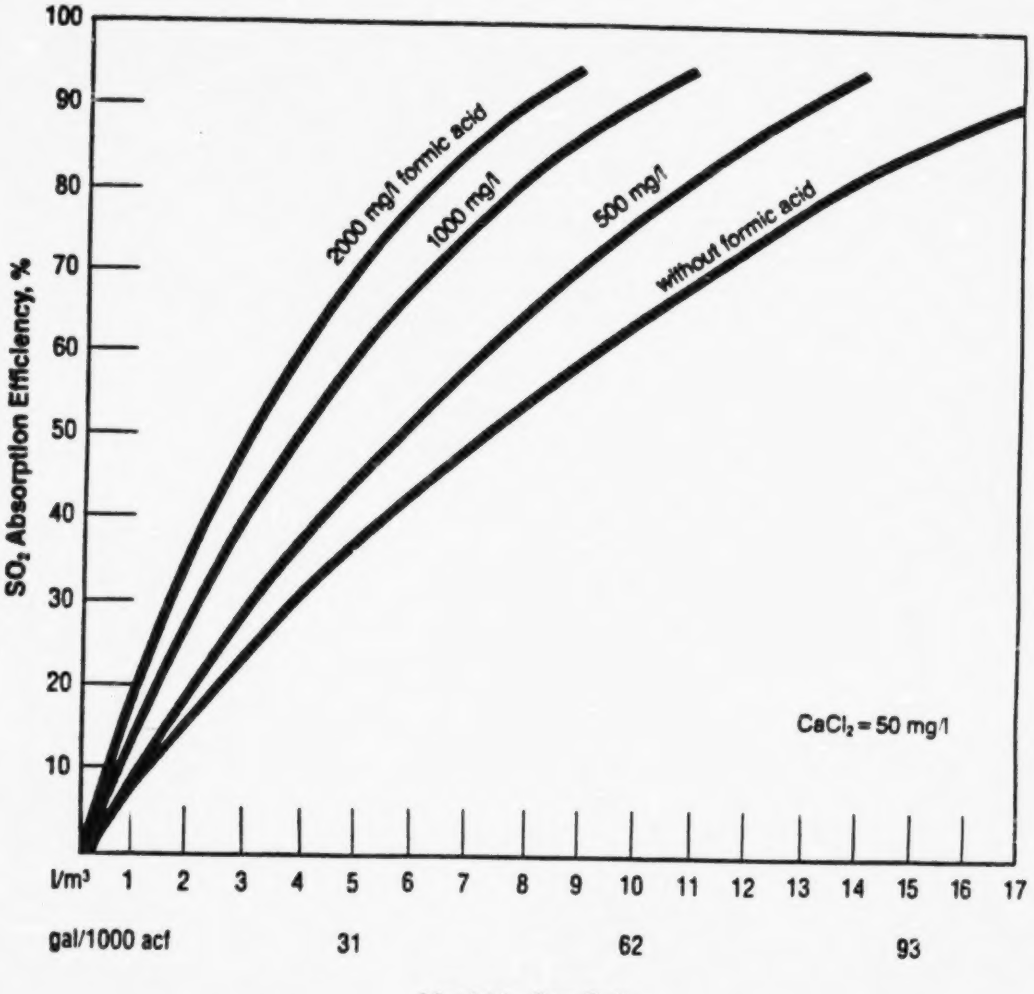

Figure 2: Effect of formic acid on SO$_2$ absorption efficiency

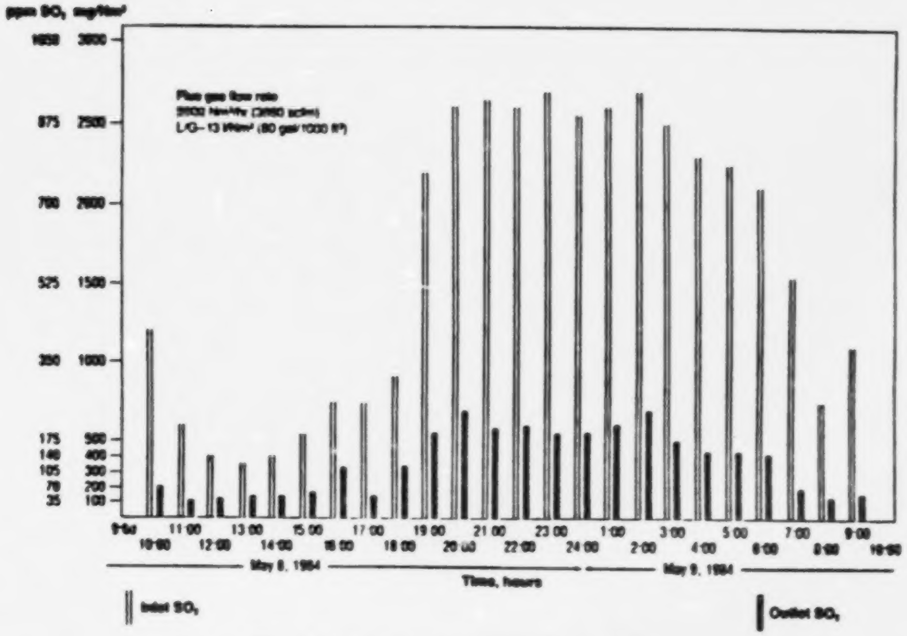

Figure 3a: SO$_2$ absorption without formic acid addition

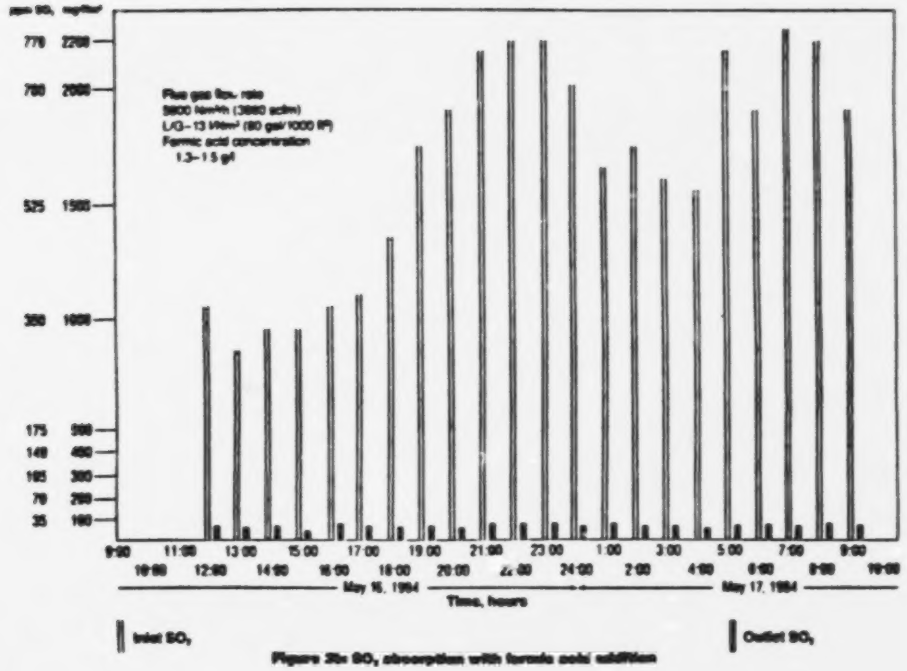

Figure 3b: SO$_2$ absorption with formic acid addition

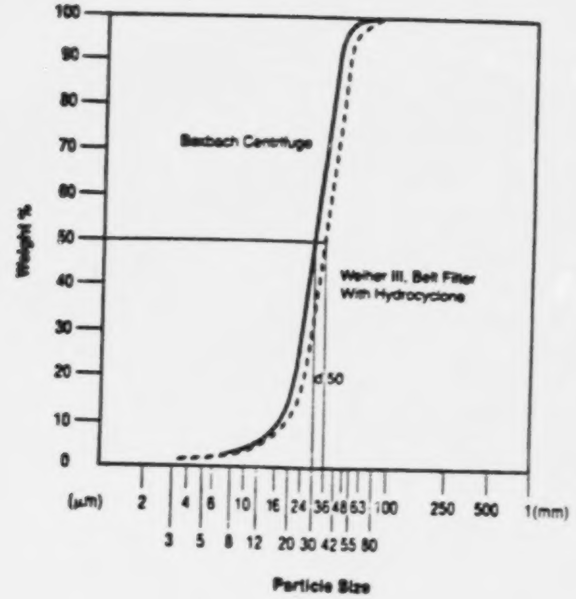

Figure 4: Size distribution of $CaSO_4 \cdot 2H_2O$

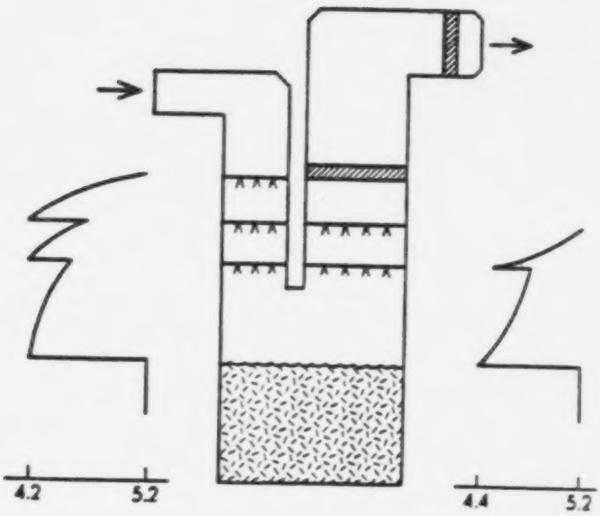

Figure 5: Typical absorber pH profile for cocurrent countercurrent scrubbing with formic acid buffering

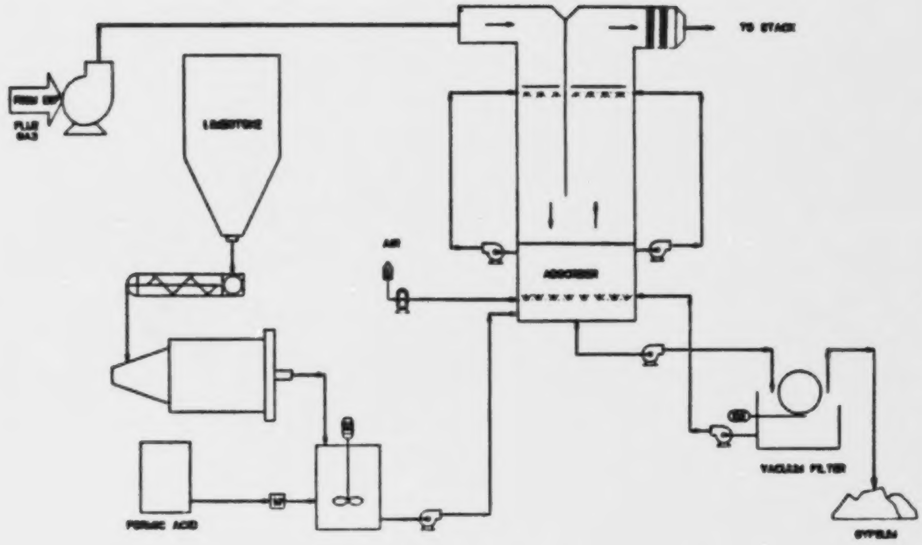
FROM ESP
FLUE GAS
LIMESTONE
TO STACK
AIR
ABSORBER
VACUUM FILTER
FORMIC ACID
GYPSUM

FIGURE 6: SAARBERG-HOLTER FLUE GAS DESULFURIZATION PROCESS

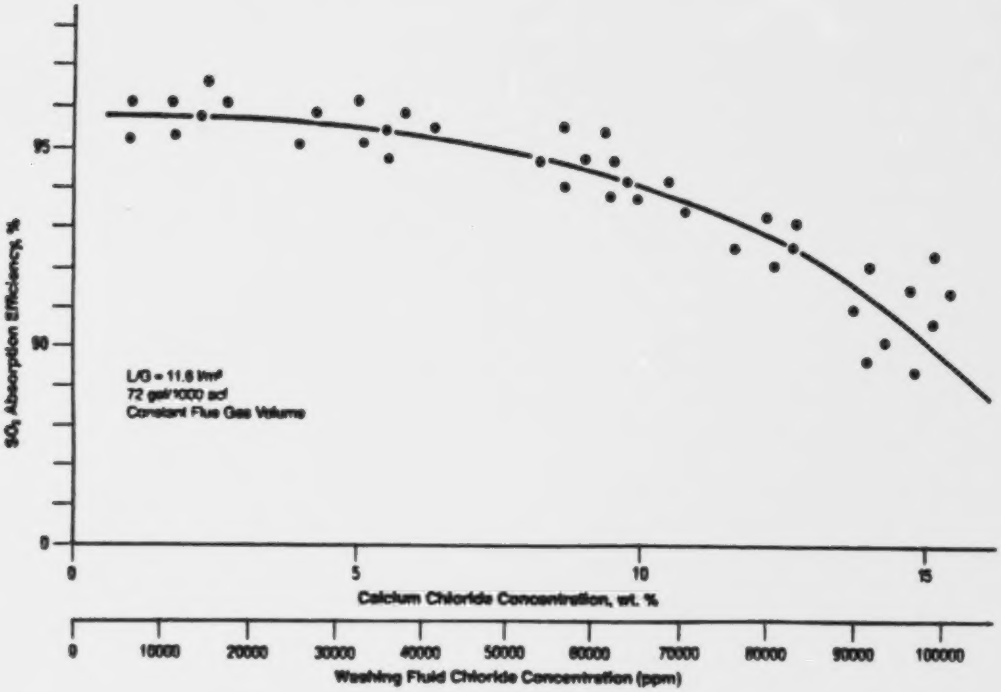

Figure 7: Effect of chloride concentration on SO_2 absorption efficiency

SESSION 6: MUNICIPAL SOLID WASTE FACILITIES

Chairman, Theodore G. Brna, EPA/AEERL

A COMPARISON OF HCL, SO_2 AND PARTICULATE EMISSIONS FROM THREE DIFFERENT MUNICIPAL SOLID WASTE-FIRED BOILERS

by: Michael A. Sandell and Vincent J. Petti
Wheelabrator Air Pollution Control
Pittsburgh, PA 15222

Timothy J. Porter
Wheelabrator Environmental Systems
Danvers, MA 01923

Joseph L. Gaines
Rust International Corporation
Birmingham, AL 35243

ABSTRACT

Wheelabrator Environmental Systems (WES) has begun operation of three refuse recovery facilities in the last 22 months. Each plant was supplied with a different Wheelabrator Air Pollution Control (WAPC) dry scrubbing system for the control of acid gas and solid particulate emissions. All three plants utilize mass burn technology to incinerate the municipal solid waste (MSW). Each facility utilizes a water wall boiler to produce high pressure steam which feeds a common turbine-generator set. The electricity produced is sold to local utilities.

A dry injection system is utilized at NH/VT Solid Waste District Facility, Claremont, NH, to control emissions from two 100-tpd MSW-fired boilers. A spray dryer/absorber-electrostatic precipitator dry scrubbing system is employed for two 750-tpd boilers at Millbury, MA. A spray dryer/absorber-fabric filter dry scrubber is utilized for three 750-tpd boilers at the WES Bridgeport, CT facility.

FACILITY DESCRIPTIONS

Each resource recovery facility utilizes mass burn technology to burn MSW. MSW is fed to a surge hopper and onto a reciprocating grate. Flue gases pass through a proprietary design boiler to the emission control equipment. Steam generated in each boiler is utilized to produce electricity in a turbine-generator set.

All three facilities are designed and built to operate 24 hour/day, 365 days/year except for periods of regularly scheduled maintenance. The design of all three facilities represents state of the art in municipal refuse processing and reflects the extensive experience Wheelabrator Environmental Systems has acquired in operating resource recovery systems since 1975. The Von Roll reciprocating stroking grate and hydraulic ram waste feed technologies are utilized at all WES facilities.

The common design features present at all three facilities include:

- Primary combustion air intakes located above the enclosed tipping floor and refuse handling area. This location provides a slight negative draft in the tipping floor to pull fugitive odors and dust into the furnaces.
- Steam coil primary air heaters to dry wet refuse prior to combustion.
- Auxiliary natural gas burners used during startup and shutdown.
- Furnace/boiler design to expose refuse and combustion gases to temperatures greater than $1800^{o}F$ for one second residence time.
- High pressure drop reciprocating grates to evenly distribute primary combustion air throughout the refuse bed.
- Overfire air supplied through front and rear wall nozzles to provide mixing, turbulence and residence time for optimum combustion.
- Fully automatic combustion control and refuse feed system.
- Turbine bypass condenser to allow full operation on all boilers during turbine outages.

The municipal refuse burned at all three facilities includes all household garbage, trash, rubbish and yard waste. Combustible agricultural, commercial and light industrial waste makes up a small portion of the refuse processed. Chemicals, oils, sludges, highly flammable substances, cesspool or other human waste, hazardous waste, hospital waste and any item which WES reasonably believes would pose a threat to health or safety or that may cause damage to the plant are excluded. White goods and large noncombustible items are removed from the refuse and disposed of separately.

CLAREMONT

The Claremont, NH facility has two 100-tpd municipal refuse processing trains. Each train consists of a Von Roll reciprocating grate, furnace and boiler, and Wheelabrator Air Pollution Control (WAPC) dry lime injection fabric filter system. Each refuse-fired system is capable of generating a maximum of 26,500 lbs/hr of 600 psig, 600°F steam at the superheater outlet. Steam from both boilers flows to a common steam driven turbine-generator nominally rated at 4 MW. Electrical power produced is transmitted to Connecticut Valley Electric Company.

Front-end loaders deliver the mixed municipal refuse to the charging hoppers. The hydraulic-operated cylinder charging rams control the refuse feed rate to the furnace. Following incineration, bottom ash is discharged into a drag-type quench conveyor. Fly ash from the fabric filter system is mechanically conveyed and combined with the bottom ash in an enclosed ash handling area. The combined ash is discharged to enclosed trucks for transportation to final disposal.

MILLBURY AND BRIDGEPORT

The Millbury facility consists of two 750-tpd refuse processing trains with WAPC spray dryer/absorber and electrostatic precipitator for flue gas emission control. The combined steam from the two units is supplied to a common turbine-generator set nominally rated at 46 MW. The Bridgeport facility consists of three 750-tpd processing trains with WAPC spray dryer/absorber-fabric filter for flue gas emission control and a common turbine-generator set nominally rated at 67 MW.

The Millbury and Bridgeport facilities use identical 750-tpd refuse processing trains. Each train consists of a Von Roll reciprocating grate and a Babcock and Wilcox/WES water wall furnace and boiler. Each boiler is rated to produce 191,600 lbs/hr of superheated steam at 825°F and 850 psig. Refuse is transported to charging hoppers using two orange peel bucket cranes. Hydraulically operated charging rams control the refuse feed into the furnace. Water-quenched bottom ash is discharged onto a common vibrating conveyor via hydraulic ram de-ashers. Spray dryer/absorber and fabric filter or electrostatic precipitator ash is drag conveyed and mixed with bottom ash in an enclosed ash handling area. The combined ash is discharged into an enclosed truck for disposal.

FACILITY OPERATING SUMMARY

Overall boiler operation and throughput tonnage at all three facilities has been as expected. A summary of facility operations is presented in Table 1. All values represent the period from startup through July 30, 1988.

The Claremont facility started up in March 1987, completed compliance testing in June 1987, and has been in continuous operation except for scheduled maintenance outages. Since startup the facility has processed a total of 77,809 tons of refuse. The nameplate usage availability since startup has been 89%.

Millbury started up in September 1987 and completed compliance testing in February 1988. The facility has processed 329,718 tons of refuse. Facility availability in terms of nameplate usage availability has been 90% since startup.

The Bridgeport facility is the latest of the Wheelabrator facilities to come on line. Since startup in January 1988 a total of 221,135 tons of refuse have been processed. Nameplate usage availability is 91% through July 30, 1988. Compliance testing was performed in June 1988.

EMISSION CONTROL SYSTEMS DESCRIPTION

CLAREMONT DRY SORBENT INJECTION SYSTEM

Dry hydrated lime (90% less than 325 mesh) is the current sorbent of choice at Claremont. It is delivered to the plant by self-unloading truck where it is conveyed pneumatically to a single storage silo with a bin vent filter for dust control. The silo employs a 60° conical hopper equipped with a bin activator to ensure smooth, uninterrupted reagent flow and a manual discharge valve. The silo is also equipped with two automatic knife gate discharge valves, one for each feeder for feeder shutdown.

Sorbent passing through the discharge valves is metered by two volumetric screw-type feeders with SCR variable speed drives. The SCR controlled valves automatically adjust the sorbent feed rate based on steam flow to provide the required amount of reagent to the pneumatic conveying system. The screw feeders are also capable of being manually set to a given discharge volume.

Rotary air lock valves feed the hydrated lime reagent into the 4-inch pipe conveying system. A separate pneumatic system (positive pressure) conveys the lime to each fabric filter venturi duct section. A common backup blower is provided. Alarms are provided for electrical and mechanical failure of the equipment. A dry particulate flow detector is also installed in the pneumatic feed lines to alarm any blockage in the lime feed stream.

The lime is injected countercurrently into the flue gas in a venturi duct section immediately upstream of the fabric filter. The venturi provides the necessary turbulence for mixing and initial acid gas absorption. A two-stage fluidization of the powdered lime was selected to provide proper fluidization and mixing over the full operating range of the boiler. The initial fluidization occurs in the conveying line and the second in the flue gas venturi. The air flow in the conveying subsystem remains constant for all boiler loads. If the lime was directly metered into the flue gas, the venturi throat gas velocities would vary with load. The lower throat velocities at reduced boiler load might not be high enough for complete fluidization.

All the equipment to store and pneumatically convey the hydrate is arranged in a three-level silo enclosure. The top level includes the hydrated lime storage silo. The second level includes the feeders and the bottom level houses the conveying system blowers and control panels.

A separate WAPC three-module, Size FA-1515 TA, Model 120, Series 6P Jet III fabric filter was supplied for each boiler train. Each module is equipped with a 60° slope pyramidal hopper designed for 100-lb/ft^3 ash load to the top of the hoppers. Each hopper has a flanged discharge to a double-dump valve, two poke holes, one access door, a high-level alarm, resistance-type heaters, and ash fluidizing pads.

Each fabric filter module is equipped with 225 bags which are constructed of woven fiberglass treated with an acid-resistant finish. Each bag is 6-inch diameter with a maximum allowable operating temperature of $500^{\circ}F$. As the flue gas leaves the boiler it enters a spark arrestor box upstream of the fabric filter. The purpose of the spark box is to drop out any large, still glowing embers prior to damaging the bags.

In order to help prevent high-high temperature excursions and subsequent bypassing of the fabric filter unit, a tempering air damper system has been installed downstream of the spark box and upstream of the fabric filter. As the flue gas temperature at the fabric filter inlet exceeds its high set point, the air tempering damper is automatically opened to allow ambient air to be drawn into the flue gas until the inlet temperature falls to the given set point. A simplified process flow diagram is presented in Figure 1.

MILLBURY SPRAY DRYER/ABSORBER-ELECTROSTATIC PRECIPITATOR SYSTEM

A separate Emission Control System (ECS) is provided for each of the two 750-tpd refuse-fired units. Each ECS is comprised of a spray dryer/absorber, followed in turn by an electrostatic precipitator, and induced draft fan equipped with a variable speed drive. A common 365-ft. concrete stack with an insulated carbon steel liner discharges the flue gas to the atmosphere. Figure 2 is a simplified process flow diagram.

Each spray dryer/absorber is a 25-ft. diameter vessel sized for a nominal 10-seconds flue gas residence time. Flue gas enters the top and passes through a roof gas disperser which uniformly distributes gas flow. Lime slurry is then atomized cocurrently into the flue gas. The flue gas is evaporatively cooled by the atomized lime slurry while SO_2 and other acid gases are simultaneously absorbed. The entrained reaction products and fly ash are ducted to the electrostatic precipitator to remove the solid particulate. Some solid material drops out in the spray dryer/absorber hopper.

The lime slurry is atomized using multiple proprietary design two-fluid nozzles. Compressed air, the second fluid, provides the energy for atomization. The nozzle design has been optimized to minimize compressed air usage and erosion. The nozzle and probe designs are also resistant to external solids accumulation which affected atomization in other nozzle designs. Nozzle/probe assemblies can be removed and replaced quickly without interrupting plant operation or significantly affecting spray dryer/absorber performance.

Slurry is prepared by slaking pebble lime in a detention-type paddle-wheel mixer slaker. The concentrated (20+ wt. %) slaked lime slurry is degritted in a vibrating screen and stored in an agitated tank. Concentrated slurry is diluted with fresh water and pumped through a final strainer into the atomizing nozzles.

The flow of diluted slurry is measured with a magnetic flow meter and modulated to maintain a constant spray dryer/absorber outlet temperature. The ratio of dilution water to concentrated slurry is automatically adjusted by a signal from the inlet-outlet SO_2 monitors. This slurry concentration control loop may be set to maintain either a constant controlled SO_2 emission limit (lb/MMBtu) or constant SO_2 removal efficiency.

Each electrostatic precipitator is a three-field rigid-discharge electrode (RDE) unit with 12-inch plate spacing. Collected particulate matter is dislodged by roof-mounted gravity impact rappers on both collecting and discharge electrodes. Particulate falls to three cross-flow trough conveyors.

All ECS equipment and ductwork are constructed of carbon steel plate with mineral wool insulation and enameled aluminum lagging. Electrostatic precipitator trough screws (augers), double-flap air locks and drag-chain conveyors remove fly ash and spray-dried acid gas reaction products from the spray dryer/absorber and electrostatic precipitator hoppers.

BRIDGEPORT SPRAY DRYER/ABSORBER-FABRIC FILTER SYSTEM

The Bridgeport facility is comprised of three identically sized 750-tpd refuse-fired units, each with its own ECS. Instead of electrostatic precipitators, each unit is equipped with a multicompartment shake/deflate fabric filter. The facility's concrete, self-supporting stack is equipped with one carbon steel, insulated flue for each ECS unit.

The spray dryer/absorbers and supporting lime slurry preparation systems are essentially identical to those provided at Millbury. The spray dryer/absorber outlet temperatures and SO_2 outlet emission rates are also controlled similarly.

Each ten-compartment spray dryer/absorber-fabric filter houses 180 8"-diameter glass fiber bags. Cleaning is accomplished one compartment at a time, first by isolating the compartment with poppet dampers and then by collapsing the bags with a reverse flow of cleaned flue gas. A gentle side-to-side shaking motion is then applied to the bags via rocking top supports. Following a "null" period during which the dislodged dust cake settles in the hoppers, the bags are slowly reinflated and the compartment is then returned to service. Any dust which is entrained in the reverse gas flow during the deflation cycle and carried backward into the inlet manifold is collected in the remaining on-line compartments.

The spray dryer/absorber, fabric filter, ductwork, ID fan and related gas handling equipment are all constructed of carbon steel plate. All external walls are insulated with mineral wool and enameled aluminum lagging. Adjoining spray dryer/absorber-fabric filter compartment walls are comprised of single-layer seal-welded carbon steel plate with rigid mineral wool insulation on one side.

Both Millbury and Bridgeport are equipped with dedicated extractive Continuous Emission Monitors (CEM's) on each boiler/ECS trains for SO_2, NO_x, CO, CO_2, O_2 and opacity. Claremont is equipped with in-situ CEM's for CO, O_2 and opacity. The Table below shows the CEM location and detector type for each facility.

	Millbury		Bridgeport		Claremont	
Gas	Inlet	Outlet	Inlet	Outlet	Inlet	Outlet
Opacity		Tran		Tran		Tran
O_2	ZrO_2	ZrO_2	ZrO_2	ZrO_2	ZrO_2	
CO_2			NDIR			
SO_2	NDUV	NDUV	NDUV	NDUV		
NO_x		ChemL		ChemL		
CO	NDIR		NDIR			GFC

The measurement devices are zirconium oxide cells (ZrO_2), chemiluminescent (ChemL), nondispersive infrared (NDIR) or nondispersive ultraviolet (NDUV), gas filter correlation (GFC) and transmissometers (Tran).

All CEM's have completed certification testing in accordance with requirements of the EPA and the respective state environmental regulatory agencies.

RESULTS/DISCUSSION

Results from the compliance testing of the three individual facilities are presented. First a discussion of the SO_2, HCl, and particulate removal performances is presented. This is followed by a presentation of the trace metals emission measurements.

PARTICULATE, HCL, SO_2

The results of the compliance testing of the Claremont facility performed in May 1987 are presented in Table 2. The design or permit limitations (whichever is more stringent) are also presented in Table 2. The Claremont facility demonstrated compliance with the permit limitations for particulate, HCl, and SO_2 easily despite higher than expected HCl and SO_2 inlet concentrations.

Results of the Millbury compliance testing are presented in Table 3 along with the design or permit conditions. The Millbury facility was tested in February 1988. Results from the CEM data indicate that the performance level demonstrated in the compliance tests has not diminished.

Table 4 presents the results and design conditions of the June 1988 Bridgeport compliance tests. Examination of Table 4 demonstrates that the Bridgeport facility met all of the air permit requirements.

The average particulate emissions reported from all three facilities were less than their respective air permit requirements. In fact, each individual test run was below the individual facility requirement; however, there was nearly a factor of 3 variation between selected test runs and unit averages. This large variation in test results, under identical operating conditions, must be taken into consideration during the permitting process.

While all three facilities met their air permit requirements, there appears to be a slight difference in particulate emission levels between the facilities. Claremont, with its pulse-jet fabric filter, produced compliance test results higher than Bridgeport compliance test results. During the compliance testing both facilities operated with approximately the same fabric filter pressure drop. A possible explanation for these relatively higher particulate loadings at Claremont is the more energetic action of the pulse-jet cleaning cycle. The particulate emissions reported from Millbury's electrostatic precipitator compliance tests were between the reported emissions of the two fabric filters.

An examination of the acid gas removal levels reveals a similar trend for HCl emissions. This is not surprising as spray dryer/absorbers are much more effective at removing acid gases than dry injection systems and fabric filters are more effective than precipitators. HCl removal efficiency for each of the three facilities was excellent with the minimum removal efficiency being 95%.

Variation in the SO_2 emission levels are present, as Millbury demonstrated a slightly higher SO_2 concentration than Claremont in the outlet gas train. However, due to the effect of the spray dryer/absorber, the amount of lime necessary to achieve approximately equal levels of SO_2 removal is less at Millbury. Bridgeport demonstrated superior SO_2 removal compared with the other two facilities at approximately the same lime feed rate as Millbury. This additional SO_2 removal is attributed to contact with the unreacted lime present in the filter cake of the fabric filter.

It should be noted from these results that at all three facilities, the HCl removal efficiency is in excess of 95% at every SO_2 removal level measured. This correlation was expected as HCl is preferentially removed over SO_2 and allows the use of SO_2 CEM's to indicate HCl removal efficiencies.

The fly ash collected from the spray dryer/absorber hoppers and the particulate control devices at all three facilities is dry and free-flowing. Difficulty in removing ash has occurred infrequently. It has been theorized that a high concentration of calcium chloride in the final spray dryer/absorber product would present a problem in ash removal. This has not been the case at Millbury or Bridgeport.

Pressure drop across the Claremont fabric filter and the Bridgeport fabric filter averages between 4-5 In. W.G. The cleaning cycle for the pulse-jet fabric filter at Claremont is typically about three hours. The 4-5 In. W.G. pressure drop for the Bridgeport shake/deflate collector is based on a 21-minute timed cycle between individual compartments which provides a 210-minute cycle for the entire fabric filter unit.

The stoichiometric ratios reported for the compliance tests are in excess of that necessary to achieve compliance. At the Claremont facility, the 90% HCl removal requirement determined the lime feed rate. It is estimated that the stoichiometric ratio could have been reduced by approximately 20% to achieve this removal requirement. For the Millbury facility, 70% SO_2 removal was the determining factor for lime feed rate setting. At Bridgeport, the lime feed rates were based conservatively on the results of the Millbury compliance tests. The lime feed rate at Bridgeport could have been reduced to achieve the 90% HCl and the 0.32 lb/MMBtu SO_2 emissions permit levels.

Preliminary testing of each facility had demonstrated wide, rapid fluctuations of inlet concentrations of HCl and SO_2. In order to ensure that the compliance limits would be met under these varying conditions, the lime feed rates were conservatively set at each facility.

METALS EMISSIONS

Table 5 presents an inventory of the metals emissions from the Millbury and Bridgeport facilities. Several of the values of the table are identified with ND followed by a "less than (<)" number. These are the worst case values where a specific element was not detected. The detection limit is used as the actual value. This is represented by the "less than (<)" sign. The beryllium and mercury values were measured using EPA Reference Methods 104 and 101A respectively. The remaining metals were determined using a combined EPA Method 5 and an EPA research and development multi-metal sampling train. This train combines EPA Method 5 and EPA Method 12 for particulate, lead, and trace metals. The trace metals were determined by runs of at least two hours in duration. Borosilicate glass probe liners and nozzles were used throughout the train to avoid any possible contamination.

An examination of Table 5 reveals that all the metals tested are present only in extremely low amounts with numerous values below the detection limit of the method. All the results are presented as Gr/SDCF at 12% CO_2 in order to make a comparison of the different facilities. Recent testing at the Bridgeport facility has shown that the removal efficiencies of the non-volatile metals listed is generally in excess of 99%.

CONCLUSION

Within the two years, WES has brought three plants into commercial operation using three different emission equipment strategies. These strategies were individualized for each specific facility location based on permit requirements and cost effectiveness. Successful compliance and performance testing at each of all facilities has demonstrated the success of each emission control strategy.

Different emission control strategies can be applied to different resource recovery projects. Each strategy must be examined with respect to facility size, location, project economics, public response, federal, state and local regulations, and specific permit requirements. Taking these factors into account, an economical and environmentally sound resource recovery facility can be designed, built, and commercially operated.

Lower than expected controlled emissions of particulate, acid gases and non-volatile metals were measured at Bridgeport. The reader is cautioned that these values may not be generally applicable to similar facilities. While the results of these individual compliance tests demonstrate that each emission control system is operating as designed, routine monitoring of the system performance over time will ensure that emission limitations are not exceeded over the expected life of the facility.

The work described in this paper was not funded by the U.S. Environmental Protection Agency and therefore the contents do not necessarily reflect the views of the Agency and no official endorsement should be inferred.

rEpEPl/eb

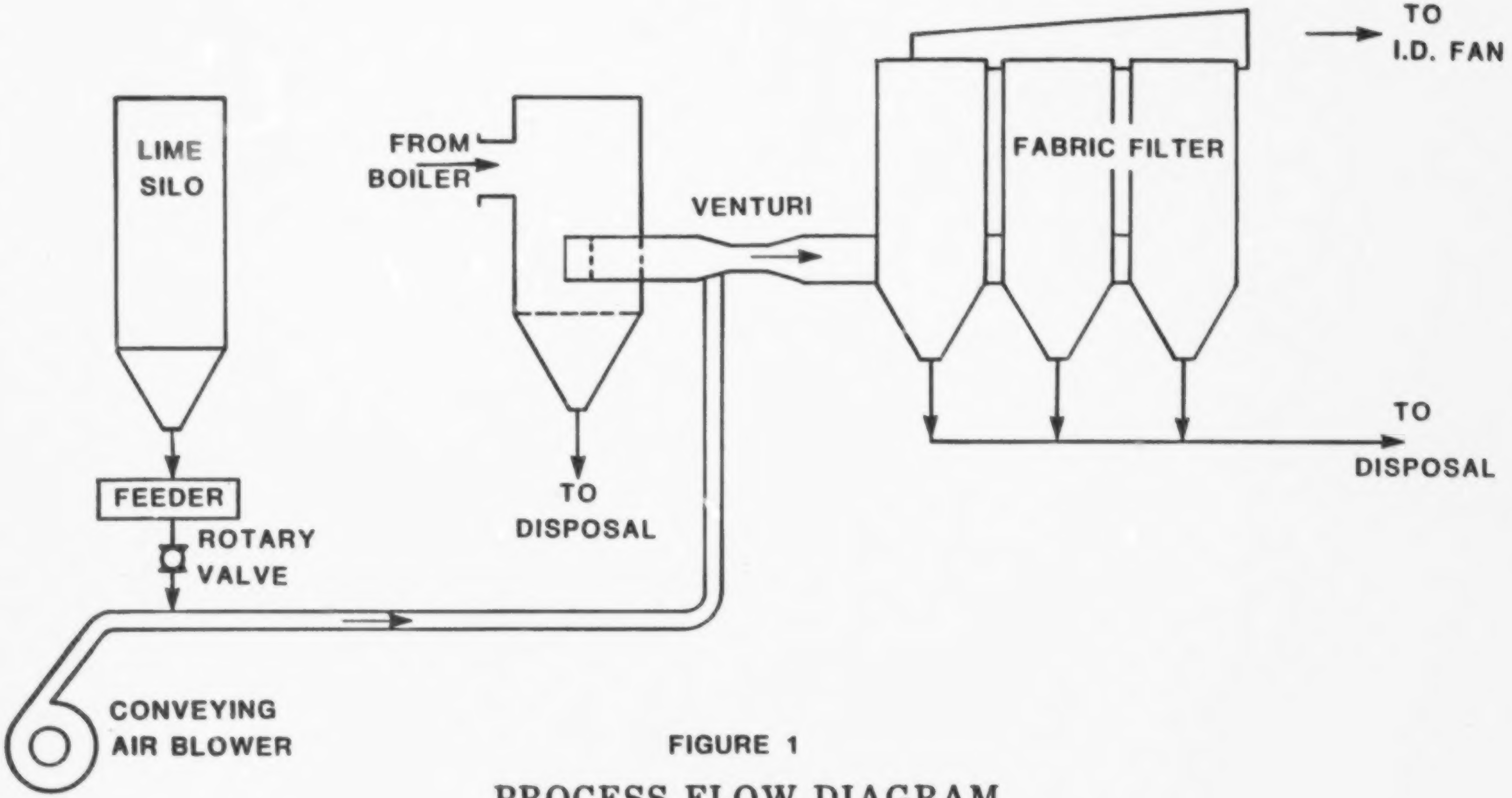
TO
I.D. FAN
LIME
SILO
FROM
BOILER
FABRIC FILTER
VENTURI
TO
DISPOSAL
FEEDER
TO
DISPOSAL
ROTARY
VALVE
CONVEYING
AIR BLOWER

FIGURE 1

PROCESS FLOW DIAGRAM
W/DRY INJECTION SYSTEM

NH/VT SOLID WASTE FACILITY
CLAREMONT, NEW HAMPSHIRE

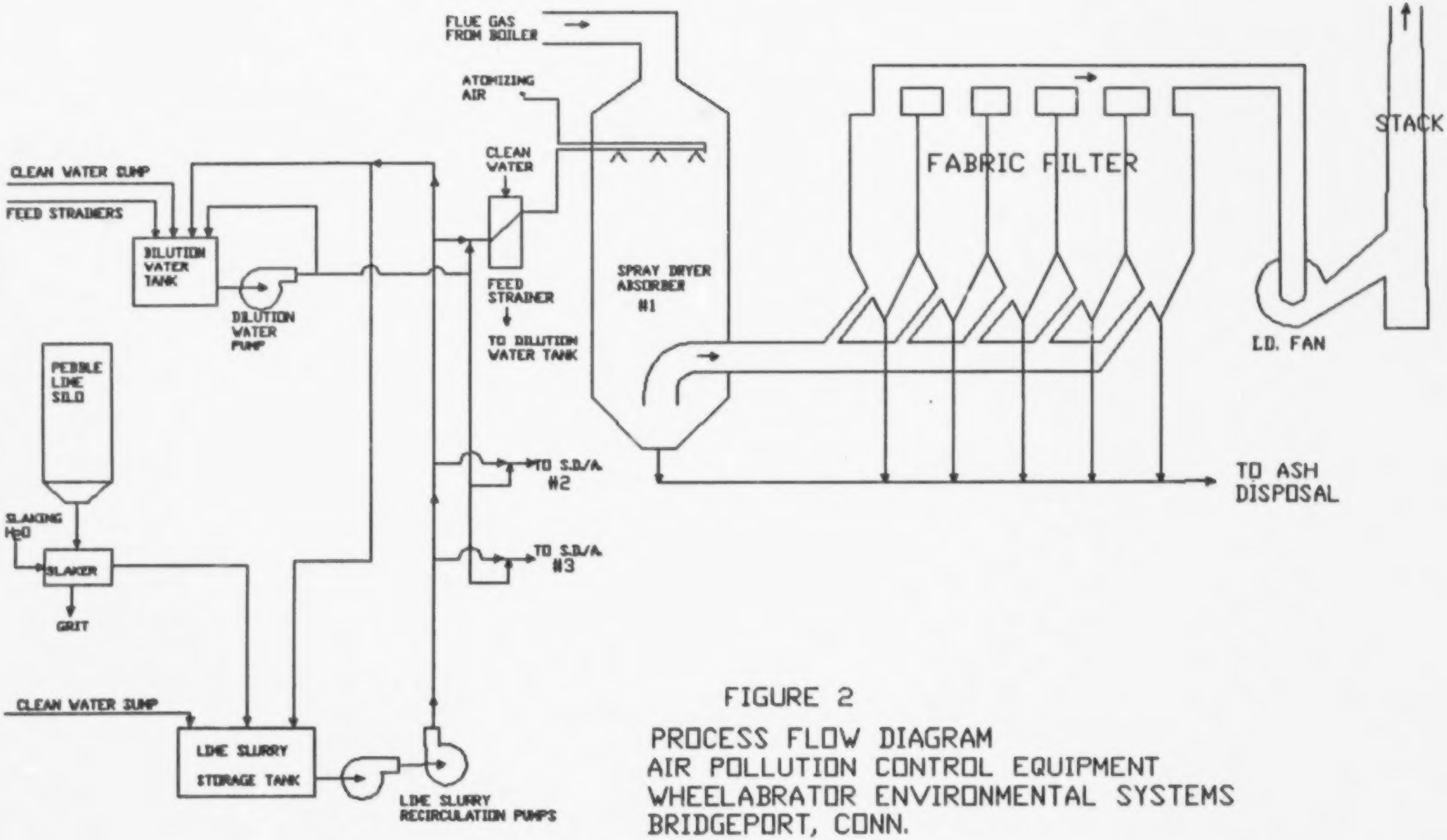
FLUE GAS FROM BOILER
ATOMIZING AIR
CLEAN WATER
FEED STRAINER
TO DILUTION WATER TANK
SPRAY DRYER ABSORBER #1
FABRIC FILTER
STACK
I.D. FAN
TO ASH DISPOSAL
CLEAN WATER SUMP
FEED STRAINERS
DILUTION WATER TANK
DILUTION WATER PUMP
PEBBLE LIME SILO
SLAKING H2O
SLAKER
GRIT
TO S.D/A. #2
TO S.D/A. #3
CLEAN WATER SUMP
LIME SLURRY STORAGE TANK
LIME SLURRY RECIRCULATION PUMPS

FIGURE 2

PROCESS FLOW DIAGRAM
AIR POLLUTION CONTROL EQUIPMENT
WHEELABRATOR ENVIRONMENTAL SYSTEMS
BRIDGEPORT, CONN.

TABLE 1
FACILITY OPERATIONAL SUMMARY

	Claremont	Millbury	Bridgeport
Startup	March 1987	Sept. 1987	Jan. 1988
Nameplate Usage	89%	90%	91%
Throughput Total	77,809 tons	329,718 tons	221,135 tons

Overall, the three facilities have processed a total of 628,662 tons of municipal solid waste.

TABLE 2
OPERATING SYSTEM EMISSIONS
WHEELABRATOR ENVIRONMENTAL SYSTEMS INC.
NEW HAMPSHIRE/VERMONT SOLID WASTE PROJECT
MAY 1987
CLAREMONT, NH

Parameter	Units	Emission Level		Design Conditions or Permit Limits
		Unit 1	Unit 2	
Steam Load	lb/hr	26,500	26,500	26,500
Oxygen	%	11.4	11.3	
Carbon Dioxide	%	8.1	7.7	
Moisture	%	11.8	13.6	
Outlet ECS Temperature		427	430	
Particulate	Gr/ACF	0.007	0.003	
@ 12% CO_2	Gr/SDCF	0.011	0.004	0.02
HCl	PPM @ 12% CO_2	32.6	39.1	
	lb/hr	1.5	2.0	7.5
SO_2	PPM @ 12% CO_2	37.5	64.0	
	lb/MMBtu			
	lb/hr	4.2	5.7	26.5
HCl Removal	%	95	95	90
SO_2 Removal	%	85	75	
Stoichiometric Ratio		3.6	3.2	

TABLE 3
OPERATING SYSTEM EMISSIONS
WHEELABRATOR ENVIRONMENTAL SYSTEMS INC.
FEBRUARY 1988
MILLBURY, MA

Parameter	Units	Emission Level Unit 1	Emission Level Unit 2	Design Conditions or Permit Limits
Steam Load	lb/hr	188,200	187,900	
Oxygen	%	9.7	9.7	
Carbon Dioxide	%	10.0	10.1	
Moisture	%	13.3	13.0	
Outlet ECS Temperature		255	241	
Particulate	Gr/ACF	0.001	0.004	
@ 12% CO_2	Gr/SDCF	0.002	0.008	0.03
HCl	PPM @ 12% CO_2	21.5	5.6	45
	lb/hr	10.0	2.6	70
SO_2	PPM @ 12% CO_2	50.2	57.0	
	lb/MMBtu	0.131	0.149	0.21
	lb/hr	42.3	45.3	137
HCl Removal	%	97	99	90
SO_2 Removal	%	73	79	70
Stoichiometric Ratio		2.2	2.8	

TABLE 4
OPERATING SYSTEM EMISSIONS
WHEELABRATOR ENVIRONMENTAL SYSTEMS INC.
JUNE 1988
BRIDGEPORT, CT

Parameter	Units	Emission Level Unit 1	 Unit 2	 Unit 3	Design Conditions or Permit Limits
Steam Load	lb/hr	191,900	191,700	191,900	
Oxygen	%	11.5	11.1	10.1	
Carbon Dioxide	%	8.5	8.9	9.8	
Moisture	%	13.0	12.4	13.2	
Outlet ECS Temperature		277	280	275	242
Particulate	Gr/ACF	<.001	<.001	<.001	
@ 12% CO_2	Gr/SDCF	0.002	0.001	0.001	0.015
HCl	PPM @ 12% CO_2	7.9	3.2	6.1	45
	lb/hr	3.6	1.7	3.2	36
SO_2	PPM @ 12% CO_2	14.1	3.2	8.2	122
	lb/MMBtu	0.0359	0.0082	0.0208	0.32
	lb/hr	10.2	2.5	6.2	104
HCl Removal	%	99	99	99	90
SO_2 Removal	%	93	98	97	45
Stoichiometric Ratio		2.4	3.0	2.4	

TABLE 5
SUMMARY
METALS EMISSIONS

	Millbury	Bridgeport
Total Particulate	0.005	0.001
Beryllium	ND (<1.84E-07)	ND (<5.61E-07)
Mercury	5.39E-04	1.26E-04
Lead	1.29E-04	ND (<1.15E-06)
Arsenic	1.72E-06	ND (<5.75E-07)
Chromium	3.12E-05	ND (<5.48E-06)
Nickel	ND (<8.18E-06)	ND (<5.43E-06)

All results are expressed as Gr/SDCF @ 12% CO_2.

DRY SCRUBBING PROCESS FOR WASTE-TO-ENERGY APPLICATIONS
OPERATING EXPERIENCE AND PERFORMANCE DATA

by: Prakash H. Dhargalkar
Research-Cottrell, Inc.
Somerville, New Jersey 08876

DISCLAIMER

The work described in this paper was not funded by the U.S. Environmental Protection Agency and therefore the contents do not necessarily reflect the views of the Agency and no official endorsement should be inferred.

ABSTRACT

Dry scrubbing process has been recently employed for control of acid gases and particulates in municipal waste-to-energy facilities. The two full-scale systems in Michigan and California have been tested extensively since the initial start-up. Emissions from both the plants are within the levels permitted by the regulatory authorities. Performance testing at the California facility showed that emissions of some pollutants - including sulfur dioxide, dioxins and furans are among the lowest reported for similar operating facilities.

This paper presents a description of the dry scrubbing emission control system installed at these plants. Key operating parameters and emission data on acid gases, particulates, heavy metals and dioxins are presented.

INTRODUCTION

Disposal of household wastes poses a major problem in many communities due to limited availability of landfill space. Most existing landfills have reached their capacities, while opening of new landfills has become an extremely tedious process due to stringent requirements. Many communities have turned to incineration of municipal garbage to reduce the amount of wastes to be landfilled. Typically, this lowers the waste quantity by 80 to 90 percent extending the useful life of the landfill by 5 to 10 times. Although waste incineration has been practiced in Europe, Japan, and the U.S.A. for many years, increasing attention is now being given to the control of emissions of various pollutants from these faciities. This paper represents data from two full-scale plants which have demonstrated extremely low emissions of various pollutants including particulates, heavy metals, acid gases, and dioxins by the use of Research-Cottrell/Teller dry scrubbing system.

CONTROL OF EMISSIONS

Until recently, the only requirement for municipal waste incenerators was the control of particulate emissions to the level of 0.04 to 0.08 grains per dry standard cubic feet of flue gas - corrected to 12% CO_2. In the early 1980's, the Japanese government imposed additional regulations for the control of hydrogen chloride (HCl) for all existing and new installations. In this country, many states have now formulated regulations for the control of HCl, sulfur dioxide (SO_2), hydrogen fluoride (HF), and nitrogen oxides (NO_X) along with lower limits for particulate emissions.

Most of the new MSW facilities under design and/or construction in the USA, Japan and Europe are required to limit the particulate emisions to less than 0.010 -.015 gr/dscf @ 12 percent CO_2. The removal efficiency for SO_2 is in the range of 70 to 90 percent, while HCl and HF removal is required at 90 to 95 percent.

In many cases, additional limits are imposed - e.g. emissions of heavy metals including cadmium, chromium, lead and mercury, dioxins/furans, fine particulates and nitrogen oxides (NO_X). Although specific regulations for these pollutants do not exist in many states, the owner/operator of a new MSW facility is required to evaluate health-risk impact as a result of these emissions.

FACILITY DESCRIPTIONS

Emission data from two waste-to-energy facilities is reported in this paper. These are - City of Commerce, operated by the County Sanitation District of Los Angeles County, and Jackson County, Michigan. A brief description of each facility follows.

CITY OF COMMERCE

This facility consists of a water wall boiler designed to produce 115,000 pounds per hour of superheated steam while combusting 320 to 380 tons per day of refuse. The steam is used in a turbine to generate 11,400 KW of electrical power of which 10,000 KW is delivered to the local utility (1).

The refuse storage and receiving area is sized to accommodate 1,200 tons of refuse which is fed to a water cooled feed chute by overhead bridge cranes. The grate system incorporates a ram feeder and three grate sections. The combustion air is drawn from the refuse storage building and supplied to the boiler by separate under-grate and over-fire fans. Manual dampers are provided to distribute the primary air to the three zones beneath the grates.

The air pollution control system consists of a Thermal DeNO$_X$ System and Teller dry scrubbing process. The deNOx System incorporates injection of ammonia through ports on both sides of the furnace. The ammonia is stored as a liquid under pressure and mixed as a vapor with compressed air prior to injection into the boiler. The flue gas leaving the economizer enters the Teller process which includes a quench reactor (dry scrubber), dry venturi and a fabric filter.

JACKSON COUNTY

The Jackson facility includes two trains each sized to burn 100 tons/day of municipal waste; provision is included to add a third train of 100 TPD capacity at a later date. Each train includes a reciprocating grate and a waterwall boiler. The combustion units supplied by Riley Stoker/Takuma are expected to maintain combustion efficiency of at least 97 percent. A natural gas-fired auxiliary burner is used during startup and shutdown to maintain proper temperature in the equipment prior to burning of solid waste. The boiler is designed to provide a minimum residence time for the combustion gases of two seconds at 1800°F (2).

The turbine generator produces up to 3.7 MW (gross) electricity from the 615 psig/650°F steam (49,000 lb/hour). Both electricity and the steam extracted from the turbine are supplied to the adjoining State Prison; excess electricity is sold to Consumers Power Company.

The air pollution control system supplied by Research-Cottrell consists of a quench reactor, a fabric filter, and reagent preparation equipment.

EMISSION REQUIREMENTS

Both Commerce and Jackson plants are required to control emissions of particulates, SO_2, HCl, NO_X and carbon monoxide (CO). These requirements are summarized in Table 1 (1, 3).

PARTICULATES

Maximum allowable limit for particulates emission is 0.016 and 0.015 grains per dry standard cubic foot of flue gas (corrected to 12 percent carbon dioxide) for Commerce and Jackson respectively. A fabric filter (baghouse) is used to achieve this requirement at both plants.

SULFUR DIOXIDE (SO_2)

Presence of sulfur-containing compounds in the waste produces sulfur dioxide (SO_2) in the combustion gases. The acid gas scrubber can remove SO_2 along with HCl. The maximum emission limit for SO_2 at Jackson is 86 ppmdv at 12 percent CO_2; a minimum of 50 percent SO_2 removal efficiency is required. For Commerce, the permit requirement is 29 ppmdv of SO_X emission at 3 percent O_2.

HYDROGEN CHLORIDE (HCl)

Studies have shown that the burning of municipal solid waste without acid gas scrubbers can result in the formation of "acid gas plumes" or fogs containing 18 to 20 percent hydrochloric acid (HCl). Such plumes can also cause severe impacts on vegetation, paint finishes, iron and other corrosible materials.

The permitted emission limit for the Jackson County facility is 105 parts per million by dry volume-corrected to 12 percent CO_2 (ppmdv) based on a three hour average, which corresponds to an emission rate of about 0.75 pounds of HCl per ton of waste. An acid gas scrubber with a design HCl removal efficiency of 90 percent is required at both plants.

NITROGEN OXIDES (NO_X)

The maximum allowable nitrogen oxide emissions rate for Jackson County is 5.43 lb per ton of waste; the emission limit is 311 ppmdv at 12 percent CO_2 based on a three-hour average. The use of staged combustion process is considered to be adequate to achieve these emission limits. The Commerce permit requires the maximum NO_X emission of less than 186 ppmdv at 3 percent O_2 which has necessitated the use of a thermal $deNO_X$ system.

CARBON MONOXIDE (C))

The discharge of carbon monoxide from the Jackson County facility is limited to 400, 113, and 63 ppm on a dry basis based on one-hour, 24-hour, and annual average respectively. These limits will assure that the steam generators are operated in a manner which will maximize combustion efficiency and minimize CO emissions in spite of variability of the refuse. The Commerce limit in 134 ppmdv at 3 percent O_2.

CADMIUM, CHROMIUM AND ARSENIC

The majority of dilute vapor phase metals such as cadmium, chromium, and arsenic are expected to condense in the dry scrubber. Since trace metals tend to be enriched on fine particulates, the fabric filter with high removal efficiency for the fine particulate should provide excellent control of these pollutants. The expected emission rates at Jackson were estimated to be half of the rates allowed by the State of Michigan.

DIOXINS AND FURANS

There are various general theories as to the source of dioxins (PCDDs) and furans (PCDFs) from resource recovery facilities, although the mechanisms involved in the formation of dioxins are not thoroughly understood.

The allowed PCDD and PCDF emission rates, and the rates used in the risk assessment performed by the State of Michigan, are based on a literature survey done by Arthur D. Little in 1981. Jackson County has elected to use these conservative estimates in order to provide a margin of safety with compliance limits due to the limited amount of available data. These rates are 0.52 micrograms per dry standard cubic meter, based on a 3 hour average for PCDD, and 0.50 micrograms per dry standard cubic meter, based on a 3 hour average for PCDF.

DRY SCRUBBING SYSTEM

An air quality control system (AQCS) consisting of a dry scrubber and a fabric filter was supplied by Research-Cottrell for the Jackson facility for control of acid gases and particulate emissions. The system is based on the Teller process developed in early 1980's and applied in various waste incinerator facilities throughout the world (See Figure 1).

The flue gas exiting the boiler enters the quench reactor (dry scrubber) where larger particulates are removed via cyclonic forces in the inlet section. The gas is then contacted with lime slurry which is atomized into fine droplet by mixing with compressed air in the injection nozzles. The lime slurry neutralizes the acid components and also quenches the flue gas simultaneously.

$$Ca(OH)_2 + 2HCl \longrightarrow CaCl_2 + 2H_2O$$
$$Ca(OH)_2 + 2HF \longrightarrow CaF_2 + 2H_2O$$
$$Ca(OH)_2 + SO_2 \longrightarrow CaSO_3 + H_2O$$

The quenched gas then flows through a fabric filter (baghouse) for removal of particulates which include fly ash, acid neutralization products and any unreacted reagent. In the fabric filter, the cake deposited on the bags also acts as a fixed bed reactor for further acid neutralization. The clean gas exits the system via the induced draft fan and stack.

The Teller dry scrubbing process at Commerce is similar with the exception of a dry venturi which is located between the quench reactor and the fabric filter. Tesisorb, a dry crystalline product, is injected in the dry venturi along with carrier air. The annular throat of the dry venturi provides an intimate contact zone between the Tesisorb and the flue gas where the fine particulates are agglomerated on the Tesisorb by inertial impaction. This results in enhanced fabric filter performance (i.e. lower pressure drop, longer cleaning cycle, etc.)

QUENCH REACTOR

The quench reactor is the proprietary Research-Cottrell/Teller design with upflow configuration. It is equipped with a single or multiple nozzles for injection of lime slurry which is atomized into fine droplets by compressed air. The nozzle may be withdrawn for inspection and service while the system is in operation. The upflow design provides longer residence time compared to a downflow configuration for evaporation of large droplets due to counteracting forces of gravity and gas flow. This ensures complete drying of slurry droplets before the gas exits the quench reactor.

FABRIC FILTER

The fabric filter at Jackson is of pulse-jet design with three modules per train, each of which can be isolated independently for cleaning and maintenance. The bags are made of fiberglass with an acid-resistant coating to protect against acid corrosion. Cleaning of the bags is initiated automatically using dry compressed air at a preset time interval or at a preset value for differential pressure across the fabric filter. The Commerce plant has an eight module reverse-air fabric filter.

REAGENT SYSTEM

The reagent system consists of a silo for storage of pebble lime (CaO). The lime is fed to the slaker where it is mixed with water to produce a slurry of calcium hydroxide [$Ca(OH)_2$]. A vibrating screen is used to separate the grits and other impurities from the lime slurry. The degritted slurry is stored in a storage tank where it is mixed with water to maintain the slurry concentration required for proper operation of the quench reactor. The lime slurry is injected through the quench reactor nozzle at a controlled rate to achieve the required acid gas removal efficiencies.

The Commerce facility also includes a Tesisorb silo and a pneumatic system for injection of Tesisorb in the dry venturi.

EMISSION DATA

Emission data on particulates, SO_2, HCl, HF, heavy metals and dioxins/furans from Commerce and Jackson facilities is presented in Tables 2-5 (1, 4, 5). The Commerce data is from a comprehensive series of tests conducted in May and June 1987 to demonstrate compliance with the permit conditions of the South Coast Air Quality Management District. At both facilities, measurements for particulates,

SO_2, HCl, and HF were made at the inlet to the quench reactor and at the fabric filter outlet or in the stack.

At Jackson, a performance test was conducted on both trains at full and reduced load in February 1988 to determine the removal efficiency and/or emission levels of particulates, SO_2, HCl and HF. In April 1988, a compliance test was conducted to determine the emissions of particulates, SO_2, HCl, CO, NOx, nonmethane hydrocarbons, certain heavy metals, dioxins and furans. Measurements were made only at AQCS stack of Units 1 and 2. The data presented in Table 4 for this compliance test should be considered as "preliminary" subject to further analysis and evaluation.

COMMERCE - PARTICULATE EMISSIONS

Particulate emission rate at Commerce was measured at 0.0043 gr/dscf at 12 percent CO_2 (see Table 2). The Southern Coast Air Quality Management District defines particulates as "any material, except uncombined water, which exists in a finely divided form as a liquid or solid at standard conditions." This definition includes any components which would condense as the flue gas is cooled.

The particulate mass emission rate was 1.44 lbs/hr which was almost one-fourth the permit limit of 5.5 lbs/hr. The fine particulate - less than 10 microns - emission was 7.2×10^{-5} grain dscf at 12 percent CO_2 which is less than 2 percent of the total particulates emission (6). With efficient removal of fine particulates, it is possible to control the heavy metal emissions which is further discussed below.

COMMERCE - ACID GAS EMISSIONS

The Commerce plant demonstrated excellent removal efficiency for both SO_2 and HCl - in excess of 98.8 percent (see Table 2). Emissions of SO_2 and HCl were were very low - less than 2 ppmdv and 12 ppmdv at 3 percent O_2 respectively.

It should be noted that the commercial waste burned at Commerce results in significantly higher concentrations of SO_2 and HCl in the flue gas. For example, the average concentrations during the test at the quench reactor inlet were 250 ppmdv of SO_2 and 1152 ppmdv of HCl @ 3 percent O_2. These values are almost twice those reported for typical household garbage. (Note that the concentrations expressed at 12 percent CO_2 are approximately 10 percent O_2 lower than the values reported at 3 percent O_2).

Even with these high loadings, the outlet emissions were extremely low 2 ppmdv for SO_2 and 11 ppmdv for HCl. These emissions (which correspond to almost 99 percent removal) are significantly lower than the permit limits. HF emission was measured at 0.05 ppmdv - corresponding to 99.7 percent removal with measured inlet concentration of 20 ppmdv.

The thermal deNOx process achieved about 45 percent reduction of NOx. The measured emission level of 116 ppmdv (@ 3 percent O_2) was lower than the permit limit of 186 ppmdv.

The CO emission of 20 ppmdv (@ 3 percent O_2) was significantly lower than the permit limit of 134 ppmdv.

JACKSON - PARTICULATE EMISSIONS

Data on emissions and removal efficiency from the performance test is sumarized in Table 3. Preliminary data from the compliance test is shown in Table 4.

Particulate emissions were significantly lower than the design value - ranging from 0.0010 grains per dry standard cubic foot (at 12 percent CO_2) to 0.0079 gr/dscf. The average was 0.0029 gr/dscf for Unit 1 and 0.0020 for Unit 2.

Similar tests were conducted on both units at "reduced" load (approximately 80-85 percent). Average particulate emission was 0.0024 gr/dscf during these tests. During the compliance test, particulate emissions ere again found to be significantly lower than expected by almost a factor of ten. The measured emission levels ranged from 0.0010 to 0.0018 gr/dscf (see Table 4).

JACKSON - ACID GAS EMISSIONS

Both HCl and SO_2 emissions were significantly lower than the design values. For four of the six tests, emissions of both these acid gases were less than 10 ppmdv corrected to 12 percent CO_2; corresponding removal efficiency for these runs was 95-97 percent for SO_2 and 98-99 percent for HCl.

The highest HCl concentration at the quench reactor inlet was 936 ppmdv at 12 percent CO_2; for this run the outlet was 36 ppmdv which corresponds to about 96 percent removal. During the same run, SO_2 concentrations was also the highest at 106 ppm. The outlet SO_2 for this run was 26 ppm yielding 75.4 percent SO_2 removal. It should be noted that these excellent removal efficiencies were achieved even though the flue gas temperature at the AQCS inlet was much lower than expected. The average inlet temperature was only 359°F compared to "nominally" expected 400°F.

Average HF emission was less than 0.5 ppmdv with removal efficiency in the range of 50 to 93 percent. For a typical municipal waste incinerator, HF concentration is expected to be very low (less than 5 ppm); thus emission levels should also be corresponding low when a dry scrubber is employed.

During the compliance test also, both HCl and SO_2 emissions were low - about 20 ppmdv for HCl and 2 ppmdv for SO_2. Removal efficiency across the dry scrubbing system cannot be calculated since no measurements were made at the system inlet during the compliance test. Assuming the inlet concentrations of HCl and SO_2 were similar to the average values measured in the earlier performance test e.g., 600 ppm for HCl and 80 ppm for SO_2, the corresponding removal efficiencies would be in the range of 95 to 97.5 percent.

The NOx and carbon monoxide (CO) emissions average of 153 and 30 ppmdv respectively reflect the combustion process operation since these are not controlled in the dry scrubbing system.

HEAVY METALS

The Commerce tests included heavy metal measurements at the boiler exit and in the stack. Thirteen elements were analyzed - antimony, arsenic, beryllium, cadmium, chromium, copper, lead, mercury, nickel, selenium, silver, thallium and zinc. Outlet emissions were found to be below the detection limits except for lead and mercury. Based on the measurements made at upstream and downstream of the dry scrubbing system, it can be projected that the removal efficiency for each heavy metal (except mercury and thallium) would be in the range of 97 to 99 percent. Total heavy metal emission was lower than 0.1 lb/hr accounting for less than 7 percent of the total particulate emission. Most of the heavy metal emission is attributed to mercury vapors which can be removed in the dry scrubbing process only by the use of a suitable adsorbing agent.

At Jackson, concentrations of arsenic, chromium and cadmium were measured in the stack during the compliance test. The preliminary values indicate emission level of around 0.01 milligrams per normal cubic meter (mg/nm^3) for each of these three metals.

DIOXINS/FURANS

Dioxin/furan (PCDD/PCDF) measurements were made at Commerce according to the draft California Air Resources Board Modified Method 5 (Semi-VOST). Tetra- through octa - PCDD's and PCDF's were measured including all 2,3,7,8 isomers. The data is summarized in Table 5.

For the largely commercial waste, the total PCDD/PCDF emissions in the stack averaged 1.82 nanograms per normal cubic meter @ 12% CO_2. This corresponds to a reduction of 93.6 percent in the Teller process based on the average boiler exhaust at 28.5 ng/nm^3 @ 12% CO_2. Another test was conducted with typical residential fuel which also showed similar results.

For both types of wastes, the 2,3,7,8 - TCDD toxic equivalent emission was less than 0.075 ng/nm^3 @ 12% CO_2 using the California DOHS - Method IV. The corresponding values based on the Swedish and U.S. EPA method were 0.023 and 0.014 ng/nm^3 @ 12% CO_2 respectively for the residential waste. For all three methods, the measured values for toxic equivalents were far below the current detection limits. The Commerce data supports the previous findings that significant reductions in dioxin/furan emissions are achieved with a dry scrubber/fabric filter (3).

Preliminary data from Jackson shows similarly low emissions. The total 2,3,7,8 - TCDD equivalent for Units 1 and 2 averaged less than 0.03 and 0.02 ng/nm^3 at 12 percent CO_2 respectively based on the U.S. EPA method.

CONCLUSIONS

The data presented in this report confirms that the required emission levels of particulates, SO_2, HCl and HF for municipal waste incineration facilities can be achieved with a properly designed quench reactor (dry scrubber)/fabric filter system. The process has been demonstrated successfully in full-scale facilities of various configurations including those designed for recovery of energy. Emissions of dioxins/furans and heavy metals are also reduced significantly when a dry scrubber/fabric filter system is employed.

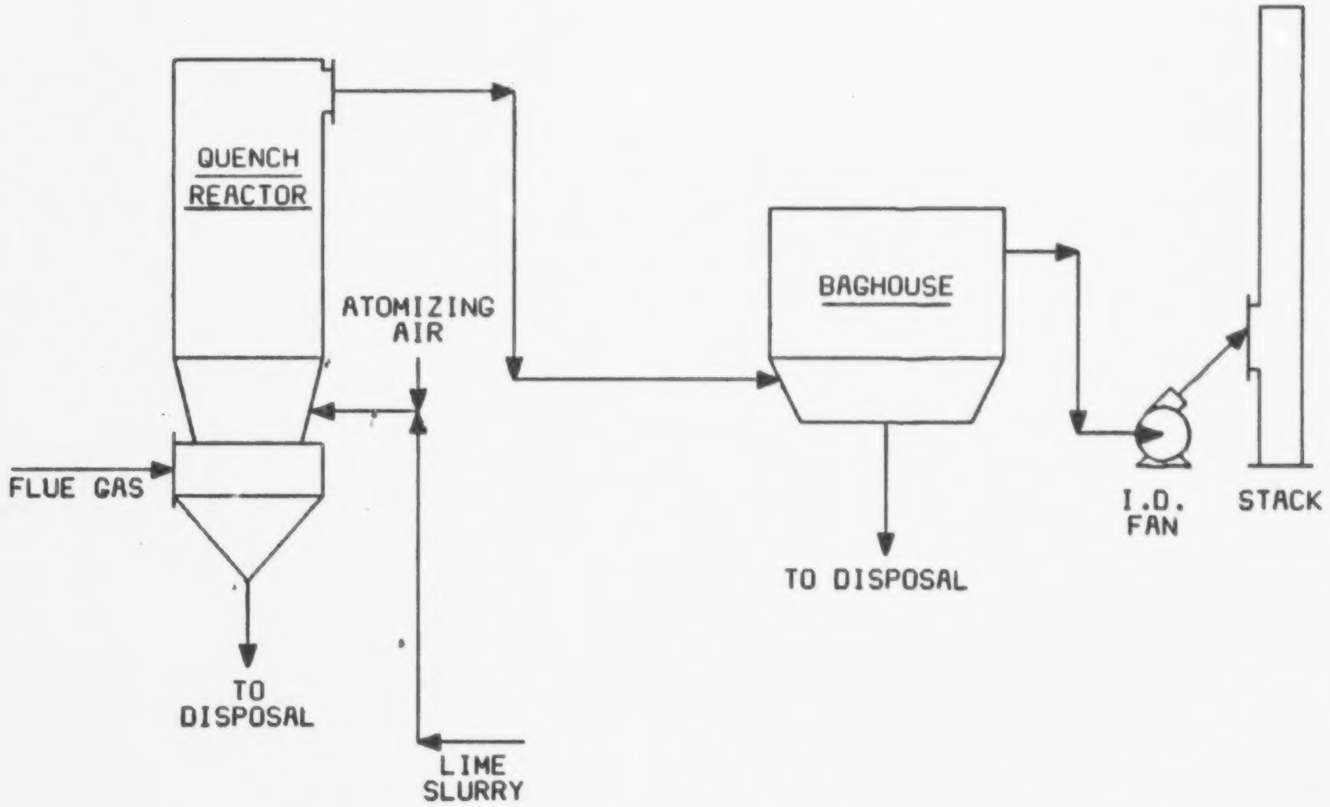
QUENCH
REACTOR
FLUE GAS
TO
DISPOSAL
ATOMIZING
AIR
LIME
SLURRY
BAGHOUSE
TO DISPOSAL
I.D.
FAN
STACK

FIGURE 1: RESEARCH-COTTRELL - AIR QUALITY CONTROL SYSTEM

TABLE 1. REQUIREMENTS FOR COMMERCE AND JACKSON

Pollutant	Emission/Removal (a)	Commerce	Jackson
Particulates	Emissions gr/dscf	0.016	0.015
SO_2	Emission, ppmdv	29 (b)	86
	Removal, percent	80	50
HCl	Emission, ppmdv	30	105
	Removal, percent	90	90
NO_x	Emission, ppmdv	186 (b)	311
CO	Emission, ppmdv	134 (b)	113 (c)

NOTE: (a) All emissions values are at 12 percent CO_2 except those identified in (b) below.

(b) At 3 percent O_2

(c) 24 hour average.

TABLE 2. COMMERCE - PARTICULATE/ACID GAS EMISSIONS

INCINERATOR CAPACITY: 300 - 380 TPD
FLUE GAS FLOW: 89,000 ACFM @ 430°F

	CONCENTRATION IN FLUE GAS		
Pollutant	Boiler Exit	Stack	Removal Efficiency Percent
Particulates, gr/dscf @ 12% CO_2	2.01	0.0043	99.8
SO_2, ppmdv @ 3% O_2	300	<2	>99
HCl, ppmdv @ 3% O_2	1,150	<12	98.8
HF, ppmdv @ 3% O_2	20	0.05	99.7
NOx, ppmdv @ 3% O_2	209	116	44.5

TABLE 3. JACKSON - PARTICULATE/ACID GAS EMISSION

TEST: PERFORMANCE TEST
OPERATING LOAD: EACH TRAIN @ 100 TPD
FLUE GAS FLOW: 21,500 ACFM @ 345-360°F

Pollutant	CONCENTRATION IN FLUE GAS (a) Boiler Exit	Stack Average (b)	Removal Efficiency Percent
Particulates, gr/dscf	1.0 - 1.5	0.0025	99.7 - 99.9
SO_2, ppmdv	80 - 110	11	67 - 97
HCl, ppmdv	200 - 940	14	88 - 99
HF, ppmdv	0 - 9	<0.5	50 - 93

NOTE: (a) All concentrations at 12 percent CO_2 by dry volume.
(b) Average for both trains; three tests per train.

TABLE 4. JACKSON - PARTICULATE/ACID GAS EMISSIONS
COMPLIANCE TEST AT FULL LOAD

Pollutant (a,b)	Unit 1	Unit 2
Particulates, gr/dscf	0.0015	0.0013
SO_2, ppmdv	1.5	1.1
HCl, ppmdv	22	17
NOx, ppmdv	156	150
CO, ppmdv	30	30

NOTES: (a) All data at full load, average of three tests per train.
(b) All values based on dry gas volume, corrected to 12 percent CO_2.

TABLE 5. DIOXIN/FURAN EMISSIONS AT COMMERCE

	Total Concentration ng/nm^3 @ 12% CO_2		Reduction In Quench Reactor/ Fabric Filter	2,3,7,8 - Toxic Equivalent ng/nm^3 @ 12% CO_2 (a)	
Waste	Boiler Exhaust	Stack	Percent	Stack Emission	Detection Limit
Commercial	28.5	1.82	93.6	0.075	0.109
Residential	28.5	3.5	87.7	0.076	0.125

NOTE: (a) California DOHS Method IV.

REFERENCES

1. Wheless, Edwin, "Air Emission Testing at the Commerce Refuse-to-Energy Facility," September 1987.

2. Vansant, Carl A. and O'Meara, Robert G. - "Waste-to-Energy Project Design: Jackson County, Michigan," presented at American Power Conference, Chicago, April 1987.

3. Jackson County Resource Recovery Facility, Descriptive Brochure, 1986.

4. Report on Performance Testing performed at Jackson County Resource Recovery Facility by Clean Air Engineering, April 1988.

5. Report (Preliminary) on Compliance Testing performed at Jackson County Resource Recovery Facility by Clean Air Engineering, June 1988.

6. Air Emission Tests at Commerce Refuse-to-Energy Facility by Energy System Associates, July 1987.

CHARACTERIZATION OF EMISSIONS FOR A MUNICIPAL SOLID WASTE INCINERATOR WITH A DRY SCRUBBER

by: Theodore G. Brna and Charles B. Sedman
U.S. Environmental Protection Agency
Air and Energy Engineering Research Laboratory
Research Triangle Park, North Carolina 27711

and

Clyde E. Riley
U.S. Environmental Protection Agency
Office of Air Quality Planning and Standards
Research Triangle Park, North Carolina 27711

ABSTRACT

Short-term tests were made to characterize air emissions control on a 249-tonne/day (275-ton/day) municipal solid waste incinerator at the Marion County Solid-Waste-to-Energy Plant in Brooks, Oregon. A lime spray dryer absorber plus fabric filter (Teller) system treats flue gas from the boiler to control HCl, SO_2, particulate matter, and other emissions. HCl, SO_2, CO, CO_2, O_2, and NO_x were measured to characterize flue gas cleaning system operation under normal and selected off-design incinerator load and air supply conditions and spray dryer absorber outlet temperature. Ash was sampled at various collection points for determination of dioxin and furan contents. In addition, tests were run during the shutdown and start-up of the incinerator to study transient operation.

Results reported include HCl, SO_2, and NO_x control by the flue gas cleaning system as well as dioxin and furan levels in ashes. The effect of off-design incinerator operation on air emissions control is also reported.

This paper has been reviewed in accordance with the U.S. Environmental Protection Agency's peer and administrative review policies and approved for presentation and publication.

INTRODUCTION

As part of a program to gather information on municipal waste combustor (MWC) emissions and control technologies for a report to Congress (1), the U.S. Environmental Protection Agency (EPA) has been collecting data on four categories of air pollutants in MWC emissions: criteria pollutants [SO_2, CO, NO_x, total hydrocarbons (THC), particulate matter, and lead], acid gases (HCl, SO_2), trace organic compounds (including dioxins and furans), and trace metals.

The testing described in this paper (June 1987) was performed prior to the EPA Administrator's decision to further regulate MWCs under Section 111 of the Clean Air Act, and was planned as part of a two-phase effort to collect additional data on a mass burn MWC equipped with a spray dryer absorber (quench reactor)/fabric filter flue gas cleaning system. Phase 1, the characterization test program, is described here; Phase 2, the performance test program component originally planned for early 1988, was cancelled in July 1988 because of delays in control modifications to the flue gas cleaning system. The results from this effort will supplement earlier pilot-scale data on a mass burn MWC and were to aid data collection planning for other MWC tests.(2) Data on refuse-derived fuel (RDF) MWCs equipped with acid gas flue gas cleaning will also be obtained as part of EPA's data collection on MWCs, and a joint EPA/Environment Canada project currently involves characterization and performance testing at a U.S. site.

The principal objectives of the tests discussed here were to:

1. Evaluate control efficiency of a spray dryer absorber/fabric filter (SDA/FF) for selected air emissions (such as HCl and SO_2) within the normal operating range.

2. Determine the SDA/FF control efficiency for selected emissions as a function of the flue gas cleaning system set point (outlet gas temperature of the spray dryer).

3. Obtain operating and emissions data during start-up and shutdown.

4. Identify combustor design or operating parameters (such as CO and furnace temperature) which can be monitored and controlled to minimize selected emissions and which, in turn, may minimize the products of incomplete combustion (PICs).

The results discussed here focus primarily on the work related to the first three objectives; tests for obtaining these results were performed at the Marion County Solid-Waste-to-Energy Facility.

SYSTEM DESCRIPTION

The Marion County Solid-Waste-to-Energy Facility in Brooks, Oregon, was constructed at a cost of $47,500,000, and shakedown operation began in April 1986. Commercial operation of the facility, which has a design capacity of 154,000 tonnes/yr (170,000 tons/yr), stipulates a guaranteed waste delivery of 132,000 tonnes/yr (145,000 tons/yr) for its two units in combination. (3)

Unit 1 of the facility was the test unit. This unit, one of two identical units [see Figure 1 (3)] at this facility, is a mass burn, reverse reciprocating grate incinerator with a waterwall multi-pass boiler.(3,4) The unit has a refuse burning capacity of 249 tonnes/day (275 tons/day) and a steam generation rate of 29,900 kg/h (66,000 lb/h) at 4.52 MPa/371°C (655 psig/700°F), assuming the refuse burned has a higher heating value of 10,700 kJ/kg (4600 Btu/lb). A single turbogenerator receiving steam from both units is rated at 13.1 MW and has a net generation of about 11 MW which is sold to the Portland General Electric Company. The flue gas cleaning system is designed to remove at least 90% of the HCl and 70% of the SO_2 and to limit particulate matter (PM) emission to 0.08 g/Nm^3 (0.03 gr/dscf) corrected to 12% CO_2.

The facility refuse is typical residential and commercial solid waste. The waste is not sorted or shredded prior to incineration; however, the refuse may be mixed in the pit using one of the two (100% spare) manually operated overhead cranes prior to transferring refuse to the charging chute of the incinerator. Following these tests, the wastes have been screened as required by Oregon's Department of Environmental Quality, and materials causing high SO_2 emissions have been removed. Thus, the SO_2 emissions are believed to have decreased from values reported here.

TEST SYSTEM

EQUIPMENT

The flue gas cleaning system for each combustion unit is a Teller system (5) with a quench reactor (spray dryer absorber), dry venturi, and reverse-air-cleaned baghouse. Lime slurry, which is fed to multiple two-fluid (air/slurry) nozzles near the inlet of the spray dryer absorber, is prepared by slaking pebble lime in a paste slaker and diluting this mixture further with water to the desired feed solids concentration. The resultant feed slurry is apportioned (about equally at equal unit steam loading) to the single spray dryer absorber serving each facility unit. Similarly, the Tesisorb supplied to each venturi originates from a common storage/feed system which apportions the feed to each venturi. A six-compartment fabric filter (120 bags/compartment) removes particulate matter from the flue gas, using fiberglass bags capable of operation at gas temperatures up to 268°C (515°F). (3)

Atomized slurry from the nozzles travels concurrently upward with the flue gas into the spray dryer absorber. The heavier dry solids formed from the slurry droplet/flue gas component reactions or by other mechanisms in the spray dryer absorber (such as metals condensation on ash/solids during flue gas cooling, organics adsorption on particles, or surface reactions on particles) gravitate to the collecting chamber below the spray dryer absorber along with cyclonically removed particulate from the flue gas just below the spray dryer absorber inlet.

Tesisorb, a filter aid consisting of cement kiln dust or equivalent, is injected into the venturi downstream of the spray dryer absorber, and increases the porosity of the dust layer or cake on the filter bags. This permits less frequent cleaning of the bags and provides more time for unreacted sorbent in the cake to react with pollutants in the flue gas. During the tests reported here, each compartment was cleaned once per 8-h shift.

Design criteria for the flue gas cleaning system include a normal lime supply rate of 56.7 kg/h (125 lb/h) [maximum rate of 193 kg/h (425 lb/h)], Tesisorb feed rate of 24 kg/h (53 lb/h), a gross air-to-cloth ratio of 0.515:1 m^3/min.-m^2 (1.69:1 cfm/ft^2), and a net value of 0.713:1 m^3/min.-m^2 (2.34:1 cfm/ft^2). As noted earlier, this system is required to remove 90% HCl and 70% SO_2 and achieve a particulate emission of 0.08/Nm^3 (0.03 gr/dscf).

INSTRUMENTATION

The flue gas components monitored with continuous emission monitors (CEMs) during the tests were: HCl, SO_2, CO, CO_2, NO_x, O_2, and total hydrocarbons (THC) (see Table 1).(6,7) Of these, the CO was monitored only at the inlet to the spray dryer absorber. The NO_x was measured at the inlet to the spray dryer absorber and at the outlet of the baghouse. Because of the low outlet THC concentrations, measurement of this quantity was not obtained for all test runs. All CEMs were operated in accordance with EPA-approved methods, except those for HCl for which there currently is no published method.

Manual methods were used to determine flue gas flow rate and HCl concentrations, as well as moisture, O_2, and CO_2 content. Process data, such as steam flow, air flows, flue gas temperatures, and pressures/pressure drops, were determined from recorders in the facility's control room.

TEST PROGRAM

Table 2 summarizes the test program and schedule.(6) Runs 1-9 were for baseline (normal) operation, variation of combustion conditions (including excess air and overfire/underfire air distribution), and operation with low steam load. Runs 10-11B concerned operation of the flue gas cleaning system under various baghouse inlet temperatures, controlled by the feed slurry flow to the spray dryer absorber. Since the lime slurry was prepared for a fixed solids percentage, changing the slurry feed to control the baghouse inlet gas temperature also varied the reagent (stoichiometric) ratio. The test ranges for both the combustion and flue gas cleaning test runs were the maximum consistent with unit operating limitations. Generally, data were collected for 3 to 3-1/2 hours during each run.

In addition to the above testing, the start-up and shutdown of Unit 1 were monitored.(8) During this facet of the test program, samples (EPA Modified Method 5) were taken at the inlet and outlet of the flue gas cleaning system to evaluate chlorinated dibenzo-p-dioxin/chlorinated dibenzofuran (CDD/CDF) emissions.

DISCUSSION OF DATA AND RESULTS

COMBUSTOR AND FLUE GAS CLEANING SYSTEM TESTS

The continuous monitor outputs were supplied as computer inputs so that the data could be averaged over the time period desired. Normally, the data were recorded as 1-minute and test-run averages. Tables 3-9 present data averaged over each of the 14 "steady" test runs. The concentrations are on a dry basis and have been corrected to 12% CO_2 in Tables 5-9.(6) Table 10 gives hourly (CEM) concentrations for HCl (not corrected to 12% CO_2) for Run 10 along with the range of the 1-minute average concentrations, while Figure 2 plots these average concentrations for the period of this test run.(7) While the HCl data indicate midpoint concentrations, the effect of lime caking, which was observed during cleaning after each test run, on the midpoint (spray dryer outlet) HCl values is not known. Particulate also passed through the fritted filter and collected on the critical orifice inside the dilution probe, changing the dilution ratio for the midpoint monitoring system. The dilution ratio recorded during the calibration drift tests changed as the calibration gas was diluted through the probe.

Figures 3-6 show the HCl and SO_2 concentrations averaged over each test run (3-h duration) as a function of test runs. The inlet ppmv SO_2 concentration varied by a factor of almost five (558.5/120.2), while the HCl variation was less than two (814.4/495.6). The overall HCl removal met or exceeded the design goal of 90% for normal operation of the spray dryer absorber in 8 of the 11 runs, achieving 89+% in 10 of these runs. Since the spray dryer absorber outlet temperature was above normal for Runs 11A and 11B, the resulting higher approach to saturation temperature for these runs was expected to lower HCl removal. However, the amount of the decrease with increasing spray dryer absorber outlet temperature (and, hence, increasing approach to saturation temperature) was unknown. While the fixed solids content of the slurry resulted in a lower lime-to-HCl ratio as the slurry flow rate was decreased to permit a higher than normal spray dryer absorber gas outlet temperature, no quantitative measure of this ratio was possible on the flue gas cleaning system as operated. An estimate of this ratio made by assuming equal dry lime feed and acid gas component (HCl and SO_2) flow rates to the two flue gas cleaning units indicated values ranging from 1.02 to 2.5 in average value for the individual runs. However, the estimated ratio for Run 11B (highest midpoint temperature and lowest slurry feed rate) was significantly greater (1.65 vs 1.02) than Run 10 (lowest midpoint temperature and highest slurry flow rate) and points out the hazard of using this approach to determine the reagent (stoichiometric) ratio.

Figures 3-6 seem to confirm the higher reactivity of HCl with lime than SO_2 with lime. The overall SO_2 removal is 70% or greater in only three of the runs in Figures 4 and 6. [SO_2 data for Runs 11A and 11B were not plotted in these figures because of suspected instrument malfunctions or other errors since the SO_2 concentrations increase, rather than decrease, from inlet to outlet (see Table 5).] The SO_2 removal is also seen to vary widely from run to run, in sharp contrast to the HCl removal. While the accuracy of the HCl removal in the spray dryer may be uncertain due to lime collection in the midpoint sampling filter, the data in Figure 5 suggest, as do similar SO_2 data in Figure 6, that, generally, 75% or more of the overall HCl and SO_2 removals occur in the spray dryer.

Other conclusions from the data and results are:

1. The maximum average CO concentration was 17 ppmv (corrected to 12% CO_2). This value corresponded to high excess air (102% vs the normal value of 90%). The next highest average concentration was 16.9 ppmv at the lowest load (72.7% of design) and highest excess air observed (149%) during these tests. The CO concentrations are considerably below the 50 ppmv guideline value of Reference 9.

2. The NO_x removal in the gas cleaning system was insignificant.

3. The average total hydrocarbons were 2.4 ppmv (corrected to 12% CO_2) or less at the inlet to the spray dryer absorber for the runs sampled. Outlet values from the baghouse were 0.9 ppmv or less (corrected to 12% CO_2) for the runs sampled (see Table 8). These low values correspond with the low CO concentrations noted above.

4. Typical total chlorinated dibenzo-p-dioxins (CDD) plus total chlorinated dibenzofurans (CDF) were typically 10-15 ppb in the baghouse ash and 2-10 ppb in the other ash samples (see Figure 7).(6) Other than the suspiciously high CDD/CDF level for Run 4, the general trend was that the CDD/CDF concentrations in the baghouse ash were the highest, suggesting that significant condensation/removal of these organic pollutants was taking place in the flue gas cleaning system. The long particulate residence time in the baghouse (8-h compartment cleaning cycle) and low flue gas temperature probably aided solids collection on the fabric filter surface.

SHUTDOWN AND START-UP

In addition to the CEM and process data collection, CDD/CDF samples were collected from the flue gas at the inlet to the spray dryer absorber and in the stack. The average test conditions during shutdown and start-up were a steam load of 19,200 kg/h (42,400 lb/h) and 25,400 kg/h (56,000 lb/h), excess air of 139.5% and 77.9%, and CO of 6.9 and 8.0 ppmv (dry), respectively. Similar values for baseline operation were 30,400 kg/h (67,100 lb/h), 74.7%, and 10.2 ppmv (dry).

The average CEM results for Run 12 (shutdown) and Run 13 (start-up) are shown in Table 11. Figures 8 and 9 show the HCl and SO_2 concentrations during shutdown, while Figures 10 and 11 are for start-up. The HCl and SO_2 reductions during shutdown averaged 91.9% and 65.8%, respectively. Since auxiliary fuel (natural gas) was fired during both shutdown and start-up to control the cooling and heating rate, the figures noted portray trends in the HCl and SO_2 concentrations. However, these removals compare favorably with those of the baseline values of 90.4% and 69.2% for HCl and SO_2, respectively.

During shutdown, inlet CDD/CDF concentrations were obtained with and without sootblowing using two separate sampling trains. After sootblowing, the inlet (uncontrolled) CDD/CDF concentration was 62.1 ng/dscm, and with sootblowing the concentration was 121 ng/dscm. At the outlet of the baghouse (controlled emissions), the total CDD/CDF concentrations in the flue gas were 0.98 and 6.00 ng/dscm, respectively, for the two trains used (see Table 12). The controlled CDD/CDF emission averaged 3.47 ng/dscm. All CDD/CDF values given have been referenced to 12% CO_2. Thus, during the period including sootblowing for about 30 minutes, the CDD/CDF removal in the flue gas cleaning system was 95.0%, and for the period after sootblowing, the removal was 98.4%. Overall, the total CDD/CDF removal during shutdown was 98.2%.

Inlet total CDD/CDF concentrations during start-up were 790 and 206 ng/dscm, respectively, during the first and second half of the 3-h test period, respectively (see Table 13). The outlet, or controlled, CDD/CDF concentration was 11.7 ng/dscm for a single sampling train; the results from the second train were questionable because of the very low recovery of internal standards. The corresponding total CDD/CDF removals were 98.5% during the first half of start-up and 94.3% over the second half. For the start-up period, the total CDD/CDF removal was 97.4%.

The total CDD/CDF removals during the shutdown and start-up tests compare well with the baseline value of 99.2% obtained in earlier tests. In terms of 2378-TCDD equivalencies (EPA method), the outlet concentration during shutdown was 0.008 ng/dscm, and 0.013 and 0.062 ng/dscm during start-up and baseline operation, respectively, all referenced to 12% CO_2. The corresponding inlet concentrations for shutdown were 0.282 (without sootblowing) and 0.666 ng/dscm (with sootblowing), while for start-up, they were 7.06 (first half) and 1.16 ng/dscm (second half).

Based on the results presented here, the lime spray dryer absorber/baghouse system can effectively control CDD/CDF emissions even when the furnace is operating at unsteady state conditions. This is desired because the formation of these pollutants is especially favored by start-up conditions.

CONCLUSIONS

The characterization tests performed on the Marion County Solid-Waste-to-Energy Unit 1 indicated that:

1. The CO emission from the furnace was 17 ppmv or less over the normally expected operating condition range.

2. The spray dryer absorber/baghouse system generally removed 90% or more HCl over the range of expected combustor operating conditions when the spray dryer absorber outlet temperature was held at or below 149°C (300°F). However, under these same conditions, the SO_2 removal was below 70%. Under the controls for this system, the lime stoichiometry and spray dryer absorber outlet temperature were not independent, with the lime solids content being fixed in the feed slurry and slurry feed rate being used to control the gas temperature at the spray dryer outlet. The inlet SO_2 variation was high (up to a factor of 5), while the inlet HCl variation was less than a factor of 2. Since the inlet concentrations of both HCl and SO_2 exceeded the unit's design values, the slurry feed and residual sorbent on the fabric filter were inadequate to remove the HCl and SO_2 to the desired levels of 90 and 70%, respectively, at the high concentrations experienced.

3. The total CDD/CDF levels in the ash samples from the characterization test runs were 15 ppb or less. The baghouse solids had the highest concentrations, suggesting that the baghouse is effective in removing these pollutants.

4. Under transient conditions (shutdown and start-up), the flue gas cleaning system removed 94% or more of the total CDD/CDF. This system was as effective in controlling these pollutants during shutdown when the inlet concentration to the spray dryer absorber ranged from 62.1 (after sootblowing) to 121 ng/dscm (with sootblowing) as well as during start-up when the concentration was 206 to 790 ng/dscm.

ACKNOWLEDGEMENTS

The authors express their thanks to the Radian Corporation and Entropy Environmentalists, Inc., EPA's contractors for the tests reported here. Special thanks are expressed to Winton Kelly of Radian Corporation and Ron Jernigan of Entropy and their associates for their dedicated and effective performance during the testing and report preparation. The authors express their appreciation to Jeffrey Hahn of Ogden Projects, Inc. and Fred Engelhardt and Russ Johnson of the Marion County Solid-Waste-to-Energy Facility, Inc. for their cooperation and assistance while planning and conducting these tests. The cooperation of their employers is also acknowledged in making these tests possible. The assistance of C.A. Vogel of EPA's Air and Energy Engineering Research Laboratory in reducing the data and correlating results is gratefully acknowledged.

REFERENCES

1. Municipal Waste Combustion Study: Report to Congress, EPA/530-SW-021a (PB87-206074), June 1987, U.S. Environmental Protection Agency, Office of Solid Waste, Washington, DC.

2. Municipal Waste Combustion Study: Flue Gas Cleaning Technology, EPA/530-SW-87-021d (PB87-206116), June 1987, U.S. Environmental Protection Agency, Office of Solid Waste, Washington, DC.

3. Marion County Fact Sheet, Ogden Martin Systems, Inc., 40 Lane Road, Fairfield, NJ.

4. Scherrer, Richard and David I. Juran, "Air Pollution Control Considerations for Municipal-Solid-Waste-to-Energy Facilities," Paper No. 86-JPGCEC-12, The American Society of Mechanical Engineers, New York, NY. (1986)

5. Teller, A. J., "The Landmark Framingham, Massachusetts, Incinerator." Presented at the Hazardous Materials Management Conference, Philadelphia, PA, June 5-7, 1984.

6. Municipal Waste Combustion Multipollutant Study, Characterization Emissions Test Report, Marion County Solid-Waste-to-Energy Facility, Ogden Martin Systems of Marion, Inc., Brooks, OR, EMB Report No. 86-MIN-04, September 1988, OAQPS, U.S. Environmental Protection Agency, Research Triangle Park, NC.

7. Entropy Environmentalists, Inc., HCl Monitoring for Characterization Test Program, Marion County Solid-Waste-to-Energy Facility, Inc. OAQPS Draft Emission Test Report, August 3, 1987. Prepared under Work Assignment No. 11, EPA Contract No. 68-02-4336, U.S. Environmental Protection Agency, Research Triangle Park, NC.

8. Municipal Waste Combustion Multipollutant Study, Shutdown/Startup Emission Test Report, Marion County, Solid-Waste-to-Energy Facility, Ogden Martin Systems of Marion, Inc., Brooks, OR, EMB Report No. 87-MIN-04A, September 1988, OAQPS, Environmental Protection Agency, Research Triangle Park, NC.

9. Municipal Waste Combustion Study: Combustion Control of Organic Emissions, EPA/530-SW-021c (PB87-206090), June 1987, U.S. Environmental Protection Agency, Office of Solid Waste, Washington, DC.

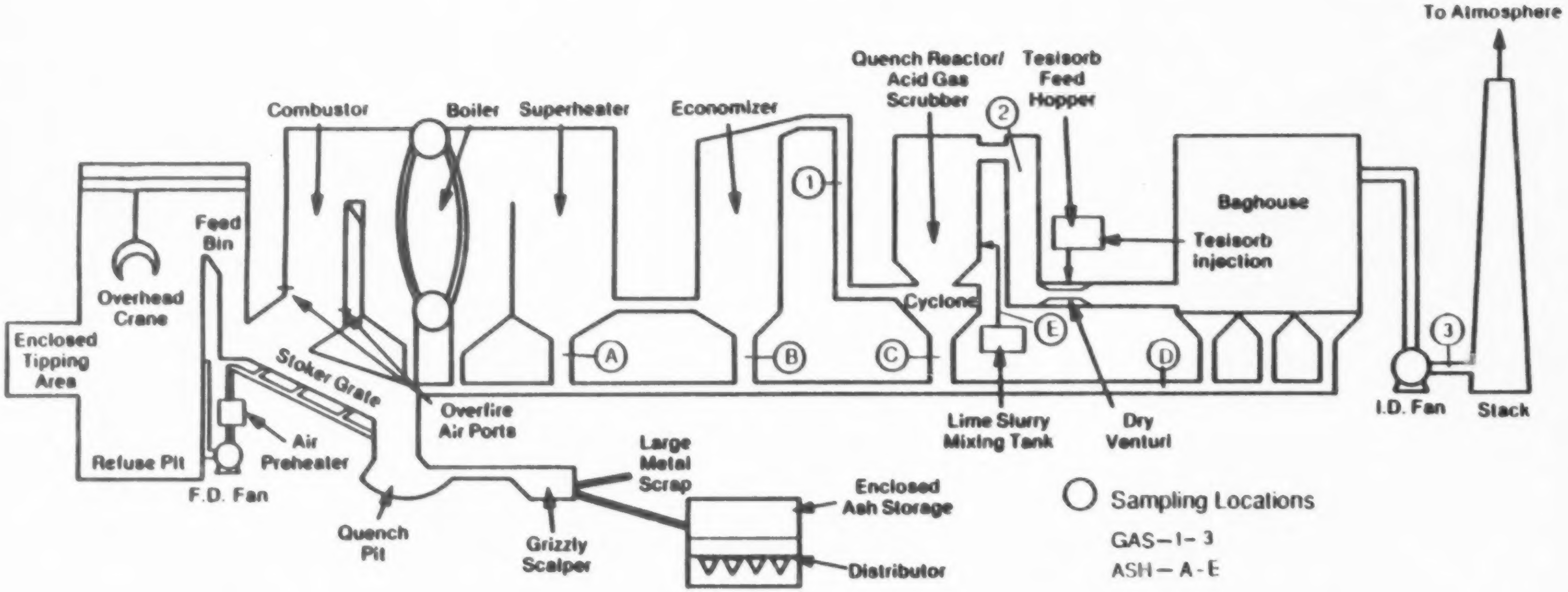
To Atmosphere
Combustor
Boiler
Superheater
Economizer
Quench Reactor/ Acid Gas Scrubber
Tesisorb Feed Hopper
Baghouse
Tesisorb injection
Feed Bin
Overhead Crane
Enclosed Tipping Area
Refuse Pit
F.D. Fan
Air Preheater
Stoker Grate
Overfire Air Ports
Quench Pit
Grizzly Scalper
Large Metal Scrap
Enclosed Ash Storage
Distributor
Cyclone
Lime Slurry Mixing Tank
Dry Venturi
I.D. Fan
Stack
1
2
3
A
B
C
D
E
Sampling Locations
GAS—1-3
ASH—A-E

Figure 1. Flow diagram for incinerator unit of the Marion County Solid-Waste-to-Energy Facility. (3)

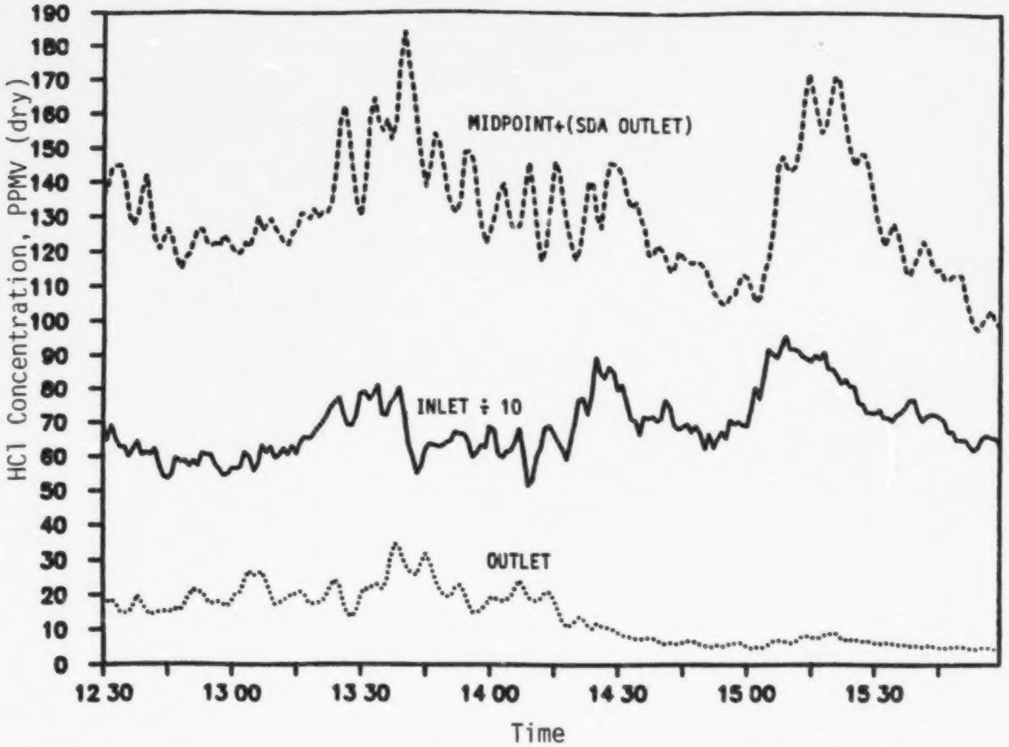

Figure 2. HCl concentrations for the spray dryer absorber/baghouse (Run 10). (7)

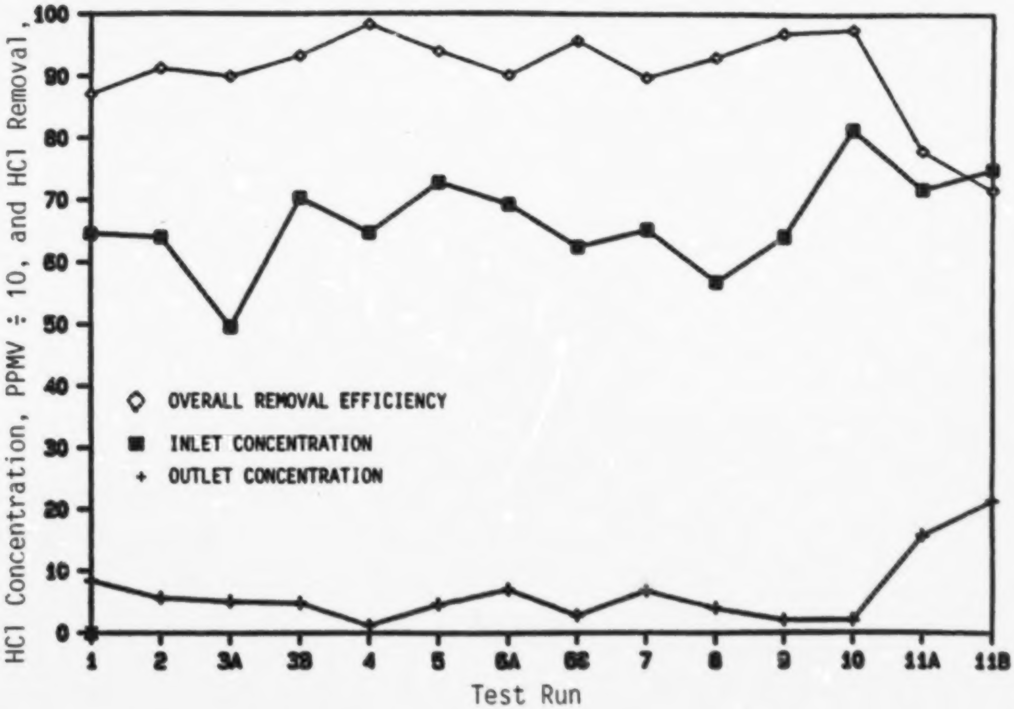

Figure 3. HCl concentrations (corrected to 12% CO_2) and removal in spray dryer absorber/baghouse. (7)

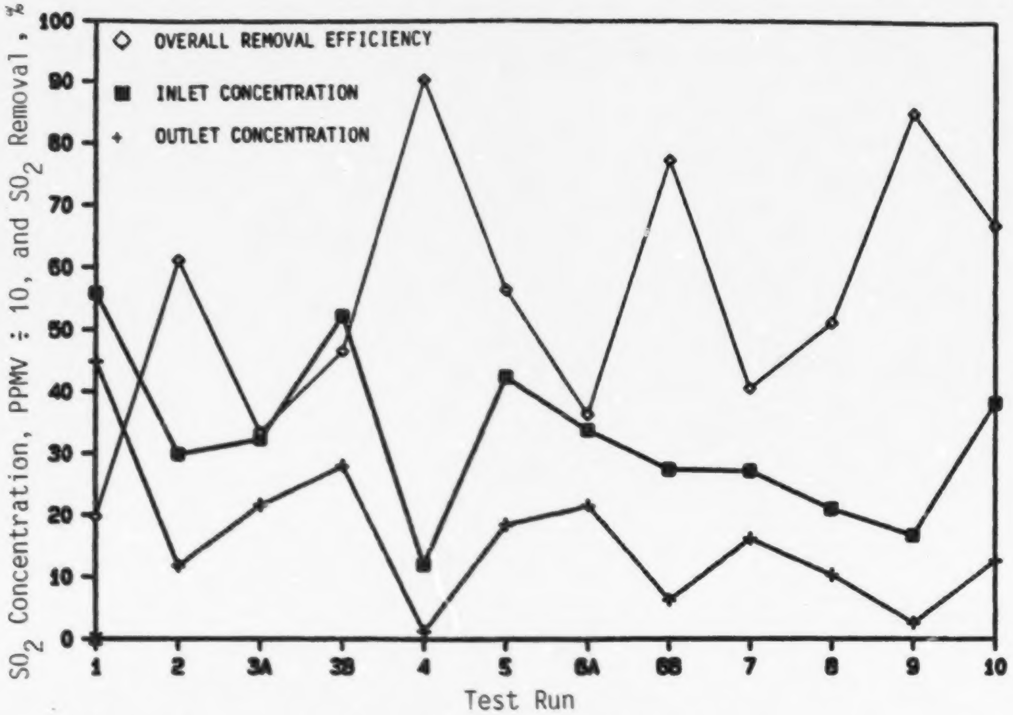

Figure 4. SO_2 concentrations (corrected to 12% CO_2) and removal in spray dryer absorber/baghouse. (6)

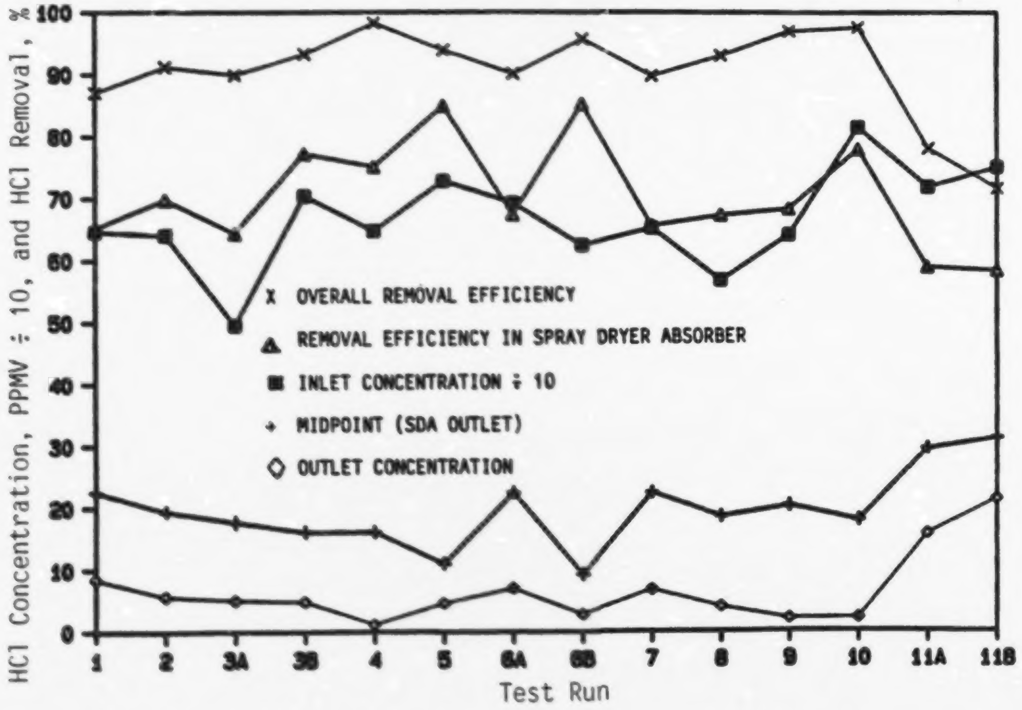

Figure 5. HCl concentrations (corrected to 12% CO_2) and removal for spray dryer absorber (SDA) and spray dryer absorber/baghouse. (7)

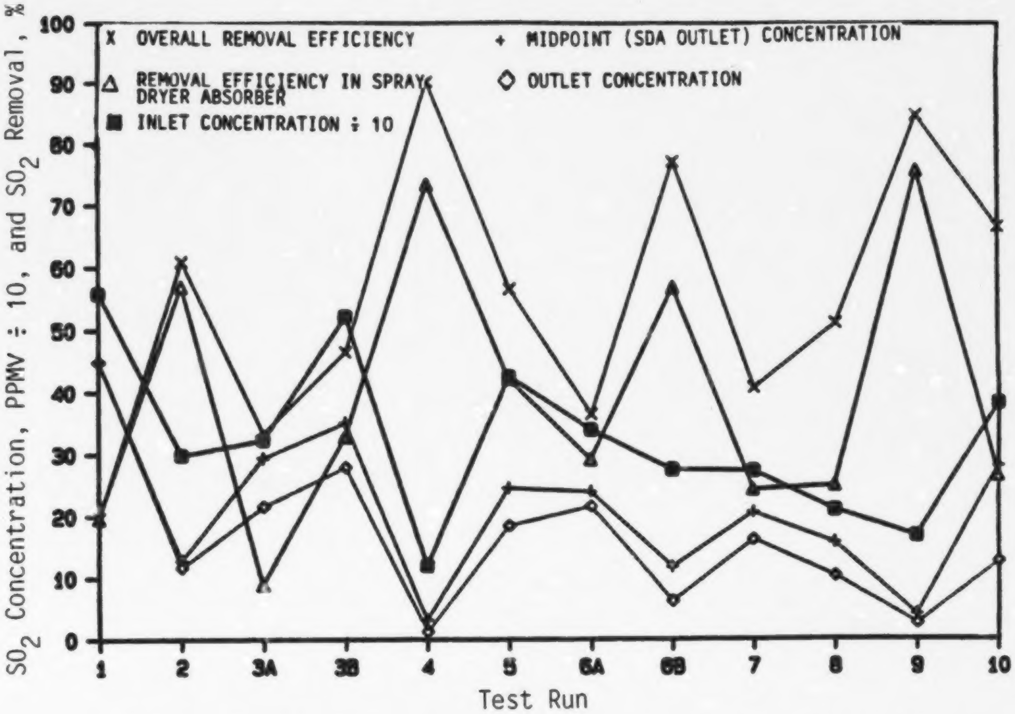

Figure 6. SO_2 concentrations (corrected to 12% CO_2) and removal for spray dryer absorber (SDA) and spray dryer absorber/baghouse. (6)

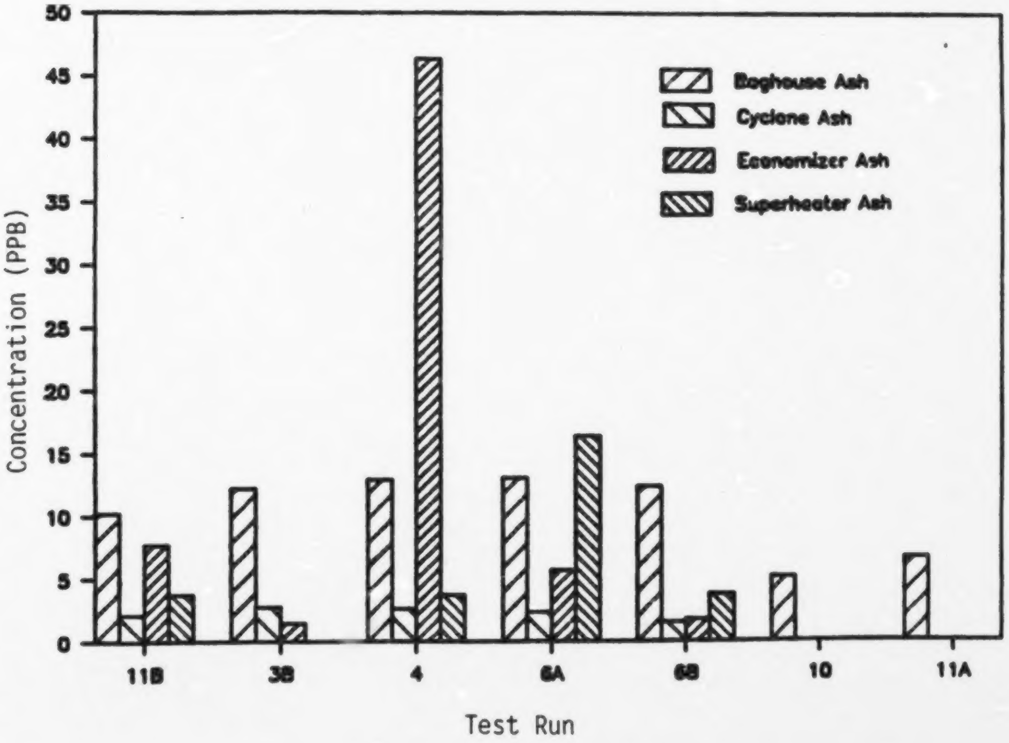

Figure 7. Summary of ash total CDD/CDF concentrations. (6)

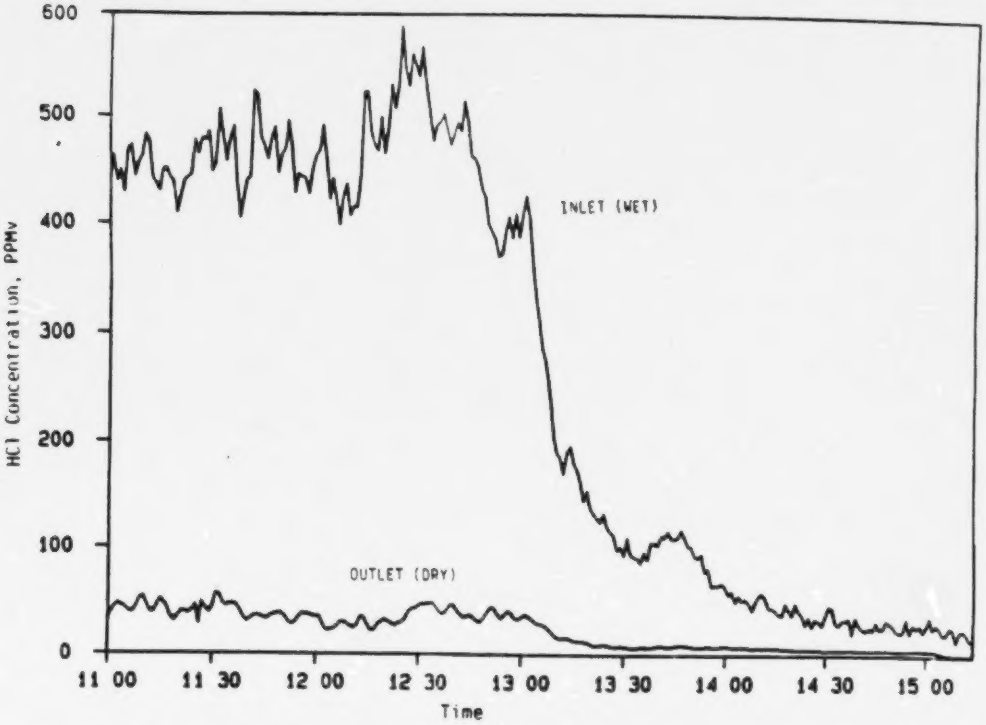

Figure 8. HCl concentration across spray dryer absorber/baghouse during shutdown test. (7)

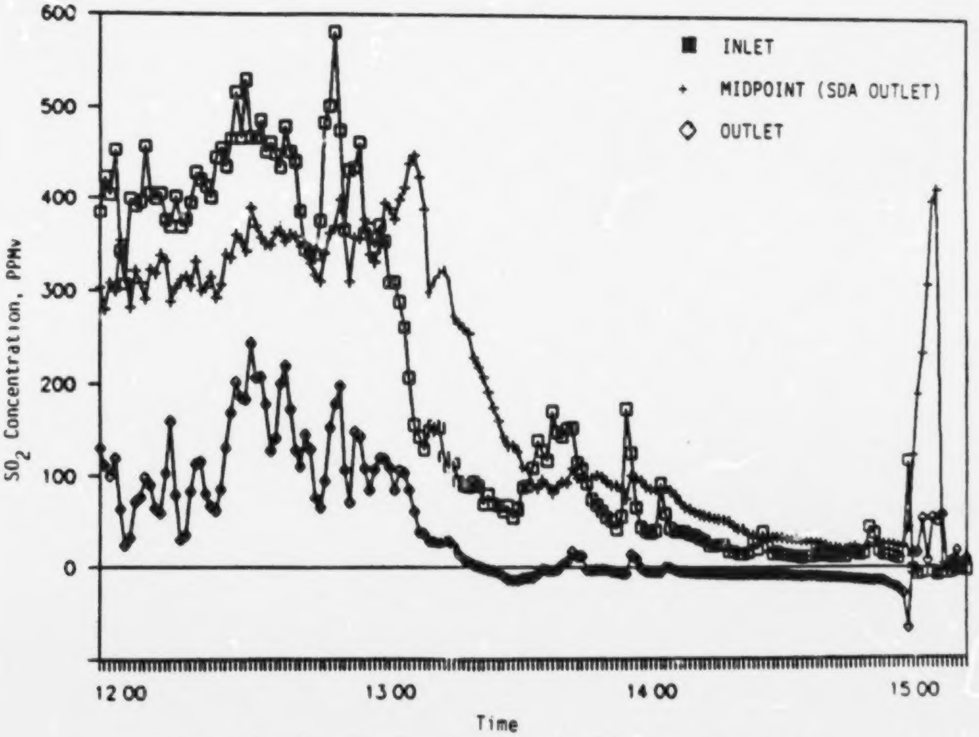

Figure 9. SO_2 concentrations for spray dryer absorber (SDA)/ baghouse during shutdown. (6)

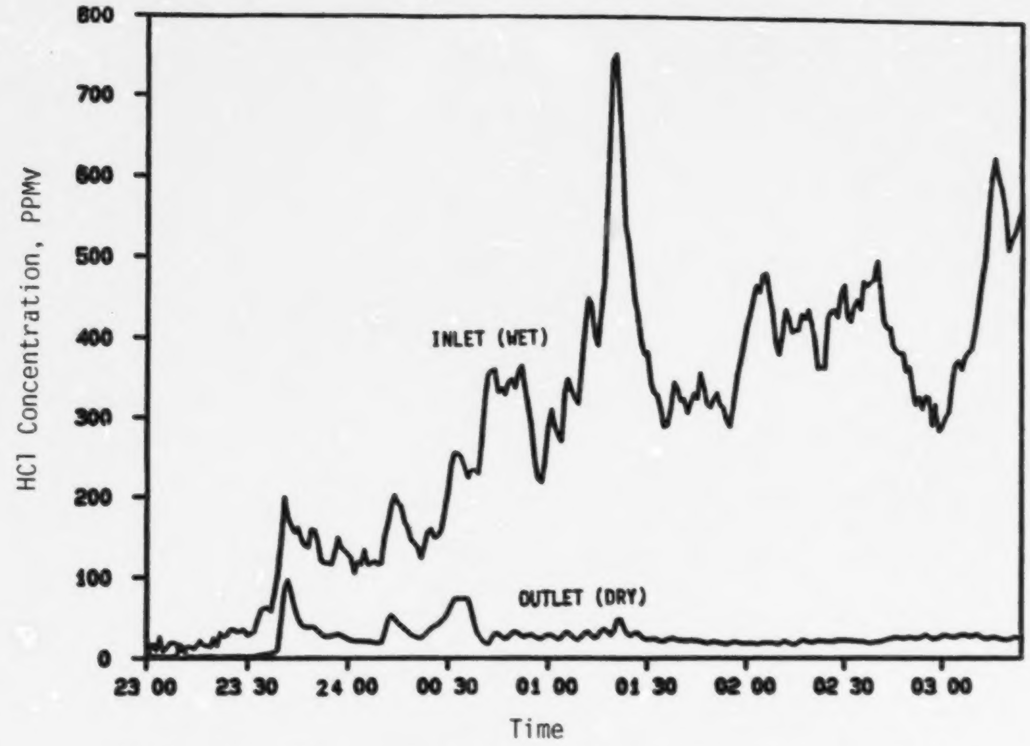

Figure 10. HCl concentration across spray dryer absorber/ baghouse during start-up. (7)

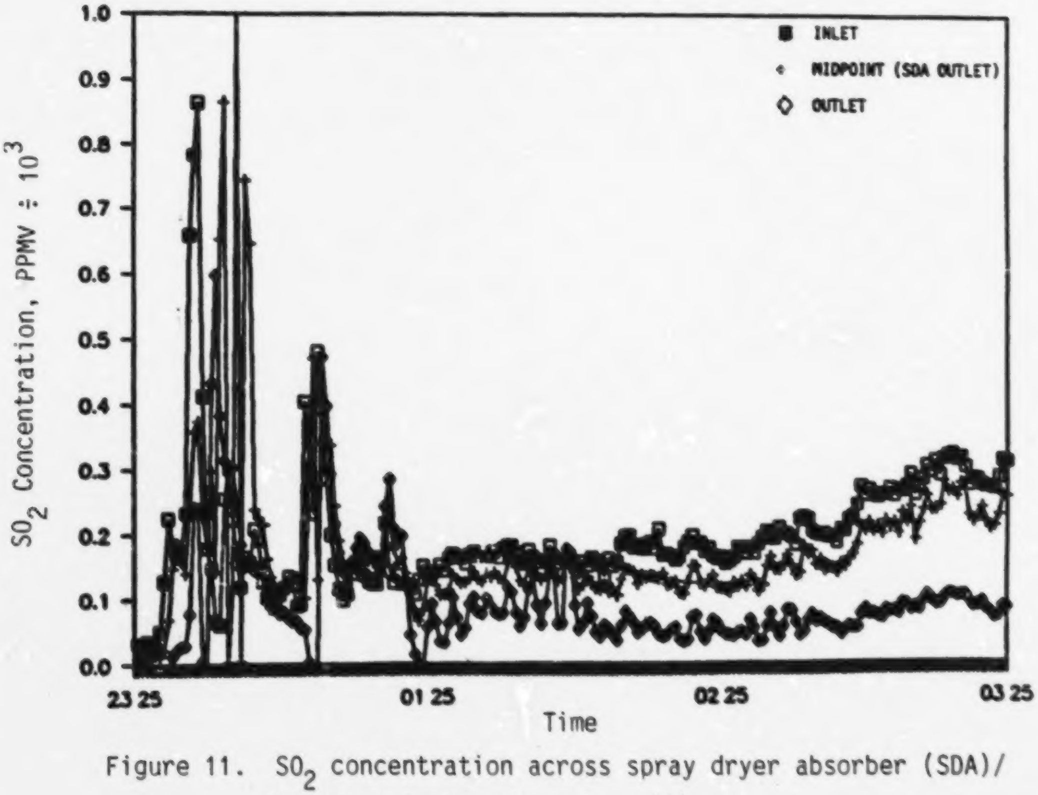

Figure 11. SO$_2$ concentration across spray dryer absorber (SDA)/ baghouse during start-up. (6)

TABLE 1. CONTINUOUS EMISSION MONITOR AND MEASUREMENT

Variable	Monitor	Measurement[a]
Oxygen	Thermox Model WDG III	Inlet concentration, % volume
"	Beckman Model 755	Midpoint concentration, % volume
"	Thermox Model WDG III	Outlet concentration, % volume
Carbon Dioxide	Beckman Model 865	Inlet concentration, % volume
" "	Anarad Model AR412	Midpoint concentration, % volume
" "	Beckman Model 865	Outlet concentration, % volume
Sulfur Dioxide	Western Model 721A	Inlet concentration, ppmv
" "	Thermo Electron (TECO) Model 40	Midpoint concentration, ppmv
" "	Thermo Electron (TECO) Model 45	Outlet concentration, ppmv
Carbon Monoxide	Thermo Electron (TECO) Model 48	Inlet concentration, ppmv
Nitrogen Oxides	Thermo Electron (TECO) Model 10AR	Inlet concentration, ppmv
" "	Thermo Electron (TECO) Model 10AR	Outlet concentration, ppmv
Average Total Hydrocarbons	Beckman Model 402	Inlet concentration, ppmv
"	Beckman Model 400	Outlet concentration, ppmv
Hydrogen Chloride	Thermo Electron (TECO) Model 15 with Model 200 dilution system	Inlet concentration, ppmv
" "	Lear Siegler (LSI) Model TGM with Compur Model 4330 dilution probe	Midpoint concentration, ppmv
" "	Bodenseewerk Model 6577	Outlet concentration, ppmv

---

[a] Inlet refers to spray dryer absorber inlet, midpoint is the spray dryer adsorber outlet, and outlet is the baghouse outlet.

TABLE 2. SUMMARY OF CHARACTERIZATION TEST PROGRAM AT MARION COUNTY, OREGON, SOLID-WASTE-TO-ENERGY FACILITY, JUNE 1987

Test Run	Date	Purpose	Test Conditions
1	6/4/87	Baseline Data	Steam generation rate = 30,500 kg/h (67,100 lb/h); Excess air = 90%: 25% overfire and 75% underfire air; Spray absorber outlet temperature = 149°C (300°F)
2	6/5/87	" "	See Run No. 1
3A	6/6/87	Combustor Data	Low excess air = 37.3%: 25% overfire; 97.0% design load; spray absorber outlet temperature = 148°C (299°F)
3B	6/6/87	" "	High excess air = 102%: 25% overfire; 96.8% design load; spray absorber outlet temperature = 149°C (300°F)
4	6/8/87	" "	Low overfire/underfire air: 100% underfire; 99.2% design load; spray absorber outlet temperature = 149°C (300°F)
5	6/9/87	" "	High overfire/underfire air: 70.7% excess air: NA[b] overfire; 104.5% design load; spray absorber outlet temperature = 148°C (299°F)
6A	6/10/87	" "	Low load = 77.6% of design load; 72.1% excess air: 25% overfire; spray absorber outlet temperature = 150°C (302°F)
6B	6/10/87	" "	Low load = 72.7% of design load; high excess air = 149%: NA[b] overfire; spray absorber outlet temperature = 149°C (300°F)
7	6/11/87	" "	Low load = 78.2% of design load; low excess air = 59.1%: 25% overfire; spray absorber outlet temperature = 142°C (288°F)
8	6/12/87	" "	Low load = 75.6% of design load; low excess air = 87.5%: low overfire/underfire, NA[b] overfire; spray absorber outlet temperature = 148°C (298°F)
9	6/12/87	" "	Low load = 78.5% of design load; high overfire/underfire, NA[b] overfire; spray absorber outlet temperature = 148°C (299°F)
10	6/15/87	Flue Gas Cleaning System Data	Low spray absorber outlet temperature = 127°C (262°F); 101.7% design load; 81% excess air: 25% overfire
11A	6/16/87	"	High spray absorber outlet temperature = 166°C (330°F); 102.7% design load; 73.6% excess air: 25% overfire
11B	6/16/87	"	High spray absorber outlet temperature = 182°C (360°F); 100.2% design load; 78.0% excess air: 25% overfire
12	6/21/87	Shutdown	
13	6/22-23/87	Start-up	Unit was not completely cold.

---

[a] This steam generation rate is 101.8% of the design load: 29,900 kg/h (66,000 lb/h).(6)
[b] N/A - not available

TABLE 3. SUMMARY OF OXYGEN CONCENTRATIONS, MARION COUNTY UNIT 1 CHARACTERIZATION TEST (6)

Test Run	Oxygen Concentration, % Volume		
	Inlet	Midpoint	Outlet
1	9.0	10.9	11.7
2	8.8	10.7	11.9
3A	5.7	8.5	10.1
3B	10.6	11.9	13.2
4	8.8	9.9	12.2
5	8.7	10.2	12.0
6A	8.8	10.7	11.8
6B	12.5	13.5	15.0
7	7.8	9.9	11.3
8	9.8	11.4	12.8
9	10.1	11.4	13.1
10	9.4	10.6	11.7
11A	8.9	10.9	11.9
11B	9.2	11	12

TABLE 4. SUMMARY OF CARBON DIOXIDE CONCENTRATIONS, MARION COUNTY UNIT 1 CHARACTERIZATION TEST (6)

Test Run	Carbon Dioxide Concentration, % Volume		
	Inlet	Midpoint	Outlet
1	10.4	8.6	8.0
2	11.0	9.0	8.1
3A	13.1	11.1	10.2
3B	8.9	8.5	7.4
4	10.3	8.8	7.5
5	10.5	8.9	8.2
6A	10.3	8.8	8.4
6B	7.3	6.2	5.6
7	11.6	9.4	8.8
8	9.8	8.2	7.6
9	9.5	7.9	7.2
10	10.3	8.8	8.1
11A	10.6	8.8	7.9
11B	11	8.6	7.8

TABLE 5. SUMMARY OF SULFUR DIOXIDE CONCENTRATIONS, MARION COUNTY UNIT 1 CHARACTERIZATION TEST (6)

Test Run	Average Sulfur Dioxide Concentration, ppmv (Corrected to 12% CO2)		
	Inlet	Midpoint	Outlet
1	558.5	449.3	448.5
2	298.9	128.4	116.6
3A	323.5	294.5	215.6
3B	522.7	351.2	279.4
4	120.2	31.9	11.7
5	425.0	246.6	185.0
6A	339.6	240.5	216.1
6B	275.2	118.8	62.6
7	273.1	206.8	162.3
8	210.6	158.0	102.9
9	168.0	40.3	25.2
10	382.1	280.9	126.5
11A	470.2	522.5	567.5
11B	118.0	177.5	192.9

TABLE 6. SUMMARY OF CARBON MONOXIDE CONCENTRATIONS, MARION COUNTY UNIT 1 CHARACTERIZATION TEST (6)

Test Run	Average Carbon Monoxide Concentration, ppmv (Corrected to 12% CO2)	
	Inlet	Outlet[a]
1	11.5	
2	11.2	
3A	5.1	
3B	17.0	
4	13.2	
5	7.9	
6A	2.0	
6B	16.9	
7	2.2	
8	6.9	
9	10.7	
10	10.8	
11A	8.9	
11B	14.5	

[a] Not monitored.

TABLE 7. SUMMARY OF NO_x CONCENTRATIONS, MARION COUNTY Unit 1 CHARACTERIZATION TEST (6)

	Average Nitrogen Oxides Concentration, ppmv (Corrected to 12% CO2)	
Test Run	Inlet	Outlet
1	304.6	306.0
2	285.4	304.3
3A	199.5	194.6
3B	310.2	304.4
4	221.4	238.7
5	274.2	274.1
6A	256.4	243.3
6B	233.3	270.4
7	190.3	201.8
8	183.7	176.8
9	276.6	283.3
10	265.6	287.4
11A	247.0	250.2
11B	261.9	301.7

TABLE 8. SUMMARY OF TOTAL HYDROCARBONS CONCENTRATIONS, MARION COUNTY UNIT 1 CHARACTERIZATION TEST (6)

	Average Total Hydrocarbon Concentration, ppmv (Corrected to 12% CO2)	
Test Run	Inlet[a]	Outlet
1		0.9
2	0.8	0.6
3A		0.7
3B		0.6
4	0.6	0.6
5		
6A	1.9	
6B	1.5	
7		
8	1.6	
9	1.5	
10	2.3	
11A	2.4	
11B	1.7	

[a] Blanks indicate no reading available.

TABLE 9. SUMMARY OF THE HYDROGEN CHLORIDE CONCENTRATIONS, MARION COUNTY UNIT 1 CHARACTERIZATION TEST (MANUAL SAMPLING) (6)

Test Run	Average Hydrogen Chloride Concentration, ppmv (Corrected to 12% CO2) Inlet	 Midpoint	 Outlet
1	646.2	224.7	83.7
2	640.4	193.6	56.4
3A	495.6	176.6	49.9
3B	703.8	160.4	47.7
4	647.8	161.5	11.5
5	728.8	110.2	45.5
6A	693.1	225.0	69.6
6B	624.8	92.5	27.4
7	652.8	224.7	67.2
8	568.2	185.9	39.5
9	641.7	203.5	19.7
10	814.4	180.0	20.4
11A	718.2	295.4	157.7
11B	750.0	313.1	213.8

TABLE 10. HCl MONITORING RESULTS - TEST RUN (7)

Hour	Time	INLET ppm HCl (dry)	MIDPOINT ppm HCl (dry)	OUTLET ppm HCl (dry)
1	12 30-13 30	629.3	130.0	18.9
2	13 30-14 30	690.0	141.1	20.1
3	14 30-15 30	778.1	132.4	6.8
4	15 30-16 00	700.6	114.0	5.4
3.5-Hour Average		699.3	131.6	13.9
Highest 1-Minute Average		958.9	184.0	35.1
Lowest 1-Minute Average		522.1	97.7	4.4

TABLE 11. SUMMARY OF AVERAGE CEM RESULTS

Test Run	Parameter	Concentration		
		Inlet	Midpoint[a]	Outlet
12	Oxygen, %volume	12.5	14.1	14.8
13	Oxygen, %volume	9.4	12.2	12.8
12	Carbon Dioxide, %volume	6.2	5.1	4.1
13	Carbon Dioxide, %volume	9.3	6.9	6.8
12	Sulfur Dioxide, ppmv @12% CO_2	262.1	235.3	79.6
13	Sulfur Dioxide, ppmv @12% CO_2	215.6	169.4	95.1
12	Carbon Monoxide, ppmv @12% CO_2	13.4	--	37.8
13	Carbon Monoxide, ppmv @12% CO_2	10.3	--	48.4
12	Nitrogen Oxides, ppmv @12% CO_2	210.4	--	245.9
13	Nitrogen Oxides, ppmv @12% CO_2	231.1	--	243.2
12	Total Hydrocarbons, ppmv @12% CO_2	2.7	--	2.9
13	Total Hydrocarbons, ppmv @12% CO_2	3.7	--	1.1
12	Hydrogen Chloride, ppmv @ 12% CO_2	454.3	--	49.8
13	Hydrogen Chloride, ppmv @ 12% CO_2	471.4	--	49.1

[a] CO, NO_x, HD, and HCl measurements not made at midpoint.

TABLE 12. FLUE GAS CDD/CDF RESULTS: SHUTDOWN TEST (8)

	Concentration (ng/dscm at 12% CO_2)					2378-TCDD Toxic Equivalancies[f]				
	Uncontrolled			Controlled		Uncontrolled			Controlled	
	Baseline[a]	with sootblowing[b]	without sootblowing[c]	Baseline[d]	Average of Trains A & B[e]	Baseline	with sootblowing	without sootblowing	Baseline	Average of Trains A & B
Total CDD	31.2	65.7	28.5	1.01	1.18	0.795	0.465	0.197	0.060	0.001
Total CDF	150	54.9	33.6	1.19	2.29	1.16	0.201	0.085	0.002	0.006
Total CDD + CDF	181.2	121.6	62.1	2.20	3.47	1.96	0.666	0.282	0.062	0.007

[a] Average of Runs 1-4 collected by EPA in February 1987.

[b] Train A included two sootblowing cycles lasting 34 minutes of the 200 minutes that this train was operated.

[c] Train B was begun after sootblowing and operated simultaneously afterwards with Train A.

[d] Average of Runs 2 and 3 collected by Ogden Projects in September 1986. The results shown have been adjusted to 68°F and 1 atm.

[e] Train A and Train B were traversed simultaneously in Ports A and B, respectively.

[f] EPA toxic equivalency factors used.

TABLE 13. FLUE GAS CDD/CDF RESULTS: START-UP TEST (8)

	Concentration (ng/dscm at 12% CO_2)					2378-TCDD Toxic Equivalencies[d]				
	Uncontrolled			Controlled		Uncontrolled			Controlled	
	Baseline[a]	Start-up		Baseline[b]	Start-up[c]	Baseline	Start-up		Baseline	Start-up
		1st half	2nd half				1st half	2nd half		
Total CDD	31.2	450	85.2	1.01	2.16	0.795	4.70	0.569	0.060	0.005
Total CDF	150	340	121	1.19	9.56	1.16	2.36	0.590	0.002	0.008
Total CDD + CDF	101.6	790	206.2	2.20	11.72	1.96	7.06	1.16	0.062	0.013

[a] Average of Runs 1-4 collected by EPA in February 1987.

[b] Average of Runs 2 and 3 collected by Ogden Projects in September 1986, but adjusted to 68°F and 1 atm.

[c] Two trains operated simultaneously in two parts, but results reported are for a single train because of extremely low internal standard recoveries in other train.

[d] EPA toxic equivalency factors used.

OPERATING EXPERIENCE WITH A SPRAY DRY SCRUBBING SYSTEM ON AN RDF FIRED BOILER

by: G. E. Bresowar
D. J. Collins
J. I. Accortt
Combustion Engineering, Inc.
Environmental Systems Division
Birmingham, Alabama 35243

ABSTRACT

Flue gas emissions control from multi-fuel waste-to-energy facilities like the Mid-Connecticut Resource Recovery Plant can present a myriad of design and operational challenges. This paper describes the special design features and early operational experience with the rotary-atomized spray dry flue gas cleaning system at Mid-Connecticut. Operational since the Fall of 1987, the flue gas cleaning system has shown a wide range of capability and a high degree of reliability. The test data collected in the Summer of 1988 shows the Mid-Connecticut plant emissions are far below the permitted requirements and indeed among the lowest values measured for any waste-to-energy plant.

INTRODUCTION

The Mid-Connecticut Resource Recovery Plant is a 2,000 TPD Refuse Derived Fuel (RDF) and/or coal-fired municipal waste-to-energy plant located in the Hartford area. It consists of a facility to process non-hazardous waste into RDF, a coal receiving and handling facility, and three power block systems. Each power block system consists of a Combustion Engineering (C-E) VU-40 boiler, a spray dry absorber (SDA) for treating the flue gas with lime slurry reagent, and a reverse-air fabric filter system. The VU-40 boilers are equipped with customized fuel feed and air supply systems for firing RDF, coal or any combination thereof. Both the spray dry absorber and the fabric filter systems are of C-E design. A complete description of the plant can be found in previous reports. (1,2)

DESCRIPTION OF AIR POLLUTION CONTROL SYSTEM

The air pollution control system receives flue gas from the boiler's tubular air heater as shown in the equipment arrangement of Figure 1. Flue gas is routed to the inlet of the spray dryer absorber where it is swirled and contacted with lime slurry which has been finely atomized in a high-speed, rotary spray machine. The spray dryer absorber is a large, open vessel with no internals whatsoever. Beneath the rotary spray machine, a spray cloud is formed as the slurry and flue gas mix. The cloud of droplets dries to form entrained dust. In the process of drying, the acid and other soluble or condensible gases are largely removed from the gas phase while the entrained particulate matter entering the spray dryer absorber is considerably agglomerated within the spray cloud. The entire mass of entrained particulate matter and dry reaction product passes out through the bottom of the spray dryer absorber to the fabric filter. No solids collection is required under the spray dryer absorber.

The particulate laden flue gas from the absorber enters a 12-compartment, reverse-air fabric filter which has a design gross air-to-cloth ratio of 1.54:1 ft^2/ACFM. Each compartment has 168 bags, eight (8) inches in diameter, installed on a bag-to-bag centerline of 9.5 inches. The total filter area is 96,768 ft^2.

The ash collected in the fabric filter hoppers is transported via a drag flight conveyor to the ash treatment and storage system.

The slurry processing system is best understood by examining the process flow diagram of Figure 2. Pebble quicklime is conveyed by truck-mounted blower from the transporting truck to the lime storage silo. The silo has the capacity to hold about 160 tons of quicklime.

Lime is fed from the lime storage silo to one of two 100% redundant paste slakers. Either of these slakers is capable of supplying the entire plant's requirements when firing 2.0% sulfur coal. The lime requirements for RDF firing are considerably less than that required for 100% coal firing, consequently the slaker system is considerably over-designed for the plant's design operating mode.

The lime paste from the slaker reactor is further diluted to produce a 15-22 wt% lime slurry. The slurry is stored in a single 15,000 gallon capacity tank. From this tank, additive is pumped as needed to the three individual additive feed tanks associated with the three power block systems. Additive supply to the additive tanks is manually adjusted based on continuously monitored sulfur dioxide emission level for each of the power block systems. The design emission control scheme includes a computer-generated feed-forward signal which is calculated from three process signals: F.D. fan load, absorber inlet SO_2 concentration, and additive slurry density. The purpose of this feed-forward signal is to facilitate close acid gas control during load or fuel changes.

Feed slurry from an additive feed tank is fed to a spray machine at a rate automatically controlled to maintain the outlet temperature of the spray dryer absorber at an operator-designated target. The design outlet temperatures for this unit are 220°F when firing 100% RDF and 153°F when firing 100% coal. As with the additive slurry control scheme, the SDA outlet temperature control scheme incorporates a feed-forward signal based on boiler load and scrubber inlet temperature to help provide smooth outlet temperature control during load or temperature swings.

Because of the high degree of slurry atomization attainable by the C-E spray machine, the outlet temperature can be maintained at a relatively low approach to saturation without any adverse affects on the absorber operation. This low approach to saturation has been proven with pilot and full scale testing to have a major impact on acid gas removal and lime utilization, therefore, the ability to maintain operation at this low approach has become a key design parameter.

There was concern early in the design phase, that the fabric filter should be protected from sustained low temperature operation. To keep the fabric filter outlet temperature above 175°F or 40°F above the expected dewpoint, a steam-heated ambient air reheat system was added.

The air pollution control system is designed for a high degree of reliability and operational flexibility since it must accommodate flue gas generated from coal and RDF firing, as well as blends of both these fuels. The compositions and flowrates for the resultant flue gases can vary widely as shown in Table 1.

SYSTEM FEATURES

The most significant features of the spray dry scrubbing system are the spray machine, the gas inlet design, and the absorber gas outlet.

SPRAY MACHINE

The spray machine (Figure 3) is composed of a 200 H.P. 3,600 RPM induction motor, a flexible disk-type coupling, a two-stage speed-increasing gearbox, a dynamically flexible shaft for absorbing imbalance-induced vibrations, a slurry distributor, and the atomizing wheel.

FLEXIBLE SHAFT

The flexible shaft connecting the gearbox to the atomizer wheel is a most important component of the C-E spray machine. This shaft reduces the magnitude of the lateral forces which would otherwise be exerted on the shaft bearing as a result of normal atomizer wheel imbalance. The reduction in force can amount to 60:1 in many instances. Without this force reduction, high speed bearing wear and failure would be the major cause of reduced spray machine availability. The flexible shaft works by dynamically flexing as imbalance loads are applied and absorbing the energy with a viscous, or "squeeze-film" damper. A schematic illustrating the mechanism is shown in Figure 4.

Basically, the flexible shaft is two shafts, one within the other. The inner shaft supports the atomizer wheel, rotating at 12,300 RPM. The outer shaft is connected to the gearbox by means of a lubricated spline coupling. The inner and outer shafts are connected to each other rigidly at the gearbox coupling and flexibly via a cage spring near the wheel. The inner race of the high-speed support bearing is mounted to the outer shaft. The outer race is flexibly mounted to the stationary shaft housing by means of a second cage spring. Hence, the bearing carrier is free to move slightly with respect to the housing. Accelerations due to lateral forces on the bearing carrier cause oscillations in this two-spring arrangement. The magnitude of the oscillations is controlled with a "squeeze-film" damper arrangement on the bearing carrier. Movement of the bearing carrier beyond a predefined limit will cause an automatic machine shutdown, thus preventing damage to the shaft or gearbox. As a result of this flexible shaft, the spray machines at Mid-Connecticut and other C-E installations are capable of very high reliability.

The entire flexible shaft assembly, as shown in Figure 5, is easily removed and replaced without the necessity of lowering the spray machine from the SDA penthouse work area. The coupling between the shaft and the gearbox is a lubricated spline type, facilitating easy changeout. With the high reliability and low maintenance associated with the flex shaft design, one spare has thus far been more than adequate to assure spray machine availability.

SPRAY DRYER INLET DISTRIBUTOR

The Mid-Connecticut spray dryer absorbers are designed to handle a range of flue gas flow from 163,000 ACFM to 41,000 ACFM. Further, they must accommodate this wide range at close approach to saturation (as low as 25°F) without adverse effects such as wall, ceiling, or outlet transition deposits. These requirements called for close control of the spray cloud shape, shown in Figure 6. In large scale testing the spray cloud shape was found to be a function of the slurry-to-gas momentum ratio which is a weighted scalar ratio of momentum vector components. A high ratio can cause the spray cloud to rise and impinge on ceiling and high wall surfaces, while a low ratio can produce a cloud shape which is quite narrow and non-conducive to gas/slurry contact. For Mid-Connecticut, a moderately low ratio of 0.35 produces the cloud shape shown in Figure 6.

The ratio can increase to 0.7 or more and the cloud shape widen unacceptably as the boiler fuel is changed from RDF to coal and the unit steaming rate is decreased, unless something is done to increase the gas momentum. This is the purpose of the patented 40/60 inlet.

The inlet is named "40/60" simply because at design load, the inlet allows 40% of the flue gas to enter through the primary swirl chamber while 60% is admitted through the secondary swirl chamber. The secondary chamber is concentrically outside the primary and further from the atomizer wheel. As the gas flow is decreased, the proportion going to the secondary swirl chamber is automatically decreased as well, maintaining a relatively constant flow to the primary swirl chamber. Constant flow is accomplished by throttling the gas through a louver control damper in a manner which maintains a constant pressure differential between the inlet to the primary swirl chamber and the main vessel chamber. Thus, the gas momentum in the vicinity close to the atomizer wheel is maintained to produce an optimum cloud shape at all loads.

SPRAY DRYER ABSROBER OUTLET

Like all of C-E's units, the Mid-Connecticut spray dryer absorber design features a bottom gas drawoff without ash removal as shown in Figure 8.

This type of design is useful because it eliminates the potential problem areas of the ash hopper and the ash removal system under the spray dryer absorber. With proper atomization and cloud shape control, deposits seldom occur in the absorber. However, should they occur during periods of extreme upset conditions, the normal corrective action is to restore routine operation and allow the deposits to dry and drop off into the outlet vanes. The gas velocity in the outlet vane area is high enough to erode and reentrain dislodged wall deposits. Of all the lime-based spray dryer absorbers built according to this design, there have been no incidents where a dryer required cleaning in order to restore normal operation.

START UP EXPERIENCE WITH THE AIR POLLUTION CONTROL SYSTEM

The spray dryer absorber/fabric filter system at Mid-Connecticut was first put into operation in September 1987. While the basic system design has been proven over many years of operation at other coal-fired power plants, this was a first-of-its kind application on a boiler which is fully capable of burning a wide variety of fuels with large load variations. A detailed analysis of this start-up experience is very worthwhile.

SLURRY SYSTEMS

The additive slurry preparation system, consisting of dual 100% paste slakers, performed very well right from the start. However, the lime slaker grit removal system operated erratically at first and seemed to plug routinely during the start-up period. It was found that two 45 degree elbows in the grit discharge line were the culprits. Once the elbows were replaced with an eight-inch completely vertical PVC line, the plugging ceased to occur.

Grit is discharged into mobile bins on the floor within the slaker building. While this has been shown to be an acceptable and practical approach to grit disposal, it definitely has forced a higher level of attention to housekeeping in the slaker building itself. Housekeeping has been somewhat hampered in this area due to the location and type of electrical compartments and termination boxes. In future plants, a preferred practice will be placement of the grit bins outside the slaker building.

Preinstallation concerns about ash and water mixing in the flyash recycle slurry tank seem to be unfounded. However, this system has seen only limited service to date because the boilers have a priority of firing RDF in lieu of coal, thus limiting the availability of coal-fired baghouse solids. Only coal-fired baghouse solids are used for recycle slurry preparation due to the high concentration of chlorides in RDF-fired baghouse solids. Since calcium chloride is more difficult to dry than other reaction products, it is important to avoid recycling and concentrating calcium chloride in the feed slurry.

SPRAY MACHINES

The spray machines, associated lube oil skids, and atomizer wheels have all performed extremely well. The atomizer wheels have shown very little wear from abrasion. It should be noted, however, that most of the run time so far has only been with lime slurry. Feed slurry containing recycle solids can be expected to be much more abrasive. The C-E atomizer wheel is designed to accommodate this more abrasive slurry through specialized material selection and a conservative maintenance/inspection schedule. This schedule stipulates monthly inspection and cleaning of all wear parts and wheel balancing as required. The Mid-Connecticut spray machines have been retrofitted with runtime meters to allow closer monitoring of each machine's usage and strict adherence to prescribed maintenance intervals.

SPRAY DRYER VESSELS

Several absorber vessel inspections during the start-up phase showed that C-E's design which incorporates the "40/60" swirl inlet and sweep-clean bottom gas discharge is very satisfactory for preventing solids buildup on the vessel wall, ceiling, and outlet duct transition.

Only two incidences of vessel flooding or wetting have occurred since start up, both of these which resulted from operator oversight regarding the operation of the absorber total bypass duct. In both incidences feed slurry flow was initiated to the atomizer while all or part of the flue gas was flowing through the bypass. Whenever a situation such as this occurs, insufficient heat is available to evaporate the atomized feed slurry, and deposits accumulate in the SDA outlet duct. C-E recommends that a total bypass duct not be required on future systems since it is not necessary for the process, represents added expense, and acts as a catalyst for operational mishap.

FABRIC FILTERS

The reverse-air fabric filters, designed and manufactured by the Air Preheater Company of Combustion Engineering, operated extremely well from the start when the boilers were firing only coal. Soon after the firing of RDF, however, stress corrosion failures occurred in tension springs and bag clamps which were fabricated from 300-series stainless steel. These same type of failures had occurred somewhat earlier under similar conditions in the EPRI Arapahoe Test Facility, thus reinforcing the assertion that 300-series stainless steel materials should not be used in baghouses following spray dry absorbers on MSW or RDF incinerators.

Another area that is requiring close attention is baghouse wall corrosion. Significant attention is being focused on baghouse insulation, especially near doors, to limit the occurrence of wall cold spots which will lead to corrosion. It has also been determined at Mid-Connecticut that wall coatings are effective at curtailing compartment wall corrosion. Limited testing to date has shown that both standard high temperature paint and valspar zinc paint yield significantly more corrosion resistance than bare carbon steel.

TEST RESULTS

The emission compliance tests performed between May and July of 1988 at the Mid-Connecticut Resource Recovery Facility demonstrated that when firing 100% coal, 100% RDF, coal plus trace RDF, and 80% RDF plus 20% coal, the Combustion Engineering VU-40/SDA/FF system emitted pollutant levels far below all applicable emissions limits or standards. Testing was conducted for seventeen pollutants and the average measured emission levels of each are presented in Table 2.

All testing was conducted by an independent testing agency whose test methods were closely scrutinized and whose quality assurance program was soundly based on accepted EPA methodology. (3) Triplicate samples were collected for each fuel combination.

PCDD/PCDF and PAH sampling was performed using an EPA Modified Method 5 sampling train with a controlled condensation module and an XAD-2 sorbent module. Each PCDD/PCDF and PAH sample was collected isokinetically for seven minutes at each of twenty-five traverse points, making for a total sample collection time of 175 mintues.

Sampling for particulate, heavy metals, HCl, and F^- was also done by 25-point traverse, but with a basically standard EPA train. Total sample time was 75 mintues. HCl was analyzed using a mecuric nitrate titration, F^- by ion specific electrode, and heavy metals (Pb, Cr, Ni, As) were analyzed using EPA Method 12 and 108 guidelines and atomic absorption spectrophotometry.

Sulfuric acid mist was collected using a modified EPA Method 8 train. Mercury emissions were determined in accordance with EPA Method 101A while beryllium was determined using EPA Method 104.

Vinyl chloride, O_2, and CO_2 samples were drawn into a Tedlar bag. Vinyl chloride was determined in accordance with EPA Method 106 using GC/FID. O_2 and CO_2 were determined by Orsat analysis.

Continuous emission monitors (CEM's) were operated during each emission test for determining NO_x, SO_2, CO, VOC, O_2, and CO_2.

The test results in Table 2 compare favorably to the lowest emissions from a wide range of emissions from municipal waste combustors (MWC) reported by EPA in a June 1987 report to Congress. (4) The EPA report was based on a comprehensive study of all types of existing incinerators, most of which only incorporated particulate control devices, while the Mid-Connecticut plant is an example of what is generally considered to be best available control technology, that is high efficiency particulate control along with scrubbers for acid gas control.

A summary of the results from the EPA report are presented in Table 3 along with the results from testing at Mid-Connecticut. To facilitate comparison, RDF-fired NO_x, CO, and SO_2 emissions from Table 2 are converted to ppmdv at 12% CO_2.

Table 3 shows the Mid-Connecticut test results to generally be near the low end of the range of reported emissions from the 1987 EPA Report, except for NO_x, which is not generally absorbed by the flue gas cleaning system. Except for one unexplained low value, the EPA database from the 1987 report shows NO_x levels ranging from 100-380 ppmdv. The database has no data from MWC systems with advanced NO_x control like thermal de-NO_x. With these qualifications, the Mid-Connecticut test results are on the low end of the NO_x emissions range for facilities without thermal-deNO_x.

Finally, it should be noted that the Mid-Connecticut test results for chromium and beryllium are below the detection limits of the analytical procedure used for the tests. The tests will be repeated for these metals, using longer sampling times, and it is anticipated that the results will be at least one order of magnitude lower for chromium and at least two orders of magnitude lower for beryllium.

The overview of data presented above supports the assertion that this spray dry absorber/fabric filter system is among the best available control technology for acid gas and particulate emissions and should be among the industry standard installations for RDF and/or coal burning facilities of the future.

DISCLAIMER

The work described in this paper was not funded by the U.S. Environmental Protection Agency and therefore the contents do not necessarily reflect the views of the Agency and no official endorsement should be inferred.

REFERENCES

1. Mirolli, M.D., Ferguson, W.B., and Bump, D.L., "Mid-Connecticut Resource Recovery Project", paper presented at the 1986 Joint Power Generation Conference, Portland, Oregon, October 19-23, 1986.

2. Ferguson, W.B., Borio, D.C., and Bump, D.L., "Equipment Design Considerations for the Control of Emissions from Waste-to-Energy Facilities", Combustion Engineering Technical Information Paper TIS-8189.

3. EPA, Quality Assurance Handbook Air Pollution Measurement Systems, Volume III (EPA-600/4-7-027b).

4. EPA, Municipal Waste Combustor Study: Emissions Data Base of Municipal Waste Combustors, (EPA/530 SW-87-021C), June 1987.

FIGURE 1
ARRANGEMENT OF COMBUSTION ENGINEERING SPRAY DRY SCRUBBING SYSTEM
MID-CONNECTICUT RESOURCE RECOVERY PLANT

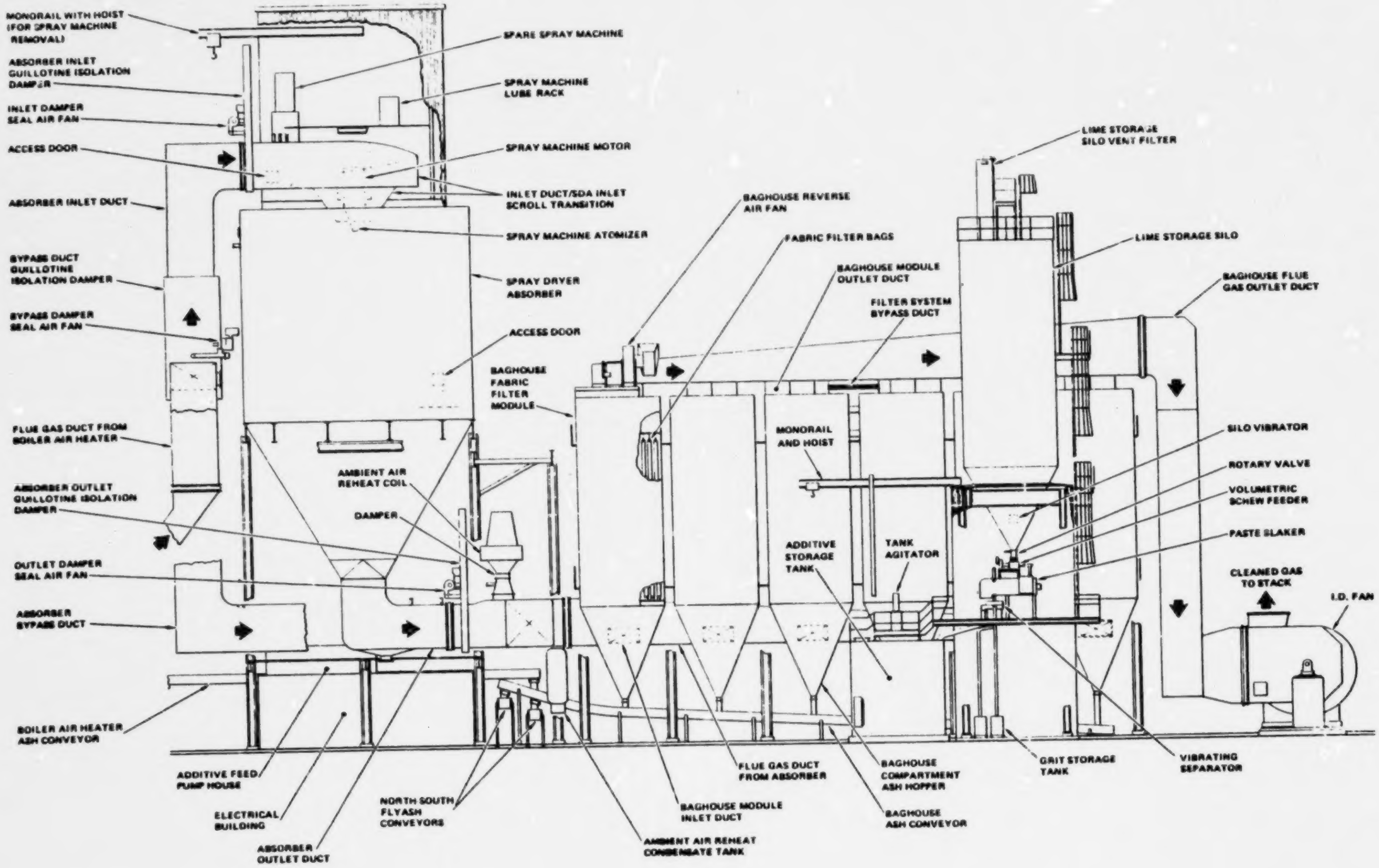
MONORAIL WITH HOIST (FOR SPRAY MACHINE REMOVAL)
ABSORBER INLET GUILLOTINE ISOLATION DAMPER
INLET DAMPER SEAL AIR FAN
ACCESS DOOR
ABSORBER INLET DUCT
BYPASS DUCT GUILLOTINE ISOLATION DAMPER
BYPASS DAMPER SEAL AIR FAN
FLUE GAS DUCT FROM BOILER AIR HEATER
ABSORBER OUTLET GUILLOTINE ISOLATION DAMPER
OUTLET DAMPER SEAL AIR FAN
ABSORBER BYPASS DUCT
BOILER AIR HEATER ASH CONVEYOR
ADDITIVE FEED PUMP HOUSE
ELECTRICAL BUILDING
ABSORBER OUTLET DUCT
NORTH SOUTH FLYASH CONVEYORS
AMBIENT AIR REHEAT CONDENSATE TANK
BAGHOUSE MODULE INLET DUCT
FLUE GAS DUCT FROM ABSORBER
BAGHOUSE COMPARTMENT ASH HOPPER
BAGHOUSE ASH CONVEYOR
GRIT STORAGE TANK
VIBRATING SEPARATOR
SPARE SPRAY MACHINE
SPRAY MACHINE LUBE RACK
SPRAY MACHINE MOTOR
INLET DUCT/SDA INLET SCROLL TRANSITION
SPRAY MACHINE ATOMIZER
SPRAY DRYER ABSORBER
ACCESS DOOR
BAGHOUSE FABRIC FILTER MODULE
AMBIENT AIR REHEAT COIL
DAMPER
BAGHOUSE REVERSE AIR FAN
FABRIC FILTER BAGS
BAGHOUSE MODULE OUTLET DUCT
FILTER SYSTEM BYPASS DUCT
MONORAIL AND HOIST
ADDITIVE STORAGE TANK
TANK AGITATOR
LIME STORAGE SILO VENT FILTER
LIME STORAGE SILO
BAGHOUSE FLUE GAS OUTLET DUCT
SILO VIBRATOR
ROTARY VALVE
VOLUMETRIC SCREW FEEDER
PASTE SLAKER
CLEANED GAS TO STACK
I.D. FAN

Reproduced from
best available copy.

FIGURE 2
PROCESS FLOW FOR COMBUSTION ENGINEERING SPRAY DRY SCRUBBING SYSTEM
MID-CONNECTICUT RESOURCE RECOVERY PLANT

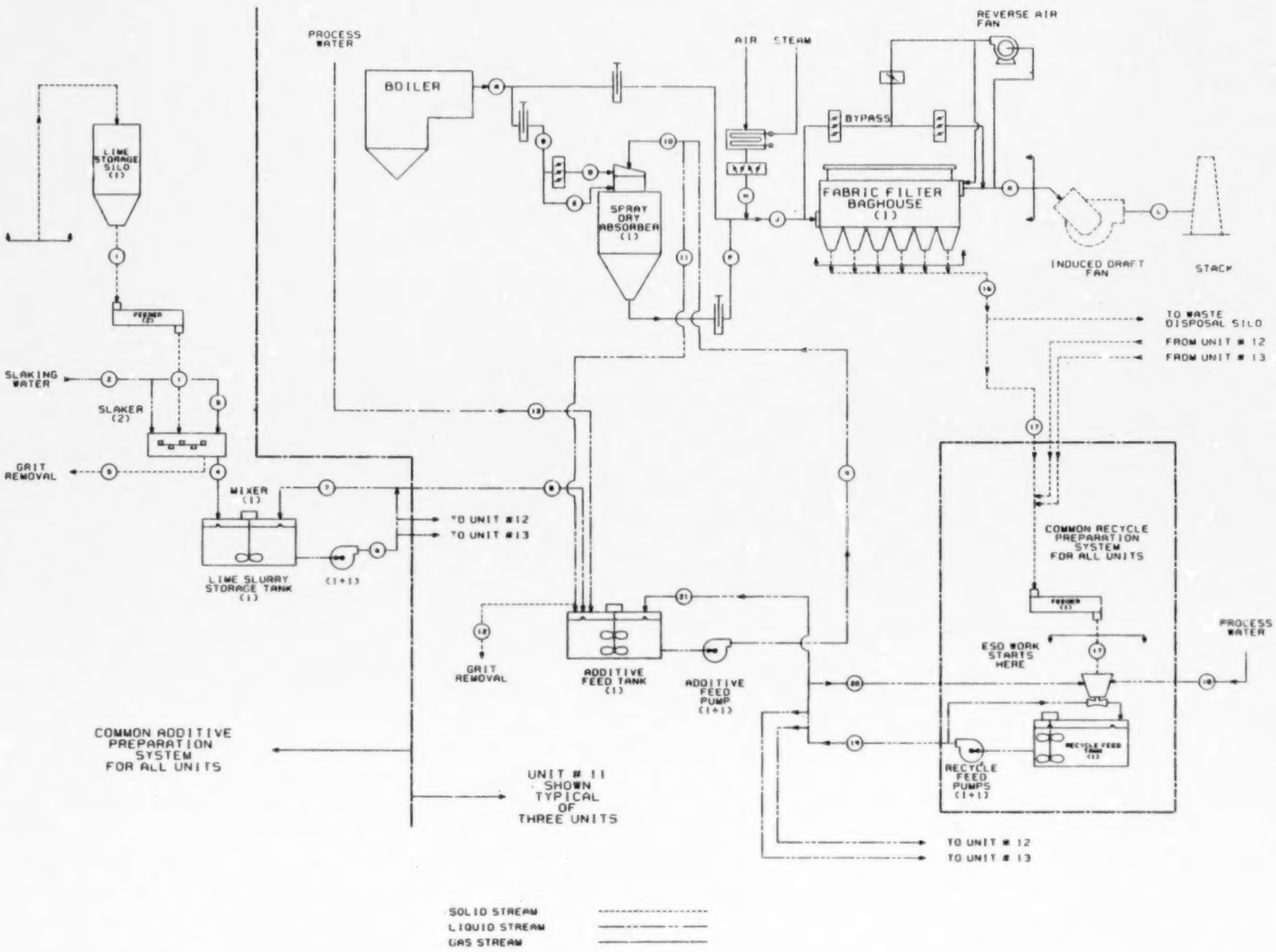

LIME STORAGE SILO (1)
FEEDER (2)
SLAKING WATER
SLAKER (2)
GRIT REMOVAL
MIXER (1)
LIME SLURRY STORAGE TANK (1)
(1+1)
TO UNIT #12
TO UNIT #13
PROCESS WATER
BOILER
SPRAY DRY ABSORBER (1)
AIR
STEAM
BYPASS
REVERSE AIR FAN
FABRIC FILTER BAGHOUSE (1)
INDUCED DRAFT FAN
STACK
TO WASTE DISPOSAL SILO
FROM UNIT # 12
FROM UNIT # 13
COMMON RECYCLE PREPARATION SYSTEM FOR ALL UNITS
FEEDER (1)
ESD WORK STARTS HERE
PROCESS WATER
RECYCLE FEED TANK (1)
RECYCLE FEED PUMPS (1+1)
TO UNIT # 12
TO UNIT # 13
GRIT REMOVAL
ADDITIVE FEED TANK (1)
ADDITIVE FEED PUMP (1+1)
COMMON ADDITIVE PREPARATION SYSTEM FOR ALL UNITS
UNIT # 11 SHOWN TYPICAL OF THREE UNITS
SOLID STREAM
LIQUID STREAM
GAS STREAM

Reproduced from
best available copy.

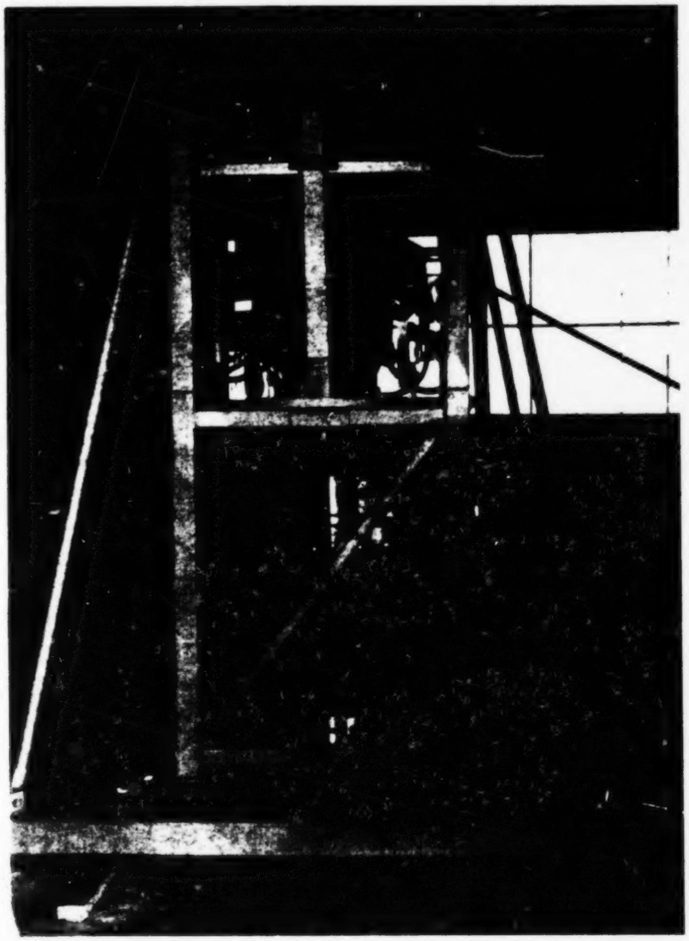

FIGURE 3
MID-CONNECTICUT SPRAY DRYER ABSORBER SPRAY MACHINE

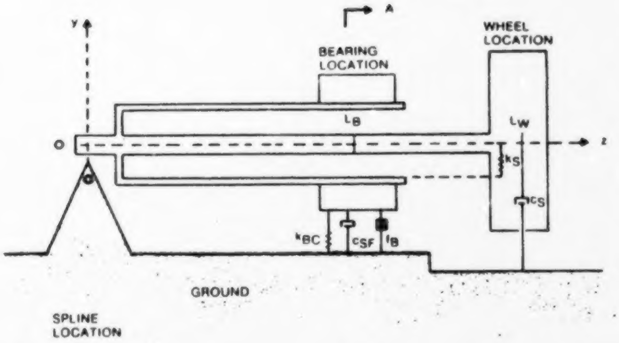
A
WHEEL LOCATION
BEARING LOCATION
y
L_B
L_W
O
z
k_S
c_S
k_{BC}
c_{SF}
f_B
GROUND
SPLINE LOCATION

FIGURE 4
SCHEMATIC OF THE VIBRATION-ABSORBING FLEXIBLE SHAFT

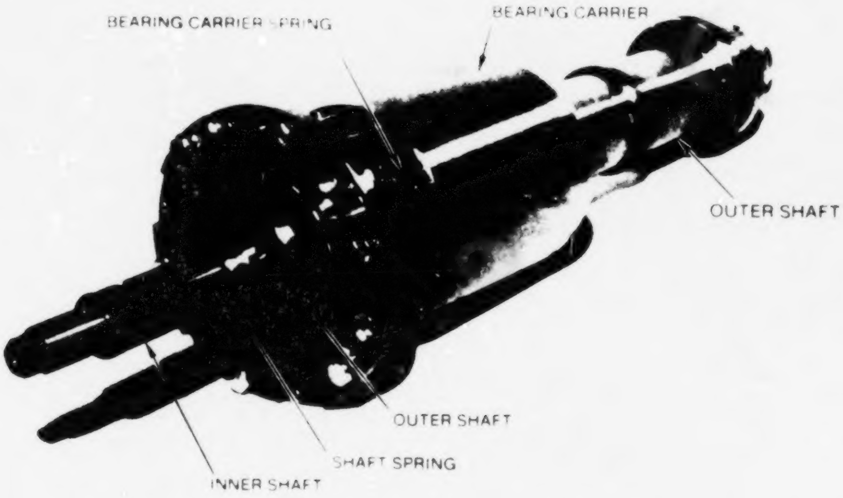
BEARING CARRIER SPRING
BEARING CARRIER
OUTER SHAFT
OUTER SHAFT
SHAFT SPRING
INNER SHAFT

FIGURE 5
FLEXIBLE SHAFT ASSEMBLY REMOVED FOR INSPECTION

FIGURE 6
MID-CONNECTICUT SPRAY CLOUD AT DESIGN MOMENTUM RATIO OF 0.35

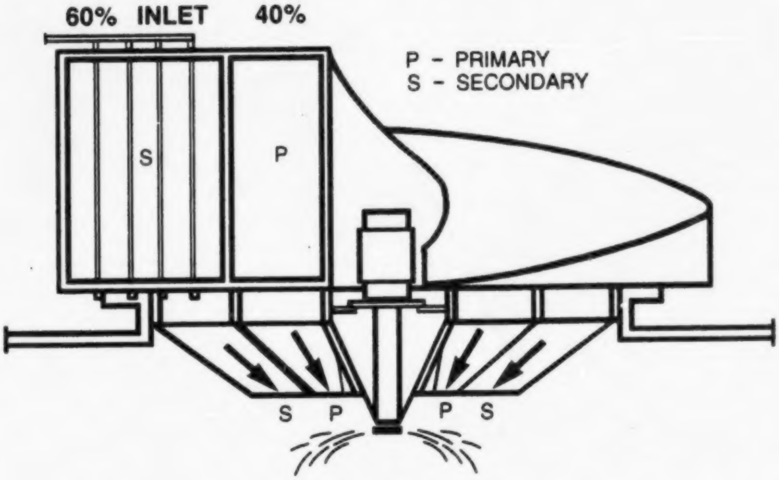
60% INLET 40%
P - PRIMARY
S - SECONDARY
S
P
S P P S

FIGURE 7
PATENTED "40/60" SPRAY DRYER INLET FOR HIGH TURNDOWN OPERATION

FIGURE 8
SPRAY DRYER ABSORBER OUTLET AT MID-CONNECTICUT

TABLE 1
DESIGN SCRUBBER INLET FLUE GAS FLOWS AND COMPOSITIONS FOR MID-CONNECTICUT

Fuel Type	RDF	Coal
Gas Flow, ACFM	163,000	82,000
Gas Temperature, °F	340	350
SO_2, ppmvw	223	1,384
HCl, ppmvw	705	31
Saturation Temperature, °F	150	128

TABLE 2
SUMMARY OF MEASURED EMISSIONS
MID-CONNECTICUT RESOURCE RECOVERY FACILITY

POLLUTANT	UNITS[A]	100%[B] COAL	100%[B] RDF	COAL PLUS[B] TRACE RDF	80% RDF[B] 20% COAL
PCDD/PCDF[C]	ng/Nm^3		<.03	<.08	<.01
Particulate	gr/DSCF	.009	.006	.006	.005
HCl	D		99.5/2	99.6/1	98.6/6
SO_2	lb/MBTU	.240	.010	.110	.006
NO_x	lb/MBTU	.36	.34	.28	.34
CO/CO_2	Ratio	.0006	.0016	.0007	.0008
VOC	ppmdv		<1	<1	<1
F	μg/Nm^3		<16	<125	<10
H_2SO_4	μg/Nm^3		674	1,510	<352
Pb	μg/Nm^3		20	<13	100
Hg	μg/Nm^3		24	18	1
Be	μg/Nm^3		<.76	<1.81	1.51
As	μg/Nm^3		<2.9	<1.5	<2.9
Ni	μg/Nm^3		213	<71	<18
Cr	μg/Nm^3		<45	<19	<6
PAH	μg/Nm^3		<4.1	<16.2	<0.6
Vinyl Chlorides	μg/Nm^3		<260	<2,600	1,190

A - volumes are corrected to 12% CO_2
B - "<" indicates that the value presented is the detection limit. Actual value is between zero and this limit.
C - 2,3,7,8 - TCDD toxic equivalent units
D - % removal/ppmwv

TABLE 3
COMPARISON OF MID-CONNECTICUT TEST RESULTS TO RANGE OF EMISSIONS FROM OTHER INCINERATORS

POLLUTANT	UNITS[A]	EPA-MWC STUDY EMISSION RANGE	MID-CONNECTICUT TEST RESULTS
Dioxin (TEQ)[B]	ng/Nm³	.01 ↔ >5,960	<.03
Particulate	gr/DSCF	.002 ↔ >.6	.006
HCl	ppmdv	7.5 ↔ 1270	2.0
NO_x	ppmdv	39 ↔ 380	184
CO	ppmdv	3.2 ↔ 1,350	188
SO_2	ppmdv	.04 ↔ 401	4.3
Lead	µg/Nm³	25 ↔ 15,500	20
Mercury	µg/Nm³	9 ↔ 2,200	24
Nickel	µg/Nm³	2 ↔ 3,600	213
Chromium	µg/Nm³	3.6 ↔ 6,700	<45
Beryllium	µg/Nm³	.0005 ↔ 21	<.76

A = volumes connected to 12% CO_2
B = 2,3,7,8 - TCDD toxic equivalent units